GEOLOGY OF THE CENTRAL JURA AND THE MOLASSE BASIN:

NEW INSIGHT INTO AN EVAPORITE-BASED FORELAND FOLD AND THRUST BELT

ANNA SOMMARUGA

Dr ès Sciences

MÉMOIRE DE LA SOCIÉTÉ NEUCHÂTELOISE DES SCIENCES NATURELLES

NEUCHÂTEL 1997 TOME XII

Editeur: Société neuchâteloise des Sciences naturelles, p.a. Bibliothèque publique et universitaire de la Ville,
2000 Neuchâtel, Suisse.

Rédacteur: Willy Matthey

Rédacteur technique: Jacques Ayer

ISBN 2-88347-001-4

Imprimé en Suisse

Photo de couverture: Eric Leuba (Photo-Report, La Chaux-de-Fonds)

Photo panoramique à 140 degrés, 2000 m au-dessus du sol. Vue du Jura neuchâtelois en direction du Nord-Est. A gauche, les villes du Locle et de la Chaux-de-Fonds, la Vallée de La Sagne et des Ponts; au centre l'anticlinal du Mont-Racine et le synclinal losangique du Val de Ruz; à droite les Rochers-des-Miroirs et la Montagne de Boudry, le lac de Neuchâtel; à l'horizon le lac de Morat et le Plateau suisse (Bassin molassique).

GEOLOGY OF THE CENTRAL JURA AND THE MOLASSE BASIN:

NEW INSIGHT INTO AN EVAPORITE-BASED FORELAND FOLD AND THRUST BELT

IMPRIMATUR POUR LA THÈSE

Géologie du Jura central et du bassin molassique: nouveaux aspects aur une chaîne d'avant-paya plissée et décollée aur des couchea d'évaporitea

de Mme Anna Sommaruga Mosar

UNIVERSITÉ DE NEUCHÂTEL

FACULTÉ DES SCIENCES

La Faculté des sciences de l'Université de Neuchâtel sur le rapport des membres du jury,

MM. M. Burkhard (directeur de thèse), J.-P. Schaer, G. Gorin (Genève), D. Roberts (Londres) et A.W. Bally (Houston, USA)

autorise l'impression de la présente thèse.

Neuchâtel, le 2 octobre 1997

Le doyen:

R. Dändliker

R. Dändliker

GEOLOGY OF THE CENTRAL JURA AND THE MOLASSE BASIN:

NEW INSIGHT INTO AN EVAPORITE-BASED FORELAND FOLD AND THRUST BELT

GÉOLOGIE DU JURA CENTRAL ET DU BASSIN MOLASSIQUE:

NOUVEAUX ASPECTS D'UNE CHAÎNE D'AVANT-PAYS PLISSÉE ET DÉCOLLÉE SUR DES COUCHES D'ÉVAPORITES

ANNA SOMMARUGA

Dr ès Sciences

Lauréate 1996 du Prix de la Conférence AIH-AISH de Lausanne 1990

Schweizerische Akademie der Naturwissenschaften SANW
Académie suisse des sciences naturelles ASSN
Swiss Academy of Sciences SAS

SN
SN

MÉMOIRE DE LA SOCIÉTÉ NEUCHÂTELOISE DES SCIENCES NATURELLES

TOME XII

REMERCIEMENTS:

Le présent travail a été soutenu par le Fonds National Suisse de la Recherche Scientifique (requêtes N° 4020-031533; 21-37366.93) et par l'Institut de Géologie de l'Université de Neuchâtel.

Je tiens à remercier les compagnies pétrolières et les institutions, propriétaires des profils sismiques et des logs de forages, d'avoir autorisé l'accès, l'utilisation, ainsi que la publication d'une partie de leurs données dans ce mémoire:

- British Petroleum Exploration Operating Company (Angleterre), en la personne du Dr David G. Roberts
- Forces Motrices Neuchâteloises S.A. (Canton de Neuchâtel), en la personne de J. Rossat
- Musée géologique du Canton de Vaud à Lausanne, en la personne de son directeur Dr Aymon Baud
- Office de l'économie hydraulique et énergétique du Canton de Berne
- SEAG (A.G. für schweizerisches Erdöl)
- Shell International Exploration and Production B.V. (Pays-Bas), en la personne du Dr Harry Doust.

La publication de ce mémoire a pu être réalisée grâce au soutien financier de nombreuses institutions, fondations et sociétés, auxquelles je témoigne toute ma reconnaissance:

- Académie Suisse des Sciences Naturelles (Berne)
- British Petroleum Exploration Operating Company (Angleterre)
- CEDRA, Société coopérative nationale pour l'entreposage de déchets radioactifs (Canton d'Argovie)
- Conférence de l'Assoc. internat. des hydrogéol. et des sci. hydrolog. (AIH-AISH) de Lausanne 1990 (Prix 1996)
- Département de l'Instruction publique de la République et du Canton de Neuchâtel
- Fondation Dr Joachim de Giacomi (Canton de Bâle)
- Forces Motrices Neuchâteloises S.A. (Canton de Neuchâtel)
- Schweizer Rheinsalinen (Canton de Bâle)
- Société Neuchâteloise des Sciences Naturelles.

AVANT-PROPOS

"En traitant de la géologie du Jura neuchâtelois, nous ne saurions avoir la prétention d'intéresser par la nouveauté du sujet. Il est peu de chaînes de montagnes qui soient aujourd'hui aussi bien connues que le Jura ...". C'est en ces termes que Desor & Gressly, en 1859, introduisent leurs "Etudes géologiques sur le Jura Neuchâtelois", publiées dans le tome IV de cette même série des Mémoires de la Société Neuchâteloise des Sciences Naturelles. Cent trente-huit ans plus tard, le Jura n'a pas encore cessé d'intéresser les géologues du monde entier et fait toujours partie des chaînes de montagnes les plus étudiées. En effet, il n'est guère d'ouvrages, traitant de la tectonique ou de la géologie structurale, où ne figurent soit les plis du Jura, soit sa structure arquée. Durant toutes ces années, de nouveaux concepts et méthodes géologiques ont été développés, appliqués et testés dans cette petite chaîne modèle, localisée au coeur de l'Europe.

Aujourd'hui, tout comme au temps de Desor et de Gressly, de nouvelles données géologiques ont fourni une "occasion ... de vérifier la justesse de nos théories" (op. cit. p. V). A l'époque, il s'agissait du creusement du tunnel ferroviaire sous la Vue des Alpes, tandis qu'aujourd'hui, ce sont les résultats de sondages par la méthode de "sismique réflexion", qui permettent de compléter nos connaissances et nos visions de la structure profonde du Jura. Depuis la Deuxième Guerre mondiale, le Bassin molassique et le Jura ont été examinés sous l'aspect de leur potentiel pétrolier, d'abord par des études classiques de géologie de surface et ensuite à partir des années 70, à l'aide d'une nouvelle technologie, telle que la "sismique réflexion". Cette méthode, comparable à une radiographie du sous-sol, permet d'identifier la nature des couches et leurs structures, notamment celles qui pourraient piéger du pétrole. A présent, tous ces résultats accompagnés d'une quarantaine de forages n'ont pas fourni de succès tangibles du point de vue pétrolier.

Une des dernières campagnes d'exploration pétrolière en Suisse a été entreprise en 1988 par la compagnie British Petroleum associée aux Forces Motrices Neuchâteloises. Elle a permis d'acquérir environ 300 km de profils de "sismique réflexion", dans le seul canton de Neuchâtel, sondé pour la première fois par cette méthode. L'Institut de Géologie de l'Université de Neuchâtel a eu la possibilité d'examiner les résultats de cette campagne et les premières interprétations réalisées par British Petroleum. Celles-ci ont d'ailleurs conduit à l'abandon du projet d'une exploration pétrolière dans le canton. A notre demande, les propriétaires de ces données ont eu la générosité de donner accès à l'ensemble des profils sismiques à des fins non-commerciales. C'est ainsi, que Anna Sommaruga alors doctorante en géologie, a pu disposer d'un matériel scientifique de grande valeur pour l'étude de la structure profonde et de l'évolution tectonique du Jura central. Pour se perfectionner dans l'interprétation des profils sismiques, un domaine encore peu enseigné dans les universités suisses, A. Sommaruga a effectué deux stages à l'Université de Rice à Houston chez le Prof. A.W. Bally. Excellent connaisseur de la géologie de la Suisse et du Monde, ce dernier fut aussitôt intéressé par ce projet et accepta de parrainer la thèse d'Anna Sommaruga. Vu depuis le Texas, où "everything is big", le canton de Neuchâtel apparaissait cependant comme assez petit et des efforts supplémentaires furent entrepris pour étendre le réseau des profils sismiques au Bassin molassique suisse ainsi que du coté du Jura français, deux régions où la compagnie Shell, avec divers partenaires locaux, avait entrepris préalablement des campagnes de prospection pétrolière. Finalement, grâce à Shell et à Swisspetrol (SEAG), qui ont ouvert leurs archives jusqu'alors confidentielles, un vaste réseau de plus de 1500 km de profils sismiques a été mis à disposition. Il a permis d'analyser la géométrie des structures profondes s'étendant du Jura externe, à travers la Haute Chaîne du Jura plissé, du Bassin molassique jusqu'à la bordure des Alpes. Anna Sommaruga ne s'est pas perdue dans les montagnes de papiers que représentent les originaux de ces profils, elle a réussi à en condenser l'information et à en tirer les points essentiels pour la tectonique de nos régions.

De nouveaux éléments de réponse ont pu être apportés aux questions classiques concernant la formation de la chaîne jurassienne. Parmi les plus importantes, la théorie du "Fernschub", trouve une très belle confirmation dans le présent mémoire. Proposée en 1907 par Buxtorf, elle explique le plissement du Jura par une poussée lointaine horizontale depuis les Alpes, avec un décollement de la couverture sédimentaire au sein des roches évaporitiques du Trias. Bien que cette théorie soit largement acceptée aujourd'hui, il restait bien des points de détail à éclaircir quant aux relations géométriques entre le socle et la couverture. C'est pour la première fois que la profondeur du socle et sa

géométrie lisse sous le Jura et le Bassin molassique ont pu être cartographiées. Ces données excluent une implication considérable du socle dans la formation des plis du Jura. Ces mêmes données sismiques ont permis de mettre en évidence deux types de plis, interprétés comme des stades d'évolution successifs du plissement de la couverture. Les profils sismiques de British Petroleum dans le canton de Neuchâtel fournissent pour la première fois une image complète et très claire des structures profondes, notamment sous le Creux du Van.

Enfin, la Société Neuchâteloise des Sciences Naturelles a accepté de publier ce travail dans la série de ses Mémoires, par lesquels, traditionnellement, les nouvelles données géologiques sur le Jura ont été diffusées. La parution coïncide avec la réunion annuelle de l'Académie Suisse des Sciences Naturelles à La Chaux-de-Fonds en automne 1997; son thème général "Paysage calcaires de l'Arc jurassien: du minéral au vivant" s'accorde parfaitement avec celui de ce nouveau mémoire.

Prof. Martin Burkhard
Institut de Géologie, Université de Neuchâtel

Avertissement au lecteur

Ce mémoire s'articule en deux parties: un volume texte avec de nombreuses figures et une série de planches et de panneaux hors-texte. Ces documents, de différents formats, sont cités dans le texte et leurs légendes se situent à la fin du mémoire.

TABLE OF CONTENTS

ACKNOWLEDGMENTS

This research is the result of a collaboration and cooperation with many individuals and institutions. I would like to express my gratitude to all those who have helped or supported me.

Firstly, I would like to thank Prof. Jean-Paul Schaer, who asked me, four and half years ago, to participate in a one year PNR20 project interpreting four seismic reflection lines (30 km) crossing the Val de Ruz. At the time we would not have imagined that this research was to continue in a thesis focusing on the interpretation of more than 1500 km of seismic lines! I also thank him for introducing me to seismic interpretation, advising me to go to Rice University for a short stay and again for having shared all his precious knowledge on the historical and regional geology of the Jura Mountains.

To Prof. Martin Burkhard, my advisor, to whom I owe countless discussions about structural geology, regional geology of the Jura and some ideas presented in this work. I thank him for his general enthusiasm, his generosity providing me with the necessary means for developing this research and for his encouragement and confidence in my work.

All my gratitude goes to Prof. Albert Bally who has kindly invited me twice to Rice University in Houston as visiting student (January-August 1993, Summer 1994) and has introduced me to the fascinating world of seismic interpretation. During his lectures he taught me the regional geology of many areas around the world as well as *Occam's Razor* philosophical maxime. I thank him for the numerous discussions on foreland fold belts and salt tectonics, which gave me a new insight on the Jura. Furthermore, he helped me to obtain most of the seismic data which I have been working on during my thesis.

I am grateful to Dr David Roberts from British Petroleum, who kindly provided the data from the Neuchâtel Jura which made it possible to broaden considerably the initial scope of my thesis.

My thanks go to Prof. Georges Gorin who gave me the first advice on seismic interpretation and correlation with well logs.

I am indebted to Dr Peter Lehner and Dr Hans Andreas Jordi for stimulating discussions on the interpretation of seismic lines from the Jura and Molasse Basin.

To the whole staff of Professors, assistants, students and personnel from the Institut de Géologie de Neuchâtel who has contributed to a familial atmosphere at the Department. I particularly remember the same year PhD students (Pierre Lambert, Essaïd Zeroual, Marie-Caroline Blanc-Aletru, Marc Rolli, Philippe Mouchet), with whom I have shared the same preoccupation and amount of stress during the last months of our theses. I thank Gregor Schönborn for sharing with me his knowledge about the regional geology of the eastern Jura and about thrust tectonics and for his precious advice. I am indebted to Xavier Tschanz who, during the first year of my thesis, took me to many field trips in the Neuchâtel Jura. To my officemate and friend Thierry Baudin, many thanks for countless "philosophical" discussions about geology and life and also for his encouragement. I do not forget all my friends from the "barrio" (Gabor Tari, Joan Flinch, Norbert Pralle, CJ Liu, Sebastian Galeazzi, ...) or from the Geology Department of Rice University (Laura De Santis, Phil Bart, Olivier Aubert, Klaus Holliger, ...) who have helped me during my stay in Houston.

I also owe my gratitude to Julie Schaer and David Hindle, who kindly helped me improve my knowledge in english.

I would like to thank A.W. Bally, M. Burkhard, G. Gorin, D. Roberts and J.-P. Schaer for critical review of this manuscript.

Many thanks to Jacques Ayer, who considerably helped with the final editing of this work.

I am grateful to my parents and my brothers and sisters, who encouraged me to do my studies and helped me put things back into perspective during difficult moments.

I also thank all my friends for their support and I would especially like to thank Jon for his understanding during the last months of my thesis. I appreciated his numerous and humorous encouragement during my "up side down" moments.

RÉSUMÉ ÉTENDU

Géologie du Jura central et du Bassin molassique: nouveaux aspects d'une chaîne d'avant-pays plissée et décollée sur des couches d'évaporites.

INTRODUCTION

But du travail

La chaîne du Jura ainsi que le Bassin molassique sont généralement considérés comme une chaîne plissée d'avant-pays, représentant la zone de déformation la plus externe d'âge tardi-Miocène des Alpes du Nord-Ouest. La formation de cette chaîne est un sujet classique, discuté depuis le début de ce siècle par de nombreux auteurs (Fig. 1.7). Dans ce travail, plus de 1500 km de profils sismiques réflexion ont été interprétés. Ils sont localisés dans les Jura suisses neuchâtelois et vaudois, dans le Jura français et dans le Bassin molassique occidental, et ont été mis à disposition par l'industrie pétrolière (British Petroleum, Shell Switzerland, Société anonyme des Hydrocarbures, Shellrex, Fig. 1.4) et le Musée de Géologie de Lausanne. De plus, la grille sismique est contrainte par les résultats d'une vingtaine de forages. Cette analyse a permis d'approfondir nos connaissances sur la stratigraphie et la géométrie des couches enfouies et par la suite de tester différents modèles concernant la formation de la chaîne du Jura et du Bassin molassique.

La géométrie en profondeur des structures du Jura et du Bassin molassique (plis, chevauchements, décrochements) procure des informations importantes sur leur développement et sur la formation de l'avant-pays alpin. Les sujets principaux discutés dans cette thèse sont: les corrélations entre les observations géologiques de surface et les données de la subsurface, l'épaisseur stratigraphique des couches enfouies, la géométrie des plis et des chevauchements et leur développement, les relations socle-couverture et la structure du socle.

L'interprétation des profils sismiques démontre que la couverture mésozoïque et cénozoïque du Jura et du Bassin molassique a été déformée au-dessus d'un niveau de décollement basal et déplacée de quelques 20 à 25 km vers le NW. Le socle sous la région étudiée montre une surface relativement plane et plonge de quelques degrés (1° à 3°) vers le S-SE.

Situation géologique

Le Jura

Le Jura représente une chaîne d'avant-pays localisée au front de la partie Ouest de l'arc alpin (Fig. 1.1). Cette chaîne a donné son nom aux couches du Jurassique, qui affleurent essentiellement dans ces montagnes.

La chaîne du Jura est entourée par des bassins tertiaires de différents types: au Nord, le Graben (ou fossé) du Rhin, à l'Ouest le Graben de la Bresse et au SSE le Bassin molassique (Fig. 1.2). Les Grabens du Rhin et de la Bresse sont associés au rifting ouest-européen d'âge Oligocène, tandis que le Bassin molassique correspond à un bassin d'avant-pays d'âge Olígo-Miocène, qui s'est développé au front des Alpes. Le Jura et le Bassin molassique représentent la zone de déformation la plus externe et la plus jeune des Alpes occidentales.

Dans toute la Suisse, le socle est composé de roches métamorphiques et de roches plutoniques associées à l'orogenèse hercynienne. A la fin de celle-ci, de nombreux fossés (grabens) allongés se sont formés et ont été par la suite remplis par des séries lacustres et fluviatiles d'âge Carbonifère et Permien. Bien que quelques uns de ces fossés, orientés E-W, soient bien localisés grâce aux résultats des forages ou aux affleurements de massifs voisins, ils en restent encore beaucoup à découvrir sous le Jura et le Bassin molassique où les sondages sont peu nombreux. Le socle cristallin n'affleure jamais dans le Jura et le Bassin molassique. Cependant, il a été pénétré par plusieurs forages et latéralement il affleure: au Nord, dans les Vosges et la Forêt Noire et au Sud, dans les massifs cristallins externes.

Le cycle alpin commence au début du Trias avec la formation d'une pénéplaine et la transgression de la mer, lorsque les bords du Jura et le Bassin molassique commencent à faire partie de la marge passive de la mer téthysienne alpine. Au cours du Trias, plus d'un kilomètre d'évaporites et d'argiles sont déposées dans un bassin à forme légèrement elliptique avec un dépôt-centre sous le futur arc jurassien. Les calcaires

des couches du Malm forment l'ossature des plis et affleurent dans le Jura oriental et central. Cependant, les calcaires des séries du Crétacé inférieur forment les crêtes des anticlinaux du Jura occidental. Au cours de l'Oligocène et du Miocène, des sédiments fluviatiles, lacustres et marins des séries de la Molasse se sont déposés dans l'avant-pays alpin ("foredeep basin"). Ces couches transgressent progressivement vers le Nord les couches du Mésozoïque sous-jacent. L'épaisseur du prisme tertiaire décroît du Sud (plus de 4 km) vers le Nord (quelques centaines de mètres). Ces séries affleurent essentiellement dans le Bassin molassique, mais sont aussi préservées dans les synclinaux du Jura. La limite entre le Bassin molassique et la chaîne du Jura est donc une limite naturelle d'érosion.

Le Jura est divisé en deux parties dont le style structural est très différent: a) le Jura externe et b) le Jura interne (Fig. 1.2).

a) Le Jura externe consiste en des régions légèrement faillées et sans grand relief, appelées les Plateaux. Ils sont séparés les uns des autres par les Faisceaux, qui représentent des zones très étroites et fortement déformées, caractérisées par des décrochements et des imbrications.

b) Le Jura interne, aussi nommé la Haute Chaîne, consiste en une succession de plis bien développés. A grande échelle, la déformation est caractérisée par des plis, des chevauchements et des décrochements. Les plis sont en relation avec des chevauchements et leur orientation varie de 90° au sein de la chaîne. Leur continuation latérale est limitée soit progressivement par un plongement axial, soit plus brusquement par un décrochement. Des décrochements sénestres recoupent d'un fort angle les axes de plis; leur orientation dessine un éventail le long de la chaîne. Les parties septentrionales de la Haute Chaîne chevauchent les Plateaux du Jura externe, tandis que le bord méridional plonge progressivement sous les sédiments tertiaires de la Molasse.

Une troisième zone, le Jura tabulaire est souvent associée à la chaîne du Jura. Cette zone est localisée à l'extérieur de l'arc jurassien et représente la couverture mésozoïque du socle cristallin de la Forêt Noire et des Vosges. Le Jura tabulaire représente la transition des grabens du Rhin et de la Bresse au Bassin de Paris.

Le Bassin molassique

Le Bassin molassique (sensu lato) représente un bassin d'avant-pays, qui s'étend sur plus de 700 km de la Savoie (France) à l'Ouest, à la région de Linz (Autriche) à l'Est (Figs. 1.1 et 1.2). Il s'étend parallèlement au front alpin et s'ouvre progressivement vers l'Est. La sédimentation dans le Bassin a été continue depuis le début de l'Oligocène jusqu'au Serravallien. Le Bassin molassique est subdivisé en trois unités tectoniques: la Molasse du Jura, la Molasse du Plateau et la Molasse subalpine.

La Molasse du Jura représente la partie septentrionale du Bassin qui a été passivement impliquée dans le plissement du Jura. Seuls quelques affleurements de Molasse sont préservés au sein des synclinaux du Jura interne.

La Molasse du Plateau, qui constitue la partie essentielle du Bassin molassique, présente un style structural bien différent entre la région occidentale et orientale. Les plis de faible amplitude, orientés NW-SE, et les décrochements soulignent les structures principales à l'Ouest, tandis qu'à l'Est, on observe quelques failles normales orientées WSW-ENE parallèles au Basin et affectant les couches du Mésozoïque et du Cénozoïque.

La Molasse subalpine représente une zone étroite le long du bord méridional du Bassin molassique (Fig. 1.2). Cette zone est caractérisée par une succession d'écailles composées de sédiments tertiaires et décollées à la base des couches tertiaires. La limite méridionale de cette zone correspond au front alpin d'âge Oligocène, représenté par les nappes alpines (Préalpes, Helvétique, ...).

Le changement de style structural le long du Bassin molassique est influencé par la présence d'un niveau de décollement au sein des évaporites du Trias. La partie occidentale du Bassin molassique est détachée de son substratum cristallin ou Permo-Carbonifère; la déformation s'est développée du Sud en direction de la chaîne du Jura. Cependant, dans la partie orientale du Bassin molassique, il n'y a aucune évidence pour admettre un niveau de décollement, car les niveaux d'évaporites du Trias sont absents.

Conditions pour la formation de la chaîne plissée et chevauchée du Jura

La formation d'une chaîne plissée et la nature du plissement dépendent considérablement des conditions aux limites. Pour le Jura, les conditions aux limites régionales les plus importantes sont les suivantes: la présence de couches évaporitiques du Trias agissant comme zone de décollement basal; la présence d'un socle rigide plongeant de 1° à 3° vers le Sud et situé sous une zone de décollement tendre; la rhéologie des couches de la couverture: l'épaisseur des couches compétentes croît du NE vers le SE, tandis que les couches incompétentes décroissent vers le SE; la structure en forme de prisme de l'avant-pays jurassien: une faible pente plongeant vers le NW à la surface tandis qu'à la base, elle plonge vers le SE (socle); la structure en forme de prisme du Bassin molassique: l'épaisseur des couches augmente considérablement du Nord au Sud; les structures héritées d'âge Oligocène au sein de la couverture.

Formation du Jura: questions ouvertes

Le développement de la chaîne du Jura reste toujours un sujet de discussion avec deux points de vue fondamentalement différents (Fig. 1.7). Plusieurs auteurs considèrent la chaîne du Jura comme autochtone, i.e. une couverture plissée et solidaire à un socle déformé par des grands décrochements et des chevauchements intra-cristallins ou recoupant la couverture. D'autres auteurs stipulent que les plis de la couverture du Jura et les chevauchements associés se sont développés au-dessus d'un niveau de décollement et ont été déplacés sur de longues distances, grâce à la poussée des Alpes transmise à travers le Bassin molassique ("Hypothèse du Fernschub"). Bien que des arguments d'équilibrage favorisent la deuxième théorie, certains auteurs ont quand même utilisé des données sismiques pour relancer le débat et proposer un décollement au sein du socle plutôt qu'à la base de la couverture.

Données et méthodologie de travail

Les données de surface consistent en un nombre considérable de cartes géologiques publiées et non publiées (Tab. 1.1), de coupes géologiques de faible profondeur et de logs lithostratigraphiques. Les données de subsurface comportent des profils de sismique réflexion et des forages provenant de l'industrie pétrolière. Elles ont été fournies soit directement par les compagnies pétrolières, soit par le Musée de Géologie de Lausanne où sont déposés la plupart des documents concernant les activités de sismique réflexion effectuées sur le territoire du Canton de Vaud.

L'élaboration de ce travail a nécessité plusieurs étapes, dont voici les principales: compilation des données préexistantes, travaux de terrain, interprétation sismique, conversion en profondeur (mètres) des profils sismiques (en temps), cartes, coupes géologiques semi-équilibrées et équilibrées.

STRATIGRAPHIE

Unités sismiques

L'interprétation géologique d'une grille sismique est basée sur la corrélation de réflecteurs sismiques. Dans les roches sédimentaires, ces réflecteurs correspondent à des discontinuités lithologiques, qui peuvent être calibrées stratigraphiquement grâce aux informations contenues dans les logs de forages. En général, il est préférable de sélectionner des unités de stratigraphie sismique limitées par de forts réflecteurs, plutôt que de définir et de corréler chaque réflecteur sismique. Dans ce travail, huit unités sismiques comprises entre deux intenses réflecteurs (ces derniers sont numérotés par les lettres de A à I, voir Tab. 2.1) ont été définies; chacune représente un intervalle, caractérisé par une lithologie prépondérante. La discordance tertiaire basale de l'avant-pays ("basal foredeep unconformity") est la seule discordance évidente visible sur nos profils sismiques.

Les profils sismiques ont permis d'éclaircir la stratigraphie en profondeur tout particulièrement pour les couches d'âge triasique, qui n'affleurent pas dans la région étudiée. Deux unités ont été définies pour le Trias sur la base des interprétations des profils sismiques: (de haut en bas) l'Unité 1 qui surmonte l'Unité 2. L'Unité 1 est bien litée avec des réflecteurs réguliers et continus; elle montre une épaisseur à peu près constante autour de 200 m. L'Unité 2 contraste fortement avec l'Unité sus-jacente: elle présente des réflecteurs discontinus et obliques. L'épaisseur de cette Unité varie fortement d'une ligne à l'autre en fonction de la position structurale: les épaississements sont visibles sous les anticlinaux, tandis que les amincissements se localisent sous les synclinaux.

Le toit du socle correspond aux derniers réflecteurs intenses, qui contrastent fortement avec le socle cristallin d'apparence transparent (sans réflecteur). Au sein du socle, il est toutefois possible par endroit de reconnaître quelques réflecteurs, interprétés soit comme multiples, soit comme des sédiments permo-carbonifères.

Les profils sismiques longitudinaux, c'est-à-dire parallèles aux synclinaux, sont d'une grande utilité, puisqu'ils montrent des réflecteurs sub-horizontaux, nécessaires pour l'interprétation stratigraphique. Les profils sismiques transversaux, c'est-à-dire perpendiculaires aux structures, sont par contre de moins bonne qualité et montrent des réflecteurs discontinus, probablement à cause du fort pendage des couches et des structures complexes.

Cartes des isopaques

Des cartes d'isopaques (courbe de même épaisseur) ont été construites pour chaque unité du Mésozoïque au sein du Bassin molassique (Figs. 2.24 à 2.29). Les cartes d'isopaques sont basées sur la conversion en profondeur (en mètres) des profils sismiques (en temps) et calibrées sur les forages. Une vitesse sismique a été attribuée à chaque intervalle sismique (voir Appendix 3). Les cartes d'isopaques permettent de déterminer des changements, même mineurs, des épaisseurs des couches. Ces changements sont intéressants pour l'analyse des mécanismes de subsidence, ainsi que pour une réflexion sur la rhéologie des couches. Bien que ces cartes ne soient pas précises quant au taux de subsidence, elles ont l'avantage d'être basées sur une large grille sismique donnant

une haute résolution spatiale et elles permettent de révéler les tendances des variations de la subsidence et l'existence de failles syn-sédimentaires au cours du Mésozoïque.

Durant le Trias, plus de 1000 m de sédiments se sont accumulés dans la région de la future chaîne du Jura, tandis que 60 km plus au Sud, au sein des parties septentrionales du domaine Helvétique, moins de 50 m de sédiments se sont déposés au cours du même laps de temps. Malgré cette considérable variation latérale, aucune évidence pour des failles syn-sédimentaires n'a été trouvée. D'importantes variations latérales d'épaisseur dans les couches du Trias sont en relation avec la déformation d'âge Miocène et l'importante redistribution des évaporites dans ces couches. D'aspect tendre, elles ont agit comme zone de décollement durant la formation du Jura. Pendant la période du Jurassique, les variations latérales de subsidence sont significatives, mais moins importantes que celles durant le Trias; aucune tendance régionale persistante n'a été identifiée. Quelques petits changements d'épaisseurs dans la région d'Yverdon peuvent être le résultat de failles syn-sédimentaires, mais une évidence directe est obscurcie par la présence de décrochements d'âge Miocène. En guise de synthèse, durant tout le Mésozoïque, la région étudiée était un domaine avec une subsidence très lente, située entre le Bassin de Paris au Nord-Ouest et la mer alpine téthysienne au Sud.

Stratigraphie rhéologique

L'épaisseur stratigraphique et la continuité latérale des formations compétentes et incompétentes au sein d'une colonne stratigraphique joue un rôle essentiel dans l'évolution tectonique d'une chaîne plissée. La rhéologie de chaque couche dépend principalement de la composition minéralogique de la roche, de la texture et de la température de déformation. Aux conditions de déformation du Jura, la compétence pour les sédiments impliqués dans la colonne stratigraphique augmente de la manière suivante: sel, gypse, anhydrite, argile, marne, grès de la Molasse, calcaire, dolomie. Trois degrés de compétence ont été définis au sein des unités stratigraphiques étudiées (Fig. 2.30): 1) dur (forte viscosité); 2) tendre (faible viscosité); 3) très tendre (très faible viscosité). Les calcaires du Crétacé et du Malm supérieur représentent principalement les niveaux durs, tandis que les argiles et les marnes du Malm inférieur (Argovien) et du Lias, ainsi que l'Unité 1 du Trias, représentent les niveaux tendres. Enfin, les évaporites de l'Unité 2 du Trias caractérisent les niveaux les plus tendres. C'est d'ailleurs dans cette dernière Unité que se localise la zone du décollement du Jura.

STRUCTURES

L'interprétation des profils sismiques a permis de mettre en évidence deux types de plis différents: d'une part, des plis larges, de grande longueur d'onde et de faible amplitude localisés dans le Bassin molassique et les Plateaux jurassiens; d'autre part, des plis de forte amplitude, situés dans la Haute Chaîne jurassienne.

Plis associés à des évaporites: les Plateaux jurassiens et le Bassin molassique

Les plis des Plateaux jurassiens et du Bassin molassique sont remarquablement bien visibles sur les profils sismiques transversaux grâce aux changements de l'épaisseur de l'Unité 2 du Trias. Ces plis sont contrôlés par des épaississements, dus à des empilements d'évaporites appelés coussins d'évaporites ou anticlinaux d'évaporites, localisés à l'intérieur de l'Unité 2 des couches du Trias. Ces empilements d'évaporites montrent, sur certains exemples des structures en forme de duplex. Le pli de Laveron, dans les Plateaux jurassiens, présente une épaisseur de plus de 1000 m, confirmée par forage, pour les couches de l'Unité 2 du Trias et correspond au plus grand épaississement reconnu dans la région étudiée. Il faut souligner qu'aucun chevauchement et qu'aucune répétition au sein des couches du Mésozoïque, en association avec les plis, n'ont été observés sur les profils sismiques provenant du Bassin molassique et des Plateaux du Jura. Les cartes d'isopaques du Bassin molassique occidental montrent que les coussins d'évaporites sont alignés NE-SW, parallèlement à la direction des structures majeures du Jura. Les anticlinaux décrits ci-dessus sont tout à fait comparables aux plis de faible amplitude, en relation avec des épaississements de sel de Melville Island dans les territoires arctiques du Canada.

Plis associés à un chevauchement: la Haute Chaîne jurassienne (Jura neuchâtelois et vaudois, Jura français)

Les plis de grande amplitude de la Haute Chaîne jurassienne sont en relation avec des chevauchements à vergence vers le NW ou le SE. Ils montrent un déplacement d'ordre kilométrique qui se traduit par le redoublement de toute la séquence jurassique. Ces chevauchements montent depuis la zone de décollement principale (Unité 2 du Trias) à travers toute la série mésozoïque et cénozoïque. La répétition des unités de stratigraphie sismique est la principale évidence sismique pour déterminer ce type de plis.

Les Jura neuchâtelois et vaudois (région du Risoux) de la Haute Chaîne jurassienne montrent les plus beaux exemples de plis associés à des chevauchements. Dans le Jura neuchâtelois, la continuité latérale des anticlinaux est de 10 km pour la région de l'Est ou 15 km à 20 km pour la région de l'Ouest. Les anticlinaux sont orientés soit ENE-WSW ou NNE-SSW et se terminent principalement contre des failles décrochantes. La combinaison des deux orientations résulte en des structures de forme losangique, comme par exemple le Val de Ruz ou le synclinal du Locle. Au contraire, le Jura vaudois et la région du Risoux (France) présentent une structure très régulière avec des anticlinaux orientés NE-SW (Mt-Tendre, Mt-Risoux), qui s'étendent latéralement sans discontinuité majeure sur plus de 30 km.

Les décrochements

Les décrochements sont bien définis dans le Jura, car la plupart s'expriment par une dépression morphologique bien visible sur les cartes topographiques. Les décrochements les plus importants montrent un mouvement sénestre et sont orientés NW-SE dans la partie méridionale du Jura, NNW-SSE à N-S dans le Jura central (par exemple Pontarlier, La Tourne, La Ferrière-Vue des Alpes) et NNE-SSW dans le Jura oriental. Des décrochements conjugués, avec un mouvement dextre, leur sont très souvent associés. Les cartes géologiques présentent aussi des évidences pour déceler les décrochements: les axes de plis ont tendance à se terminer brusquement contre les failles décrochantes, sans présenter une corrélation évidente de part et d'autre de la faille. Les évidences géophysiques pour déterminer les décrochements sur les profils sismiques consistent en une large zone transparente (sans réflecteur), en une succession stratigraphique différente de part et d'autre de la faille et en un décalage des unités sismiques. Les principaux décrochements observés (Pontarlier, Morez, Mt Chamblon-Treycovagnes, La Ferrière-Vue des Alpes) affectent l'ensemble de la couverture mésozoïque et ne décalent pas le toit du socle d'un côté à l'autre de la faille. Aucun élément valable n'a été observé pour étendre ces failles dans le socle. Ces failles décrochantes sont alors, soit des décrochements limités à la couverture ("tear faults"), soit des rampes latérales.

SYNTHÈSE ET CONCLUSIONS

L'interprétation d'un réseau de profils sismiques a permis de réfléchir sur la formation des plis du Jura et du Bassin molassique et de présenter une évolution dans le temps. Les plis des Plateaux jurassiens, localisés dans l'avant-pays, sont interprétés comme des plis de flambage correspondant à un stade précoce de la déformation. En augmentant la déformation, une rampe se génère et ce type de pli se développe en association avec un chevauchement, comme ceux observés dans la Haute Chaîne. La déformation augmente, donc, vers l'arrière-pays au sein de la chaîne plissée et chevauchée du Jura. Dans le Bassin molassique, les plis de faible amplitude représentent, cependant, un stade précoce, qui n'a pas pu évoluer à cause de la surcharge importante des sédiments tertiaires.

Afin de synthétiser toutes les données, une carte du toit du socle (Fig. 5.1) de la région étudiée a été réalisée à l'aide des résultats de la conversion en profondeur des profils sismiques. Cette carte montre un socle plat et lisse plongeant de 1° à 3° vers le S-SE. Aucun changement important de profondeur et de direction, qui affecterait les couches de la couverture sédimentaire, n'a pu être décelé sous les décrochements principaux. Aucune relation structurale n'a pu être déduite entre la carte d'isopaques de l'Unité 2 du Trias et celle des contours du toit du socle. Le socle n'est donc pas impliqué dans la formation des plis, des chevauchements et des décrochements du Jura central et du Bassin molassique. A l'échelle de la chaîne de montagne, il existe une très bonne corrélation entre la distribution des couches du Trias et l'étendue de la couverture déformée du Jura. Il semble donc que la forme arquée de la chaîne du Jura est étroitement dépendante de la présence d'évaporites du Trias à la base de la couverture.

En conclusion, l'interprétation des profils sismiques démontre, que la couverture mésozoïque et cénozoïque du Jura et du Bassin molassique a été déformée, au-dessus d'un niveau de décollement basal, et déplacée de quelques 20 à 25 km vers le NW.

1. INTRODUCTION

1.1 AIM AND SCOPE OF THE PRESENT STUDY

The Jura, together with the Molasse Basin, is generally considered a foreland fold and thrust belt representing the most external, late Miocene deformation zone of the northwestern Alps. The development of this belt is still a matter of debate. The availability of more than 1500 km of seismic lines has provided the opportunity to extend our knowledge about the subsurface stratigraphy and the geometry of the Jura and Molasse Basin folds in depth.

The geometry in depth of the Jura and Molasse Basin structures (folds, thrust faults and tear faults) provides important constraints on their development and the formation of the Alpine foreland. The main subjects addressed in this thesis are:

- the correlation between the surface geological observations and subsurface data
- the stratigraphic thickness of the buried strata
- the geometry of the folds and thrusts and their development
- the cover-basement relationship
- the structure of the basement.

Few public seismic reflection data are available to date within the Jura arc. A small seismic survey has been carried out by the NAGRA (National Cooperative for the Storage of Radioactive Waste) in the eastern Jura, whereas in the western Jura one profile has been shot by the ECORS group. The availability of recent industry seismic lines (Fig. 1.4) in the Neuchâtel Jura and older lines in the Risoux Jura, the French Jura and the western Molasse Basin has allowed infilling an important data gap for the central part of the Alpine foreland.

This manuscript is organized into six chapters, providing information and illustrations about stratigraphy and tectonics of the central Jura and the western Molasse Basin. Subsurface, as well as surface geology are presented to offer an integrated regional geologic interpretation.

Chapter 1 presents a general introduction, which exposes the aim of the study, the geological and historical setting and the methodology. Chapter 2 concerns stratigraphy. Although this thesis is focused on structure, stratigraphy is discussed because it is necessary to understand structural development for example: regional overview, outcrop and subsurface stratigraphy from well logs, seismic stratigraphic units and their correlation through the whole grid, isopach maps and rheological stratigraphy. Chapter 3 presents an overview of the structures (evaporite-related anticlines, thrust-related anticlines and tear faults), illustrated by seismic profiles. The most remarkable structures are evaporite stacks within the Triassic layers, controlling the anticline formation of the Molasse Basin and the Plateau Jura. The Haute Chaîne Jura folds, on the other hand, are leading to duplication of Mesozoic strata beneath the Haute Chaîne Jura thrust-related folds. Chapter 4 presents the regional geology of the central Jura and the western Molasse Basin, highlighted by seismic interpretation (line drawings), tectonic maps, cross-sections of specific areas and structural contour maps within the Molasse Basin. The depth to the basement map of the central Jura and Molasse Basin, derived from depth conversion of the whole seismic grid, as well as the isopach map of the Triassic beds of the Molasse Basin, will be the key for the general discussion on the formation of the Jura fold and thrust belt (Chapter 5). Chapter 6 will summarize the main conclusions of this work.

1.2. GEOLOGICAL SETTING

1.2.1. The Jura

The Jura is a small arcuate fold belt located in front of the western Alpine arc (Fig. 1.1). This chain has given its name to the Jurassic layers, because they represent the major part of the outcropping rocks in the Jura.

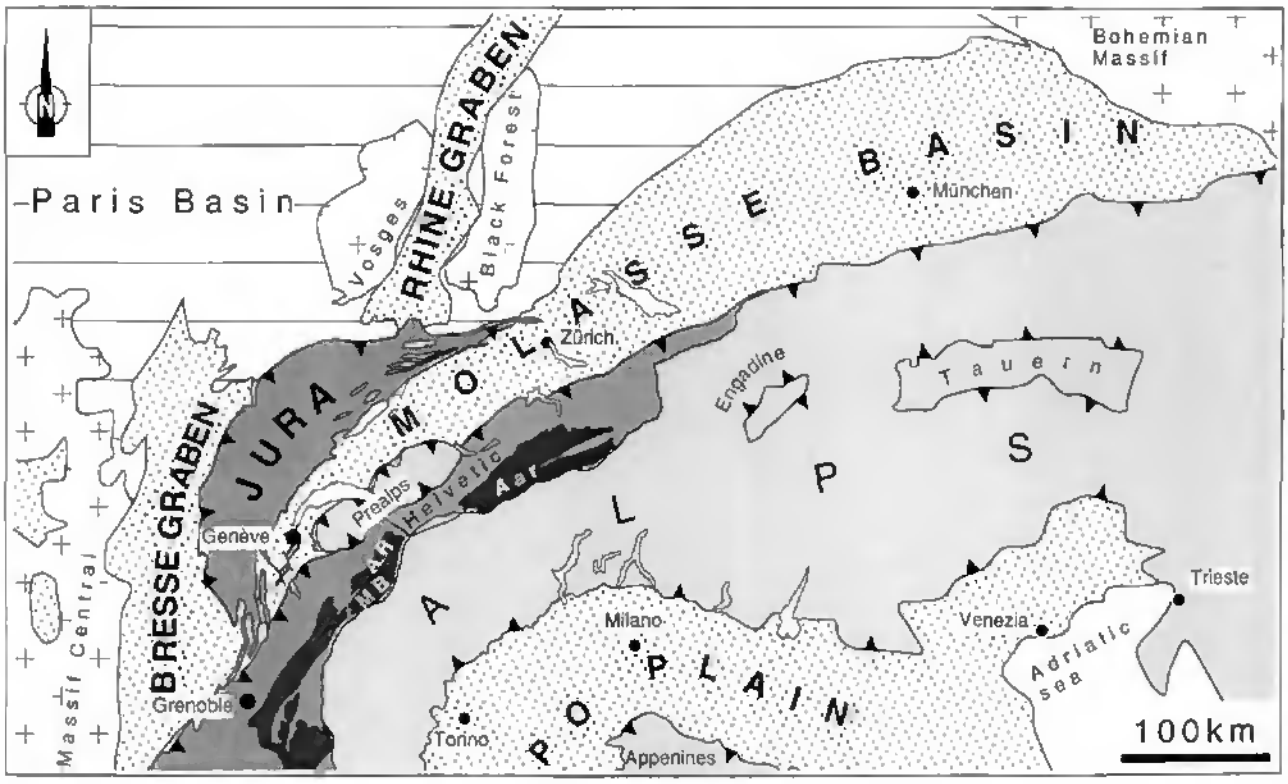

Figure 1.1: Location of the Jura arc with respect to the major Cenozoic sedimentary basins (Rhine-Bresse Grabens, Molasse Basin, Po Plain) and the Alps. Late alpine culminations and external crystalline massifs are highlighted in dark grey. AR = Aiguilles Rouges massif; MB = Mont-Blanc Massif.

Situation de l'arc jurassien par rapport aux bassins sédimentaires tertiaires avoisinants (Grabens du Rhin et de la Bresse, Bassin molassique, Plaine du Pô) et aux Alpes. Les culminations alpines tardives et les massifs cristallins externes sont soulignés en gris foncé. AR = Massif des Aiguilles Rouges; MB = Massif du Mont-Blanc.

The outer arc of the Jura is 400 km long and the inner arc 340 km. The width between both arcs varies from 0 km at the eastern end, to 65 km between Neuchâtel and Besançon (Switzerland-France). The Jura arc is surrounded by Tertiary basins of different types: to the N, the Rhine Graben, to the W the Bresse Graben and to the SSE the Molasse Basin (Fig. 1.2). The Rhine and Bresse Grabens are associated with the Oligocene, West-European rift system, whereas the Molasse Basin corresponds to an Oligo-Miocene foredeep, which developed in front of the Alpine orogen. During the Mesozoic, the Jura and Molasse Basin realm was part of the Alpine Tethys passive margin and comprises a total thickness of up to 2 km of alternating limestones and marls. Limestones of Malm age crop out in the central Jura, whereas the Cretaceous limestones (Barremian) form the crests of the western Jura anticlines. During the Oligocene and Miocene, alternating fluvial, lacustrine and marine clastic Molasse sediments were deposited. They progressively onlap the underlying Mesozoic rocks towards the Northwest. The thickness of this sedimentary wedge decreases from the South (up to 4 km) to the North (a few hundred meters). These series crop out mainly within the Molasse Basin, but they are also preserved in many Jura synclines (Val de Ruz, La Chaux-de-Fonds - Le Locle, Val de Travers, Delémont Basin, ...) (Fig. 1.3).

The Jura and the Molasse Basin consist of folded Mesozoic and Cenozoic beds, which are detached from the pre-Triassic basement. The latter crystalline basement is never exposed in the Jura and Molasse Basin. It has, however, been penetrated by a few drill holes and laterally it crops out in the Vosges and Black Forest to the North, in the alpine external crystalline massifs to the South and in some small isolated outcrops along the northwestern external border of the Jura Mountains (Serre Massif).

At its southern termination, the Jura belt merges with the Subalpine Chains, which were folded contemporaneously. Along its western border, the Jura over-thrusts the Bresse Graben, whereas in the

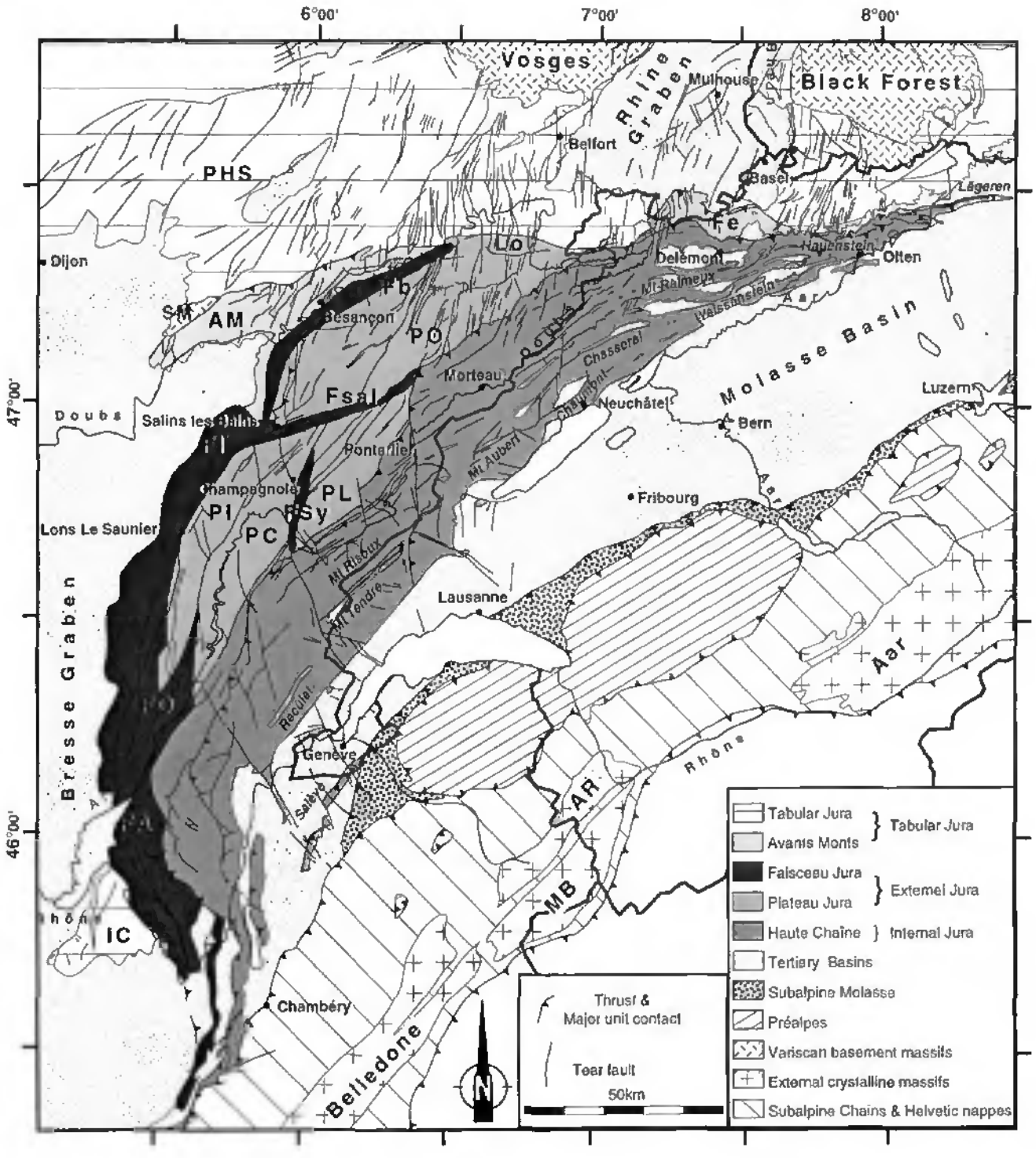

Figure 1.2: Tectonic sketch of the Jura arc with main structural units. Legend: PHS = Plateau de Haute-Saône; IC = Ile Crémieu; AM = Avants-Monts; Fe = Ferrette; FA = Faisceau d'Ambérieu; Fb = Faisceau bisontin; Fl = Faisceau lédonien; FO = Faisceau d'Orgelet; Fsal = Faisceau salinois; FSy = Faisceau de Syam; Lo = Lomont; PC = Plateau de Champagnole; PL = Plateau de Levier; Pl = Plateau lédonien; PO = Plateau d'Ornans; AR = Aiguilles Rouges; MB = Mont Blanc. Modified from SOMMARUGA (1995).

Carte tectonique de l'arc jurassien avec les unités structurales majeures. Légende: PHS = Plateau de Haute-Saône; IC = Ile Crémieu; AM = Avants-Monts; Fe = Ferrette; FA = Faisceau d'Ambérieu; Fb = Faisceau bisontin; Fl = Faisceau lédonien; FO = Faisceau d'Orgelet; Fsal = Faisceau salinois; FSy = Faisceau de Syam; Lo = Lomont; PC = Plateau de Champagnole; PL = Plateau de Levier; Pl = Plateau lédonien; PO = Plateau d'Ornans; AR = Aiguilles Rouges; MB = Mont Blanc. Modifiée de SOMMARUGA (1995).

North, it overrides the Tabular Jura. At its eastern end, the last Jura fold (Lägern) dies out within the Molasse Basin.

The Jura itself is divided into the external Jura and the internal Jura (CHAUVE *et al.*, 1980).

a) The external Jura

The external Jura (Fig. 1.2) consists of flat areas, Plateaus, limited to the North and separated from each other by the so called "Faisceaux" (from North to South: F. bisontin, F. salinois, F. lédonien, F. de Syam, F. d'Orgelet and F. d'Amberieu). These are narrow, strongly deformed fold bundles characterized by a succession of numerous small-scale imbricates and tear faults. The Plateaux (P. d'Ornans, P. lédonien, P. Champagnole and P. Levier) correspond to weakly faulted, horizontal or slightly SE dipping areas.

b) The internal Jura

The internal Jura, often called the folded Jura, "Haute Chaîne" or "Faisceau helvétique" consists of a well developed fold train representing a natural present-day northern limit to the Molasse Basin. On a large scale, deformation is characterized by major folds, thrusts and tear faults. The amplitude of the Jura folds depends on the cover thickness (800 m-2000 m) and the degree of shortening, which is highest in the internal part of the central Jura and decreases outwards. Folds are thrust-related and end laterally either with plunging axes or abruptly against tear faults. Some major sinistral tear faults cutting the whole cover are recognized; their orientation is N-S in the eastern Jura and changes gradually along the chain to a WNW-ESE direction at the western end. The outer border of the folded Jura is thrust over the Plateau Jura. At the southern border, the Mesozoic beds dip below the Oligo-Miocene sediments of the Molasse Basin.

A third zone, the Tabular Jura, is often associated with the Jura. This zone is located outside of the Jura arc and represents the Mesozoic cover of the southern Black Forest and Vosges basement. The Tabular Jura represents the transition from the Rhine-Bresse Graben to the Paris Basin. Strata are subhorizontal and cut by a N-S or NE-SW Oligocene fault system. The Avant-Monts and the Ferrette areas represent the deformed cover of this Tabular Jura. At the southern end of the arc, the Ile Crémieu is the southern counterpart of the Tabular Jura.

1.2.2. The Molasse Basin

The whole Molasse Basin (sensu lato) represents a foreland basin which extends over more than 700 km, from the French Savoy in the West (Chambéry, Figs. 1.1 and 1.2) to Linz (Austria) in the East. It runs parallel to the Alpine front and widens progressively to the East, from 50 km in the Neuchâtel traverse to some 150 km in southern Germany. Sedimentation in the foreland basin was continuous from earliest Oligocene to Serravallian time and took place in alternating marine, fluvial and lacustrine environments. The thickness of this sedimentary wedge decreases from some 4 km in the South to a few hundred meters in the North.

The clastic wedge of the Molasse Basin is subdivided into three geological units, the Jura Molasse, the Plateau Molasse and the Subalpine Molasse (HOMEWOOD *et al.*, 1989).

a) The Jura Molasse

The Jura Molasse represents the northern feather edge of the Molasse Basin that has been passively involved in Jura folding and thrusting. Only isolated patches of Molasse are preserved within major synclines of the internal Jura.

b) The Plateau Molasse

The Plateau Molasse, representing the major part of the Molasse Basin, shows contrasting structural styles between the western and eastern parts.

In the western Swiss part, the structures consist of broad anticlines oriented NE-SW and tear faults trending N-S, NW-SE and WNW-ESE. The northern limit of the Plateau Molasse corresponds to an erosion limit along the most internal, high amplitude folds of the Jura belt.

In eastern Switzerland and Bavaria, surface geological outcrops show the onlap towards the North of the Tertiary wedge over the Tabular Jura (Franconian Platform) (BACHMANN *et al.*, 1987). The only known deformation is characterized by small normal faults oriented WSW-ENE, parallel to the basin and affecting the Mesozoic and Cenozoic strata (BACHMANN *et al.*, 1982).

c) The Subalpine Molasse

The Subalpine Molasse represents a narrow zone located along the southern border of the Molasse

Basin (Fig. 1.2). This zone is characterized by a stack of thrust sheets of Tertiary sediments, detached along a décollement zone within these Cenozoic layers ("Grisigen shales") (TRÜMPY, 1980). The southern limit of this zone corresponds to the Oligocene Alpine front represented by the Alpine nappe stack (Prealps, Helvetic nappes, ...) which overthrusts the Molasse sediments. The northern limit of this unit, corresponding to the transition between the Subalpine- and the Plateau Molasse, is structurally an important triangle zone (BACHMANN *et al.*, 1982; VOLLMAYR & WENDT, 1987; MÜLLER *et al.*, 1988; VOLLMAYR, 1992).

According to ALLEN *et al.* (1986), HOMEWOOD (1986) and VANN *et al.* (1986), the change in structural style along the strike of the Molasse Basin is related to the presence of a décollement zone within the Triassic evaporites. The entire Basin in the western and central parts is considered to be detached from its crystalline or Permo-Carboniferous substratum.

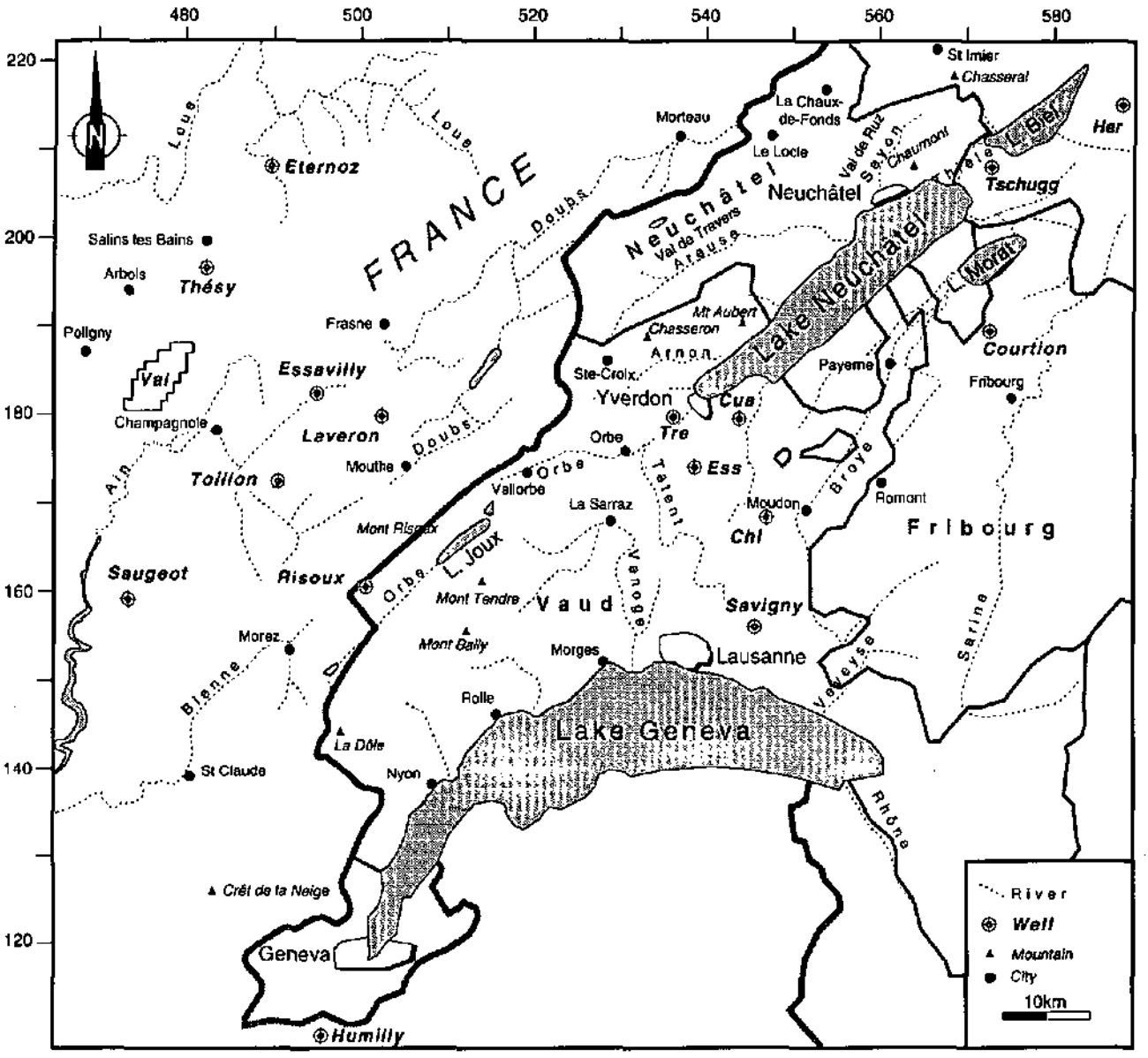

Figure 1.3: General geographical index map of the investigated area (cities, rivers, mountains and wells). Legend: Chl = Chapelle; Cua = Cuarny; Ess = Essertines; Her = Hermrigen; Tre = Treycovagnes; Val = Valempoulières.

Carte géographique générale de la région étudiée (villes, rivières, montagnes et forages). Légende: Chl = Chapelle; Cua = Cuarny; Ess = Essertines; Her = Hermrigen; Tre = Treycovagnes; Val = Valempoulières.

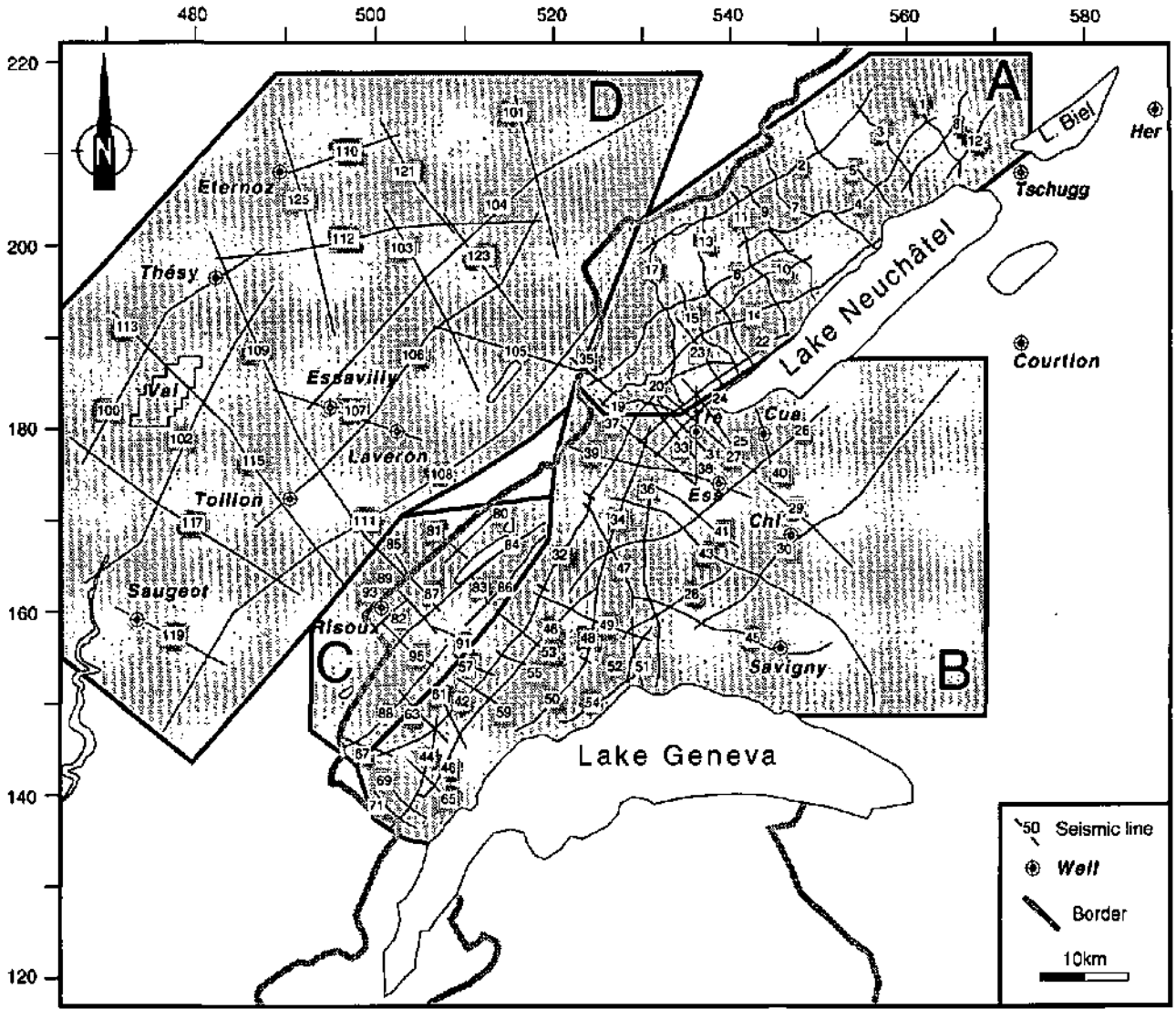

Figure 1.4: Seismic data used in this work. Location of the various sectors: A = Neuchâtel and Vaud Jura Mountains, Panels 1, 2, 3. B= Molasse Basin, Panels 4, 5, 6. C = Mt- Risoux Jura Mountains, Panels 8, 9. D = Champagnole-Mouthe Jura Mountains, Panel 10. Legend: Chl = Chapelle; Cua = Cuarny; Ess = Essertines; Her = Hermrigen; Tre = Treycovagnes; Val = Valempoulières.

Profils sismiques interprétés dans ce travail. Localisation des différents secteurs: A = Jura neuchâtelois et vaudois, Panneaux 1, 2, 3. B= Basin molassique, Panneaux 4, 5, 6. C = Région jurassienne du Mt- Risoux , Panneaux 8, 9. D = Région jurassienne de Champagnole-Mouthe, Panneau 10. Légende: Chl = Chapelle; Cua = Cuarny; Ess = Essertines; Her = Hermrigen; Tre = Treycovagnes; Val = Valempoulières.

The deformation propagated from the South into the Jura belt, whereas to the East there is as yet no evidence for a décollement zone. Thick evaporite horizons in Triassic strata are present beneath the Jura and the Swiss Molasse Basin (RIGASSI, 1977) (see also Fig. 2.5). Triassic beds progressively onlap basement to the North-East and are entirely absent beneath the Molasse Basin in Germany, where Jurassic strata lie unconformably on the basement; here, even where the Triassic is preserved, evaporite series are absent (BACHMANN *et al.*, 1987).

1.3. REGIONAL BOUNDARY CONDITIONS TO THE FORMATION OF THE JURA FOLD AND THRUST BELT

The formation of a fold and thrust belt and the nature of folding are intimately dependent on the existing boundary conditions. For the Jura belt, the major regional boundary conditions can be summarized as follows:

- the presence of Triassic evaporite beds serving as basal décollement level;

- the presence of a rigid basement dipping 1° to 3° towards the South and underlying a weak décollement level (BUXTORF, 1907);

- the rheological stratigraphy in the cover (§2.6. and Fig. 2.30): the thickness of strong competent rocks (Malm and Dogger limestones) increases from NE to SW, whereas the weak incompetent beds above the décollement decrease towards the SE;

- the small overburden and hence the weak burial depth: depths ranging from few hundreds of meters to a maximum of 2500 m in the southern Jura create low temperature conditions for the deformation of the rocks;

- the wedge shape of the whole Jura foreland: the shallow surface slope towards the NW and the basal dip towards the SE;

- the wedge shape of the Tertiary Molasse Basin: the thickness of the sediments increases strongly from the North to the South;

- the inherited Oligocene structures within the cover: the West-European rift system results in the formation of the Rhine-Bresse Grabens and also in N-S to NE-SW faults affecting the cover and the basement. These faults are especially located in the external and eastern regions of the Jura arc.

1.4. FORMATION OF THE JURA: SHORT REVIEW AND OPEN QUESTIONS

The Jura Mountains have drawn the interest of structural geologists and paleontologists since the beginning of the last century. In the early years, research was focused on stratigraphy and paleontology. Among the few early geological cross-sections that were drawn, the one of Von Buch (1806) in VON BUCH (1867) is remarkable for its time. He presented a geological section from the Aar Massif to the Serre Massif (Fig. 1.2), where the so called limestone cover rocks of the Prealps, the Molasse Basin and the Jura chain overly granite rocks. On his section, the latter crop out in the Aar and Serre Massifs, the southern and the northern borders, respectively. The major issues of the formation of the Jura are already included in this early 19th century cross-section: what are the cover-basement relationships within the Jura and the Molasse Basin and where is the Jura cover shortening compensated in the basement ?

Since the beginning of this century, many authors have attempted to answer these questions. In the following sections, we will give a short review of various interpretation of the Jura formation illustrated by some published cross-sections (Fig. 1.5) and some conceptual models (Fig. 1.7) modified from BURKHARD (1990). For the Jura, two fundamentally different assumptions dominate the debate i.e. basement involved folding versus décollement of the sedimentary cover. Basement, here, includes all rocks older than the Triassic anhydrites. The viability of these models will be discussed later in the Chapter 5 together with the main results of this thesis.

For a more detailed review on the evolution of the ideas during the first 50 years of this century, the reader should refer to CAIRE (1963).

Basement involvement beneath the Jura: proponents

Many authors have argued in favor of basement involvement. They regard the Jura as an essentially autochthonous cover, which has been deformed in response to deformation in the underlying basement so that the shortening of the Jura folds is taken up in the underlying basement. AUBERT (1945) proposed disharmonic folding of the Jura cover in the Muschelkalk anhydrites due to basement slices penetrating into the cover (Fig. 1.5, section 3). This idea was inspired by the cross-sections of STAUB (1924) in the Alps. Fifteen years later, AUBERT (1959) reconsidered his theory taking into account the work of GLANGEAUD (1949) and especially new field work results in the Pontarlier strike slip fault area (Figs. 1.2 and 3.19). The latter fault, like all Jura strike slip faults, is considered in this model as deep Oligocene age strike-slip faults rooting in the basement. The contraction of the strike-slip faults of the Jura has induced some major folding in the overlying cover ("contraction du socle" theory, Fig. 1.7). Following the results of the Risoux well, with its large scale duplication of Mesozoic strata, AUBERT (1971) changed his views to conclude that the Jura cover is allochthonous.

The influence of deep seated strike-slip faults is also central to PAVONI's (1961) theory of folding related to basement involved wrench faulting (Fig. 1.7). Based on a series of experiments, Pavoni demonstrated a possible connection between the relative movement and strike of the wrench faults and the resulting fold structures. In this model, the Jura folding results from horizontal shortening oblique to the general trend of the fold axes.

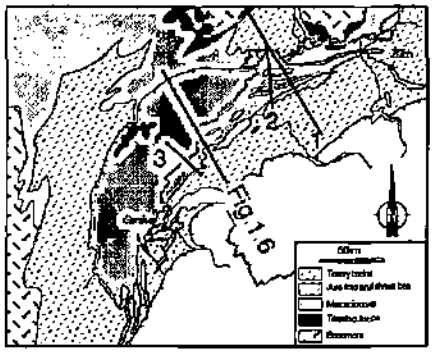

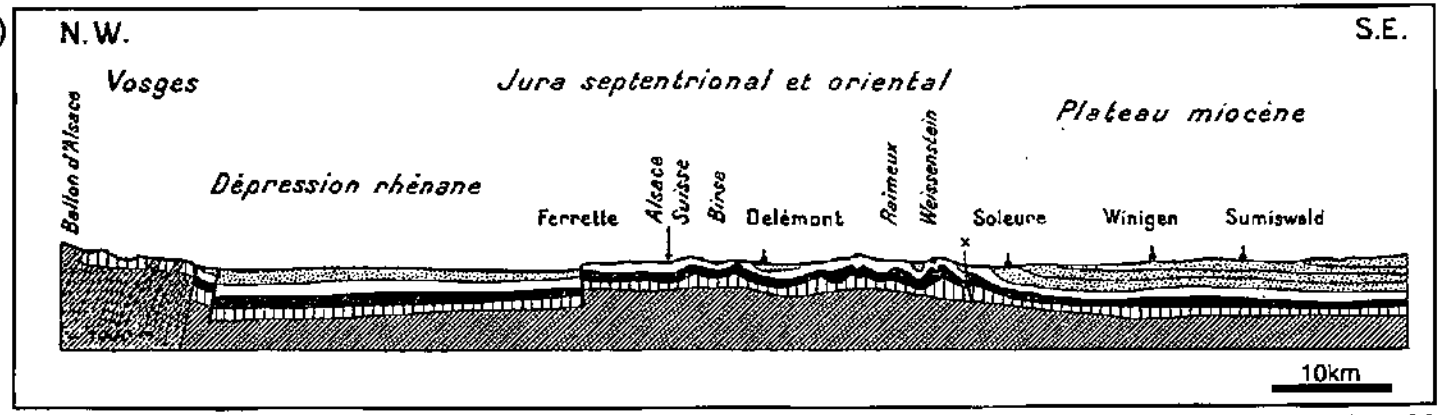

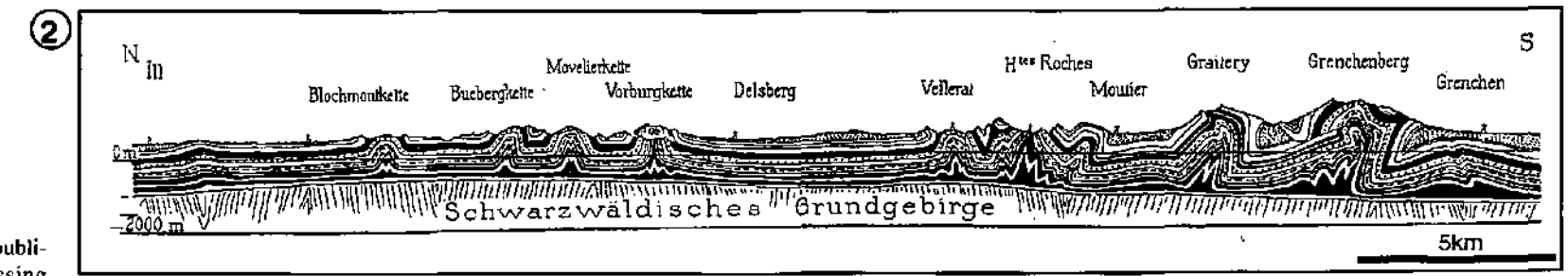

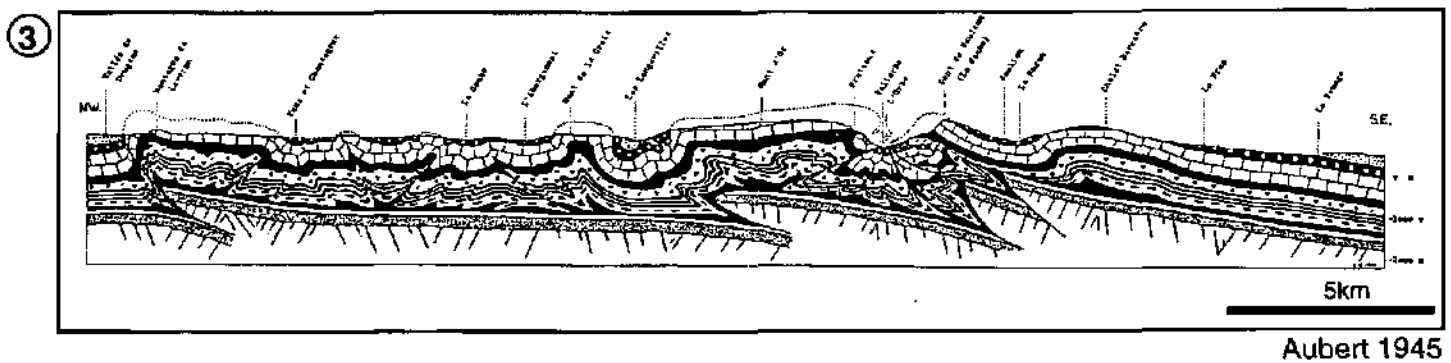

Figure 1.5: Selection of published cross-sections crossing the Jura fold and thrust belt. 1) From SCHARDT (1906, pl.VI); 2) From BUXTORF (1916); 3) From AUBERT (1945).

Coupes géologiques publiées recoupant la chaîne du Jura. 1) Tirée de SCHARDT (1906, pl.VI); 2) Tirée de BUXTORF (1916); 3) Tirée de AUBERT (1945).

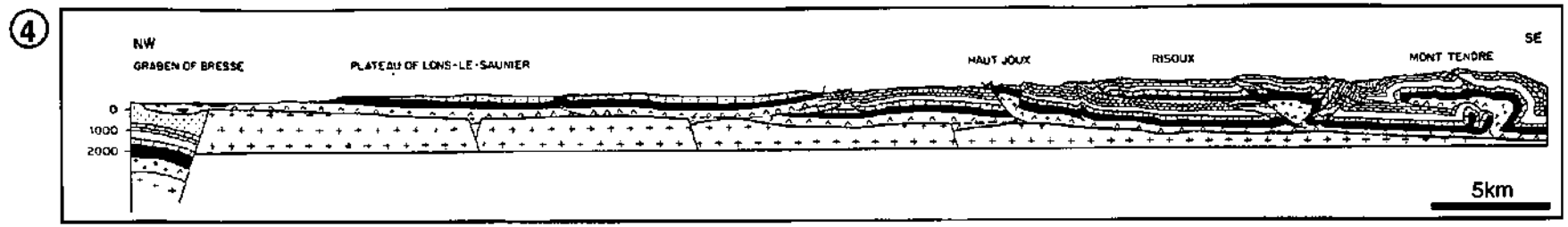

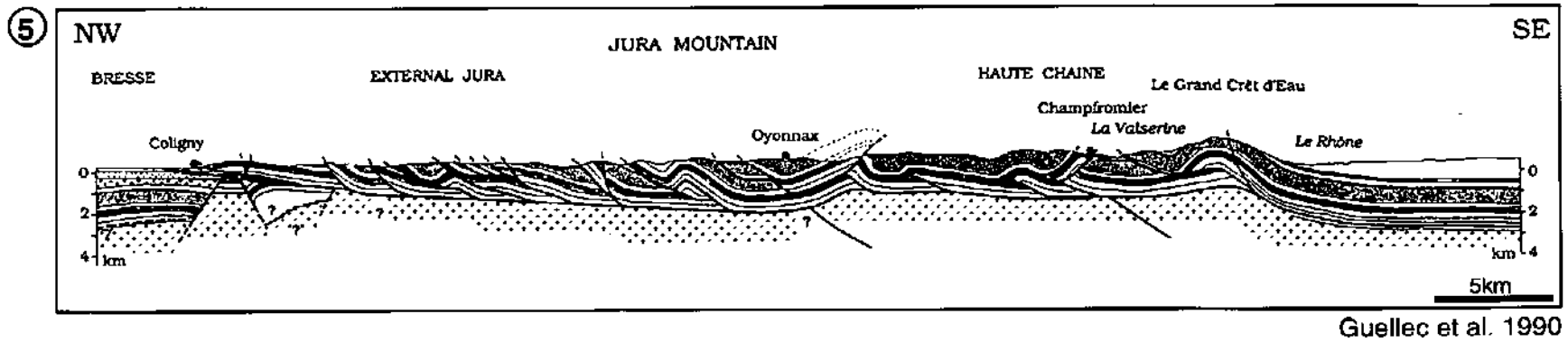

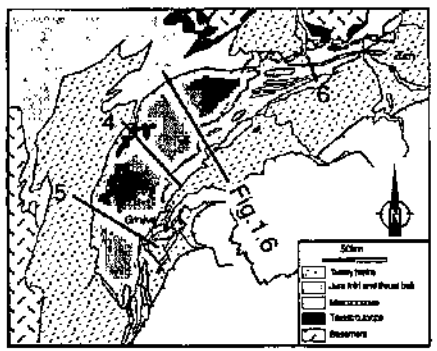

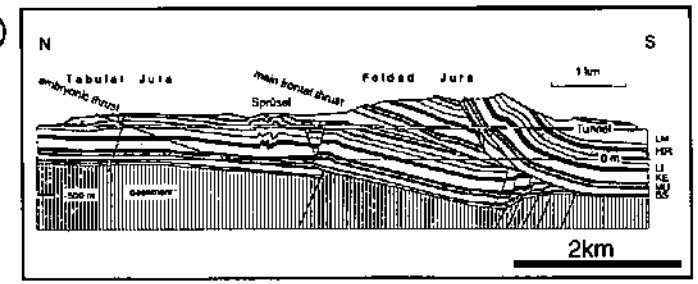

Figure 1.5: Selection of published cross-sections crossing the Jura fold and thrust belt. 4) From LAUBSCHER (1965); 5) From GUELLEC *et al.* (1990); 6) From LAUBSCHER (1992).

Coupes géologiques publiées recoupant la chaîne du Jura. 4) Tirée de LAUBSCHER (1965); 5) Tirée de GUELLEC et al. (1990); 6) Tirée de LAUBSCHER (1992).

Stretching in this model is essentially subhorizontal as expressed by the presence of conjugate systems of strike-slip faults. A wrench fold concept was also discussed by WEGMANN (1963), who suggested that the crystalline basement was broken by N-S trending horsts and grabens and by NE-SW trending antithetical faults. Accordingly, major tear-faults of the Jura resulted from the movement of the basement and concentrated along narrow zones. Folding resulted from more diffuse movements in the cover.

The availability of seismic reflection and well log data induced some authors (ZIEGLER, 1982; GORIN *et al.*, 1993) to further develop arguments in favor of an autochthonous cover. ZIEGLER (1982) argues that seismic reflection data show that the Molasse Basin is transected by a set of basement-involving normal and wrench-faults. These faults die out in the Oligocene or Miocene sediments and were active during the folding of the Jura fold and thrust belt. On the seismic lines, basement appears much deeper in the hinterland part of the Jura than below the Molasse Basin. Based on these data, ZIEGLER (1982, Fig. 26) suggests, that "*... the southern margin of the Jura belt is associated with a major basement imbrication along which the bulk of the shortening evident in the Jura-thrust belt is taken up. ... The configuration of the Molasse Basin implies that the postulated basement imbrication is carried out by a gently southeast-dipping thrust fault that possibly soles out within the crust. ...*". This thick-skinned allochthonous model suggests that the folding of the Jura belt was associated with crustal delaminations (Fig. 1.7). Recently, GORIN *et al.* (1993) have published structural interpretations of industry seismic lines from the western Swiss Molasse Basin. According to these authors the "*... foothills of the Jura Mountains are marked by a considerable thickening of the Triassic evaporites, which has been related by BITTERLI (1972) to salt flowage, but also coincides with a deep-seated Paleozoic lineament. ...*". These lineaments would have been active during that time and reactivated several times until the present day. Gorin *et al.* then argued that the geometry of these faults did not permit the translation of the cover and therefore the latter is autochthonous.

PFIFFNER *et al.* (1997a) have also suggested recently that the presence of inverted Permo-Carboniferous grabens argues in favor of a thick-skin deformation. A first detachment would be located within the Triassic evaporites and a second detachment horizon would be present within the basement. An inverted Permo-Carboniferous graben has been interpreted on one seismic reflection line in the central Molasse Basin (Hermrigen) (Fig. 1.3) and another one has been postulated in order to balance a geological cross-section in the central Jura (Chasseral anticline) (KÜHNI, 1993) (Fig. 1.7). This model agrees with that of GUELLEC *et al.* (1990) based on a ECORS deep seismic line as well as surface and subsurface data, who propose a shallow décollement in the Triassic evaporites layers and a deeper one within the basement (Fig. 1.5, section 5). According to them, "*... basement shortening is often required to account for the late deformation of the overlying but allochthonous sedimentary cover.*"

A similar interpretation of the Jura in terms of "thick-skinned" tectonics is given by JOUANNE *et al.* (1994) based on the comparisons of triangulations and present day vertical uplift rates (JOUANNE & MÉNARD, 1994).

Basement involvement beneath the Jura: opponents

Many other authors have explained the formation of the Jura belt as folded above a main décollement level within Triassic evaporite series. This hypothesis supposes an allochthonous cover and no basement involvement. For these authors, the discussion centres around the question of where the shortening of Jura and Molasse Basin cover is compensated in the basement ? The review presented here is based on a discussion by BURKHARD (1990) with the addition of some new references.

BUXTORF (1907) was among the first to interpret the Jura fold and thrust belt as an allochthonous cover deformation, resulting from a distant Alpine push (= "Fernschub" in German) transmitted through Mesozoic and Cenozoic strata of the Molasse Basin. The cover would be detached from the basement in the Triassic anhydrite beds. BUXTORF (1907; 1916) based his hypothesis on the observation of Triassic rocks in railway tunnel cut through anticlines (Fig. 1.5, section 2). The earlier section of SCHARDT (1906), shows that the Jura as an allochthonous cover folded over a slightly warped basement, stating a décollement zone between the cover and the basement (SCHARDT, 1906, 1908).

Gravity sliding for the whole Jura belt was proposed as early as 1892 by REYER (1892) and later more clearly expressed by LUGEON (1941, p. 9) for whom, the Jura resulted from the lateral migration of the evaporite layers from the Molasse Basin,

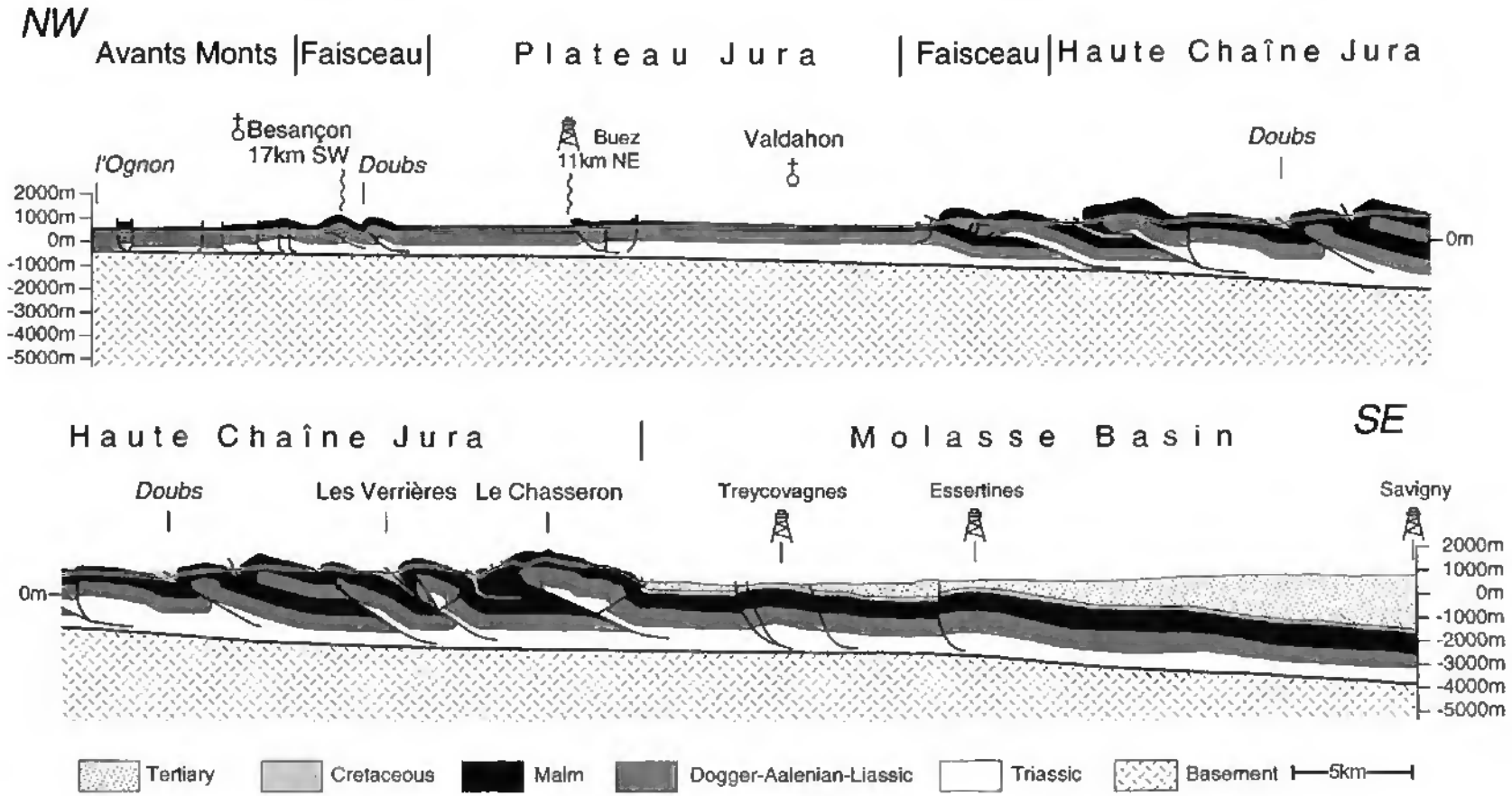

Figure 1.6: Line length balanced cross-section across the Jura and the Molasse Basin. This figure corresponds to the enlargement of the northern part of the large scale cross-section in Plate 9. For location, see geological map of Figure 1.5.

Coupe équilibrée à travers le Jura et le Bassin molassique. Cette figure correspond à l'agrandissement de la partie septentrionale de la coupe à grande échelle de la Planche 9. Pour la localisation, voir la carte géologique de la Figure 1.5.

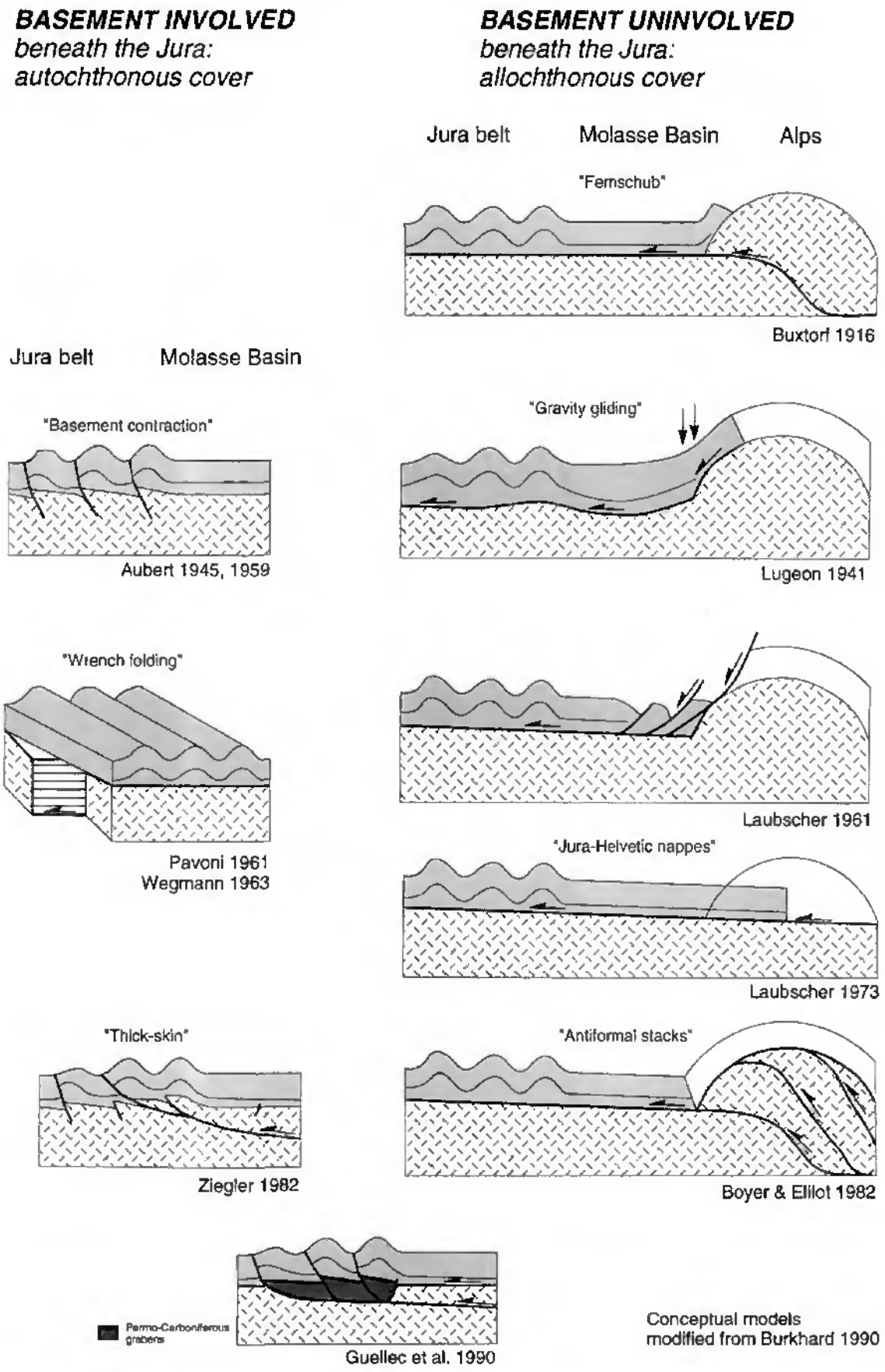

Figure 1.7: Review of conceptual models of the formation of the Jura fold and thrust. Modified from BURKHARD (1990).

Présentation de plusieurs modèles conceptuels expliquant la formation de la chaîne plissée du Jura. Modifié de BURKHARD (1990).

under a vertical loading stress (Fig. 1.7). The first model of LAUBSCHER (1961, 1965) also suggested that gravity sliding played an important role (Fig. 1.7). The Mesozoic cover together with the overlying Tertiary Molasse is folded and thrusted towards the NW from 2 to 25 km and rotated 8° around its northern tip, above a main décollement horizon located within the Triassic evaporite beds (Fig. 1.5, section 4). This model assumed a smooth underlying basement dipping 2° to 3° towards the South. Later, LAUBSCHER (1973b) presented a kinematic model of the Jura-Helvetic system, where the main Jura décollement level was connected to the basal Helvetic thrust; as a result the uplift of the external crystalline massifs would postdate the formation of the Jura thrust and fold belt. BURKHARD (1990) referring to fission track data from the Alps (SCHAER *et al.*, 1975; HURFORD, 1986) argues that "*... the uplift of the Central Alps must have started at the Early Miocene time, when the Molasse Basin was still subsiding. .... This means that during the thrusting of the Jura, there existed already an Aar massif culmination that had about half its present amplitude ...*". Consequently, the Jura basal thrust must root below or in the front of the external crystalline massifs (BOYER & ELLIOTT, 1982) and it cannot connect with the basal Helvetic thrusts (Fig. 1.7).

Recently, several seismic reflection lines have been shot and a series of drill holes have been made in the northeastern Swiss Jura by the NAGRA (Cooperative for the Storage of Radioactive Waste) (DIEBOLD *et al.*, 1991). This work has led to the discovery of an important Permo-Carboniferous trough. In addition the basement top seems to be affected by E-W trending normal faults with throws of some tens of meters. However, these faults are not important enough to impede a basal detachment within the thick Triassic beds (LAUBSCHER, 1992) (Fig. 1.5, section 6).

1.5. SOURCES OF DATA

Surface geological information, reflection seismic data and wells provide the data sets for this research.

1.5.1. Surface geological data

The surface geology data consist of a large number of published and unpublished geological maps, near-surface cross-sections and lithostratigraphic logs. In Switzerland, the studied area is more or less covered by 1:25'000 scale geological maps published by the Swiss Geological and Hydrological Survey and in France by 1:50'000 scale maps published by the French BRGM (Bureau de recherches géologiques et minières). Several unpublished original maps and cross-sections (diploma, PhD theses and private contracts) deposited at the Geology Department of Neuchâtel University, have been very useful for understanding structures. All maps used in this investigation are listed in Table 1.1.

1.5.2. Subsurface data

Industry seismic reflection surveys were conducted in the study area between 1970 and 1988 by different companies: British Petroleum (sector A in Figure 1.4), Shell Switzerland (sector B et C), Société anonyme des Hydrocarbures (sector B) and Shellrex (sector D). This subsurface data set consists of more than 1500 km of migrated or unmigrated seismic profiles and lithology- and velocity-logs of some twenty wells. The parameters (acquisition and processing) of the seismic set are more or less consistent, depending on each survey and especially on the date of exploration (Tab. 1.2). The Neuchâtel Jura and French Jura data sets were provided directly by the oil companies. Most of the industry seismic lines and well data from the Canton Vaud area are deposited at the Musée de Géologie at Lausanne, who kindly gave access to this information. The data sets include a migrated or unmigrated stack copy on paper.

Appendix 1 presents an inventory of seismic lines with the renumbering adopted in this thesis. In this new line numbering scheme (see Tab. 1.2 thesis numbering and sector), even numbers denote strike lines (NE-SW), whereas odd numbers denote dip lines (NW-SE). For a wider area, SWISSPETROL (1992) and BITTERLI (1972) present a general location map with a seismic grid and survey names from the Jura arc and the Molasse Basin.

Data from some twenty drill holes could be used for calibration of the seismic lines. These data include lithology and velocity logs (Appendix 2) coming essentially from the literature or provided by the Musée de Géologie in Lausanne.

1.6. METHODOLOGY

This subchapter present a short view of the important steps involved in the elaboration of this research.

Title	Location	Scale	Authors
Val de Ruz	NE, CH	1: 25'000	Bourquin et al. (1968)
Bieler See	BE, NE, CH	1: 25'000	Schär (1971)
Neuchâtel	NE, CH	1: 25'000	Frei et al. (1974)
Le Locle- La Chaux-de-Fonds	NE, CH	1: 25'000	Rollier & Favre (1910)
Chaumont (East sector)	NE, CH	1: 5'000	Schaer (1956)
Chaumont (West sector)	NE, CH	1: 5'000	Margot (1962)
Le Pâquier	NE, CH	1: 25'000	Aragno (1994)
Mont Amin Kette	NE, CH	1: 5'000	Baer (1959)
Biaufond-...-Saint-Imier	NE, JU, CH	1: 25'000	Bourquin & Suter (1946)
Les Verrières	NE, CH	1: 25'000	Mühlethaler (1930)
Val de Travers	NE, CH	1: 25'000	Rickenbach (1925)
Travers	NE, CH	1: 25'000	Thiébaud (1936)
Solmont	NE, CH	1: 25'000	Frei (1942)
Les Gorges de l'Areuse	NE, CH	1: 15'000	Schardt & Dubois (1903)
Les Gorges de l'Areuse	NE, CH	1: 25'000	Meia (1986)
Creux du Van	NE, CH	1: 10'000	Müller (1958)
Ponts-de-Martel	NE, CH	1: 5'000	De Pury (1963)
La Tourne	NE, CH	1: 5'000	Schwaar (1959)
Mt-Aubert	VD, NE, CH	1: 25'000	Meia (1969)
Les Gorges de La Vaux	VD, CH	1: 5'000	Dessoulavy (1952)
Ste-Croix	VD, CH	1: 25'000	Rigassi & Jaccard (1995)
Yverdon	VD, CH	1: 25'000	Jordi (1994)
Orbe	VD, CH	1: 25'000	Aubert & Dreyfuss (1963)
Cossonay	VD, CH	1: 25'000	Custer & Aubert (1935)
Jorat	VD, CH	1: 25'000	Bersier (1952)
Morges	VD, CH	1: 25'000	Vernet (1972)
Lausanne	VD, CH	1: 25'000	Weidmann (1988)
Châtel-St.-Denis	VD, FR, CH	1: 25'000	Weidmann (1992)
Marchairuz	VD, CH	1: 25'000	Falconnier (1950)
Vallée de Joux	VD, CH	1: 25'000	Aubert (1941)
Baume-Les-Dames	F	1:50'000	BRGM (1972)
Chalon-sur-Sâone	F	1: 250'000	BRGM (1987a)
Champagnole	F	1: 50'000	BRGM (1965a)
Dijon	F	1: 250'000	BRGM (1989)
Dôle	F	1:50'000	BRGM (1979)
Lons-Le-Saunier	F	1:50'000	BRGM (1966)
Morez-Bois d'Amont	F	1:50'000	BRGM (1968a)
Morteau	F	1: 50'000	BRGM (1968b)
Mouthe	F	1: 50'000	BRGM (1964)
Ornans	F	1: 50'000	BRGM (1963)
Poligny	F	1:50'000	BRGM (1981)
Pontarlier	F	1: 50'000	BRGM (1969)
Quingey	F	1:50'000	BRGM (1975)
Salins-Les-Bains	F	1:50'000	BRGM (1967)
Thonon-Les-Bains	F	1: 250'000	BRGM (1987b)
Vercel	F	1: 50'000	BRGM (1965b)

Table 1.1: List of geological maps from the studied area. Cantons: NE = Neuchâtel; BE = Bern; VD = Vaud; FR = Fribourg. Countries: CH = Switzerland; F = France.

Liste des cartes géologiques utilisées dans cette étude. Cantons: NE = Neuchâtel; BE = Bern; VD = Vaud; FR = Fribourg. Pays: CH = Suisse; F = France.

- *Compilation of existing data*

A large amount of data on the Central Jura and Molasse Basin exists, but few of these are easily accessible. Tools for documenting this study include: geological maps, dip data, cross-sections, drill hole data and seismic reflection lines. Different petroleum companies have shot thousands of kilometers of seismic reflection lines and drilled many wells in the project area. Many of them are neither published nor in the public domain. However, upon request BP and SHELL oil companies kindly provided many useful seismic lines and drill logs.

- *Field work*

Field work was conducted in order to collect additional dip data for the cross-sections.

- *Seismic interpretation*

More than 1500 km of seismic lines were interpreted for this work (Fig. 1.4). Surface data from geological maps of the central Jura and additional data collected in the field have been integrated with seismic profiles and well logs. Knowledge about stratigraphy is essential for seismic interpretation. As first step drill hole logs were therefore compiled. Based on wells, seismic stratigraphic units have been defined and correlated through the whole seismic grid, with jump correlations if necessary, because good data in synclines are often interrupted by bad data across anticlines and tear faults. Due to the good quality of strike lines, mainly shot along synclines, it was possible to constrain the stratigraphic column at depth. This has been especially important for unexposed Triassic formations. Each intersection of the seismic profiles was checked to obtain an internally consistent interpretation.

- *Depth conversion and contour maps*

Seismic time lines (two way time in seconds) were converted to depth (meters), in order to construct contour and isopach maps. Seismic velocities were constrained by nearby drill hole velocities. In the Jura itself, a simple velocity model was used for depth conversion, whereas in the Molasse Basin region, powerlaw or linear functions, dependent on depth were used (Appendices 3).

- *Cross-sections*

One line length balanced cross-section across the whole Jura and Molasse Basin (Fig. 1.6 and Plate 9) and two more regional cross-sections across the Neuchâtel Jura (Val de Ruz: Fig. 4.5; Val de Travers: Fig. 4.8) were drawn. These sections are based on the depth conversions of the nearest seismic lines and constructed using modern concepts of structural geology (WOODWARD *et al.*, 1989).

Survey	Year	Migration	Quantity	Sector	Lenght	Source	D. P.	Thesis numbering
British Petroleum	1988	yes	17	A	300km	vibroseis	500m	1-19
Shell Switzerland	1973-1978		11	B	450km	vibroseis	500m	20-
SADH *)	1972-1979		34	B	200km	vibroseis	500m	-71
Shell Switzerland	1972-1974	yes	14	C	100km	vibroseis	500m	80-95
Shellrex	1970-1974	mostly	20	D	600km	vibroseis	800m	100-125

Table 1.2: Seismic data parameters for each survey. For sectors, see Figure 1.4. D.P. = Datum Plane. *) SADH = Société anonyme des Hydrocarbures.

*Paramètres sismiques caractérisant chaque campagne sismique. Pour les secteurs, voir Figure 1.4. D.P. = Niveau de référence sismique. *) SADH = Société anonyme des Hydrocarbures.*

2. STRATIGRAPHY

2.1. INTRODUCTION

The geological interpretation of a seismic grid is based on the correlation of major seismic reflectors throughout the whole area. In sedimentary rocks, reflectors correspond to major lithological discontinuities. The stratigraphic calibration of the reflectors is done with the information obtained from the interpretation of drill hole logs. This chapter will first provide a regional overview and then present a synthetic stratigraphic column for the Neuchâtel Jura. Selected reflectors and seismic units used for the interpretation of the lines will then be presented taking into account the lithostratigraphic considerations. This chapter will also offer a series of isopach maps of the major stratigraphic units below the Molasse Basin and a rheological framework, which are both crucial for the understanding of the structures.

2.2. REGIONAL OVERVIEW

2.2.1. Introduction

The evolution of the Molasse and Jura basins during Mesozoic and Cenozoic times is here discussed in the larger geographic and tectonic context of central Europe. The following summary is not based on seismic data, but mostly on surface geology and wells, as reported in published books, guides or papers, that discuss the setting and the stratigraphic evolution of the sedimentary cover. Key references are listed below:

DIESLER (1914), HEIM (1921), JEANNET (Plate IV) in FAVRE & JEANNET (1934), GUILLAUME (1966), DEBELMAS (1974), CHAUVE (1975), AUBERT (1975), TRÜMPY (1980), DEBRAND-PASSARD *et al.* (1984), DEBRAND-PASSARD & COURBOULEIX (1984), HOMEWOOD (1986), GYGI & PERSOZ (1986, 1987), MARTIN (1987), ZIEGLER (1982, 1988, 1990), HOMEWOOD *et al.* (1989), KELLER (1989).

Formation names in quotation marks are given in French or German to avoid confusion associated with translation.

2.2.2. The basement: Paleozoic or older rocks

Paleozoic and older rocks underlie the Mesozoic strata of the Jura and the Molasse Basin. Crystalline basement crops out in the Vosges and Black Forest massifs (migmatitic gneisses), in the Serre massif and in the external Alpine massifs (Fig. 1.2). Permo-Carboniferous sediments are locally preserved in graben-like structures in all of these areas. Both kinds of rocks have been penetrated by wells underneath the Jura and the Molasse Basin.

The crystalline basement (metamorphic rocks) was formed during the Variscan (or Hercynian) orogeny. The latter is considered the product of the collision between the Gondwana and the Laurasia continents during lower Carboniferous time. Syn-kinematic granitic intrusion is associated with Variscan structures; post-kinematic granitic intrusion is related to crustal extension beginning in the upper Carboniferous. The latter corresponds to the final stage of the Hercynian orogeny, which is characterized by presumed crustal thinning along low angle normal faults and widespread strike-slip faults. Transtensional basins (pull-aparts, grabens), volcanism and hydrothermal activity is obviously the result of extension tectonics. Detrital fluvial sediments derived from high relief areas filled the basins and a luxuriant continental vegetation developed in warm climatic conditions. Coal seams result from the burial of this organic matter and Permian red sandstones and conglomerates ("Rotliegendes") overlie the coal-bearing strata. Important subsurface basins occur at the edge of the Jura: one example is the Lons-le-Saunier basin located at the western edge of the Jura (Fig. 1.2) and another basin located in the northern part of Switzerland was discovered in 1983 by the Swiss NAGRA (National Cooperative for the Storage of Radioactive Waste). Peneplanation followed the end of the Hercynian orogeny.

The basement is therefore characterized by two major unconformities: one below the Carboniferous sediments and second below the Triassic rocks.

2.2.3. Mesozoic

During the Mesozoic, an epicontinental sea developed in the area of the future Jura Mountains. Interlayered marl and limestone beds were deposited in a platform or lagoonal environment. An important facies limit (barrier or barrier reefs) appears to be located today approximately along the internal part of the Haute Chaîne Jura (TRÜMPY, 1980; PERSOZ, 1982; MOUCHET, 1995). In the Molasse Basin, more basinal facies have been recognized (PERSOZ, 1982).

Three typical stratigraphic columns of the Mesozoic formations, outcropping along the Swiss Jura, are presented on Figure 2.1. This figure shows the most important lateral changes in thickness and facies of the formations along the Swiss Jura.

2.2.3.1. Triassic

The Triassic is not exposed in the study area, except in the "Faisceaux" Jura of France. Triassic also crops out in the eastern Jura of Switzerland and it also has been drilled (Figs. 2.11 to 2.13) in the French Jura, in the Molasse Basin and in the Bresse Graben.

The stratigraphy of the Triassic layers is difficult to establish in the subsurface of the Jura and the Molasse Basin, because tectonic complications occur within these formations. As mentioned earlier (Chapter 1), the cover has been deformed over a main Triassic décollement level. Tectonic thickening, thinning and doubling of beds make it difficult to establish a detailed stratigraphy. Figure 2.2 presents a composite geological profile through the Triassic décollement level as interpreted from the well data of Schafisheim (Canton Aargau, Switzerland) (MATTER *et al.*, 1988). This area, located in the eastern Swiss Molasse Basin and a few kilometers south of the easternmost fold of the Haute Chaîne Jura, is structurally less complicated than the French Jura Plateau or the Haute Chaîne Jura. Even if the classic German Triassic and its stratigraphic framework is presented here, the area remains difficult to correlate with the limited and tectonically complicated data provided by the Jura and the Molasse Basin drill holes. The terms Keuper and Muschelkalk are not used in this work in view of the lack of reliable biostratigraphy and the tectonic considerations discussed above. Instead, we have adopted Triassic Unit 1 and Triassic Unit 2 as main subdivisions, based on seismic correlation (§2.4.3.7. and §2.4.3.8.).

At the beginning of the Mesozoic, the peneplaned basement was invaded by a marine transgression. An epicontinental shallow water sea developed with a depocenter in northern Germany (Fig. 2.3). The basin was almost completely landlocked. During times of limited connection with the Tethys, continental clastics and evaporites were deposited. During marine ingression huge lowland areas were flooded and carbonates were precipitated. The Triassic deposits in the Jura are of Germanic type and traditionally subdivided into three lithostratigraphic units (Fig. 2.4): the "Buntsandstein" consists of sandstones or conglomerates also called the "Grès bigarrés" formation; the "Muschelkalk" begins with the "Wellen-gebirge", marine sandstones, marls and dolomites and is followed by the "Anhydritgruppe" with its salt and evaporites suggesting only a restricted connection between the Germanic inland sea and the Tethys (Fig. 2.3) and terminates with the "Hauptmuschelkalk" and its marine shelly limestones; the last of the trilogy, the "Keuper", starts with the marker bed "Lettenkhole", containing lignite and dolomite and continues mainly with evaporites ("Gipskeuper") and marls. The overlying Rhaetian is represented by sandstones and marls.

The total thickness of the Triassic series (Fig. 2.5) is less than 500 m outside of the Jura fold and thrust belt and appears to increase progressively towards the center of the chain (internal Jura), reaching more than 1000 m. The formation of the Jura fold and thrust belt seems to be closely related to the thickness distribution of the Triassic layers and will be discussed later in Chapter 5.

2.2.3.2. Jurassic

Early Jurassic: Liassic

The lower Jurassic formations, like those of the Triassic, crop out in the Tabular Jura, along the northern margin of the Folded Jura and in France along the western margin of the Jura.

The Early Jurassic was characterized by a transgression. The environment was a platform or a low energy shallow basin (Fig. 2.6). The studied area is too small to be a distinct paleogeographic domain itself, although it shows influences from the Alpine (Tethys basin), Swabish and Paris basins. Several positive areas of low relief, represented by anorogenic highs (i.e. Massif Central, London-Brabant massif, Rhenish massif, Bohemian massif, ...) surround these basins. The southern part of the Molasse Basin was occupied by one of these islands called

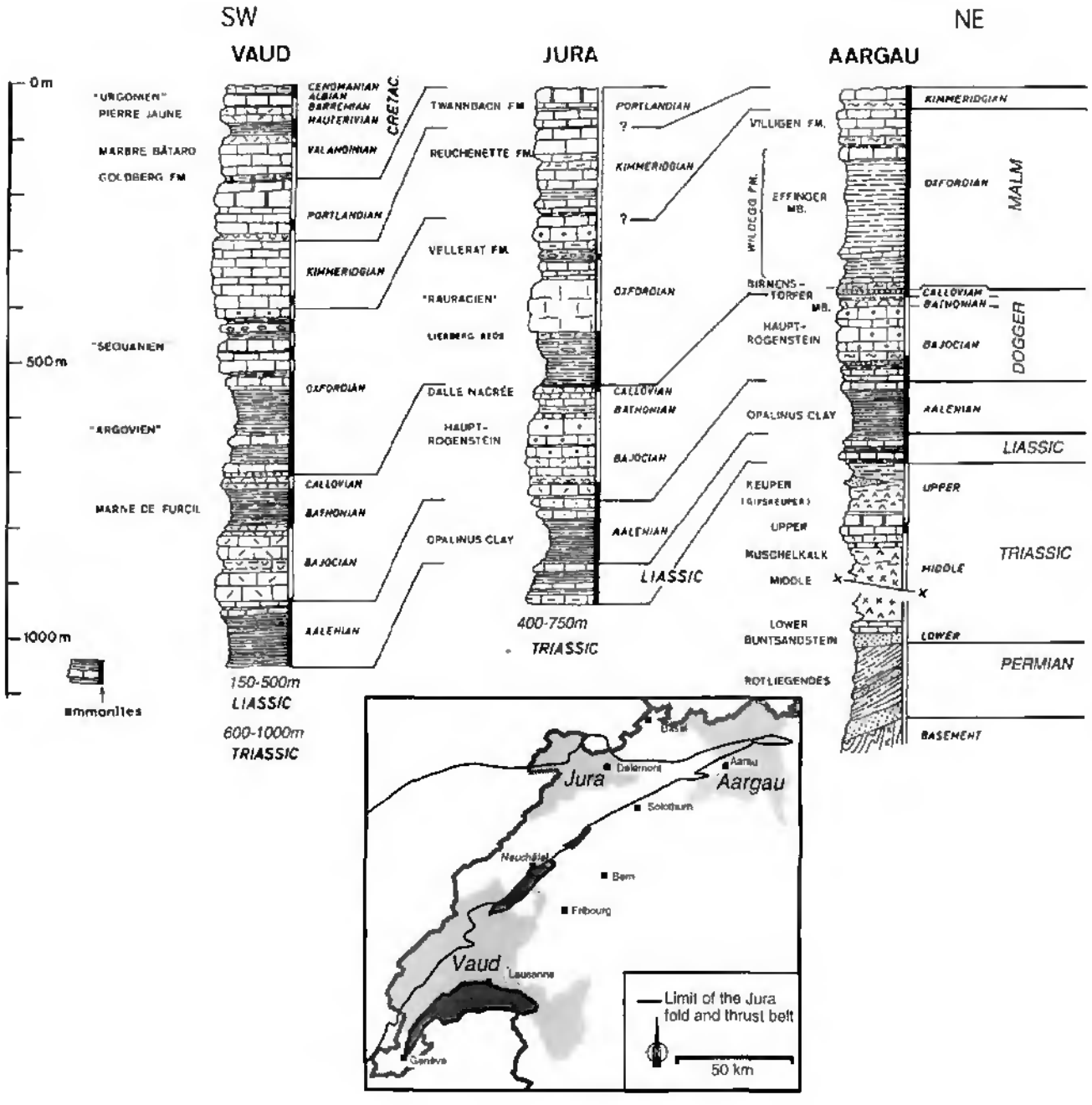

Figure 2.1: Stratigraphic sections of the Mesozoic formations in the Swiss Jura. Vaud, Jura and Aargau correspond to three Swiss Cantons, their location is given on the small adjoining map. Modified from TRÜMPY (1980).

Coupes stratigraphiques des formations mésozoïques du Jura suisse. Vaud, Jura et Aargau représentent trois cantons suisses. Modifié de TRÜMPY (1980).

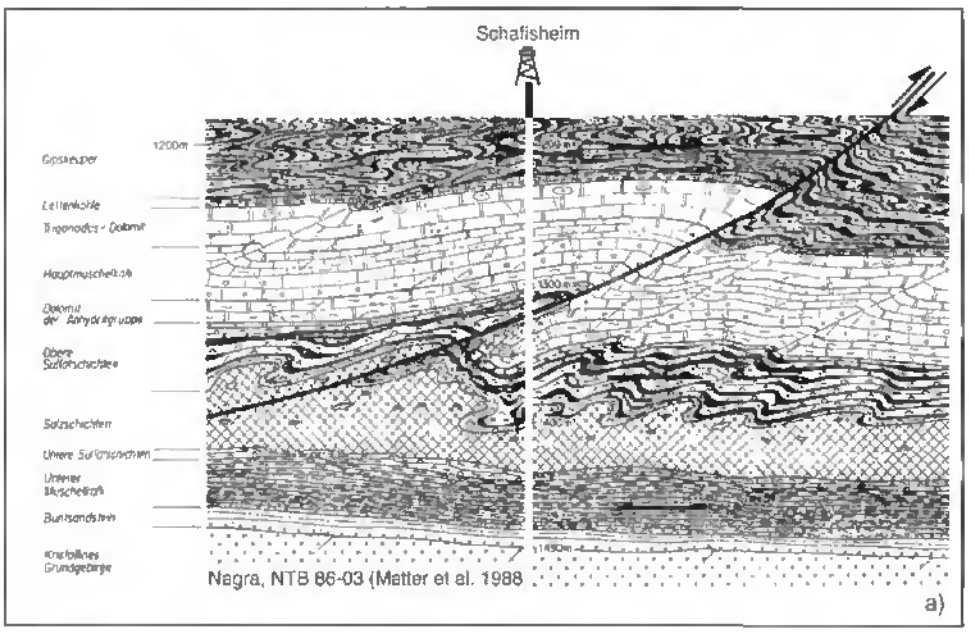

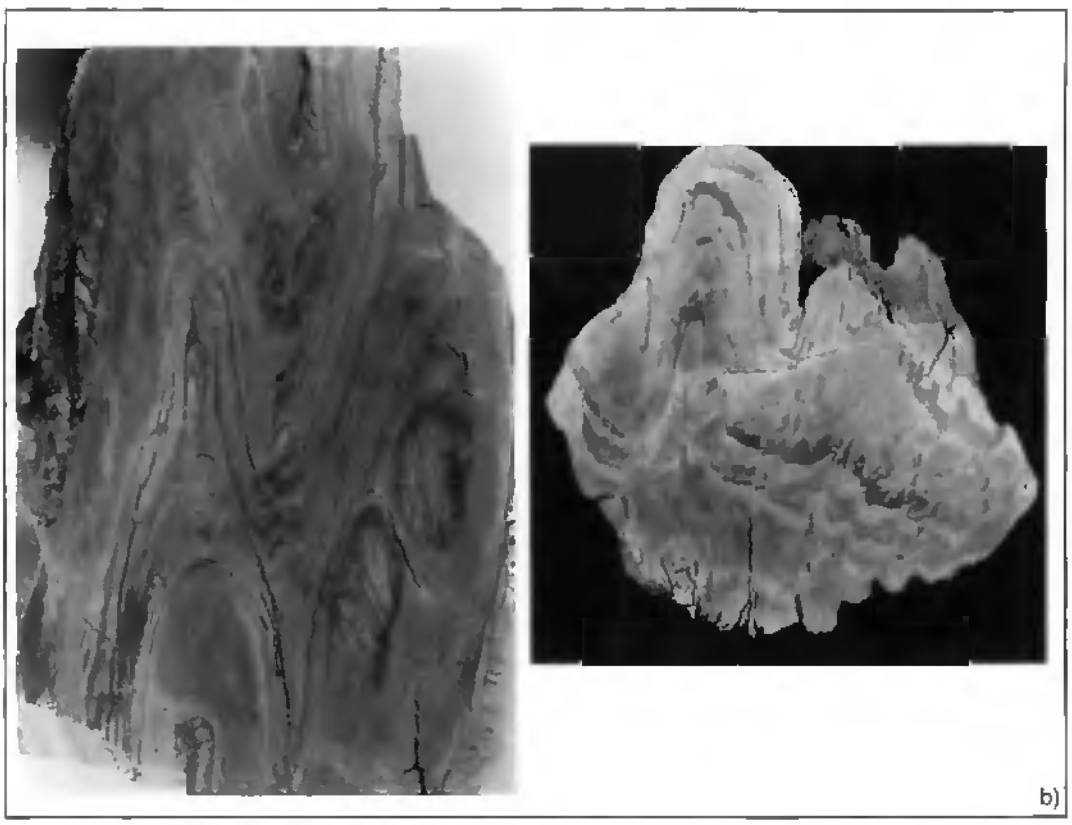

Figure 2.2a): Composite geological profile through the Triassic décollement zone. This section, based on the Schafisheim drill hole data, highlights the tectonically disturbed stratigraphy in the Triassic layers. From MATTER *et al.* (1988).

Coupe géologique à travers la zone de décollement du Trias. Ce profil, basé sur les données du forage de Schafisheim, souligne les perturbations tectoniques qui affectent la succession des couches du Trias. Tiré de MATTER *et al.* (1988).

Figure 2.2b): Type of folds observed in the Triassic evaporites in the Riepel quarry from Aargau Jura (645'200 m / 253'900 m, Swiss geographical reference).

Types de plis observés dans les niveaux évaporitiques du Trias de la carrière de Riepel, Jura argovien (645'200 m / 253'900 m, coordonnées géographiques suisses).

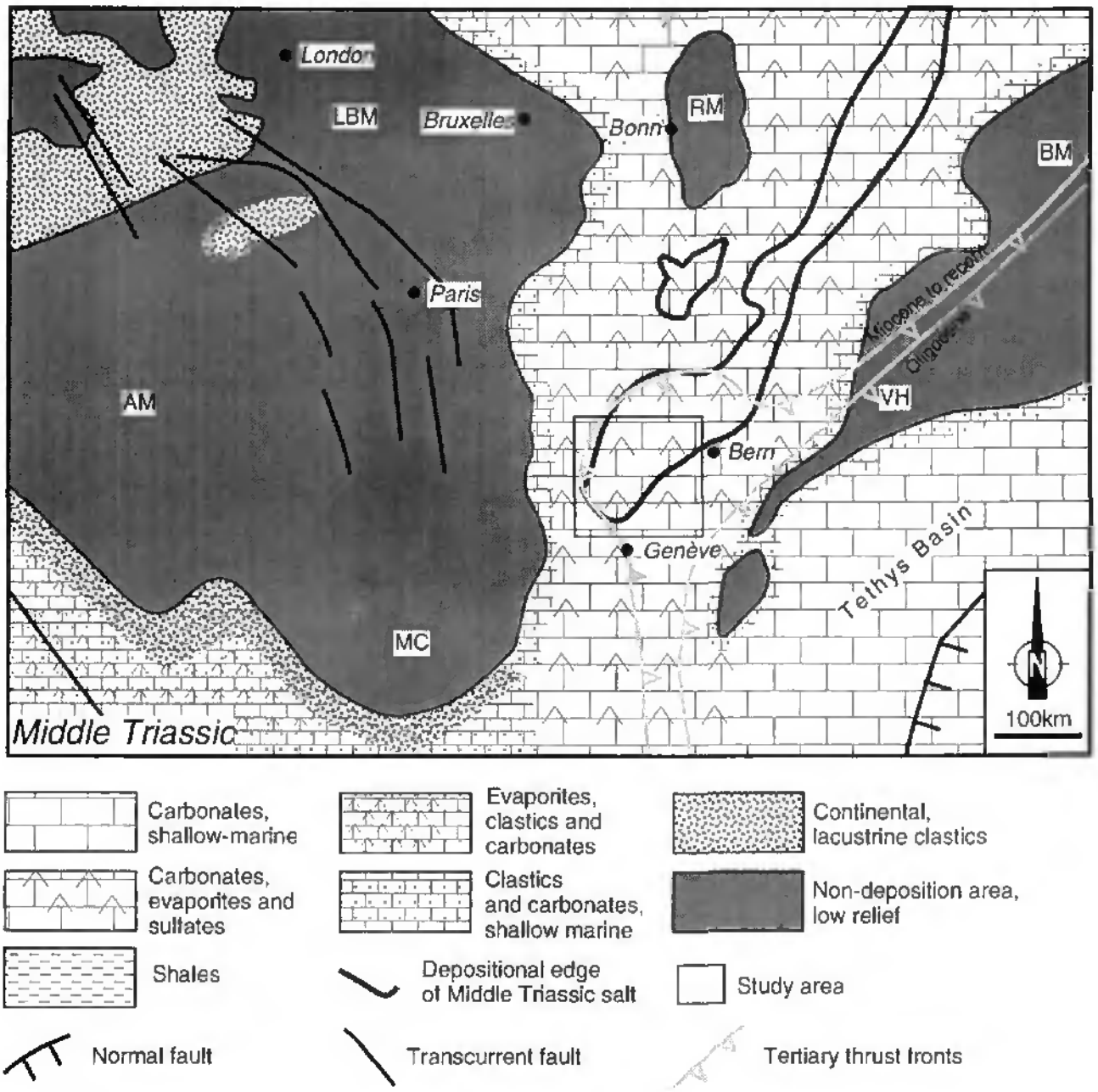

Figure 2.3: Paleogeographic map of Central Europe (not restored) in Middle Triassic times ("Muschelkalk"). AM = Armorican massif; BM = Bohemian massif; LBM = London-Brabant massif; MC = Massif Central, RM = Rhenish massif; VH = Vindelician High. Modified from ZIEGLER (1988, 1990). The square corresponds to the studied area.

Carte paléogéographique de l'Europe centrale (non reconstruite) au Trias moyen ("Muschelkalk"). AM = Massif armoricain; BM = Massif de Bohême; LBM = Massif de Londres-Brabant; MC = Massif Central, RM = Massif rhénan; VH = Seuil vindélicien. Modifiée de ZIEGLER (1988, 1990). Le carré représente la région étudiée.

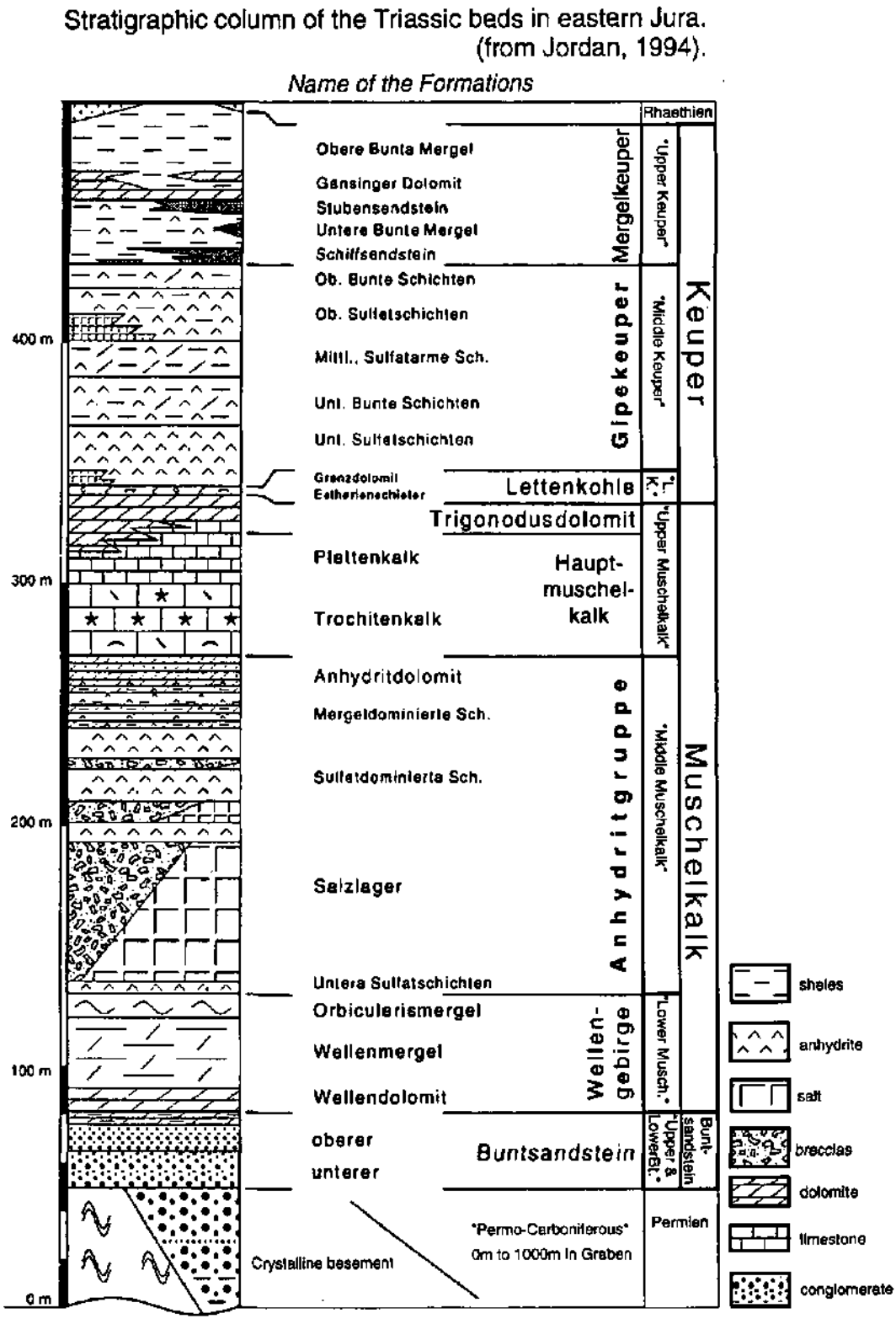

Figure 2.4: Composite stratigraphic column of the Triassic series as based on outcrops and drill hole data of the eastern Swiss Jura. Modified from JORDAN (1994).

Coupe stratigraphique des séries du Trias, reconstituée à partir des informations de la surface (affleurements) et de la subsurface (forages) de l'Est du Jura. Modifiée de JORDAN (1994).

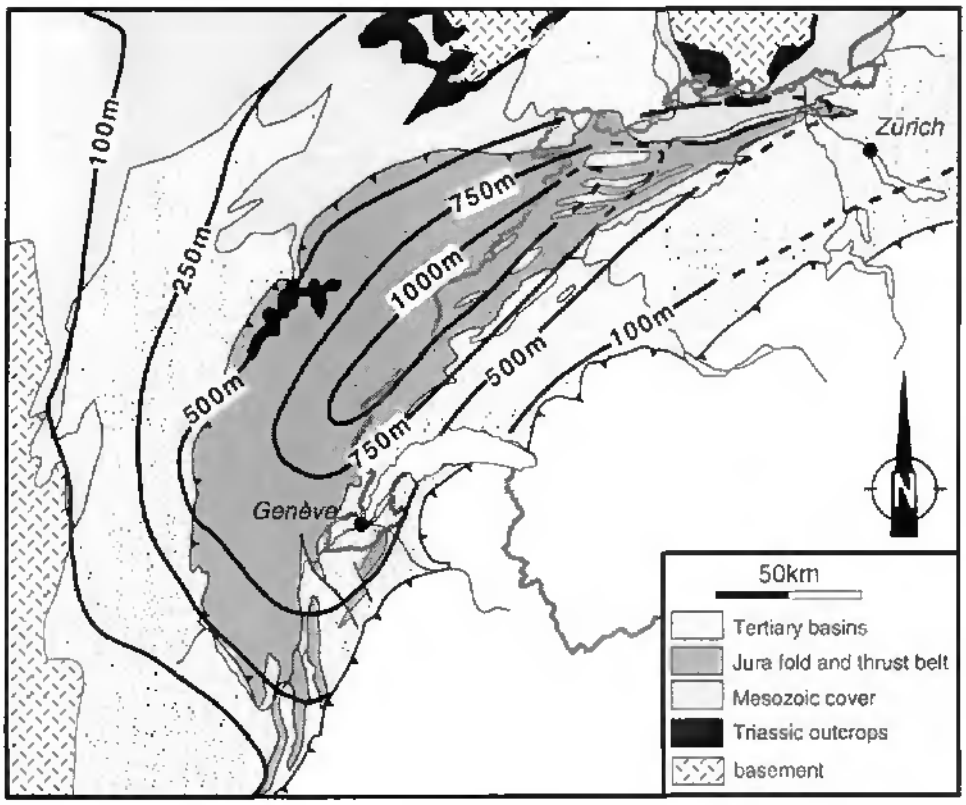

Figure 2.5: Isopachs (in meters) of the Triassic layers (minus Buntsandstein) in the Jura fold and thrust belt and adjoining areas. Thicknesses are compiled from many authors (Winnock *et al.*, 1967; Debrand-Passard & Courbouleix, 1984; Bachmann *et al.*, 1987; Bitterli, 1992).

Carte des isopaches (en mètres) des couches du Trias (Buntsandstein non compris) de la chaîne du Jura et des ses régions avoisinantes. Les épaisseurs sont compilées de plusieurs auteurs (Winnock et al., 1967; Debrand-Passard & Courbouleix, 1984; Bachmann et al., 1987; Bitterli, 1992).

the Alemannic high (Fig. 2.6). Coarse (mm size) quartz sands derived from this high occur in the Liassic series encountered in bore holes.

Middle Jurassic: Dogger

These are the oldest formations seen at outcrop throughout the Jura. By the beginning of mid-Jurassic times, the Alemannic high was flooded, but remained an area of minimal sedimentation until the late Middle Jurassic.

Lateral and vertical facies changes in the Liassic suggest differentiation of the Jura platform into different facies realms, which persisted throughout the Middle and Late Jurassic. The northwestern region was a shallow-water platform, whereas to the Southeast more muddy sedimentation prevailed in a low-energy hydrodynamic regime. The boundary between the two realms shifted repeatedly, but never corresponded to a single major shelf margin scarp; it is located along the axis Bern-Genève on the paleogeographic map of the Early Jurassic times (Fig. 2.6).

Late Jurassic: lower and upper Malm

The difference between an eastern and western domain still persisted. The boundary between the two domains shifted towards the SE during Late Jurassic times. The former Alemannic high began to subside. Sub-euxinic limestones extend beyond the Molasse Basin into the Helvetic domain (Fig. 2.7).

The Late Jurassic began with a condensed facies, represented by few centimeters of iron ooliths with Cephalopods, but was then characterized by a shallow-water platform with development of biohermal reefs. The boundary between the platform and basinal domains was marked by a discontinuous belt of patch reefs and oolitic bars. At the end of the upper Malm time, the sedimentary environment changed

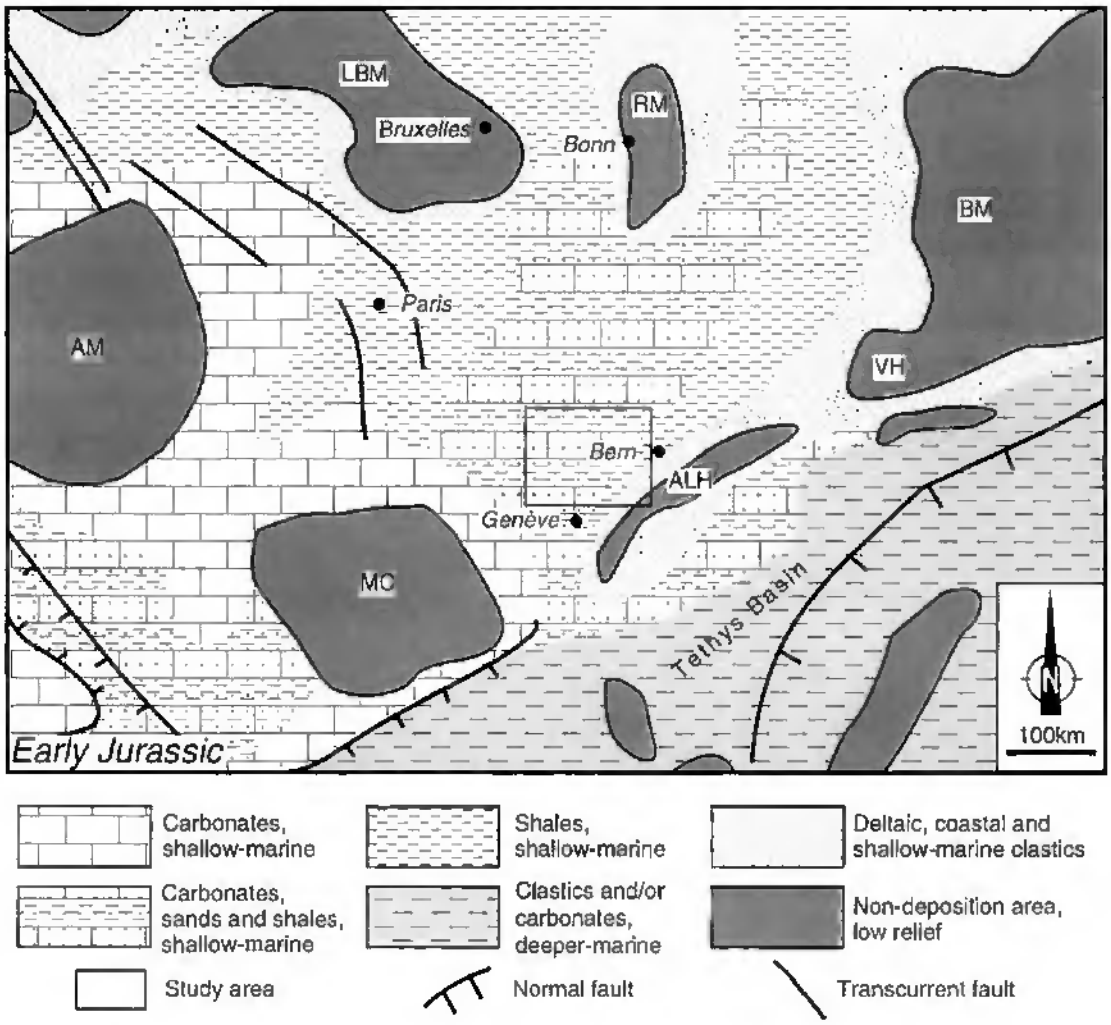

Figure 2.6: Paleogeographic map (not restored) of Central Europe in Early Jurassic times (Sinemurian - Aalenian). AM = Armorican massif; ALH = Alemannic high; BM = Bohemian massif; LBM = London-Brabant massif; MC = Massif Central, RM = Rhenish massif; VH = Vindelician High. Modified from ZIEGLER (1988, 1990). The square corresponds to the studied area.

Carte paléogéographique de l'Europe centrale (non reconstruite) au début du Jurassique (Sinémurien - Aalénien). AM = Massif armoricain; ALH = Seuil alémanique; BM = Massif de Bohême; LBM = Massif de Londres-Brabant; MC = Massif Central, RM = Massif rhénan; VH = Seuil vindélicien. Modifiée de ZIEGLER (1988, 1990). Le carré représente la région étudiée.

from a margino-littoral facies to a supratidal facies with emersion episodes, leading to a marine brackish facies. These changes occurred as the result of a widespread regression, which affected western Europe by the end of the Jurassic.

2.2.3.3. Cretaceous

The Early Cretaceous is well developed in the Haute Chaîne Jura, whereas the Late Cretaceous is discontinuous, due to Tertiary erosion. At the beginning of Cretaceous time, a new marine incursion covered the southern Jura. During the Early Cretaceous, the Jura formed a platform with sediments deposited in shallow waters (neritic environment) close to emersion conditions. A paleogeographic border was located along the internal zone of the Haute Chaîne Jura. The Early Cretaceous deposits are limestones or calcareous marls. During the Cenomanian-Turonian stage, the "Craie" (chalk) facies invaded the Jura from the Paris Basin. Detrital facies migrated progressively towards the South and the Jura became part of the Paris Basin. Late Cretaceous limestones are locally preserved in karst pockets. All Cretaceous formations thin towards N or NE and disappear totally eastward of Biel. This raises the question whether Cretaceous sediments were removed by erosion or if they were never deposited? The answer is still open (Thierry Adatte, Neuchâtel, personal communication), but it

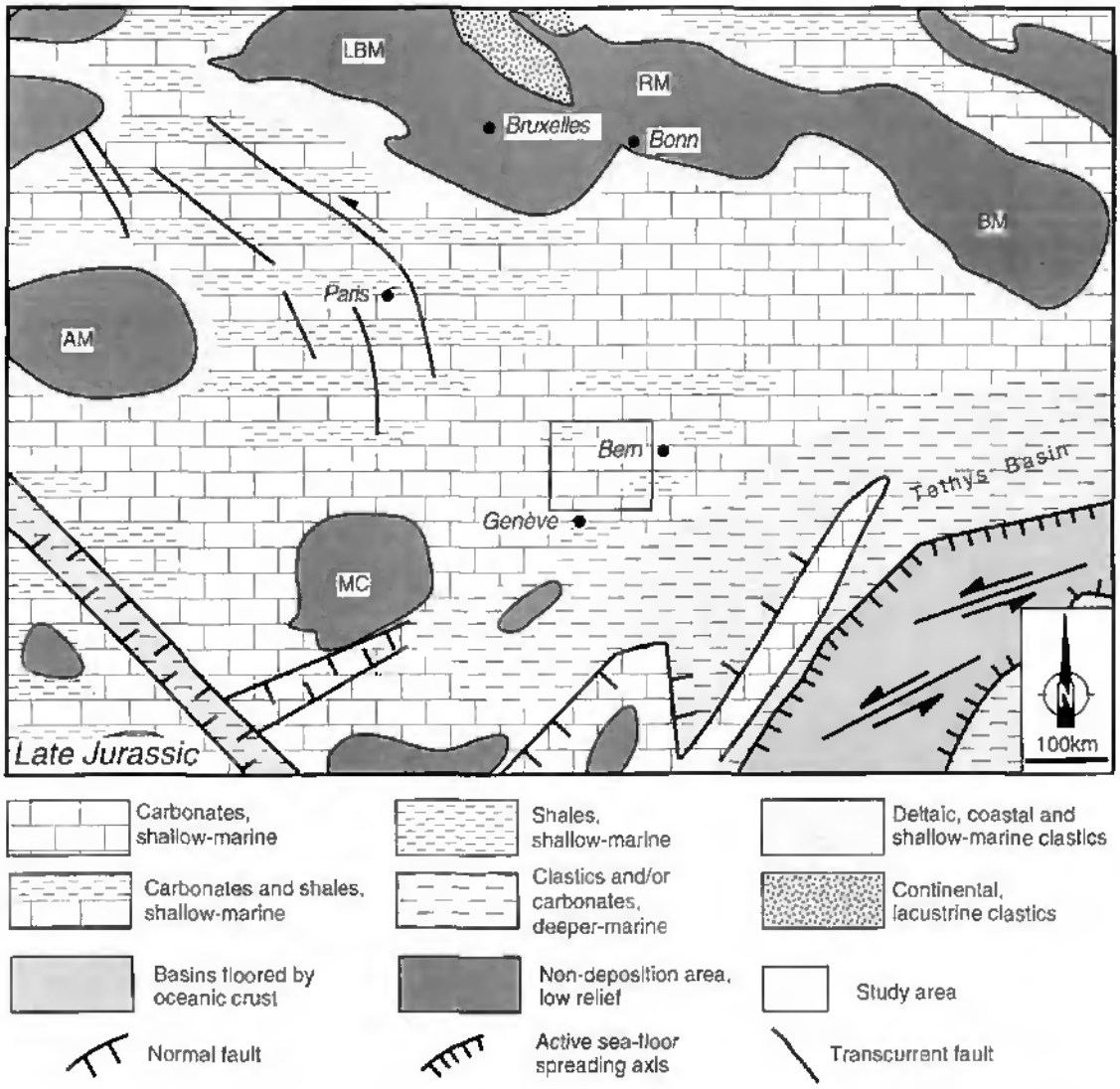

Figure 2.7: Paleogeographic map of Central Europe (not restored) in Late Jurassic times (Kimmeridgian - Tithonian). AM = Armorican massif; BM = Bohemian massif; LBM = London-Brabant massif; MC = Massif Central, RM = Rhenish massif. Modified from ZIEGLER (1988, 1990). The square corresponds to the studied area.

Carte paléogéographique de l'Europe centrale (non reconstruite) à la fin du Jurassique (Kimméridgien - Tithonique). AM = Massif armoricain; BM = Massif de Bohême; LBM = Massif de Londres-Brabant; MC = Massif Central, RM = Massif rhénan. Modifiée de ZIEGLER (1988, 1990). Le carré représente la région étudiée.

appears very likely that Cretaceous sediments were deposited in the Jura area (POMEROL, 1975; ZIEGLER, 1982) and subsequently eroded. The strong erosion is related to basement uplift in connection with the Oligocene Vosges-Black Forest mantle dome (TRÖMPY, 1980; KARNER & WATTS, 1983; NAEF *et al.*, 1985).

2.2.4. Cenozoic: Tertiary

The Tertiary of the Molasse Basin and the Jura record the late stages of the Alpine deformation. A profound erosion surface separates various subcropping Mesozoic formations (Cretaceous, Late Jurassic and even Middle Jurassic in the East) from the onlapping Neogene (Fig. 2.8). The Eocene sediments are only known in karst pockets filled with red lateritic clays and ferrigeneous ooliths ("Bohnerz formation"). The Oligocene and Miocene successions are influenced by two major events affecting the foreland: the WNW-ESE extension of the Rhine Graben subsidence (Priabonian to Aquitanian age) and the uplift of the Black Forest - Vosges dome (LAUBSCHER, 1992).

In the study area, the Tertiary is commonly referred to as Molasse. The Tertiary stratigraphy of the Jura and the Molasse Basin has been reviewed by HOMEWOOD *et al.* (1989), KELLER (1990) and

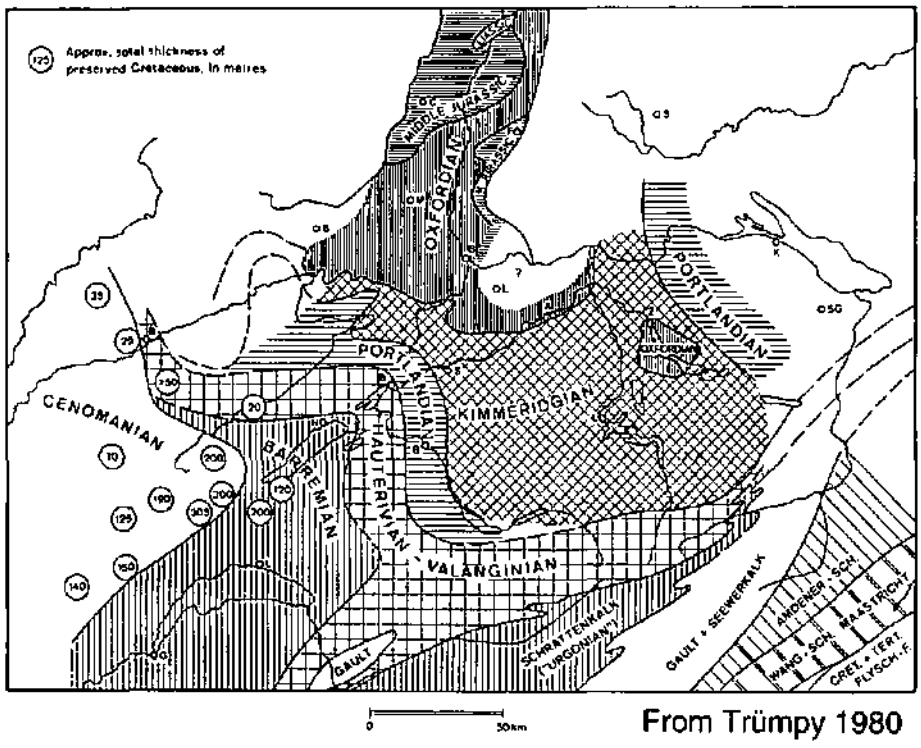

Figure 2.8: Tertiary subcrop map of the Jura and the Molasse Basin. The total thickness of preserved Cretaceous (in meters) decreases towards the SE. From TRÜMPY (1980) with Courtesy of Shell Oil Co.

Carte paléogéographique à la base du Tertiaire. Les chiffres dans les cercles correspondent à l'épaisseur totale approximative (en mètres) des couches préservées du Crétacé. Tirée de TRÜMPY (1980), courtoisie de Shell Oil Co.

BERGER (1992). Figure 2.9 relates the traditional nomenclature to more modern usage. The Molasse is essentially a clastic wedge prograding from the Alps towards the NW. Sediments are derived from the rising Alps, with only a minor detrital influx from the NW. Four lithostratigraphic groups are distinguished traditionally (Fig. 2.9): UMM ("Untere Meeresmolasse" = Lower marine water sediments), USM ("Untere Süsswassermolasse" = Lower freshwater Molasse), OMM ("Obere Meeresmolasse" = Upper marine water Molasse) and OSM ("Obere Süsswassermolasse" = Upper freshwater Molasse). Continental environments were represented by alluvial fans, gently sloping flood-plains with river channels and braided streams, lakes and coal swamps, whereas shallow current swept seas, paralic deltas and tidal flats represent marine to brackish environments.

Outcrops of the Lower marine Molasse group (UMM) are found in the Subalpine Molasse. The formation is represented by marine and brackish shales and sandstones. They correspond to a thick turbidite sequence at the base, followed by storm, wave and tide deposits and finally by a regressive littoral series. Along the southern rim of the Jura mountains, some thin continental deposits are time-equivalent to the UMM (AUBERT, 1975). The northern limit of the marine "Rupelian" deposits lies not far north from the present day Alpine front along a line Lausanne-Lucerne. Savigny (LEMCKE, 1963) is the only well in the study area yielding UMM sediments in cuttings.

During the "Chattian" - "Aquitanian" stages (USM), the sea retreated from the Molasse depression and the Alps began to rise strongly at rates of almost 1 mm/year (TRÜMPY, 1980). According to BERGER (1992), "Chattian" and "Aquitanian" stage terms, as used locally, are imprecise chronostratigraphic terms and should be used only as "local units". A part of the USM is surely of Rupelian age (BERGER, 1992). The Plateau Molasse landscape at late Oligocene times is dominated by at least seven gravel fans, at the northern margin of the Alps. Thick alluvial-fan conglomerates and sandstones were deposited grading northwards into multicolored sandstones and claystones representing meandering rivers, lakes and floodplain deposits. The USM conglomerates are derived from Mesozoic carbonates, flysch, igneous metamorphic and ophiolite clasts from Prealpine and Austroalpine nappes. In the Jura Molasse domain, the Oligocene fresh water transgression was influenced by the Rhine-Bresse graben extension and the Plateau Molasse subsidence; outcrops are isolated and some Gasteropods and Charas (algae) fossils give evidence for lacustrine facies (AUBERT, 1975).

The "Burdigalian" and the "Helvetian" stages (OMM) are characterized by a marine transgression. Shallow seas flooded the Molasse Basin and rocks

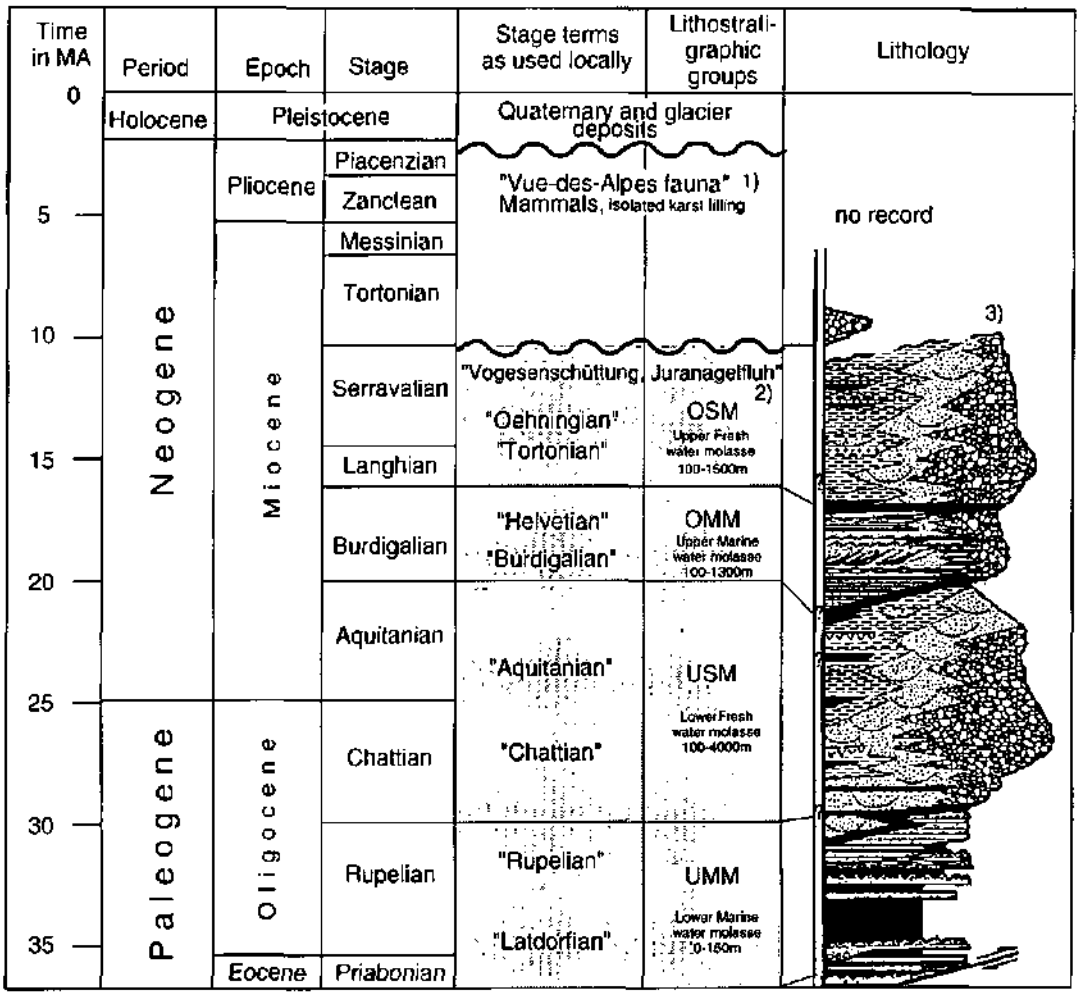

Figure 2.9: Tertiary stratigraphy and formation names as used in the Jura and the Molasse Basin. Modified from TRÜMPY (1980) and HOMEWOOD *et al.* (1989). 1) Data from BOLLIGER *et al.* (1993); 2) Data from KÄLIN (1993, 1997); 3) Lithological column from KELLER (1990).

Coupe stratigraphique et nom des formations du Tertiaire du Jura et du Bassin molassique. Modifié de TRÜMPY (1980) et HOMEWOOD et al. (1989). 1) Résultats de BOLLIGER et al. (1993); 2) Résultats de KÄLIN (1993, 1997). 3) Colonne lithologique de KELLER (1990).

consist of marine glauconitic sandstones with siliceous and calcareous grains with some thin marl layers alternating with sandstones. The transgression of the OMM is relatively well constrained by mammal ages from the underlying USM (BERGER, 1992). In the Jura Mountains, the diachronous character of the OMM-base can only be deduced from indirect correlation and from geological patterns (more detailed information on the Jura area is given by AUBERT, 1975). During these stages the Bresse-Graben subsidence stopped and basins were by then filled with Oligocene sediments.

During the "Tortonian" - "Oehningian" stages (OSM), the sea withdrew permanently, arguably not synchronously because of depocenter migration and variable relief created by alluvial fans (BERGER, 1992). Sedimentation continued in the floodplains beyond and between the gravel fans, providing fluviatile sandstones in channels and silty shales. Freshwater limestones formed in local basins. In the Neuchâtel Jura, a complete series is preserved in the Le Locle syncline (FAVRE, 1911; FAVRE *et al.*, 1937) (Figs. 1.3 and 4.3) and has a thickness of some 200 m, of which 165 m are lacustrine chalks (KÜBLER, 1962a, 1962b). The extension of this lake was small and limited to Les Verrières, La Brévine, Morteau, Le Locle and La Chaux-de-Fonds area (Fig. 4.3).

The top of the OSM is marked, in the internal part of the Molasse Basin, by an erosional boundary covered generally by Quaternary sediments, whereas in the external part (Jura Mountains, Delémont Basin) a discordance covered by conglomerates, sands and gravels ("Vogesenschüttung, Juranagelfluh", "Hipparion and Dinotherium sands", Fig. 2.9) of MN9 Mammals age (~11 M.y.) (KÄLIN, 1993) is present.

2.3. OUTCROP AND SUBSURFACE STRATIGRAPHY

2.3.1. Introduction

Facies and thickness variations cannot be presented in one single synthetic lithostratigraphic log valid for the whole region. Therefore a key area will be described first (§2.3.2.), followed by a discussion of lateral variations (§2.3.3.). The reference profile will be described in some detail, while the drill hole data and their correlation will be synthesized with respect to the seismic units described in §2.4. The key area is the Neuchâtel Jura and it has been chosen, because it presents one of the most complete profiles (from Tertiary to Aalenian rocks). Correlation and lateral variations will be based on drill hole data (Figs. 2.11 to 2.13), which show a continuous log from surface to Triassic and the basement.

The following profile and the drill hole lithostratigraphy will be described going from the youngest rocks to the oldest (i.e. from top to bottom), and will be followed stepwise on seismic lines. The key stratigraphic column is presented on Figure 2.10 and is compared with drill holes on Figure 2.12.

2.3.2. A stratigraphic column for the Neuchâtel Jura

The Tertiary Molasse is preserved in the Val de Ruz, Val de Travers and La Chaux-de-Fonds - Le Locle synclines below fluvio-glacial Quaternary sediments (Fig. 2.9). The youngest sediments are late Middle Miocene ("Oehningian", OSM) lacustrine deposits (KÜBLER, 1962a), which occur in the La Chaux-de-Fonds - Le Locle syncline. By contrast in the Val de Ruz, the youngest preserved Molasse formations are USM (lower freshwater Molasse) (MORNOD, 1970; AUBERT, 1975; MATHEY, 1976), which rest directly on the Early Cretaceous with an intermediate Eocene Laterite ("Bohnerz") formation, which fills a karst surface. In the Val de Ruz, the total thickness of Tertiary Molasse increases from 100 m in the NW (MORNOD, 1970) to about 200 m in the SE (SCHNEGG *et al.*, 1983; SCHNEGG & SOMMARUGA, 1995). In the Val de Travers, the Molasse reaches 235 m (MEIA, 1969).

The Cretaceous is of special importance for the Neuchâtel Jura because the Neocomian, Valanginian and Hauterivian stages have been defined in this area (THURMANN, 1836b; DESOR, 1854; RENEVIER, 1894). Early Cretaceous is represented by a well-layered 150-200 m thick series of limestones and marls. Cenomanian chalky limestones overlie Albian blue marls rich in Ammonites and Aptian glauconitic limestones and marls. The underlying Barremian, Hauterivian, Valanginian and Berriasian rocks consist from top to bottom (Fig. 2.10) of: the "upper Urgonian" oolitic limestones, the "lower Urgonian" spathic limestones with intercalated marls, the "Pierre jaune d'Hauterive de Neuchâtel", detrital and spathic limestones with ooliths and Echinids, the "Marnes bleues d'Hauterive" blue colored marls, the "Calcaire roux valanginien" limonitic reddish limestones and the "Marbre bâtard valanginien" oolitic limestones (REMANE, 1982). In the upper Urgonian formation, asphalt deposits have been mined in the Val de Travers from 1713 to 1986 (MEIA, 1987). The source bed of these asphalt deposits is still unknown, but the asphalt must have migrated before the deformation of the Jura (ZWEIDLER, 1985). The transition from Cretaceous to Jurassic rocks is highlighted by the 10-30 m thick Purbeckian facies (Berriasian in age), consisting of brackish marls.

In contrast to the well layered Cretaceous sequence, the underlying 350 to 400 m thick upper Malm limestones are homogeneous and massive (PERSOZ & REMANE, 1973). The Portlandian consists of 100 m of dolomites and limestones. The "Banc à Nérinées" is used as the top of the Kimmeridgian, with white massive platform limestones (150-170 m). The Sequanian represents a barrier facies, with oolitic limestones (100-120 m). The transition to the underlying Argovian marls (150-200 m) is gradational and shows a progressive decrease in layer thickness and an increase in the percentage of marly interbeds. It represents the Argovian facies sensu stricto, comprising three members (GYGI & PERSOZ, 1986): the "Couches de Geissberg" at the top, corresponding to a regional calcareous facies, the

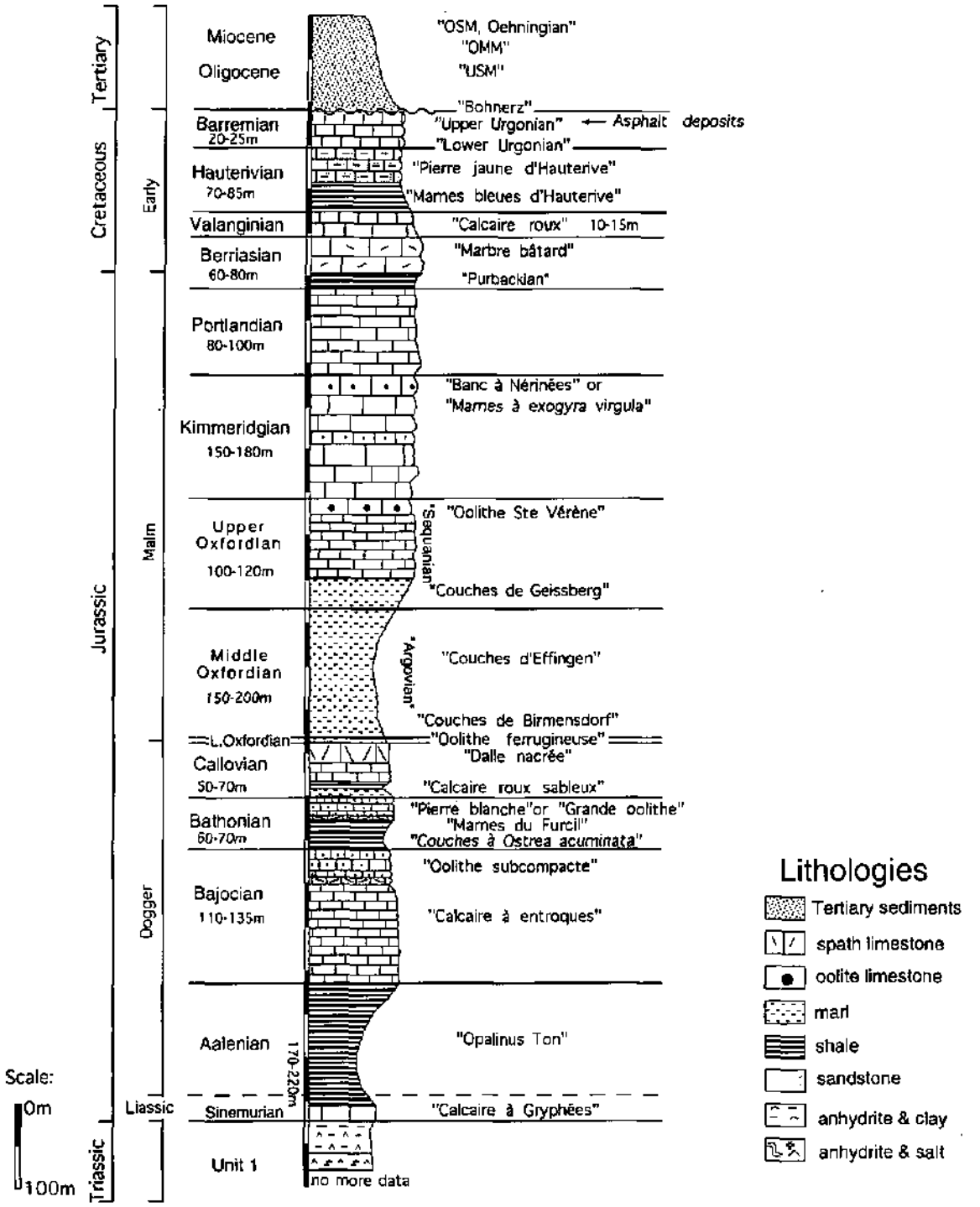

Figure 2.10: Stratigraphic profile of the Neuchâtel Jura (Val de Ruz and Val de Travers). The position of the formations mentioned in the text is given on the right hand side.

Profil stratigraphique du Jura neuchâtelois (Val de Ruz et Val de Travers). La position des formations décrites dans le texte est donnée sur le coté droit du log.

"Couches d'Effingen" consisting of marls with a wide range in carbonate content and the "Couches de Birmensdorf" composed of biostroms made of siliceous sponges and rich in Ammonites.

The Dogger is formed by at least 250 m of a well bedded coarse grained limestones subdivided into various formations: "Dalle nacrée, Calcaire roux sableux, Grande Oolithe, Marnes blanches, Oolithe subcompacte" and "Calcaire à entroques". The Aalenian black shales, corresponding to the "Opalinus Ton" of the eastern Jura, strongly contrast with the overlying Dogger limestones.

The Liassic and upper Triassic formations have been penetrated during a recent geotechnical drilling campaign near Neuchâtel (MEIA, 1992). These layers are strongly tectonized and do not allow measurement of precise stratigraphic thicknesses. The apparent thicknesses are: 160 m for the Aalenian and Liassic series and more than 100 m for the Triassic Unit 1. The Liassic is represented by bituminous shales and the "Calcaire à Gryphées" formation, whereas the Triassic consists of marls, evaporites, salt and dolomites. By comparison with the nearest well, Courtion (Fig. 2.13), the thickness of Unit 1 below the Neuchâtel Jura is expected to be of the order of 200 m of anhydrite and shales, underlain by some 60 m of dolomites. The thickness of the Triassic Unit 2 evaporites is not constrained by nearby drill holes; based on depth conversion from seismic lines, it ranges from 400 m to 1000 m.

2.3.3. Surface and well log correlation

2.3.3.1. Introduction

The upper 400-500 m of the stratigraphic section outcrops in the central Jura Mountains and the subsurface stratigraphy is known from wells, as shown on Figures 2.11, 2.12 and 2.13. Appendix 2 is a compilation of well data from the literature or unpublished documents in which some detailed and many summary log descriptions with elevation of tops are available. The lithostratigraphy of wells has not been reinvestigated here. Log descriptions are mainly based on cuttings and the lithological descriptions or nomenclature adopted by the different authors is not always consistent. The correlation of units and stratigraphic ages is approximate. The holes were drilled by the industry in the search of oil, gas or hot water. Most of the wells were drilled on anticlines (Risoux, Laveron, Treycovagnes, Essertines, Courtion, Hermrigen, Cuarny). Because no drill hole data exist in synclinal structures, the stratigraphic thicknesses reported from wells could be exaggerated by a few 10 to 100 m, due to thrusting, tectonic thickening and or salt flowage. This is especially true for the Triassic evaporite units.

The top Triassic is used as a datum for wells shown on Figures 2.11 to 2.13. In these figures, the thickness of the Tertiary, Cretaceous, Malm, Dogger and Liassic units corresponds to that listed in Appendix 2. However, the thickness of the Triassic Unit 1 and Unit 2 of the Triassic layers has been modified based on seismic interpretations. Details are given in subchapter 2.4.3.7. and 2.4.3.8.

Figure 2.11 is a SW-NE correlation of the lithostratigraphy of the Valempoulières, Eternoz, Buez and Buix drill holes, which are located in the external Jura. Figure 2.12 presents the Risoux, Toillon, Essavilly, Laveron drill holes and the Val de Travers and Val de Ruz profiles (Neuchâtel Jura), which are all located in the Haute Chaîne and Plateau Jura. Figure 2.13 includes Humilly 2, Treycovagnes, Essertines, Courtion and Hermrigen located in the Molasse Basin.

For previous compilations and correlations of wells in the Jura Mountains and Molasse Basin compare with BÜCHI *et al.* (1965a), WINNOCK *et al.* (1967), ZIMMERMANN *et al.* (1976), RIGASSI (1977), BÜCHI & ETHZ (1981), PERSOZ (1982), JORDAN (1992), LOUP (1992a).

2.3.3.2. Tertiary

Tertiary sediments have been encountered only in drill holes located in the Molasse Basin (Fig. 2.13). Tertiary stratigraphic subdivisions have not been distinguished, because the low resolution for this interval on seismic lines did not allow correlation of different horizons. The present-day thickness of the Tertiary strata in the project area ranges from 0 in the Jura Mountains anticlines to 2500 m in the Subalpine Molasse (South of Savigny). The wedge-shaped Tertiary sediments overlie and onlap a major erosional discordance (Fig. 2.8).

2.3.3.3. Cretaceous

The present distribution of Cretaceous outcrops (Fig. 2.14) outlines the structure of the Jura Mountains. The outcrop pattern is the result of the combined effects of Eocene erosion, Jura folding, and post- Miocene erosion. Cretaceous strata do not exist in the external and eastern Jura (Figs. 2.8 and 2.14 and see discussion §2.2.3.3.). The thickness

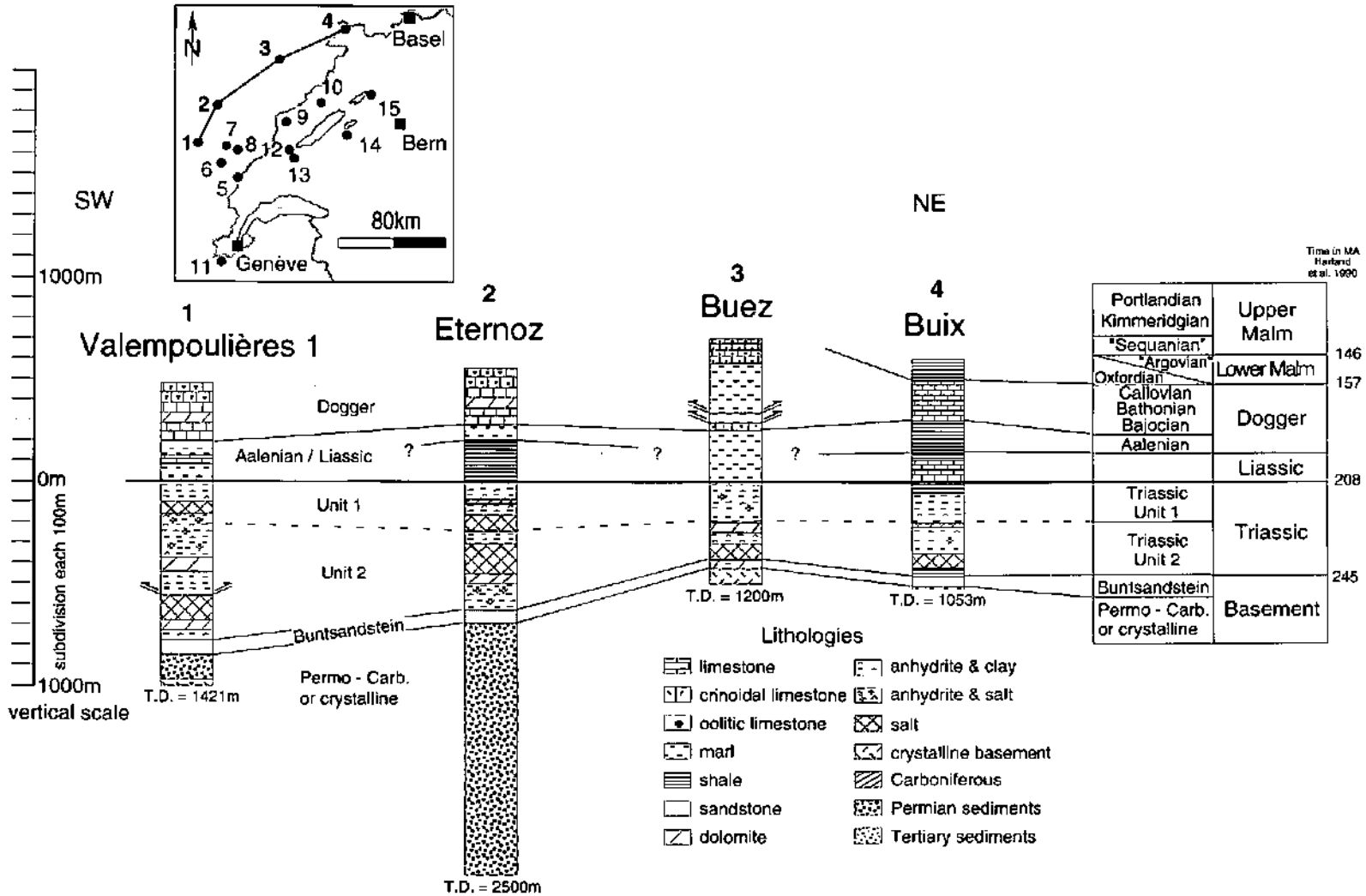

Figure 2.11: SW-NE correlation of main lithostratigraphic formations between the following wells: Valempoulières (BITTERLI, 1972), Eternoz (BRGM. 1975), Buez (BITTERLI, 1972) and Buix (SCHMIDT *et al.*, 1924). Datum plane is top of Triassic series. Plain lines represent correlation based on well data, whereas dashed lines correspond to correlation based on seismic lines. Time scale is from HARLAND *et al.* (1990).

Corrélation SW-NE des principales formations lithostratigraphiques des forages suivants: Valempoulières (BITTERLI, 1972), Eternoz (BRGM. 1975), Buez (BITTERLI, 1972) et Buix (SCHMIDT et al., 1924). Le niveau de référence correspond au toit des séries du Trias. Les lignes en trait plein correspondent aux corrélations basées sur les données de forages: les lignes en tireté correspondent aux corrélations basées sur les interprétations sismiques. L'échelle de temps est de HARLAND et al. (1990).

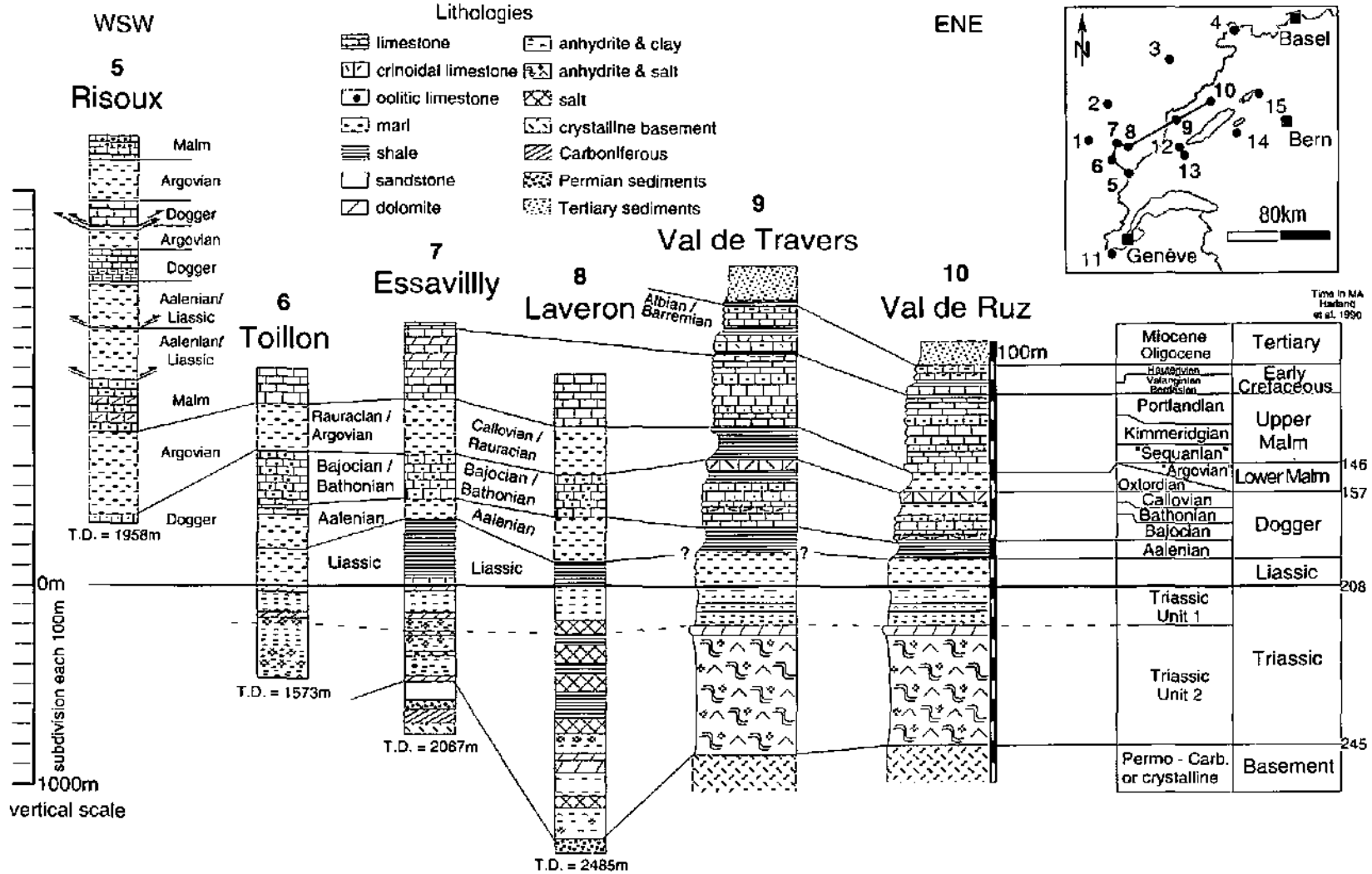

Figure 2.12: WSW-ENE correlation of main lithostratigraphic formations between the Val de Ruz and Val de Travers areas using the following wells: Risoux (WINNOCK, 1961), Toillon (BRGM, 1965a), Essavilly (BRGM, 1965a) and Laveron (BRGM, 1964). Datum plane is top of Triassic series. Plain lines represent correlation based on well data, whereas dashed lines correspond to correlation based on seismic lines.

Corrélation WSW-ENE des principales formations lithostratigraphiques entre la région du Val de Ruz et du Val de Travaers et les forages suivants: Risoux (WINNOCK, 1961). Toillon (BRGM, 1965a). Essavilly (BRGM, 1965a) et Laveron (BRGM, 1964). Le niveau de référence correspond au toit des séries du Trias. Les lignes en trait plein correspondent aux corrélations basées sur les données de forages; les lignes en tireté correspondent aux corrélations basées sur les interprétations sismiques.

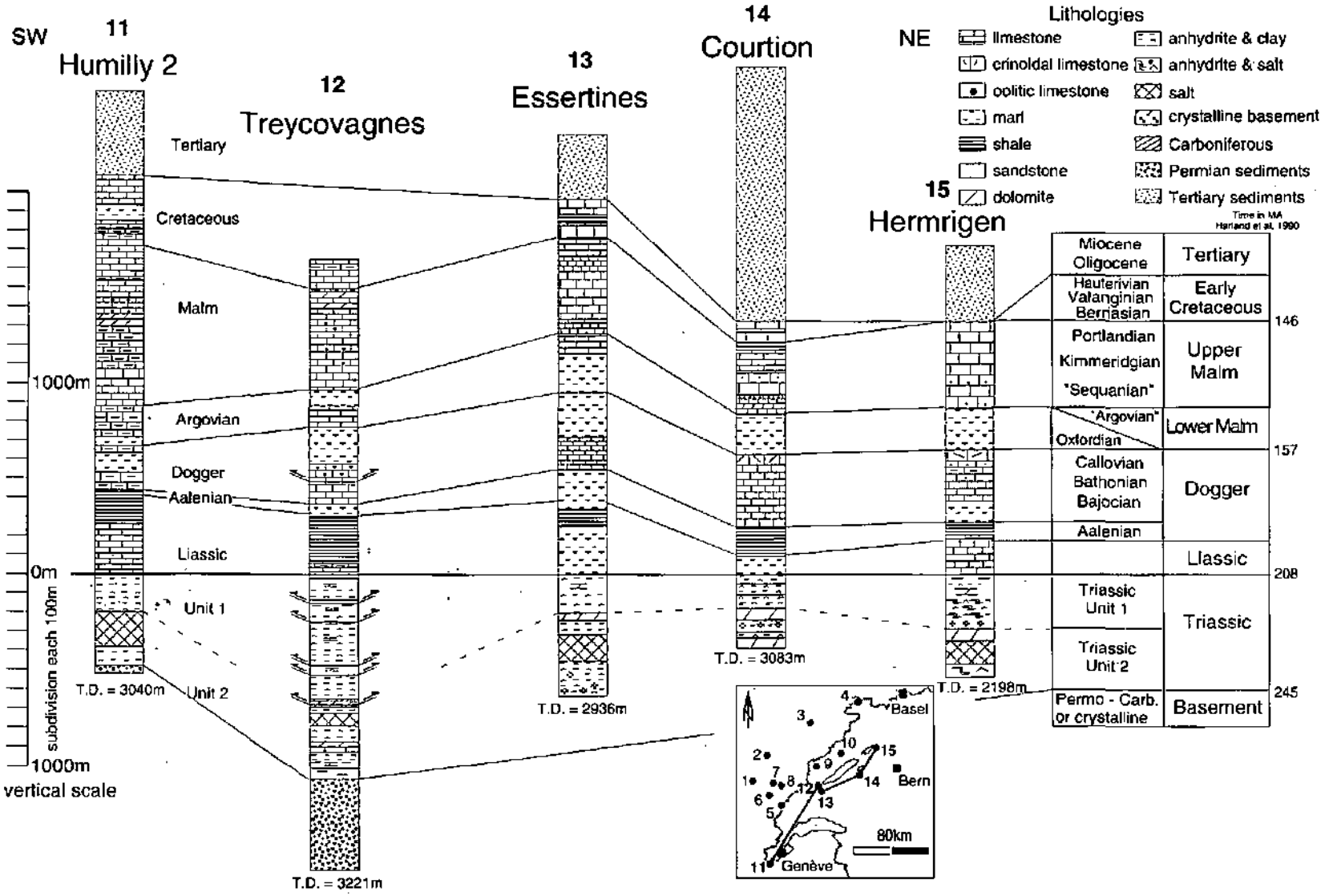

Figure 2.13: SW-NE correlation of main lithostratigraphic formations between the following wells: Humilly 2 (PERSOZ, 1982; WILDI *et al.*, 1991; JENNY *et al.*, 1995), Treycovagnes (Report deposited in Lausanne at the Musée géologique du Canton de Vaud), Essertines (BÜCHI *et al.*, 1965b), Courtion (FISCHER & LUTERBACHER, 1963) and Hermrigen (HOUSSE, 1982). Datum plane is top of Triassic series. Plain lines represent correlation based on wells data, whereas dashed lines correspond to correlation based on seismic lines.

Corrélation SW-NE des principales formations lithostratigraphiques des forages suivants: Humilly 2 (PERSOZ, 1982; WILDI et al., 1991; JENNY et al., 1995). Treycovagnes (Rapport déposé à Lausanne au Musée géologique du Canton de Vaud), Essertines (BÜCHI et al., 1965b). Courtion (FISCHER & LUTERBACHER, 1963) and Hermrigen (HOUSSE, 1982). Le niveau de référence correspond au toit des séries du Trias. Les lignes en trait plein correspondent aux corrélations basées sur les données de forages; les lignes en tireté correspondent aux corrélations basées sur les interprétations sismiques.

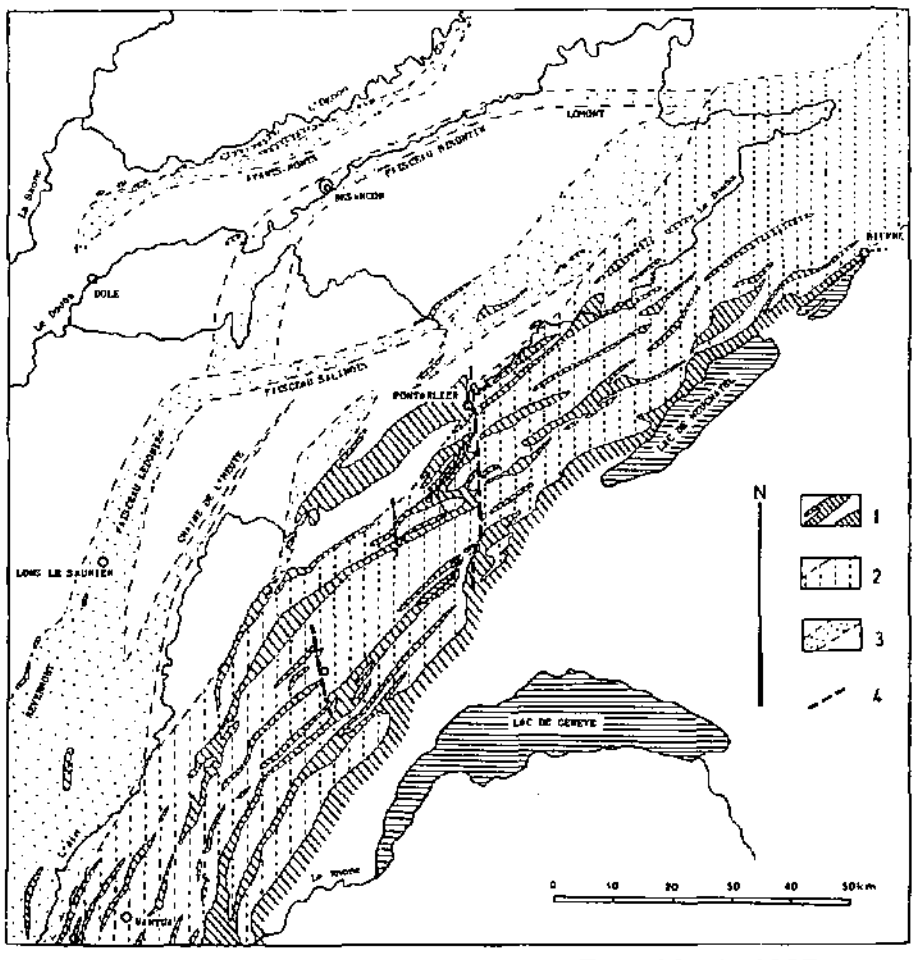

From Martin 1987

Figure 2.14: Outcrop pattern of Cretaceous erosional remnants in the central Jura. 1 = Cretaceous; 2 = Haute Chaîne Jura; 3 = Faisceau Jura; 4 = Tear faults. From MARTIN (1987).

Affleurements de Crétacé dans le Jura central. 1 = Crétacé; 2 = Haute Chaîne jurassienne; 3 = Faisceau jurassien; 4 = Décrochements. Tiré de MARTIN (1987).

increases from N to S, e.g. from the French Jura (0-70 m) to Humilly (374 m) (Fig. 2.13). It shows also the wedging out of Cretaceous strata 20 km eastwards and northwards from Neuchâtel, e.g. the Hermrigen drill hole did not encounter any Cretaceous beds.

Late Cretaceous limestones are locally preserved in karst pockets. The Albian stage is only represented in the internal zone. There is a transition from the basal limestone to the top glauconitic sandstone. Albian sediments include quartzitic and shaly sands sometimes interbedded with conglomerates and biodetrital limestones. The Barremian series begins with yellow bioclastic limestones overlain with white, oolitic, biohermal limestones. During the Hauterivian stage, a shallow sea covered the whole Jura platform. The lower part consists of fossiliferous marls ("Marnes bleues d'Hauterive"), whereas the upper part is characterized by the "Pierre jaune de Neuchâtel" with its cross-bedded spathic limestone, rich in shells and glauconite. The maximum of the Early Cretaceous transgression (Valanginian stage) reached the "Faisceau salinois" area, where the "Calcaire Roux" sediments were deposited. They contain ooliths, Echinoderms and Bryozoan debris and show cross-bedded stratification. The underlying "Marbre bâtard" consists of oolitic, bioclastic and marly calcareous.

The yellow color of the Cretaceous rocks is due to post-depositional oxidation of the iron and contrasts strongly with the white Jurassic limestones.

2.3.3.4. Upper Malm

The upper Malm thins by erosional truncation in the northern Jura area e.g. in the Laveron, Toillon and Risoux wells. In the southern Jura, the thickness of the complete series is around 350-400 m, whereas in the Molasse Basin it increases from 400 m in the Northnortheast to 850 m in the Southsoutheast (Humilly).

The top of the upper Malm series consists of Portlandian limestones, representing a marginal-littoral facies. The underlying Kimmeridgian is characterized by thick beds of back-reef limestones and

dolomites. A discontinuous belt of patch reefs and oolite bars represents the boundary between sedimentation domains. The Sequanian rocks consist of biohermal Spongiae limestones.

2.3.3.5. Lower Malm

The lower Malm corresponds to Oxfordian age beds represented by the "Rauracian, Argovian and Oxfordian s.s." facies. With the overlying upper Malm strata, it is partly eroded in the external regions. The rocks are marly or calcareous in the West (Humilly, Treycovagnes, Toillon, Essavilly, Laveron) and more shaly in the East (Val de Travers, Val de Ruz, Courtion).

The upper series consists generally of biohermal limestones (Rauracian facies) of upper Oxfordian age. During the middle Oxfordian stage several facies developed. Along the Haute Chaîne, the Argovian facies sensu stricto consists of interbedded marly limestones of the "Couches de Birmensdorf", Couches d'Effingen" and "Couches de Geissberg" (Fig. 2.1, Vaud and Aargau stratigraphic columns). These rocks were deposited in a starved basin of about 100 m of water depth (GYGI & PERSOZ, 1987). In the external Jura (Franche-Comté), the Argovian rocks consist of Brachiopod rich limestones replaced within the Canton Jura (Fig. 2.1) by the Rauracian facies, consisting of massive limestones, with a well preserved fauna of corals, Echinids and Gasteropods. The lower Oxfordian is condensed everywhere and consists of iron ooliths with Cephalopods. Shales were deposited only in the northwestern Jura.

As a historical note, GRESSLY (1837-41) studied Oxfordian strata in the Solothurn Jura. Detailed observations of coral bioherm and coeval fine-grained sediments (near St-Ursanne, Canton Jura) inspired him to introduce the concept of facies.

2.3.3.6. Dogger

The Dogger (Callovian, Bathonian, Bajocian stages) is the oldest formation exposed in the central and western Jura and it consists of 250-300 m thick limestones. At the top of the Dogger, the "Dalle nacrée" formation occurs almost everywhere, except in the Essavilly well, where the Callovian has been grouped with the Oxfordian layers.

The Callovian "Dalle nacrée" formation consists of biodetrital limestones deposited in a reducing high energy environment. This condensed facies extended far beyond the Swiss Molasse Plateau and even into the Helvetic domain. It corresponds to a time of increasing water depth associated with a starved basin. Eastern Swiss Jura deposits are composed of argillaceous shales. During the Bathonian, shales and crinoidal limestones were deposited in the East, giving way to oolitic and micritic limestones to the West. The upper Bajocian consists of marly shales with few layers of crinoidal limestones and iron ooliths to the Southwest, but of light colored oolitic limestones, called the "Hauptrogenstein" to the Northeast. In Bajocian strata, several Ostrea and Bryozoa hardgrounds are observed. The lower Bajocian consists of crinoidal limestones to the West (Vaud stratigraphic section, Fig. 2.1) and sandy limestones with iron ooliths to the East (Jura and Aargau sections). These beds are underlain by alternating limestone and marl horizons.

At the base of the Dogger, argillaceous beds of Aalenian age, i.e. the "Opalinus Ton" of eastern Switzerland are observed in the internal Jura (Fig. 2.1, Jura and Aargau stratigraphic columns). In the French Jura, shallow-water limestones are interbedded with ferrugineous horizons.

2.3.3.7. Aalenian - Liassic

The Aalenian - Liassic transition is poorly defined on the drill hole logs, because the rocks from Aalenian to Liassic stages show a progressive change from shales at the top to calcareous beds at the base.

From top to bottom, the Liassic series consists of: Posidonia shales and oolitic limestones, rich in nektonic and planktonic fauna (Ammonites, reptiles and fish), bituminous shales and oyster limestones, the "Calcaire à Gryphées" formation.

2.3.3.8. Triassic Unit 1

Triassic Unit 1 represents the top of the Triassic. It consists of marls and evaporites. The correlation from one well log to the other, expressed on Figures 2.11 to 2.13 by dashed lines, is based on seismic data. A good reflector can be followed between a more or less constant interval identified as Triassic Unit 1 and an underlying layer showing major thickness variations (see §2.4.3.7. and §2.4.3.8.). The Triassic is the most ductile sequence of the sedimentary cover (JORDAN, 1992), whose intense deformation results in difficulty in defining a clear stratigraphy based on cuttings.

2.3.3.9. Triassic Unit 2

The Triassic Unit 2 thickness ranges from 300 m to 1200 m. This unit is strongly influenced by evaporites and salt tectonics. Thickening and thinning are interpreted in terms of Neogene tectonics. Thickening is localized under anticlines, which trend parallel to the Jura structures. This aspect will be discussed in greater detail in Chapter 3 and 5. Repetitions or tectonic complications within the Triassic units are particularly clear in the Valempoulières and Treycovagnes wells.

2.3.3.10. Basement

Basement is defined to include all formations that occur below the sole thrust, i.e. the units which, according to the Fernschub theory, are not involved in the late Miocene deformation of the Jura and the Molasse Basin. The basement includes the Triassic "Buntsandstein" formation, downfaulted Carboniferous and Permian sediments overlying older crystalline rocks. The basement was reached in the French Jura wells (Valempoulières, Eternoz, Bucz, Essavilly, Laveron) and in one recent Molasse well (Treycovagnes). In the latter, Permian conglomerates or sandstones were found. In Eternoz these clastics appear to be more than 1 km thick. Carboniferous coals have been encountered in Essavilly. To date, no Permo-Carboniferous graben, such as the one in Lons-Le-Saunier (DEBRAND-PASSARD *et al.*, 1984) or in northwestern Switzerland (DIEBOLD *et al.*, 1991), has been identified in the studied area. Small grabens are locally visible on the seismic lines of the Molasse Basin, however (§2.4.3.9.). Such grabens have been identified also in the Geneva area in a recent paper by SIGNER & GORIN (1995) and in Germany (BACHMANN *et al.*, 1987).

2.3.4. Conclusions

In summary, the Mesozoic stratigraphic column of the Val de Ruz area from the top of the Cretaceous to the base of Unit 2 of the Triassic appears to be about 2000 m thick, with an estimated uncertainty of about 200 m. The overall thickness increases toward the SW (Humilly, more than 2500 m).

Toward the West, the thickness of the Dogger and Malm of Neuchâtel is quite similar to that of the French Jura. However, lower Jurassic age units vary from one area to another. The lithostratigraphy of Neuchâtel is very similar to that further to the South in the Molasse Basin. For all post-Liassic formations, PERSOZ (1982) has shown a good correlation of whole rock and clay mineralogy, as well as lithofacies, between the Courtion well and the Val de Ruz. The thickness of the Malm and the Cretaceous beds increases regularly from Neuchâtel toward the SW. The Triassic Unit 1 sequence seems to increase slightly toward the W. The thickness of the Triassic Unit 2 changes considerably in response to "salt tectonics".

2.4. SEISMIC UNITS

Like surface studies that depend on the correct identification of lithological units and their contacts, seismic stratigraphic units require correct identification and definition. To interpret a seismic grid, however, it is not necessary to define and correlate each reflector. It is more appropriate to select seismic units bounded by robust continuous reflectors. Seismic units correlated here do not then represent sequences as defined by MITCHUM & VAIL (1977), i.e. a conformable succession of strata bounded above and below by unconformities. Our seismic data are not sufficiently differentiated to allow for sequence stratigraphic interpretation. As used here, a seismic unit is sandwiched between two strong reflectors (labeled from A to I). In general, these units represent an interval, characterized by a dominant lithology. The Tertiary basal foredeep unconformity is the only well visible unconformity on our seismic lines. The main reflectors used for seismic correlation are shown on Table 2.1.

Strike profiles across the study area are good to excellent and show subparallel reflectors that are most useful for the stratigraphic interpretation. The main reflectors correspond to major impedance (lithology) changes, i.e. marl/limestone or shale/limestone, as seen in the preceding sub-chapter. Dip profiles are less continuous, due to steep to vertical dips, complicated structures and rugged topography.

This sub-chapter is organized similarly to the subchapter on outcrop and subsurface stratigraphy. First a key area (Fig. 2.15) and also some well log data (Figs. 2.16 to 2.19) will be introduced and then lateral variations (Figs. 2.20 to 2.22) will be discussed. The key area is again the Neuchâtel Jura, more specifically the Val de Ruz syncline, because seismic intervals have been defined first on strike line 8 from this area (Fig. 1.4) (SOMMARUGA & BURKHARD, 1997).

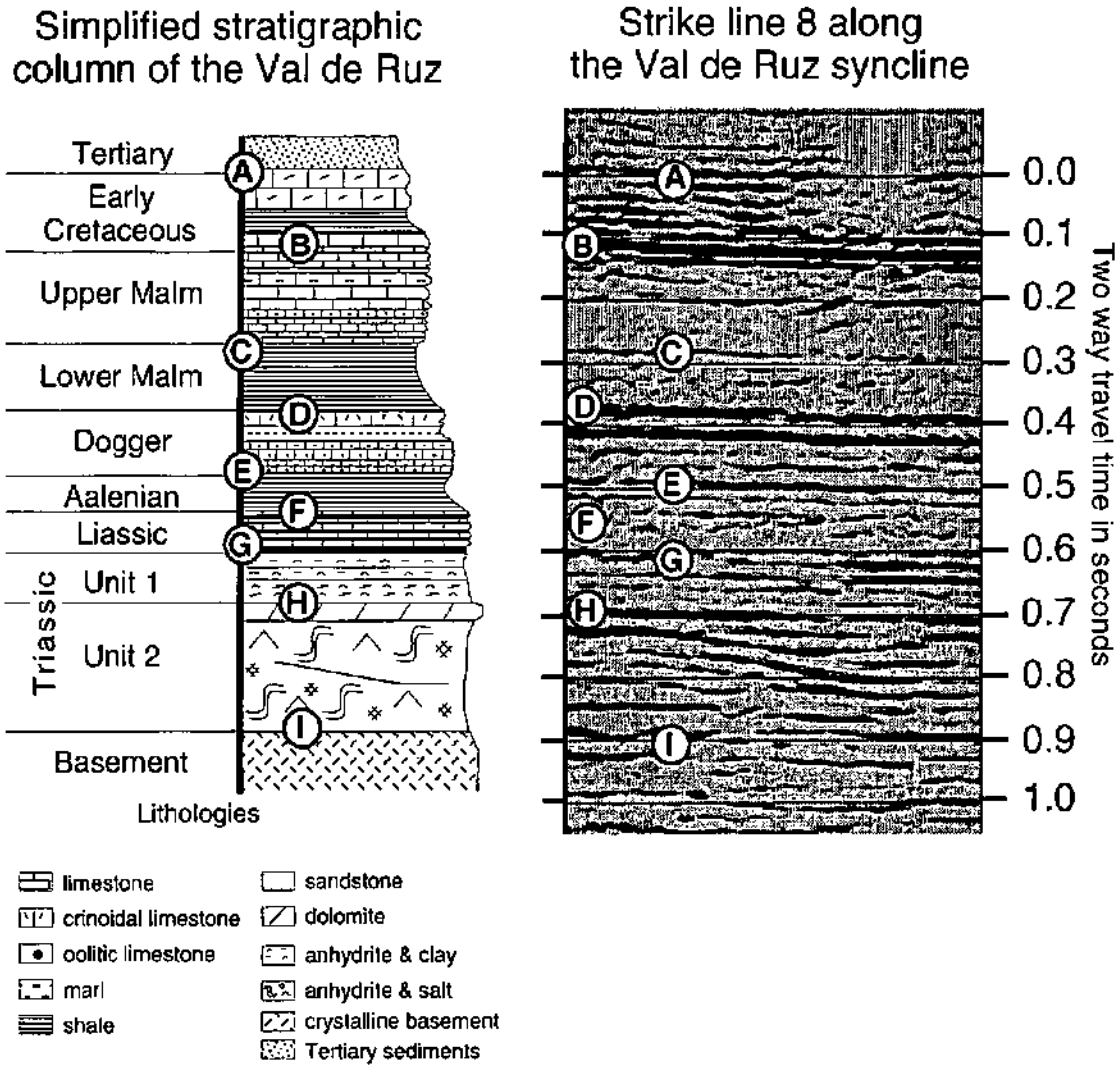

Figure 2.15: Correlation of seismic reflectors (line 8, vertical scale in seconds, TWT) with simplified stratigraphic column of the Val de Ruz. For oblique reflectors in Triassic Units, see discusions in §3.4. Legend for the letters A, B, C, ... is explained in Table 2.1.

Corrélation entre les réflecteurs sismiques (ligne 8, échelle verticale en secondes, temps double) et une colonne stratigraphique simplifiée du Val de Ruz. Concernant les réflecteurs obliques dans les unités du Trias, voir §3.4. La signification des lettres A, B, C, ...est expliquée dans le Tableau 2.1.

2.4.1. Neuchâtel (Val de Ruz) seismic line

Figure 2.15 illustrates the calibration of the seismic reflectors followed throughout the whole area. The calibration is based on stratigraphic thicknesses and lithologies known from the surface and from nearby wells. The stratigraphic column of the Val de Ruz shown in Figure 2.15 is a simplified version of that in Figure 2.10.

The Tertiary Molasse is preserved within many synclines and often buried underneath a thick fluvio-glacial Quaternary cover. The important unconformity between the top Cretaceous and the base of the Tertiary (A) is not easily recognized on the seismic section shown in Figure 2.15. The Early Cretaceous beds between reflectors A and B consist of interbedded limestones ("Pierre jaune d'Hauterive", "Marbre bâtard") and marls ("Marnes bleues d'Hauterive"). The underlying, 350 to 400 m thick, upper Malm limestones form a homogeneous, massive bed. The strong reflector B corresponds to the top of the upper Malm limestones, which are transparent on seismic profiles. The transition from pure, massive limestones to the underlying, increasingly marly sediments of the "Argovian" (lower Malm), appears as weak reflector C. The strong reflector D is one of the most prominent marker horizons in the region and corresponds to the "Dalle

Labelling of the major seismic reflectors

This work	Naef & Diebold (Nagra Bulletin 1990)
Ⓐ Top Cretaceous	Ⓐ Base Tertiary
Ⓑ Top upper Malm	
Ⓒ Top lower Malm, Argovian	Ⓒ within Malm
Ⓓ Top Dogger	Ⓓ Base Malm
Ⓔ Top Aalenian	
	Ⓖ within "Opalinus Ton"
Ⓕ Top Liassic	Ⓗ Top Liassic
Ⓖ Top Triassic Unit 1	
Ⓗ Top Triassic Unit 2	Ⓜ Top Hauptmuschelkalk
Ⓘ Top Basement	Ⓟ Top Permian
	Ⓠ Carboniferous

Table 2.1: Labeling of major seismic reflectors used in this work and correlation with the NAGRA tops (NAEF & DIEBOLD, 1990).

Numérotation par une lettre des réflecteurs sismiques importants et comparaison avec la numérotation de la CEDRA (NAEF & DIEBOLD, 1990).

nacrée" formation, the top of the Dogger series, comprising some 250 m of well layered coarse grained limestones. The Aalenian black shales corresponding to the "Opalinus Ton" (shales), contrast strongly with the overlying Dogger limestones. Thus, strong reflector E corresponds to the top Aalenian (base Dogger), in contrast to the weaker top Liassic F reflector. Between 0.6 and 0.65 s TWT, a series of layered reflectors is interpreted as Liassic limestones. The top of the Triassic Units is reflector G and corresponds to the transition from the early Liassic "Calcaire à gryphées" formation to the underlying anhydrite and shales. Below reflector G, a strong, continuous reflector H most probably corresponds to the top of Triassic Unit 2, which may be the "Hauptmuschelkalk" dolomite or the "Lettenkohle" formation. Below this formation, oblique reflectors, between 0.73 and 0.85 s TWT, constitute a most remarkable feature on several strike lines. Their interpretation will be discussed later. The top basement (I) is not as a strong continuous reflector on this profile. Reflectors below I may represent Permo-Carboniferous; however, the deeper reflectors (below 1 s) are, almost certainly, multiples.

2.4.2. Seismic lines and well log data

Figures 2.16 (Essertines) and 2.17 (Treycovagnes) present the correlation between the seismic line, the sonic log and the lithology. The availability of a scale in meters and in seconds for both wells allows direct correlation of the lithology log (in meters) and the seismic line (in seconds).

At the Essertines well location on the seismic line, good reflectors correspond to contrasts of lithology that are also highlighted by the sonic log (Fig. 2.16). Five good reflectors are observed: 1) within the Cretaceous; 2) C, top Argovian; 3) D, top Dogger; 4) F, top Liassic and 5) H, top Triassic Unit 2. The Jurassic interval is represented by a well bedded sequence, whereas both Triassic units consist of discontinuous reflectors.

The Treycovagnes well log is characterized by multiple duplication of the stratigraphy (Fig. 2.17) within the Aalenian and the Triassic. The Dogger and the Triassic Unit 1 intervals show the best reflectors, whereas the Cretaceous, the Malm and the Triassic Unit 2 intervals are transparent zones, due to uniform lithology.

The figures of the Courtion (Fig. 2.18) and Risoux (Fig. 2.19) well logs present a correlation between the sonic log and the lithology data. These logs are useful in terms of lithology and especially seismic velocities, which were used to depth convert the lines and are presented in Appendices 3.

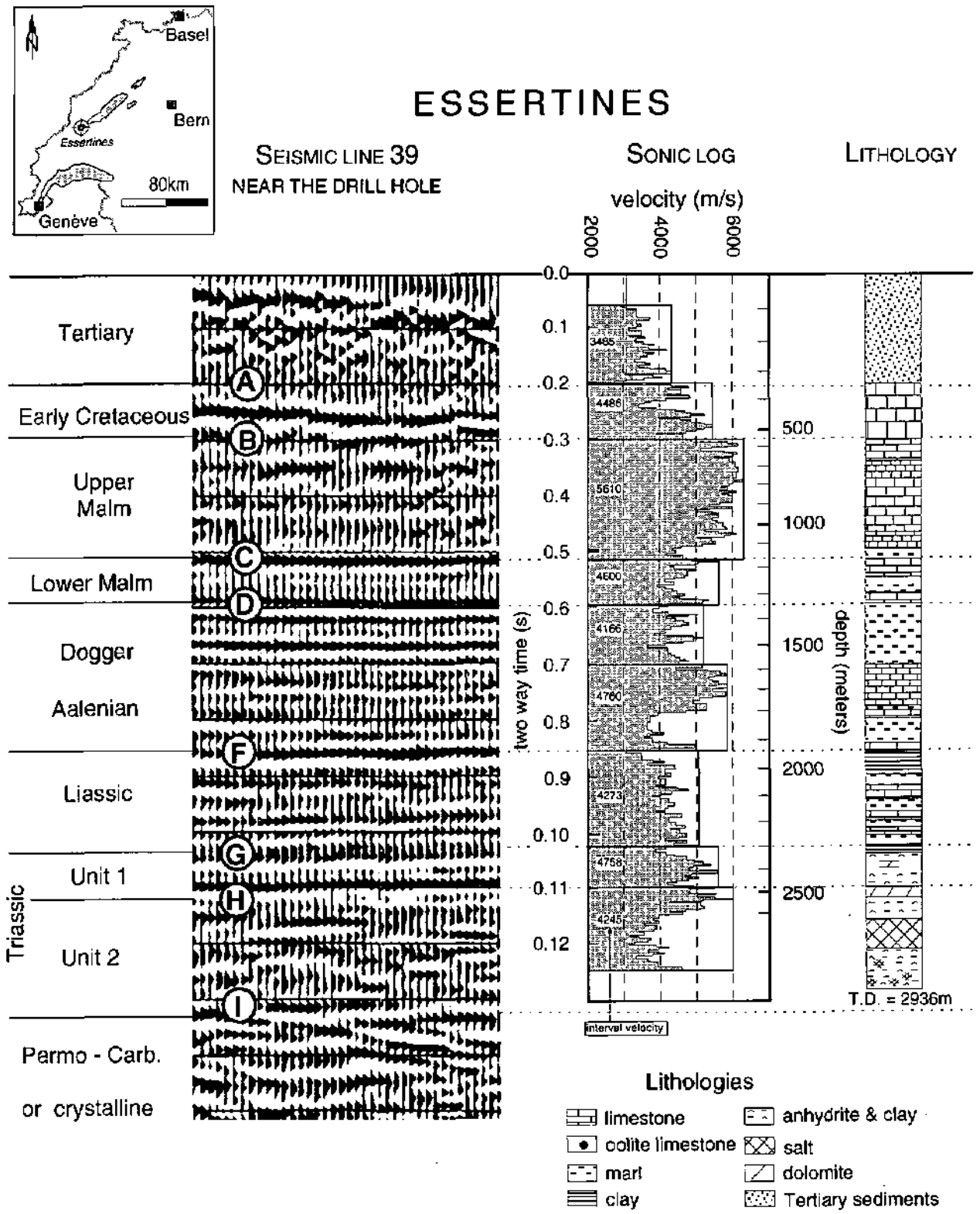

Figure 2.16: Correlation between the Essertines (BÜCHI *et al.*, 1965b) well lithology, the sonic log (GORIN *et al.*, 1993) and a nearby seismic line.

Corrélation entre le litholog du forage d'Essertines (BÜCHI et al., 1965b), le log sonique (GORIN et al., 1993) et un profil sismique voisin.

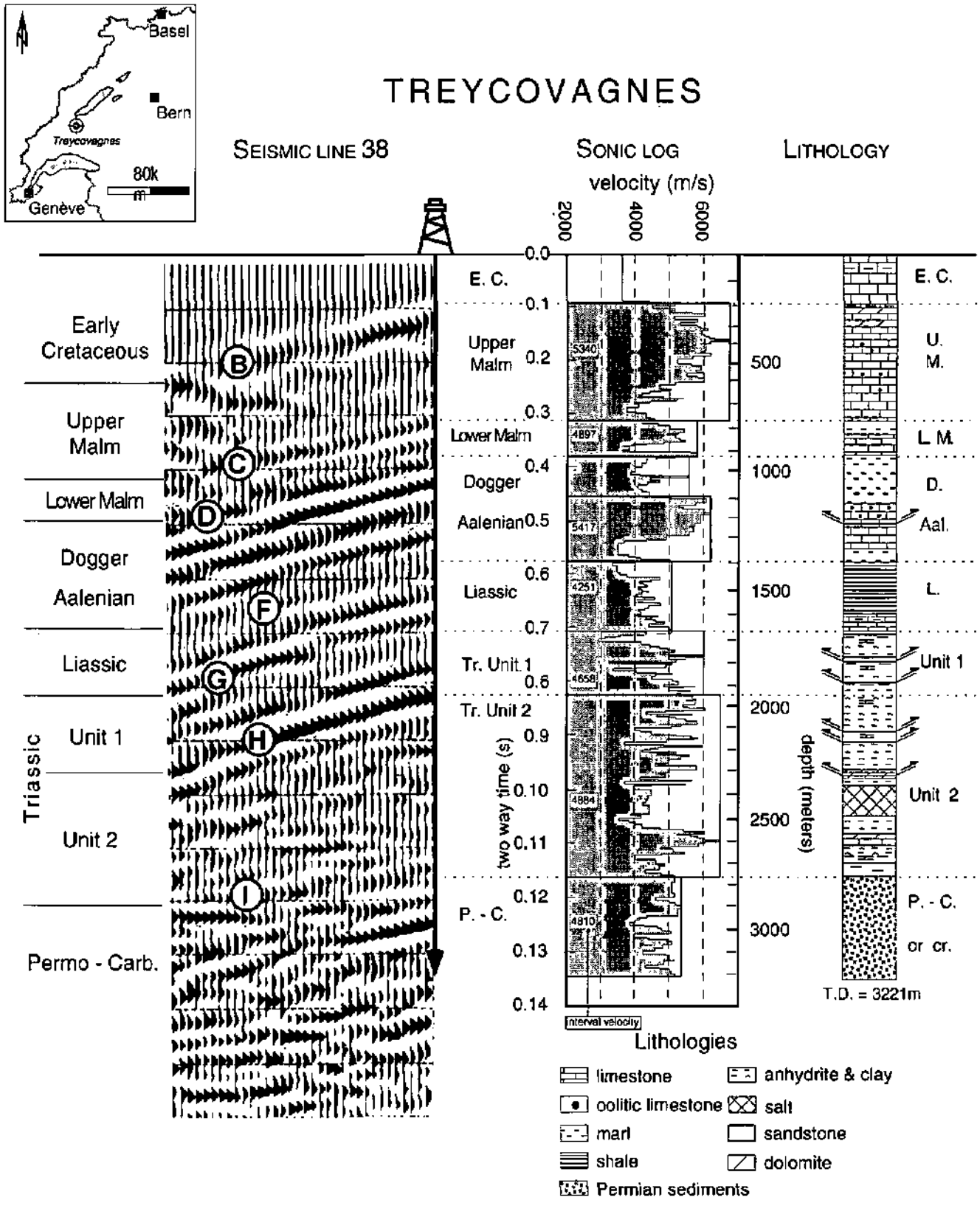

Figure 2.17: Correlation between the Treycovagnes well lithology (SCHEGG *et al.*, 1997), the sonic log (report deposited in Lausanne at the Musée géologique du Canton de Vaud) and a nearby seismic line.

Corrélation entre le litholog du forage de Treycovagnes (SCHEGG et al., 1997), le log sonique (rapport déposé à Lausanne au Musée géologique du Canton de Vaud) et un profil sismique voisin.

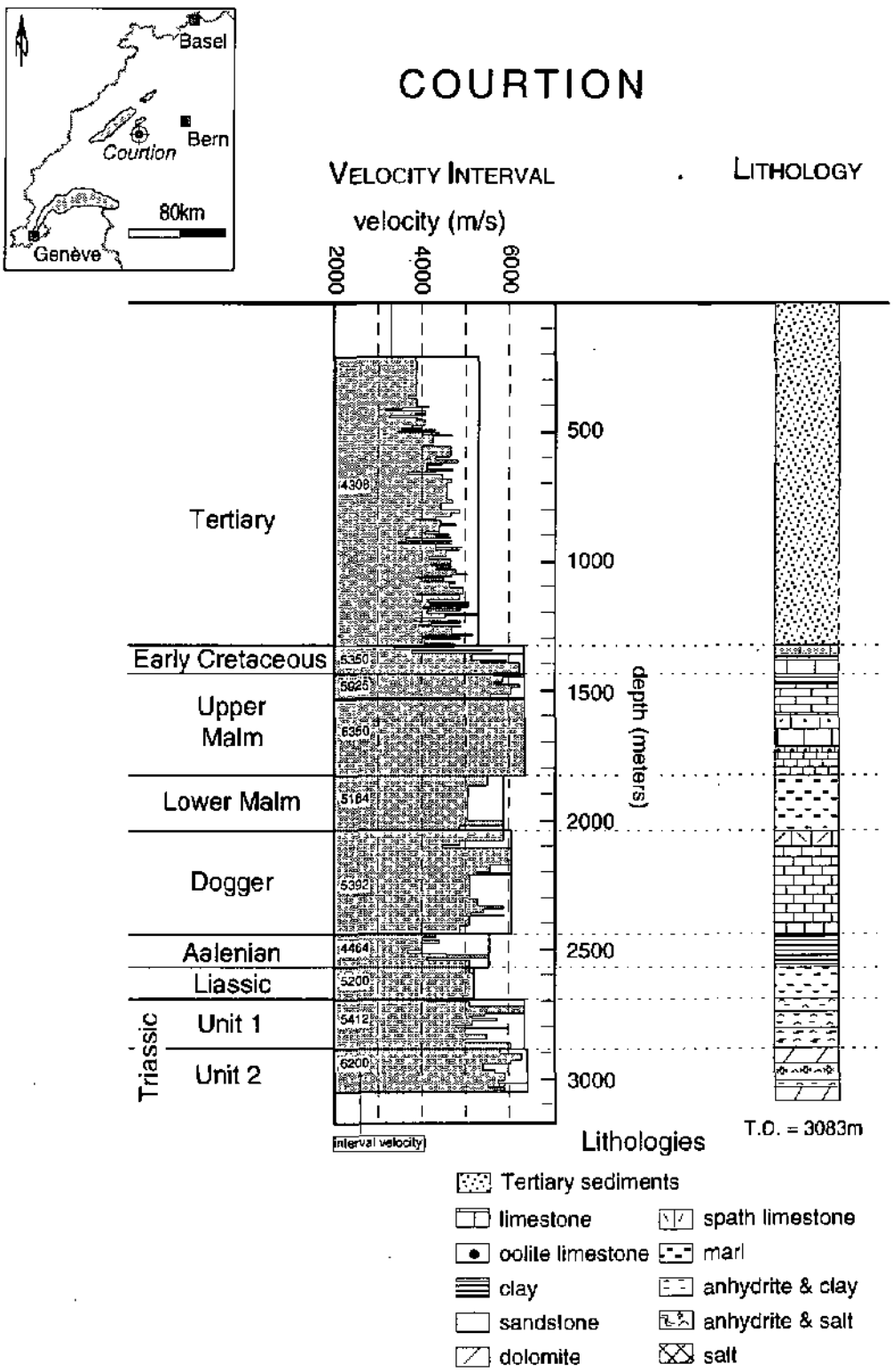

Figure 2.18: Correlation between the Courtion well lithology (FISCHER & LUTERBACHER, 1963) and the sonic log.

Corrélation entre le litholog (FISCHER & LUTERBACHER, 1963) et le log sonique du forage de Courtion.

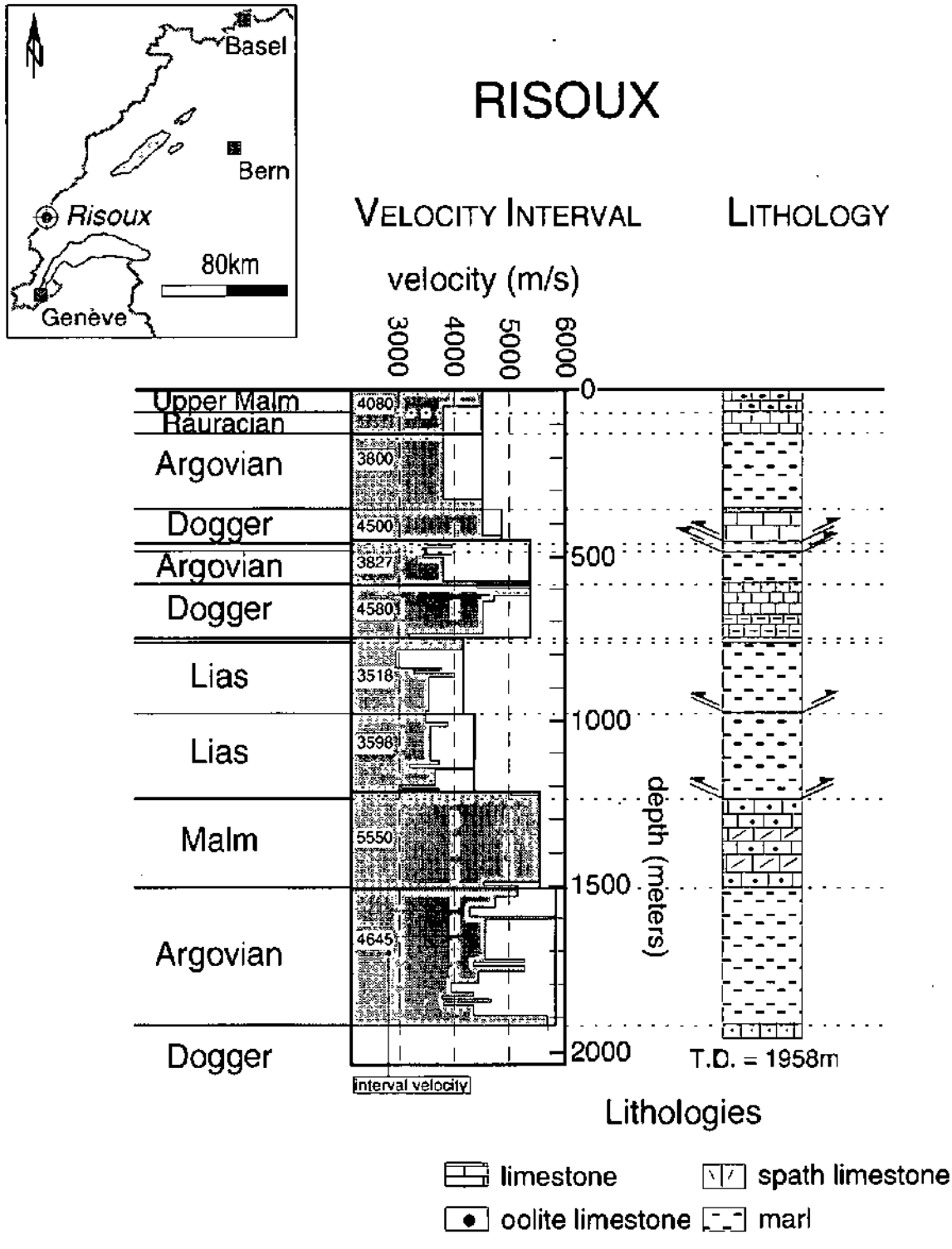

Figure 2.19: Correlation between the Risoux well lithology (WINNOCK, 1961) and the sonic log.

Corrélation entre le litholog du forage du Risoux (WINNOCK, 1961) et le log sonique.

2.4.3. Correlation ocross the seismic grid: "jump correlation"

2.4.3.1. Definition of "jump correlation"

Seismic jump correlation methods have to be used in the interpretation of the profiles, because typically good data in synclines are interrupted by poor data areas underneath anticlines. The stratigraphy of adjacent synclines could be confidently correlated by juxtaposing and matching the best reflectors between adjacent synclines. Thus the major reflectors A to I were all traced and tied to the better quality strike lines. In general thickness variations were negligible from one syncline to another, as is supported by the outcrop data. Three figures (Figs. 2.20 to 2.22) illustrate seismic jump correlations. Note seismic segments, but reflectors can still be traced easily using neighboring lines. Figure 2.20 shows the West-East correlation of seismic units through the Haute Chaîne and Plateau Jura lines. Figure 2.21 shows the Southwest-Northeast correlation of seismic units through the Plateau Molasse and Figure 2.22 presents North-South dip comparisons from the Neuchâtel folded Jura to the Subalpine Molasse.

2.4.3.2. Tertiary unit

The Tertiary unit is mainly present in the Molasse Basin and in some Jura synclines (Fig. 2.20, line 6, 4 and close to Tschugg). The onlap of Tertiary sediments to the underlying Mesozoic layers (Fig. 2.22 line 45) corresponds to the basal foredeep unconformity (BALLY, 1989), which is best visible on lines 45 and 43. The age of the onlapping sediments becomes younger from the South to the North, as explained in §2.2.4. Unfortunately no Molasse-interval subdivision could be distinguished.

2.4.3.3. Cretaceous unit: from reflector A to B

The base Tertiary or top Cretaceous layer is highlighted by reflector A (white reflector). For more convenience, the black reflector has been chosen for the correlations. This missmatch may represent an offset of 0.04 s. The Cretaceous unit is a well layered sequence of marls and limestones, especially in the Molasse Basin.

2.4.3.4. Upper Malm unit: from reflector B to C

The massive platform limestone of the upper Malm is typically devoid of reflectors. To the SW, the lower part of the unit is more reflective (Line 46), due to the appearance of well-bedded limestones. Reflector B, the top of the Malm, may correspond either to the Purbeckian brackish facies or to the Portlandian limestones. TWT isopachs increase considerably towards SW and S, as shown on Figure 2.22.

2.4.3.5. Lower Malm (Argovian): from reflector C to D

Argovian and Rauracian units have been highlighted in gray in Figures 2.20 to 2.22. This sequence is bounded by two strong reflectors, C at the top and D at the base. In the Jura, the sequence is unreflective where it corresponds to marls, but is more reflective to the Southwest, where the marly facies becomes intercalated with limestones. TWT isopachs are constant on Northeast-Southwest profiles, but thin southsouthwestward to disappear on section 45 and then 43; seismic line 45 clearly confirms this change. A stratigraphical log (TRÜMPY, 1980) of the autochtonous cover of the Aiguilles Rouges unit (the adjacent unit paleogeographically) shows well developed upper Malm layers and no lower Malm strata and is in agreement with the disappearance of the Argovian as seen on seismic lines.

2.4.3.6. Dogger-Aalenian-Liassic unit: from reflector D to G

The strong reflector D characterized by considerable lateral continuity throughout the seismic grid, corresponds to the top of the Dogger series, the "Dalle nacrée" formation. The Dogger is represented by two, three, or in places, four strong reflectors. The underlying transparent zone of the Aalenian contrasts with the Liassic reflective zone. This contrast is due to facies differences, between the Aalenian "Opalinus Ton" beds (shales) and the Liassic limestones. The top Liassic is a good reflector only within the Molasse Basin. The time interval thickness of this unit increases towards the Southwest (Fig. 2.21) and decreases toward the South (Fig. 2.22). The southern part of the Molasse Basin corresponds to an island (Alemannic high) during the Lower Jurassic, which explains the decrease in sediment thickness.

2.4.3.7. Triassic Unit 1: from reflector G to H

The strength of reflector G, marking the top of the Triassic beds, is due to the contrast between the early Liassic "Calcaire à Gryphées" formation and the Triassic evaporites or Rhaetian marls. Triassic Unit 1, highlighted in gray in Figures 2.20 to 2.22, is well layered with regular and continuous reflections and contrasts strongly with the underlying unit. The correlation of the base of this unit is based only on seismic interpretation.

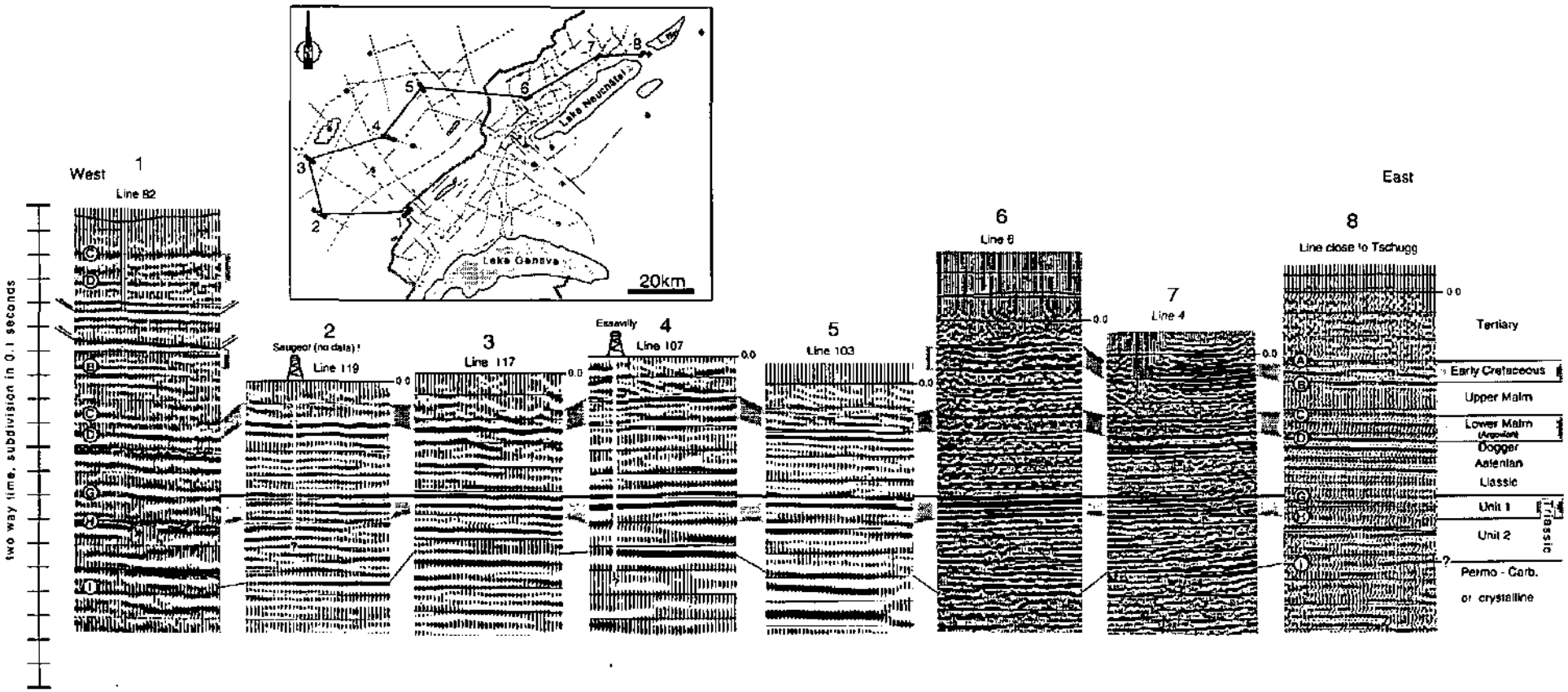

Figure 2.20: W-E correlation of seismic stratigraphic units between small portions of strike lines located in the Plateau Jura and the folded Jura. Datum plane is top of Triassic Unit 1 as in Figures 2.11 to 2.13.

Corrélation W-E des unités sismiques entre des petites portions de profils sismiques longitudinaux situés dans les Plateaux jurassiens et le Jura plissé. Le niveau de référence correspond au toit de l'Unité 1 du Trias comme dans les Figures 2.11 à 2.13.

Figure 2.21: SW-NE correlation of seismic stratigraphic units between portions of strike lines located in the Plateau Molasse. Datum plane is top of Triassic Unit 1 as in Figures. 2.11 to 2.13.

Corrélation SW-NE des unités sismiques entre des petites portions de profils sismiques longitudinaux situés dans le Bassin molassique. Le niveau de référence correspond au toit de l'Unité 1 du Trias comme dans les Figures 2.11 à 2.13.

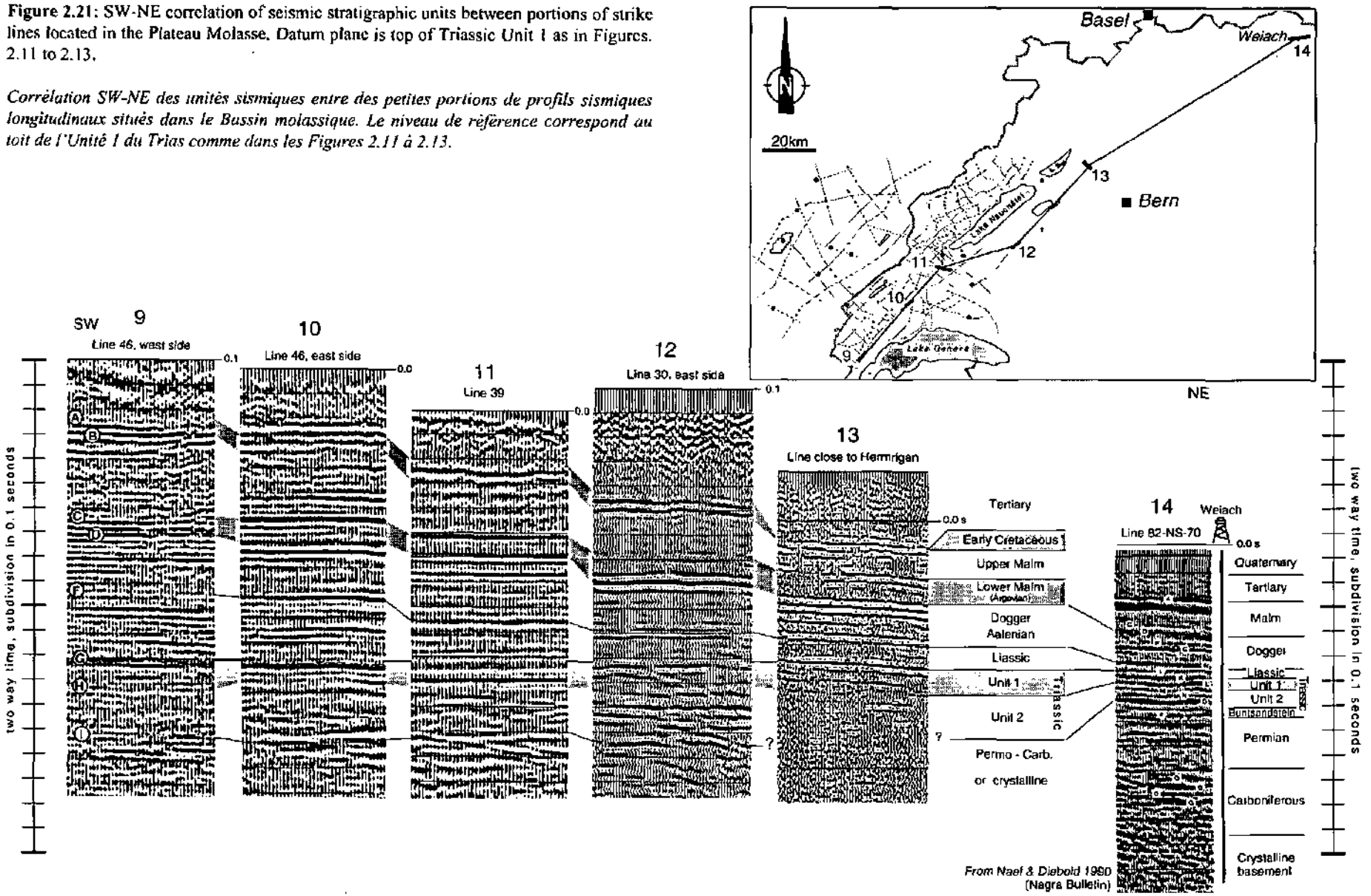

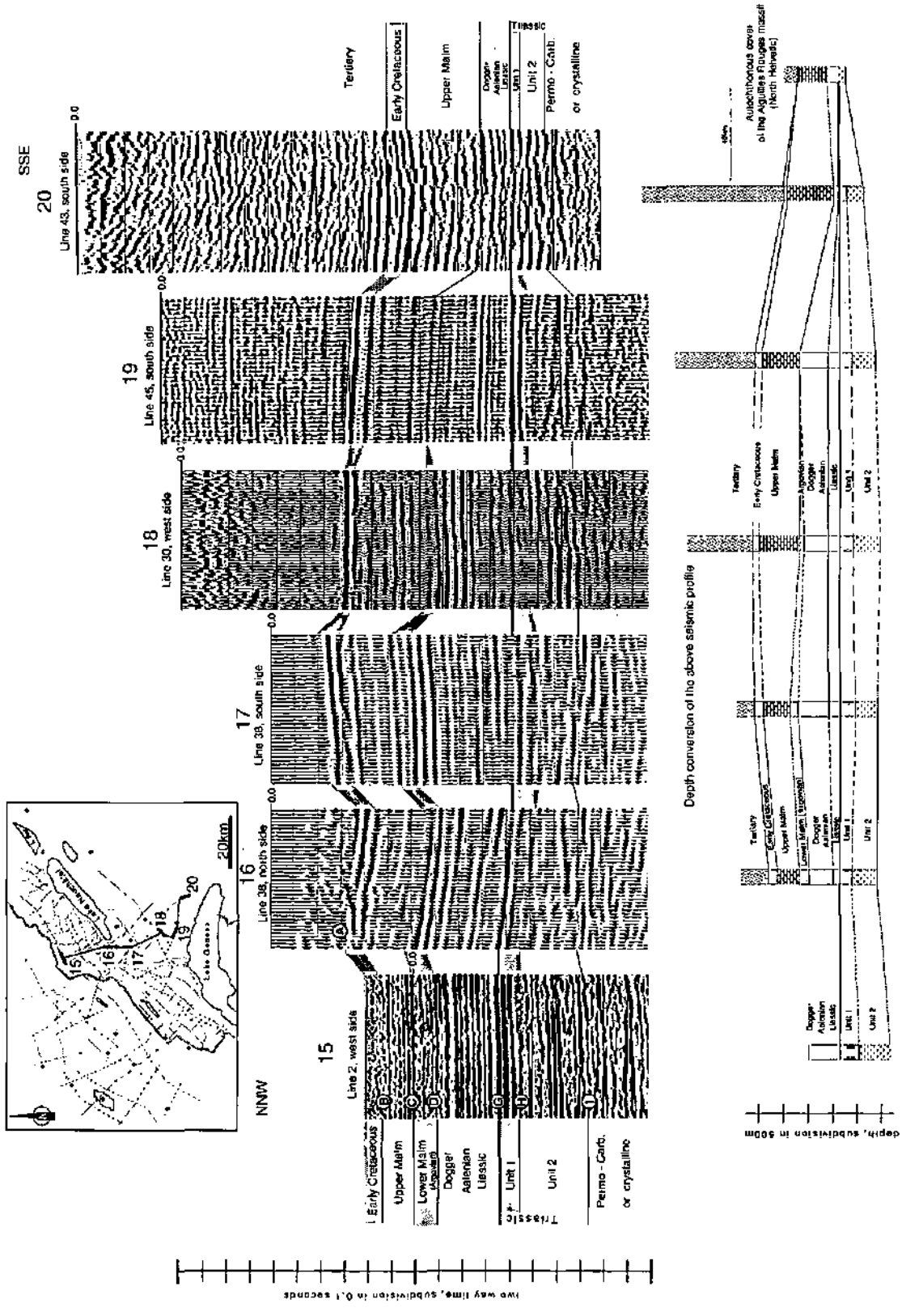

Figure 2.22: NNW-SSE correlation of seismic stratigraphic units between portions of lines located in the folded Jura and Molasse Basin. Correlation of depth converted seismic units underlie the seismic lines. Datum plane is top of Triassic Unit 1 as in Figures 2.11 to 2.13. The stratigraphic thickness of the southern part of the Molasse Basin is compared to the autochthonous cover of the Aiguilles Rouges massifs (TRÜMPY, 1980).

Corrélation NNW-SSE des unités sismiques entre des petites portions de profils sismiques situés dans le Jura plissé et le Bassin molassique. Le niveau de référence correspond au toit de l'Unité 1 du Trias comme dans les Figures 2.11 à 2.13. L'épaisseur de la partie méridional du Bassin molassique est comparée directement à celle de la couverture autochtone du massif des Aiguilles Rouges (TRÜMPY, 1980).

2.4.3.8. Triassic Unit 2: from reflector H to I

Reflector H defines the top of Triassic Unit 2. In the East, it may represent the "Hauptmuschelkalk dolomite" formation, while toward the West, it corresponds to the "Lettenkohle" beds. This sequence shows discontinuous and oblique reflectors, especially visible on lines 30, 39, 6, 119, Tschugg, 2 and 38. The origin of these reflections is not obvious and will be discussed later (Chapter 3). This unit is clearly differentiated from the Triassic Unit 1 and has led to the correlation (dashed lines on Figures 2.20 to 2.22) of the top of Triassic Unit 2.

The time interval varies strongly from one line to another, depending on the structural position: thickening is observed in anticlines and thinning in synclines.

2.4.3.9. Basement: from I reflector to downward

The top of the basement corresponds to the base of the last strong reflection, that contrasts with the unreflective crystalline basement below (NAEF & DIEBOLD, 1990). Occasionally however, reflections are present below I. These are either multiples (line 103, 117) or Permo-Carboniferous sediments (Fig. 2.23). Identifiable Permo-Carboniferous sediments are characterized by discontinuous strong reflectors, that contrast with the unreflective crystalline basement.

2.5. ISOPACH MAPS

2.5.1. Introduction

A series of isopach maps for individual Mesozoic units has been constructed for the western Molasse Basin (Figs. 2.24 to 2.29). Isopach maps are a powerful tool to depict even slight lateral thickness variations. Such changes are interesting for the analysis of subsidence mechanisms as well as for rheological considerations. The subsidence has been analyzed in detail (LOUP, 1992a, 1992b) for the western Molasse Basin and Helvetic realm. His study was based on well logs and stratigraphic profiles which were corrected for compaction, depositional water depth and eustatic sea level changes. The maps presented here cannot compete with Loup's analysis as far as time resolution and accuracy in subsidence rates are concerned, but is complementary, however. Based on a large seismic grid with continuous profiles, this analysis has the advantage of a wide spatial resolution with the potential to reveal subsidence trends, synsedimentary faults and also anomalies not penetrated by wells.

Isopach maps presented herein are based on the depth conversion of the interpreted seismic lines and calibrated by wells. Only data below the datum plane (D.P.) of 500 m a.s.l. have been included in the contour maps, which do not extend to the folded and thrusted Jura. The velocities assigned to each seismic unit are described in Appendices 3. Contouring has been performed by computer, using the Uniras/ Unimap package. The chosen bi-linear interpolation (to a uniform grid 1 km by 1 km) between individual points (with a spacing of 1 to 2 km along seismic profiles) results in a conservative extrapolation in areas with no data. Major tear faults, as known from surface mapping, have been introduced as discontinuities. Contouring is performed independently on either side of such faults. The advantage of this automatic contouring are no "observer-bias" and the capability to treat large data sets very rapidly. Disadvantages are interpolation artifacts in areas with little data coverage, e.g. close to faults or region borders, as well as crooked contour lines around isolated data points (an interpreter might have smoothed them out or else reviewed the basic data input). Blank holes appear where data density was insufficient for contouring. Actual data points are superimposed on the contours together with the tear faults.

2.5.2. Isopachs of the upper Malm unit

These isopachs represent the depth converted interval from reflector B to C (see §2.4.3.4.). The isopach map of the upper Malm layer (Fig. 2.24) confirms a progressive increase in thickness from N to S. No abrupt changes are visible on this map. The thickness of the complete unit is around 350-400 m in the southern Jura, whereas in the Molasse Basin it increases from 400 m in the Northnortheast to 850 m in the Southsoutheast (Humilly). Some contour intervals are offset by tear faults, whose sense of offset is consistent with field observation of sinistral N-S tear faults and dextral WNW-ESE tear faults.

2.5.3. Isopachs of the "Argovian" unit (lower Malm)

This isopach is the depth conversion of the "Argovian" seismic unit between reflector C and D (see §2.4.3.5.). The thickness ranges from 150 to 300 m and decreases gently from the Northwest to the Southeast and is close to zero near Savigny (southeastern edge) (Fig. 2.25). This decrease is well expressed also on the dip transect of Figure 2.22. No major changes across tear faults are noticeable.

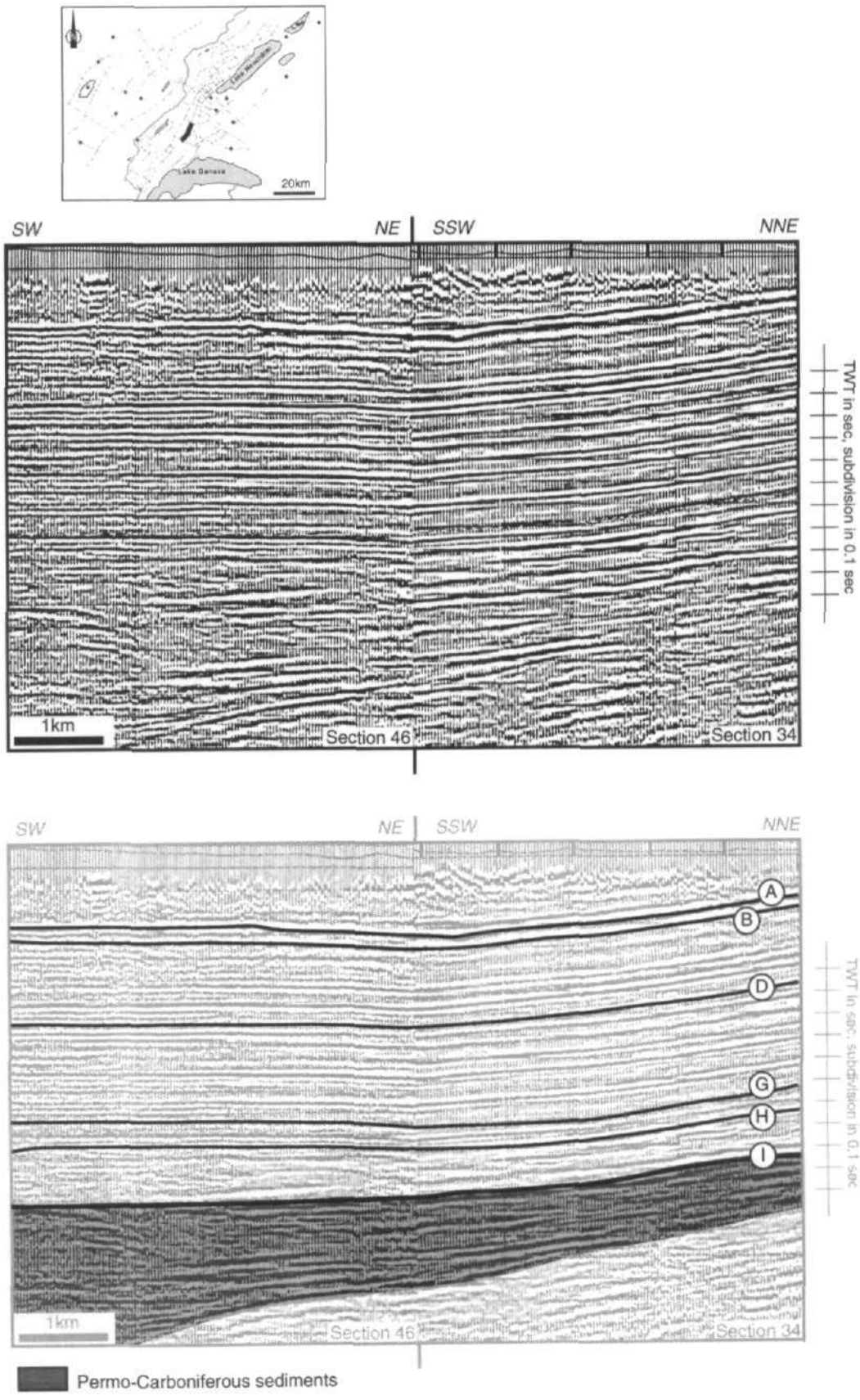

Figure 2.23: Seismic section (intersection between lines 46 and 34) showing Permo-Carboniferous sediments under the Mesozoic cover. Letters A to I label the reflectors (see Tab. 2.1).

Profil sismique (intersection entre les lignes 46 et 34) montrant des sédiments Permo-Carbonifères sous la couverture mésozoïque. Les lettres de A à I soulignent des réflecteurs importants (voir Tab. 2.1).

2.5.4. Isopachs of the Dogger unit

The isopachs of the Dogger unit (including the Aalenian unit), between reflectors D and F, are shown in Figure 2.26. In the Molasse Basin, the Dogger thickness is maximum along the W-E trending zone Treycovagnes - Essertines - Courtion (600 m) and decreases towards the SW (Humilly, 200 m). The same trends can also be seen on Dogger subsidence rate maps presented by Loup (1992a). Abrupt changes are observable on the Treycovagnes-Essertines transects (see also Figure 4.18). These changes may be explained by a facies change either related or not to a synsedimentary normal fault. The Treycovagnes-Yverdon area will be discussed and illustrated in Chapter 4 (Regional geology of the Yverdon area, Fig. 4.18).

2.5.5. Isopachs of the Liassic unit

These isopachs represent the depth converted interval from reflectors F to G. The thickness increases from 200 m (Neuchâtel Jura) to 500 m (Essertines, Humilly) (Fig. 2.27). Changes observable on the Treycovagnes-Essertines or Essavilly-Laveron transects (see Appendix 2 for well data) can be explained either by tectonic thickening of these ductile beds during the Miocene deformation (e.g. in the Laveron area), or by facies changes (Yverdon area).

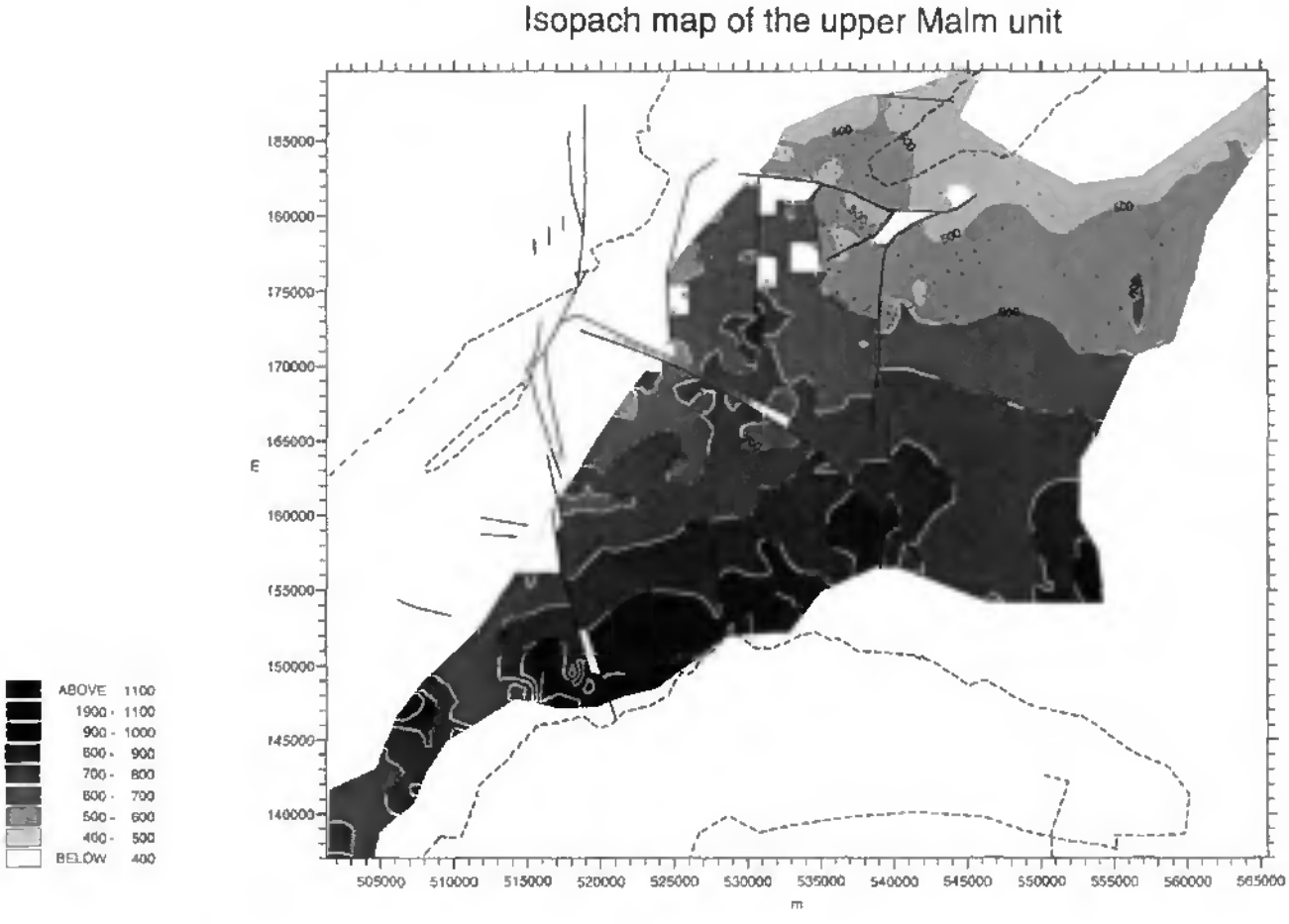

Figure 2.24: Isopach map of the upper Malm unit of the western Molasse Basin. Thickness is in meter. Black dots are shotpoints used for depth control of contour map. Note that blank areas and tight closed circles are computer-related artefacts in areas of sparse control. Numbers on the side and bottom are in meters, that relate to the national Swiss geographical coordinate system. Lakes Geneva and Neuchâtel are outlined for general reference.

Carte des isopaches (en mètres) des couches du Malm supérieur du Bassin molassique occidental. Les points noirs représentent la position géographique des points de tir, utilisés pour le contrôle des profondeurs de la carte de contours. Les zones vides et les petits cercles fermés sont des artefacts, dus au programme de contourage, dans des régions où la densité des données est faible. Les coordonnées géographiques (en mètres) se réfèrent à la grille suisse. Les lacs Léman et de Neuchâtel permettent une localisation générale de la carte.

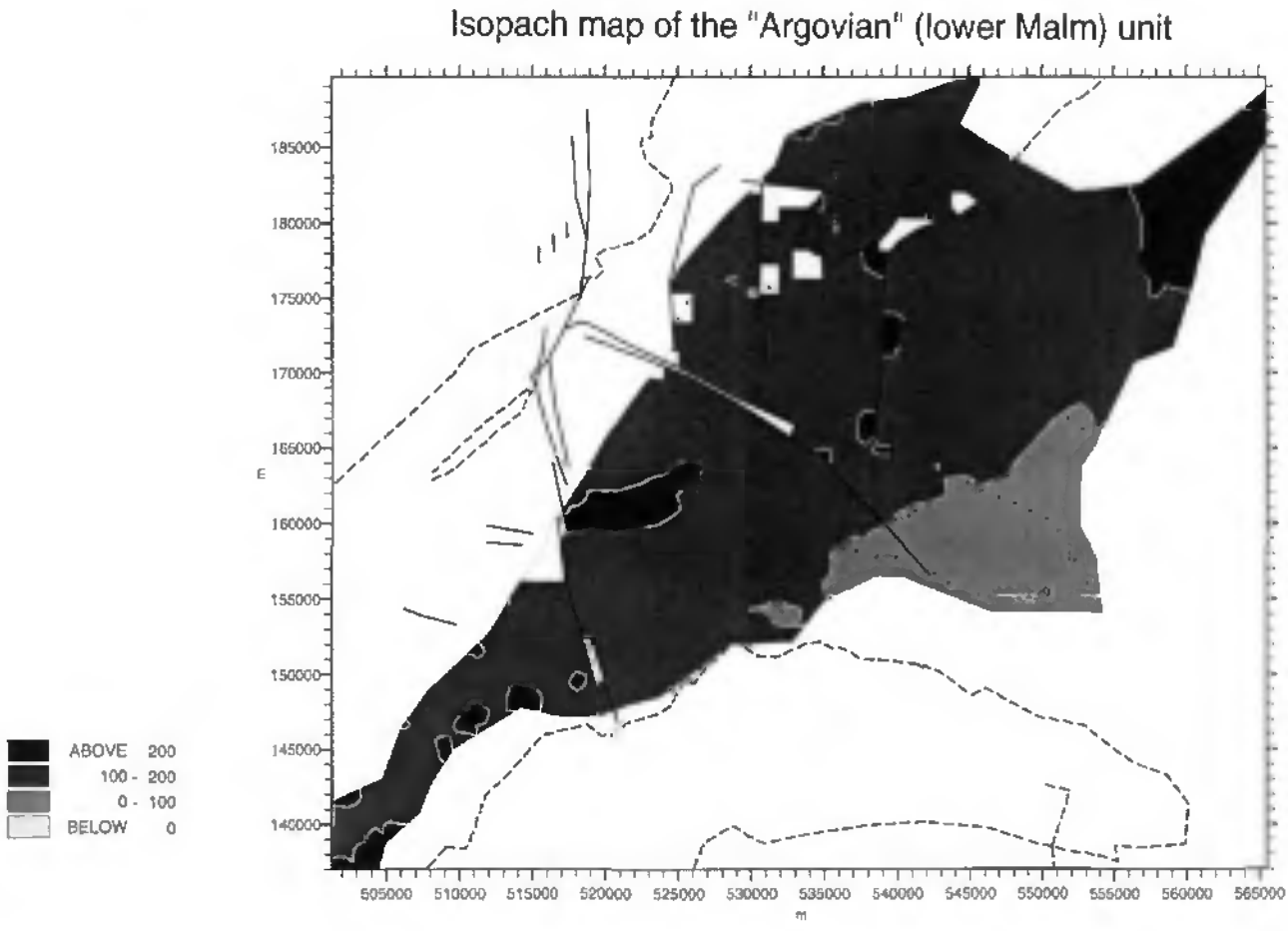

Figure 2.25: Isopach map of the "Argovian" unit (lower Malm) of the western Molasse Basin. Thickness is in meter. For explanation see legend of Figure 2.24.

Carte des isopaches (en mètres) des couches de l'"Argovien" (Malm inférieur) du Bassin molassique occidental. Pour les explications, voir la légende de la Figure 2.24.

Figure 2.26 (page 67, top): Isopach map of the Dogger-Aalenian unit of the western Molasse Basin. Thickness is in meter. For explanation see legend of Figure 2.24.

Carte des isopaches (en mètres) des couches du Dogger-Aalénien du Bassin molassique occidental. Pour les explications, voir la légende de la Figure 2.24.

Figure 2.27 (page 67, bottom): Isopach map of the Liassic unit of the western Molasse Basin. Thickness is in meter. For explanation see legend of Figure 2.24.

Carte des isopaches (en mètres) des couches du Lias du Bassin molassique occidental. Pour les explications, voir la légende de la Figure 2.24.

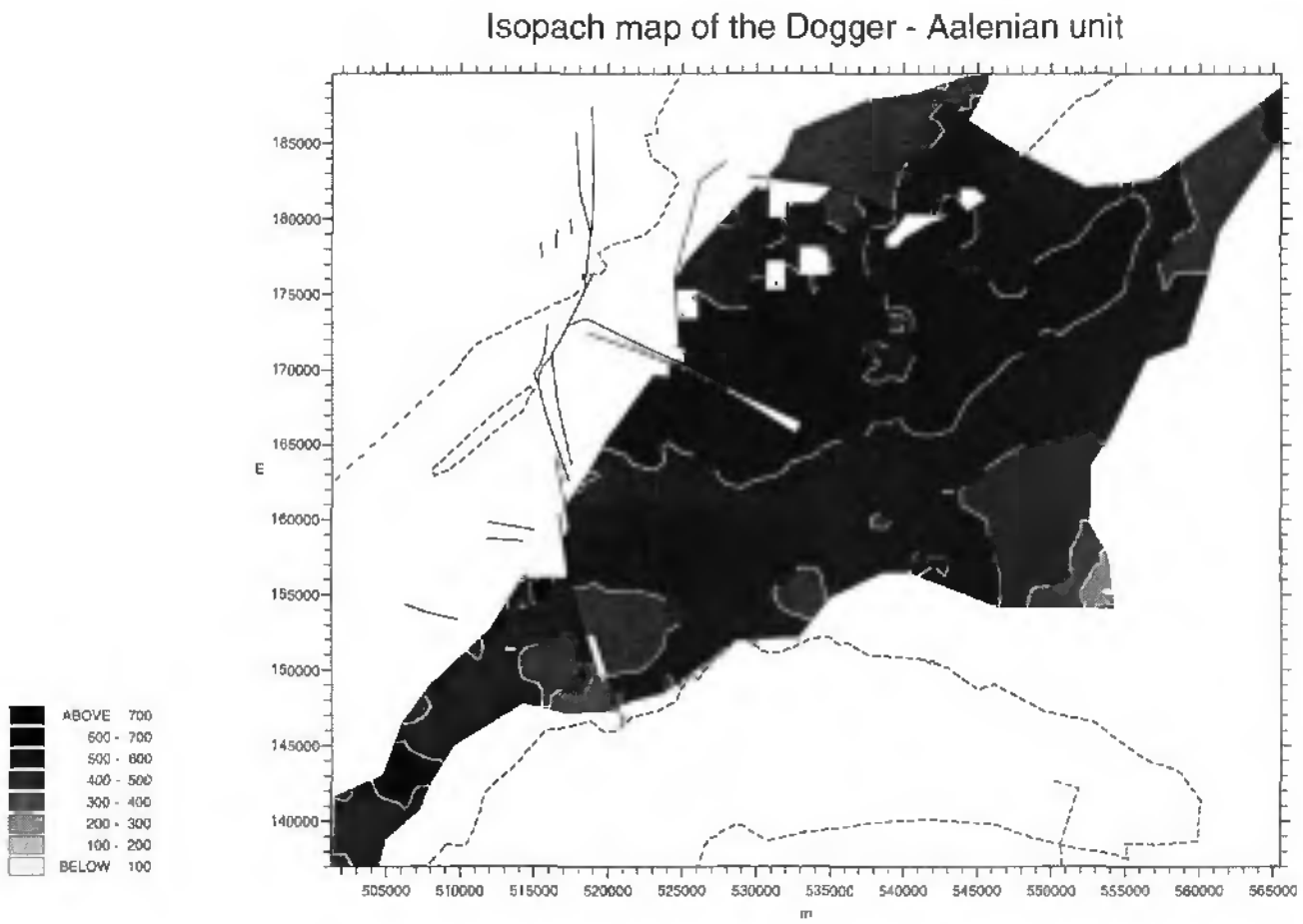

Figure 2.26

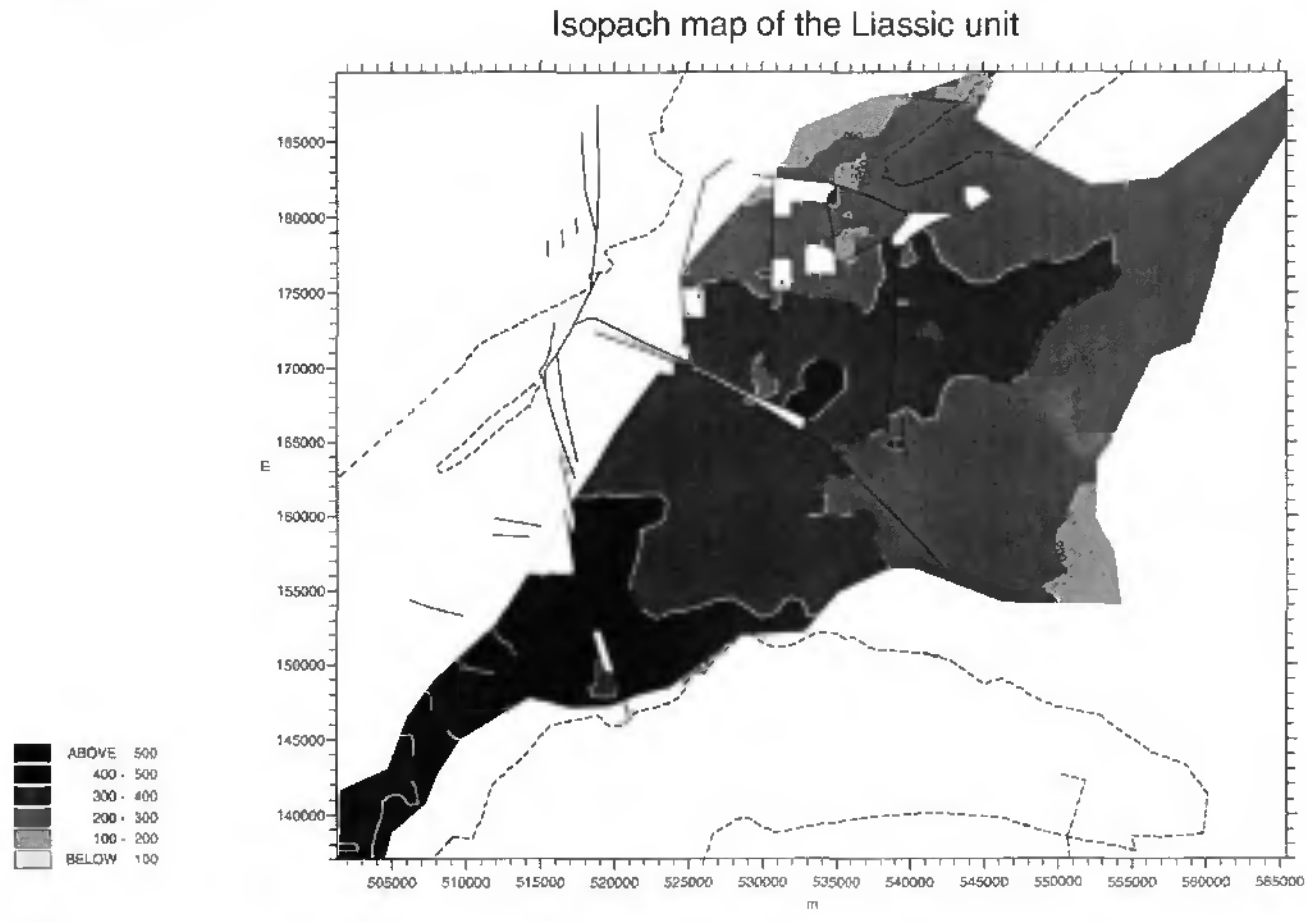

Figure 2.27

2.5.6. Isopachs of the Triassic Unit 1

These isopachs represent the depth converted interval from reflector G to H (see §2.4.3.7.). The thickness of Triassic Unit 1 ranges from 400 m to 200 m, decreasing progressively toward the ESE (Fig. 2.28). The well thicknesses do not match with this map, because of the new correlation based on our seismic interpretation (for more details see §2.4.3.7. and §2.4.3.8.).

2.5.7. Isopachs of the Triassic Unit 2

These isopachs consist of the depth converted interval from reflector H to I (see §2.4.3.8). The thickness varies considerably and ranges from 300 m to 1200 m (Fig. 2.29). In addition to a general trend of thickening towards the NW, this isopach map shows a conspicuous series of lows and highs, which alternate on the 10 km scale with a weak NE-SW trend, parallel to the Jura folds further to the North. A hand contoured version of this map is presented in Chapter 3 (Fig. 3.6). The highs are interpreted in terms of stacks of evaporites, clays and salt and will be discussed in detail in Chapter 3.

2.5.8. Summary

Thicknesses of individual stratigraphic intervals have been mapped from the interpretation of seismic lines and allow assessment of some gross regional trends in the Mesozoic subsidence pattern.

During the Triassic, more than 1000 meters of tectonically thickened sediments were accumulated in the area of the future Jura arc, whereas some 60 km further south, in the North Helvetic domain, less than 50 m of sediments were deposited in the same time span. Despite this considerable lateral variation, no evidence for synsedimentary faults has been detected. Important lateral thickness variations in the Triassic on the scale of about 10 km are related to Miocene deformation and material redistribution within this weak layer, which served as the major décollement horizon for Jura tectonics.

During Liassic and Jurassic times, lateral variations in subsidence were significant, but less important than during the Triassic. Depocenters shifted in an irregular manner over the study area, but no persistent trends were found. Some small abrupt thickness changes in the Yverdon region may be the result of synsedimentary faults, but direct evidence is obscured by Miocene tear faults.

Throughout the Mesozoic, the studied area was a slowly subsiding region intermediate between the Paris basin to the NW and the Alpine Tethys to the South. According to Loup (1992b), the subsidence was polyphase and cannot easily be described in terms of a single Mesozoic event. Modeling the subsidence curves yields stretching factors for Triassic, Liassic and Late Jurassic rifting events on the order of 1.05 to 1.20. Subsidence ceased during the upper Cretaceous.

Figure 2.28 (page 69, top): Isopach map of the Triassic Unit 1 of the western Molasse Basin. Thickness is in meter. For explanation see legend of Figure 2.24.

Carte des isopaches (en mètres) des couches de l'Unité 1 du Trias du Bassin molassique occidental. Pour les explications, voir la légende de la Figure 2.24.

Figure 2.29 (page 69, bottom): Isopach map of the Triassic Unit 2 of the western Molasse Basin. Thickness is in meter. For explanation see legend of Figure 2.24.

Carte des isopaches (en mètres) des couches de l'Unité 2 du Trias du Bassin molassique occidental. Pour les explications, voir la légende de la Figure 2.24.

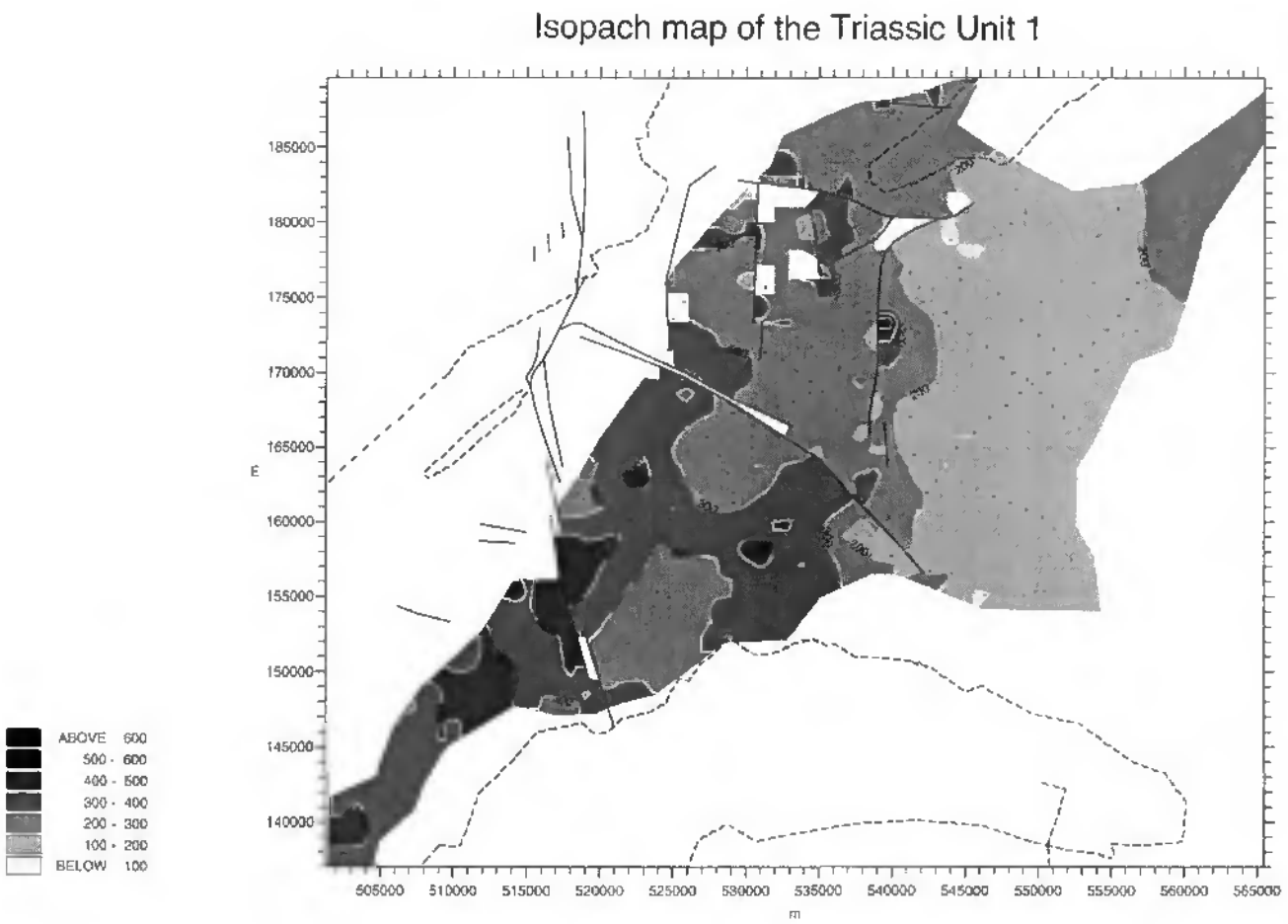

Figure 2.28

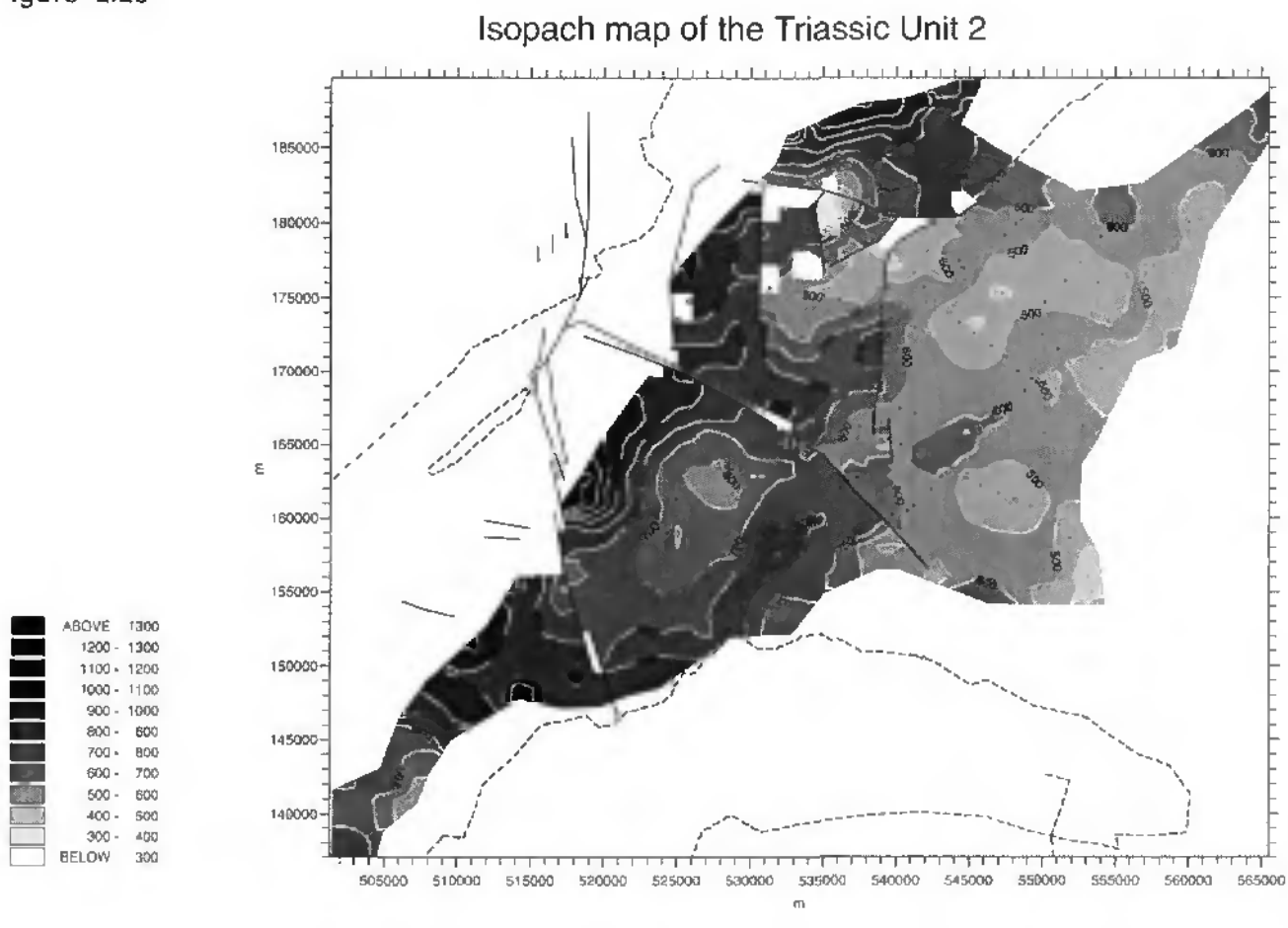

Figure 2.29

2.6. RHEOLOGICAL STRATIGRAPHY

2.6.1. General comments

The stratigraphic thickness and lateral continuity of competent and incompetent formations within the stratigraphic column plays a key role in the tectonic evolution of foreland fold and thrust belts. The rheology of individual layers is primarily dependent on the mineralogical composition of the rock, the texture and the deformation temperature. In the case of a sedimentary cover consisting of alternating competent and incompetent beds, the relative thickness of these layers also plays an important role in the style of deformation (RAMSAY, 1967). Variations in any of these parameters across a foreland area will strongly influence the tectonic and structural style.

Given a maximum total thickness of less than 1.5 km of Mesozoic and Cenozoic cover rocks in the northern Jura, increasing to 2 km in the central Jura and to more than 3 km at the southern rim of the Molasse Basin, maximum temperatures at the base of the cover series can be estimated to be between 60°C and 130°C respectively (JORDAN, 1992). Under these very low temperature conditions, the relative competence of the sediments present in the stratigraphic column increases by orders of magnitude in the following estimated order (from weakest to strongest): salt, gypsum, anhydrite, shale, marl, Molasse sandstone, limestone, dolomite (NÜESCH, 1991; TWISS & MOORES, 1992; JORDAN, 1994). Although the entire area lies in the low temperature field, a slight southward temperature increase is important insofar, because the rheology of gypsum and anhydrite are very sensitive in this temperature range (OLGAARD & DELL'ANGELO, 1991).

2.6.2. Rheological behavior of rocks from the Jura

The following rheological behavior of individual layers in the Jura can be expected and has been confirmed by detailed structural observations from outcrops and experiments:

2.6.2.1. Salt

Laboratory data (CARTER & HANSEN, 1983) indicate that pure rock salt is by far the most ductile lithology at low temperature. For reasonable geological strain rates, salt will deform plastically by dislocation - glide and - climb, as well as pressure solution mechanisms. This behavior has been confirmed by observation in samples of the Schafisheim drill cores (MATTER *et al.*, 1988; JORDAN & NÜESCH, 1989a). Experimental work (CARTER & HANSEN, 1983) on halite, with a similar grain size to the Jura halite, yields very low shear strengths, especially in the presence of pore fluids. In the Jura, pure salt thicknesses are generally thin and vary between 20 m and 300 m in the Laveron drill hole (Figs. 2.11 to 2.13; see also JORDAN, 1992).

In terms of rheology, salt behavior will be the same for a 10 m or a 100 m thick salt layer. There seems to be little or no justification for trying to establish some critical minimum thickness of salt (JENYON, 1986). The difference will reside in the shape and the size of the features resulting from thinning or thickening. Thus a very thin salt layer will probably act as a lubricant between floor and roof sequences, once thrust or décollement movement has been initiated.

2.6.2.2. Gypsum / Anhydrite

At the depth of the main Jura décollement, gypsum is expected to be transformed into anhydrite (HEARD & RUBEY, 1966). This transition is important for the rheological behavior, since anhydrite is somewhat stronger than gypsum. The transformation of gypsum to anhydrite involves dewatering, a reaction which in turn, could have weakened the associated clay rich rocks by creating higher than hydrostatic fluid pressures. Outcrops of Triassic gypsum/anhydrite series show compelling evidence for the ductile behavior of anhydrite layers during Jura deformation (Fig. 2.2b).

Deformation within the anhydrite shear zones from the eastern Jura has been studied by JORDAN (1994). Even at moderate temperatures and shallow depths, anhydrite is in an intracrystalline glide deformation regime in combination with grain boundary migration. Fluids are responsible for the early onset of grain boundary migration and therefore for the weakening of the anhydrite (fluid enhanced flow). Highly deformed anhydrite tectonites show evidence for diffusion and grain boundary gliding processes (OLGAARD & DELL'ANGELO, 1991).

Fluids seem to have been omnipresent in the Triassic evaporites during the deformation of the Jura belt. This appears to be reasonably correlated with the experimental results of HEARD & RUBEY (1966) on the dehydration of the gypsum transformed to anhydrite and water and other experiments

on clays (JORDAN & NÜESCH, 1989b). Dehydration increases fluid pressure and decreases the rock strength.

During an initial stage, strain was mainly accommodated by ductile flow of anhydrite, while at a later subsurface stage, main shear deformation changed into new-grown gypsum and finally into fault breccias. Comparable behavior has been observed in Triassic imbrications outcropping in the northeastern Jura (JORDAN *et al.*, 1990).

2.6.2.3. Shales / shaly Marls

It is commonly accepted, that shales are efficient décollement horizons. Their competence, however is strongly dependent on porosity, fluid pressure and anisotropy. Dry, compacted shales, at low temperature, may be almost as strong as limestone, whereas wet, overpressured shales can be weaker than evaporites.

Experimental results confirm the existence of a regime of low-strength pervasive cataclastic-type deformation in shales not known in other rock types (JORDAN & NÜESCH, 1989b). Such a deformation regime is explained by the ability of clay minerals to adsorb and to retain water. This interlayer water decreases the strength of clay and hence that of shales significantly.

Observations on the naturally deformed shale layers of the eastern Jura show that deformation is generally friction controlled. Shales interbedded with evaporites on the other hand show plastic deformation behavior, interpreted as controlled by sulfate lubrication (JORDAN & NÜESCH, 1989b). Therefore, in the Jura, deformation of the Opalinus shales (Aalenian layers of the eastern Jura, Fig. 2.30) is predominantly brittle, due to the lack of lubricant, whereas in the Triassic evaporites the deformation is dominantly plastic.

In the Jura, shale interlayers within the evaporites result in two types of deformation, depending on burial depth. The domains of deformation are separated by the inversion of relative competence of shale and anhydrite and the onset of gypsification (JORDAN & NÜESCH, 1989b). In deeper domains, strain is focused on slickensides, which are often coated with sulfate that acts as a lubricant. Anhydrite is ductily deformed and shale interlayers are boudinaged. In shallower domains, and especially in domains with significant exposure to water, strain becomes pervasive and very low strength ductile shale-gypsum tectonites are formed. The deformation is characterized by boudinaged brittle anhydrite layers within highly ductile shale-gypsum cataclasites. Such tectonites are restricted to areas of little overburden and to domains of significant water content.

2.6.2.4. Limestones

At low temperature, dry limestones are very strong compared to the above mentioned lithologies, because intracrystalline deformation mechanisms are not operative below temperatures of about 200 °C (RUTTER, 1974). From this, an entirely brittle behavior would be expected for a limestone succession. In the presence of water, however, pressure solution and recrystallization play an important role (GRATIER, 1984). This mechanism impairs some apparent macroscopic plasticity to the rock, although in terms of rheological behavior, limestones at low temperature must be regarded rather as brittle than ductile.

2.6.3. Rheological profiles for the central and eastern Jura

The more theoretical considerations discussed above, together with outcrop observations and data from seismic lines, allow construction of a composite rheological stratigraphic profile (Fig. 2.30). The Jurassic and Cretaceous stratigraphic columns from Vaud, Jura and Aargau are taken from TRÜMPY (1980). The Neuchâtel stratigraphic log and the Triassic log are compiled from the literature and from subsurface data respectively. In the four sections, three degrees of competence have been distinguished : 1) strong (limestone dominated); 2) weak (shale and marl dominated); 3) very weak (evaporite dominated).

The main incompetent formations are the Lower Cretaceous shales ("Marnes bleues d'Hauterive" in the Neuchâtel Jura), the "Purbeckian" formation at the transition of Malm to Cretaceous strata, the Lower Malm marls ("Argovian" formation in the northwestern part of the Swiss Jura), the Aalenian shales ("Opalinuston") and the evaporitic levels of the Triassic Unit 1 and Unit 2. Based on interpretation of seismic lines and on well data, Triassic Unit 2 appears as the most ductile zone or weakest zone of the whole stratigraphic column in the central Jura and the western Swiss Molasse Basin. Field observations (eastern Jura) and core sample observations

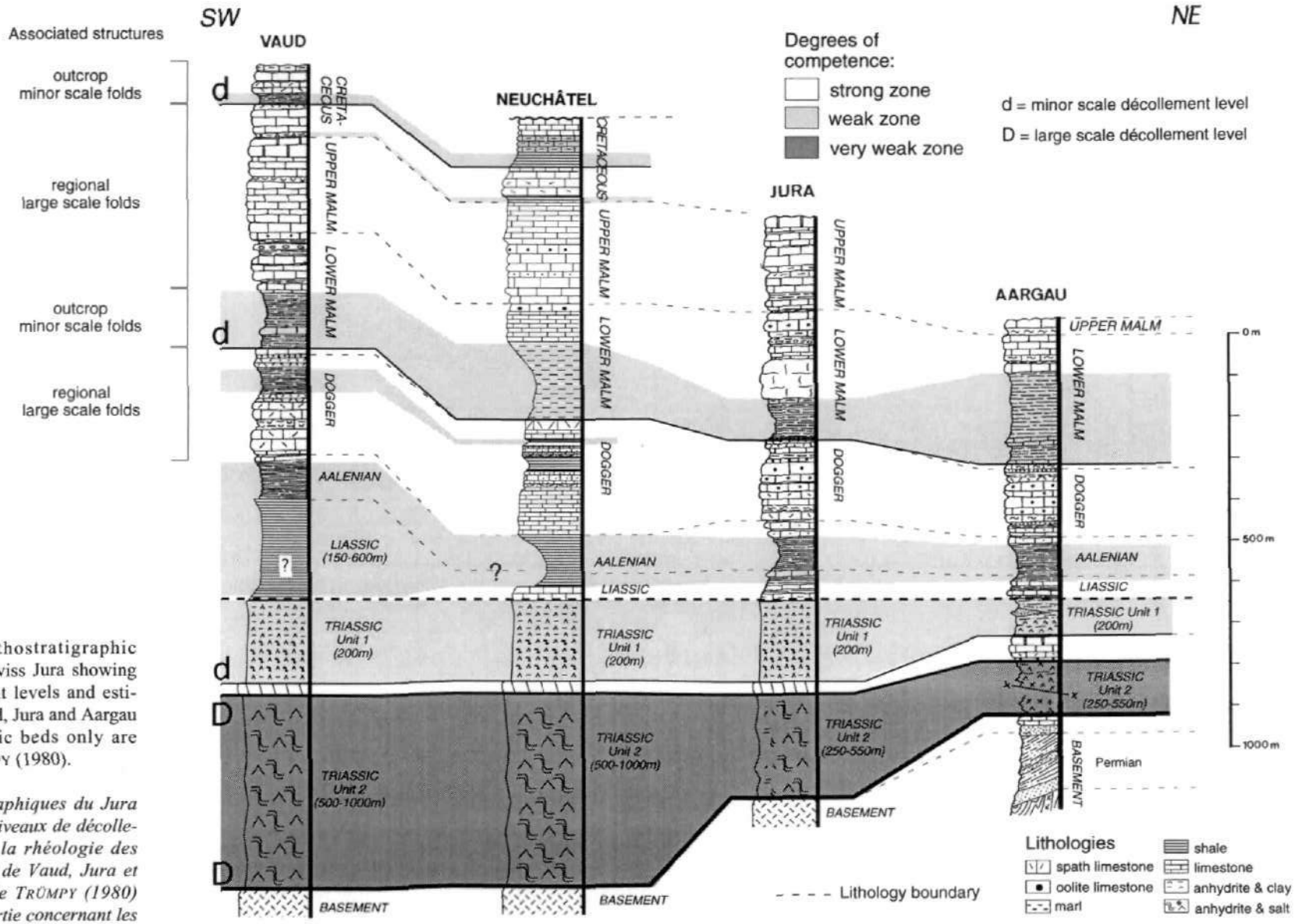

Figure 2.30: Lithostratigraphic columns from the Swiss Jura showing potential décollement levels and estimated rheology. Vaud, Jura and Aargau columns for Jurassic beds only are modified from TRÜMPY (1980).

Profils lithostratigraphiques du Jura suisse montrant les niveaux de décollements potentiels et la rhéologie des couches. Les profils de Vaud, Jura et Aargau sont tirés de TRÜMPY (1980) seulement pour la partie concernant les couches du Jurassique.

show several shear zones and ductile deformation in the Triassic evaporites (WEBER *et al.*, 1986; JORDAN & NÜESCH, 1989a; JORDAN *et al.*, 1990; HAUBER, 1993; JORDAN, 1994). The mineralogical composition of this unit consists of anhydrite, gypsum, salt, clay, calcite and dolomite. Salt has been recognized in all wells, but pure rock salt thicknesses are difficult to establish. There were variations of rheological behavior of the individual layers during compressional deformation, ranging from low strength viscous flow within pure halite and anhydrite layers, to rigid behavior or high-strength cataclastic flow in pure shales, marls and carbonates (JORDAN & NÜESCH, 1989a). The shear zones tend to be localized in pure halite and anhydrite layers.

The rigid layers are the upper Malm limestones (especially in the West) and the Dogger bioclastic limestones. The net thickness of these layers determines the wavelength of the first order folds. The ratio between competent and incompetent layers in the Mesozoic cover decreases from SW toward NE i.e. from 2:1 in the southern Jura to 1:2 in the eastern Jura, passing through 1:1 in the central Jura. The total cover thickness has a major influence on the structural relief which also decreases from SW to NE.

Major and minor potential décollement levels are indicated in Figure 2.30 with thick and thin black lines respectively. Minor décollement horizons include Triassic Unit 1 evaporites, Aalenian black shales, Argovian marls and lower Cretaceous marls. Deformation and structures resulting from minor décollement along these levels is discussed in §3.2.3.4. Among these, the most important in the Neuchâtel and Vaud Jura is the lower Cretaceous horizon. A strong decoupling level within the Cretaceous is observed in many outcrops (DROXLER, 1978; MARTIN *et al.*, 1991), where a strong disharmony in folding style is observed between the large folds of the Malm and small scale folds in the Cretaceous. The latter are too small to be resolved on seismic lines. The same may be true for the slightly disharmonic folding observed within the Argovian (PFIFFNER, 1990) (see Figure 3.17). However, only one case has been found on the examined seismic lines (Section 71, Fig. 3.2), where the Argovian acts as a significant décollement level for the overlying fold.

The major décollement zone is located in the Triassic Unit 2. This appears clearly from the interpretation of seismic lines. This zone is bound both by a roof décollement and a basal décollement and the style of deformation within this zone is very different from the underlying rigid basement and from the overlying Triassic Unit 1 and especially the Jurassic layers. HARRISON & BALLY (1988), in the salt-based Melville Island fold and thrust belt, preferred to define the whole interval as a ductile zone, (although the processes are not truly plastic at microscopic scale), instead of a décollement zone, because the term décollement refers to a single weak plane. In this work we will interchangeably use ductile zone or décollement zone, keeping in mind that this décollement is represented by a thick zone and not by one single weak plane. The envelope of the ductile zone corresponds to the décollement level. Previously SCHARDT (1908) expressed this very same idea: "... *Il serait plus juste de parler d'une zone de glissement. Il est en effet peu probable que la poussée venant des Alpes ait produit un glissement sur un plan déterminé; mais ce sont certainement les couches marneuses dans leur ensemble qui ont servi de lits mobiles en se déformant dans toute leur masse.* ...".

The presence of a weak continuous basal décollement horizon or zone is a primary condition for the development of any foreland fold and thrust belt. In the case of the Jura arc, the original paleogeographical extent of Triassic evaporite series (Fig. 2.5), with salt, gypsum and/or anhydrite and clays, seems to be responsible for the shape of the external and lateral limits of the fold thrust belt. These outer limits are interpreted mainly as due to the disappearance of a suitable basal décollement horizon, i.e. the Triassic evaporites. Note that in Bavaria (Germany), where no Triassic evaporites exist, there is no lateral equivalent to the Jura and the Alpine deformation front remains tens of kilometers further back at the southern border of the Molasse Basin (BACHMANN *et al.*, 1987; LEMCKE, 1988; BURKHARD, 1990).

3. STRUCTURES:
OVERVIEW, EXAMPLES AND INTERPRETATION

3.1. INTRODUCTION

The Jura arc on a large scale shows all characteristic features of a foreland fold and thrust belt developed above a weak basal décollement (DAVIS & ENGELDER, 1985; RODGERS, 1990; LAUBSCHER, 1992; TWISS & MOORES, 1992). These features include the arcuate outward convex shape, folds, thrusts and tear faults, that are all kinematically compatible with a tectonic transport in a general NW direction.

Seismic lines have allowed lateral correlation of the well known surface structures from the Haute Chaîne Jura to the less well known adjacent areas of the Molasse Basin hinterland and the Plateau Jura foreland (Fig. 1.2). Different types of folding styles have thus been identified: the Molasse Basin and the external Plateau Jura present broad, long wavelength, low amplitude folds cored by Triassic evaporites; by contrast, the Haute Chaîne Jura is characterized by high amplitude folds which formed above thrust faults stepping up from the basal Triassic décollement. Despite the fact that seismic lines across such folds are of mediocre quality as compared to Melville Island (HARRISON, 1995), they provide important geometric constraints which are most helpful in the construction of viable kinematics model.

The characteristics and particularities of the Jura fold thrust belt and its connection with the Molasse Basin are the result of a series of boundary conditions (see also Chapter 1); the most important are summarized below :

1) presence and thickness variations of a suitable basal décollement zone laid down in form of evaporites and shales during the Triassic (compare Fig. 2.5)

2) the rheological stratigraphy of the Mesozoic carbonate cover with alternating competent limestones and incompetent marl series (Fig. 2.30)

3) the overall wedge shape of the Mesozoic and Cenozoic cover in the Alpine foreland - a result mainly of the Oligocene collision which produced a pronounced foreland basin filled with the clastic Tertiary Molasse wedge.

In this Chapter, a brief theoretical introduction to folds will be given prior to presentation of the actual structures observed. The seismic expression of compressional structures developed in the Jura fold and thrust belt and in the Molasse Basin during the Miocene are discussed. The most prominent structures are high amplitude, thrust-related folds of the Haute Chaîne Jura as well as low amplitude, broad buckle folds developed in the Plateau Jura and the Molasse Basin. Folds and thrusts are intimately linked with the concomitant formation of tear faults. Seismic examples of these structures are compared with field observations on various scales. The lateral continuity of the structures described below will be discussed further in a regional context in the next Chapter 4.

3.2. FOLDS AND THRUSTS

3.2.1. Geometry and mechanisms: definitions

Apart from thrust faults, folds are the most prominent structures developed in the compressional tectonic regime. Folds are ubiquitous from the grain scale (e.g. kinked mica flakes) to kilometers (folded sedimentary series), to the scale of some hundred kilometers (lithosphere flexure). Reflecting this wide range, there is an overwhelming amount of literature which discusses the geometry, kinematics and mechanisms of folds and folding e.g. RAMSAY (1967), SUPPE (1985), TWISS & MOORES (1992), JOHNSON & FLETCHER (1994) and many others. Despite the apparent similarities of folds developed at various scales and in widely different materials, there seems to be no common classification between folds developed plastically, without failure (e.g. in high temperature deformed terranes) and folds developed brittly and often related to faults (e.g. low temperature terranes). Therefore, before describing the Jura and Molasse Basin folds, a summary of definitions and concepts related with folds and folding is given.

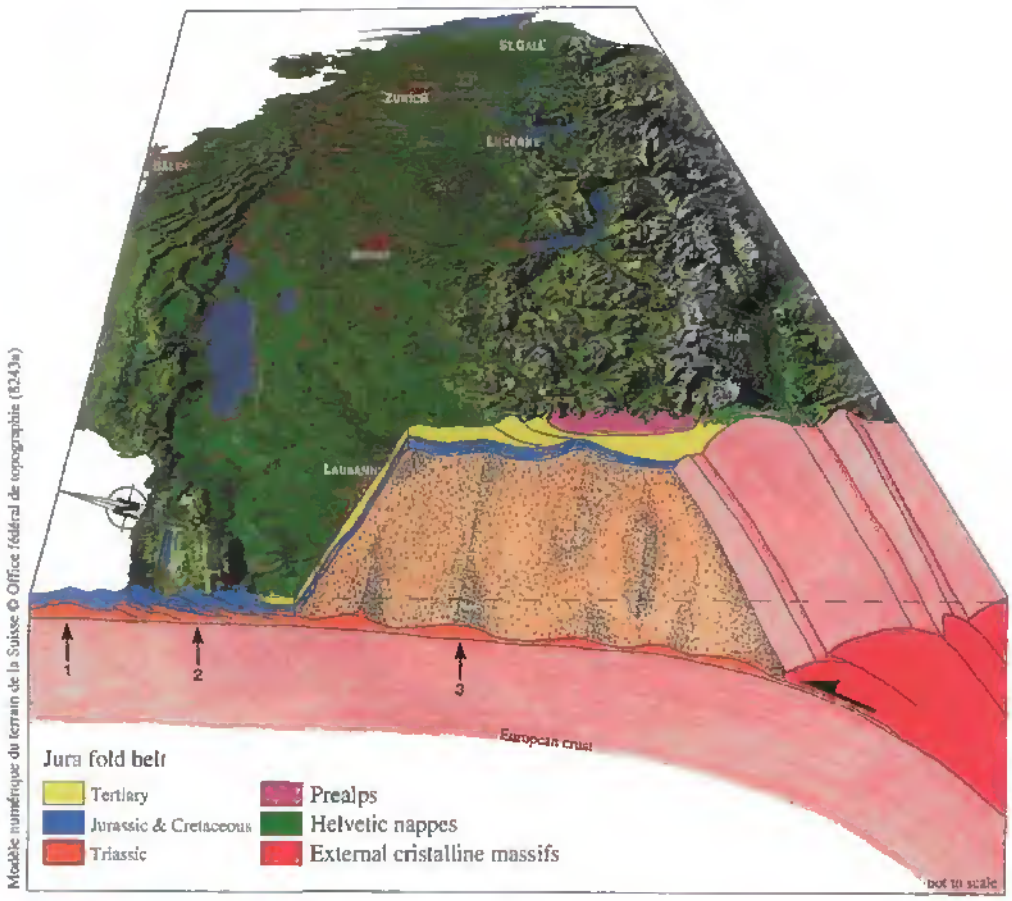

Figure 3.1: Schematic cross-section and bloc-diagram crossing the Jura fold and thrust belt from the foreland to the hinterland. The 3 styles of folds are represented: 1) evaporite-related anticline from the Plateau Jura, 2) thrust- related anticline from the Haute Chaine Jura, 3) evaporites-related pillow from the Molasse Basin. From SOMMARUGA (1995).

Bloc diagramme schématique recoupant la chaîne plissée du Jura depuis l'avant-pays aux parties internes. Trois styles de plis sont représentés: 1) dans les Plateaux jurassiens, un anticlinal associé à un empilement d'évaporites, 2) dans la Haute Chaine jurassienne, un anticlinal associé à une rampe de chevauchement, 3) dans le Bassin molassique, un coussin d'évaporites. Tiré de SOMMARUGA (1995).

3.2.1.1. Geometric classifications of folds

Different geometric classifications of folds have been proposed. The most popular fold classification scheme was introduced by RAMSAY (1967) and is based on the comparison of the two surfaces of one layer using any of the following parameters : orthogonal thickness, thickness parallel to the axial plane and the angle of dip isogons with respect to the axial plane. An alternative method by TWISS & MOORES (1992, p.229) describes the style of a fold using its aspect ratio (ratio between the amplitude of a fold and the distance measured between the adjacent inflection points), tightness (interlimb angle) and bluntness (curvature of the fold). The latter and other purely mathematical descriptions (Fourier transform series) have not gained much attention among structural geologists. Although these classifications are purely descriptive and not genetic, they are clearly designed for the description of continuous smoothly folded layers i.e. buckle folds and do not include in their description any discontinuities such as associated thrust faults.

Fault-related folds on the other hand are classified in a totally different, genetic classification scheme. Three end members of fault-related folds, which result in distinct fold-thrust (ramp) interactions, are generally agreed (JAMISON, 1987; MITRA, 1992) (Fig. 3.2):

- fault-bend folds (Fig. 3.2a): folds generated in the hangingwall rocks by movement of a thrust sheet over a ramp (RICH, 1934; SUPPE, 1983). The décollement ramps from a lower structural level over a higher stratigraphic level. The fold develops as a result of the underlying flat-ramp geometry. Fault

bend folds were described first by Rich, in the Pine Mountain thrust region of the Appalachians. He recognized that this fold style developed broad flat-topped symmetric anticlines.

- fault-propagation folds (Fig. 3.2b): asymmetric folds, with one steep or overturned frontal limb associated with a thrust fault. These are generated at the tip of contemporaneously developing thrusts, which propagate into undeformed strata (SUPPE, 1985). As long as the structure has not been faulted through (breakthrough), fault slip is consumed by folding of the overlying strata.
- detachment folds (Fig. 3.2c, d): symmetric or asymmetric folds developed above the termination of a detachment or a bedding parallel thrust fault. The folding does not require a ramp and thus the detachment folds are not associated with ramp thrusts (JAMISON, 1987; MITRA, 1992). Lift-off folds, chevron type (Fig. 3.2e) or box type folds (Fig. 3.2f) are a particular expression of fault-propagation folds and detachment folds. The beds and the detachment are isoclinally folded in the core of the anticline (MITRA & NAMSON, 1989).

The important parameters used for the geometric description of these fault-related folds are the angular relationships between the forelimb, the ramp and the backlimb dip. The emphasis in this classification scheme lies on the description of the geometry of the thrust fault and the overall shape of the fold above.

The consideration of a temporal relationship between folding and faulting is implicit in the description of these folds. Whereas the fault-bend folds develop subsequent to ramp formation, fault-propagation folds and detachment folds develop simultaneously with the ramp or the décollement propagation, respectively. Detachment folds like fault-propagation folds develop at the termination of a thrust fault.

In addition to the three basic end member fault-related fold types, a virtually endless and somewhat confusing terminology has been introduced for the geometric description of networks of thrust faults. The reader is referred to BOYER & ELLIOT (1982) and the glossary by MCCLAY (1992).

3.2.1.2. Mechanisms and kinematics of folding

Folds are the result of compression in a layered material where compression is applied in a direction subparallel to the anisotropy i.e. along the length of the layers. Two fundamentally different mechanisms lead thereby to the formation of folds :

1) Buckling
2) Fault-related folding

Buckling and buckle folds

Buckling results from the application of compressive stresses in layered materials with contrasting viscosities (rheologies), where both the strong and the weak materials are plastically deformed without failure. Above a certain threshold of compressive stress, the stiffest layers become unstable and buckle into a fold. Buckling is the dominant folding mechanism at relatively higher temperatures and confining pressures, where deformation is essentially plastic (flowing) and pervasive, although strongly partitioned into the weaker layers. Buckling is the most discussed mechanism in the literature and was first proposed by HALL (1815) and later treated in many text books e.g. BIOT (1957), RAMBERG (1964), RAMSAY (1967), JOHNSON & FLETCHER (1994).

Buckle folds (Fig. 3.2g) may be developed in a single layer or in a multilayer stack. Folding of a single layer means that the layer is embedded in viscous media. The layer has two interfaces and if the two interfaces deflect in the same direction the resulting structure is called a buckle fold. The development of buckle folds in single-or multi-layers has been studied by mathematical and analog models (JOHNSON & FLETCHER, 1994). The most important parameters which control the development of buckle folds are: the viscosity contrast of the materials, the layer thicknesses, as well as the cohesion between layers. The main results can be summarized as follows:

- competent (stiff) layers are less deformed internally than the incompetent matrix
- in stiff layers, deformation is concentrated in fold hinges
- limbs of stiff layers show little internal deformation
- hinges are formed early and remain fixed in the material
- wavelength is determined by the viscosity contrast and the thickness of the stiff layer

in a multilayer:

- strong layers influence each other

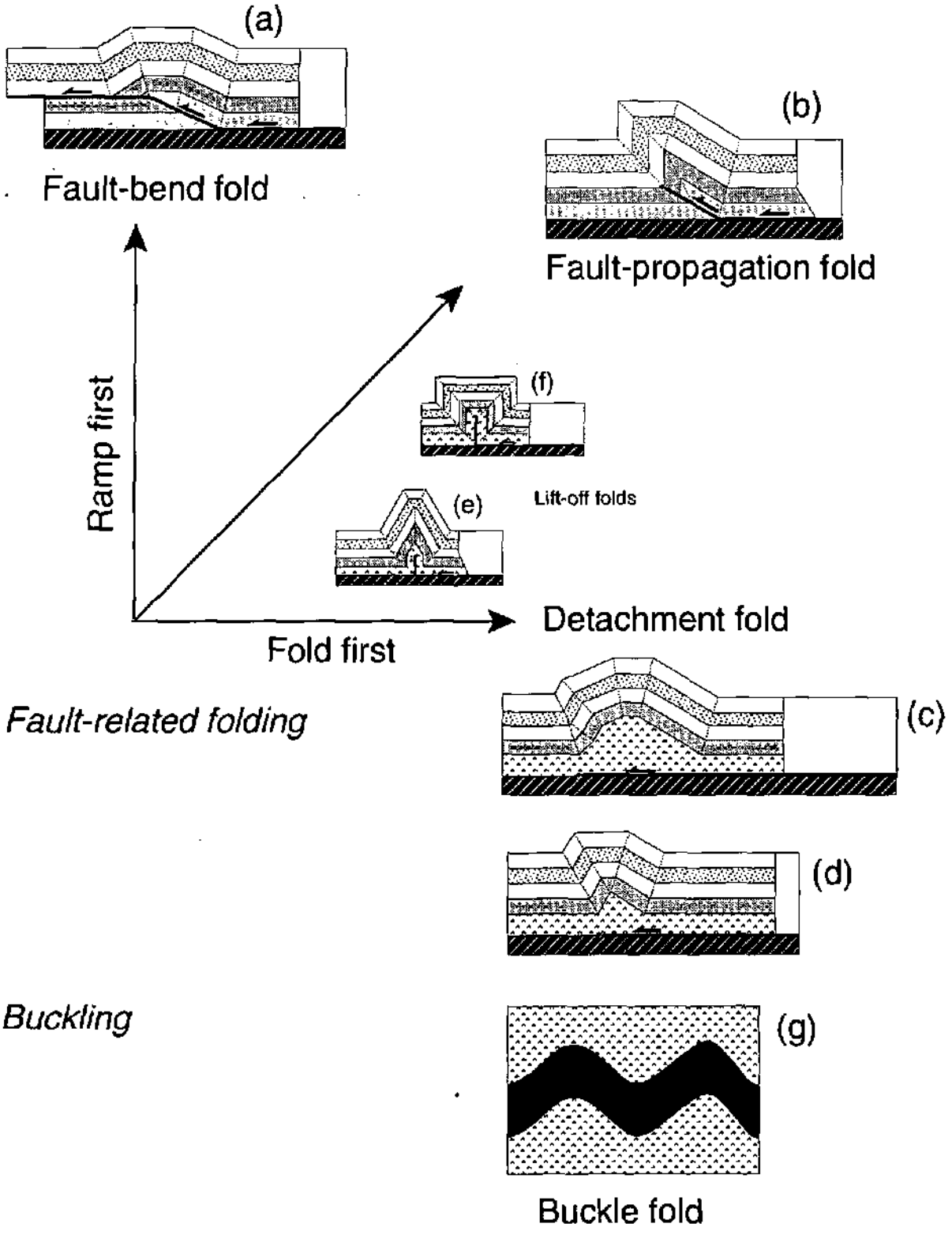

Figure 3.2: Geometry of folds (see text for discussion). Classification of fault-related folds: a) fault-bend fold (RICH, 1934; SUPPE, 1983); b) fault-propagation fold (SUPPE, 1985; SUPPE & MEDWEDEFF, 1990; MOSAR & SUPPE, 1992); c) detachment fold from MITRA (1992); d) detachment fold from JAMISON (1987); e) chevron type of lift-off fold (MITRA & NAMSON, 1989); f) box fold type of lift-off fold. Classification of buckle fold: g) buckle fold with a single layer.

Géométrie des plis (voir texte pour discussion). Classification des plis associés à une faille: a) fault- bend fold (RICH, 1934; SUPPE, 1983); b) fault-propagation fold (SUPPE, 1985; SUPPE & MEDWEDEFF, 1990; MOSAR & SUPPE, 1992); c) detachment fold de MITRA (1992); d) detachment fold de JAMISON (1987); e) type chevron du lift-off fold (MITRA & NAMSON, 1989); f) type coffré du lift-off fold. Classification des plis de flambage: g) pli de flambage à une seule couche.

- the most resistant (viscosity and thickness) layer dictates the dominant wavelength

Multilayer sequences contain layers of widely different strength and thickness. According to experiments, the form of the folds depends upon several parameters: the relative stiffness of the multilayer and its confinement; the relative thickness and stiffness of adjacent layers within a multilayer; the properties of the contacts between layers; the degree of cohesion between layers. Experimental measurements (JOHNSON & BERGER, 1989) in sedimentary rocks shows that if there are too few ductile layers in a multilayer stack, the stack will fail by faulting before it buckles into folds.

Fault-related folding and fault-related folds

The second mechanism of fault-related folding requires a fault to be active prior to and/or during fold formation. This mechanism does not require any viscosity contrast, nor does anisotropy have to be present in the material other than that of a localized thrust fault. This mechanism develops in the low temperature regime, where deformation is predominantly brittle.

Folds related to a ramp active prior to folding (Fault-bend folds) were first described by RICH (1934). He proposed that the thrust surface followed some zone of easy gliding, such as shale until frictional resistance became too great and then sheared diagonally up across bedding forming a ramp to another shale, then following the shale for some distance, to shear across the bedding at another ramp to the ground surface. This mechanism (ramp folding) was later discussed more precisely by WILTSCHKO (1979) and by JOHNSON & BERGER (1989). A ramp fold is the result of duplication of strata at the ramp fault and along the detachment surface beyond the ramp fault. Folds are consequently formed passively by translation of a thrust sheet over a ramp. In this model, the thrust is clearly implied to develop first and the fold is a product of passive accommodation. The model has the advantage of being easy to analyze in a rigorous geometrical way. A problem with this model is the location of the ramp.

Another model is represented by folds which develop simultaneously with the ramp portion of a stepped thrust fault (fault-propagation folds). The mechanisms of those folds are not so well understood as yet.

Fault-related folds are developed in a multilayer sequence assuming bedding plane slip between the layers. Fault-bend and fault-propagation folds are formed over a discrete sole thrust and represent a folded multilayer sequence with a very low viscosity contrast between layers. Detachment folds require a weak décollement layer (e.g. salt or shale layer), which can infill the space generated at the base of the fold. The latter have all the characteristics of a buckle folds.

The nucleation of the faults is an interesting question. Models proposed by DIXON & LIU (1992) based on centrifuge modeling, suggests that, in a stratigraphic sequence with high contrast of viscosity between layers, the thrust ramps are localized solely by earlier stage of low amplitude folds. Early buckling would be responsible for the localization of the ramps.

Criteria to distinguish buckle and fault related folds ?

The most obvious criterion for the distinction of the two folding mechanisms is the identification of a thrust fault which can genetically be related to the fold formation. In the case of folds observed in foreland fold and thrust belts, this usually requires a detailed knowledge of the subsurface geometry, which may often not be available.

The fold profile may provide some information about the relative competency of layers. However, there is no information regarding the underlying dominant folding mechanism (buckling vs. fault-related folding).

A detailed knowledge of the internal deformation along the entire fold profile, in individual key layers, may provide other critical information about the folding mechanism: deformation can be expected to be concentrated within fold hinges of competent layers of buckle folds, whereas intricate but predictable patterns of high and low strain zones (possibly several superposed incremental strain "events") may be expected throughout in fault-related fold models, where material has to move through certain axial planes.

Transitions between buckle folds and fault-related folds

Transitions from buckling to fault-related folding mechanisms are commonplace and accordingly, there is no clear cut limit between the two end mem-

ber mechanisms of folding. Folding may start by buckling of a competent layer to a certain amount of shortening, before deformation is localized into thrust faults (DIXON & LIU, 1992). Alternatively, a sedimentary wedge may start to deforme by thrust faulting and then be buckled at later stages. Moreover transitions between the two models of fault-related folding (fault-propagation folds to fault-bend folds) are also possible.

3.2.1.3. Kinematic sequences associated to salt flow

The presence of weak layer in a multilayer sequence has a strong influence on the mechanisms of folding. Rock salt, one of the weakest material known in sedimentary sequences, is responsible for a particular set of deformation structures.

Salt tectonics (syn. halotectonics) refers to any tectonic deformation involving salt or other evaporites as a substratum or a source layer (JACKSON & TALBOT, 1994). Halokinesis, on the other hand, designates the formation of salt structures which are the result of salt flow under the influence of gravity alone, without any significant lateral tectonic forces (TRUSHEIM, 1957, 1960).

In the studied area, gravity forces are not unique and probably not the most important. A major lateral push of the Alps towards the NW appears to be responsible for the formation of the Jura foreland fold and thrust belt. This stress is well known under the German term "Fernschub" (= distant push) defined by LAUBSCHER (1961).

In sedimentary environments, the continuous deposition of layers during salt movements may record the timing and the character of the salt flow. Three kinematic sequences have been distinguished (Fig. 3.3). The prekinematic sequence is deposited before the salt starts to flow; the synkinematic sequence is deposited during the salt flow and shows internal onlaps or truncations; the postkinematic sequence is deposited after the salt stopped flowing. The recognition of these sequences in a mountain belt, may give many information on the timing of deformation. In the field, evidence may also be furnished by thickness changes and truncations or onlaps. High quality seismic lines may be required to reveal all the subtleties of such salt structures and their relation with the surrounding rocks.

3.2.2. Evaporite-related folds (low amplitude)

3.2.2.1. General comments

Low amplitude folds may be difficult to recognize on geological maps or in the field. The low limb dip and the low structural relief make these structures inconspicuous and difficult to observe at outcrops. Seismic lines are more useful in documenting the geometry of this fold type at depth.

Interpretations of seismic lines across the Plateau Jura and the Molasse Basin, show a series of broad and gentle anticlines which are controlled by evaporite, salt and clay stacks within the ductile Unit 2 of the Triassic layers.

In the scientific literature, this type of anticline is termed salt anticline or salt welt (HARRISON & BALLY, 1988) also defined by JACKSON & TALBOT (1994) as "an elongated upwelling of salt with concordant overburden". The term salt pillow has the same meaning, but is used for subcircular shapes (Fig. 3.4). In this work, we prefer to use the terms evaporite anticline and evaporite pillow, due to the uncertainty about the amount of pure salt in the Triassic layers. Conventional salt pillows, as first visualized by TRUSHEIM (1960), are today often interpreted in an overall extensional context (VENDEVILLE & JACKSON, 1992). In a compressional context, ideally, the evaporites pinch out in the adjacent synclines and flow into anticlinal evaporite ridges (HARRISON, 1995).

It is important not to confuse the term salt welt with the term salt weld, which describes a surface or zone of adjacent strata originally separated by autochthonous or allochthonous salt (JACKSON & TALBOT, 1989). Compressional salt welds occur when all ductile material has migrated from the syncline to the core of the anticline.

3.2.2.2. Geophysical evidence from seismic profiles

Geophysical evidence for evaporite stacks include thickness variations of a seismic unit, which are spatially associated with broad folds in the overlying formations and velocity anomalies. The latter generally consist of a positive deflection of the reflectors (velocity pull-up) beneath anticlines, caused by the thickening of the Triassic evaporite unit of supposedly high velocity. This velocity pull-up is further enhanced by a velocity pull-down in the synclines,

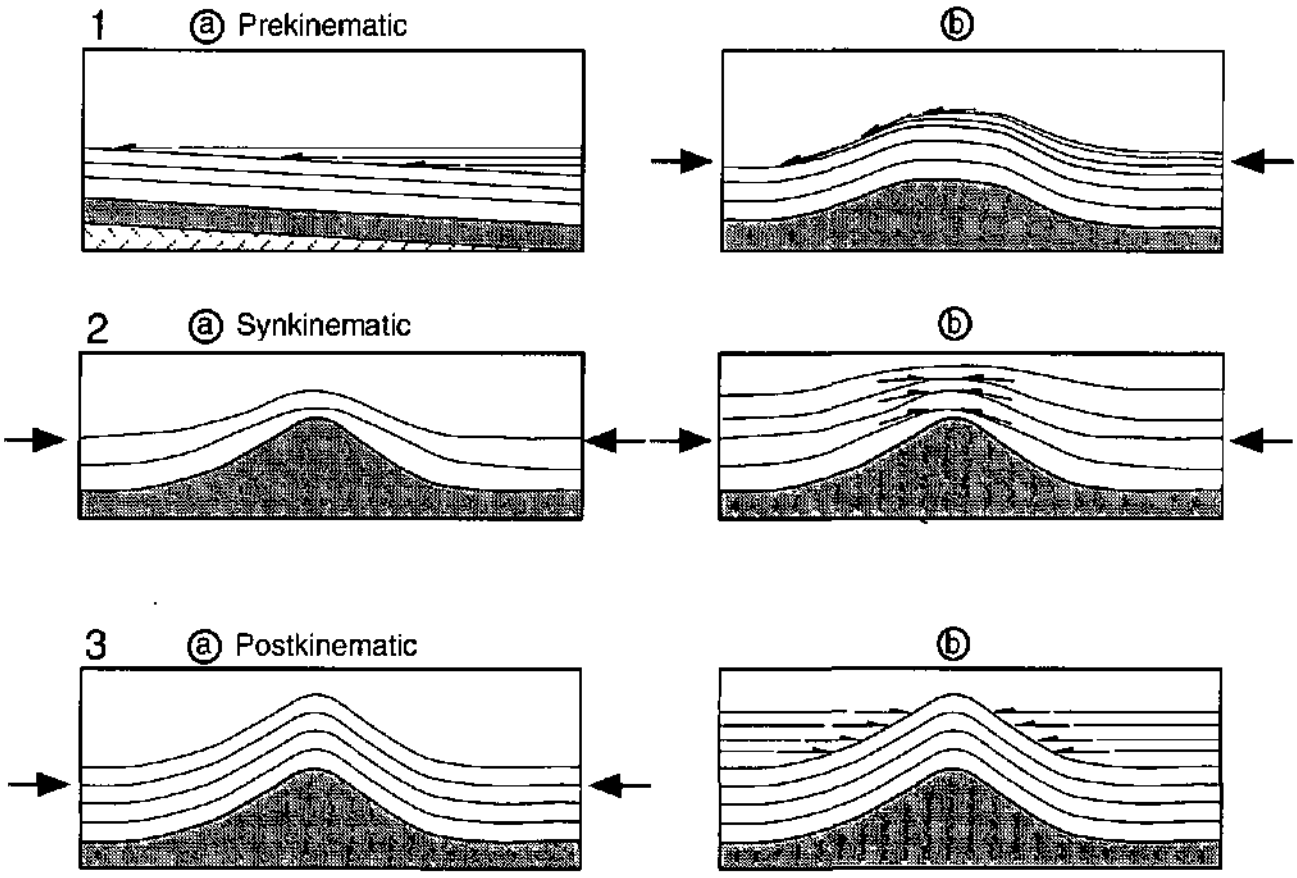

Figure 3.3: Sedimentary record of salt flow during shortening. Three kinematic sequences are inferred from the relation salt flow and sedimentary record. 1) Prekinematic sequence; 2) Synkinematic sequence; 3) Postkinematic sequence. Inspired from JACKSON & TALBOT (1994).

Enregistrement syn-sédimentaire du fluage du sel durant un raccourcissement. Trois séquences cinématiques sont déduites des relations entre le fluage du sel et l'enregistrement sédimentaire. 1) Anté- cinématique; 2) Syn-cinématique; 3) Post-cinématique. Inspiré de JACKSON & TALBOT (1994).

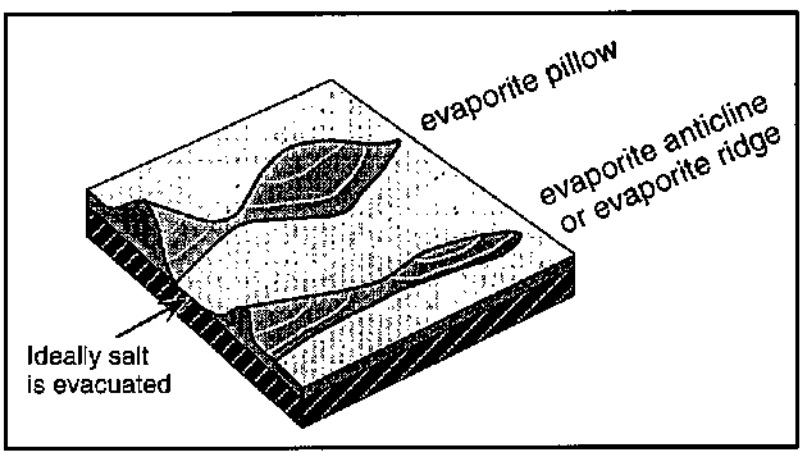

Figure 3.4: Difference between evaporite anticline and evaporite pillow. An evaporite anticline has an elongated shape, whereas the evaporite pillow has a sub-circular shape. Modified from JACKSON & TALBOT (1994).

Différence morphologique entre un anticlinal associé à des évaporites et un coussin associé à des évaporites. Un anticlinal d'évaporites est caractérisé par une forme allongée, tandis qu'un coussin d'évaporites montre une forme sub-circulaire. Schéma inspiré de JACKSON & TALBOT (1994).

due to the low velocity of the thick Tertiary sediments (Fig. 3.8, Essertines anticline). As described in §2.4.3.8. the Triassic Unit 2 shows discontinuous and oblique reflectors, whereas the overlying unit (Triassic Unit 1) displays well layered, laterally continuous reflectors. Triassic Unit 1 does not present thickness changes and seems therefore to be tectonically undisturbed.

3.2.2.3. Examples illustrated by seismic profiles

The Plateau Jura evaporite anticlines

The Plateau Jura broad folds are illustrated on the northern part of the dip Section 111 (Panel 9 and Plate 8) and Sections 107, 115 and 117 (Panel 10). These folds display two long asymmetric limbs dipping with a very low angle towards the North and the South respectively. This geometry is illustrated by a well layered series of reflectors in the middle of the Mesozoic cover series (Fig. 3.5). This sequence represents the evaporites of the Triassic Unit 1. Beneath this unit, we observe discontinuous reflectors belonging to the Triassic Unit 2. Some of these reflectors onlap the last strong and continuous reflection, which represents the top of the basement (either crystalline rocks or Permo-Carboniferous sediments). The Triassic Unit 2, highlighted in dark gray on Figure 3.5, shows a thickness increasing from NW to SE. This thickening, due to evaporite stacking, appears clearly on dip seismic lines (Plate 8, Panel 10 and Fig. 3.5). It is the thickest stack of evaporites observed so far in the studied area and has been confirmed by the Laveron drill hole (BRGM, 1964). The Laveron fold (Fig. 3.5 and Section 107 on Panel 10) is a clear seismic expression of what is here termed evaporite anticline. BITTERLI (1972), over twenty years ago, presented an interpretation referring to halokinetic movements.

Few Plateau Jura anticlines are symmetric. Most, typically exhibit a limb grading progressively into a syncline (thinning of Triassic Unit 2), whereas the opposite limb ends against faults. On Section 107 (Panel 10), the Laveron anticline stops against the Mouthe tear fault trending N-S. On Section 117 (Panel 10), the evaporite anticline disappears towards the South in a transparent zone. The latter corresponds to the transition between the Haute Chaîne Jura and the Plateau Jura, as well as to the intersection between the Morez tear fault, oriented NNW-SSE and the "Faisceau de Syam", a strongly deformed zone oriented NNE-SSW (Figs. 1.2, 4.1 and Panel 10).

It has to be emphasized, that thrust faults (ramp or flat) and repetition within the Mesozoic strata are not recognizable. Sections 111 to 85 (Panel 9) clearly show the geometrical contrast between high amplitude Haute Chaîne Jura folds, related to thrust faults and low amplitude Plateau Jura folds, related to evaporite stacks.

The Molasse Basin pillow structures

In the Molasse Basin, broad anticlines are known from outcrop geology. Interpreted subsurface data (Panel 4, strike lines; Panels 5 and 6, dip lines; Plates 6 and 7) present a succession of low amplitude folds, with slightly dipping limbs. Folds with a high degree of symmetry have been found in the southern region, whereas further to the North they are either foreland- (NW) or hinterland- (SE) verging. The same anticline may also change its vergence laterally (Figs. 3.6, 3.7 and 3.8). The geometry of the folds is highlighted by a well layered series of reflectors representing Cretaceous, Malm, Dogger, Liassic and upper Triassic strata. The core of these folds is filled with thickened Triassic Unit 2 beds and their geometry is shown in detail on the six seismic examples (Figs. 3.7 to 3.12). The location of these parts of seismic lines is shown on Figure 3.6, which represents an isopach map of Unit 2 of the Triassic beds of the western Swiss Molasse Basin. This map highlights elongated or elliptical thickening of the Triassic Unit 2 along a NE-SW trend. The consequential interpretation of these structures and their pattern on formation of the Jura is discussed in Chapter 5.

Triassic Unit 2 is colored in dark gray on the seismic interpretations of Figures 3.7 to 3.12. These examples illustrate the considerable thickness variations and also the internal pattern of the unit. Thickening is located underneath broad anticlines and the maximum thickness coincides with the most internal Jura anticlines (compare Fig. 3.6 and Fig. 3.11). Generally, Unit 2 displays discontinuous reflectors, which are either flat or oblique, bounded by a basal and roof reflector. Examples 2, 5 and 6 (Figs. 3.8, 3.11 and 3.12) show a succession of oblique reflectors within Triassic Unit 2, that dip toward the South. These reflectors may be interpreted as small thrust faults imbricating parts of the unit, to result in an overall thickening. Such structures are named duplexes in the literature (MITRA, 1986; MCCLAY, 1992). Duplexes are bounded by a roof thrust, e.g. below reflector H (Top Triassic Unit 2) and a basal thrust, e.g. above the top of the basement in our study area.

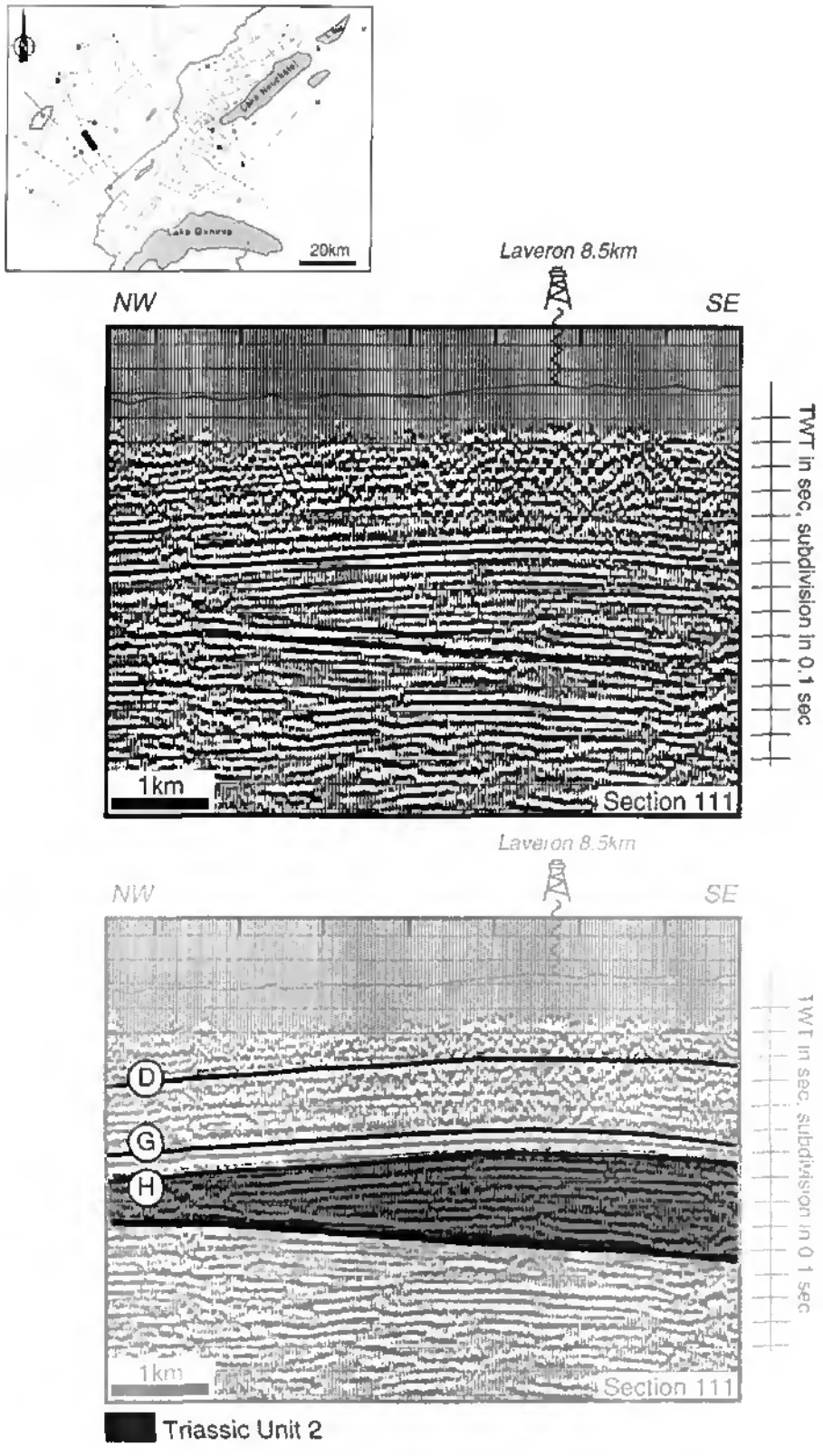

Figure 3.5: Northern part of the dip seismic Section 111 located in the Plateau Jura (external zone). The interpretation displays a broad anticline related to thickening of the Triassic Unit 2. Laveron drill hole (projection), which reaches the top of the Buntsandstein strata, confirms the seismic interpretation. Legend for the top of the layers: D = Dogger; G = Triassic Unit 1, H = Triassic Unit 2.

Partie septentrionale du profil sismique 111 transversal localisé dans les Plateaux jurassiens (zone externe). L'interprétation montre un large anticlinal associé à un épaississement dans l'Unité 2 du Trias. Le forage de Laveron (projeté de 8,5 km) atteint le toit des couches du Buntsandstein et confirme l'interprétation sismique. Légende pour le toit des couches: D = Dogger; G = Unité 1 du Trias, H = Unité 2 du Trias.

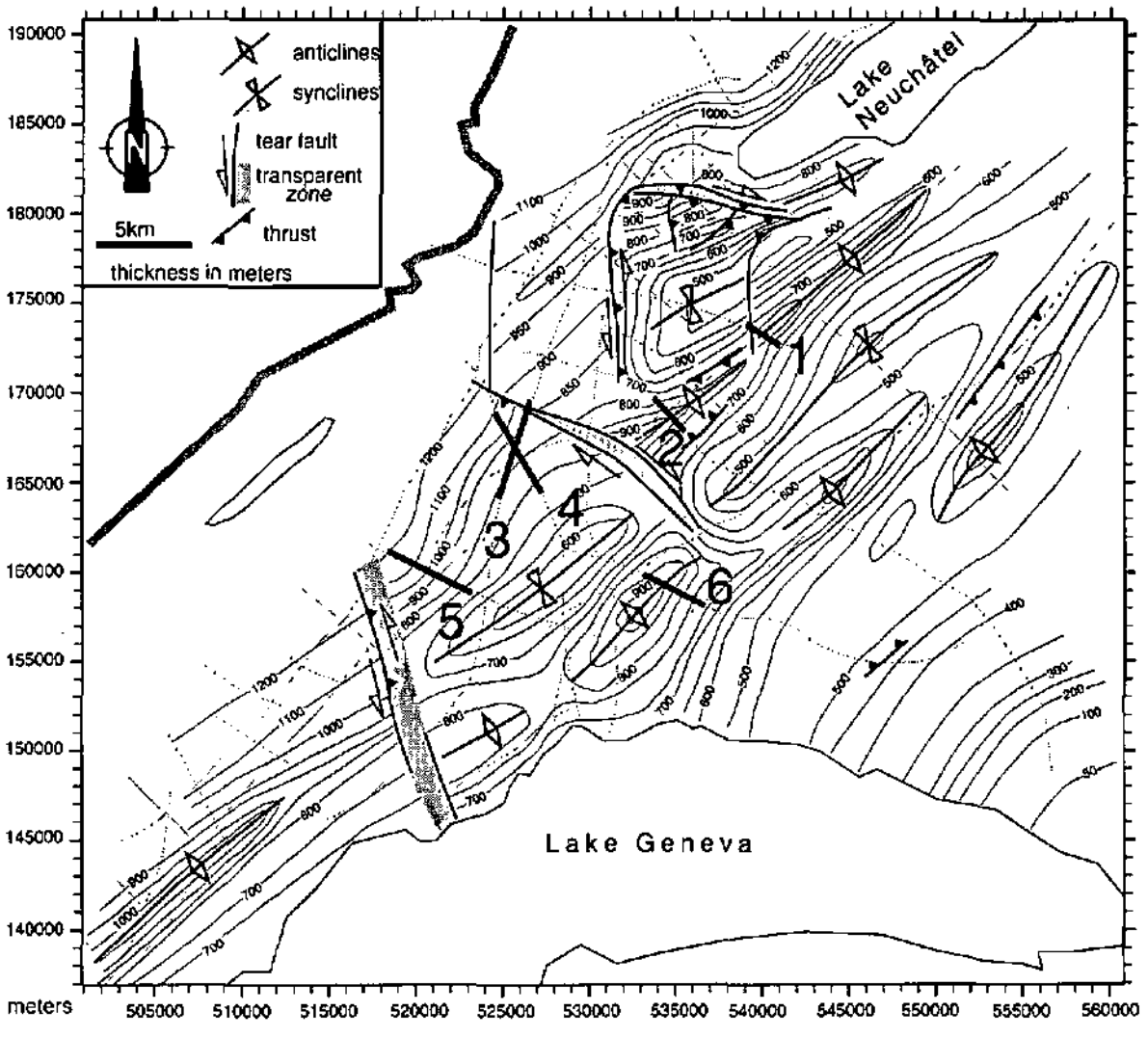

Figure 3.6: Isopach map of the Triassic Unit 2 beds from the western Molasse Basin (hand contouring). Compare with Figure 2.29. Anticline axes emphasize thick zones, syncline axes show thin zones. Location of six examples (Figs. 3.7 to 3.12) of evaporite stacks in the Triassic Unit 2. Coordinates in meters are according to the Swiss geographic reference grid. Modified from SOMMARUGA (1995).

Carte des isopaches de l'Unité 2 des couches du Trias du Bassin molassique occidental. Méthode de contourage à la main, comparer avec la Figure 2.29. Les axes des anticlinaux indiquent les zones très épaisses, les axes des synclinaux soulignent les zones peu épaisses. Localisation de six exemples (Figs. 3.7 à 3.12) d'empilements d'évaporites dans l'Unité 2 du Trias. Les coordonnées en mètres correspondent à la grille de référence géographique de la Suisse. Modifié de SOMMARUGA (1995).

3.2.2.4. Interpretation of the evaporite anticlines or pillows

The kinematic sequences in the central Jura and the Molasse Basin lines can be recognized on a number of examples of evaporite anticlines (Fig. 3.5 and Figs. 3.7 to 3.12).

Broad folds from the Plateau Jura and the Molasse Basin show in their core, thickening of evaporites, salt and clays within the Triassic Unit 2 (Panel 10 and Panel 5), which result in folding of the overlying layers. However, the Cretaceous, Jurassic and Triassic Unit 1 intervals maintain an apparently more constant thickness. Maybe because the seismic data are not of high quality, especially in the Plateau Jura, no truncations are visible within these strata. In some dip lines, located in the southern Molasse Basin e.g. Section 43 on Panel 5, Tertiary sediments onlap clearly the underlying strata. Onlaps have been observed mostly on south dipping limbs.

The interpretation of these onlaps is not clear. On the one hand, these onlaps may be due to salt flow to the NW and may thus be interpreted as evidence of salt movements since the beginning of Cenozoic time. To confirm this hypothesis, however, there

should be some onlaps onto North dipping limbs (there is only one case on strike Section 26, where onlaps are recognized to the SW). No onlap has been found on a north dipping limb, however. On the other hand, updip truncations toward the foreland may be interpreted as the foredeep unconformity. This major unconformity was induced by the subduction of the distal part of the European plate (BALLY, 1989, see also Chapter 5). This second hypothesis appears the most likely. In the central Jura and Molasse Basin, the Mesozoic layers, with the Oligocene and early Miocene sediments represent the prekinematic sequence. No synkinematic series has been observed on seismic lines. Evaporite flow was most likely contemporaneous to the main deformation, of late Miocene age in the Jura (LAUBSCHER, 1961). No evidence for growth anticlines, involving deposition of Tertiary Molasse sediments, has been found so far in the Jura or the Molasse Basin.

The detailed internal structure of swells within Triassic Unit 2 is unknown, since few evaporite-related anticlines have been drilled (Laveron, Essertines) and most other wells do not reach the Triassic Unit 2. In the Jura and Molasse Basin, the evolution stage is similar for all broad anticlines and it is thus difficult to describe the evolution of the deformation. Salt flow and/or stacking of thrust sheets (duplexes) are possible explanations for the observed swells.

True salt flow producing the so called salt pillows or salt anticlines is not really proven in the Jura fold and thrust belt, nor in the Molasse Basin. The Laveron stratigraphic well log, which shows more than 300 m of pure salt in Triassic layers, is the thickest pillow observed in the studied area and salt flow seems a reasonable assumption to explain this pillow (Fig. 3.5). The Triassic Unit 2 interval shows either discontinuous reflectors parallel to the overlying strata or no reflectivity (transparent zone). The reflectors do not highlight any structural relationships. The thick amount of salt and the absence of structural features suggest that the thickening within the Triassic Unit 2 is indeed the result of an accumulation of salt and evaporite by lateral flow. This flow occurs in a compressional regime and is not to be confused with conventional salt diapirism, which often occurs in an extensional context. It is important to underline, however, that no salt diapir has been observed, to date, in the Jura belt and the Molasse Basin. This is probably due the scarcity and thinness of pure rock salt layers present in the Triassic.

Low amplitude anticlines related to salt welts (see 3.2.2.1.) are well illustrated by HARRISON & BALLY (1988) and HARRISON (1995) on high quality seismic data from the Parry Islands Fold Belt (Melville Island, Canadian Arctic, Fig. 3.13). The increasing intensity of deformation toward the hinterland can be viewed as representing progressive stages of deformation and, as result, gives insight into the evolution of deformation within large anticlines. The first stage illustrates a salt welt, i.e. a significant triangular disharmony in the salt layer overlying the less disturbed unit. The triangular envelope of this salt welt is made of decoupling surfaces. In common language (BALLY, oral communication), this structure has been called "Napoleon's hat", due to the strong similarity in shape. With increasing shortening, the competent layers overlying the ductile zone respond by brittle behavior and the incompetent shales respond by flow (shale welt). The response to deformation varies, both laterally and vertically in the strata, as a function of the distribution of detachment levels and the relative thickness and competence of different formations. In the Melville Island case, thrust faults appear to be progressively younger from bottom to top. In comparison, the Jura Plateau and the Molasse Basin folds seem to be less evolved, since no obvious wedging is observed above the salt welts.

In the Molasse Basin, many broad anticlines present structural features within the Triassic Unit 2 layer (best examples are in Fig. 3.8 and Fig. 3.12). Strong reflectors dipping toward the South crosscut the whole unit. These can be interpreted as small imbricate thrust faults linking the floor thrust to the roof thrust (below reflector H). According to the classification of BOYER & ELLIOT (1982), these structures may correspond to hinterland dipping duplexes within an anticlinal core. These structures, confined to the lower unit just above the basement, result in folding of the mainly unfaulted overlying layers. The roof thrust of the duplex (just below reflector H) separates two different styles of deformation: the overlying layers are folded, whereas the underlying are faulted (thrusts) and/or ductily deformed.

In the Appalachian Plateau (Pennsylvania), MITRA (1986) presents a seismic line example of a duplex in the core of a major anticline (Fig. 3.14). The Lower to Upper Devonian units are folded into a broad unfaulted anticlinal arch. The Middle Ordovician carbonates (Trenton Formation) are affected by a series of imbricate thrusts that constitute a duplex. Additional thickening occurs within

the Upper Ordovician to Silurian units, but no reflectors are visible, due to the poor quality of the seismic lines. The basal Cambrian unit is not affected by the deformation. Imbricate thrust systems of this sort, have attracted much interest among petroleum geologists, since they constitute potential hydrocarbon traps.

In the eastern Jura, seismic sections show also important thickening within Triassic strata, as shown in the strike line presented on Figure 3.15. This seismic line crosses a low amplitude anticline (Born anticline), which is surrounded by Tertiary Molasse sediments. Beneath the broad anticline, the layer thickness increases between the reflectors representing the base of the Mesozoic and the top of the Muschelkalk (in gray color on Figure 3.15). This interval corresponds to the Triassic Unit 2 of the central Jura. This anticline is located between the Haute Chaîne Jura (Folded Jura) and the Plateau Molasse unit. The structural style of this evaporite-related anticline may be compared to the examples of the Figures 3.10 and 3.11, located in the most internal part of the folded Jura.

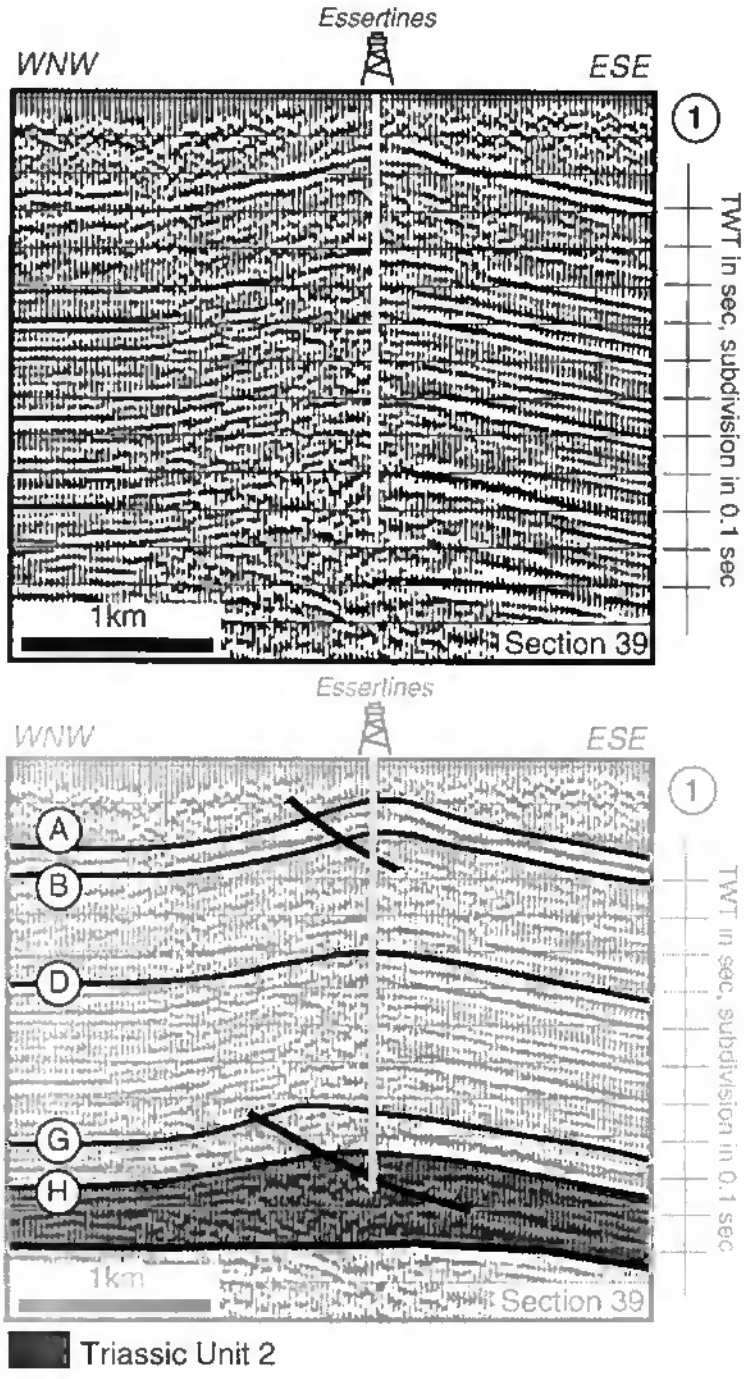

Figure 3.7: Southern part of the dip seismic Section 39 from the western Swiss Molasse Basin. For location, see example 1 on Figure 3.6. The interpretation, calibrated on the Essertines drill hole, shows a low amplitude fold related to a thickening within the Triassic Unit 2. Legend for the top of the layers: A = Lower Cretaceous or base Tertiary; B = upper Malm; D = Dogger; G = Triassic Unit 1, H = Triassic Unit 2.

Partie méridionale du profil sismique 39 transversal, situé dans le Bassin molassique suisse. Pour la localisation, voir exemple 1 sur la Figure 3.6. L'interprétation, calibrée sur le forage d'Essertines, montre un pli de faible amplitude associé à un épaississement dans les couches de l'Unité 2 du Trias. Légende pour le toit des couches: A = Crétacé inférieur ou base du Tertiaire; B = Malm supérieur; D = Dogger; G = Unité 1 du Trias, H = Unité 2 du Trias.

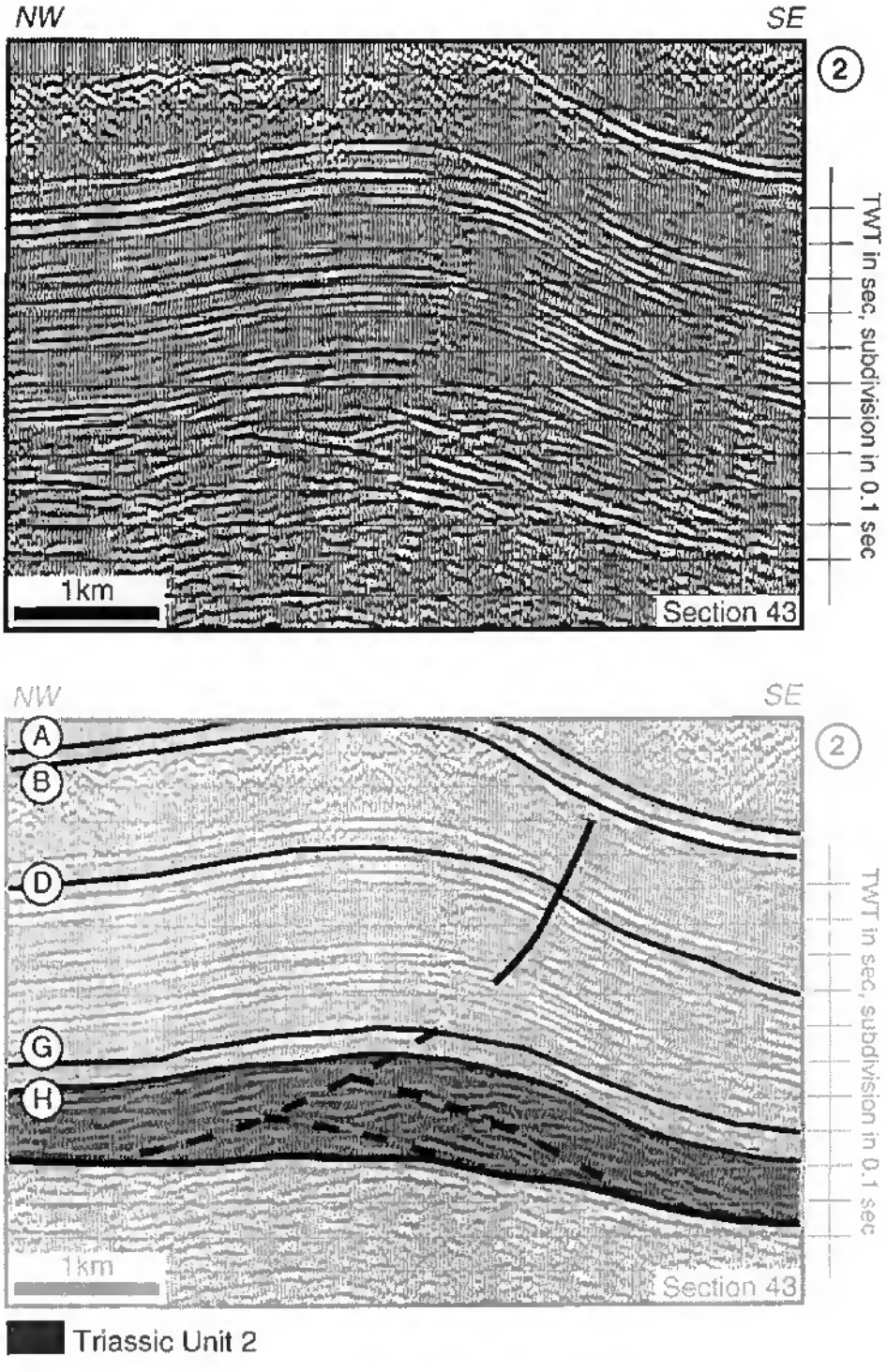

Figure 3.8: Northern part of the dip seismic Section 43 from the western Swiss Molasse Basin. For location, see example 2 on Figure 3.6. The interpretation shows a hinterland-vergent fold related to a thickening within the Triassic Unit 2. The thickening may be due to duplex structures. Legend for the top of the layers: A = Lower Cretaceous or base Tertiary; B = upper Malm; D = Dogger; G = Triassic Unit 1, H = Triassic Unit 2.

Partie septentrionale du profil sismique 43 transversal, situé dans le Bassin molassique suisse. Pour la localisation, voir exemple 2 sur la Figure 3.6. L'interprétation montre un pli à vergence vers le Sud, associé à un épaississement dans les couches de l'Unité 2 du Trias. L'épaississement est probablement dû à des structures imbriquées en duplex. Légende pour le toit des couches: A = Crétacé inférieur ou base du Tertiaire; B = Malm supérieur; D = Dogger; G = Unité 1 du Trias, H = Unité 2 du Trias.

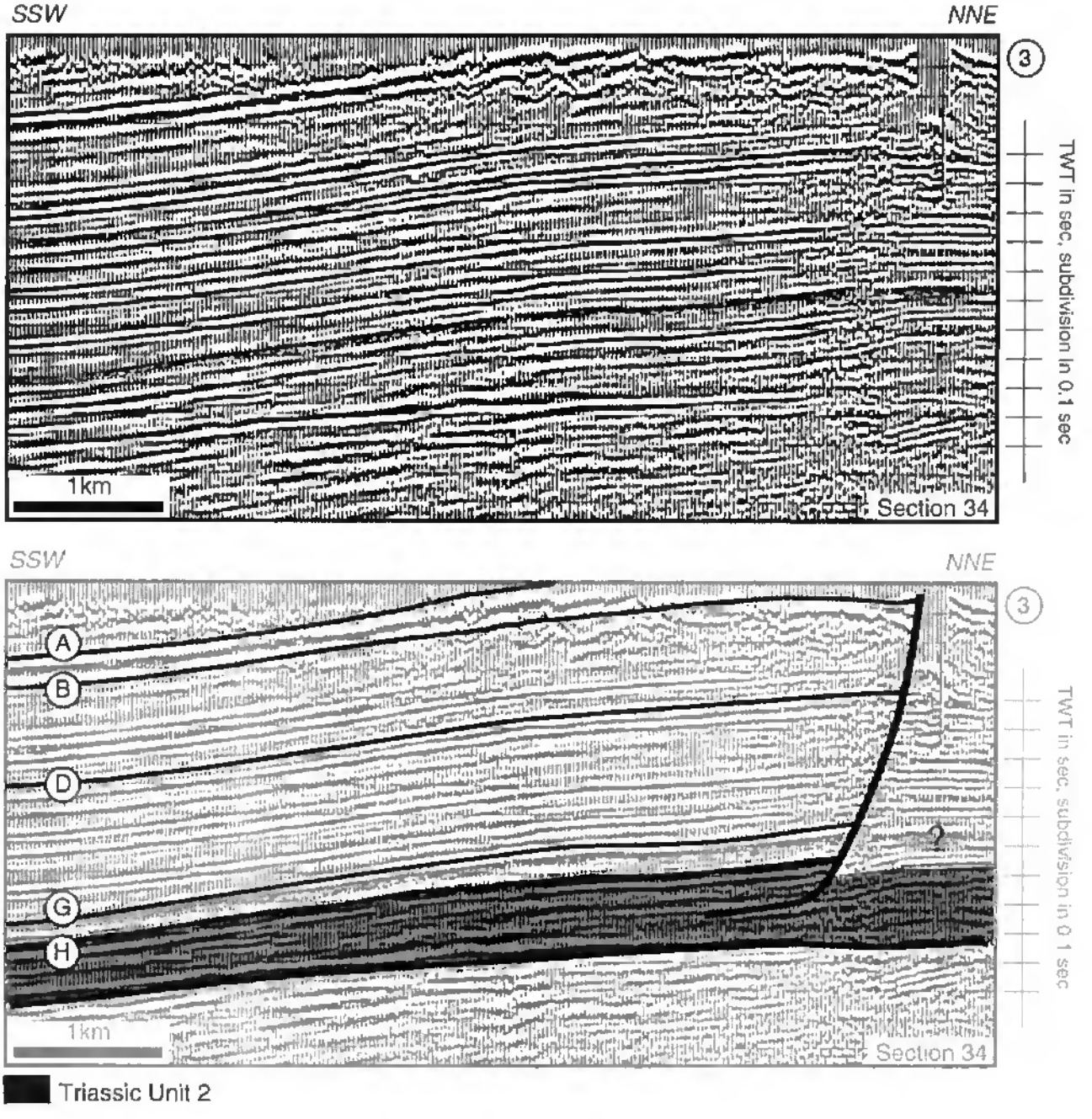

Figure 3.9: Southern part of the seismic Section 34 from the western Swiss Molasse Basin. For location, see example 3 on Figure 3.6. The interpretation shows a foreland-vergent fold related to a thickening within the Triassic Unit 2. A tear fault crosscuts the evaporite anticline (compare map of Figure 3.6). Legend for the top of the layers: A = Lower Cretaceous or base Tertiary; B = upper Malm; D = Dogger; G = Triassic Unit 1, H = Triassic Unit 2.

Partie méridionale du profil sismique 34, situé dans le Bassin molassique suisse. Pour la localisation, voir exemple 3 sur la Figure 3.6. L'interprétation montre un pli à vergence vers l'avant-pays, associé à un épaississement dans les couches de l'Unité 2 du Trias. Un décrochement recoupe l'anticlinal (comparer avec la carte de la Figure 3.6). Légende pour le toit des couches: A = Crétacé inférieur ou base du Tertiaire; B = Malm supérieur; D = Dogger; G = Unité 1 du Trias, H = Unité 2 du Trias.

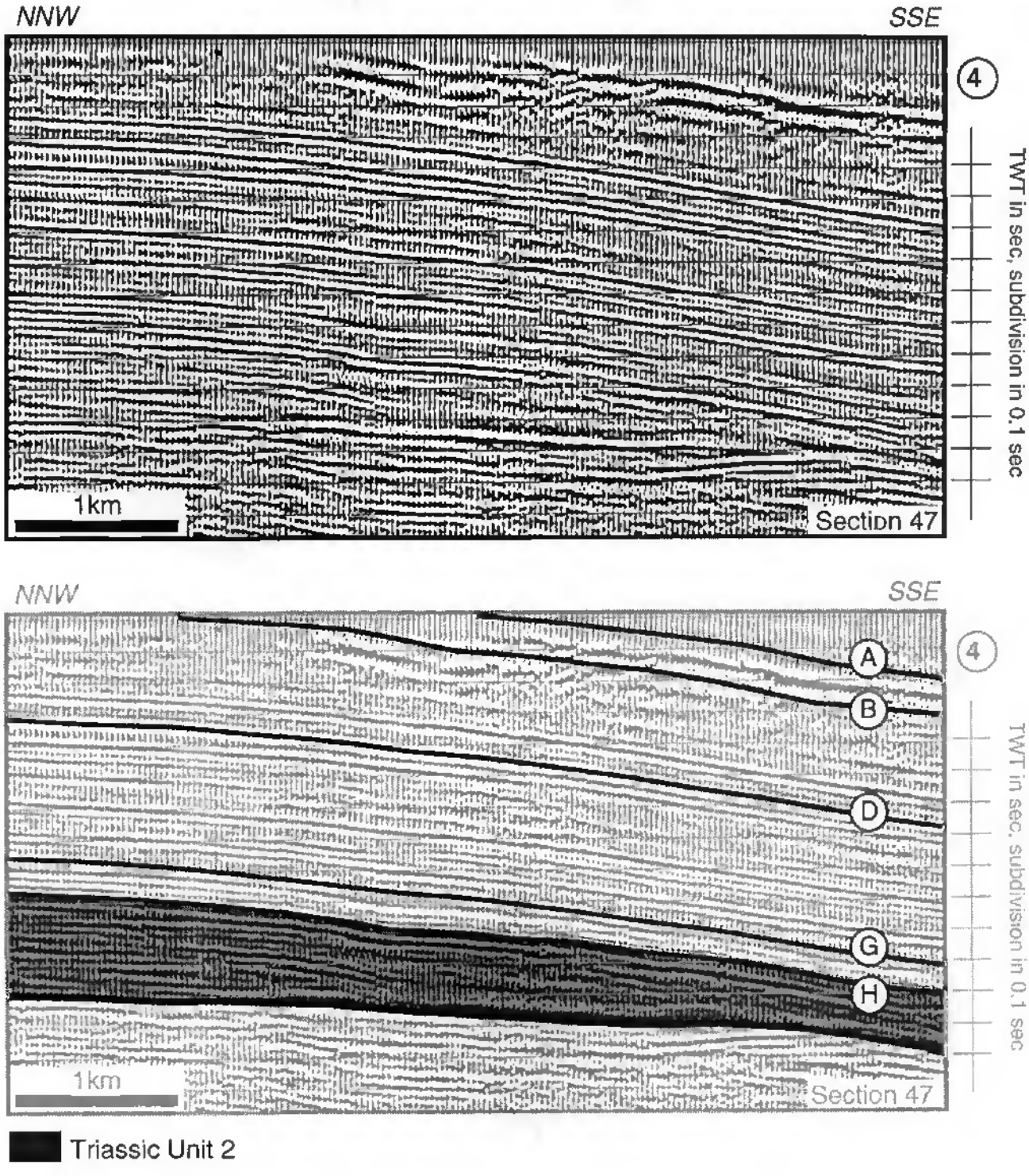

Figure 3.10: Northern part of the dip seismic Section 47 from the western Swiss Molasse Basin. For location, see example 4 on Figure 3.6. The interpretation shows a foreland-vergent fold related to a thickening within the Triassic Unit 2. Legend for the top of the layers: A = Lower Cretaceous or base Tertiary; B = upper Malm; D = Dogger; G = Triassic Unit 1, H = Triassic Unit 2.

Partie septentrionale du profil sismique 47 transversal, situé dans le Bassin molassique suisse. Pour la localisation, voir exemple 4 sur la Figure 3.6. L'interprétation montre un pli à vergence vers le NW, associé à un épaississement dans les couches de l'Unité 2 du Trias. Légende pour le toit des couches: A = Crétacé inférieur ou base du Tertiaire; B = Malm supérieur; D = Dogger; G = Unité 1 du Trias, H = Unité 2 du Trias.

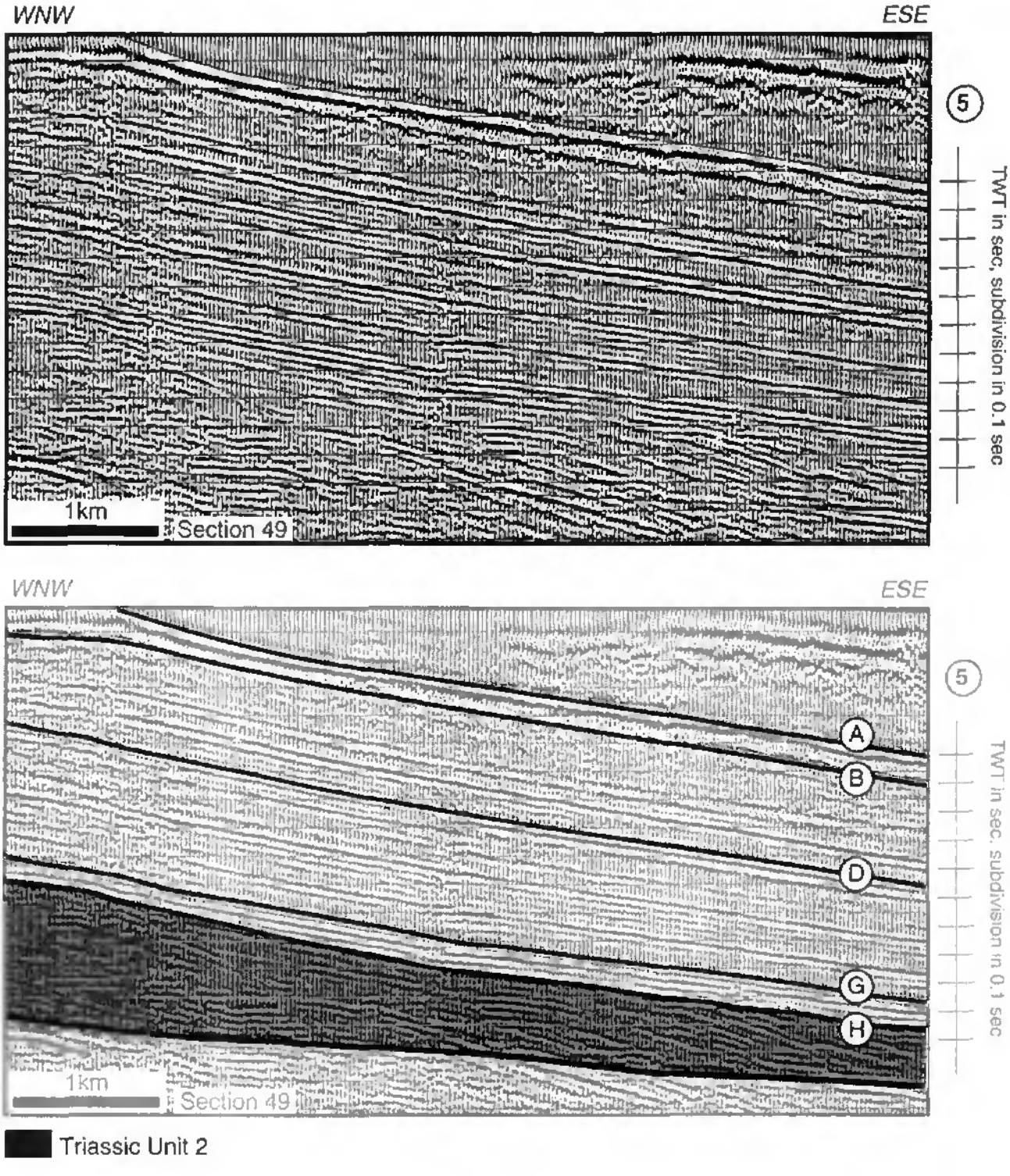

Figure 3.11: Northern part of the dip seismic Section 49 from the western Swiss Molasse Basin. For location, see example 5 on Figure 3.6. The interpretation shows a foreland-vergent fold related to a thickening within the Triassic Unit 2. The thickening may be due to duplex structures. Legend for the top of the layers: A = Lower Cretaceous or base Tertiary; B = upper Malm; D = Dogger; G = Triassic Unit 1, H = Triassic Unit 2.

Partie septentrionale du profil sismique 49 transversal, situé dans le Bassin molassique suisse. Pour la localisation, voir exemple 5 sur la Figure 3.6. L'interprétation montre un pli à vergence vers le Nord, associé à un épaississement dans les couches de l'Unité 2 du Trias. L'épaississement est peut-être dû à des structures imbriquées en duplex. Légende pour le toit des couches: A = Crétacé inférieur ou base du Tertiaire; B = Malm supérieur; D = Dogger; G = Unité 1 du Trias, H = Unité 2 du Trias.

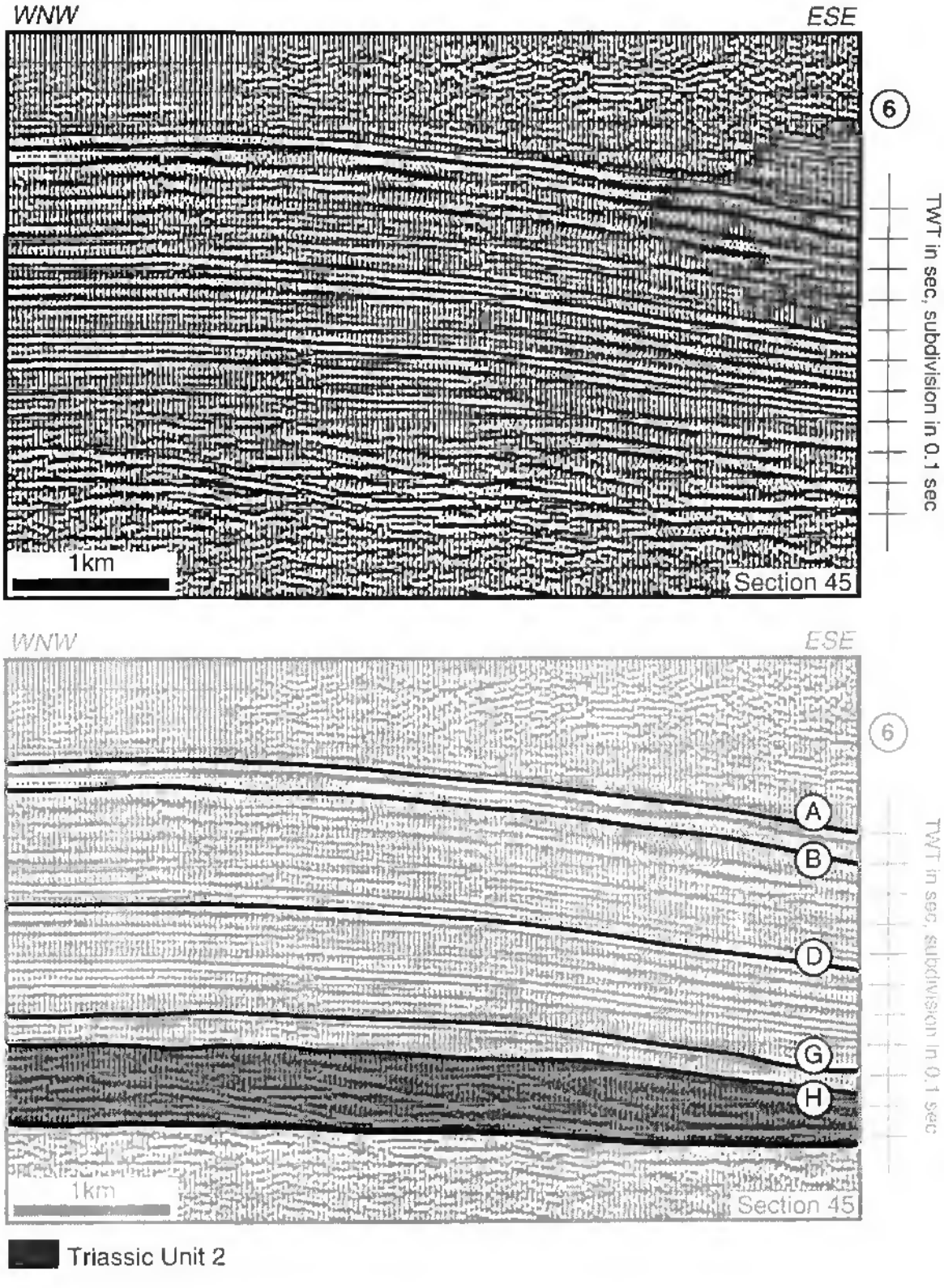

Figure 3.12: Northern part of the dip seismic Section 45 from the western Swiss Molasse Basin. For location, see example 6 on Figure 3.6. The interpretation shows a foreland-vergent fold related to a thickening within the Triassic Unit 2. The thickening may be due to duplex structures. Legend for the top of the layers: A = Lower Cretaceous or base Tertiary; B = upper Malm; D = Dogger; G = Triassic Unit 1, H = Triassic Unit 2.

Partie septentrionale du profil sismique 45 transversal, situé dans le Bassin molassique suisse. Pour la localisation, voir exemple 6 sur la Figure 3.6. L'interprétation montre un pli à vergence vers l'avant-pays, associé à un épaississement dans les couches de l'Unité 2 du Trias. L'épaississement est peut-être dû à des structures imbriquées en duplex. Légende pour le toit des couches: A = Crétacé inférieur ou base du Tertiaire; B = Malm supérieur; D = Dogger; G = Unité 1 du Trias, H = Unité 2 du Trias.

a)

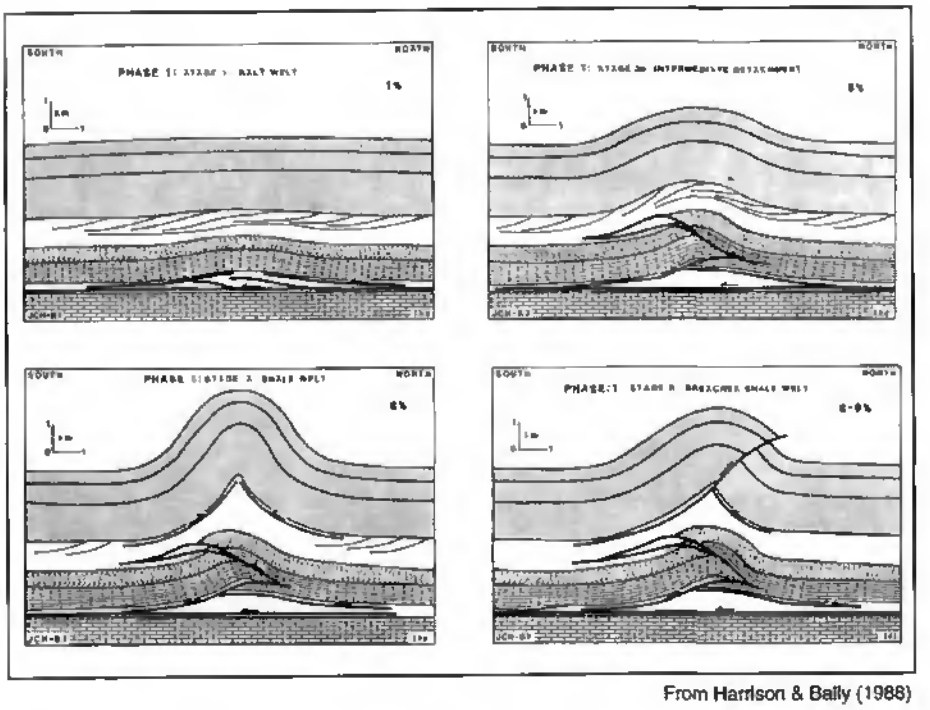

From Harrison & Bally (1988)

b)

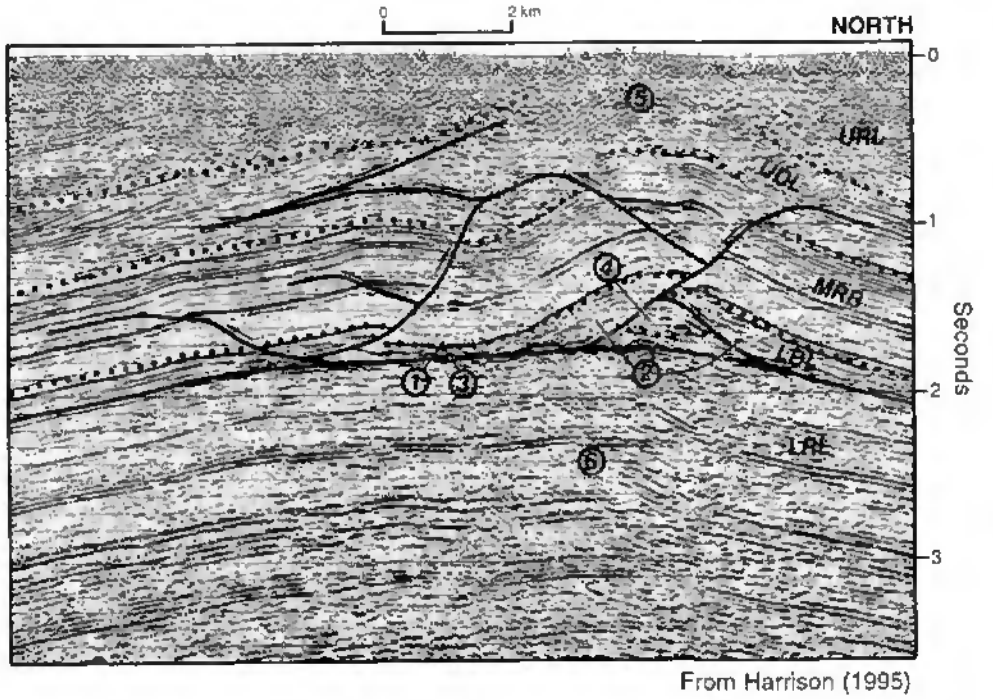

From Harrison (1995)

Figure 3.13:
a) Stages from the evolution of an anticline in the salt-based Parry Islands Fold Belt (Melville Island). Modified from HARRISON & BALLY (1988).

Evolution d'un anticlinal dans la chaîne plissée de l'île de Melville (territoires arctiques). Modifié de HARRISON & BALLY (1988).

b) Example of an anticline from Melville Island. LRL = lower rigid layer; LDL = lower ductile layer; MRB = medial rigid beam; UDL = upper ductile layer; URL = upper rigid layer; 1 = footwall syncline; 2 = a compound anticlinal salt welt with a faulted and indistinct hinge saddle; 3 = dramatic local thinning of the lower Bay beam is encapsulated by evaporites; 5 = some anticlinal hinge thickening of mud rock is indicated for the Cape de Bray formation; 6 = the crest of structures at deeper level. From HARRISON (1995, Figure 123).

Exemple d'un anticlinal de l'île de Meville. LRL = couche rigide inférieure; LDL = couche ductile inférieure; MRB = niveau rigide moyen; UDL = couche ductile supérieure; URL = couche rigide supérieure; 1 = synclinal dans le mur; 2 = anticlinal composite avec une charnière faillée en forme de selle; 3 = important amincissement du niveau "lower Bay" enveloppé par des évaporites; 5 = un faible épaississement de la charnière par des roches argileuses est montré pour la formation du Cape de Bray ; 6 = crête des structures localisées à un niveau inférieur. Tiré de HARRISON (1995, Figure 123).

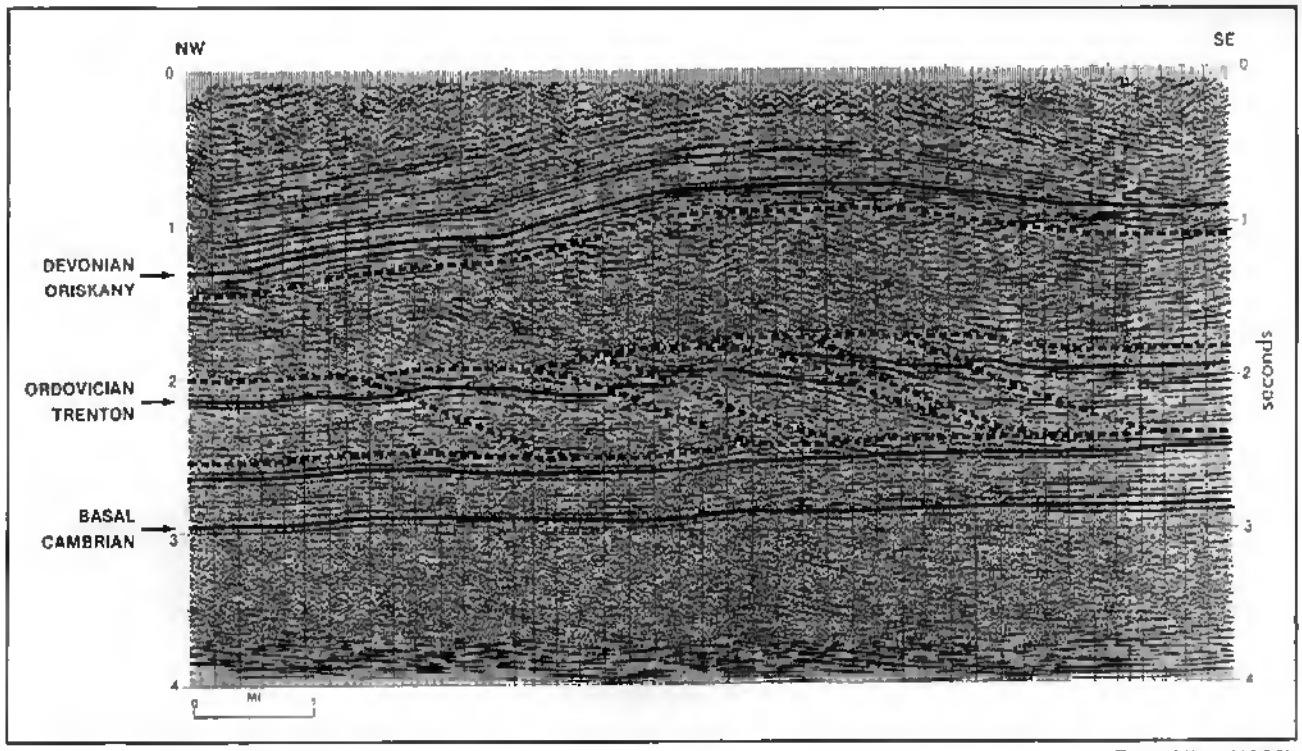

From Mitra (1986)

Figure 3.14: Migrated seismic profile across an anticline in the Appalachian Plateau (Pennsylvania). Devonian units are folded into a broad anticlinal arch cored by duplexes in Ordovician carbonates. Interpretation and figure are from MITRA (©1986, Figure 27, reprinted by the permission of the "American Association of Petroleum Geologists").

Profil sismique migré d'un anticlinal du Plateau appalachien (Pennsylvanie). Les unités du Dévonien forment une large arche anticlinale, remplie par des imbrications en duplex dans les carbonates de l'Ordovicien. L'interprétation et la figure sont tirées de MITRA (©1986, Figure 27, reproduite avec la permission de l'"American Association of Petroleum Geologists").

Concluding on the evaporite-related folds, it is suggested that the broad anticlines from the Plateau Jura are related to salt flow within the Triassic Unit 2, whereas Molasse Basin anticlines are related to well organized evaporite duplexes within the Triassic Unit 2. This difference is probably related to mineralogical composition and hence to the rheology of the Triassic evaporites. In the northern parts, considerable amounts of pure salt seem to be present within this formation, whereas in the southern parts its presence is not yet proven. Duplexes seem to have formed within the slightly more competent Triassic Unit 2 of the Jura internal parts and of the Molasse Basin.

In the preceding paragraphs, the geometry and the kinematics of evaporite pillows have been discussed. In terms of mechanism, buckling seems the most adequate for the observed structural style and rheology. The Triassic Unit 2, which consists of salt, evaporite and clay rocks, has a low viscosity in comparison with the overlying alternating carbonate and shale layers. These rheological conditions favor folding by flexural-flow. The weakest layer, Triassic Unit 2 (see Figure 2.30), flows into the core of the anticline presenting thickening of the unit, whereas the strong layers buckle without any thickness changes (concentric folds).

3.2.3. Thrust-related folds (high amplitude)

3.2.3.1. General comments

The sinusoidal shape of the Jura folds drawn by earlier geologists e.g. in DE MARGERIE (1922), HEIM (1921), RICKENBACH (1925), SUTER & LÜTHI (1969) (see Chapter 4 Regional geology) has been shown to be an oversimplification, not only in the central Jura, but also in the eastern (LAUBSCHER, 1977) and western Jura (PHILIPPE, 1994). In most places, at the surface, a veneer of Quaternary sediments obscures the critical relationships between strata and thrust faults. Seismic data have, however, confirmed that folds are related to major thrust faults. This relationship has been already suggested by different authors in the eastern and western part of the Jura (BUXTORF, 1916; LAUBSCHER, 1985; DIEBOLD *et al.*, 1991; PHILIPPE, 1994).

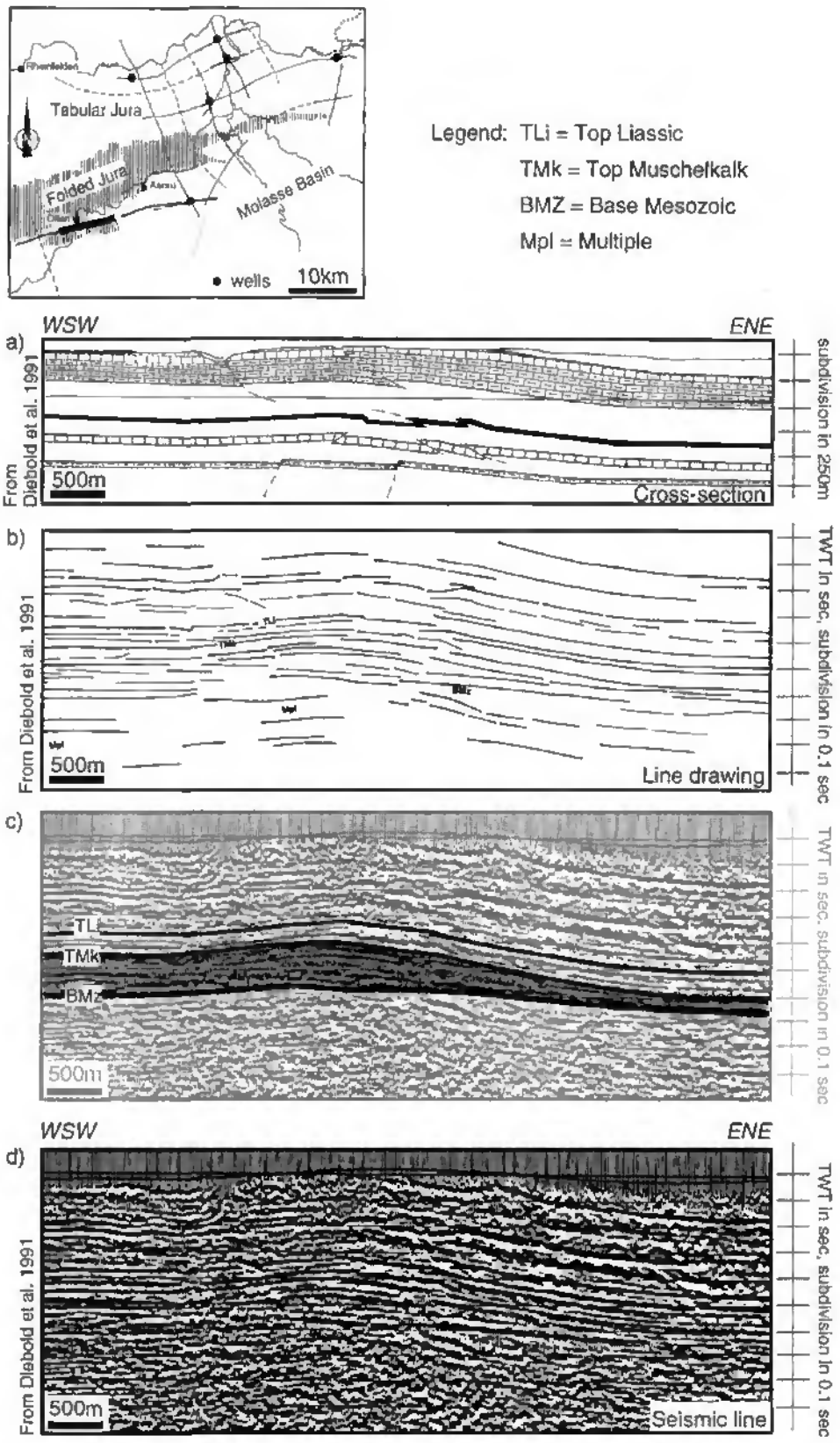

Figure 3.15: Strike seismic line from the Nagra work located in the eastern Jura (southern side). a) Geological cross-section. b) Line drawing of the seismic section. c) Interpretation of the seismic line. "Muschelkalk" layers, highlighted in gray, present a thickening (evaporite pillow) beneath the broad anticline. d) Seismic profile. The location is shown on the map. The seismic line, the line drawing and the cross-section are from DIEBOLD *et al.* (1991).

Profil sismique longitudinal et coupe géologique localisés dans le Jura oriental (partie méridionale). a) Coupe géologique. b) Réflecteurs du profil sismique. c) Interprétation du profil sismique. Les couches du "Muschelkalk", soulignées en gris, montrent un épaississement (coussin d'évaporites) sous le large anticlinal. d) Profil sismique, voir localisation sur la carte. Le profil sismique, le dessin et la coupe géologique sont tirés de DIEBOLD *et al. (1991).*

The observed scale of folding ranges from kilometers to meters. The first corresponds to large anticlines (regional scale), whereas the second consists of disharmonic folds, with metric wavelength (outcrop or minor scale). The latter are developed contemporaneously with the large scale structures. Disharmonic folding is observed between the stiff limestone beds and the weak marl layers (Fig. 2.30).

3.2.3.2. Geophysical evidence from seismic profiles

Generally the geophysical evidence for large subsurface thrusts includes duplication of coherent successions of seismic stratigraphic reflectors and velocity anomalies caused by tectonic duplication of strata higher in the section.

On many profiles, velocity anomalies are observed. The anomaly is usually a low positive deflection of the reflectors beneath anticlines (velocity pull-up) and a negative deflection beneath synclines (velocity pull-down). The dip Section 1 (Panel 1 and Plate 1) and Section 3 (Panel 1 and Plate 2) and the strike Section 8 (Panel 3 and Plate 3) from the Neuchâtel Jura illustrate such anomalies.

Recognition of repeated seismic stratigraphic reflections is the most common and evident form of identification of subsurface thrusts. Repetition, more obvious on lines parallel to the trend of the structures (strike lines), is one major reason for careful interpretation of seismic stratigraphy on strike lines. The lack of resolution often observed on dip profiles below the anticlines can be explained by many structural complications, but also by the steep topography. Strike Section 14 (Panel 3 and Plate 5) and dip Section 11 (Panel 2 and Plate 4) from the Neuchâtel Jura and strike Sections 80, 82 and 84 (Panel 8) and dip Sections 81, 83, 85, 87, 93 from the Risoux Jura document clearly duplication of reflectors. The Mt-Risoux anticline on Section 93 also shows duplication of the Jurassic series, confirmed by a well (WINNOCK, 1961) (Fig. 2.19).

3.2.3.3. Geometry of large scale folds illustrated by seismic profiles

Transverse lines crossing the Jura, oriented perpendicularly to the fold axes (NW-SE), allow to constrain of the fold geometry at depth. Line drawings of dip sections on panels 1, 2, and 9 illustrate the type of folds from the Haute Chaîne Jura (see Figure 1.2, for location on geological map). These high amplitude folds, which are asymmetric and are clearly related to thrust faults, root in the basal décollement zone located within the evaporites of the Triassic Unit 2. These thrust-related anticlines cause duplication of these Mesozoic stratigraphic layers. Thrust-related anticlines are separated by broad or tight synclines, Val de Ruz (Panel 1) and Val de Travers (Panel 2) respectively, which display flat lying, parallel layers.

Many thrust faults are NW (NNW) verging, like the main thrust system (foreland-vergent thrust). SE (SSE) vergent thrust faults are considered as backthrusts (hinterland-vergent thrusts). Thrust faults include both flats and ramps, e.g. Section 1 on Panel 1 or Plate 1, Sections 11 (Nouvelle Censière anticline, Plate 4, see also Fig. 4.7b), 13, 17 on Panel 2 (Neuchâtel Jura) and Sections 85, 111 (Mt-Risoux anticline, Plate 8), 95 on Panel 9 (Vaud and France Jura). In the flats, thrust faults are parallel to the overlying layers or parallel to the main décollement plane, whereas, in the ramps, the thrust fault cuts across the layers. All seismically mapped thrust faults are throughgoing to the surface, breaking through the structures in the steep frontal limbs e.g. Sections 1, 3 on Panel 1 and Section 11 on Panel 2. The leading edge of the thrust sheet may also show some imbrications e.g. Sections 5 and 7 on Panel 1.

Many backthrusts are associated with foreland-vergent thrust faults. They seem to be localized in kink or steep dip data zones, identified on geological maps e.g. Section 3 on Panel 1, Sections 11, 13, 17 on Panel 2 and Section 111 on Panel 9, but also appear to be connected to a main thrust fault at the transition between a flat and a ramp portion. Foreland-vergent thrusts have a kilometric dipslip displacement (e.g. Section 11 on Panel 2 and Section 111 -southern part- on Panel 9) and hinterland-vergent thrusts generally have few tens or hundreds of meters of displacements. Sometimes, as in the backthrust of the Mt-Risoux anticline (Sections 85, 111 -southern part- on Panel 9), a kilometric displacement can be observed.

The foreland-vergent thrust ramps have step-up angles between 20° and 30° (sometimes more), whereas backthrusts in the Neuchâtel Jura are much steeper (±60°) or else much shallower, as in the Vaud Jura (Mt-Risoux, Sections 85 and 111, southern part). These angles are approximate, because they are deduced from the seismic interpretations, which are displayed in TWT (seconds).

The Triassic Unit 2 evaporite layers are considered as the major regional décollement zone. The thrust ramps of the anticlines described above, root in this zone. Triassic Unit 2 layers appear very thick on the seismic lines (see line drawings on panels and Figure 2.30 of §2.6.). Formations beneath this very weak zone represent the basement. The term basement includes any rocks or sediments not involved in the formation of the overlying folds. The top of the basement appears as a smooth and flat surface dipping 1° to 3° to the S-SE (Fig. 5.1).

Some smaller scale thrust-related folds, e.g. the example of Figure 3.16, have a main thrust fault that roots in the lower Malm layers ("Argovian facies"). This figure is a dip line, located at the southwestern edge of the studied area, that crosses the transition from the Molasse Basin to the Jura Haute Chaîne. The thrust fault on this seismic line (Section 71, Fig. 3.16) is clearly documented by numerous flat reflectors (between B and C reflectors) cut by south-dipping reflectors. Unfortunately, this is the only example documented on seismic lines of the study area. Such minor scale folds are, however, already well known from surface geology (DROXLER, 1978; PFIFFNER, 1990) and will be discussed later.

In conclusion, the new seismic data confirm that large scale anticlines are formed above NNW vergent thrusts with kilometric dipslip displacement. Important thrusting results in duplication of the entire Jurassic stratigraphic sequence. These thrusts root in the basal décollement zone located in the evaporites of the Triassic Unit 2, which are surprisingly thick and clearly involved in the thrusting.

3.2.3.4. Minor scale deformation and disharmonic folds illustrated by outcrops

At the outcrop scale, deformation is brittle, characterized by stylolites, veins and small faults bearing slickensides. Deformation is localized within fold hinges and narrow fractured zones separating seemingly undeformed regions (limbs). Construction of a pilot tunnel below La Vue des Alpes (between the cities of Neuchâtel and La Chaux de Fonds, eastern Neuchâtel Jura, (Figs. 4.3 and 4.5) allowed Xavier Tschanz (from Neuchâtel University) to observe subsurface outcrops along a continuous profile of an anticline from the Neuchâtel Haute Chaîne Jura. This profile, running perpendicular to the fold axis and located along the same trace as the seismic Section 3 (Panel 1 and Plate 2), is more or less between intersections 4 and 2. Results from observation of fresh outcrops in the drilled tunnel are discussed in more detail in the paper by TSCHANZ & SOMMARUGA (1993). The rocks displayed surprisingly few deformation features. Vein volumes generally represent less than c.a. 0.5% of the rock and very few tectonic stylolites are present. The more intense deformations occurred only within sharp kink and hinge zones. These are characterized by an increased number of seemingly chaotic calcite veins, representing in places up to about 5% of the total rock volume. Locally, reverse and normal faults with a decimetric throw were identified. Meter scale offset faults are associated to the major kink and hinge zones. On seismic Section 3 (on Panel 1, 2 km North of intersection 4), these zones are interpreted as related to a backthrust. Bedding parallel slip surfaces are present along the whole anticline. Stylolites, veins, striae and twins are the expression of strain at the outcrop and sample scale, respectively and demonstrate strains at scales smaller than the wavelength of the folds.

At sample scale, calcite twin strain analyses in bioclastic coarse grained Dogger limestones from the Neuchâtel Jura (Val de Ruz), revealed small intracrystalline deformations on the order of 1 to 4% shortening. All twins observed in this study are thin and straight (micro-)twins. These microstructures are indicative of minor deformation at very low temperatures (<<150°C) (GROSHONG *et al.*, 1984; BURKHARD, 1993). This local study can be integrated with the regional study of TSCHANZ (1990), which presents the same results analyzed on calcite twins from the whole central Jura.

Minor scale décollement levels, producing small scale folds, observed at the base of the lower Malm marls ("Argovian" facies) and the Cretaceous (Hauterivian) marls (see Figure 2.30) are discussed in two cases below.

A detailed study at the outcrop scale has been made by PFIFFNER (1990) in lower Malm limestone and shale interlayered beds (for rheology, see Figure 2.30) at the frontal hinge of a large scale, SE-vergent anticline (St-Sulpice, western edge of the Val de Travers syncline, Neuchâtel Jura, see Figure 4.3 for location on the map). Figure 3.17 shows several zoom sections at different scales. The geological cross-section (Fig. 3.17b), located halfway between seismic Sections 13 and 15 (Fig. 3.17a), has been modified from that of Pfiffner. Seismic data has improved the geometry at depth and the thickness of the Dogger, Liassic and Triassic units.

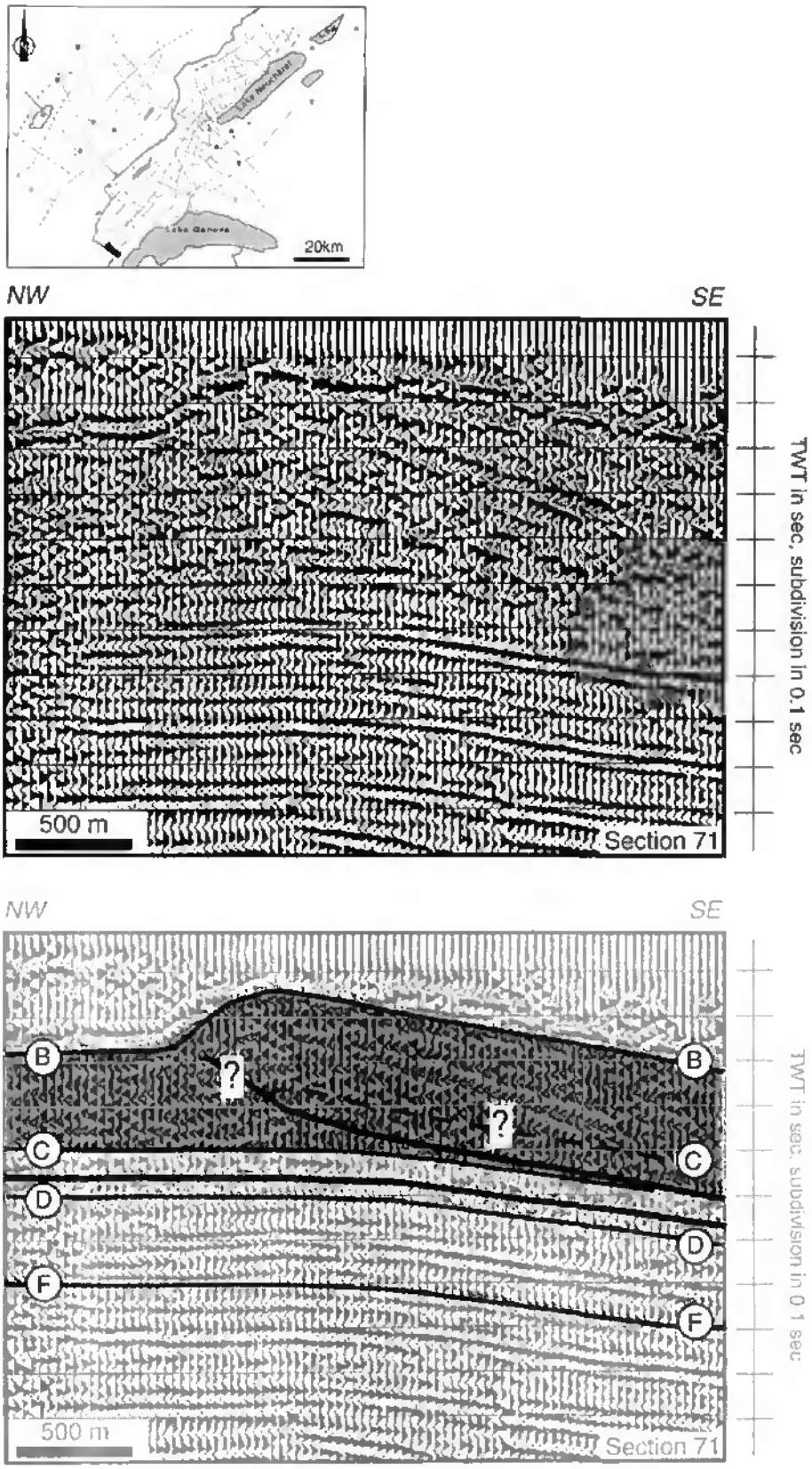

Figure 3.16: Portion of the dip seismic Section 71 located at the internal limit of the Jura Haute Chaîne. The interpretation shows a fold related to a thrust which roots in a minor décollement level at the base of the lower Malm unit ("Argovian" formation). Legend for the top of the layers: B = upper Malm; C = lower Malm; D = Dogger; F = Liassic.

Partie du profil sismique 71 transversal localisé à la limite interne de la Haute Chaîne jurassienne. L'interprétation présente un pli en relation avec un chevauchement qui s'enracine dans un niveau de décollement mineur à la base du Malm inférieur ("Argovien"). Légende pour le toit des couches: B = Malm supérieur; C = Malm inférieur; D = Dogger; F = Lias.

The seismic and geological sections show, at regional scale, a hinterland-vergent anticline related to a thrust fault, rooting in the main décollement level (Triassic Unit 2). The Val de Travers syncline shows two thrust faults in the Triassic units. This shortening is accommodated in the overlying layers by fish-tail structures. In the field, several disharmonic folds can be seen; these are of small wavelength and developed above a minor décollement level located in lower Malm shales ("Argovian") (Figs. 3.17c and 3.17d). According to PFIFFNER (1990, p.585), "individual limestone layers maintain compatibility within large scale structures by folding, bedding plane slip, conjugate contractional and extensional faults, and duplexes. The thickness of individual limestone layers appears not to be altered by a significant amount. Some of the contractional faults indicate considerable layer-parallel shortening in the early history of the folds. The ductile behavior indicated by round fold hinges is mainly linked to small scale faulting."

Metric and decimetric disharmonic folds are also common in the thin bedded limestones of the Lower Cretaceous (Hauterivian). A décollement level is present between the Cretaceous beds and the stiff Malm limestones, where strong disharmony in folding style is observed. Within the Cretaceous, décollement can also occur within the Hauterivian marls. The geometry and the kinematics of these folds have been analyzed in detail by DROXLER & SCHAER (1979) at one outcrop of the Neuchâtel Jura. According to these authors, ruptures induced by shearing and traction during the fold evolution have transformed the layers into semi-independent groups of fragments, the external geometry of which has been modified by dissolution in pressured zones. Part of the dissolved material in stylolitic planes is recrystallized in extension cracks.

These folds in the Cretaceous layers are attributed to Miocene thrusting e.g. in the Verrières syncline (Haute Chaîne Jura, France, Fig. 4.3) (MARTIN *et al.*, 1991), in contrast to the gravity sliding hypothesis ("collapse structure") suggested first by CASTANY (1947).

3.2.3.5. Interpretation of the thrust-related folds

In the Haute Chaîne Jura, high amplitude folds, though apparently simple, result from the superposition of a number of processes active at metric to kilometric scale. Stylolites, veins, striae and twins demonstrate strain at scales much smaller than the wavelength of the folds (§3.2.3.4).

Though the wavelength of the Haute Chaine fold-geometry seems to be determined by the thickness of the Malm layers, the overall rheology of the sedimentary cover (see Figure 2.30) has an important influence on the shape of Jura folds. The thickness of the sedimentary cover decreases from SW towards NE, so that higher amplitude folds are located in the southwestern area (higher topographic relief in Canton Vaud, Canton Geneva and in France), whereas in the East topographic relief is much lower (Canton Aargau and Jura).

The presence of a thick, very weak sole layer, in contrast with more competent overlying layers, also determines the fold type. The very weak zone consists of evaporites, salt and clays (see description and discussion in §2.6.2) of the Triassic Unit 2 layers. This interval shows clearly thickness changes in the Plateau Jura and the Molasse Basin. In the central part of the Haute Chaîne, this interval appears to be thick and of constant thickness in some synclines (Val de Travers and Val de Ruz, Sections 4, 6, 8 on Panel 3). In the northern part of the Neuchâtel Jura however, the La Brévine syncline (Section 2 on Panel 3) shows duplication of the Triassic Unit 2 along the whole valley, which may explain the high elevation (1000 m) of this syncline, in comparison with the Val de Travers and Val de Ruz synclines (600 m to 800 m). The poor quality of seismic data beneath anticlines does not allow for accurate interpretation. Although the combination of the interpretation of several dip and strike lines (seismic grid) suggests that the Triassic Unit 2 interval is thick, in some cases this thickness results from an obvious tectonic duplication.

The sedimentary cover of the central Jura represents a multilayer sequence with a thick and particularly weak layer at the base of the sequence, corresponding to the décollement zone. The overlying layers consist of alternating marls (incompetent layer) and limestones (competent strong layers, Fig. 2.30). A high viscosity contrast also exists between the very weak Triassic Unit 2 layer and the weak to strong overlying layers. The Haute Chaîne Jura folds were initiated first as buckle folds in response to the layer-parallel compression. Evaporites, clays and salt rock infilled the space generated at the base of the sequence by inflowing mechanisms. These first stage buckle fold, also called detachment fold, then developed into fault-propagation folds and fault-bend folds after breakthrough of thrusts, with progressive deformation. The deformation within the stiff layers is accommodated mainly by bedding-

plane slip, pressure solution and brittle faulting. The Chaumont (southern anticline on Sections 1 and 3 on Panel 1) and SomMartel anticlines (Intersection 2 on Section 5, Panel 1) are examples of detachment folds that evolved into fault-propagation style folds. On the geological cross-section of Figure 4.5, located more or less parallel to the seismic Section 3, the Chaumont anticline presents a breakthrough in the steeper forelimb (see High-Angle Breakthrough in SUPPE & MEDWEDEFF (1990). The anticlines of the Nouvelle Censière (Section 11 on Panel 2) and the Mt-Risoux (Section 111-87 on Panel 9) are examples of detachment folds developed later over a ramp - flat geometry (fault-bend fold style). Liassic marls favor minor décollement levels. Beneath the anticline, duplication of the Mesozoic cover is observed. In the study area, thrust-related folds are a mixture between the three types of fault-related folds described above.

DIXON & LIU (1992) have observed a similar evolution from centrifugal structural models; these represent a stratigraphic succession composed of six units with alternating bulk competency (low competence at the base). The models were subjected to horizontal, layer-parallel compression and show three mechanisms of shortening: layer-parallel shortening, buckling and thrust faulting. The relationship between folding and faulting evolves through time: firstly, detachment buckle folds form above a zone of décollement, secondly, a fault ramp propagates upward across the lowermost competent layers at the position of a foreland dipping limb (fault-propagation fold) and thirdly, when the fault has propagated through the competent unit its trajectory bends into the overlying incompetent unit and with further transport the hangingwall is modified by fault-bend folding. Limbs of the low-amplitude folds form shortly afterward, cut by foreland verging thrust faults.

The question, about the core infill of Jura anticlines, has been debated by geologists since the beginning of the century (BUXTORF, 1907). Using the same dip data, based on surface geology, several type of cross-sections have been drawn. As discussed by BITTERLI (1992), the core of an anticline may be filled by salt flow, duplexes, duplication of the entire cover over a thrust or thrust sheets presenting several generations of thrusting. In the absence of seismic data, several different methodologies have been tested in the Jura foreland fold and thrust belt, by different geologists, in order to answer this question: analogical modeling, comparison with other foreland belts, 2D and 3D modeling and new models of folding (BITTERLI, 1988; PHILIPPE, 1995).

In the central Jura (this work), the wealth of seismic data has allowed clarification of the geometry beneath the anticlines. The Haute Chaîne folds are first related to evaporite stacks within the Triassic layers and then evolved over thrust faults, which implies duplication of the Jurassic cover. In the Plateau Jura, the cores of the broad folds (not related to thrust) are filled with evaporite stacks.

For the southern French Jura, the recent PhD thesis of PHILIPPE (1995) interprets the evolution of folds as asymmetric detachment folds with salt flow that later evolve into fault-propagation folds. This is compared herein with analog modeling and with examples from the Canadian Rocky Mountain Foothills and Front Ranges described by DOBSON & MCCLAY (1992) and LANGENBERG (1992). Folds are first related to evaporite flow and then to thrust faults that duplicate the strata.

In the eastern Jura, cross-sections were constructed for many years in the style of lift-off folds (box folds), supported by thickening of lower Jurassic to Triassic sediments in their core, as drawn already by BUXTORF (1916) at the beginning of the century (see Figure 1.5, Section 2). However, modeling in two (balanced cross-sections) and three dimensions (block mosaic) of the geometry and the kinematics of one of these eastern anticlines (Weissenstein), has lead to a completely different interpretation (BITTERLI, 1990). The huge lift-off box folds are reinterpreted in terms of complex fault-bend folds presenting at least two generations of thrusting. However, these large thrusts are nowhere exposed at the surface.

LAUBSCHER (1986, 1992), using seismic evidence, has suggested that some of the eastern Jura box folds e.g. the Grenchenberg (Fig. 1.5) are supported by hinterland-dipping stacks, within the Middle Triassic Anhydritgruppe (= Triassic Unit 2) duplexes. Thrusts may be hidden in the subsurface.

In the eastern Jura also, JORDAN & NOACK (1992) have discussed the geometry of thrusts related to thick ductile soles. The model they propose differs from the classical fault-bend fold model, which has only a discrete sole thrust fault. The backlimb is much longer than the present ramp and has a lower backlimb angle with respect to the ramp angle. Several differences concerning rotation and migra-

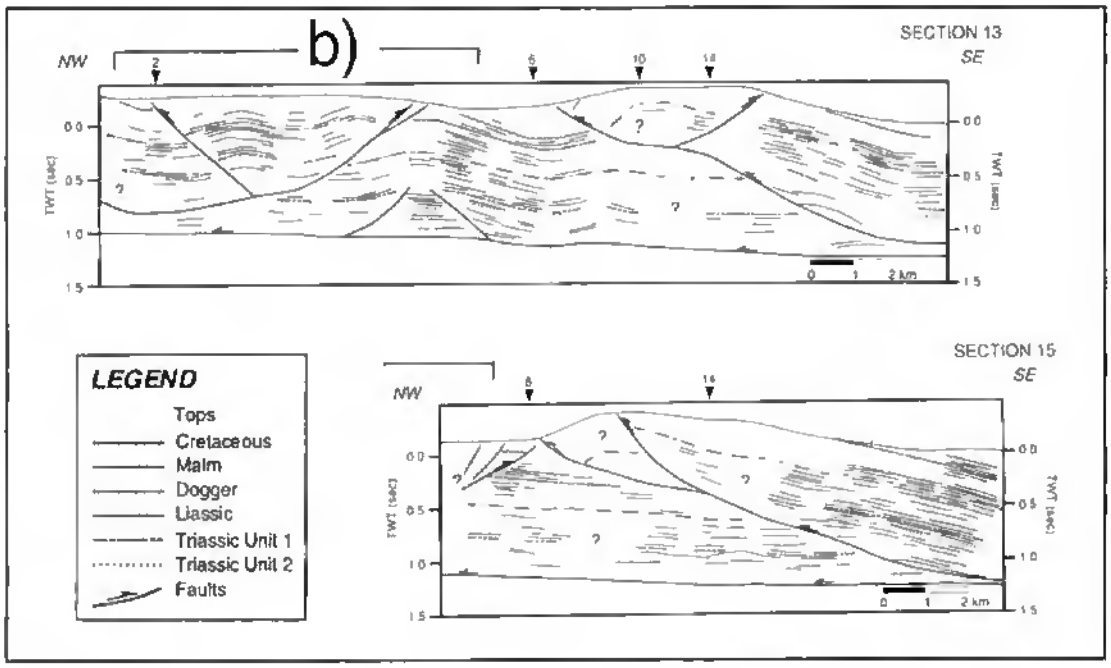

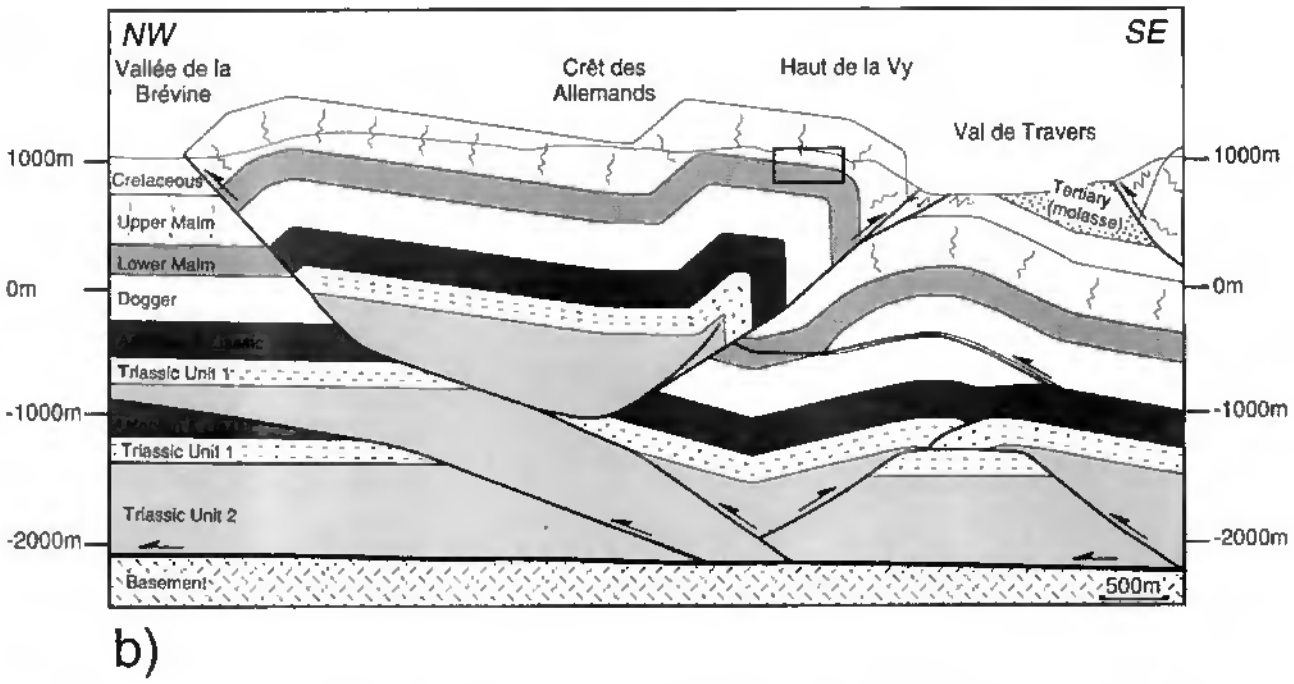

Figure 3.17 (pages 100, 101): Deformation at different scales in a hinterland-vergent anticline from the Neuchâtel Jura (Val de Travers area). Figures 3.17c and d are according to PFIFFNER (1990).

a) Line drawing (in TWT depth scale) of seismic Section 13 and 15 illustrating the regional scale.

b) Geological cross-section according to seismic interpretation and outcrop data. The rectangle shows the location of the small scale folds illustrated in Figure 3.17c. For location of the cross-section, see Figures 4.7b and 4.9.

c) Detailed cross-section showing relationships between meter scale folds and faults. Rectangle locates Figure 3.17d.

d) Detailed analysis (meter scale) of one of the small scale folds of Figure 3.17c.

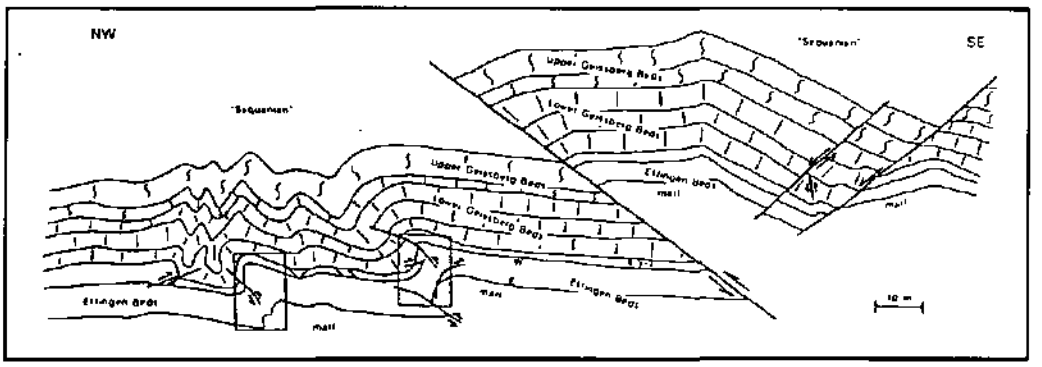

c)

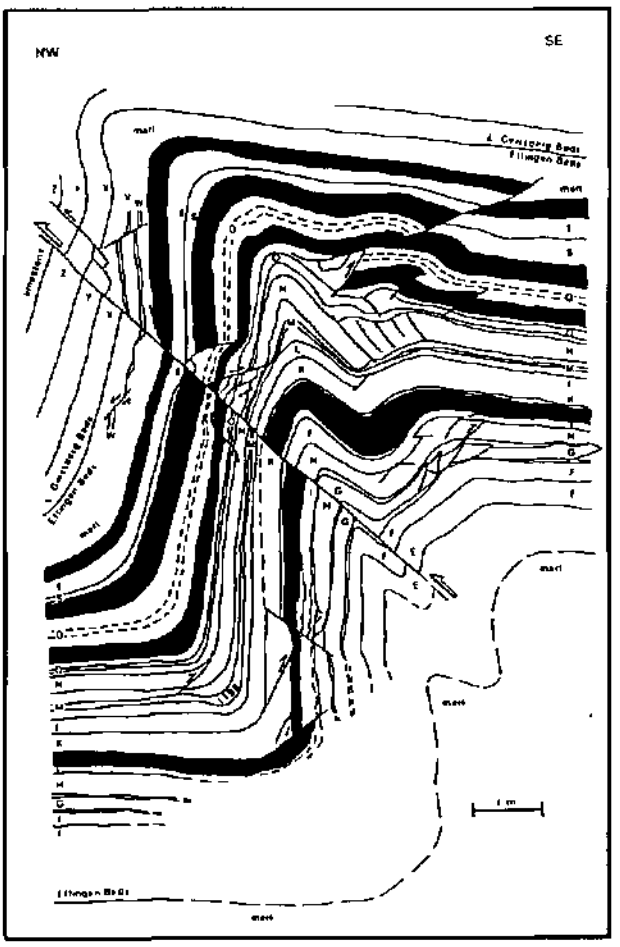

d)

Déformation à différentes échelles au sein d'un anticlinal à vergence vers le SE localisé dans le Jura neuchâtelois (Val de Travers). Figures 3.17c et d sont modifiées de PFIFFNER *(1990).*

a) Réflecteurs (profondeur en temps) des profils sismiques 13 et 15 (échelle régionale).

b) Coupe géologique en accord avec l'interprétation sismique et les données de la géologie de surface. Le rectangle montre l'emplacement des plis décamétriques illustrés dans la Figure 3.17c. Localisation de la coupe, voir Figures 4.7b et 4.9.

c) Coupe géologique détaillée montrant les relations entre les plis décamétriques et les failles. Le rectangle localise la Figure 3.17d.

d) Analyse détaillée d'un pli métrique de la Figure 3.17c.

tion of hinges are presented. In this model, a major part of the backlimb is deformed only by layer parallel slip, because it does not migrate through the flat-ramp hinge. These authors present some field evidence (a more or less intact backlimb), which seems to confirm the last point. This model also presents some features compatible with the central Jura, notably a thick ductile sole thrust and long shallow dipping backlimbs e.g. Chaumont anticline (Fig. 4.5).

In conclusion, the Haute Chaîne Jura folds of the central Jura developed first as buckle folds (detachment folds) and then evolved into fault-propagation or/and fault-bend fold types. The presence of a thick and very weak sole thrust and the final geometry of the folds has led to this model. The first stage buckle folds were most probably similar to the Plateau Jura evaporite-related folds. Seismic profiles are a good tool for understanding the geometry of the folds, but 3D kinematic modeling would allow to further constrain the geometry and also include the lateral continuation of the anticlines.

3.3. TEAR FAULTS

3.3.1. Definitions

In the following paragraphs, the general context of strike-slip faults is discussed first, followed by more specific discussion and definition of tear faults.

a) Strike-slip faults (sensu lato)

Strike-slip faults correspond to the end member of the spectrum in a kinematic classification of faults (Reid *et al.*, 1913). According to the definition of Bates & Jackson (1987), they represent "faults on which most of the movement is parallel to the faults' strike". They are generally vertical and accommodate horizontal shear within the crust or/and the lithosphere. Displacement along these faults may be either right-lateral or left-lateral. Sylvester (1988), reviewing strike-slip faults (Fig. 3.18), suggested that such faults can be classified either as transform faults, which cut the lithosphere as plate boundaries, or as transcurrent faults which are confined to the crust. The latter category, which includes indent-linked strike-slip faults, tear faults, transfer faults and intracontinental transform faults, is of particular interest in the study of thin-skinned fold belts, such as the Jura.

Indent-linked strike-slip faults juxtapose pieces of continental lithosphere, especially in zones of plate convergence and tectonic escape. They are not true transform faults, because they do not cut the lithosphere. Tear faults accommodate the differential displacement within a given allochthon or between the allochthon and adjacent structural units. They are generally oriented transverse to the strike of the deformed rocks and are sometimes called transverse faults or transcurrent faults. The term transfer fault is used for strike-slip faults that connect overstepping segments of parallel or en echelon strike-slip faults. Commonly located at the ends of pull-aparts, they transfer the displacement across a stepover from one parallel fault segment to the other. Intraplate or intracontinental transform faults are regional strike-slip faults, which are similar to indent-linked strike-slip faults in that they are restricted to the crust, but they need not to be genetically related to indentor tectonics. They typically separate regional domains of extension, shortening or shear.

Transfer faults and intracontinental transform faults are of larger scale than tear faults and also may accommodate larger amounts of slip (Twiss & Moores, 1992). Tear fault seems to be the appropriate term to characterize the strike-slip faults observed in the Jura.

b) Tear faults

To our knowledge, there is no generally admitted, precise definition of tear fault. In this paragraph, definitions proposed by different authors are presented to avoid confusion with this term.

Dahlstrom (1970) probably published one of the first definitions and classifications of tear faults: "a tear fault is a species of strike-slip fault which terminates both upwards and downwards against movement planes, that may be detachments or thrust faults or low angle normal faults". He distinguishes two basic types of tear faults: 1) transverse (primary or secondary) or oblique tear fault within a deformed thrust sheet; 2) tear fault as an integral part of a thrust sheet boundary. The first type is discussed below; for the second, one may refer to Dahlstrom's explanations.

In primary tear faults, the amount of shortening on either side is consistent, but the mechanisms may be different. Such compensated differences in rock shortening mechanisms demonstrate that the tear fault is an integral part of the structural fabric, which developed in the very early stages of deformation.

Secondary transverse tear faults provide a mechanism for transferring displacement between pairs of existent thrust faults. Such tear faults transect the intervening thrust sheet, thus permitting adjacent parts of the same thrust sheet to have markedly disparate displacements. Formation of these tear faults post-dates thrusting and they are therefore secondary phenomena.

According to the SYLVESTER's (1988) classification of strike-slip faults (Fig. 3.18), tear faults belong to the category of transcurrent faults found in intraplate settings (thin-skinned). For the exact definition of tear faults, Sylvester refers to BIDDLE & CHRISTIE-BLICK (1985): "a strike-slip fault or oblique-slip fault within or bounding an allochthon produced by either regional extension or regional shortening. Tear faults accommodate differential displacement within a given allochthon and adjacent structural units". In this classification, strike-slip fault as mentioned above, is not a specific term, but a generic term.

In structural geology books e.g. TWISS & MOORES (1992), the term tear fault is used in a general sense, describing as a small-scale, local strike-slip fault, that is commonly subsidiary to other structures such as folds, thrust faults, or normal faults. They are steeply dipping and oriented subparallel to the regional direction of displacement. They occur in the hangingwall blocks of low angle faults and accommodate different amounts of displacement, either on different parts of the fault or between the allochthon and adjacent autochthonous rocks. The discontinuity in displacement is then taken up by tear faults. Tear faults within a deformed sheet per-

CLASSIFICATION OF STRIKE-SLIP FAULTS

INTERPLATE (deep-seated)	INTRAPLATE (thin-skinned)
TRANSFORM faults (delimit plates, cut lithosphere, fully accommodate motion between plates)	**TRANSCURRENT faults** (confined to the crust)
Ridge transform faults* • Displace segments of oceanic crust having similar spreading vectors • Present examples: Owen, Romanche, and Charlie Gibbs fracture zones	Indent-linked strike-slip faults* • Separate continent-continent blocks which move with respect to one another because of plate convergence • Present examples: North Anatolian fault (Turkey); Karakorum, Altyn Tagh, and Kunlun fault (Tibet)
Boundary transform faults* • Join unlike plates which move parallel to the boundary between the plates • Present examples: San Andreas fault (California), Chaman fault (Pakistan), Alpine fault (New Zealand)	Tear faults • Accommodate differential displacement within a given allochthon, or between the allochthon and adjacent structural units (Biddle and Christie-Blick, 1985) • Present examples: northwest- and northeast-striking faults in Asiak fold-thrust belt (Canada)
Trench-linked strike-slip faults* • Accommodate horizontal component of oblique subduction; cut and may localize arc intrusions and volcanic rocks; located about 100 km inboard of trench • Present examples: Semanko fault (Burma), Atacama fault (Chile), Median Tectonic Line (Japan)	Transfer faults • Transfer horizontal slip from one segment of a major strike-slip fault to its overstepping or en echelon neighbor • Present examples: Lower Hope Valley and Upper Hurunui Valley faults between the Hope and Kakapo faults (New Zealand), Southern and Northern Diagonal faults (eastern Sinai)
	Intracontinental transform faults • Separate allochthons of different tectonic styles • Present example: Garlock fault (California)

*See Woodcock (1986, p. 20) for additional examples, both ancient and modern, and for their geometric and kinematic characteristics.

From Sylvester 1988

Figure 3.18: Classification of strike-slip faults from SYLVESTER (1988). See also WOODCOCK (1986).

Classification des décrochements (sensu lato) d'après SYLVESTER (1988). Voir aussi WOODCOCK (1986).

mit abrupt changes in the pattern of deformation through differential movement between component parts of the sheet. Displacement may be either right-lateral or left-lateral. Twiss & Moores define a strike-slip fault as a vertical fault that accommodates horizontal shear within the crust. Strike-slip faults exist on all scales, in both oceanic and continental crust.

In his glossary of thrust tectonic terms, McClay (1992) defines tear faults as strike-slip faults parallel to the thrust transport direction and separating two parts of the thrust sheet, each of which has a different displacement. He distinguishes a tear fault from a lateral ramp; the latter is a ramp in the thrust surface parallel to the direction of transport of the thrust sheet. Ramp angles are generally between 10° and 30°. He notes that if the lateral structure is vertical then it becomes a thrust transport parallel tear or strike-slip fault and should not therefore be termed a lateral ramp.

All these explanations or definitions highlight many geometric and kinematic peculiarities of tear faults admitted by most authors. In summary:

- *a tear fault belongs to an allochthonous sheet and has a transcurrent movement*
- *a tear fault terminates rightward and leftward into a thrust fault and downward into a décollement zone*
- *a tear fault is steeply dipping*:
  Lateral ramps like tear faults are subparallel to the transport direction. Tear faults have a subvertical fault plane, whereas lateral ramp fault planes dip 10° to 30° (Fig. 3.19).
- *the same amount of shortening may be accommodated differently on each side of the fault*
- *the formation of a tear fault may be earlier and contemporaneous to thrusting (primary tear fault) or subsequent (secondary tear fault)*:
  In primary tear faults, shortening may be accommodated differently on each side of the fault i.e. one thrust-related fold on one side may correspond to two thrust-related folds on the other side. In this case it is difficult to determine a sense of movement. Therefore on a geological map, the sense of movement of primary tear faults is only apparent and the true displacement will be deduced from restored maps or from fault/striae outcrops in the field. However, in the case of secondary tear faults, the sense of movement is real and fold axes are offset as passive markers.
- *the tear fault is oriented subparallel to the regional transport direction of displacement*:
  A regional transport direction is difficult to determine in fold and thrust belts, where no direct access to the basal thrust planes exists. Intuitively, transport direction is perpendicular to fold axes. But in many cases, local transport direction is oblique to the regional direction. Therefore it would be more appropriate to define the trend of the tear faults in comparison with the fold belt orientation.

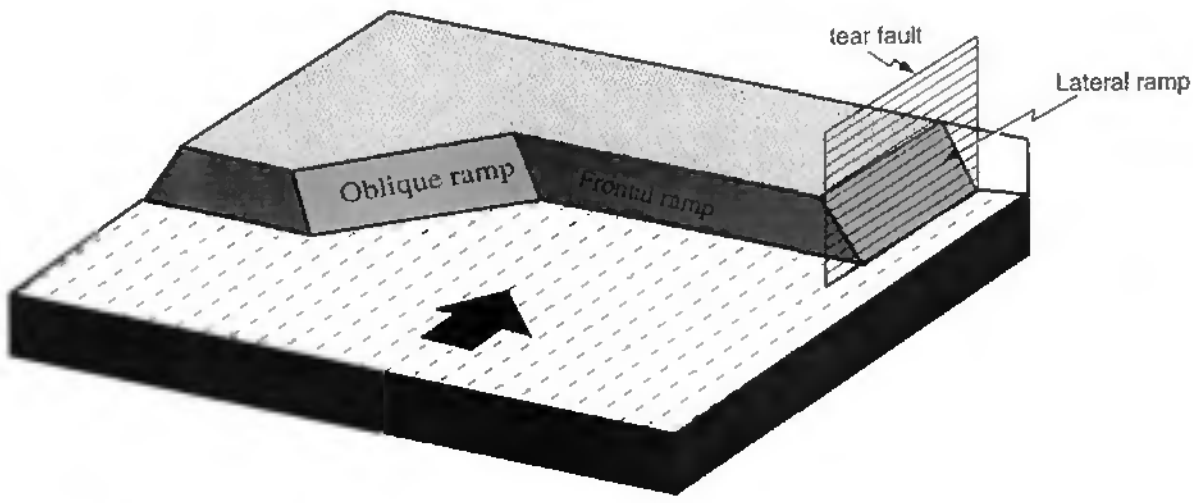

Figure 3.19: Three-dimensional view of a tear fault and different ramp types (lateral, frontal and oblique ramps).

Vue tridimensionelle d'un décrochement (sensu stricto) et de différentes rampes (rampes latérale, frontale et oblique).

Ramps are often associated with tear faults. There are basically three types of ramps: frontal, oblique and lateral (Fig. 3.19). These ramps are defined with respect to the regional transport direction, perpendicular, oblique and parallel respectively (APOTRIA *et al.*, 1992). Fault planes of these ramps generally show dips between 10° to 30°.

3.3.2. Geomorphological evidence

The tear faults in the Jura are well known from geological maps but can almost as well be recognized on topographic maps, where they have a clear morphological expression (Fig. 3.20). A close genetic relationship between folding and tear faults was postulated by HEIM (1915), who noted the radial arrangement of the tear faults when viewed on a map of the entire Jura arc. Major, apparently sinistral, tear faults are oriented NW-SE in the southern Jura, NNW-SSE to N-S in the central Jura and NNE-SSW in the eastern Jura (Fig. 3.20a). Somewhat shorter, apparently conjugate dextral tear faults are often associated. Folds, thrusts, sinistral and dextral tear faults define a set of structures compatible with a horizontal shortening in a WNW-ESE, NW-SE, and NNW-SSE direction respectively (LAUBSCHER, 1972, indenter model).

On the geomorphological map (Fig. 3.20b), tear fault traces appear to be straight lines even across rugged topography. Tear faults are marked by prominent continuous topographic features, such as narrow linear depressions. The topographically high part of the fault changes from one side to the other along the fault trace, because of the juxtaposition of different structures along the fault (synclines and anticlines) e.g. Pontarlier fault, or the juxtaposition of lithologies with different resistance to erosion. It is important to highlight this morphologic evidence, because as will be discussed below, seismic characterization of tear faults may be poor in some cases (e.g. La Ferrière fault, La Tourne fault).

In addition, geological maps present also evidence for tear faults; fold axes tend to terminate against tear faults and they do not have obvious direct correlation from one side of the fault to the other (see later discussion).

3.3.3. Geophysical evidence from seismic profiles

Generally, geophysical evidence for an important tear fault includes a transparent zone without reflections, a different succession of stratigraphic reflectors on either side of the fault and an offset of the corresponding seismic reflectors from one side to the other. The transparent zone may be wide or narrow (<1 km). On the studied lines, large transparent zones without reflectors are recognized in Panel 7 and Panel 8.

In this respect, seismic lines and cross-sections, are not ideal for the analysis of strike slip tectonics. Strike-slip faults are best analyzed on the horizontal plane of geological or geomorphological maps, which are natural sections at a high angle and contain the dominant displacement vector. Strike-slip faults may produce a series of characteristic features on seismic sections such as the well known positive and negative flower structures. Positive identification of such structures is not easy, however, and would ideally require a three-dimensional survey or at least a series of lines across the same fault zone.

3.3.4. Examples illustrated by seismic profiles

Some seismic lines cross major mappable Jura tear fault zones, e.g., the Morez (France), Mouthe (France), Pontarlier (France-Switzerland), Mt Chamblon-Treycovagnes (Canton Vaud), La Tourne and La Ferrière-Vue des Alpes (Canton Neuchâtel) zones (Fig. 3.19; Panel 3, 5, 6, 7 and 8). On seismic lines, it can be seen that these faults affect the whole Cenozoic and Mesozoic layers of the Jura and Molasse Basin cover.

In the Canton Vaud, seismic data, crossing the southern part of the major Pontarlier tear fault, are of high quality on both sides of the fault (Panel 7). Section 46 (Panel 7) displays a succession of well layered reflectors, whose stratigraphic interpretation is well constrained laterally. From one side to the other, stratigraphic thickness changes are observable within the Dogger - Liassic beds and within the Triassic Unit 2 layer. The latter is thicker on the western side of the fault, which may explain the higher elevation for the same beds on the western side of the fault. Section 50 (Panel 7) presents also a succession of layered reflectors on both sides of the tear fault. They are unfortunately not well constrained by other seismic lines (Figs. 1.4 and 4.1). The attempted interpretation shows a thickening of the Malm and the Triassic Unit 2 layers on the western side of the fault.

Further north, in the Lake Joux area (Panel 8), the quality of seismic data along the Pontarlier tear fault

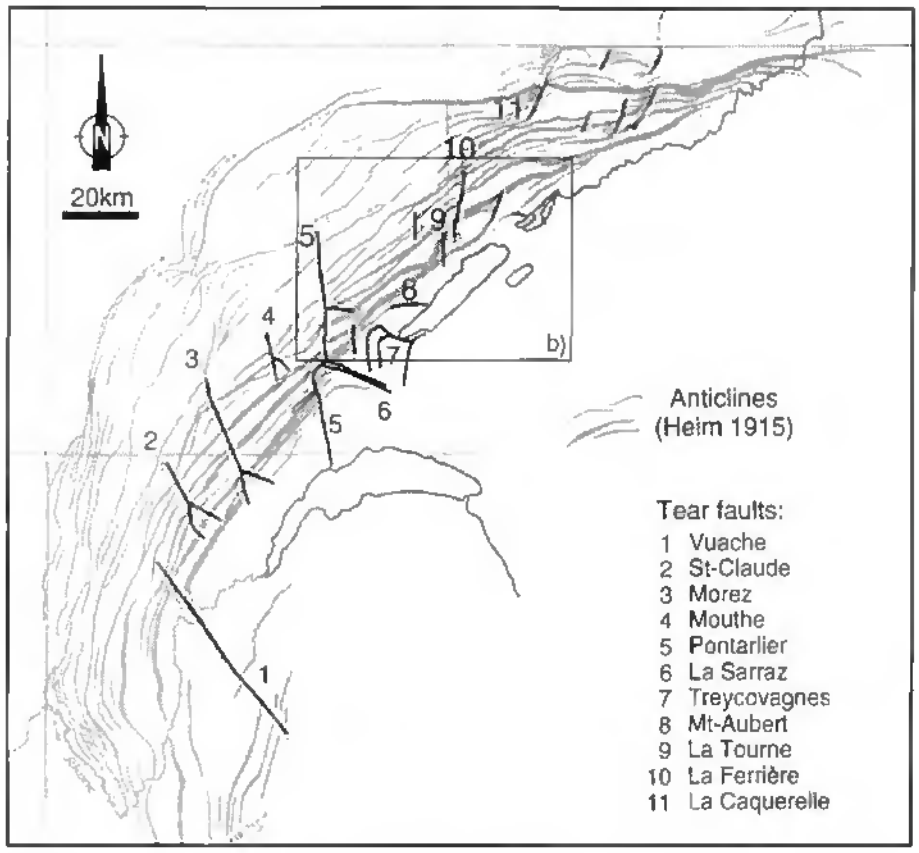

a)

b)

Figure 3.20:
a) Location of tear faults on Jura anticline map drawn by Heim (1915).
b) Geomorphological evidence of tear faults in the central Jura.

a) Situation géographique des décrochements sur une carte des axes des anticlinaux de Heim (1915) de la chaîne du Jura.
b) Evidence géomorphologique de décrochements dans le Jura central.

is poor. Unfortunately the seismic lines end close to the fault. In this case, no stratigraphic correlation is possible on the western side of the fault. The Sarraz tear fault forms the conjugate dextral system to the sinistral Pontarlier fault and is displayed on Section 26 (intersection 36, Panel 4) and on Section 36 (intersection 26, Panel 6). Along the Pontarlier tear fault, seismic data do not give evidence for basement offsets. The tear fault appears to terminate in the décollement level of Triassic Unit 2.

The Yverdon area (Figs. 1.2, 1.4 and 4.3) is another region with conjugate tear faults (JORDI, 1993). Recently, a careful structural investigation (CHYN, 1995) for hydrogeological purposes has led to a detailed interpretation of seismic lines in this region (Section 27 on Panel 5; Section 38 on Panel 6). The regional setting and results will be discussed in Chapter 4. These faults appear to be tear faults and thrust faults. The associated structure is a fold related to a northward-vergent thrust, cutting the frontal fold limb (Fig. 4.18). Thickness changes within the Dogger beds are observable, showing a thickening towards the South. This local change (not clearly visible on the regional isopach maps of the western Molasse Basin, Fig. 2.26) may be due to lateral facies changes.

In the Neuchâtel area, seismic data along tear fault zones of La Tourne (Section 7 on Panel 1 and Section 4 on Panel 3) and La Ferrière-Vue des Alpes (Section 3, Panel 1) are of poor quality, probably due to the presence of an anticline on one side of the faults. These faults appear on seismic lines as transparent zones. No offset of the basement top on either side of the fault could be detected from contour maps. Accordingly, these faults are either tear faults restricted to the cover or lateral ramps. No evidence for an extension of these faults into the basement could be found.

3.3.5. Description from outcrops

Four major, N-S oriented tear faults are found within the study area (Fig. 3.20): Pontarlier, La Tourne, La Ferrière and Treycovagnes. All these faults have apparent sinistral offsets of a few hundred meters and their traces can be followed over several kilometers. Conjugate dextral faults e.g. La Sarraz, Mt-Aubert oriented 120° are associated with them.

In addition to these large, map scale tear faults, an important number of minor faults are observed in the competent lithologies of the central Jura e.g. (LLYOD, 1964). These minor faults have a less important throw (on the meter scale) and crosscut anticlines, but they are often too small to appear on geological maps. The poor outcrop quality, in many parts of the Jura, usually prohibits the direct observation of the effect of such minor structures on geological limits.

In the Val de Ruz (Neuchâtel Canton), small scale (cm to dm offsets) striated faults are ubiquitous in limestones and most outcrops show a sufficient number (>20) of fault/slickenside pairs for statistical determination of "paleo-stress" or strain axes directions. TSCHANZ & SOMMARUGA (1993) conducted a kinematic analysis of fault/slickenside pairs using ANGELIER & MECHELER's (1977) right dihedra method. Similar observations have been made in other parts of the Jura and have led different authors (DROXLER & SCHAER, 1979; LAUBSCHER, 1979; PFIFFNER, 1990; TSCHANZ, 1990) to independently draw a comparable schematic diagram of the relation between faults and folds (Fig. 3.21). Strike-slip and thrust faulting occurs during the early stages of folding and is interpreted as due to large parallel shortening preceding folding. During fold amplification, these earlier faults are passively rotated with the fold limbs and partly reactivated to accommodate internal deformation related to folding.

Fault/slickenslide analyses from the vicinity of large strike-slip movement zones indicate systematically subhorizontal movement directions, despite variable bedding orientations. Horizontal striations on vertical fold limbs are frequently observed (e.g. La Tourne or La Ferrière-Vue des Alpes) and clearly indicate that some fault motion post-dates folding. Local maximum compression axes, determined from fault/slickenside pairs and twin strain analyses, are systematically oriented subperpendicular to the local fold axis trend, but major discrepancies exist between this general NW-SE compression direction and the map scale fold axis trends.

Fault/slickenside analyses preferentially measure late (with respect to folding) strain increments, due to the sampling of fault planes, because late, subvertical tear faults are much easier to detect in the field than supposedly earlier, layer-parallel fault planes. The predominance of subhorizontal shortening and extension directions as determined from fault/slickenside pairs is partly due to this sampling effect. Nevertheless, the results show that NNW to NW directed shortening was active throughout the fol-

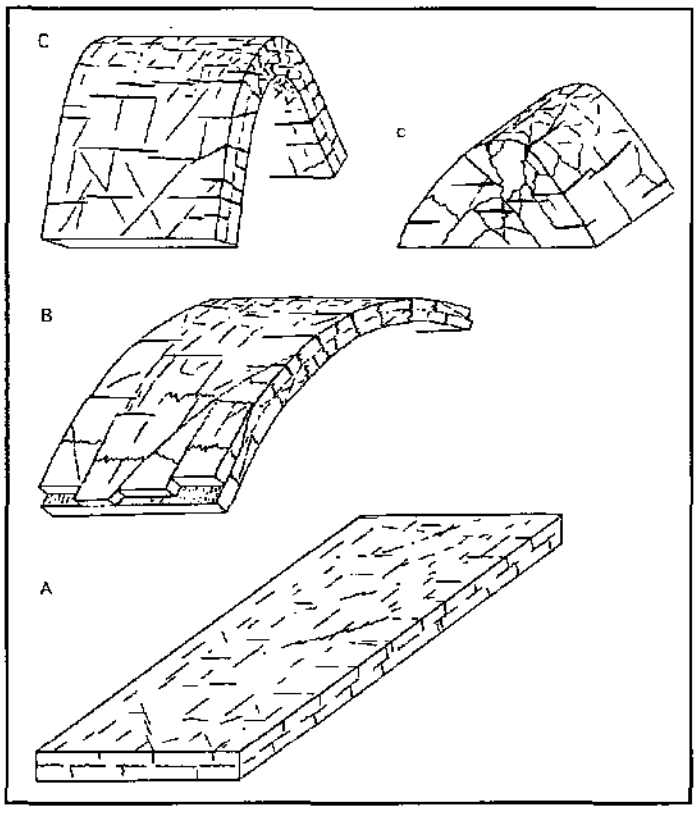

From Droxler & Schaar 1979

Figure 3.21: Relation between faults and folds during amplification of a metric fold in limestone rocks. A) Layer parallel shortening before folding; B) Fold amplification, 30% shortening; C) 60% or more shortening. From DROXLER & SCHAER (1979).

Relations géométriques entre faille et pli durant la mise en place d'un pli métrique dans des roches calcaires. A) Avant le plissement, lorsque le raccourcissement est parallèle aux couches; B) Durant l'évolution du pli, lorsque 30% de raccourcissement est observé; C) à 60% ou plus de raccourcissement. Tiré de DROXLER & SCHAER (1979).

ding history. This shortening seems to be still active today, as evidenced by in situ stress determinations (BECKER, 1987; BECKER, 1989; SCHAER *et al.*, 1990; BECKER & WERNER, 1995) and focal mechanisms from earthquakes (PAVONI, 1984; DEICHMANN, 1992). According to Deichmann, the focal mechanisms are of strike-slip or normal fault type, indicating a regional shortening with a NNW-SSE orientation, roughly perpendicular to the strike of the Alpine and Jura belt and a corresponding WSW-ENE extension parallel to the main axis of the Molasse Basin. Hypocenters below northern Switzerland are distributed throughout the entire depth range of the crust. This distribution of focal depths contrasts with what is observed below the Alps and in most other intracontinental settings.

3.3.6. Interpretation of the central Jura and Molasse Basin tear faults

Major tear faults (from West to East: Vuache, Morez, Pontarlier and La Ferrière, Fig. 3.20) cut the Jura belt at angles of 60°-70° to the fold axes. Many minor faults are associated to the major ones. All these faults have an apparent sinistral movement and change from a NW-SE to N-S trend along the Jura arc. Conjugate dextral sets of tear faults are less developed, nevertheless, the Sarraz and the Treycovagnes faults are good examples. The major tear faults are located in the Haute Chaîne Jura and are connected to thrust planes at the transition Haute Chaîne - Plateau Jura. On seismic lines these faults represent important transparent zones, indicating that these faults are characterized by broad deformation zones.

Folds tend to terminate against tear faults and do not match from on side of the fault to the other (e.g. Pontarlier fault, Fig. 3.22). AUBERT (1959), LAUBSCHER (1965), PHILIPPE (1995) and SCHÖNBORN (1995) have attempted correlation from one side of Pontarlier fault to the other. Each author has proposed a different correlation, requiring lengthy arguments to justify a far from obvious choice. Most probably, there is no match to be found because shortening was accommodated by different fold trains on either side of the fault. These observations lead to the interpretation of the Pontarlier fault as a primary tear fault, i.e. differential movements along this fault occurred during folding (DAHLSTROM, 1970). Fault/slickenside outcrop observations on tear faults cutting anticlines show that striae dip is rarely bedding parallel on the vertical limb, but is mostly horizontal. The latter observation favors post-folding movement along the fault. Although offsets of geological limits appear to be mostly

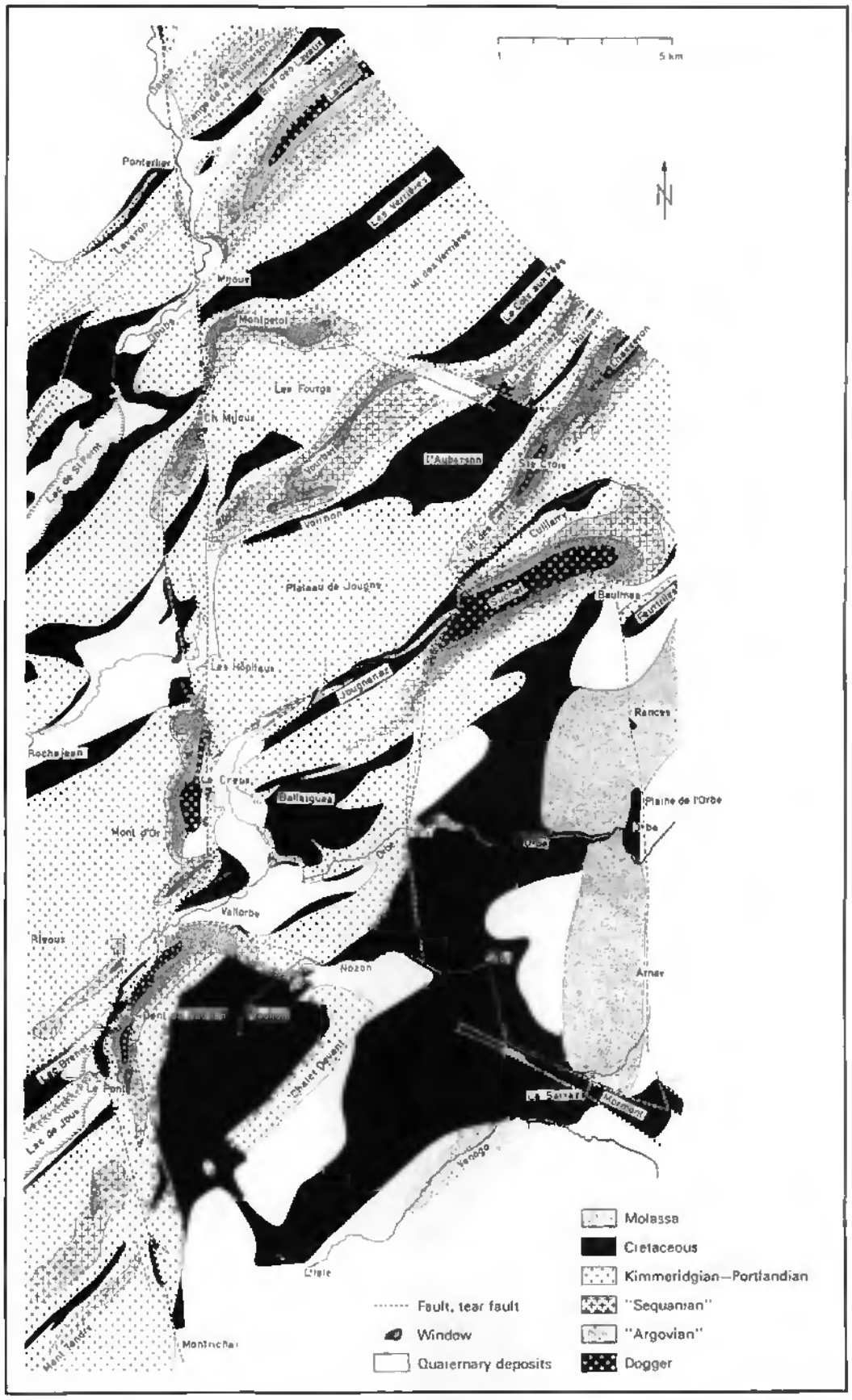

From Aubert 1959

Figure 3.22: Simplified geological map along the Pontarlier tear fault (see for location Figures 1.2 and 3.20). From AUBERT (1959).

Carte géologique simplifiée le long du décrochement de Pontarlier (pour localisation voir Figures 1.2 et 3.20). Tiré de AUBERT (1959).

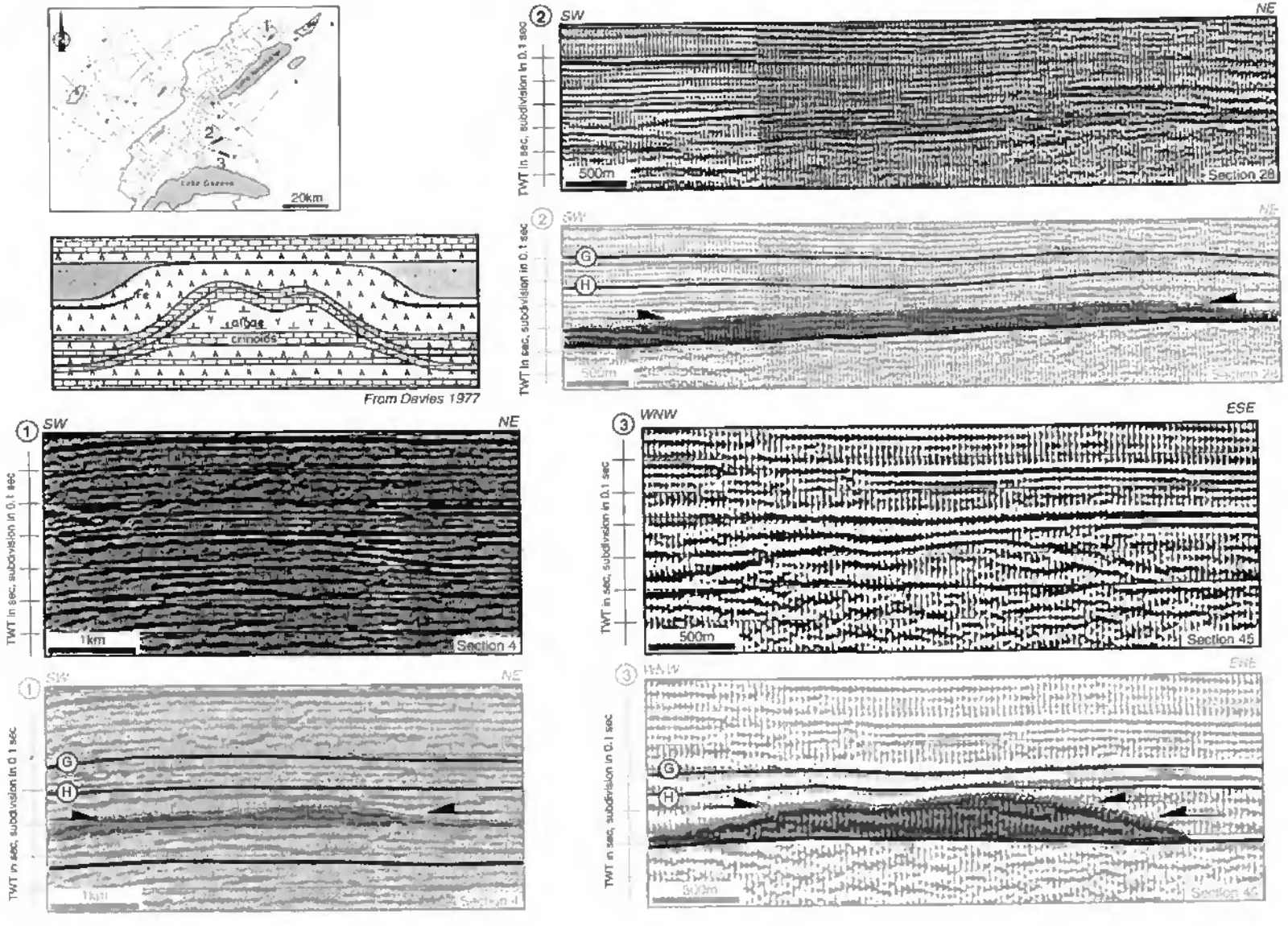

Figure 3.23: Portions of seismic lines showing oblique reflectors in the Triassic Unit 2 interval, which is not thickened. These features do not affect the overlying strata by buckling and could be interpreted as reef-like features in comparison with the algal mound developed in carbonate-anhydrite facies in the Canadian Arctic Archipelago (DAVIES, 1977) or as dissolution effects (see text for discussion). Legend for the top of the layers: G = Triassic Unit 1, H = Triassic Unit 2.

Portions de profils sismiques montrant des réflecteurs obliques dans l'intervalle de l'Unité 2 du Trias, qui n'est pas épaissie. Ces particularités dans le Trias n'affectent pas les couches sus-jacentes en les plissant. Elles peuvent être interprétées soit comme des structures récifales, en les comparant aux accumulations algaires développées dans les faciès évaporitiques carbonatés de l'Archipel arctique canadien (DAVIES, 1977), soit comme le résultat d'effets de dissolution (voir texte pour discussion). Légende pour le toit des couches: G = Unité 1 du Trias; H = Unité 2 du Trias.

sinistral on the map scale, there is no objective way to determine absolute displacements along this tear fault, because folding occurred at least partly syn-faulting. It is therefore concluded, that the Jura tear faults show mainly syn-folding and post-folding movement.

In this study, no evidence for deeply rooted strike-slip faults has been observed on the seismic sections. Faults root in the main ductile zone (Triassic Unit 2) and apparently do not offset the underlying basement. HEIM (1921, p.614) already suggested that tear faults rooted in the cover only. Consequently, these faults have been correctly named as tear faults, because they belong to an allochthonous sheet.

3.4. "REEF-LIKE" FEATURES

As explained in preceding paragraphs, the Triassic Unit 2 interval varies in thickness and often presents oblique reflectors on the seismic lines. Some of these features have been interpreted as tectonic structures (duplexes, see Figure 3.8 and Fig. 3.12) just above the main décollement horizon. They show a thickening within the Triassic Unit 2, with folds in the overlying beds. However, other examples that also show oblique reflectors in the Triassic Unit 2 layer, are not associated with thickening in the Triassic beds or buckling of the overlying strata (Fig. 3.23); accordingly, they seem to be formed during Triassic times. The nature of these features is the subject of this section.

These features resemble biogenic reef structures or algal mounds like those of Mississippian-Pennsylvanian age, found in carbonate-anhydrite facies from the Canadian Arctic Archipelago (DAVIES, 1977) (Fig. 3.23). The Zechstein salt facies also show this type of feature. JENYON & TAYLOR (1987) and TAYLOR (1993) discuss the possible confusion of such features with buildups and propose the terms "reef-like features" or "pseudo-reefs", respectively. According to Jenyon & Taylor, some of these positive features resting on basal Zechstein, consist of material of much higher velocity than salt and may be bryozoan-algal reefs from their shape and location. However, it is equally possible that they may be primary or relict pods of anhydrite resulting from dissolution and removal of the surrounding salt. For Taylor, the mound-like features are related to swelling in Zechstein evaporite intervals. Virtually all are situated below former pillows in the overlying salt and many are related to faults. Careful seismic interpretation in the Zechstein basin reveals that the reflector defining the top of these structures is broken into segments, each of which is offset. In many cases, there is no velocity anomaly beneath these pods. Therefore the included material should have more or less the same velocity as the adjacent rocks. Pure salt (~ 4500 m/s) does not have the same velocity as carbonates (~5500 m/s to more than 6000 m/s), whereas anhydrites may be in the same range of velocity as carbonates.

Algal mounds within the German Triassic facies are not known from field observations (A. Baud at the Musée de Géologie in Lausanne, oral communication). However, only very few Triassic beds crop out in the Jura Mountains and none in the Molasse Basin. Even in areas where Triassic strata crop out, such as around the rim of the Vosges and Black Forest, evaporite (NaCl)-bearing series are exceedingly rare at outcrop and always strongly perturbed by surface weathering. In the absence of high resolution seismic lines and with the sparse drill hole information available, it is impossible to discard any of these hypotheses. This issue is not without bearing on the hydrocarbon potential of the area: carbonate buildups within evaporite series, if present, may be interesting traps.

4. REGIONAL GEOLOGY

4.1. INTRODUCTION

In this Chapter the lateral continuity of structures in the central Jura and the Molasse Basin is discussed, supported by regional examples. The availability of a dense seismic grid (Fig. 4.1) has given the opportunity to follow, at large scale, the structures along their strike. Interpretation of dip and especially strike seismic lines highlights some large scale continuities and/or discontinuities in the structures. Rather than presenting lengthy details of folds, thrust faults and ramps, in order to discuss the lateral continuity of the central Jura structures, we will emphasize some characteristics of the Jura and Molasse Basin anticlines and synclines. This Chapter is subdivided into regions (Neuchâtel Jura, Risoux Jura, Champagnole-Mouthe region, western Swiss Molasse Basin; for location see Figures 1.3 and 1.4), because the structures turn out different from one area to another.

4.2. NEUCHÂTEL JURA

4.2.1. Previous studies

Too many authors have worked on the structures of the Neuchâtel Jura to give due credit to all of them and cited here are but some of the major works that have contributed to a better understanding of the geology in Neuchâtel Canton.

During the 19th century, pioneers of Jura geology are von Buch, Thurmann, De Montmollin, Desor and Gressly. VON BUCH (1867) is best known for his cross-section of 1803 from the Alps to the Jura (see comments in §1.4) and also in the Neuchâtel Jura for his drawing showing the profile and the plunge of an anticline (Chaumont). THURMANN (1836a, 1856) made a morphological map of the whole Jura and DE MONTMOLLIN (1839) published the first geological map of the whole Neuchâtel Jura. DESOR & GRESSLY (1859) presented a detailed 1:25'000 scale map. Other interesting contributions of authors working for the second Neuchâtel Academy have been recently reviewed by SCHAER (1994).

Contributions on the Jura Mountains from the beginning of this century are collected in the review of HEIM (1921), DE MARGERIE (1922, 1936) and BAILEY (1935). Key references for the Neuchâtel Jura are SCHARDT (1906), SCHARDT & DUBOIS (1903), RICKENBACH (1925), FREI (1925, 1942), THIÉBAUD (1936), KIRALY (1969) and MEIA (1969). More recently, published and unpublished works (Diploma, PhD thesis and maps deposited at the Neuchâtel University, see Tab. 1.1) have contributed to increase the knowledge of the surface and subsurface geology of the Neuchâtel Jura.

The cross-section of SCHARDT & DUBOIS (1903) (Fig. 4.2) is of particular interest for the Neuchâtel Jura, because it crosses the Creux du Van anticline and the Areuse syncline (Fig. 4.3). Beyond the fact that the Creux du Van anticline is formed over a foreland-vergent thrust, with a vertical northern limb, the top of the anticline shows an impressive steep cliff resulting from a glacier cirque development. For details about glacial deposits and the Quaternary history, the reader is referred to the appropriate literature (RITTER, 1888; DU PASQUIER, 1893; AUBERT, 1965; MATTHEY, 1971).

4.2.2. Eastern part

The geology of the Neuchâtel Jura is shown on the tectonic sketch of Figure 4.3. The geological units of this map have been compiled from several 1:200'000 scale tectonic sketches of 1:25'000 map sheets (see Tab. 1.1). Many tear faults appear in the eastern part, in contrast to the West. This is in part due to the different style of mapping from author to author. Many thrust faults have been added on this general map, following our interpretation of seismic lines, e.g. in front of the Chaumont anticline. At the surface, most thrust faults are capped by a veneer of Quaternary sediments and therefore it is sometimes difficult or impossible to locate them exactly in the field.

In the eastern part of the Neuchâtel Jura, the tectonic sketch highlights thrust-related anticlines with

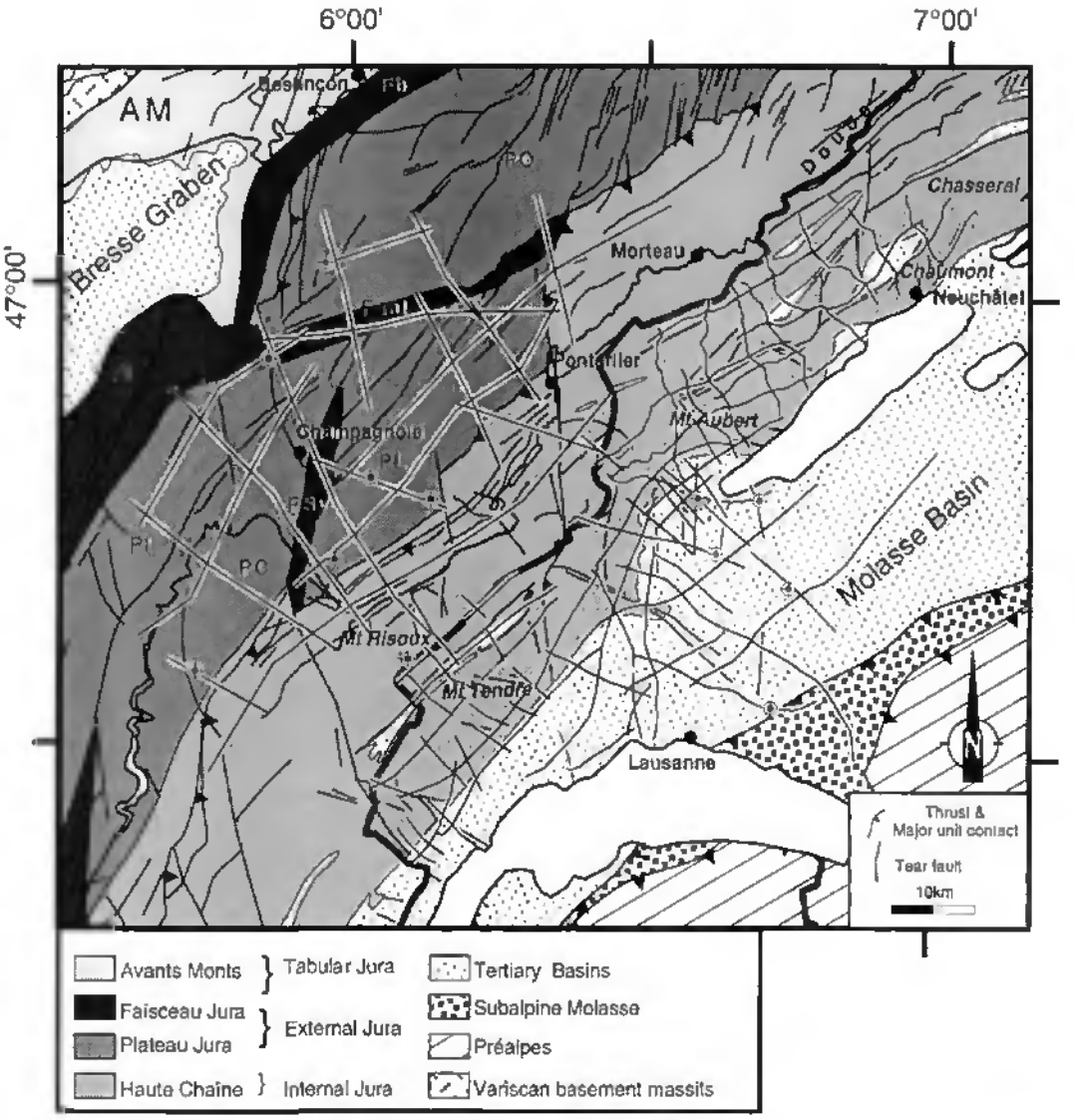

Figure 4.1: Seismic grid located on a tectonic sketch of the central Jura and the western Molasse Basin. Legend: AM = Avants-Monts; Fb = Faisceau bisontin; Fl = Faisceau lédonien; Fsal = Faisceau salinois; FSy = Faisceau de Syam; PC = Plateau de Champagnole; PL = Plateau de Levier; Pl = Plateau lédonien; PO = Plateau d'Ornans.

Grille sismique reportée sur la carte tectonique du Jura central et du Bassin molassique occidental. Légende: AM = Avants-Monts; Fb = Faisceau bisontin; Fl = Faisceau lédonien; Fsal = Faisceau salinois; FSy = Faisceau de Syam; PC = Plateau de Champagnole; PL = Plateau de Levier; Pl = Plateau lédonien; PO = Plateau d'Ornans.

a lateral continuity of about 10 km. Anticlines appear to end against tear faults (La Tourne and La Ferrière faults) and have axes oriented either ENE-WSW or NNE-SSW. The combination of both orientations results in rhomb shaped structures such as the Val de Ruz basin and the Le Locle syncline. The relationships between both trends are enhanced on the three-dimensional structural contour map representing the base of the competent upper Malm layer (top "Argovian") in the Neuchâtel Canton (Fig. 4.4a).

The rhomb shaped structure of the Val de Ruz basin, with sharp bends of more than 35°, has been analyzed at different scales by TSCHANZ & SOMMARUGA (1993) in order to better constrain the various possible models for its development. Detailed structural studies within the differently oriented portions of the anticlines show that ENE-WSE trending anticlines are formed as cylindrical folds, whereas the NNE-SSE trending anticlines are non-cylindrical, with important discrepancies of up to 30° between measurable strike (bedding and local

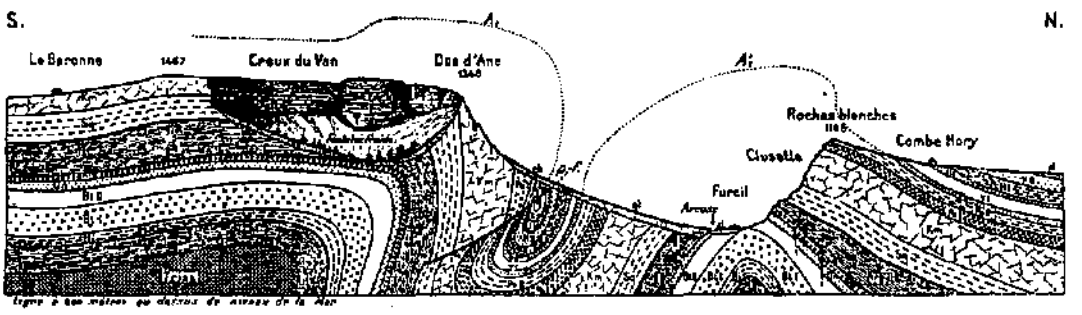

Fig. 92. — Coupe du Creux du Van et de la Vallée de l'Areuse, d'après H. Schardt et Aug. Dubois (*Eclogae Geol. Helv.*, VII, n° 5, pl. 13, Profil 1, 1903).

Échelle de l'original 1 : 15 000. Réduction à 1 : 30 000.

Légende. *Jurassique* : L. Lias; Bj. Bajocien; Bt I. Bathonien inférieur; Bt II. Bathonien supérieur; Dn. Dalle nacrée (Callovien); Arg I. Argovien inférieur (Spongitien); Arg II. Argovien supérieur; Sq. Séquanien; Km. Kimeridgien; Po I. Portlandien inférieur; Po II. Portlandien supérieur. — *Crétacique* : V I. Valangien inférieur; V II. Valangien supérieur; H I. Hauterivien inférieur; H II. Hauterivien supérieur; U I. Urgonien inférieur; U II. Urgonien supérieur. — *Tertiaire* : Aq. Aquitanien. — *Quaternaire* : gl. Moraines; al. Alluvions; eb. Eboulis.

From Schardt & Dubois 1903

Figure 4.2: Cross-section of the Creux du Van anticline and the Val de Travers (Areuse valley) syncline located in the western Neuchâtel Jura. From SCHARDT & DUBOIS (1903). For location see Figure 4.7b or Figure 4.9.

Coupe géologique de SCHARDT & DUBOIS (1903) de l'anticlinal du Creux du Van et du synclinal du Val de Travers (Gorges de l'Areuse), Jura neuchâtelois occidental (pour la localisation voir Figure 4.7b et Figure 4.9).

Figure 4.4a (page 117, top): Three-dimensional view towards the NE representing the base of Malm limestones (top of "Argovian" marls) in the Canton of Neuchâtel, based on data from a structural contour map (KIRALY, 1969). Vertical axes are in meters above sea level and horizontal axes are in kilometers (Swiss geographic coordinate grid).

Vue tridimensionnelle vers le NE, représentant la base des calcaires du Malm (toit des marnes argoviennes) dans le Canton de Neuchâtel, basée sur les données de la carte structurale de KIRALY (1969). L'axe de coordonnées vertical est exprimé en mètres au-dessus du niveau de la mer, l'axe horizontal en kilomètres (grille de référence des coordonnées géographiques suisses).

Figure 4.4b (page 117, bottom): Three-dimensional view towards the NE representing the base of Malm limestones (top of "Argovian" marls) from the Canton of Neuchâtel, the Risoux-Mt-Tendre-Pontarlier Jura area and the Molasse Basin. This three dimensional view is based on structural contour maps from KIRALY (1969, Neuchâtel area) and from AUBERT *et al.* (1979, Risoux-Mt-Tendre Pontarlier area) and from results of this work in the Molasse Basin. Vertical axes are in meters and horizontal axes are in kilometers (Swiss geographic coordinate grid). Compare the lateral continuity of the anticlines between the Neuchâtel and the Risoux-Mt-Tendre Jura.

Vue tridimensionnelle vers le NE représentant la base des calcaires du Malm (toit des marnes argoviennes) dans le Canton de Neuchâtel, dans la région jurassienne du Risoux-Mt-Tendre-Pontarlier et dans le Bassin molassique. Cette vue 3D est basée sur les données de la carte structurale de KIRALY (1969, région de Neuchâtel) et de AUBERT et al. (1979, région du Risoux-Mt-Tendre-Pontarlier). L'axe de coordonnées vertical est exprimé en mètres au-dessus du niveau de la mer, l'axe horizontal en kilomètres (grille de référence des coordonnées géographiques suisses). Comparer l'extension latérale des anticlinaux du Jura neuchâtelois et vaudois (Risoux-Mt-Tendre).

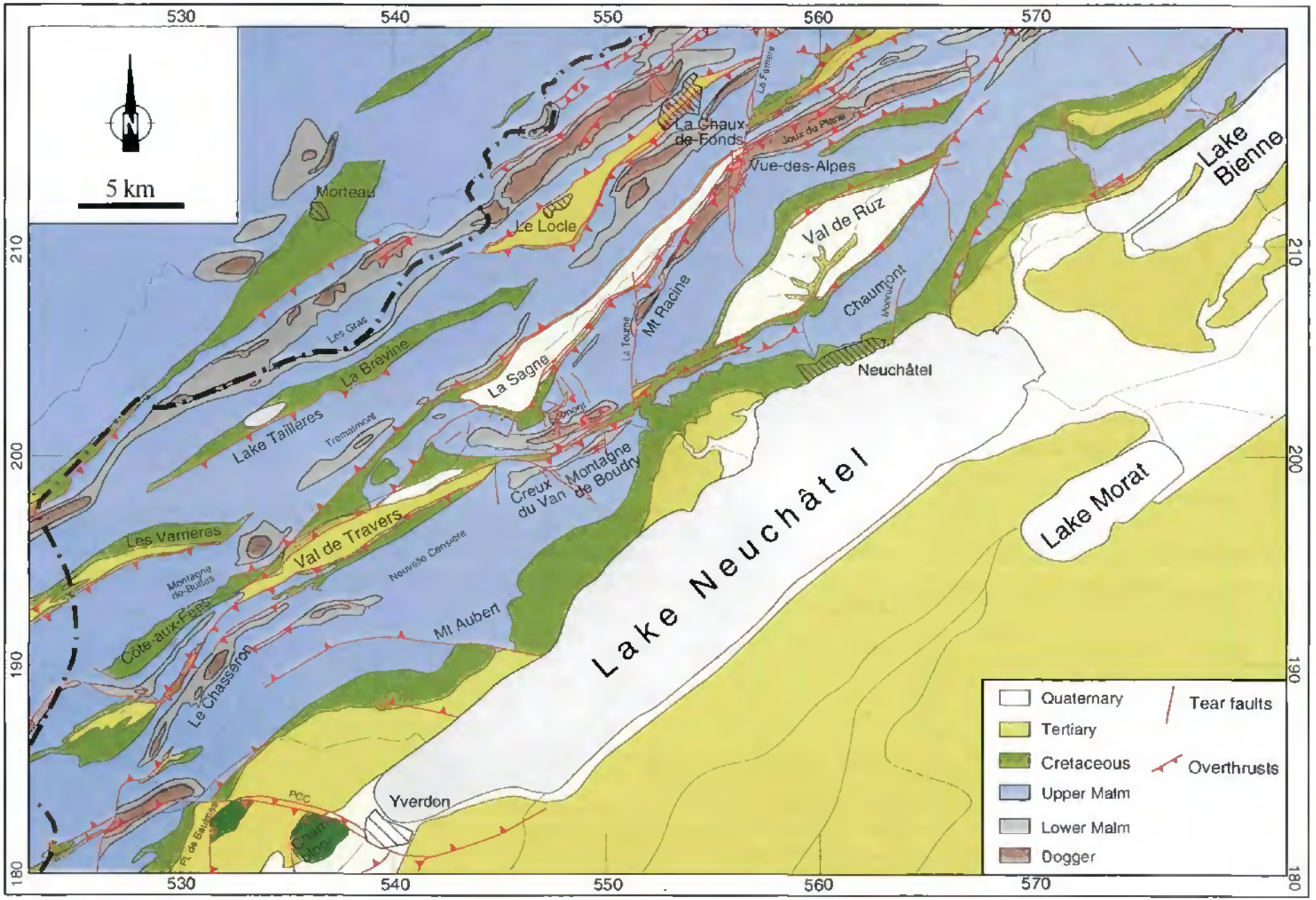

Figure 4.3: Tectonic sketch of the Neuchâtel Jura based on 1:200'000 tectonic sketches of published local maps (see texte for references).

Carte tectonique du Jura neuchâtelois basée sur les esquisses tectoniques, à l'échelle 1:200'000, des cartes régionales publiées (voir texte pour les références).

a) Structural contour map Base of Malm limestone

in the Canton of Neuchâtel area

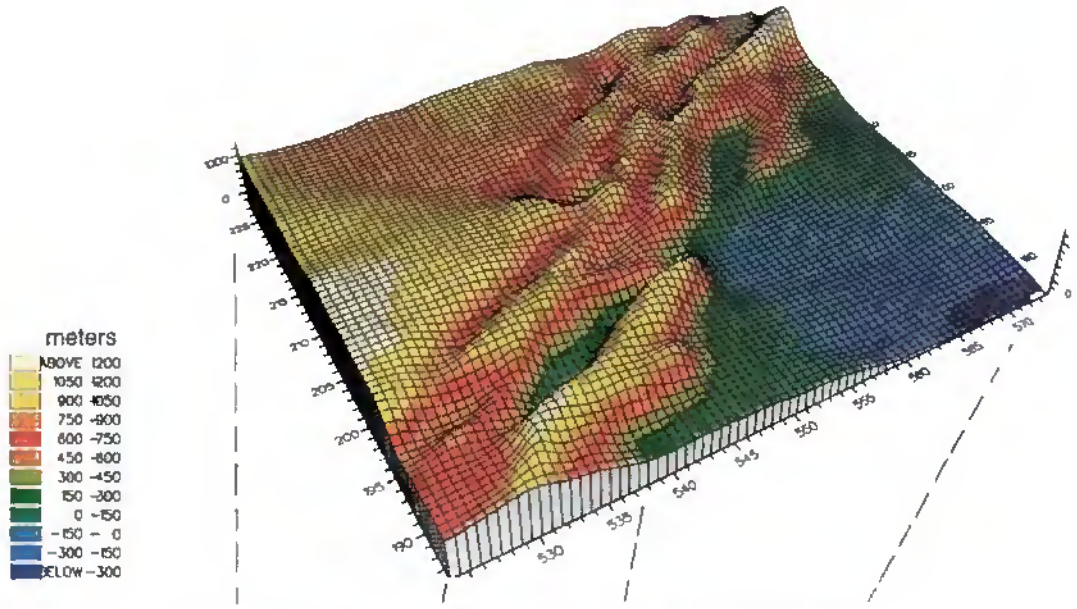

b) Neuchâtel Jura - Risoux Jura - Molasse Basin

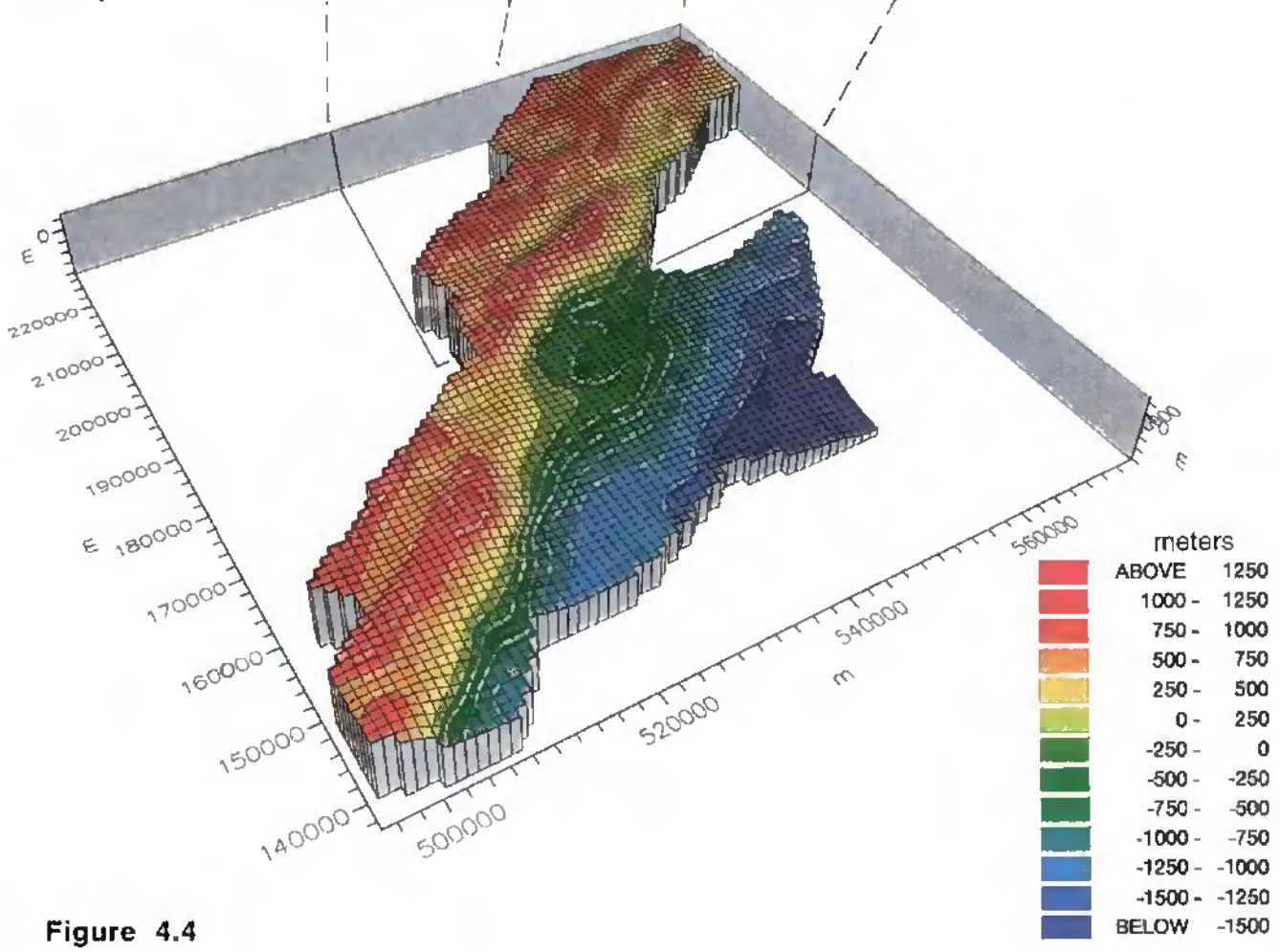

Figure 4.4

fold axes directions) and the map scale fold axes directions. The direction of map scale anticlines was determined from the geological maps of Neuchâtel and Val de Ruz at 1:25'000 scale (BOURQUIN *et al.*, 1968; FREI *et al.*, 1974) and a compiled structural contour map. Local anticline directions have been determined from dip and azimuth data compiled from several maps and then plotted on stereograms in order to obtain a best fit local fold (MANCKTELOW, 1989, Stereoplot computer software). Tschanz & Sommaruga interpret cylindrical folds as folding above a frontal ramp and non-cylindrical folds as folding above an oblique ramp, with an overall transport direction to the NNW (335°). This interpretation is corroborated by the direction of paleo-stress axes determined from fault/slickenside pairs as well as from twin strain analyses. Local maximum compression directions are invariably NNW-SSE to NW-SE oriented, regardless of the position within the rhomb shaped structure.

Strike seismic profiles within the Val de Ruz basin are of excellent quality and show strong and flat reflectors with a good lateral continuity (Section 8, and eastern part of Section 4 on Panel 3). Seismic intervals have been defined on strike Section 8 as discussed in §2.4.1 (Fig 2.15). No major structural features are recognized in those two lines. The slight bends of the basement top reflector are interpreted as velocity pull-up beneath the anticlines and pull-down beneath the Val de Ruz syncline. Due to a strong increase in thickness of Tertiary and Quaternary sediments from NNW to SSE within the syncline (MORNOD, 1970; SCHNEGG & SOMMARUGA, 1995) reflectors are pulled down in the southern part of the Val de Ruz basin. On the dip seismic lines crossing the Val de Ruz basin (Sections 1, 3, 5 on Panel 1), the changes in width of the syncline are clear: on the eastern line the syncline is already broad, in the middle it is the widest (Section 3) and then it narrows towards the West, to finally end against the La Tourne tear fault. In this area, seismic data are of poor quality, probably due to the topographic effects and/or the complexity of the structures. Therefore surface geological data are required in order to obtain a clear understanding.

Three major N-S tear faults have been mapped around the Val de Ruz syncline (Fig. 4.3): the La Tourne fault in the western part, the La Ferrière fault in the northern and central part and the Monruz fault in the south-eastern part. These faults, of kilometric length, have an apparent sinistral offset of few hundred meters on the map and coincide (especially the La Ferrière fault) with the position where the mapped fold axes change direction. This suggests that these fracture zones have possibly predetermined the position of oblique and/or lateral ramps and can thus be interpreted as faults reactivated during the late Miocene folding of the Jura. Alternatively, these faults may have developed only during folding. Fault/slickenside analyses from the vicinity of tear faults indicate that these were active still after the major folding phase, since sub-horizontal striations are frequently found on faults cross-cutting vertical bedding planes (TSCHANZ & SOMMARUGA, 1993). Directions of paleo-stress axes for the past 10 Ma are indistinguishable from present day maximum horizontal stress directions.

Seismic lines do not offer any evidence for inherited or newly developed Oligocene tear faults, as suggested by AUBERT (1972) and BERGERAT (1987). On the seismic lines, described in Chapter 3, tear faults appear as transparent zones, thus explaining why the La Ferrière and La Tourne faults are not clearly recognizable on Sections 3 and 7, respectively.

Val de Ruz cross-section

A geological cross-section (Fig. 4.5) based on surface dip data and completed at depth with information from seismic data, has been constructed parallel to seismic Section 8 (Panel 1) in the Val de Ruz area. This cross-section has been modified from that presented by SOMMARUGA & BURKHARD (1997). The availability of a dense seismic grid has better constrained the depth to the basement, which now lies at greater depth in this modified version (Fig. 4.5).

From SE to NW, the geological section crosses two major anticlines. These thrust-related anticlines, previously discussed in Chapter 3, formed firstly as detachment folds (or buckle folds) and then developed into fault-propagation or fold-bend folds, thus forming a complex structure e.g. La Vue des Alpes anticline (SOMMARUGA & BURKHARD, 1997, see map of Figure 4.3). The interpretation of the seismic line (Section 8) suggests the presence of a rather smooth thrust, separating a relatively uniform dip domain with gently SSE dipping layers in the footwall, from a more strongly folded and/or faulted hangingwall. A very good correlation between SSE-vergent kink folds at the surface and SSE vergent (blind?) thrust faults at depth is observed. The southernmost of these backthrusts seems to be located above the area where the NNW thrust branches off from the basal

décollement zone. Other backthrusts are unrelated to bends in the main thrust fault.

Further North, two more foreland vergent thrust faults have been postulated, based on surface geology in combination with interpretations of seismic lines. The La Chaux de Fonds syncline is located at a high elevation possibly due to a thrust fault within the Triassic beds. Further North (1 or 2 km), an anticline is related to this thrust fault.

The geological section (Fig. 4.5) crosses the La Ferrière fault which adds to the complexity of the broken up anticline near La Vue des Alpes. The extension of this fault at depth is unknown. In constructing the cross-section, this fault has been ignored, because no evidence for its presence has been found on seismic lines. If this tear fault represents a post folding feature only, its overall apparent sinistral offset of ca. 500 m should be compensated by a stretching of the section by a similar amount. On seismic Section 8, however, reflectors on either side of the supposed fault trace at depth could be correlated without major offset, suggesting that the La Ferrière fault could be a superficial tear fault.

4.2.3. Western part

The western part of the Neuchâtel Jura is located between two tear faults: the La Tourne fault to the East and the Pontarlier fault to the West. In its northern part, this region is characterized by anticlines and synclines oriented NE-SW with a lateral continuity of about 15 km to 20 km e.g. the La Brévine and Morteau synclines. The central part appears much more complex, as shown on the tectonic sketch (Fig. 4.3). A detailed map analysis has been conducted in the Travers region, in order to better visualize the relations between the structures. Since no 1:25'000 scale map of this region has been published yet, a compilation (Fig. 4.7a) has been made of several unpublished maps (SCHARDT & DUBOIS, 1903; RICKENBACH, 1925; THIÉBAUD, 1936; FREI, 1942; DE PURY, 1963; MEIA, 1969; FREI *et al.*, 1974; MEIA, 1986; MÜLLER, 1958).

The Travers area is characterized by several large scale structures illustrated on the tectonic sketch of Figure 4.7b. To the North, the St-Sulpice-Trémalmont-Les Combes Derniers anticline forms a continuous, NE-SW oriented, feature with lower Malm and Dogger layers outcropping in the core. This structure grades northward into the narrow, flat bottomed La Brévine syncline. In the southern part of the area, the anticline is thrust towards the South over adjacent synclinal structures along a south-vergent fault surface. To the South, the Travers area is bordered by the NE-SW trending Nouvelle Censière-Creux du Van-Montagne de Boudry anticline. This structure is large and flat topped in the SW (Nouvelle Censière), whereas in the NE erosion allows insight in the tighter anticlinal core (Creux du Van-Montagne de Boudry). Along the southern border of the Areuse valley, the core is related to a north-vergent thrust and represented by Dogger strata. In the central portion, this anticline is cut by a conjugate set of tear faults, consisting of a N-S oriented set with sinistral offset and a NW-SE oriented set with a dextral offset. This is a typical orientation for tear faults in the central Jura. Between the two anticlines, a complex set of structures has developed. The most prominent are, to the NE, the La Sagne syncline oriented NE-SW and, to the SW, the ENE-WSW trending Val de Travers syncline. Both synclines are broad, flat bottomed and covered by Tertiary and/or Quaternary sediments. They are also overridden both from the NW and the SE by south-vergent and north-vergent thrusts respectively. Along its northern limit, the Val de Travers syncline is bordered by two small synclines oriented NE-SW and oblique to the Val de Travers, but pinches out to the East. Further to the E, the very tight Areuse syncline, like the Val de Travers syncline, is overridden to the North and the South by south-vergent and north-vergent thrusts respectively. The southern thrust (along the northern limb of the Montagne de Boudry-Creux du Van anticline) extends eastward into the N-S oriented, left-lateral La Tourne tear fault. The very narrow width of the Areuse syncline is unusual for the Neuchâtel Jura, where synclines are generally quite large, as shown by the Val de Ruz-La Sagne-Le Locle Valleys (Fig. 4.3).

Most remarkably, the Solmont anticline runs NE-SW in its eastern part, changing to a WNW-ESE orientation in its western part, where it separates the La Sagne and Val de Travers synclines. Its continuation is probably the Crêt Pellaton anticline, whose central portion is cut by a fault.

Thus between two continuous NE-SW oriented major anticlines, the southern of which is related to an foreland-vergent thrust fault and the northern to a hinterland-vergent fault, we observe a complex transfer zone, where displacement is relayed between two large en echelon synclines (La Sagne, Val de Travers). Its further noteworthy, that the La Tourne tear fault grades into a north-vergent thrust at the base of the Montagne de Boudry anticline.

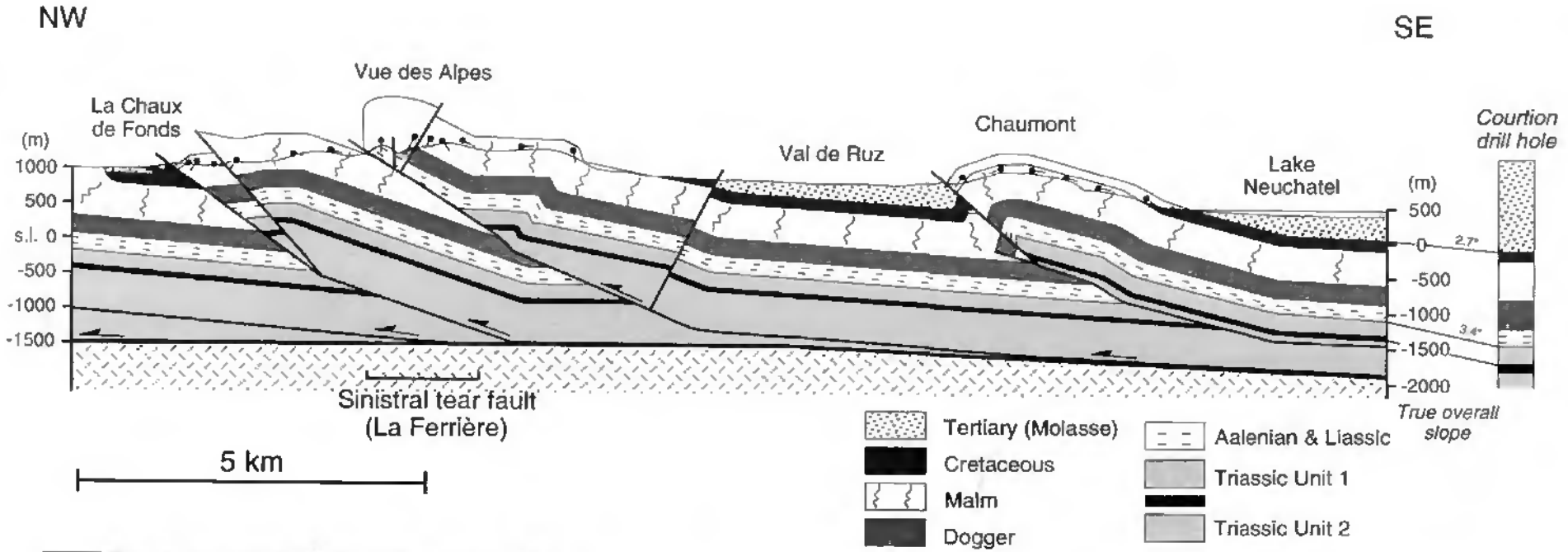

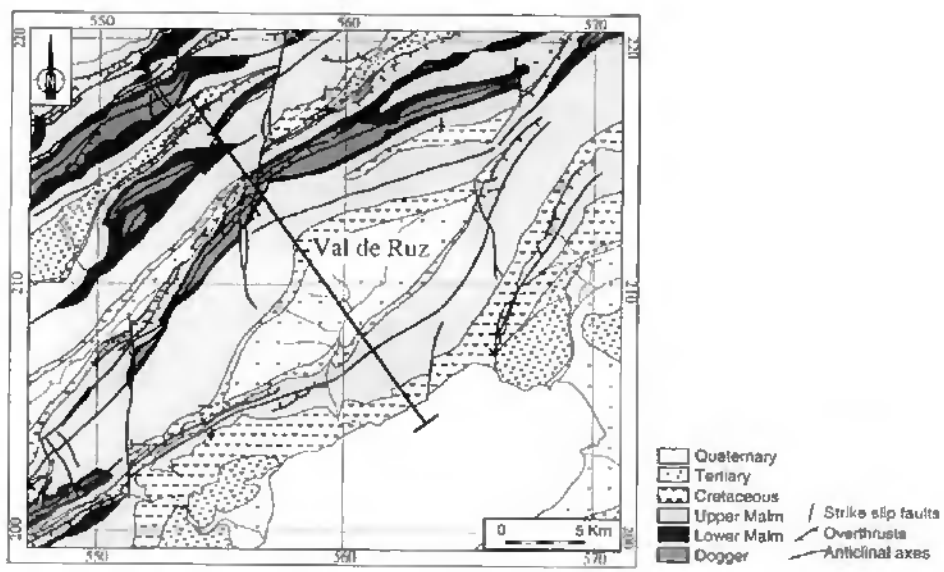

Figure 4.5: Geological cross-section based on surface data, completed at depth with information from seismic Section 3. La Ferrière tear fault is located on the cross-section. The extension of this fault at depth is unknown. During cross-section constructing, this fault has been ignored. The stratigraphy of the Val de Ruz area is correlated with the Courtion drill hole located 18 km to the SSE of the town of Neuchâtel. Modified from SOMMARUGA & BURKHARD (1997).

Coupe géologique basée sur des données de surface et complétée en profondeur avec les informations de l'interprétation du profil sismique 3. La faille de La Ferrière est localisée sur la coupe. La continuité en profondeur de cette faille étant inconnue, il n'en a pas été tenu compte pour la construction de la coupe géologique. La stratigraphie du Val de Ruz est corrélée avec les données du forage de Courtion, situé 18 km au SSE de Neuchâtel. Modifiée de SOMMARUGA & BURKHARD (1997).

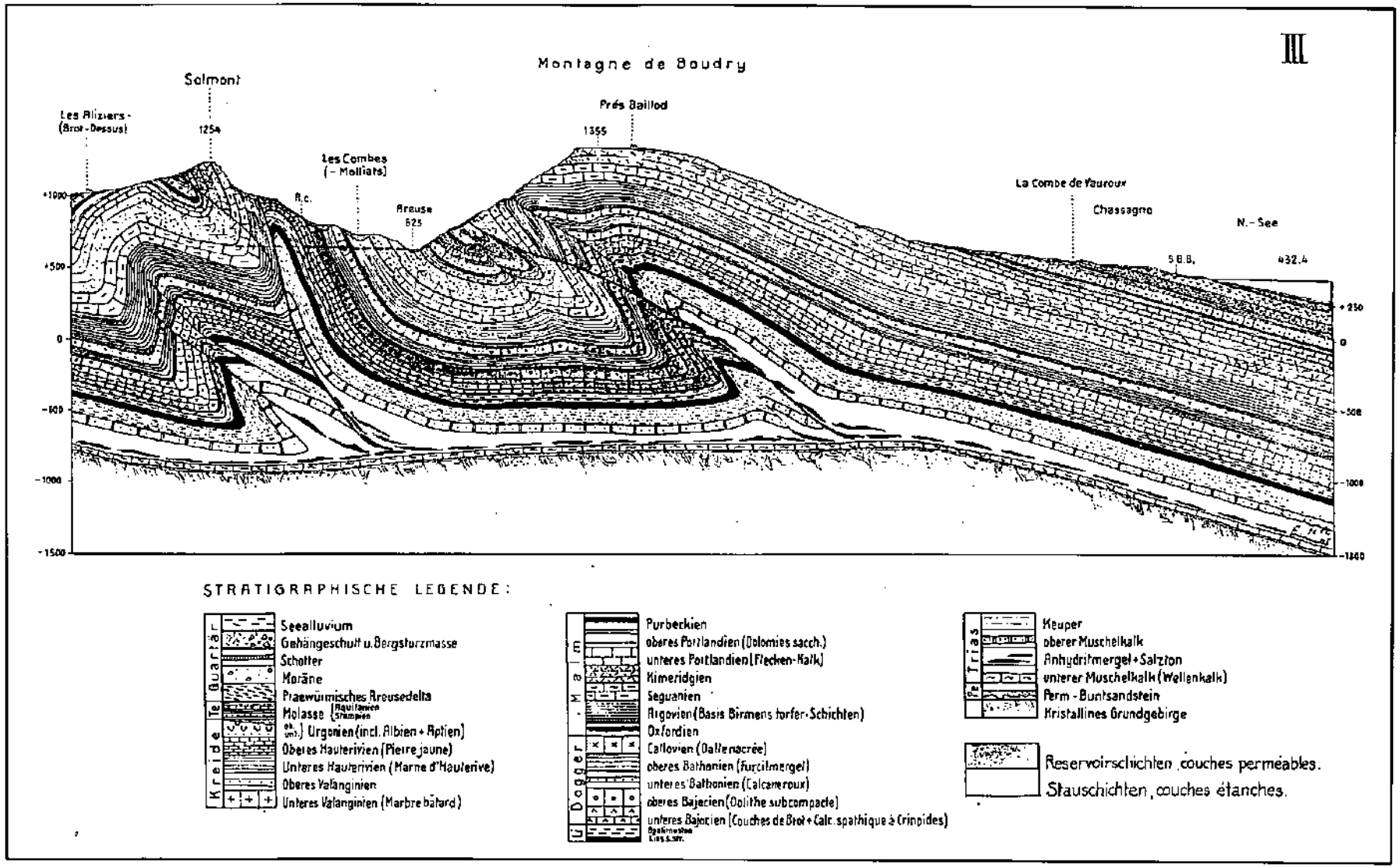

From Frei 1946

Figure 4.6: Unpublished geological cross-section of FREI (1946). The section presents an anticline (Montagne de Boudry) related to a thrust fault which roots in the anhydrite layer of the "Muschelkalk" (Triassic Unit 2). Refer to text for discussion. For location see Figure 4.7b

Coupe géologique non publiée de FREI (1946). La coupe présente un anticlinal (Montagne de Boudry) en relation avec une faille de chevauchement qui s'enracine dans les couches du "Muschelkalk" (Unité 2 du Trias). Voir texte pour discussion et Figure 4.7b pour la localisation.

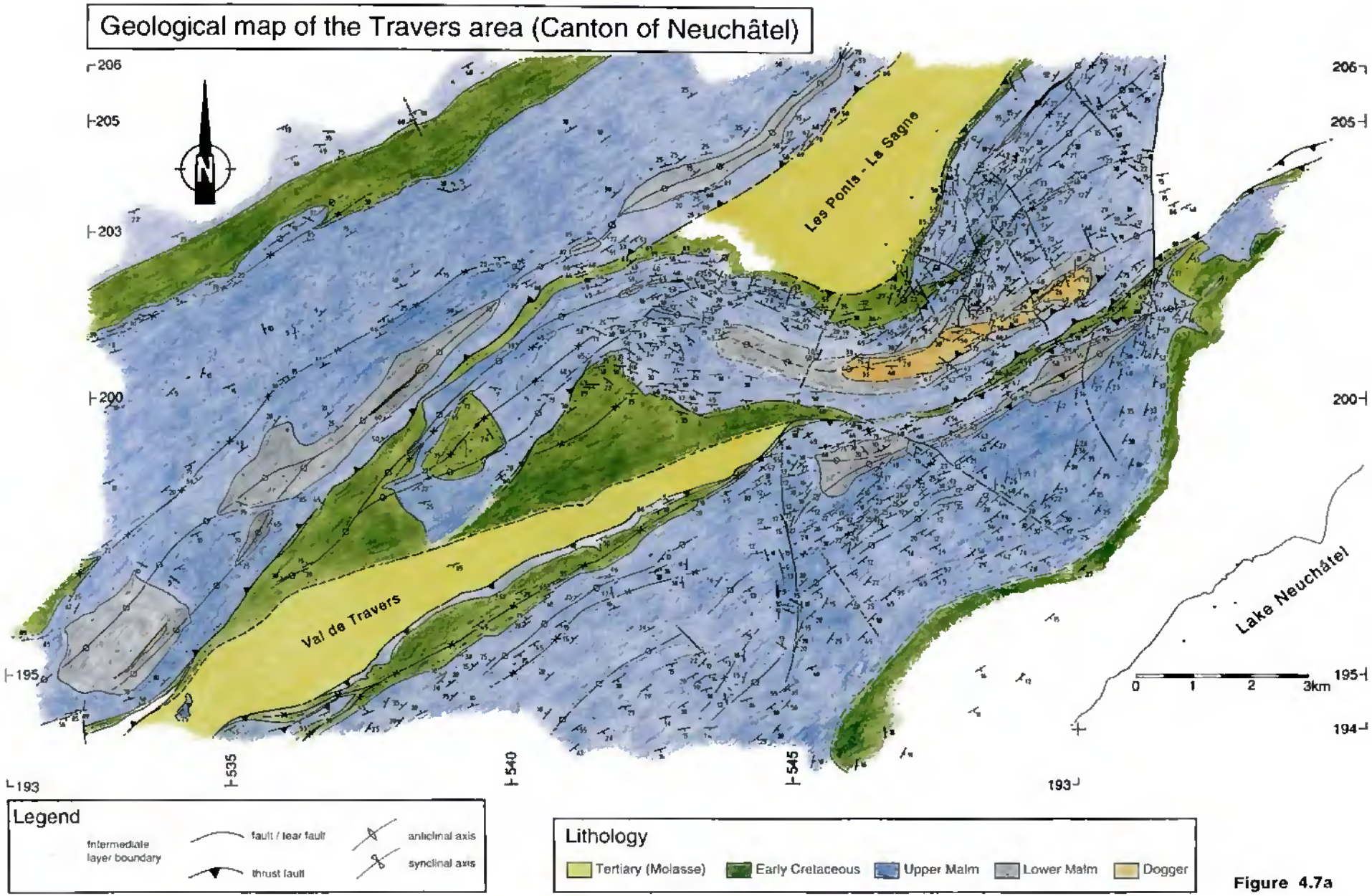
Geological map of the Travers area (Canton of Neuchâtel)
206
205
203
200
195
193
535
540
545
N
Les Ponts - La Sagne
Val de Travers
Lake Neuchâtel
0
1
2
3km
Legend
intermediate layer boundary
fault / tear fault
thrust fault
anticlinal axis
synclinal axis
Lithology
Tertiary (Molasse)
Early Cretaceous
Upper Malm
Lower Malm
Dogger

Figure 4.7a

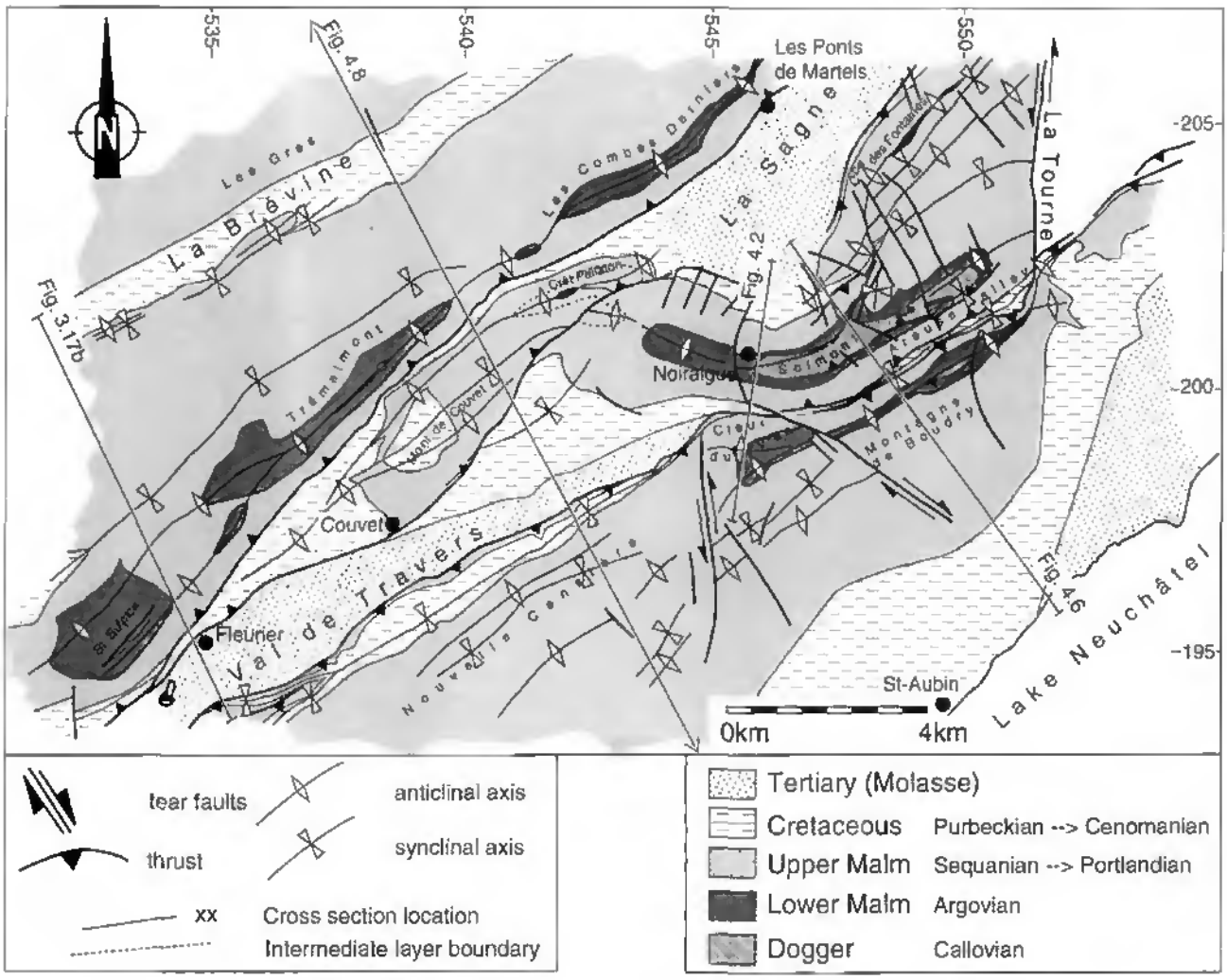

Figure 4.7b:
Tectonic sketch of the structural map of Travers presented in Figure 4.7a with location of cross-sections.

Esquisse tectonique de la carte structurale de Travers, présentée dans la Figure 4.7a. Localisation de plusieurs coupes présentées dans ce travail.

Figure 4.7a (page 122):
Structural map of the Travers region. This map is a compilation and interpretation of several published or unpublished geological maps. See text for references. Small dots (SE Les Ponts-La Sagne valley and Lake Neuchâtel) correspond to end points of three unpublished cross-sections by FREI (1946).

Carte structurale de la région de Travers. Cette carte est une compilation et une interprétation de diverses cartes géologiques publiées ou non publiées. Voir le texte pour les références. Les petits points (au SE de la vallée Les Ponts-La Sagne et dans le lac de Neuchâtel) correspondent à la fin de la trace de trois coupes géologiques non publiées de FREI (1946).

Thus, fold and thrust appear to be contemporaneous with the tear fault, at least in this specific case. Inspection of the tectonic sketch of the Neuchâtel Jura (Fig. 4.3) shows that transfer zones such as that of the Travers area are common in e.g. the Le Locle-La Brévine area or the NW of lake Biel region. However, the Travers area presents the best outcrops.

Unfortunately the seismic line crossing the Creux du Van and Solmont anticlines (Section 9, Panel 2) is of poor quality, probably due to the steep topography and the karstification of the Jurassic limestones. The geology of the Travers area has been illustrated since the beginning of the century in cross-sections by SCHARDT & DUBOIS (1903) (Fig. 4.2) and FREI (1946) (Fig. 4.6). The first section oriented N-S, crosses the western part of the Solmont anticline, the Areuse syncline and the Creux du Van anticline. On this section, the latter appears related to a thrust fault, whereas the Solmont anticline does not. The unpublished cross-section by FREI (Fig. 4.6) shows a modern structural concept, in that anticlines are related to thrust faults which root in the Middle Triassic evaporite décollement zone. The top of the basement is flat, showing a minor bend beneath the southern limb of the Montagne de Boudry anticline. Its depth is much shallower than the depth to the top basement presented in the maps of Chapter 5. The results of the seismic interpretation from the western Val de Travers area have shown that the Dogger, Liassic and especially Triassic layers are much thicker than predicted from surface geology.

The structure of the western region of the Travers area (Fig. 4.7b) is illustrated by two seismic lines (Sections 11 and 13 on Panel 2, for location see also Figure 4.3) and by two geological cross-sections (Figs. 3.17b and 4.8). The cross-section of Figure 4.8, running from Lake Neuchâtel to Morteau (for location see Figures 4.3 and 4.9), is based on surface geological data and completed at depth with information from seismic lines. From SE to NW, this section crosses different types of structure: the Mt Aubert dextral tear fault system, the periclinal end of the Mt Aubert anticline, the Nouvelle Censière anticline, the Val de Travers syncline, the Mont de Couvet anticline, the Trémalmont anticline, the Brévine syncline, the Les Gras anticline and the Morteau syncline. All the large scale anticlines are thrust-related structures. The broad Nouvelle Censière thrust-related anticline has already been discussed in Chapter 3. From the interpretation of the seismic lines, duplication of the Jura cover beneath the anticline can be demonstrated.

Dips of 35° towards the South are observed in the northern portion of the Val de Travers syncline, whereas the central portion dips gently to the S, extending far below the broad Nouvelle Censière. The Mont de Couvet area presents, at surface, two short wavelength anticlines related to a hinterland-vergent thrust fault (the southernmost of which corresponds to the Corridor aux Loups anticline). Seismic lines (Sections 11 and 13) in this region present at depth a rather broad anticline, with thickening within the Triassic layers. Both these anticlines and the steeper northern portion of the Val de Travers syncline are related to an important change in thickness of the Triassic series, which appears to originate at the point of development of a complex imbricate thrust fault system linked to the Mont de Couvet thrust fault. Further North, the Trémalmont anticline is related to a backthrust of the broad north-vergent Les Gras anticline that steps up over a ramp and flat thrust surface. This anticline also shows duplication of the Mesozoic cover series.

The Triassic series is less important below the meridional portions of the Nouvelle Censière and Les Gras anticlines. The thickness of these layers increases toward the North of these structures, especially beneath the Val de Travers and the Mont de Couvet, suggesting "flow" of the evaporites under the weight of the overriding broad anticlines.

Thickness changes are also noticeable in Dogger - Liassic strata in the hangingwall of the Nouvelle Censière thrust-anticline, as well as south of the Mont Aubert tear fault; these are thicker compared to those in the footwall, indicating that strata thicken toward the South, in general agreement with the trend of Middle Jurassic facies.

It must be emphasized that the northwestern part of the Neuchâtel Jura is characterized by synclines, that have a higher topographic elevation (e.g. La Brévine, Le Locle-La Chaux-de-Fonds, La Sagne synclines) compared to the southern synclines e.g. Val de Ruz and Val de Travers. This is well shown on the cross-sections of Figure 3.17 and Figure 4.5. Strike seismic Section 2, running parallel to La Brévine syncline, shows a succession of very strong flat reflectors, usefully constraining the seismic stratigraphy. At depth, duplication of the Triassic stratigraphy is observed, explaining the high elevation of the Jurassic, Cretaceous and Tertiary strata. The total thickness of Triassic is around 1000 m. In terms of balancing, the duplication of the Triassic beds represents an important shortening which must

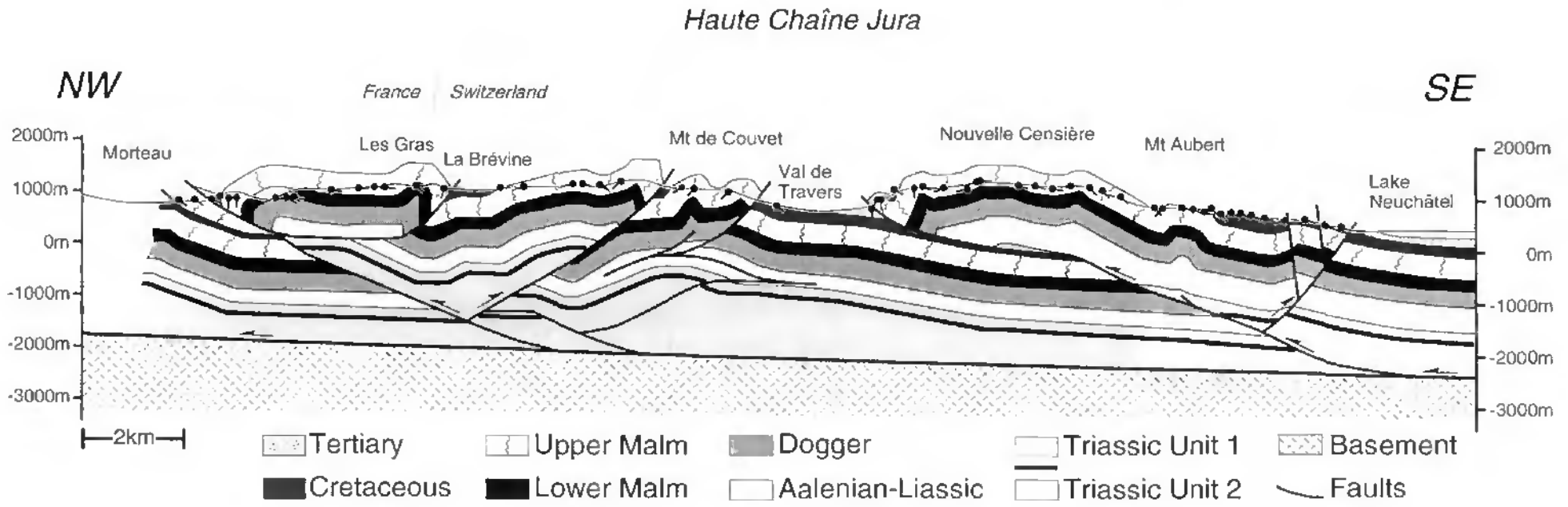

Figure 4.8: Geological cross-section from lake Neuchâtel to Morteau based on surface data and completed at depth with information from seismic Sections 11 and 13. For location see Figure 4.7b and Figure 4.9.

Coupe géologique allant du lac de Neuchâtel à Morteau, basée sur les données de la surface et complétée en profondeur par les informations des profils sismiques 11 et 13. Pour la localisation voir Figure 4.7b et Figure 4.9.

be present in higher Mesozoic rocks and has to be compensated beneath anticlines.

4.3. RISOUX JURA

The following paragraphs discuss the regional geology of the Risoux (sensu lato) area, which consists of the Mont-Risoux (sensu stricto) anticline, the Vallée de Joux syncline and the Mont-Tendre anticline.

4.3.1. Previous studies

The Risoux region located in the Haute Chaîne Jura along the Swiss-French border (Figs. 1.3 and 4.1) has been the subject of many papers. During the last century, the Mt-Risoux anticline was considered to be a simple anticline, because of the apparent lateral continuity of the structures seen at surface. At the beginning of this century, the excavation of the Mont d'Or railway tunnel, located at the eastern end of the Mt-Risoux chain, revealed some unexpected structural complexities (COLLOT, 1913) (see also cross-section 3 in Fig. 1.5). Some fifty years later, the Risoux well results (WINNOCK, 1961) showed a major thrust fault separating an upper series, ranging from Malm limestone ("Sequanian-Rauracian" facies) down to Liassic marls in the hangingwall, from a second series, ranging from Malm limestone ("Sequanian-Rauracian" facies) to Bathonian limestone in the footwall. The drill hole log data presented in Figure 2.12 and Figure 2.19 were the first formal proof of tectonic duplication of the Mesozoic cover beneath Jura anticlines. These unexpected results have considerably increased, not only, the understanding of the internal structure of the Haute Chaîne Jura anticlines, but were a major step forward in the tectonics of the Jura fold and thrust belt. The older hypothesis suggesting the Mt-Risoux anticline as "... *masse inerte à peine ébranlée par la poussée orogénique* ..." (AUBERT, 1959) was reconsidered by WINNOCK (1961), LAUBSCHER (1961, 1965) and later again by AUBERT (1971). These authors stress the presence of a basal décollement level in the Triassic as postulated much earlier by BUXTORF (1916).

Since the discovery of the tectonic duplication of the Mesozoic cover within the Risoux well, the Risoux area has become a classical region for structural studies in the Jura. Several authors have attempted to explain the geometry and especially the vergence (either foreland or hinterland) of the main overthrust in relation to the anticline using field evidence. For a short review the reader can refer to the paper by WILDI & HUGGENBERGER (1993) and for details see COLLOT (1913), AUBERT (1941, 1945), WINNOCK (1961), RIGASSI (1962), LAUBSCHER (1965), AUBERT (1971), BITTERLI (1972), RIGASSI (1977), CHAUVE *et al.* (1980), MARTIN (1987), PHILIPPE (1995).

From this literature, we have singled out the cross-section by LAUBSCHER (1965) presented in Figure 1.5 (cross-section 4) and also that of BITTERLI (1972). Laubscher's section crosses two Haute Chaîne anticlines, the Mt-Tendre and the Mt-Risoux, then the whole Plateau Jura domain to end in the Bresse Graben area. The shortening within the Mt-Risoux anticline equals 10 km and the total shortening of the sedimentary cover along the whole section amounts to 25-30 km. The latter agrees with the estimate made using his rotational model of the Jura cover (LAUBSCHER, 1965). Before Laubscher's work, the shortening of the Mesozoic cover was always underestimated. Moreover this section shows a more or less flat basement top, dipping few degrees towards the South.

The geological cross-section of Bitterli has been constructed using surface geology data and subsurface information. In 1972 some seismic lines had already been shot in the Champagnole-Mouthe area (Shellrex concession, Fig. 1.4), located North of the Risoux area. Bitterli completed the northern part of the Mt-Risoux - Mt-Tendre section at depth using these seismic data.

4.3.2. Interpretation

At the surface the Mt-Risoux (sensu stricto) chain shows a large anticline oriented NE-SW, a classical trend for a Jura anticline. It is limited towards the North by the NE-SW oriented Mouthe syncline (the Doubs valley), towards the South by the Vallée de Joux syncline, to the West by the Morez fault and towards the East by the Pontarlier fault. This anticline extends over some 30 km laterally (Fig. 4.1 and Fig. 3.20a).

The Mt-Tendre anticline, located south of the Vallée de Joux syncline (Fig. 4.4b), has a lateral extent of over 25 km and ends westward at the Morez fault and eastward at the Pontarlier fault. The lateral continuity of the Mt-Risoux and Mt-Tendre anticlines across the Morez and Pontarlier faults are not discussed in this work, because more surface

geological data are necessary. Recently, PHILIPPE (1995, PhD thesis) proposes an extension of these anticlines beyond the Morez and Pontarlier faults and considers latter faults to be secondary tear faults, where fold axes are offset as passive markers (§3.3.).

The NE-SW trend of the Mt-Tendre anticline axis, sub-parallel to the Mt-Risoux anticline, is emphasized on the three-dimensional view of Figure 4.4b, of the base of the Malm limestones. In the Risoux area the structures are parallel and aligned along one axial trend. This contrasts with the Neuchâtel Jura, where, as explained in preceding paragraphs, the NNE-SSW or ENE-WSW orientation of the anticlines results in a rhomb shaped form in the synclines.

The lateral continuity of the Risoux Jura area is also well shown on the strike profiles running along the northern limb of the Mt-Tendre anticline (Section 86, Panel 8) and the southern limb of the Mt-Risoux anticline (Section 82-80, Panel 8). These sections do not show any lateral discontinuities, except for some zones with poor seismic data quality. They are most valuable in helping to constrain the seismic stratigraphy of the dip sections, which are of poorer data quality. Moreover, these sections highlight the duplication of part of the Jurassic cover, the Dogger and Malm layers.

Four dip profiles crossing the Mt-Risoux and the Mt-Tendre anticlines are presented on Panel 9. Unfortunately, no profile crosses the entire Mt-Tendre anticlinal structure. Seismic interpretation shows that the Mt-Tendre anticline is related to a foreland vergent thrust fault that soles out in Triassic Unit 2. The thrust ramp emerges in the Vallée de Joux syncline. The Mt-Risoux anticline is also related to a major north-vergent ramp which roots in Triassic Unit 2. This ramp breaks surface in the Mouthe syncline. A major shallow dipping backthrust is associated with the frontal ramp. This thrust represents a flat of 4 km in Liassic marls that ends in the Vallée de Joux syncline. The geometrical relationships between thrust faults, syncline and anticline beneath the Vallée de Joux are not clear on the seismic lines, due to poor quality. The shortening within the Mt-Risoux and Mt-Tendre anticlines is more than kilometric, in agreement with estimates by LAUBSCHER (1965).

The interpretation of seismic lines clearly highlights (Panel 9) that the Risoux Jura (sensu lato) is characterized by a succession of two different anticlines, the Mt-Risoux (sensu stricto) and the Mt-Tendre anticline located in the northern and in the southern part, respectively. This structural view has already been expressed by LAUBSCHER (1965) (Fig. 1.5) and PHILIPPE (1995). Other authors, such as AUBERT (1971) and WILDI & HUGGENBERGER (1993) have considered the Risoux (sensu lato, i.e. Mt-Risoux and Mt-Tendre anticlines) as a single thrust sheet rooting in the Triassic evaporite layers further to the South at the border of the Haute Chaîne Jura and Molasse Basin. Their hypothesis suggests shortening of up to 20 km for the Risoux area alone.

Both the Mt-Risoux and the Mt-Tendre anticlines ride above important kilometric thrust faults, leading to a duplication of the entire Mesozoic series (Panel 8 and 9). In a recent publication, based on surface geology data, WILDI & HUGGENBERGER (1993) did not attempt to fill the core of the Risoux anticlines and invoked "volume cachés" (= hidden volumes) between the surface geology and top basement.

Seismic Section 87-85-111 (Panel 9) differs from previous interpretations in identifying an important backthrust associated with the Mt-Risoux anticline.

4.4. THE CHAMPAGNOLE-MOUTHE REGION

4.4.1. General comments

The Champagnole-Mouthe region, as discussed hereafter, extends beyond these two towns as represented on Figure 1.4 (sector D). The Champagnole-Mouthe (sensu lato) name has been chosen for this region, following the name of the seismic survey. This region is located in the Plateau and Faisceau Jura (see Chapter 1). These Plateaux represent large scale flat zones, whereas the "Faisceaux" correspond to strongly deformed zones. The main geological units of the Champagnole-Mouthe region (sensu lato) are (Figs. 1.2 and 4.1.):

- in the North, the "Faisceau bisontin" oriented NE-SW in its northern part and N-S in its southern part (between Besançon and Salins-les-Bains). The Lomont anticline in the northern part forms the link between the external and internal Jura.

- in the central part, the "Faisceau salinois" is oriented ENE-WSW and the "Faisceau de Syam" is

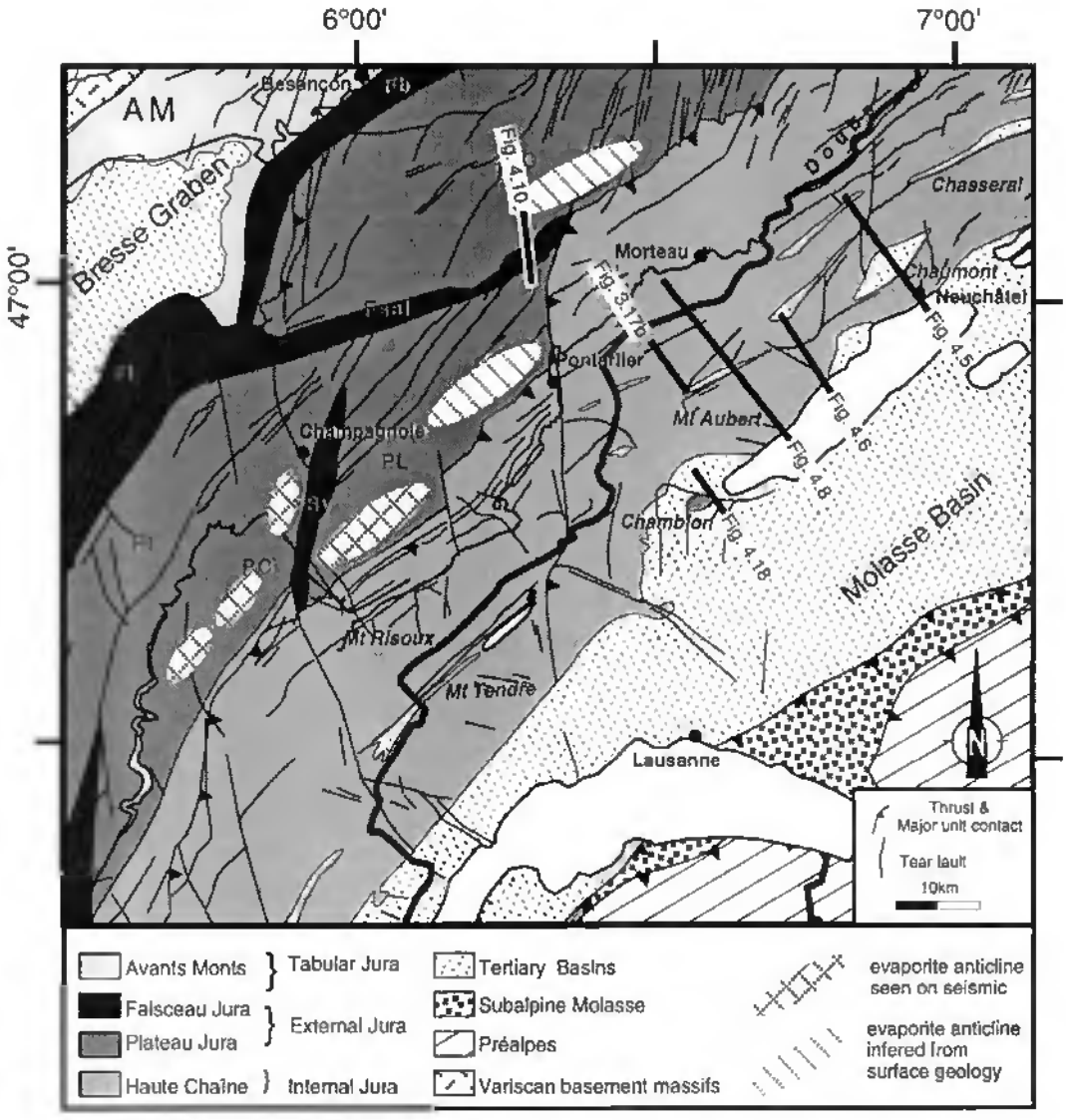

Figure 4.9: Tectonic sketch of the Jura and Molasse Basin with location of the evaporite-related anticlines of the external Jura. Geological cross-sections presented in this work are also located in this Figure. Legend: AM = Avants-Monts; Fb = Faisceau bisontin; Fl = Faisceau lédonien; Fsal = Faisceau salinois; FSy = Faisceau de Syam; PC = Plateau de Champagnole; PL = Plateau de Levier; Pl = Plateau lédonien; PO = Plateau d'Ornans.

Carte tectonique du Jura central et du Bassin molassique occidental montrant la situation des anticlinaux en relation avec les évaporites. Les coupes géologiques présentées dans ce travail sont aussi localisées sur cette figure. Légende: AM = Avants-Monts; Fb = Faisceau bisontin; Fl = Faisceau lédonien; Fsal = Faisceau salinois; FSy = Faisceau de Syam; PC = Plateau de Champagnole; PL = Plateau de Levier; Pl = Plateau lédonien; PO = Plateau d'Ornans.

oriented NNE-SSW. The latter separates two Plateaux, the "Plateau de Levier" to the East and the "Plateau de Champagnole" to the West, whereas the "Faisceaux bisontins, salinois" and the Haute-Chaîne limit the Plateau d'Ornans". The "Faisceau lédonien", corresponding to the outmost northwestern Jura unit, overthrusts the Bresse Graben by a few kilometers (5-7 km) (LIENHARDT, 1962). This important thrust does not outcrop, but has been encountered in many wells (LIENHARDT, 1962; CHAUVE *et al.*, 1988).

- in the southern part, the "Faisceau d'Orgelet and d'Ambérieu" folded and faulted units are directly linked to the Haute Chaîne Jura. No Plateau exists in this region.

4.4.2. Previous studies

The lack of published work on the external part of the Jura, in comparison with the internal part, is due to the scarce geological outcrops in this flat region.

In the northern part, the geological structures of the "Faisceau salinois and bisontin" have been studied by KILIAN (1893), GLANGEAUD (1947), GLANGEAUD & MATTAUER (1955), DREYFUSS (1960), CHAUVE *et al.* (1980; 1988), MARTIN *et al.* (1986). Martin *et al.* suggest a polyphase context for the "Faisceau salinois" formation, resulting in a kilometric translation of the cover towards the NW, concluding that the cover thus needs to be detached in the Triassic evaporites. They also postulate the reactivation of earlier Paleozoic and Oligocene faults.

At outcrop scale, the flat lying series of the Plateau areas show slight deformation: faults and striae, tensions cracks and stylolites witness a N-S to NW-SE oriented compression. These tectonic features have been studied along the whole external Jura, including the Champagnole-Mouthe area, by PLESSMANN (1972, stylolites), SOPENA & SOULAS (1973, faults and striae), BERGERAT (1987, faults and striae), LE PICHON *et al.* (1988), TSCHANZ (1990, calcite twins, stylolites, faults and striae), PHILIPPE (1995). Most of these authors infer two to three main tectonic events which are summarized in the paper of HOMBERG *et al.* (1994): 1) N-S Eocene compression; 2) Oligocene extension (WNW-ESE); 3) NW-SE Mio-Pliocene compression. These phases are recognized at large scale from the opening of the Central European Graben system (Rhine-Bresse-Rhône-Limagne) and their timing is constrained by sediments found in these grabens and from volcanic events (BECKER, 1985). Outcrop scale paleo-stress measurements cover the Jura and adjoining platforms. The third phase results in reactivation of Paleogene structures. The interpretation of these paleo-stress results is unclear, since the present day orientation of the maximum horizontal stress in the Jura Mountains is N-S in the northern Jura and NNE-SSW in the southern Jura (BECKER, 1987, 1989). Deviation of these data from the uniform NW-SE trend of the central and western European stress field (BECKER & WERNER, 1995) suggests care as required in interpreting paleo-stress results from the Jura.

4.4.3. Interpretation

Seismic lines crossing the external Jura have highlighted some important features, especially beneath the Plateau Jura. In the southern region of the "Plateau de Levier" and "Plateau de Champagnole" seismic lines show broad anticlines related to evaporite stacking (Panel 10 and Fig. 4.1), whose geometry has already been described in Chapter 3. The seismic interpretation indicates important thickening in the Triassic Unit 2. The Laveron well (Fig. 2.12) encountered up to 1400 m of Triassic strata. The location of the thick zones within the Triassic Unit 2 has been mapped on Figure 4.9, which shows two zones of aligned isopach thicks. The first, oriented NE-SW, is located in front of the Risoux area (Haute Chaîne Jura), between the "Faisceau de Syam" and the Mouthe tear fault and the second, oriented NNE-SSW, located in the Champagnole Plateau, in front of the Haute Chaîne anticline, stops against the south-western border of the "Faisceau de Syam". Apparently evaporite-anticlines are located in front of the Haute Chaîne anticlines and many stop against a tear fault or a Faisceau zone, e.g. Sections 107, 117 on Panel 10 and Section 111 on Panel 9. Unfortunately seismic lines show transparent zone across tear faults and Faisceau zones and as a result it is impossible to observe the precise relationship between evaporite-anticlines, Faisceaux and tear faults. In the northern area of the Plateaux, the quality of seismic lines does not allow interpretation of any features.

In the Faisceau zones, because of very poor seismic data quality, surface geology remains the best constraint. Along the deep cut of the Loue river, strata seen in the cliffs represent the transition from the "Faisceau salinois" to the "Plateau d'Ornans". DREYFUSS (1960) and later AUBERT *et al.* (1980) have drawn a cross-section showing the relationship between the different outcrops. Based on these surface geological data, a new cross-section has been constructed, including the entire stratigraphic succession down to the basement (Fig. 4.10, location on Figure 4.9). This geological section indicates a kilometric shortening in the cover. The south dipping Malm layers in the footwall and to the North of the main thrust (see cross-section from Dreyfuss) most likely correspond to thickening within the Triassic layers. The overload of the hangingwall to the South may induce evaporite flow toward the North. Similarly, such flowage possibly contributed to enhance the evaporite stack in the footwall of the Mt-Risoux anticline (see Section 111 on Panel 9).

The same relationship between the footwall Cretaceous layers and the faulted Jurassic hangingwall layers in the cross-section of Hautepierre (Fig. 4.10) has been well described along the southern border of the Verrières syncline by MARTIN *et al.* (1991).

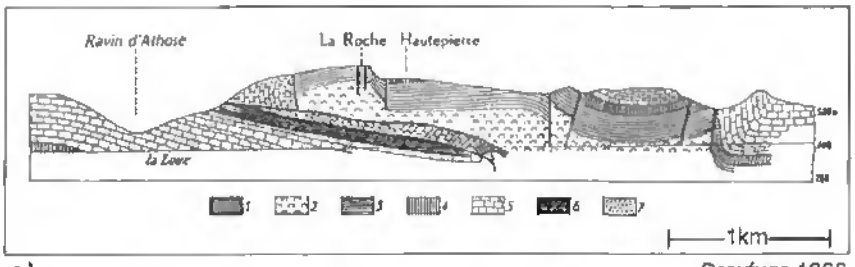

a) Dreyfuss 1960

Legend: 1 = Sinemurian; 2 = Upper and Middle Liassic; 3 = Middle Jurassic;
4 = Oxfordian and Argovian; 5 = Upper Jurassic (Rauracian); 6 = Neocomian; 7 = Albian

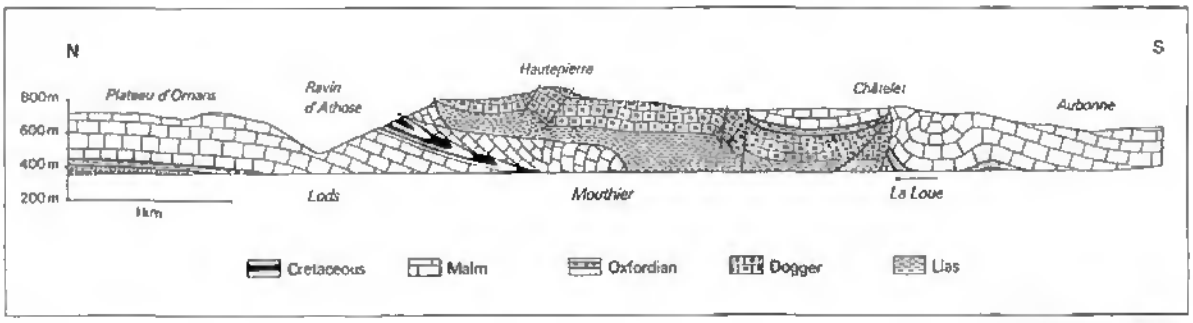

b) Aubert et al. 1980

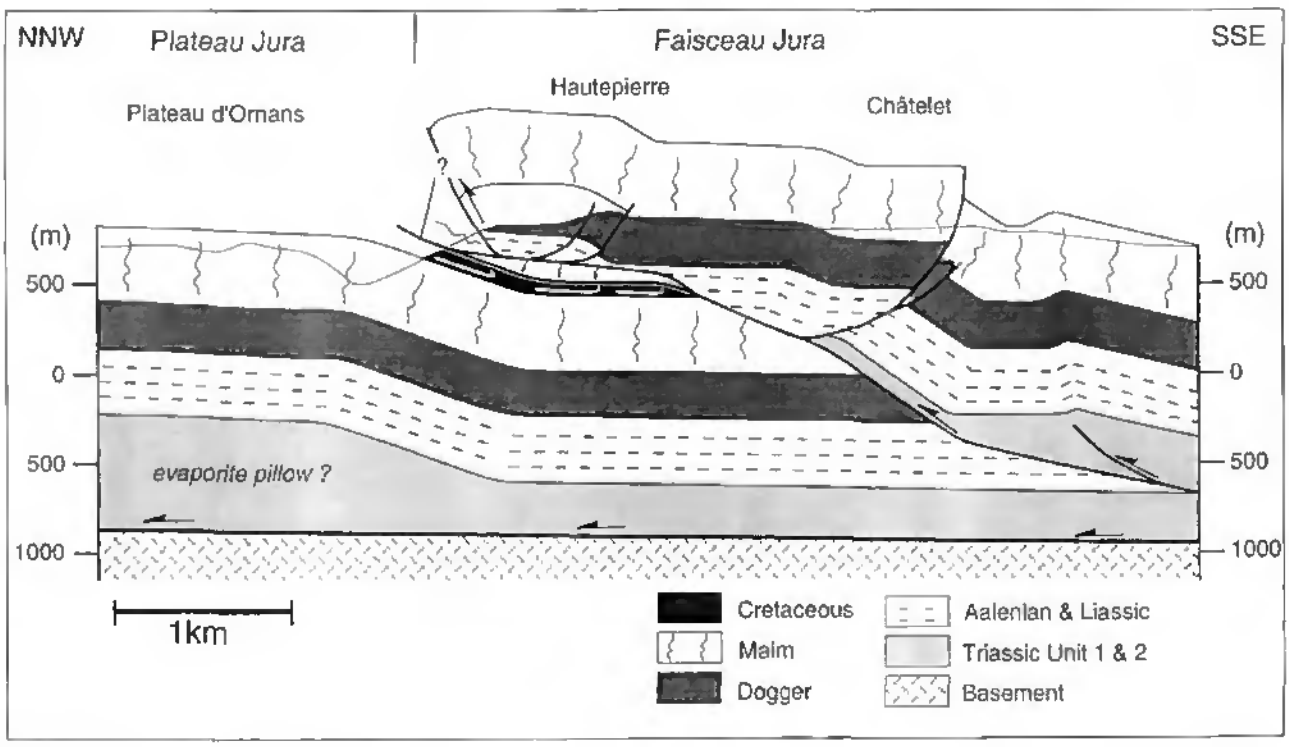

c)

Figure 4.10: Geological cross-sections of the transition from Faisceau Jura (Faisceau salinois) to Plateau Jura (Plateau d'Ornans). For location see Figure 4.9.
a) Surface geological cross-section made by DREYFUSS (1960).
b) Surface geological cross-section made by AUBERT *et al.* in TRÜMPY (1980).
c) Deep cross-section based on surface data from Dreyfuss and Aubert *et al.* and subsurface interpretation of seismic lines. The section shows a thrust-related anticline in the Faisceau Jura and an evaporite-anticline or a pillow at the front of the high amplitude anticline.

Coupes géologiques montrant la transition entre le Faisceau salinois et le Plateau d'Ornans. Pour la localisation, voir Figure 4.9.
a) Coupe géologique de surface dessinée par DREYFUSS (1960).
b) Coupe géologique de surface dessinée par AUBERT et al. dans TRÜMPY (1980).
c) Coupe géologique dessinée à partir des données de la surface de Dreyfuss et Aubert et al. et des interprétations des profils sismiques. La coupe montre dans le Faisceau jurassien un anticlinal en relation avec un chevauchement. Dans le Plateau jurassien, on observe un anticlinal d'évaporites ou un coussin d'évaporites au front d'un anticlinal de grande amplitude.

4.5. THE WESTERN MOLASSE BASIN

4.5.1. Previous studies

Research on the stratigraphy and the sedimentology in the western Molasse Basin has a long history. Lithostratigraphic logs (e.g. Fig. 2.9) have been established since the beginning of the century and detailed stratigraphic correlations along the Molasse Basin are not so straightforward, due to the lateral changes of facies and especially to the scarcity of outcrops (references concerning the stratigraphy of the western Molasse Basin have been cited in Chapter 2).

Few structural studies of the Molasse Basin have been published, due to the scarcity and poor quality of outcrops and the extensive cover by ground moraine. Furthermore, the gentle dip of the bedding requires careful collection of much data to map structures. During World War II, many Molasse areas were precisely mapped for oil exploration, resulting in detailed structural maps (ALTHAUS & RICKENBACH, 1947, 1952; SCHUPPLI, 1950), which show the main anticline and syncline structures and the major tear faults.

Recently, the availability of modern industry seismic lines has allowed elucidation of the stratigraphy and the structures beneath the Tertiary sediments. Structural interpretations and a contour map of the base of the Molasse sediments have been presented by JORDI (1990, 1993) for the Yverdon-Lake Morat region, by GORIN *et al.* (1993) for the Lausanne and Geneva Cantons region and by SIGNER & GORIN (1995) for the Geneva area. All these interpretations show that the Plateau Molasse consists of a weakly deformed Tertiary clastic wedge thinning towards the Jura belt and onlapping the top Mesozoic strata towards the N-NW.

4.5.2. Interpretations and contour maps

Surface geological maps from the Plateau- and Subalpine Molasse (ALTHAUS & RICKENBACH, 1947; SCHUPPLI, 1950; BERSIER, 1952; VERNET, 1972; WEIDMANN, 1988, 1992; JORDI, 1994) give an overview of the major structures that involve the Cenozoic and Mesozoic strata i.e. tear faults, broad folds and thrust sheets. These features have also been recognized in the subsurface and are interpreted on Panels 4, 5, 6. Seismic lines are mostly located in the Plateau Molasse, except for two lines, Sections 43 and 45, which extend into the Subalpine Molasse, because of their greater length.

In the Molasse Basin, Cenozoic strata are onlapping the Mesozoic beds. On most strike lines, they appear strictly parallel. In some dip lines, located in the southern Molasse Basin e.g. Section 43 on Panel 5, Tertiary sediments onlap clearly onto the underlying strata. Onlaps have been observed mostly on south dipping limbs of structures. The interpretation of these onlaps is discussed in Chapter 3 and Chapter 5.

At a large scale, the Mesozoic strata of the Plateau Molasse dip to the SE, as demonstrated by subcrop contour maps of the top of the Cretaceous, upper Malm, "Argovian", Dogger, Triassic Unit 1 and Triassic Unit 2 layers (Figs. 4.11 to 4.17) within the western Molasse Basin. These contours maps are based on depth conversion of the seismic lines and have been calibrated by well log data. Seismic velocities used for each seismic unit are presented in Appendices 3. Contours have been calculated by computer, using a bilinear interpolation method. Tear faults, as known from geological maps and surface data, as well as seismic interpretation, have been imposed as discontinuities in the contour calculations. As a result small zones due to insufficient data density (blank zones in the maps) appear during contouring in the vicinity of these faults. Furthermore, minor closed contours may in some cases also represent contouring artifacts. Despite these contouring artifacts, the complete original computer contoured maps are presented here, because they clearly and objectively show large scale regional trends.

All these maps highlight a hinterland-dipping Mesozoic monocline with a NE-SW structural trend, except along the south-western and northern edges which are unfortunately not well constrained by data and are crossed by several faults. Cretaceous, upper Malm and Triassic Unit 1 depth maps clearly show a depression located between the two major tear faults (on the West Pontarlier fault, on the East La Sarraz fault). This structural low has already been noted by GORIN *et al.* (1993) on their schematic Base Molasse map. This depression is located exactly above a thin thickness of Triassic Unit 2 beds (compare Figure 4.11 and Figure 3.6) and therefore seems to be related to it. Other thinning or alternatively thickening shown on the isopach map of Triassic Unit 2 beds (Fig. 2.29, Fig. 3.6) does not seem to have any direct impact for the overlying unit maps. Of course the spacing (200 m) of the depth intervals in Figures 4.11 to 4.17 is too large to resolve structures involving 100, 150 or even 200 m thickness changes.

Isopach maps of Triassic Unit 2 are presented in Figures 2.29 and 3.6. The first figure (Fig. 2.29) has been contoured automatically by computer and the second (Fig. 3.6) has been contoured by hand, but based on the same data set. Both maps highlight elongated or elliptical thickening or thinning of Triassic Unit 2 along a NE-SW trend, parallel to the general trend of the Jura fold belt. The maximal thickness coincides with the most internal Jura anticlines. Some major sinistral tear faults oriented NNW-SSE (Pontarlier fault) to N-S (Yverdon-Treycovagnes area) and the conjugate dextral system WNW-ESE (La Sarraz fault) cross-cut and offset these pillows. In the hand contoured map, computer artifacts have been neglected to produce better lateral continuity of structures and the position of geological surface structures has also been taken into account. Furthermore, the

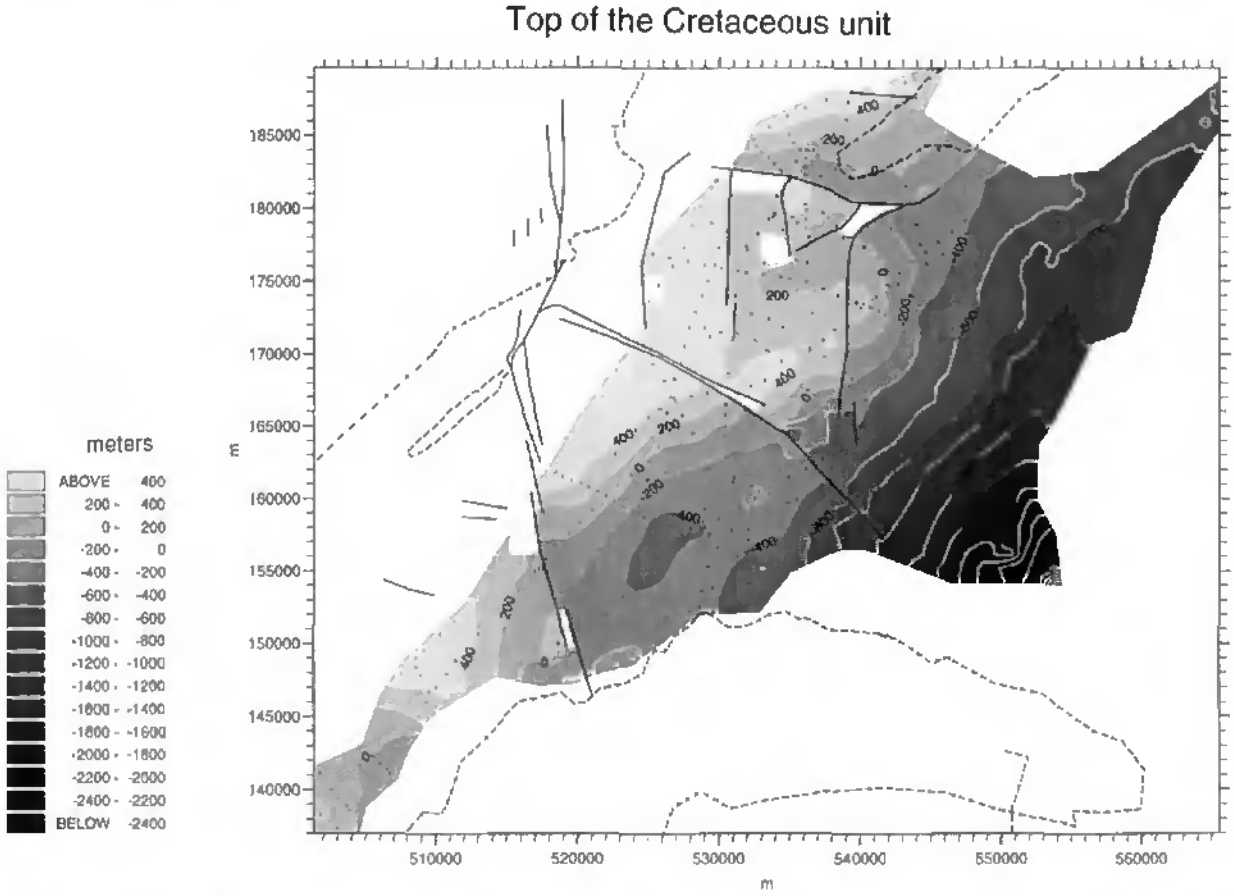

Figure 4.11: Contour map of the top Cretaceous unit in the western Molasse Basin. Depths are in meters. Black dots are shotpoints used for depth control of contour map. Note that blank areas and tight closed circles are computer-related artefacts in areas of sparse control. Numbers on the side and bottom are in meters, that relate to the Swiss national geographical coordinate system. Lakes Geneva and Neuchâtel are outlined for general reference.

Carte structurale des contours du toit des couches du Crétacé dans le Bassin molassique occidental (profondeurs en mètres). Les points noirs représentent la position géographique des points de tir, utilisés pour le contrôle des profondeurs de la carte de contours. Les zones vides et les petits cercles fermés sont des artefacts, dus au programme de contourage, dans des régions où la densité des données est faible. Les coordonnées géographiques (en mètres) se réfèrent à la grille suisse. Les lacs Léman et de Neuchâtel permettent une localisation générale de la carte.

Figure 4.12 (page 133, top): Contour map of the top upper Malm unit in the western Molasse Basin. Depths are in meters. For explanation see legend of Figure 4.11.

Carte structurale des contours du toit des couches du Malm supérieur dans le Bassin molassique occidental (profondeurs en mètres). Pour les explications, voir la légende de la Figure 4.11.

Figure 4.13 (page 133, bottom): Contour map of the top "Argovian" unit (lower Malm) in the western Molasse Basin. Depths are in meters. For explanation see legend of Figure 4.11.

Carte structurale des contours du toit des couches de l'"Argovien" (Malm inférieur) dans le Bassin molassique occidental (profondeurs en mètres). Pour les explications, voir la légende de la Figure 4.11.

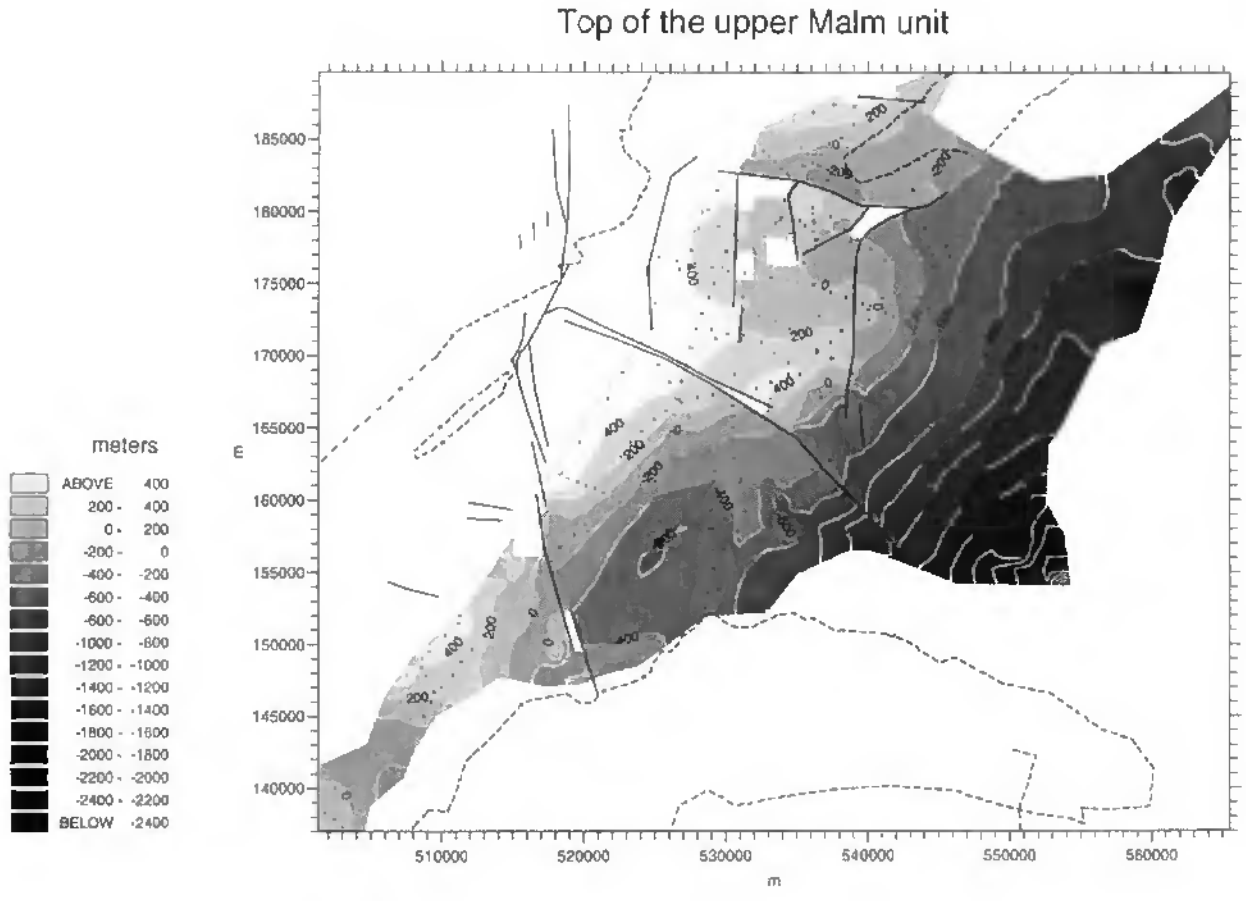

Figure 4.12

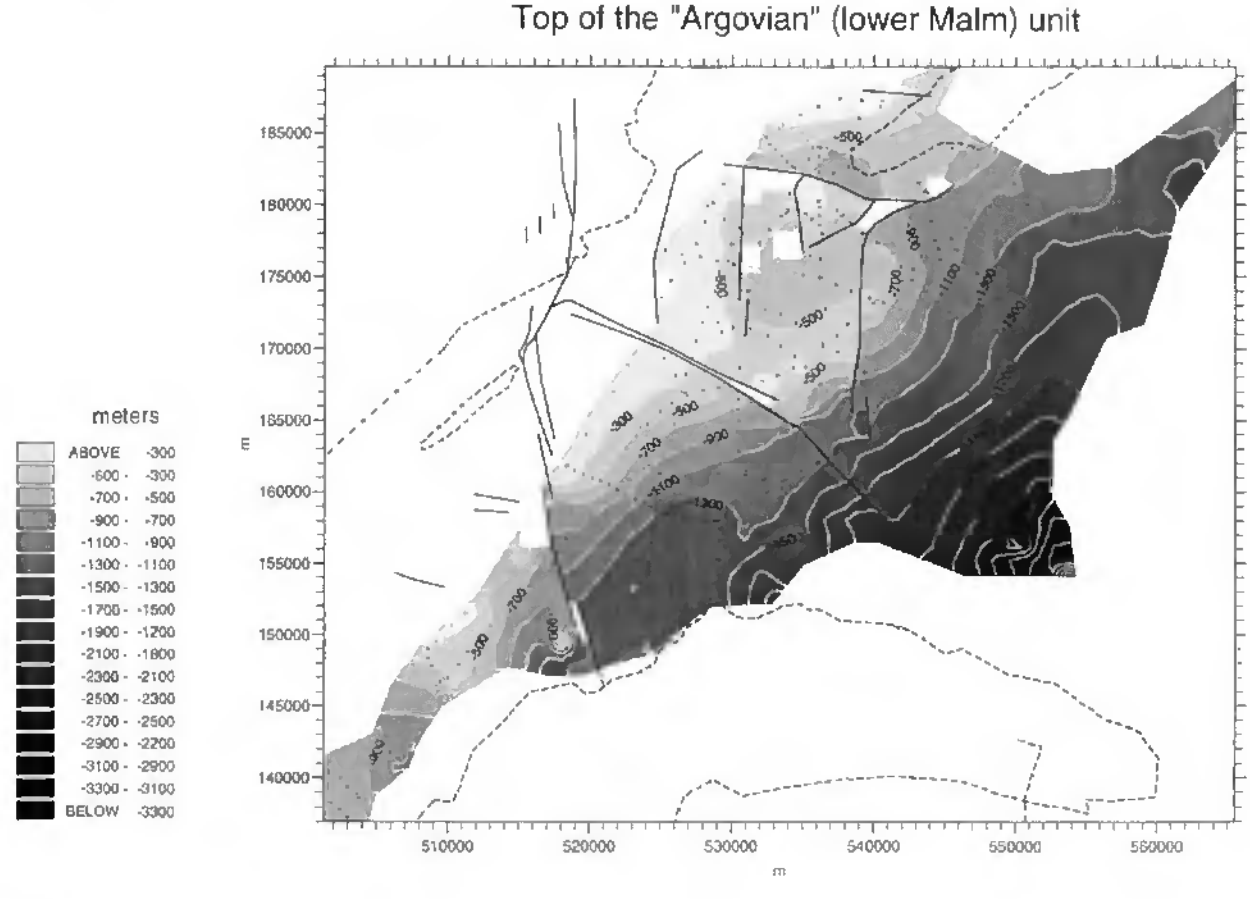

Figure 4.13

contour intervals are closer (each 50 m). The broad folds from the Plateau Molasse, observed on these maps, are due to tectonic thickening of evaporites, salt and clays within the Triassic Unit 2 (see discussion in Chapter 3).

The Subalpine Molasse is characterized by a stack of thrust sheets of Tertiary sediments detached along an incompetent décollement zone at the base of the Oligocene layers ("Grisigen shales" formation or "Schistes à Meletta" formation: TRÜMPY, 1980). Unfortunately, seismic resolution is really poor within the Molasse and therefore does not allow clear observation of these structures. Nevertheless, foreland-vergent thrust faults have been recognized on seismic lines crossing the Subalpine Molasse (Sections 43 and 45 on Panel 5; Plates 6 and 7). Beneath the Subalpine Molasse, the Mesozoic layers present small thrust faults. Furthermore, seismic Section 43 (on Panel 5)

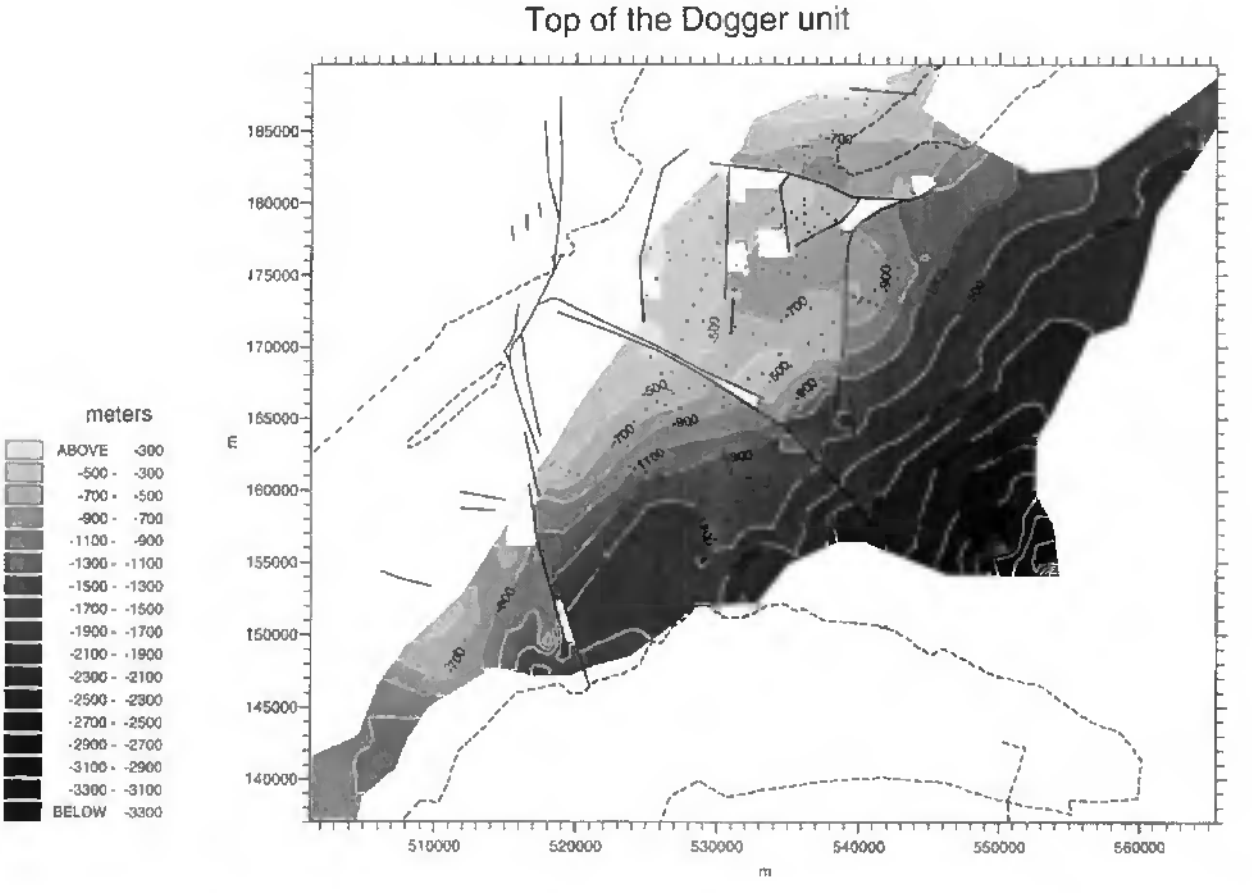

Figure 4.14: Contour map of the top Dogger unit in the western Molasse Basin. Depths are in meters. For explanation see legend of Figure 4.11.

Carte structurale des contours du toit des couches du Dogger dans le Bassin molassique occidental (profondeurs en mètres). Pour les explications, voir la légende de la Figure 4.11.

Figure 4.15 (page 135, top): Contour map of the top of the Liassic unit from the western Molasse Basin. Depths are in meters. For explanation see legend of Figure 4.11.

Carte structurale des contours du toit des couches du Lias dans le Bassin molassique occidental (profondeurs en mètres). Pour les explications, voir la légende de la Figure 4.11.

Figure 4.16 (page 135, bottom): Contour map of the top Triassic Unit 1 in the western Molasse Basin. Depths are in meters. For explanation see legend of Figure 4.11.

Carte structurale des contours du toit des couches de l'Unité 1 du Trias dans le Bassin molassique occidental (profondeurs en mètres). Pour les explications, voir la légende de la Figure 4.11.

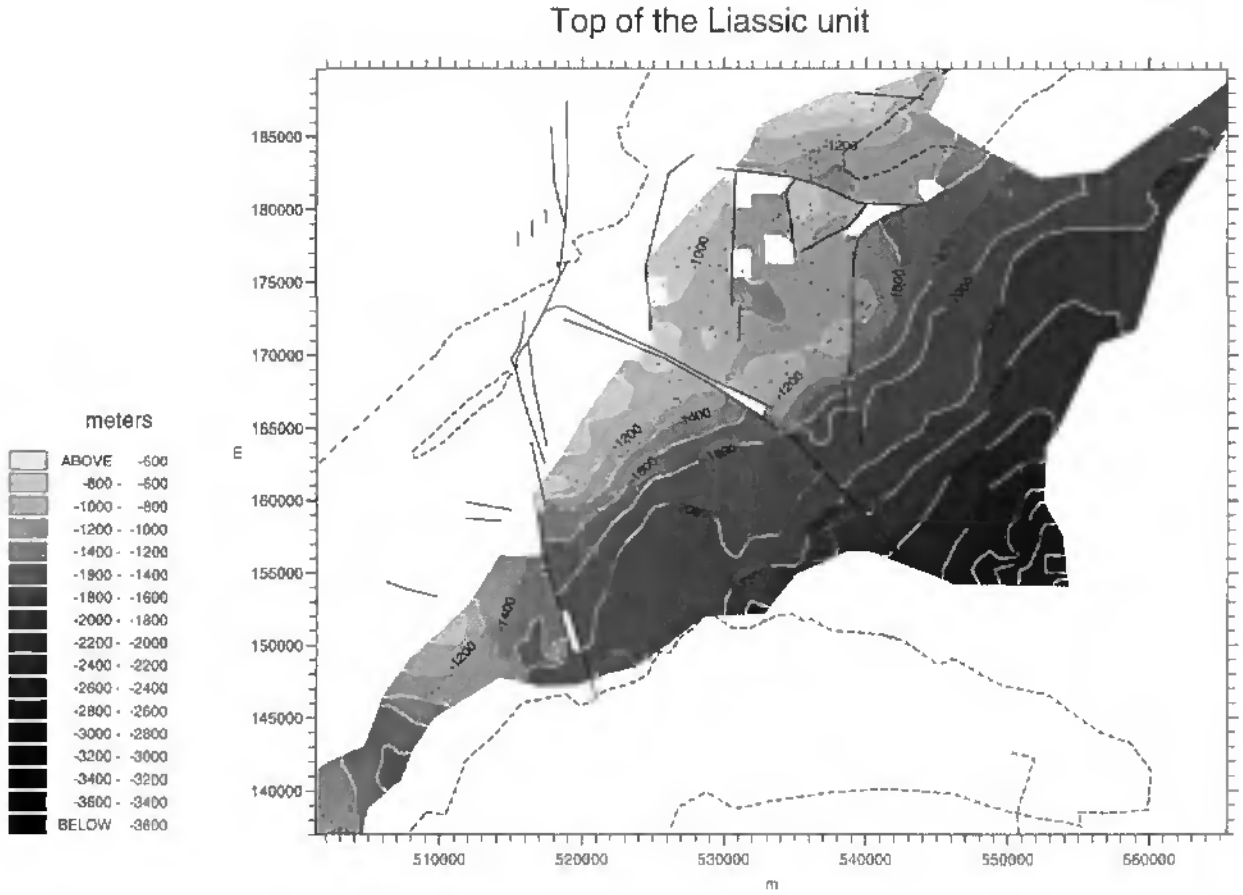

Figure 4.15

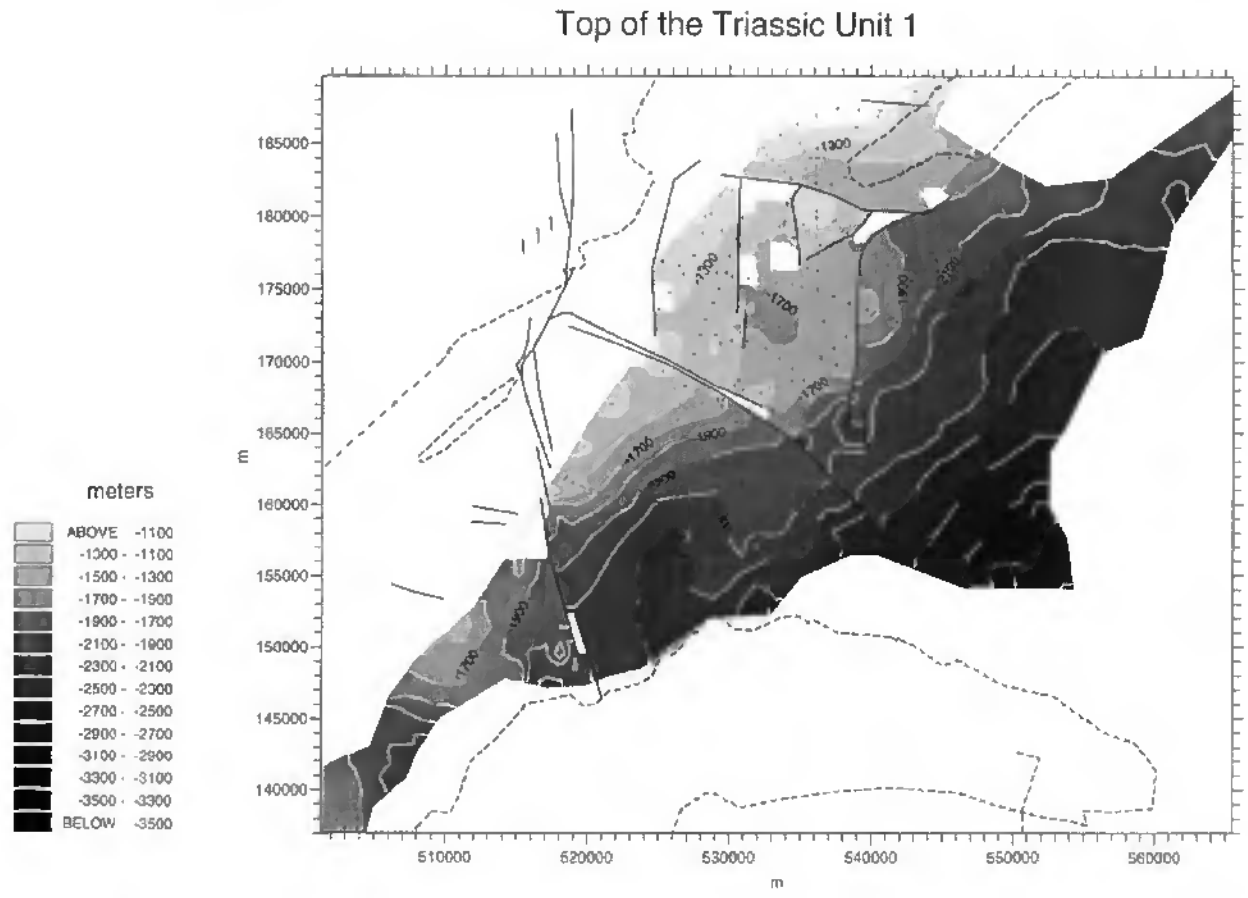

Figure 4.16

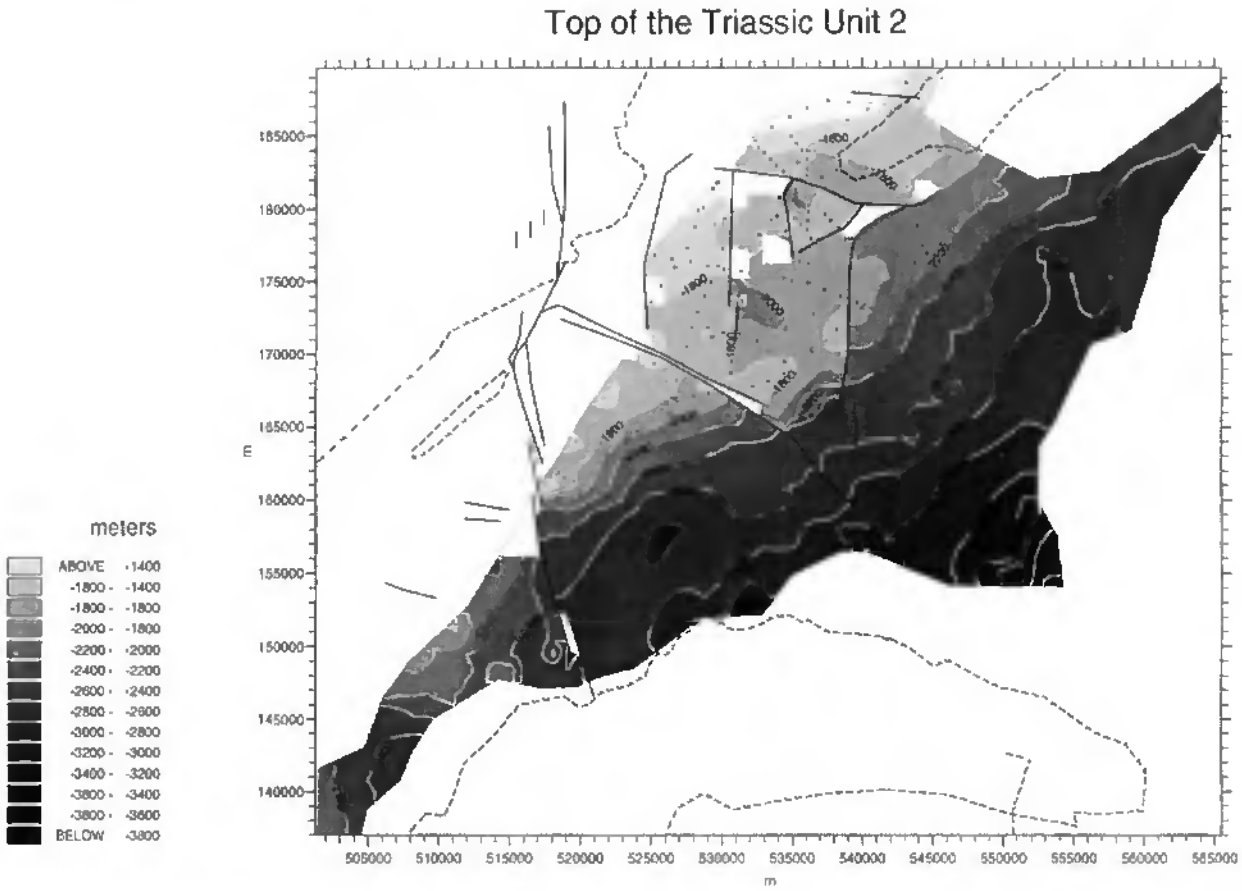

Figure 4.17: Contour map of the top Triassic Unit 2 in the western Molasse Basin. Depths are in meters. For explanation see legend of Figure 4.11.

Carte structurale des contours du toit des couches de l'Unité 2 du Trias dans le Bassin molassique occidental (profondeurs en mètres). Pour les explications, voir la légende de la Figure 4.11.

shows Cenozoic and Mesozoic foreland dipping reflectors in its southernmost part. The latter may be interpreted to be linked, through a simple, bend to the south dipping reflectors further to the North in the Molasse Basin. The interpretation of this bend is difficult and is clearly related to a structure underlying the Triassic strata. One interpretation involves a slice of basement, related to a thrust fault rooting in the basement. This thrust fault may step up from the basement into the basal Triassic evaporites and then evolves as the main decoupling zone for the Jura fold and thrust belt (MOSAR *et al.*, 1996). Another hypothesis could be that of GORIN *et al.* (1993), who proposed an inverted Permo-Carboniferous graben and a third suggestion could be a thick evaporite pillow. All these interpretations have profound implications for the formation of the Jura foreland fold and thrust belt, which will be discussed in Chapter 5. It should also be noted, that these structures occur at the end of a non migrated line that runs obliquely to the direction of local structures, cautioning against overinterpretations.

4.5.3. The Yverdon - Treycovagnes area

4.5.3.1. Previous studies

The Yverdon-les-Bains area has attracted much attention, because of hot water springs. During the 1970's, Shell conducted a seismic survey (Swisspetrol) and drilled a well (Treycovagnes, see Appendix 2) for oil exploration (Figs. 1.4 and 4.1). Besides the wells drilled by oil industry during the 1940's (Cuarny, see Appendix 2), the 1960's (Essertines) and 1970's (Treycovagnes), many shallow holes were made recently for geothermal purposes or for mineral water production (BURGER & GOHRAN, 1986).

The area has been the subject of several geological studies: the earliest were based on surface geo-

logy (RENEVIER, 1854; JORDI, 1955) and later studies were based on surface geology observations and subsurface interpretations of seismic lines and wells (JORDI, 1990, 1993, 1994, 1995).

The recent investigation of the Yverdon area for hydrogeological purposes (CHYN, 1995; MURALT *et al.*, 1997) has led to a new detailed interpretation of seismic lines in this region which is presented below.

4.5.3.2. Geological setting

The Yverdon-Treycovagnes area extends along the foot of the internal Jura, at the southern end of Lake Neuchâtel (Fig. 4.3). The region is dissected by two conjugate sets of tear faults that trend N-S (sinistral) and W-E to WNW-ESE (dextral). A complex dextral fault zone, the Pipechat-Chamblon-Chevressy fault zone (PCC, see Figure 4.3) (JORDI, 1993) with at least two distinct faults (North and South fault), is joined by several southward trending sinistral faults: one along the western border of Mont de Chamblon and a second from the Plaine de Baulmes towards the South. All these faults also have a reverse compressional component and are transpressive faults. The areas located SE of the junctions of the sinistral with the dextral faults consequently form NW-pointing "indenters". They are either uplifted above NW-vergent thrust faults (e.g. Chamblon) or depressed below SE-vergent backthrusts. Near Yverdon, major water sources are all located along these faults.

4.5.3.3. Interpretation

The interpreted seismic lines (see Figure 4.1 for the seismic grid) were depth converted according to velocities presented in Appendices 3. Compilation and correlation of all data led to a well supported structural model of the Yverdon area (Fig. 4.19), except for the faulted zone along the dextral transpressive PCC-fault. Seismic reflectors within this zone are blurred and the sparse surface data have had to be projected laterally over large distances and downwards across décollement horizons.

On all seismic lines crossing the PCC-fault, the reflectors dip gently south outside the faulted zone. Within the faulted zone, reflectors dip gently south on the westernmost line (Section 38 on Panel 6) and are subhorizontal on the next line to the East (Section 24, see Figure 1.4 for location). On both lines the reflectors within the fault zone are well displayed and thus the south-dipping faults on either side are constrained. Section 25, the next line to the east, cuts the fault zone at a highly oblique angle. The faulted zone is blurred, but a gentle northward dip of some Cretaceous-Malm reflectors can be inferred nonetheless. Since both faults have a compressional component and the hangingwall as well as footwall of the whole fault zone are clearly displayed, the inter-fault zone can be established with some confidence, once its general dip direction is known. The resulting structure (Fig. 4.18) is a fault-related fold with two faults breaking through the frontal limb. A third thrust fault is inferred at depth to account for the gentle northern dip of the strata immediately to the north of the faulted zone.

Seismic and drill hole data show thickness changes of various strata across the PCC fault zone. The Dogger sequence decreases from 420 m in the South to 290 m in the North (Fig. 4.18). This may be due to a Jurassic normal fault, reactivated during the Jura folding in late Miocene-Pliocene time. Reactivated faults often show tortuous geometries in detail, so local complexities must be expected. Such an inherited fault could also have influenced the orientation of the younger fault zone presently observed. Further, tectonic thickening of the ductile beds during the Miocene deformation cannot be excluded. In any case two different regions which were not juxtaposed during Jurassic sedimentation time, are today juxtaposed.

The interpretation and the depth conversion of the seismic lines discussed above have led to a structural model of the top of the Dogger unit. Figure 4.19 represents a structural contour map of the Dogger in the Yverdon-Treycovagnes area. This figure highlights the structure of the Chamblon area, which appears to form a NW-pointing indenter uplifted above a NW vergent-thrust fault. The vergence of the structures along the PCC fault changes further towards the East, where the northern side is uplifted above a steep southeast vergent thrust fault (Fig. 4.19).

In conclusion, the Chamblon hill (Yverdon-Treycovagnes area) shows a north-vergent fault-related fold with two to three faults breaking through the frontal limb. The thrust faults sole out in the Triassic décollement zone, but there are also suggestions that the Alpine faults reactivate earlier, possibly Liassic normal faults.

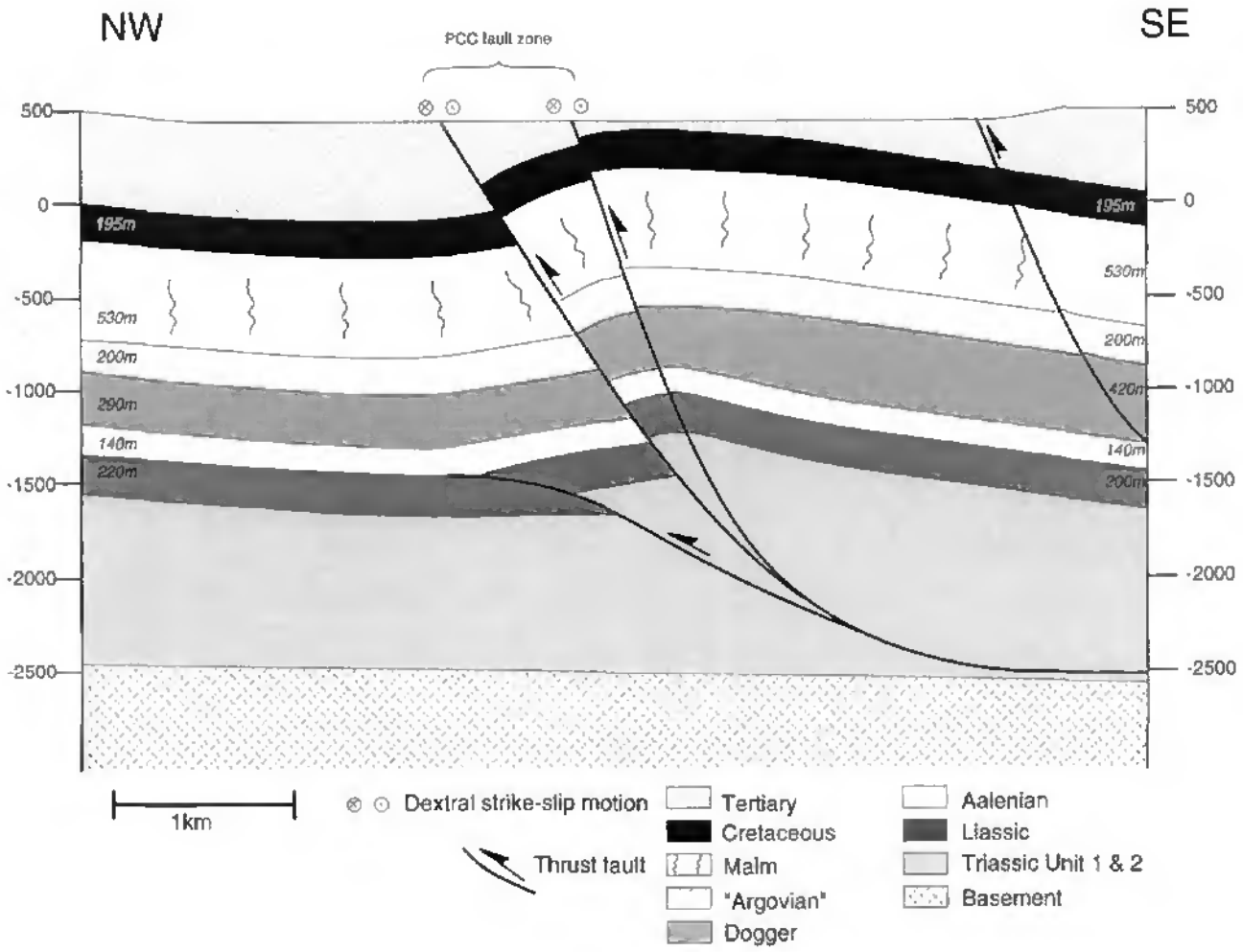

Figure 4.18: Geological cross-section oriented NW-SE based on surface geological data and completed at depth with information from seismic Section 25, Section 27 (Panel 5) and Section 38 (Panel 6). This geological section crosses the Chamblon hill (for location see Figs. 4.3 and 4.9). Modified from MURALT *et al.* (1997).

Coupe géologique orientée NW-SE construite à partir des données de la surface et complétée en profondeur par les informations des profils sismiques 25, 27 (Panneau 5) et 38 (Panneau 6). Cette coupe traverse la colline du Mont de Chamblon (pour localisation voir Figs. 4.3 et. 4.9). Modifiée de MURALT *et al. (1997).*

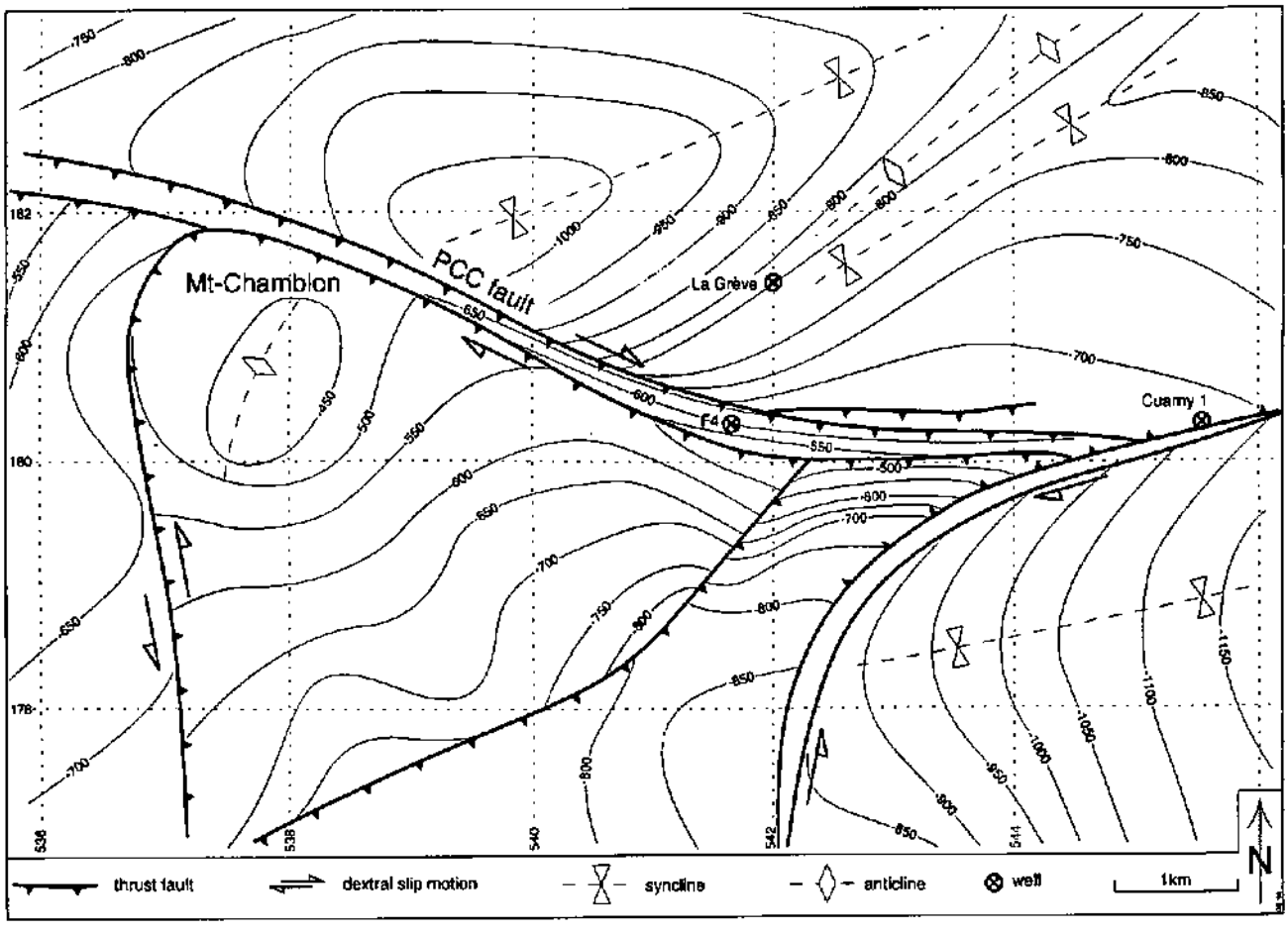

Figure 4.19: Contour map of the top Dogger in the Yverdon-Treycovagnes area, western Molasse Basin. Depths are in meters, below sea level. Numbers on the side and bottom are in kilometers that relate to the Swiss national geographical coordinate system. Modified from MURALT *et al.* (1997).

Carte structurale des contours du toit des couches Dogger dans la région d'Yverdon-Treycovagnes, Bassin molassique occidental (profondeurs en mètres, en-dessous du niveau de la mer). Les coordonnées géographiques (en kilomètres) se réfèrent à la grille suisse. Modifiée de MURALT *et al. (1997).*

5. SYNTHESIS AND DISCUSSION

The synthesis and discussion emphasize the following important points:

- the boundary conditions such as the geometry of the basement top, the distribution of the very weak décollement zone
- the geometry of structures in the Jura and the Molasse Basin
- correlation between inherited structures in the basement and in the cover
- the Molasse Basin, example of a foredeep basin
- the link from the Jura to the Alps.

Structure of the basement top

The depth conversion of all seismic lines has allowed a mapping of the depth to top basement in the central Jura and the Molasse Basin (Fig. 5.1). In the Jura area, a simple velocity model, attributing a constant velocity to each major interval (Tertiary, Cretaceous, Jurassic and Triassic), has been used. In the Molasse Basin, however, more complex depth-dependent conversion functions from NAGRA (NAEF & DIEBOLD, 1990) were used in order to account for increased velocities due to the considerable thickening and facies changes of Tertiary sediments (see Appendices 3 for seismic velocities). The contour map highlights a smooth basement that dips uniformly at 1° to 3° to the SSE. Some broad irregularities in Figure 5.1, e.g. Treycovagnes, are better illustrated in the three-dimensional view of the top basement map (Fig. 5.2). An apparently flat area (with a high at Treycovagnes) at the SW edge of Lake Neuchâtel is visible. The Treycovagnes area has been analyzed carefully (see Chapter 4) and no major basement high appears on the interpreted seismic lines. Depths from well data (e.g. Treycovagnes, Laveron, Essavilly, Valempoulières) fit to +/-200 m the depths obtained from depth converted seismic time lines. Discrepancies may be due to the use of inappropriate seismic velocities, especially in the weathering layer (SCHNEGG & SOMMARUGA, 1995). However, seismic velocities used in this work are compatible with the overall well information, but do not satisfy precisely individual drill hole data. It seems that the velocity model used here lies on the fast side (i.e. seismically obtained depths are slightly deeper than those obtained from drill holes).

The trend of the basement is E-W in the Neuchâtel Jura and NE-SW or ENE-WSW in the other regions (Risoux, external Jura and Molasse Basin, Fig. 5.1). The E-W trend of the Neuchâtel Jura differs by an angle of 30° from the orientation of structures in the Jura fold and thrust belt. The contour map presented here is coherent with the crude map from BÜCHI & ETHZ (1981). Even if the values of the contour map are not absolute, Figures 5.1 and 5.2 clearly demonstrate the morphology and orientation of the basement structures, which are important in understanding the formation of the Jura foreland fold and thrust belt.

It has to be emphasized, that the major tear faults (e.g. Pontarlier, La Sarraz) presented in Chapter 3 do not show any significant offset of the basement top. Along these faults, data are reasonably well constrained in the Molasse Basin and no major bend is visible (Fig. 5.1). The tear faults are therefore limited to the sedimentary cover of the Jura. In addition, evaporite-related folds and thrust-related folds are floored by subhorizontal layers at their base. No evidence has been found (see description in Chapter 3) for construction of thrust faults downward into the pre-Triassic basement. Nowhere in the study area has this basal décollement layer been disrupted by later thrusts.

Any irregularities which exist in the top of the basement are small compared to the thickness of Triassic Unit 2 (see Figure 3.6), which ranges from 100 m to more than 1000 m. On the south-eastern edge of the map (Fig. 5.1), near the front of the Subalpine Molasse, the basement dips toward the North showing an important uplift. The latter, highlighted by only one seismic line (Section 43), has been already discussed in Chapter 4 (§4.5). This map shows a basement high resulting either from an inversion of a Permo-Carboniferous graben or else a basement slice. No reflector appears beneath the supposed basement top and therefore it is difficult

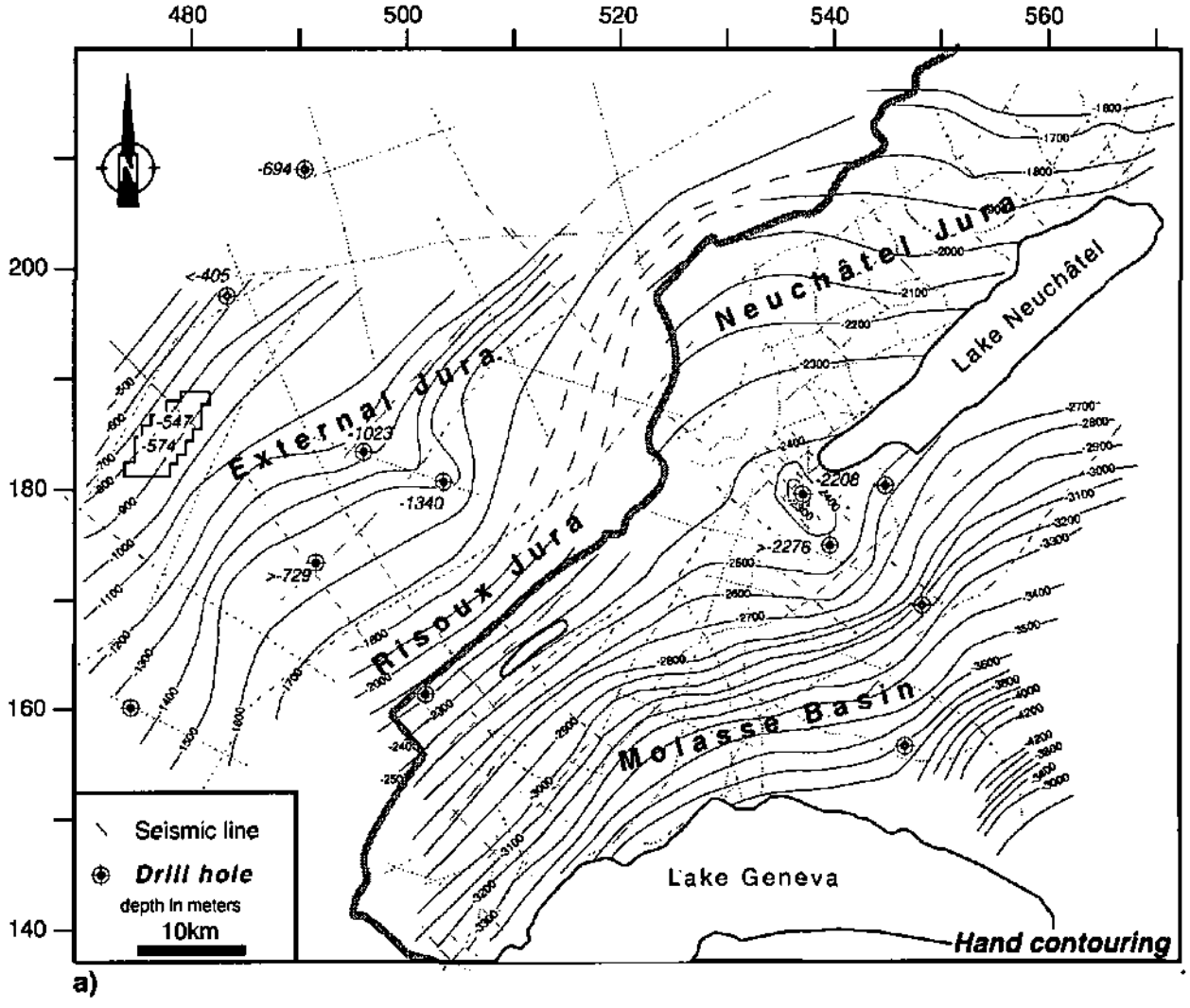

Figure 5.1 (pages 142, 143): Map of the depth to top basement in the central Jura and western Molasse Basin. Depths are in meters with reference to the sea level. Depths next to drill holes correspond to top basement depth from drill hole data. Minimal depths (>...) are from drill holes which ended within the Triassic layers. No depth indication is given for drill holes which did not reach the Triassic. Coordinates (in km) are according to the Swiss national geographical coordinate system.

a) Contours made by hand. Gray thin lines represent the seismic grid. Modified from SOMMARUGA (1995).

b) Contours made automatically by computer. Compare with Figure 5.1a. Black dots correspond to location of depth control at shot points along seismic lines.

Carte du toit du socle du Jura central et du Bassin molassique occidental. Les profondeurs sont exprimées en mètres par rapport au niveau de la mer. Les chiffres à côté des forages indiquent la profondeur du toit du socle dans le forage. Les profondeurs minimales (>...) sont indiquées pour les forages se terminant dans les couches du Trias. Aucune indication n'a été donnée pour les sondages n'atteignant pas les séries du Trias. Les coordonnées (en km) correspondent à la grille de référence géographique de la Suisse.

a) Contourage interpolé à la main. Les fines lignes grises fines représentent la grille sismique. Modifié de SOMMARUGA (1995).

b) Contourage automatique assisté par l'ordinateur. Comparer avec la Figure 5.1a. Les points noirs représentent la position géographique des points de tir, utilisée pour le contrôle des profondeurs de la carte de contours.

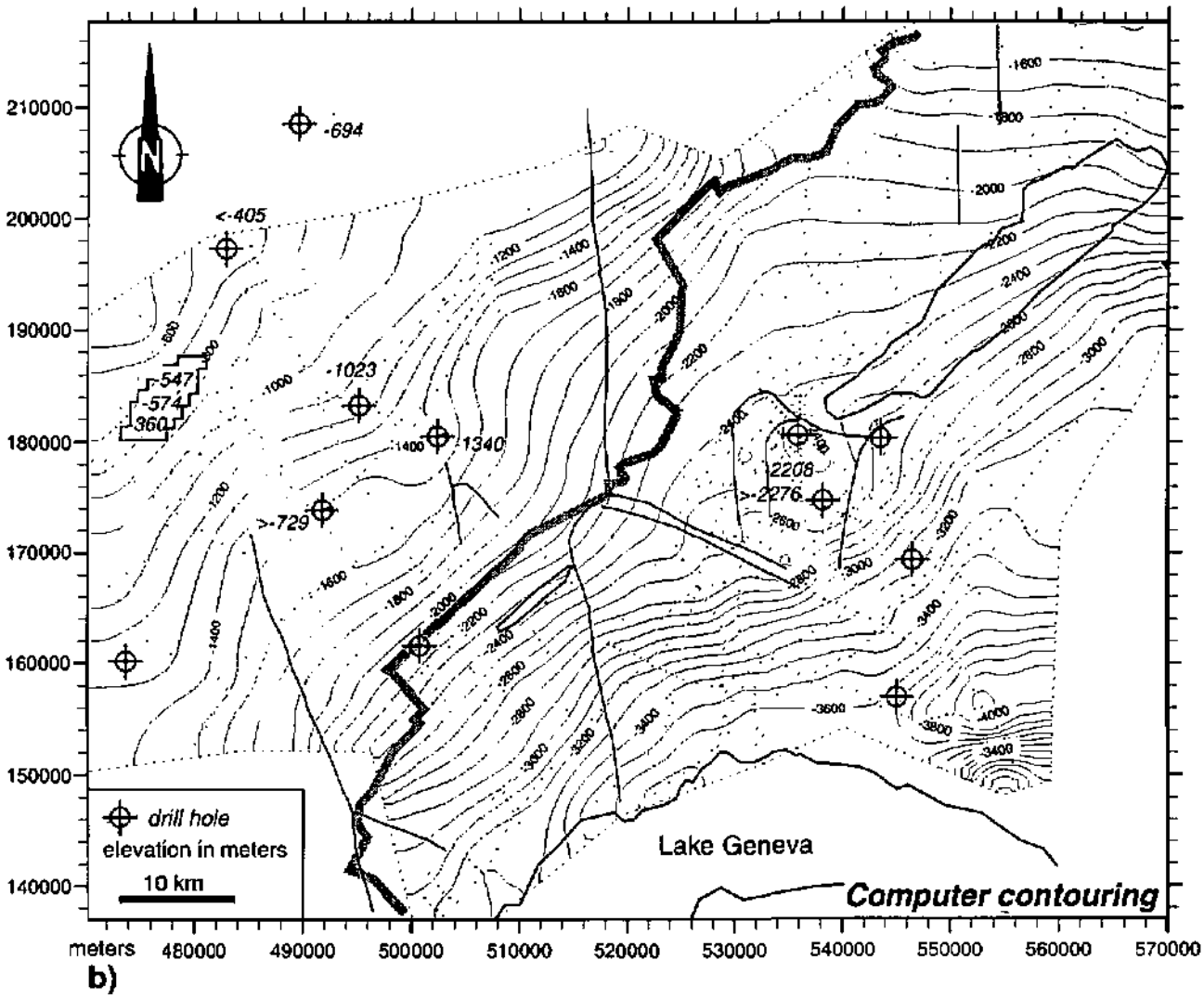

Figure 5.1b: For legend see page 142.
Pour la légende, voir page 142.

to interpret the nature of this high. It has also to be recalled, that Section 43 is a non migrated line running at a low angle to the direction of local structures and caution is required in interpretation. There is a problem related to seismic interpretation of fact or artifact.

It should be noted that the presence, beneath the Jura fold and thrust belt, of a continuous basement dipping 1° to 3° toward the South and underlying a weak décollement level was previously proposed by BUXTORF (1907) almost ninety years ago, from subcrop observations along the Grenchenberg railway tunnel (see Figure 1.5, cross-section 2).

Extension of the Triassic evaporites

In the central Jura and the Molasse Basin, the presence of the very weak (Fig. 2.30) Triassic Unit 2, at the base of the sedimentary cover has been confirmed by well data (see Figs. 2.11 to 2.13), by sample analyses (JORDAN, 1994) and also by interpretation of seismic lines. This very weak zone consists of salt, gypsum, anhydrite and clay, of which salt is by far the weakest lithology. In the Jura, thicknesses of pure salt range between 20 m and 300 m (Laveron drill hole). The Triassic Unit 2 zone is bound by two décollement horizons (roof and basal décollements). The style of deformation within this zone is very different from the overlying weak Triassic Unit 1 layer and the strong Jurassic layers, as well as from the underlying crystalline (or sedimentary) basement.

In the Molasse Basin, the isopach map of Triassic Unit 2 (Fig. 3.6) clearly shows changes in thickness along a NE-SW trend. These changes in thickness contrast significantly with the smooth and planar top basement (Fig. 5.1), suggesting "ductile" defor-

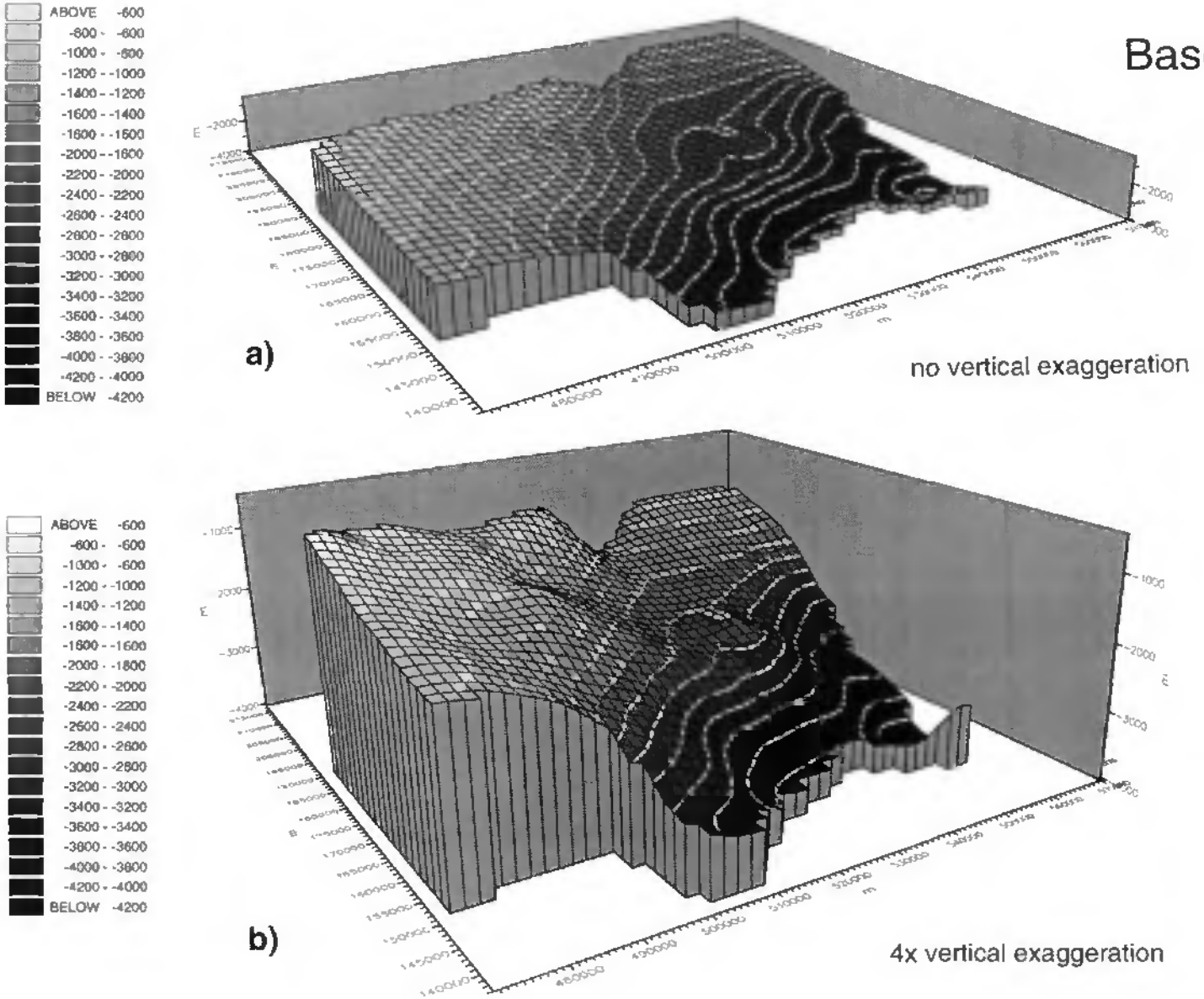

Figure 5.2: Three-dimensional view towards the NW representing the top of basement in the central Jura and the western Molasse Basin. This figure is based on data from the structural contour map presented in Figure 5.1. Vertical axes are in meters below sea level and horizontal axes are in kilometers (Swiss geographic coordinate grid).
a) No vertical exaggeration;
b) 4x vertical exaggeration.

Vue tridimensionnelle vers le NW du toit du socle dans le Jura central et le Bassin molassique occidental. Cette figure est basée sur les données de la carte structurale des contours présentée à la Figure 5.1. Les axes de coordonnées verticales et horizontales sont exprimés en mètres (grille de référence des coordonnées géographiques suisses).
a) sans exagération verticale;
b) exagération verticale de 4 x.

mation within Triassic Unit 2. In the eastern Jura, both, Triassic Unit 1 and Unit 2 layers seem to host décollement horizons. An isopach map of both Triassic Units in the Jura and its vicinity has been compiled in order to examine possible correlation between the distribution of Triassic strata and the extent of the deformed Jura cover (Fig. 2.5). A rather good correlation between both may be inferred from Figure 2.5. The thickest regions correspond to the central Haute Chaîne Jura and to the southern part of the external Jura. Towards the East (e.g. German Molasse Basin), even where Triassic sequences are preserved, they do not contain evaporites (BACHMANN *et al.*, 1987). Towards the Southwest, several drill holes have also demonstrated the absence of evaporitic layers (PHILIPPE, 1994). It therefore appears likely that the existence, as well as the arcuate shape of the Jura fold and thrust belt, is intimately linked to the presence of Triassic evaporites. Within the whole Molasse Basin, the change in structural style along strike, from a transported basin (western Molasse Basin) to an autochtonous basin (eastern Molasse Basin), is therefore due to the thinning and then absence of evaporite horizons. The presence of a thick and very weak basal layer beneath the Jura and the western Molasse Basin is thus important for the understanding of the formation of this foreland fold and thrust belt.

Characteristics of fold and thrust belts developed over a very weak basal décollement

A common feature of foreland fold and thrust belts is the presence of a basal décollement surface or zone, which dips towards the hinterland and below which relatively little deformation occurs (CHAPPLE, 1978; DAVIS & ENGELDER, 1985). The basal layer bounding the thin-skinned belt is generally composed of particularly weak rocks, e.g. salt, evaporite or shale. The undeformed sediments below this layer often do not differ much in rheology from those above the basal décollement and which have participated in the deformation. According to CHAPPLE (1978), it is not the mechanical contrast between basement and cover but rather the presence of a weak layer that seems to determine the thin-skinned nature of such folded belts.

Many fold and thrust belts around the world (e.g. Melville Island Fig. 3.13, Appalachian Plateau Fig. 3.14, Alberta and British Columbia Rocky Mountains,...) have developed above a weak basal layer (salt and/or evaporites and/or shales). A comparison of these belts has allowed some authors e.g. BALLY *et al.* (1966), DAVIS & ENGELDER (1985, 1987) to characterize these compressional terranes as broad belts with a low-angle cross-sectional taper, laterally continuous symmetric folds, broad synclines, anticlinal salt flow and forward as well as backward verging folds and thrusts.

The critical taper is the cross-sectional wedge profile maintained when an entire thrust belt is on the verge of horizontal compressive failure. The magnitude of the angle between surface topography and the décollement surface of the critical taper of belt or accretionary prism is governed by the relative magnitudes of the frictional resistance along the base and the compressive strength of the wedge material (DAHLEN, 1990). Therefore, the contrast in competence between the basal décollement zone and the overlying cover series is responsible for the minimum (and maximum) permissible critical taper angle. The critical angle is therefore the sum of the angles of the décollement dip, which is towards the hinterland, and the topographic slope towards the foreland (CHAPPLE, 1978; DAVIS & ENGELDER, 1985; DAHLEN, 1990). The lowermost permissible critical taper angle determines the locus of the thrust front in any transport parallel cross section. Propagation of this front toward the foreland is achieved by thickening at the back of the thrust wedge which results in an increase of the topographic slope.

Foreland fold and thrust belts riding above salt décollements typically have extremely low critical taper angles of less than 1° (DAHLEN *et al.*, 1984; DAVIS & ENGELDER, 1985, 1987) and in these cases topographic slopes may be virtually absent. In such a low angle taper, internal deformation of the wedge may take place by symmetric foreland- or hinterland-vergent thrusts. This is in contrast to higher angle tapers (commonly in excess of 8°), where a predominance of shallow foreland vergent thrusts is both predicted and observed (DAVIS & ENGELDER, 1985; DAHLEN, 1990). Recently PHILIPPE (1995) calculated a critical taper angle of 3,4° for the Jura fold and thrust belt, based on an angle of 1,6° for the topography and 1,8° for the basement. This is in good agreement with results herein, since an angle of 1° to 2° for the basal décollement is observed on the top of basement map (Fig. 5.1). However, the topographic slope, when considered from the toe of the Jura to the crest of the Alps, does show a conspicuous hinterland-dipping portion located at the transition from the Jura to the Molasse Basin. This hinterland-dipping slope can be explained by the important glacial erosion that occurred during

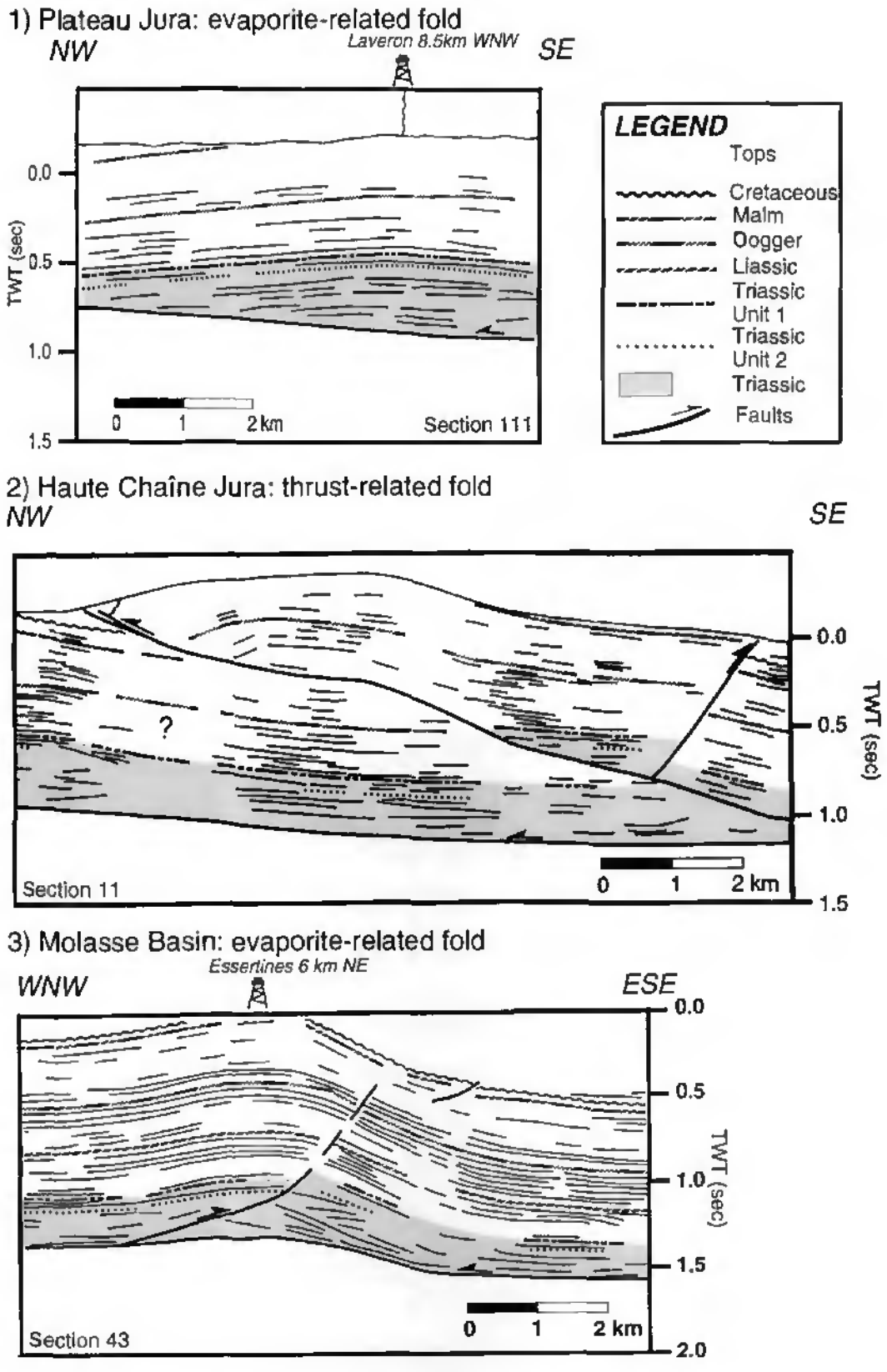

Figure 5.3: Line drawings of examples of typical fold structures in the Jura and the Molasse Basin (example numbers refer to Figure 3.1). Horizontal scale is in meters, whereas vertical scale is in seconds (two way travel time). Triassic Unit 2 is highlighted in gray. Examples 1 and 3 show low amplitude evaporite-related folds, whereas example 2 presents a high amplitude thrust-related fold. Modified from SOMMARUGA (1995).

Exemples de plis dans le Jura central et le Bassin molassique (numéros d'exemples réfèrent à la Figure 3.1). L'échelle horizontale est en mètres, par contre l'échelle verticale est en secondes (temps double). L'Unité 2 du Trias est soulignée en grisé. Les exemples 1 et 3 montrent des plis de faible amplitude en relation avec des évaporites, par contre l'exemple 2 présente un pli en relation avec un chevauchement. Modifié de SOMMARUGA (1995).

Pleistocene time in the Molasse Basin. Deformation behind this line is considerably less than in the Jura itself, apparently in contradiction with a simple foreland fold thrust belt wedge model which would predict increasing deformation intensity from the foreland to the hinterland. Perhaps the most outstanding feature of the Jura arc is its position at the outward rather than the inward side of the foreland basin, which is directly related to the Triassic evaporite distribution.

Thrust-related folds in the Haute Chaîne Jura are either foreland- or hinterland-vergent (see Panels and descriptions in Chapter 3). Most evaporite-related folds in the Molasse Basin are symmetrical, but some folds show either a forward or backward vergent asymmetry. In the Plateau Jura, most of the broad folds end against tear or thrust faults and therefore do present an aborted geometry; though some examples show entire symmetric folds (Panel 10). Anticlines and synclines have a lateral continuity over 30 km in the Risoux Jura, whereas in the Neuchâtel Jura the lateral continuity is limited to 10 km. In the Haute Chaîne Jura, synclines are mainly broad e.g. Val de Ruz, Vallée de la Sagne, but some exceptions exist (e.g. Areuse syncline in the Neuchâtel Jura).

In conclusion, the Jura presents most of the characteristics of fold and thrust belts developed above a weak basal layer.

Evolution of the central Jura and Molasse Basin folds

The surface geology and especially the seismic subsurface data of the central Jura and the Molasse Basin display two different types of folds: thrust-related folds and evaporite-related folds (Fig. 5.3). The first type is located in the Haute Chaîne Jura, whereas the second type has been observed not only in the Plateau Jura at the very front to the NE of the Haute Chaîne Jura folds, but also beneath the Molasse Basin. According to BALLY *et al.* (1966) and critical taper models (DAHLEN *et al,*. 1984) fold and thrust belts evolve by progressive deformation from the hinterland to the foreland. If we admit this consideration as a rule, the southernmost structures of the Jura fold and thrust belt should have formed first, to then have evolved into the present day structures. The northern folds should therefore represent a later stage of deformation, with less evolved geometries. This corresponds to what we have observed and inferred from the surface and especially subsurface data.

The Plateau Jura evaporite-related folds (Panel 10) may also represent an early stage of the Jura folds. The folds would have been initiated as low amplitude, apparently symmetric, buckle folds in response to layer-parallel compression. The very weak rocks of the Triassic Unit 2 infilled the space generated at the base of the sedimentary cover by flow mechanism. The core of the folds present a thickening within the very weak basal zone, whereas the strong layers buckle without any change of thickness (concentric folding). With progressive deformation, a fault ramp nucleates in the hinge area at the base of the strong layers in order to accommodate further the strain. Fault ramps will then propagate upward within the stiff layers or bend their trajectory within overlying weak or incompetent layers. With further transport the cover may be doubled, as has been observed in the present day Haute Chaîne Jura folds (e.g. Mt-Risoux or Nouvelle Censière anticlines). The spacing between adjacent early stage buckle folds should be large, since in the Haute Chaîne Jura the formation of subsequent folds does not alter the geometry of the adjacent fold.

In the northern part of the area, seismic data are poor and structures are only revealed with difficulty. Even if from geological maps no major anticlines can be inferred, it is possible that embryonic folds as described by HARRISON (1995), i.e. early stage buckle folds may exist. Moreover, the Plateau Jura buckle folds are located at the front of the high amplitude Jura folds. The Laveron well drilled into one of the Plateau Jura low amplitude folds penetrated 1400 m of Triassic strata (300 m of rock salt). This seems rather thick for an early stage Jura buckle fold compared to the Molasse Basin folds. From the location of the Plateau Jura folds, it appears that part of the thickening may be due to salt flow resulting from the load beneath the thrust-related anticlines of the Haute Chaîne (e.g. Risoux).

Folds beneath the Molasse Basin are located in a more internal position of the Alpine foreland belt than the Jura. The folds observed on the seismic lines represent typically early stage buckle folds and their cores seem to be filled with reasonably well organized evaporite duplexes, whereas those of the Plateau Jura suggest salt flow features. The question remains as to why the Molasse Basin folds did not further evolve into thrust-related folds as did the Haute Chaîne folds? The most obvious reason seems to be the load of Tertiary sediments. The Tertiary Molasse Basin has a wedge shape, with

strong thickening of the sediments from North to South. Furthermore, the amplitude of folds within the Molasse Basin increases toward the Northeast, i.e. toward the Jura belt (e.g. Section 43 and Section 45). There may be two explanations for this: on the one hand, the thickness of Tertiary sediments decreases towards the North and on the other hand the thickness of Triassic sediments decreases slightly towards the South in the Molasse Basin (see Figure 2.22). With progressive erosion and deformation of the Tertiary wedge, it can be supposed that the Molasse Basin anticlines may evolve into Jura folds supported by antiformal duplexes, such as is seen in examples from the eastern Jura (NOACK, 1989; LAUBSCHER, 1992).

Inherited structures and their consequences

The décollement at the base of a fold and thrust belt follows frequently the contact between the crystalline basement and sedimentary cover (BUXTORF, 1907; BALLY *et al.*, 1966; RODGERS, 1990). Pre-existing structures along this contact may form an important boundary condition and play a role in the location of thrust faults during the deformation of the sedimentary cover. Local irregularities in the basal décollement may act as stress concentrators to determine instabilities in the sedimentary cover and therefore act as a nucleation point for a thrust fault (LAUBSCHER, 1977). In the eastern Jura fold and thrust belt, many authors have seen a relation between thrust nucleation and inherited structures e.g. Paleozoic graben system or Oligocene N-S oriented normal faults related to the Rhine-Bresse graben system (LAUBSCHER, 1985; 1986; NAEF & DIEBOLD, 1990; NOACK, 1995). In the western Molasse Basin, especially the Geneva area, recent work based on seismic data (GORIN *et al.*, 1993; SIGNER & GORIN, 1995) highlights the presence of NE-SW and NW-SE trending Permo-Carboniferous lineaments which would have been reactivated several times until the present day. Further East in the Molasse Basin (Bern area), the Hermrigen anticline (for location see Figs. 1.3 and 1.4) is interpreted by some authors as a result of inversion tectonics, reactivating a Permo-Carboniferous graben (PFIFFNER, 1994; PFIFFNER *et al.*, 1997a). This latter interpretation, based on one dip seismic line only, is however not well constrained and an alternate interpretation of an evaporite pillow in the Triassic beds, has been suggested by Erard (oral communication).

In this study area, thickening in the Triassic Unit 2 and duplication of the Mesozoic cover represent the only clear tectonic features visible beneath the anticlines. Reflections attributed to Permo-Carboniferous sediments have been recognized beneath the Molasse Basin. In the Neuchâtel Jura, many reflectors, visible beneath the top of the basement, may represent either Permo-Carboniferous strata or multiples. Seismic data interpreted in this work do not present any positive evidence for inversion of Permo-Carboniferous grabens or for thrust fault nucleation related to inhomogeneities in the basement.

Clear evidence for normal faults on seismic data has been observed within the Bavarian Molasse Basin (BACHMANN *et al.*, 1982; BACHMANN *et al.*, 1987), whereas in the Swiss Molasse Basin no distinct evidence is visible. Early interpretations by VOLLMAYR & WENDT (1987) in the central Swiss Molasse Basin showed many normal faults of presumably Oligocene-Early Miocene age offsetting the whole Mesozoic cover. These authors later reconsidered their interpretation and replaced the normal faults by an embryonic thrust system, as illustrated and discussed by LAUBSCHER (1992). However, normal faults, confined below the Middle Muschelkalk Triassic layers, have been identified by HAUBER (1993) from drill hole data in the Rhine valley of northern Switzerland. These faults have offsets of 50 m or less (Fig. 5.4) that which would corresponds to 0.01s or 0.02s TWT on the seismic lines (more or less one reflector). Unfortunately, the resolution of the seismic lines is too low to observe such faults.

N-S oriented tear faults in the North Alpine foreland are interpreted by many authors as inherited features related to the Oligocene opening of the Rhine-Bresse Graben system (LAUBSCHER, 1973a; ELMOHANDES, 1981; ILLIES, 1981; BERGERAT, 1987; LAUBSCHER, 1992). AUBERT (1972) was indeed able to identify N-S oriented karst crevasses with Oligocene Molasse infill in the Pontarlier region. Accordingly, AUBERT (1972) postulated an Oligocene age for these N-S trending structures, without being specific about their tectonic significance. During Miocene folding and thrusting of the Jura, preexisting faults and joints represented major anisotropies within the Mesozoic cover. They were reactivated during and after folding and played an important role in localizing bends and discontinuities in folds during shortening deformation. The N-S orientation of preexisting faults and joints thereby induced a reactivation with sinistral transcurrent deformation, compatible with the overall N to NW directed Alpine push (LAUBSCHER, 1972). However,

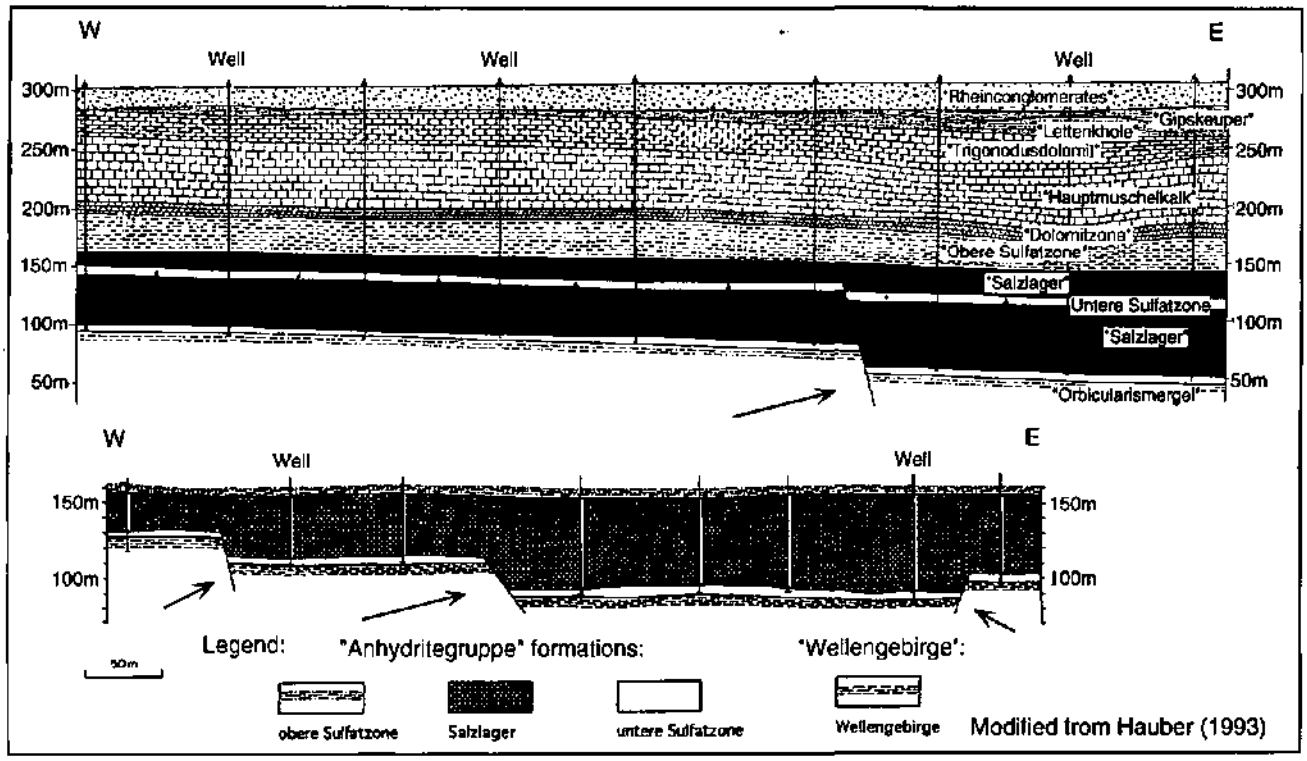

Figure 5.4: Geological cross-sections exhibiting normal faults within the Triassic layers calibrated from drill holes (Rhine Valley of northern Switzerland). Modified from HAUBER (1993).

Coupes géologiques montrant des failles normales au sein des couches du Trias, calibrées à partir de forages (Vallée du Rhin, Nord de la Suisse). Modifié de HAUBER (1993).

seismic lines in the central Jura do not present, in general, arguments in favor or against inherited faults. In the Treycovagnes area, minor thickness changes within the Liassic and Dogger beds are visible from one side of the fault to the other one (MURALT *et al.*, 1997). These thickness changes may be due to Liassic synsedimentary normal faults, which may have been reactivated during the Miocene deformation.

The Molasse Basin: a faredeep basin

The wedge shaped Molasse Basin is presently considered to be a foreland basin. Foredeep or foreland basins are defined as sedimentary basins, located between the front of a mountain chain (orogen) and the adjacent crafon and developed in the context of a A-type subduction (BALLY & SNELSON, 1980). PRICE (1973) and BEAUMONT (1981) suggested that foredeep basins result from lithospheric flexuring in response to overthrust loading in the mountain chain. Foreland basins are characterized by a downwarp flexure, the foredeep basin, and an upwarp flexure or forebulge located in the foreland. Models predict an outward-migrating peripheral bulge, which is often responsible for a characteristic basal foredeep unconformity. Because the thrust load is inherently mobile, the foreland basin itself becomes eventualy involved in deformation.

DICKINSON (1974) was the first to define the North Alpine Tertiary Molasse Basin as a peripheral foreland basin located against the outer arc of the orogen. The Alpine Molasse Basin system extends from the Jura to the Prealps and even to the Helvetic nappes. Therefore the Jura and especially Plateau Molasse subsurface data interpreted in this work, represent only the distal parts of the North Alpine foreland basin system. According to BALLY (1989, idealized foredeep Figure 4), foredeep basins present many common features and units. These are recognized on seismic lines crossing the Plateau Molasse: (1) a basement: a crystalline basement has been confirmed by drill holes in the Jura and has been inferred from seismic interpretation beneath the Molasse Basin Mesozoic strata; (2) a rifling

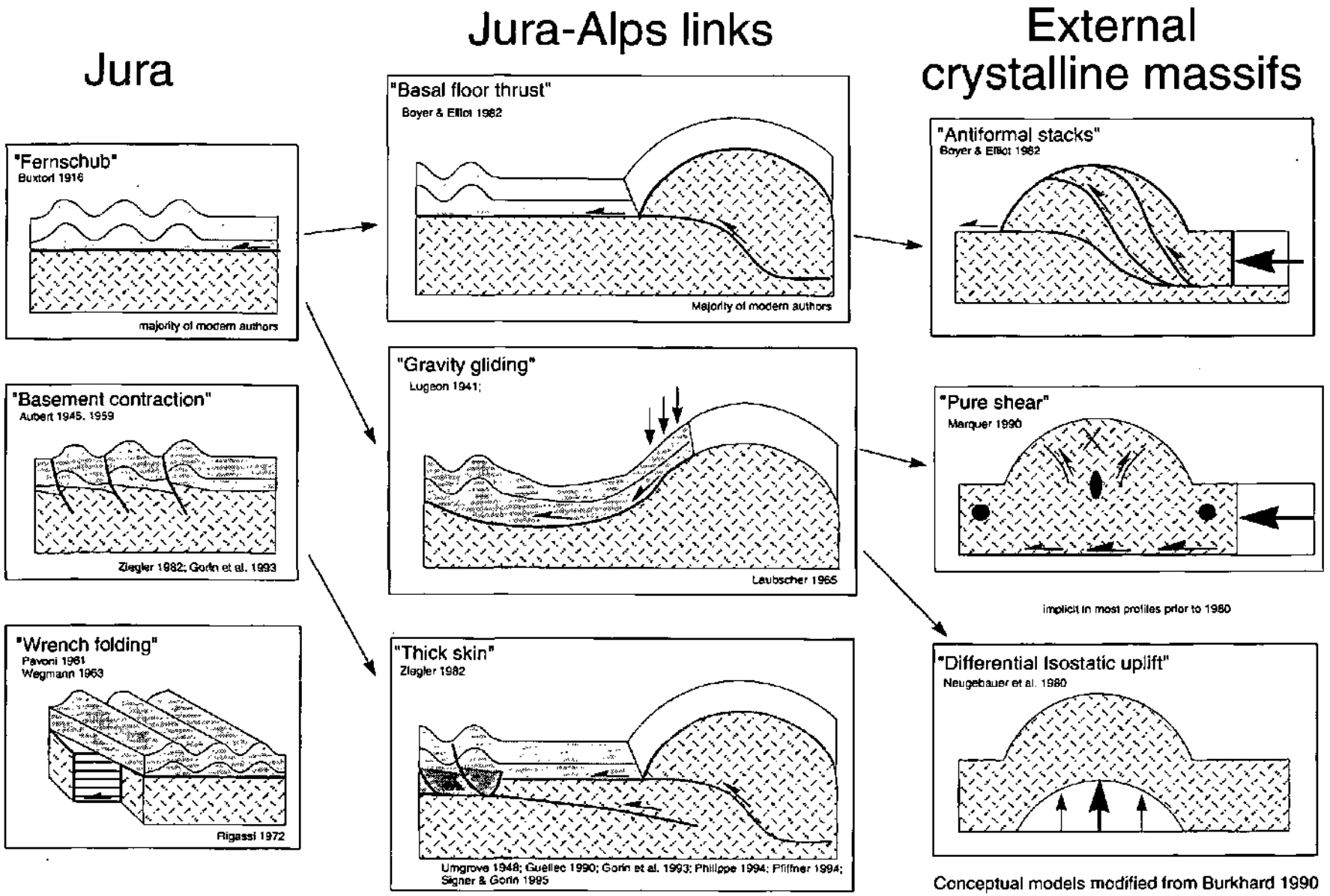

Figure 5.5: Conceptual models on the formation of the Jura fold and thrust belt and its links to the Alps (external crystalline massifs). Modified from BURKHARD (1990).

Modèles conceptuels sur la formation de la chaîne plissée du Jura et son lien avec les Alpes (massifs cristallins externes). Modifié de BURKHARD (1990).

sequence: no real rift sequence has been identified on the seismic lines, although Permo-Carboniferous grabens present characteristics of extension tectonics; (3) a passive margin or platform sequence: during the Triassic an epicontinental shallow water environment developed and then during the Jurassic and Cretaceous interlayered marl and limestone beds were deposited in a platform or lagoonal environment. These strata, 1 to 3 km thick, overly the basement; (4) a deep water phase representing the inception of the foredeep: this early sequence consists of deposits located in the hinterland parts of the Molasse Basin. In Switzerland, the oldest deposits of the foreland basin are Flysch series, which are involved in the Helvetic nappes. Moreover the Molasse underlies the Prealpine klippen. This unit is not visible on the Plateau Molasse seismic lines; (5) a prograding sequence: the sequence of Tertiary shallow water Molasse sediments has been observed on the seismic lines.

These five units are separated by basically different unconformity types (see also BALLY, 1989): (a) The pre-rift unconformity at the base of the Permo-Carboniferous grabens. (b) The breakup unconformity at the base of the Mesozoic strata. Unconformities (a) and (b) are inherited and are not related directly to the formation of the foredeep. (c) The basal foredeep unconformity which marks the beginning of the flexural response to the Alpine loading of the European plate. Subhorizontal Tertiary sediments onlap the Cretaceous (Mesozoic) strata dipping a few degrees (the same dip as the basement) toward the South. This unconformity is the most obvious on all Molasse Basin seismic lines. Unfortunately reflections are poor within this sequence and do not give the possibility to recognize minor unconformities due to sea level changes. The possibility of interpreting the Tertiary sediment onlaps in relation to salt flow deformation has been discussed in Chapter 3. However it appears most reasonable to attribute them to the basal foredeep unconformity.

Evidence that the Molasse Basin represents a flexural basin has already been provided, based on stratigraphy, sedimentology, subsidence profiles and gravity anomaly studies (LEMCKE, 1974; KARNER & WATTS, 1983; NAEF *et al.*, 1985; HOMEWOOD *et al.*, 1986). LAUBSCHER (1992) suggested that the forebulge developed during two different phases: the Helvetic phase (Late Oligocene-Early Miocene) and the Jura phase (Middle to Late Miocene). Recently CRAMPTON & ALLEN (1995), using modeling work and surface outcrop data, proposed the existence of the forebulge flexure throughout the early evolution of the Alpine foreland basin, although its topographic expression has changed over time. It is beyond the scope of this work to join this discussion. Further arguments of the evolution of the Molasse Basin and its structural relations with the Jura and the Alps are developed by BURKHARD & SOMMARUGA (in press). The present work, nevertheless, shows what was previously inferred, that the basement is homoclinal and can be followed with reasonable continuity from the foreland to the Alps beneath the foreland basins. The foreland basement (the Jura basement) is the shared link with the Alpine belt.

Jura - Alps links

The two fundamental questions, i.e. the cover-basement relationships within the Jura and the Molasse Basin and the compensation of the Jura cover shortening, were discussed in a short review in Chapter 1. The review shows that answers to both questions remain open and various authors still argue the possibility of shortening the basement beneath the Jura and the Molasse Basin, based on debatable seismic evidences (ZIEGLER, 1982; GUELLEC *et al.*, 1990; GORIN *et al.*, 1993; PFIFFNER, 1994; SIGNER & GORIN, 1995; PFIFFNER *et al.*, 1997a).

However, the interpretation of more than 1500 km of seismic reflection lines across all the Jura tectonic units (external Jura: Plateau and Faisceau; internal Jura: Haute Chaîne) and also the Molasse Basin tectonic units (Plateau- and Subalpine-Molasse) has not revealed any obvious examples where cover structures can be related to observable, reliable deformation in the underlying basement. No deformation features are observed in the basement, instead the overlying Triassic Unit 2 layers are deformed, showing mainly evaporite swells. Any irregularities which might exist in the top of the basement (Fig. 5.1) are small compared to the thickness of Triassic Unit 2. This leads to the key conclusion that the Jura and Molasse Basin cover has been deformed over a main décollement zone located in Triassic Unit 2. This conclusion corresponds to the "Fernschub theory" formulated at the beginning of the century by BUXTORF (1916). Nevertheless the link between the Jura fold and thrust belt and the Alps chain remains an item for discussion. Many authors have proposed various hypotheses (Fig. 5.5) based on field work, fission track data, balancing

concepts and recently refraction or reflection seismic data (see also review by BURKHARD, 1990; LAUBSCHER, 1992). One hypothesis connects the Jura basal thrust to the basal Helvetic thrust and implies that uplift of the external crystalline massifs would post-date the Jura-thrusting (LAUBSCHER, 1973b). The internal deformation within the external crystalline massifs would be explained by vertical pure shear (MARQUER, 1990) or by differential isostatic uplift (NEUGEBAUER *et al.*, 1980). Another hypothesis, first expressed by BOYER & ELLIOT (1982), states that the Jura basal thrust continues beneath the Molasse Basin and then roots in the frontal part of the external crystalline massifs. This hypothesis is the most widely accepted today, even if some authors see contrary seismic evidence. This work provides a map of the basement top showing a basement dipping gently towards the South underneath the Jura and the Molasse Basin but does not provide new critical information beneath the external crystalline massifs. Therefore it is beyond the scope of this work to embark in a detailed discussion of the large scale relationship of the Jura - Alps system. The relationship of the Jura system to the deeper parts of the crust and the mantle has been elucidated by the results of the NFP20 research projects (PFIFFNER *et al.*, 1997b) and has been discussed recently by LAUBSCHER (1992).

6. CONCLUSIONS

Apart from some stratigraphic observations within the Jurassic and Cretaceous layers for which the reader can refer to Chapter 2, the interpretation and correlation of more than 1500 km seismic reflection lines has revealed some major structural elements, which have a considerable consequences for the understanding of the formation of the Jura foreland fold and thrust belt.

This work has confirmed that the cover of the central Jura and the western Molasse Basin has been deformed over a smooth basement surface dipping 1° to 3° to the S-SE, within the limited constraints of seismic resolution. This pre-Triassic basement is not significantly affected by the deformation of structures such as the folds, thrust faults and tear faults observed in the cover. The contrast in deformation between the basement and the cover is due to an unexpectedly thick and very weak décollement zone. This zone, composed essentially of evaporite and salt rocks belonging to seismic Triassic Unit 2 defined in this work (corresponding ± to Middle Triassic age), represents the lowermost seismic stratigraphic unit involved in the deformation of the cover. The regional thickness of this unit ranges from 200 m at the NW periphery of the Jura belt to more than 1000 m in the central part of the Jura, due to structural thickening. Thus Triassic evaporites control the development of the Jura and the Molasse Basin folds during the Late Miocene as well as the arcuate shape of the fold belt.

The analyses of the geometry of structures within the central Jura and the Molasse Basin has shown two types of folds:

1) Evaporite-related folds, located in the Molasse Basin and the external Plateau Jura. The development of these low amplitude buckle folds is related to evaporite stacks within the Triassic Unit 2 layer. The axis of these folds is oriented NW-SE, parallel to the general trend of the Jura belt structures.

2) Thrust-related folds, located within the Haute Chaîne Jura. These high amplitude folds are related to NW- or SW-vergent thrusts of at least kilometric dipslip displacement, that results in a duplication of the entire Mesozoic sequence. These thrusts step up from the main décollement zone (Triassic Unit 2) through the entire Mesozoic and Cenozoic cover series.

These two types of folds are respectively interpreted as embryonic and evolved stages of the Late Miocene cover deformation. The Haute Chaîne Jura folds began as buckle folds, to then evolve into the present thrust-related folds. In the Molasse Basin, however, low amplitude folds represent an early stage which did not evolve because of loading by the overlying thick Tertiary sedimentary wedge. Both types of folds show that the Triassic Unit 2 is clearly involved in the development of fold and thrust structures in the cover of the Jura and controlled their formation.

Furthermore, the cover structures are also influenced by the rheology of the whole stratigraphic column. The increase of the thickness ratio between strong (competent) and weak (incompetent) layers, associated with an increase of the Mesozoic stratigraphic column from the north-eastern towards the south-western Jura, results in the development of low relief box-folds or detachment folds in the eastern Jura and high relief thrust-related folds in the western Jura.

Some seismic lines cross major tear faults which, within the limit of seismic resolution, do not show any significant offset of the basement top from one side to the other. These faults are restricted to the cover and do not present evidence of an offset basement.

In conclusion, interpretation of the seismic lines confirms the "Fernschub" hypothesis concerning the formation of the Jura: the Mesozoic cover of the Jura foreland fold and thrust belt and the Molasse Basin has been pushed to the NW over a main décollement zone. The seismic lines have not shown evidence for inverted Permo-Carboniferous grabens or thrust faults continuing downwards into the pre-Triassic basement. Therefore, the shortening of the

basement is compensated, not beneath the Jura, but probably under the external crystalline massifs of the Alps.

This work has provided the opportunity to complete the surface geological observations with subsurface data and thus has allowed to present a regional "three-dimensional view" of basement to cover relationships. Thanks to the subsurface data, new light has been shed on the formation of the Jura, which remains a classical evaporite foreland fold and thrust belt.

ABSTRACT

Geology of the central Jura and the Molasse Basin: new insight into an evaporite-based foreland fold and thrust belt.

More than 1500 km of industry seismic reflection lines in the Neuchâtel and Vaud Jura of Switzerland, the French Jura and the Swiss western Molasse Basin have been interpreted. Through the seismic grid, constrained by drill hole data, each intersection of seismic profiles was controlled in order to obtain an internally consistent interpretation. These new data have shed new light on the stratigraphy of the buried Mesozoic layers and the deformation style of the subsurface structures from the Subalpine Molasse to the external Jura. Interpretation of the seismic lines demonstrates that the Mesozoic and Cenozoic cover of the Jura fold and thrust belt and the adjacent Molasse Basin has been deformed over a weak basal décollement and displaced for many kilometers toward the NW.

Folding and thrusting took place above a very weak décollement zone within the thick seismic Triassic Unit 2 (Middle Triassic age) composed essentially of evaporites, salt and clays. The thickness of this interval ranges from 200 m at the NW periphery of the Jura belt to more than 1000 m in the central part of the Jura. The low amplitude broad folds of the Molasse Basin and the external Plateau Jura are controlled by evaporite pillows or anticlines within Triassic Unit 2. As seen on an isopach map, these structures are aligned along a NE-SW trend parallel to the general trend of the Jura fold and thrust belt. The high amplitude folds of the Haute Chaîne Jura, however, are related to NW- or SE-vergent thrusts with at least kilometric dipslip displacement that result in doubling of the entire Jurassic sequence. These thrusts step up from the main décollement zone through the entire Mesozoic and Cenozoic cover series. The Plateau Jura evaporite-related folds located in the foreland are interpreted as early stage buckle folds. With progressive deformation a fault ramp nucleates and this fold type develops into thrust-related folds as observed in the Haute Chaîne. Thus, within the Jura fold and thrust belt, deformation increases toward the hinterland. In the Molasse Basin, however, low amplitude folds represent an early stage which could not develop further due to load of the overlying thick Tertiary clastic wedge.

The depth to the basement map of the studied area derived from depth conversion of the seismic lines, shows a smooth flat basement dipping 1° to 3° to the S-SE. No significant change in depth and trend of the basement top can be seen below major tear faults which affect the layers of the sedimentary cover. No structural relation can be detected, when comparing isopach map of Triassic Unit 2 series and the basement top contour map. A key conclusion is therefore, that basement is not involved in the formation of folds, thrusts and tear faults in the central Jura and the Molasse Basin.

RÉSUMÉ

**Géologie du Jura central et du Bassin molassique:
nouveaux aspects d'une chaîne d'avant-pays plissée et décollée sur des couches d'évaporites.**

Plus de 1500 km de profils sismiques mis à disposition par l'industrie pétrolière, provenant du Jura suisse neuchâtelois et vaudois, du Jura français et du Bassin molassique occidental ont été interprétées. Chaque intersection du profil sismique a été contrôlée à travers le réseau de profil sismique et calibrée sur les données de forage, afin d'obtenir une interprétation cohérente. Ces nouvelles données ont apporté des connaissances plus approfondies sur la stratigraphie des couches mésozoïques et sur le style de déformation des structures de la subsurface depuis la région de la Molasse subalpine au Jura externe. L'interprétation des profils sismiques démontre, que la couverture mésozoïque et cénozoïque de la chaîne plissée et chevauchée du Jura et du Bassin molassique a été déformée au-dessus d'un décollement basal et a été déplacée de plusieurs kilomètres vers le NW.

Les plis et les chevauchements se sont développés au-dessus d'une zone de décollement à faible viscosité, localisée dans les couches du Trias moyen (Unité 2 du Trias) et composée essentiellement d'évaporites, de sel et d'argiles. L'épaisseur de cet intervalle varie entre 200 m à la périphérie NW de la chaîne du Jura et 1000 m dans la partie centrale du Jura. Les plis de faible amplitude du Bassin molassique et des Plateaux jurassiens sont contrôlés par des coussins d'évaporites ou des anticlinaux d'évaporites au sein de l'Unité 2 des couches du Trias. Comme cela a été démontré sur une carte d'isopaques, ces structures sont alignées NE-SW parallèlement à la direction des structures majeures du Jura. Les plis de grande amplitude de la Haute Chaîne jurassienne sont, cependant, en relation avec des chevauchements à vergence vers le NW ou le SE montrant un déplacement d'ordre kilométrique qui se traduit par le redoublement de toute la séquence jurassique. Ces chevauchements montent depuis la zone de décollement principale à travers toute la série mésozoïque et cénozoïque. Les plis des Plateaux jurassiens, localisés dans l'avant-pays, sont interprétés comme des plis de flambage correspondant à un stade précoce de la déformation. En augmentant la déformation, une rampe se génère et ce type de pli se développe associé à un chevauchement comme ceux observés dans la Haute Chaîne. La déformation augmente, donc, vers l'arrière-pays au sein de la chaîne plissée et chevauchée du Jura. Dans le Bassin molassique, les plis de faible amplitude représentent, cependant, un stade précoce, qui n'a pas pu évoluer à cause de la surcharge de sédiments tertiaires.

Une carte du toit du socle de la région étudiée a pu être réalisée grâce à la conversion en profondeur des profils sismiques. Cette carte montre un socle plat et lisse plongeant de 1° à 3° vers le S-SE. Aucun changement important de profondeur et de direction, qui affecterait les couches de la couverture sédimentaire, n'a pu être décelé sous les décrochements principaux. Aucune relation structurale n'a pu être déduite entre la carte d'isopaches de l'Unité 2 du Trias et celle des contours du toit du socle. Le socle n'est donc pas impliqué dans la formation des plis, des chevauchements et des décrochements du Jura central et du Bassin molassique.

RIASSUNTO

**Geologia del Giura centrale e del Bacino della Molassa:
nuovi sviluppi sulla conoscenza dell'avampaese di una catena a falde e pieghe al tetto sulle evaporiti triassiche.**

In questo lavoro sono state interpretate oltre 1500 km di linee sismiche acquisite dall'industria petrolifera nel Giura Svizzero (Cantone Vaud e Neuchâtel), nel Giura francese e nel Bacino occidentale della Molassa. La correlazione degli orizzonti da una linea sismica all'altra, attraverso tutta la maglia dei profili, ha reso possibile un'analisi strutturale a scala regionale, calibrata dalle informazioni stratigrafiche provenienti dai pozzi. Questi nuovi dati hanno permesso di approfondire le conoscenze scientifiche sulla stratigrafia dei sedimenti mesozoici attualmente sepolti e sullo stile di deformazione delle strutture profonde, dalla regione della Molassa subalpina al Giura esterno.

Dall'interpretazione delle linee sismiche emerge che la copertura mesozoica e cenozoica della Catena a pieghe del Giura e del Bacino della Molassa si sono deformate al di sopra di un livello di scollamento basale e sono state dislocate per diversi chilometri verso NW. Le pieghe e gli accavallamenti si sono sviluppati al tetto di una zona di scollamento molto duttile, localizzata entro l'Unità 2 del Triassico medio e costituita soprattutto da evaporiti (prevalentemente sale) ed argille. Lo spessore di questa unità varia da 200 m, alla periferia NW del Giura, a 1000 m, nella parte centrale del Giura. Le pieghe che si sono formate nel Bacino della Molassa e negli altipiani del Giura ("Plateaux jurassiens") hanno bassa ampiezza a causa della presenza di cuscini ed anticlinali di evaporiti nell'Unita 2 del Triassico. Come si puo notare dalle carte delle isopache, queste strutture hanno la stessa direzione delle strutture principali del Giura, allineate NE-SW.

Nella parte alta della Catena del Giura ("Haute Chaîne") le pieghe hanno un'ampiezza maggiore e sono

associate ad accavallamenti vergenti sia verso NW che SE, che causano uno spostamento superiore al chilometro ed il raddoppio di tutta la sequenza giurassica. Questi accavallamenti si originano lungo la zona di scollamanto principale e risalgono verso la superfice, interessando tutta la serie mesozoica e cenozoica. Le pieghe degli altipiani del Giura ("Plateaux jurassiens"), che si trovano nella parte frontale della Catena, sono interpretate come pieghe di buckling formatesi durante uno stadio iniziale della deformazione. All'aumentare della deformazione si forma generalmente una rampa e le pieghe di buckling evolvono in pieghe associate ad un accavallamento. Simili pieghe sono state osservate nella Haute Chaîne e questo viene interpretato come indice dell'aumento della deformazione verso le zone interne della Catena. Le pieghe a piccola ampiezza osservate nel Bacino della Molassa rappresentano uno stadio precoce della deformazione che non si è potuta evolvere ulteriormente, a causa del carico dei sedimenti terziari della Molassa.

Nella regione studiata, la carta del tetto del basamento, compilata dalla conversione in profondità delle linee sismiche, evidenzia un basamento con una superfice planare, leggermente inclinata (da 1 a 3°) verso S-SE. Il basamento che si trova al di sotto delle zone in cui la copertura sedimentaria è notevolmente disturbata da faglie trascorrenti non mostra nessuna variazione strutturale significativa. Non si nota inoltre nessuna relazione strutturale tra la carta delle isopache dell'Unità 2 del Triassico e la carta del tetto del basamento. Importanti conclusioni di questo lavoro sono che il basamento non è coinvolto nel piegamento e nell'accavallamento che hanno prodotto la Catena del Giura ed inoltre che il basamento non risulta essere interessato dalle faglie trascorrenti del Giura centrale e del Bacino della Molassa.

ZUSAMMENFASSUNG

Geologie des Zentraljuras und des Molassebeckens:
Neue Erkenntnisse zu einem Evaporitverbundenen Vorland Uberschiebungs - und Faltengebirge.

Mehr als 1500 km seismische Reflexionsprofile der Erdölindustrie aus dem neuenburger und dem waadtländer Jura, sowie aus dem französischen Jura und dem westlichen Schweizer Molasse Becken, wurden interpretiert. Um eine kohärente Gesamtinterpretation zu erreichen, wurden die Schnittstellen der verschiedenen Profile im gesamten Netz kontrolliert und mit Bohrlochdaten korrelliert. Die daraus gewonnenen Daten haben es ermöglicht neue Erkenntnisse über die Stratigraphie der nicht aufgeschlossenen mesozoischen Horizonte, sowie des Deformationstils zwischen der subalpinen Molasse und dem äußeren Jura zu gewinnen. Die Auswertung der seismischen Profile zeigt, daß die mesozoischen und känozoischen Deckschichten des Jura Faltengebirges und des angrenzenden Molasse Beckens über einer plastischen Basiszone abgeschert wurden und viele Kilometer nach NW überschoben wurden.

Falten und Überschiebungen entstanden in dieser schwachen Abscherzone innerhalb der mächtigen "Trias Unit 2" (mittleres Trias), welche im wesentlichen aus Evaporiten, Salz und Tonen besteht. Die Mächtigkeit dieses Intervalls schwankt zwischen 200 m, am NW-Ende der Jurakette, und 1000 m im zentralen Teil des Jura Gebirges. Die Evaporit "pillows" oder Antiklinalen in der "Trias Unit 2" verursachen breite Falten mit schwachen Amplituden im Molasse Becken, sowie im äußeren Plateau Jura. Auf den Mächtigkeitskarten erkennt man daß die Strukturen NE-SW, parallel zum allgemeinen Trend des Jura Deckengebirges streichen. Die Falten mit großen Amplituden im "Haute Chaîne" Jura, sind mit NW oder SW vergenten Überschiebungen verbunden. Die Überschiebungsbeträge im Kilometerbereich führen zu einer Verdopplung der gesamten jurassischen Serien. Die Überschiebungsflächen steigen von der Basisüberschiebung auf und durchschlagen die gesamten mesozoischen und känozoischen Deckensedimente.

Die sich im Vorland befindenden, mit Evaporit verbundenen Falten werden als "buckle" Falten in einem frühen Entwicklungsstadium interpretiert. Mit anhaltender Deformation und Verkürzung entsteht ein Rampenbruch und der sich entwickelnde Faltenstil entspricht einer Überschiebungs-verbundenen Falte, wie man es in der "Haute Chaîne" beobachten kann. Im Jura Faltengebirge ist die Deformation also größer in Richtung Hinterland. Im Molasse Becken dagegen, entsprechen die Falten mit schwacher Amplitude einem frühen Stadium der Deformation, die sich wegen der darüber liegenden Mächtigkeit der tertiären Sedimente nicht weiter entwickeln konnte.

Im untersuchten Gebiet zeigt die Tiefenkarte zur Oberfläche des Sockels, basierend auf Tiefenkonversionen von seismischen Linien, eine flache 1°-3° nach S-SE hin geneigte Oberfläche. Unter den Blattverschiebungsflächen die die Deckschichten durchschneiden, gibt es keine Veränderungen im Streichen und in der Tiefe der Sockeloberfläche. Eine strukturelle Verbindung wird vom Vergleich der Mächtigkeitskarte der Trias Unit 2 und der Sockeloberfläche, ausgeschlossen.

Die Schlußfolgerung daraus schließt eine Beteiligung des Sockels in der Entwicklung der Falten, Überschiebungen und Blattverschiebungen im zentralen Jura und im Molasse Becken aus.

APPENDICES

APPENDIX 1

	Thesis Numbering	Survey Numbering	Line trend
British Petroleum,	1	SW88-16	NW-SE, dip
Sector A	2	SW88-12	NE-SW, strike
Neuchatel Jura	3	SW88-14	NW-SE, dip
	6	SW88-04W	NE-SW, strike
	5	SW88-15	NW-SE, dip
	4	SW88-04E	NE-SW, strike
	7	SW88-01	NW-SE, dip
	8	SW88-17	NE-SW, strike
	9	SW88-09	NW-SE, dip
	10	SW88-11	NE-SW, strike
	11	SW88-07	NW-SE, dip
	12	SW88-18	NE-SW, strike
	13	SW88-06	NW-SE, dip
	14	SW88-10	NE-SW, strike
	15	SW88-20	NW-SE, dip
	17	SW88-03	NW-SE, dip
	19	SW88-19	NW-SE, dip
Shell Switzerland	20	73VD01	NE-SW, strike
and SADH	21	73VD04	NW-SE, dip
Sector B	22	73VD02-73VD34	NE-SW, strike
Molasse Basin	23	74VD33	NW-SE, dip
	24	74VD35	NE-SW
	25	74VD30	NE-SW
	26	78SADH21	NE-SW
	27	73VD05-74VD36-74SADH08	NW-SE, dip
	28	76SADH18	NE-SW, strike
	29	78SADH22	NW-SE
	30	79SADH27	NE-SW
	31	74VD31	NW-SE, dip
	32	72SADH07	NE-SW, strike
	33	74VD29	NW-SE, dip
	34	74VD38-74SADH09	NNE-SSW
	35	74VD40	NW-SE, dip
	36	74SADH14	N-S
	37	73VD06	NW-SE, dip
	38	75VD55	N-S
	39	73VD07	WNW-ESE
	40	76SADH15	NNW-SSE
	41	74SADH11	NW-SE
	42	73VD23	NE-SW
	43	79SADH24	NW-SE
	44	73VD21-73VD18	NNE-SSW
	45	76SADH16	WNW-ESE
	46	74SADH06-74VD52-N6	NE-SW, strike
	47	76SADH17	NNW-SSE
	48	76VD57	N-S
	49	76VD67	NW-SE

Appendix 1 (pages 157, 158): Inventory of seismic lines. Sector A, B, C, D refers to Figure 1.4.

Inventaire des profils sismiques. Se référer à la Figure 1.4 pour la définition des secteurs A, B, C, D.

	50	76VD58	strike, NE-SW
	51	76VD69	N-S
	52	78VD81	NE-SW
	53	73VD26	NW-SE, dip
	54	78VD76	NE-SW
	55	73VD24	NW-SE, dip
	57	73VD19	NW-SE, dip
	59	73VD22	NW-SE, dip
	61	73VD25	NW-SE, dip
	63	73VD14	NW-SE, dip
	65	73VD20	NW-SE, dip
	67	73VD15	NW-SE, dip
	69	73VD16	NW-SE, dip
	71	73VD17	NW-SE, dip
	22-34-	73VD02-73VD34-74VD38-74SADH09-	NNE-SSW
	46-44	74SADH08-74VD52-N6-73VD18	NNE-SSW
	35-37-39	74VD40-73VD06-73VD07	NW-SE
	42-32-20-22	73VD23-72SADH07-73VD01-73VD02	NE-SW, strike
	50-48-34-39	76VD58-76VD57-74SADH09-74VD38-(-73VD07)	S-N after W-E
Shell	80	74VD49	NE-SW, strike
Sector C	81	74VD48	NW-SE, dip
Mt-Risoux	82	74VD44	NE-SW, strike
	83	74VD42	NW-SE, dip
	84	73VD09-74VD53-73VD10	NE-SW, strike
	85	74VD45	NW-SE, dip
	86	73VD12	NE-SW, strike
	87	73VD08	NW-SE, dip
	88	73VD13	NE-SW, strike
	89	74VD46	NW-SE, dip
	91	72M2	NW-SE, dip
	93	74VD43	NW-SE, dip
	95	74VD41	NW-SE, dip
	111	CM7	NW-SE, dip
	93-95-61	73VD43-73VD41-73VD25	NW-SE, dip
	89-91-55	74VD46-72M2-73VD24	NW-SE, dip
	111-85-87-91-55	CM7-74VD45-73VD08-72M2-73VD24	NW-SE, dip
Shellrex	100	CM20-CM20N	strike
Sector D	101	CM13	dip
Champagnole-	102	CM19Sud-CM19Nord	strike
Mouthe	103	CM1	dip
	104	CM11-CM11Nord	strike
	105	CM42	dip
	106	CM3Sud-CM3centre-CM3Nord (à double)	strike
	107	CM4	dip
	108	CM5-CM5Sud-CMV7	strike
	109	CM6	dip
	110	CM10	strike
	111	CM7	dip
	112	CM2	strike
	113	CM16Nord	dip
	115	CM16Sud	dip
	117	CM17	dip
	119	CM18	dip
	121	CM9	dip
	123	CMV6	dip
	125	CM14	dip

Appendix 1 (pages 157, 158): Legend on page 157.

Légende à la page 157.

APPENDIX 2

exploration company

1) Courtion

BP, 1960 T.D. = 3083m

elevation	x	y
599m	572'415m	189'420m

top of ...

Formation	depth m	elevation m	thickness m
Tertiary	0	599	1322
Cretaceous	-1322	-723	112
Malm	-1434	-835	388
Argovian	-1822	-1223	216
Dogger	-2038	-1439	400
Aalenian	-2438	-1839	152
Liassic	-2590	-1991	100
Keuper	-2690	-2091	180
MK dolom.	-2870	-2271	63
MK evap.	-2933	-2334	150
T.D.	-3083	-2484	

Fischer & Luterbacher 1963

3) Hermrigen

Elf Aquitaine, 1982 T.D. = 2198m

elevation	x	y
480m	*587'790m*	*214'900m*

top of ...

Formation	depth m	elevation m	thickness m
Tertiary	0	480	395
Cretaceous	-395	85	8
Malm	-403	77	436
Argovian	-839	-359	239
Dogger	-1078	-598	380
Aalenian	-1458	-978	92
Liassic	-1550	-1070	177
Keuper	-1727	-1247	280
MK dolom.	-2007	-1527	79
MK evap.	-2086	-1606	112
T.D.	-2198	-1718	

Housse 1982

exploration company

2) Tschugg

KUS, 1976 T.D. = 704m

elevation	x	y
463m	572'610m	207'910m

top of ...

Formation	depth m	elevation m	thickness m
Tertiary	0	463	509
Cretaceous	-509	-46	129
Jurassic	*-638*	*-175*	*66*
T.D.	-704	-241	

Schnegg 1992

4) Essertines

SADH, 1963 T.D. = 2936m

elevation	x	y
660m	539'775m	173'490m

top of ...

Formation	depth m	elevation m	thickness m
Tertiary	0	660	337
Cretaceous	-337	323	194
Malm	-531	129	501
Argovian	-1032	-372	314
Dogger	-1346	-686	406
Aalenian	-1752	-1092	153
Liassic	-1905	-1245	397
Keuper	-2302	-1642	634
T.D.	-2936	-2276	

Büchi et al. 1965b

5) Cuarny

Vingerhoets, 1940 T.D. = 2229m

elevation	x	y
562m	543'540m	180'380m

top of ...

Formation	depth m	elevation m	thickness m
Tertiary	0	562	480
Cretaceous	-480	82	240
Malm	-720	-158	1240
Dogger	-1960	-1398	269
T.D.	-2229	-1667	

Althaus & Rickenbach 1947

Appendix 2 (pages 159-162): Compilation of well data as found in the literature or in unpublished reports. Lithologies and abbreviations are explained at the end of the table. Drilling company and year are mentioned for each hole. Total depth (T.D.) corresponds to the depth reached and corrected for deviations from vertical. Elevations are indicated above or below (-) sea level. Location coordinate X and Y refers to the Swiss coordinate system. All data are in meters.

Données de forages compilées de la littérature ou de rapports non publiés. Les lithologies et les abréviations sont expliquées à la fin de cet annexe. Les compagnies et l'année de forage sont mentionnées pour chaque puits. La profondeur (T.D.) correspond à la profondeur maximale atteinte et corrigée par rapport aux déviations de la verticale. Les altitudes sont indiquées par rapport au niveau de la mer. Les coordonnées X et Y se réfèrent au système suisse de coordonnées géographiques. Toutes les données sont en mètres.

6) Treycovagnes Shell, 1978 T.D. = 3221m

elevation	x	y
473m	536'135m	180'273m

top of ... Formation	depth m	elevation m	thickness m
Cretaceous	0	473	177
Malm	-177	296	514
Argovian	-691	-218	203
Dogger	-894	-421	404
Aalenian	-1298	-825	66
Liassic	-1364	-891	308
Keuper	-1672	-1199	858
MK dolom.	-2530	-2057	30
MK evap.	-2560	-2087	121
Buntsandstein	-2681	-2208	62
Permian	-2743	-2270	478
T.D.	-3221	-2748	

Report deposited at the Musée géologique du Canton de Vaud in Lausanne; Schegg et al. 1997

8) Savigny SADH, 1960 T.D. = 2486m

elevation	x	y
839m	546'271m	155'312m

top of ... Formation	depth m	elevation m	thickness m
Tertiary	0	839	2331
Cretaceous	-2331	-1492	155
T.D.	-2486	-1647	

Lemcke 1963

10) Risoux PREPA, 1960 T.D. = 1958m

elevation	x	y
1350m	500'310m	161'020m

top of ... Formation	depth m	elevation m	thickness m
Upper Malm	0	1350	123
Argovian	-123	1227	205
Dogger	-328	1022	125
Argovian	-453	897	129
Dogger	-582	768	160
Aalenian	-742	608	15
Lias	-757	593	218
Lias	-975		259
Malm	-1234	116	265
Argovian	-1499	-149	417
Dogger	-1916	-566	42
T.D.	-1958	-608	

Winnock 1961

7) Chapelle SADH, 1958 T.D. = 1540m

elevation	x	y
764m	547'305m	168'359m

top of ... Formation	depth m	elevation m	thickness m
Tertiary	0	764	1506
Cretaceous	-1506	-742	25
T.D.	-1531	-767	

Lemcke 1959

9) Laveron PREPA, 1959 T.D. = 2485

elevation	x	y
1080m	503'000m	180'600m

top of ... Formation	depth m	elevation m	thickness m
Malm	0	1080	266
Raur. /Argov.	-266	814	243
Dogger	-509	571	220
Aalenian	-729	351	228
Liassic	-957	123	118
Rhaetian / Keup.	-1075	5	882
Lettenkohle	-1957	-877	23
MK dolom	-1980	-900	63
MK evap.	-2043	-963	377
Buntsandstein	-2420	-1340	65
T.D.	-2485	-1405	

BRGM, Mouthe 1964

11) Eternoz T.D. = 2500m

elevation	x	y
521m	491'800m	207'200m

top of ... Formation	depth m	elevation m	thickness m
Bath./Baj.	0	521	278
Aalenian	-278	243	79
Liassic	-357	164	196
Keuper	-553	-32	456
Lettenkohle	-1009	-488	18
MK dolom.	-1027	-506	57
MK evap.	-1084	-563	131
Buntsandstein	-1215	-694	65
Permian	-1280	-759	1220
T.D.	-2500	-1979	

BRGM, Quingey 1975

Appendix 2 (pages 159-162): Legend on page 159.

Légende à la page 159.

12) Essavilly SNPA, 1964 T.D. = 2067m

elevation	x	y
795m	496'400m	183'000m

top of ...

Formation	depth m	elevation m	thickness m
Cretaceous	0	795	36
Portlandian	-36	759	359
Raur./Callov.	-395	400	279
Baj./Bath.	-674	121	226
Aalenian	-900	-105	102
Lw Aal. / Lias.	-1002	-207	333
Rh./Keuper	-1335	-540	327
Lett./MK dolom.	-1662	-867	45
MK evap.	-1707	-912	111
Buntsandstein	-1818	-1023	92
Permian	-1910	-1115	46
Carboniferous	-1956	-1161	68
Basement	-2024	-1229	43
T.D.	-2067	-1272	

BRGM, Champagnole 1965a

13) Toillon PREPA. T.D. = 1573m

elevation	x	y
844m	492'100m	174'000m

top of ...

Formation	depth m	elevation m	thickness m
Malm	0	844	180
Argovian	-180	664	240
Dogger	-420	424	270
Aalenian	-690	154	225
Liassic	-915	-71	193
Keuper	-1108	-264	465
T.D.	-1573	-729	

BRGM, Champagnole 1965a

14) Valempoulières 1 PREPA. 1961 T.D. = 1421m

elevation	x	y
653m	481'400m	186'500m

top of ...

Formation	depth m	elevation m	thickness m
Dogger	0	653	280
Aalenian / Lias.	-280	373	190
Keuper	-470	183	370
Lettenkhole	-840	-187	30
MK evap.	-870	-217	115
Keuper	-985	-332	120
MK evap.	-1105	-452	95
Buntsandstein	-1200	-547	72
Permian	-1272	-619	118
Basement	-1390	-737	31
T.D.	-1421	-768	

Bitterli 1972

15) Valempoulières 2 PREPA. 1962 T.D. = 1252m

elevation	x	y
643m	480'600m	186'000m

top of ...

Formation	depth m	elevation m	thickness m
Rh./Keuper	-466	177	361
Lettenkohle	-827	-184	208
Middle Triassic	-1035	-392	182
Lower Triassic	-1217	-574	35
T.D.	-1252	-609	

Bitterli 1972

16) Thésy T.D. = 1108m
Cristalline rock

elevation	x	y
703m	484'200m	196'800m

17) Saugeot T.D. = 1307m

elevation	x	y
m	476'000m	162'000m

18) Salins-Les-Bains T.D. = 267m
Keuper

elevation
347m

19) Buez T.D. = 1200m

elevation	x	y
685m	522'400m	235'800m

top of ...

Formation	depth m	elevation m	thickness m
Dogger	0	685	125
Aalenian/Lias.	-125	560	225
Rhaetian	-350	335	50
Dogger	-400	285	30
Aalenian/Lias.	-430	255	250
Keuper	-680	5	175
Lettenkohle	-855	-170	25
MK dolom.	-880	-195	25
MK evap.	-905	-220	200
Buntsandstein	-1105	-420	75
Basement	-1180	-495	20
T.D.	-1200	-515	

Bitterli 1972

Appendix 2 (pages 159-162): Legend on page 159.

Légende à la page 159.

20) Humilly 2 T.D. = 3040m

SNPA 1969

elevation	x	y
629m	480'500m	108'250m

top of ...

Formation	depth m	elevation m	thickness m
Tertiary	0	629	438
Cretaceous	-438	191	374
Malm	-812	-183	832
Argovian	-1644	-1015	211
Dogger	-1855	-1226	233
Aalenian	-2088	-1459	28
Liassic	-2116	-1487	410
Keuper	-2526	-1897	383
MK evap.	-2909	-2280	131
T.D.	-3040	-2411	

Persoz 1982, Wildi et al. 1991, Jenny et al. 1995

21) Buix T.D. = 1053m

elevation	x	y
395m	568'780m	258'620m

top of ...

Formation	depth m	elevation m	thickness m
Oxfordian	0	395	103
Dogger	-103	292	195
Aalenian	-298	97	158
Liassic	-456	-61	106
Keuper	-562	-167	186
Lett.	-748	-353	3
MK dolom.	-751	-356	20
MK evap.	-771	-376	221
Buntsandstein	-992	-597	51
Permian	-1043	-648	10
T.D.	-1053	-658	

Schmidt et al. 1924

Lithologies:

Raur. = Rauracian; Argov. = Argovian; Lias. = Liassic;
Bath. = Bathonian; Baj. = Bajocian
Lett. = Lettenkohle; MK = Muschelkalk;
MK dolom. = Muschelkalk dolomite;
MK evap. = Muschelkalk evaporites

Companies:

PREPA = Société de Prospections, Recherches et Etudes Pétrolifères en Alsace
SNPA = Société Nationale des Pétroles d'Aquitaine
SADH = Société anonyme des Hydrocarbures, Lausanne
KUS = Konsortium Untertagespeicher
RAP = Régie autonome des Pétroles

Appendix 2 (pages 159-162): Legend on page 159.

Légende à la page 159.

APPENDIX 3.1

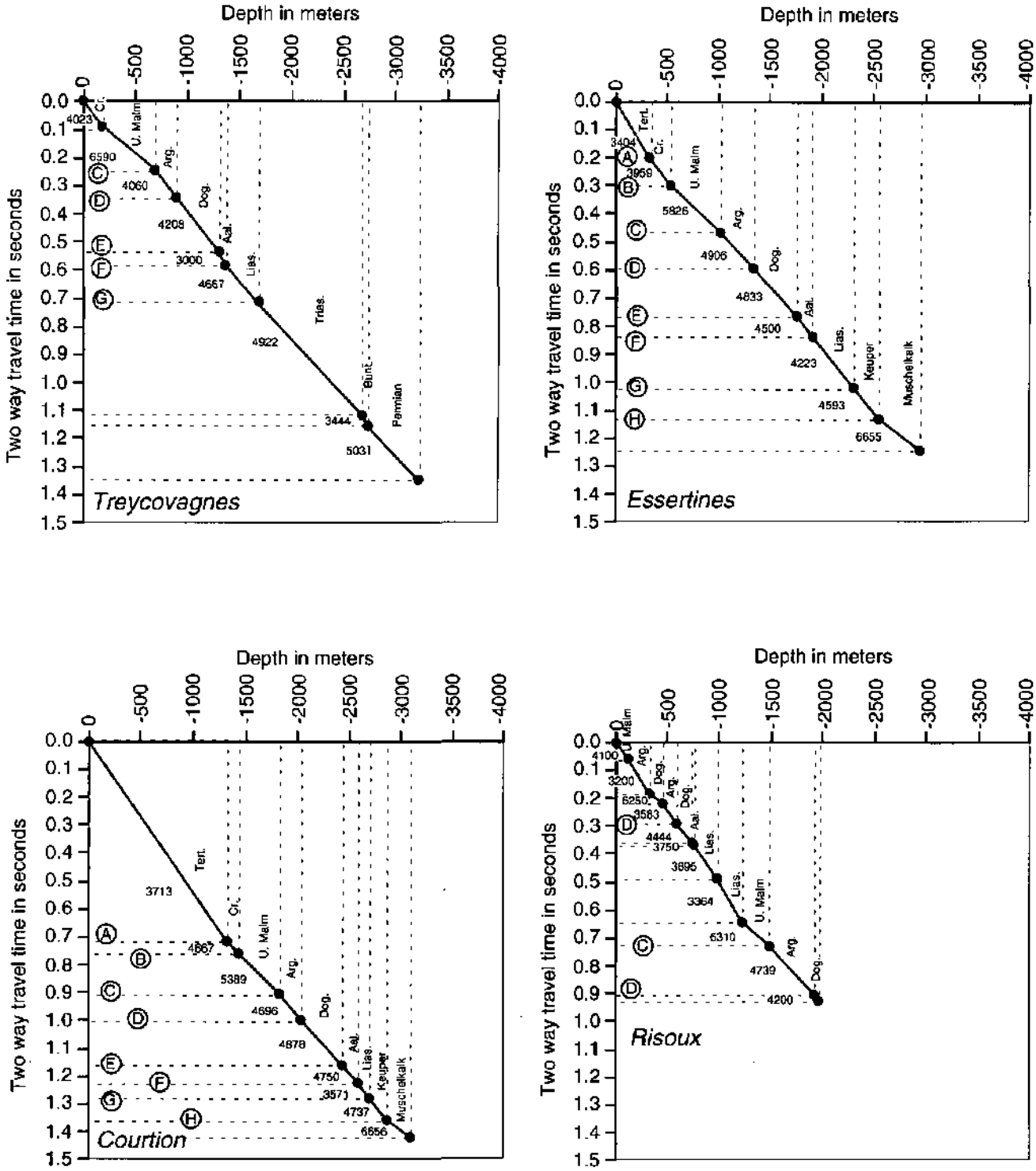

Appendix 3.1: Seismic velocities deduced from correlation of seismic two way time interval (in seconds) and stratigraphic thicknesses (in meters) based on well log data.

Vitesses sismiques déduites de la corrélation entre les intervalles sismiques (en temps double, en secondes) et les épaisseurs stratigraphiques (en mètres) basées sur les données de forages.

APPENDIX 3.2

	A	B	B	C	C	D	E
	Neuchâtel Jura	Molasse Basin	interval	Treycovagnes area	interval	Risoux area	C.M. area
	BP	Shell/SADH	min-max veloc.	Shell/SADH	min-max veloc.	Shell	Shellrex
	1988	1973-1976		1973-1976		1973-1974	1970-1974
Formation	m/s	m/s	m/s	m/s	m/s	m/s	m/s
Tertiary	2500	4119* z^0.133	2500-4300	3000	3000	-	-
Cretaceous	3500	4370+0.477 z	4370-5700	4370+0.477 z	4370-5000	-	-
Malm	4800	5015+0.393 z	5015-6217	5015+0.393 z	5015-5500	4600	4800
Argovian	4800	1864* z^0.12	3240-5042	1864* z^0.12	3931-4500	4600	4800
Dog. & Aal.	4800	4370+z^0.477	4418-6276	4800	4800	4600	4800
Liassic	4800	995* z^0.17	2178-4107	995* z^0.17	3300-3800	4600	4800
Keuper	5500	5435+0.184z	5453-6224	5500	5500	5500	5000
MK evap.	5500	5435+0.184z	5453-6252	5500	5500	5500	5000

A, B, C, D, E: refers to velocity sector in Appendix 3.3
*: *multiplication function*
^: exponential function

Appendix 3.2: Table of seismic velocities used in this work. In the Jura area a simple velocity model attributing a constant velocity to each major interval (Tertiary, Cretaceous, Jurassic and Triassic) was used. In the Molasse Basin, however, more complex depth-dependent conversion functions from NAGRA (NAEF & DIEBOLD, 1990) were used in order to account for increased velocities due to the considerable thickening and facies changes of Tertiary sediments. See also Appendix 3.3.

Tableau des vitesses sismiques utilisées dans ce travail. Dans la région jurassienne, un modèle simple attribuant une vitesse constante à chaque intervalle majeur (Tertiaire, Crétacé, Jurassique et Trias) a été appliqué. Dans la région du Bassin molassique, on a utilisé un modèle plus complexe, nécessitant des fonctions qui tiennent compte de la profondeur des couches (NAEF & DIEBOLD, 1990, CEDRA). Voir aussi Annexe 3.3.

APPENDIX 3.3

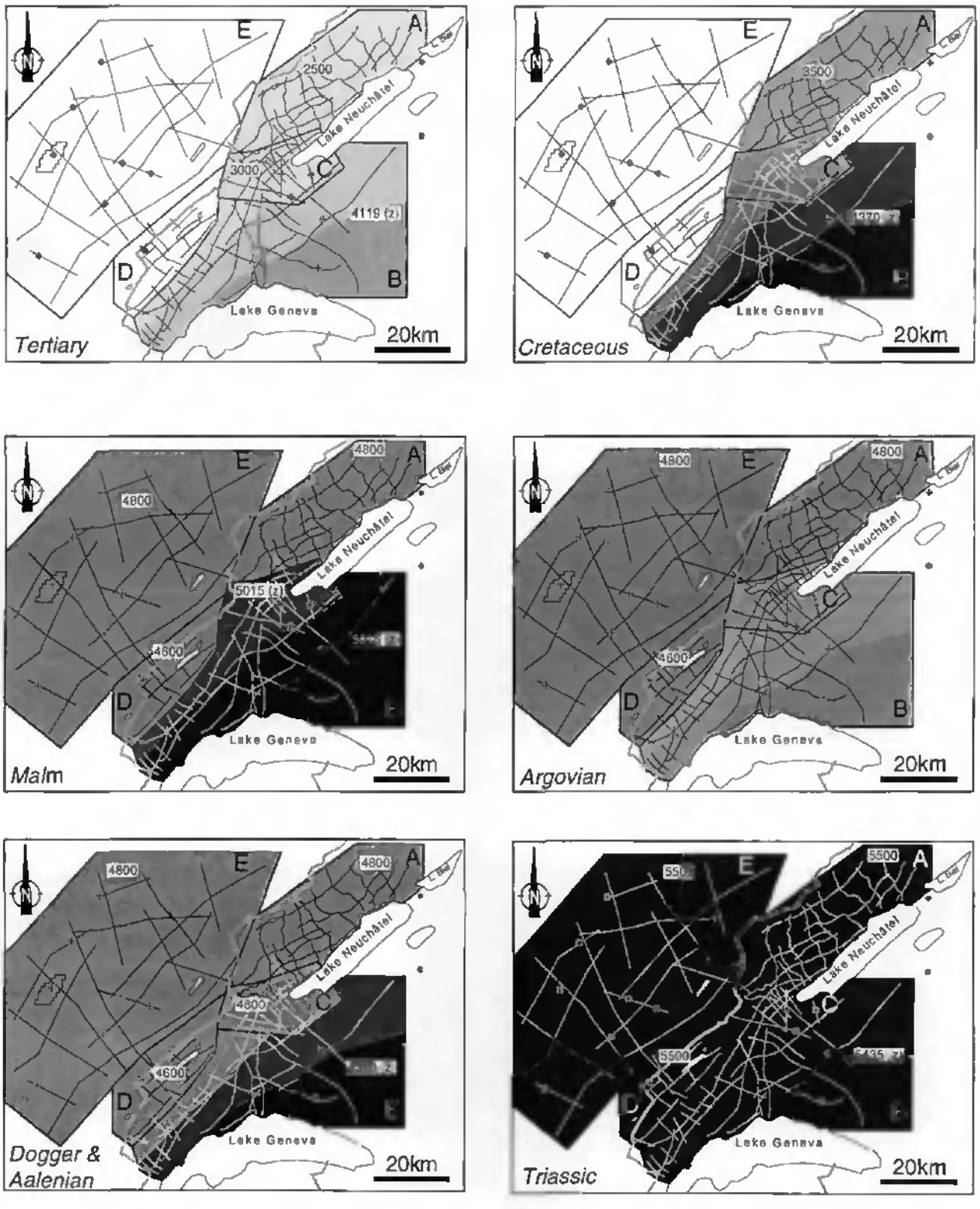

Appendix 3.3: Map showing the seismic velocities used for the depth conversion of the seismic lines.

Carte montrant les vitesses sismiques utilisées pour la conversion en profondeur (en mètres) des profils sismiques (en secondes).

REFERENCES

ALLEN, P.A., HOMEWOOD, P. & WILLIAMS, G.D. 1986. Foreland basins: an introduction. In: ALLEN, P.A. & HOMEWOOD, P.A. (eds.). Foreland basins, 8, 3-12. *Spec. Publ. int. Ass. sediment.*

ALTHAUS, H.E. & RICKENBACH, E. 1947. Erdölgeologische Untersuchungen in der Schweiz, 1. Teil. *Beitr. Geol. Schweiz. Geotechn. Ser.* 26, 88 pp.

ALTHAUS, H.E. & RICKENBACH, E. 1952: Erdölgeologische Untersuchungen in der Schweiz, IV. Teil. *Beitr. Geol. Schweiz, Geotechn. Ser.* 26, 79 pp.

ANGELIER, J. & MECHLER, P. 1977. Sur une méthode graphique de recherche des contraintes principales également utilisable en tectonique et en séismologie: la méthode des dièdres droits. *Bull. Soc. géol. France* 19, 1309-1318.

APOTRIA, T.G., SNEDDEN, W.T., SPANG, J.H. & WILTSCHKO, D.V. 1992. Kinematic models of deformation at an oblique ramp. In: McClay, K.R. (ed.). Thrust tectonics, 141-154. *Chapman & Hall, London*

ARAGNO, P.O. 1994. Etude de la terminaison Ouest de l'anticlinal de Chasseral. *Travail de Diplôme, Université de Neuchâtel.*

AUBERT, D. 1941. Vallée de Joux. Atlas géol. Suisse, feuille N°17. *Commission Géologique Suisse. Berne.*

AUBERT, D. 1945. Le Jura et la tectonique d'écoulement. *Mém. soc. vaudoise des sci. nat.* 8, 217-236.

AUBERT, D. 1959. Le décrochement de Pontarlier et l'orogénèse du Jura. *Mém. soc. vaudoise des sci. nat.* 12, 93-152.

AUBERT, D. 1965. Calotte glaciaire et morphologie jurasienne. *Eclogae geol. Helv.* 58, 555-578.

AUBERT, D. 1971. Le Risoux, un charriage jurassien de grandes dimensions. *Eclogae geol. Helv.* 64, 151-156.

AUBERT, D. 1972. Le lapié fossile des Verrières (Doubs). *Ann. sci. Univ. Besançon* 3, 85-88.

AUBERT, D. 1975. L'évolution du relief jurassien. *Eclogae geol. Helv.* 68, 1-64.

AUBERT, D., AYRTON, S., BEARTH, P., BURRI, M., CARON, C., ESCHER, A., SCHAER, J.-P. & WEIDMANN, M. 1980. Excursion N°11: Geotraverse of Western Switzerland. In: COMMISSION GÉOLOGIQUE SUISSE (ed.). Geology of Switzerland - a guide-book. Part B: Geological excursions, 155-181. *Wepf, Basel, New York.*

AUBERT, D., BADOUX, H. & LAVANCHY, Y. 1979. La carte structurale et les sources du Jura vaudois. *Bull. Soc. Vaud. Sc. Nat.* 74, 333-343.

AUBERT, D. & DREYFUSS, M. 1963. Orbe. Atlas géol. Suisse, feuille N°42. *Commission Géologique Suisse. Berne.*

BACHMANN, G.H., DOHR, G. & MÜLLER, M. 1982. Exploration in a classic thrust belt and its foreland: Bavarian Alps, Germany. *Amer. Ass. Petrol. Geol. Bull.* 66, 2529-2542.

BACHMANN, G.H., MÜLLER, M. & WEGGEN, K. 1987. Evolution of the Molasse Basin (Germany, Switzerland). *Tectonophysics* 137, 77-92.

BAER, A. 1959. Carte géologique des environs de la Vue des Alpes. Unpublished. *Deposited at Neuchâtel University.*

BAILEY, E.B. 1935. Tectonic Essays, Mainly Alpine. *Oxford University Press, Oxford,* 200 pp.

BALLY, A.W. 1989. Phanerozoic basins of North America. In: BALLY, A.W. & PALMER, A.R. (eds.). The geology of North America - An overview. Vol. A, 397-446. *Geological Society of America, Boulder, Colorado.*

BALLY, A.W., GORDY, P.L. & STEWART, G.A. 1966. Structure, seismic data and orogenic evolution of southern Canadian Rocky Mountains. *Can. Soc. Petrol. Geol. Bull.* 14, 337-381.

BALLY, A.W. & SNELSON, S. 1980. Realms of subsidence. In: MIALL, A.D. (ed.). Facts and Principles of World Petroleum Occurence, 6, 9-75. *Can. Soc. Petrol. Geol. Mem., Calgary.*

BATES, R.L. & JACKSON, J.A. 1987. Glossary of geology (3rd edition). *American Geological Institute, Alexandria (Virginia),* 788 pp.

BAUMANN, M. 1994. Three-dimensional modeling of the crust-mantle boundary in the alpine region. *Thèse de Doctorat, ETH Zurich.*

BEAUMONT, C. 1981. Foreland basins. *Geophys. J. r. astron. Soc.* 55, 471-498.

BECKER, A. 1985. Messung und Interpretation oberflächennaher in situ- Spannungen am Südost-Ende des Oberrheingrabens und im Tafeljura. *Thèse de Doctorat, Université de Karlsruhe.*

BECKER, A. 1987. Recent stress field and neotectonics in the eastern Jura Mountains. *Tectonophysics* 135, 277-288.

BECKER, A. 1989. Detached neotectonic stress field in the northern Jura mountains, Switzerland. *Geol. Rdsch.* 78, 459-475.

BECKER, A. & WERNER, D. 1995. Neotectonic state of stress in the Jura Mountains. *Geodinamica Acta (Paris)* 8, 99-111.

BERGER, J.-P. 1992. Correlative chart of the European Oligocene and Miocene: Application to the Swiss Molasse Basin. *Eclogae geol. Helv.* 85, 573-609.

BERGERAT, F. 1987. Paléo-champs de contrainte tertiaires dans la plate-forme européenne au front de l'orogène alpin. *Bull. Soc. géol. France* 8, 611-620.

BERSIER, A. 1952. Jorat. Atlas géol. Suisse, feuille N°27. *Commission Géologique Suisse. Berne.*

BIDDLE, K.T. & CHRISTIE-BLICK, N. 1985. Glossary: Strike-slip deformation, Basin formation and Sedimentation. *Spec. Publ. Soc. econ. Paleont. Mineral.* 37, 375-385.

BIOT, M.A. 1957. Folding instability of a layered viscoelastic medium under compression. *Proc. r. Soc. London* 242, 211-228.

BITTERLI, P. 1972. Erdölgeologische Forschungen im Jura. *Bull. Ver. Schweizer. Petrol.-Geol. u. Ing.* 39, 13-28.

BITTERLI, T. 1988. Die dreidimensionale Massenbilanz - ein wichtiges Hilfsmittel zum Verständnis der regionalen Kinematik (Schuppenzone von Reigoldswil, Faltenjura). *Eclogae geol. Helv.* 81, 415-431.

BITTERLI, T. 1990. The kinematic evolution of a classical Jura fold: a reinterpretation based on 3-dimensional balancing techniques (Weissenstein Anticline, Jura Mountains, Switzerland). *Eclogae geol. Helv.* 83, 493-511.

BITTERLI, T. 1992. Die Anwendung der tektonischen Materialbilanz im östlichen Faltenjura. *Thèse de Doctorat, Université de Bâle.*

BOLLIGER, T., ENGESSER, B. & WEIDMANN, M. 1993. Première découverte de mammifères pliocènes dans le Jura neuchâtelois. *Eclogae geol. Helv.* 86, 1031-1068.

BOURQUIN, P., BUXTORF, R., FREI, E., LÜTHI, E., MUHLENTHALER, C., RYNIKER, K. & SUTER, H. 1968. Val de Ruz. Atlas géol. Suisse, feuille N°51. *Commission Géologique Suisse. Berne.*

BOURQUIN, P. & SUTER, H. 1946. Biaufond - Les Bois - La Ferrière - St-Imier. Atlas géol. Suisse, feuille N°15. *Commission Géologique Suisse. Berne.*

BOYER, S.E. & ELLIOTT, D. 1982. Thrust systems. *Amer. Ass. Petrol. Geol. Bull.* 66, 1196-1230.

BRGM 1963. Ornans. Carte géologique détaillée de la France 1:50'000, feuille N°530. *Service Carte géol. France. Orléans.*

BRGM 1964. Mouthe. Carte géologique détaillée de la France 1:50'000, feuille N°583. *Service Carte géol. France. Orléans.*

BRGM 1965a. Champagnole. Carte géologique détaillée de la France 1:50'000, feuille N°582. *Service Carte géol. France. Orléans.*

BRGM 1965b. Vercel. Carte géologique détaillée de la France 1:50'000, feuille N°503. *Service Carte géol. France. Orléans.*

BRGM 1966. Lons-Le-Saunier. Carte géologique détaillée de la France 1:50'000, feuille N°581. *Service Carte géol. France. Orléans.*

BRGM 1967. Salins-Les-Bains. Carte géologique détaillée de la France 1:50'000, feuille N°556. *Service Carte géol. France. Orléans.*

BRGM 1968a. Morez - Bois d'Amont. Carte géologique détaillée de la France 1:50'000, feuille N°605. *Service Carte géol. France. Orléans.*

BRGM 1968b. Morteau. Carte géologique détaillée de la France 1:50'000, feuille N°531. *Service Carte géol. France. Orléans.*

BRGM 1969. Pontarlier. Carte géologique détaillée de la France 1:50'000, feuille N°557. *Service Carte géol. France. Orléans.*

BRGM 1972. Baume-Les-Dames. Carte géologique détaillée de la France 1:50'000, feuille N°473. *Service Carte géol. France. Orléans.*

BRGM 1975. Quingey. Carte géologique détaillée de la France 1:50'000, feuille N°529. *Service Carte géol. France. Orléans.*

BRGM 1979. Dôle. Carte géologique détaillée de la France 1:50'000, feuille N°528. *Service Carte géol. France. Orléans.*

BRGM 1981. Poligny. Carte géologique détaillée de la France 1:50'000, feuille N°555. *Service Carte géol. France. Orléans.*

BRGM 1987a. Chalon-sur-Saône. Carte géologique de la France 1:250'000, feuille N°24. *Service Carte géol. France. Orléans.*

BRGM 1987b. Thonon-Les-Bains. Carte géologique de la France 1:250'000, feuille N°25. *Service Carte géol. France. Orléans.*

BRGM 1989. Dijon. Carte géologique de la France 1:250'000, feuille N°19. *Service Carte géol. France. Orléans.*

BÜCHI, U.P. & ETHZ 1981. Geothermische Datensynthese der Schweiz. (Schriftreihe N°. 26). *Bundesamtes für Energiewirtschaft.*

BÜCHI, U.P., WIENER, G. & HOFMANN, F. 1965a. Neue Erkenntnisse im Molassebecken auf Grund von Erdöltiefbohrungen in der Zentral- und Ostschweiz. *Eclogae geol. Helv.* 58, 87-108.

BÜCHI, U.P., LEMCKE, K., WIENER, G. & ZIMDARS, J. 1965b. Geologische Ergebnisse der Erdölexploration auf das Mesozoikum im Untergrund des schweizerischen Molassebeckens. *Bull. Ver. Schweizer. Petrol.-Geol. u. Ing.* 32, 7-38.

BURGER, A. & GOHRAN, H.L. 1986. Prospection géothermique le long du pied sud du Jura. *Bull. Centre Hydrogéol.* 6, 91-227.

BURKHARD, M. 1990. Aspects of the large scale Miocene deformation in the most external part of the Swiss Alps (Subalpine Molasse to Jura fold belt). *Eclogae geol. Helv.* 83, 559-583.

BURKHARD, M. 1993. Calcite twins, their geometry, appearance, significance as stress/strain markers and indicators of tectonic regime, a review. *Journal Structural Geology* 15, 351-368.

BURKHARD, M. & SOMMARUGA, A. (in press). Evolution of the western Swiss Molasse basin: structural relations with the Alps and the Jura belt. *Spec. Publ. Geol. Soc. London.*

BUXTORF, A. 1907. Zur Tektonik des Kettenjura. *Ber. Vers. oberrh. geol. Vers.* 30/40, 79-111.

BUXTORF, A. 1916. Prognosen und Befunde beim Hauensteinbasis- und Grenchenberg-tunnel und die Bedeutung der letzteren für die Geologie des Juragebirges. *Verh. Naturforsch. Ges. Basel* 27, 184-205.

CAIRE, A. 1963. Problèmes de tectonique et de morphologie jurassiennes. In: Livre Mém. Prof. P. Fallot (Ed. by *Soc. Géol. France*). Mém. hors-série 1, 105-158.

CARTER, N.L. & HANSEN, F.D. 1983. Creep of Rocksalt. *Tectonophysics* 92, 275-333.

CASTANY, G. 1947. Le synclinal des Verrières (Jura) et la "Collapse Structure". *Bull. Soc. géol. France* 5, 199-207.

CHAPPLE, W.M. 1978. Mechanics of thin-skinned fold-and-thrust belts. *Geol. Soc. Amer. Bull.* 89, 1189-1198.

CHAUVE, P. 1975. Jura. *Masson & Cie. Paris*, 216 pp.

CHAUVE, P., ENAY, R., FLUCK, P. & SITTLER, C. 1980. L'Est de la France (Vosges, Fossé Rhénan, Bresse, Jura). In: 26e Congrès Géologie International, Paris. *Ann. Sci. Univ. Besançon Géol.* 4 /1, 3-80.

CHAUVE, P., MARTIN, J., PETITJEANSEQ, E. & SEQUEIROS, F. 1988. Le chevauchement du Jura sur la Bresse. Données nouvelles et réinterprétation des sondages. *Bull. Soc. géol. France* 8, 861-870.

CHYN 1995. Etude hydrogéologique pour la réalisation d'un forage profond au Dogger à Yverdon-les-Bains. *Rapport du Centre d'hydrogéologie, Université de Neuchâtel.*

COLLOT, L. 1913. Le Mont-D'Or et le Tunnel de la ligne Frasne-Vallorbe. In: *Assoc. Fr. Av. Sc., Tunis.* 325-330.

CRAMPTON, S.L. & ALLEN, P.A. 1995. Recognition of Forebulge Unconformities Associated with Early Stage Foreland Basin Development: Example from the North Alpine Foreland Basin. *Amer. Ass. Petrol. Geol. Bull.* 79, 1495-1514.

CUSTER, W. & AUBERT, D. 1935. Mont-la-Ville -La Sarraz - Montricher - Cossonay. Atlas géol. Suisse, feuille N°5. *Commission Géologique Suisse. Berne.*

DAHLEN, F.A. 1990. Critical taper model of fold-and-thrust belts and accretionary wedges. *Ann. Rev. Earth Planet. Sci.* 18, 55-99.

DAHLEN, F.A., SUPPE, J. & DAVIS, D.M. 1984: Mechanics of fold-and-thrust belts and accretionary wedges (continued): Cohesive Coulomb theory. *J. Geophys. Res.* 88, 1153-1172.

DAHLSTROM, C.D.A. 1970. Structural geology in the eastern margin of the Canadian Rocky Mountains. *Bull. Can. Petrol. Geol.* 18, 332-406.

DAVIES, G.R. 1977. Carbonate-Anhydrite Facies Relationships. Otto Fiord Formation (Mississippian-Pennsylvanian), Canadian Arctic Archipelago. *Amer. Ass. Petrol. Geol. Studies in Geology* 5, 145-167.

DAVIS, D.M. & ENGELDER, T. 1985. The role of salt in fold-and-thrust belts. *Tectonophysics* 119, 67-88.

DAVIS, D.M. & ENGELDER, T. 1987. Thin-skinned deformation over salt. In: LERCHE, I. & O'BRIEN, J.J. (eds.). Dynamical Geology of Salt and Related Structures, 301-337. *Academic Press, Inc., Orlando, Florida.*

DEBELMAS, J. 1974. Géologie de la France. Les Chaînes plissées du cycle alpin et leur avant-pays. *Doin, Paris*, 480-500.

DEBRAND-PASSARD, S. & COURBOULEIX, S. & LIENHARDT, M.-J. 1984. Synthèse géologique du Sud-Est de la France. Stratigraphie et Paléogéographie. Volume 1. *BRGM, Orléans*, 615 pp.

DEBRAND-PASSARD, S. & COURBOULEIX, S. 1984. Synthèse géologique du Sud-Est de la France. Atlas. Volume 2. *BRGM, Orléans.*

DEICHMANN, N. 1992. Recent seismicity of the northern Alpine foreland of Switzerland. *Eclogae geol. Helv.* 85, 701-705.

DE MARGERIE, E. 1922. Le Jura. Première Partie: Bibliographie sommaire du Jura français et suisse (orographe, tectonique et morphologie). *Ministère des Travaux publics, Paris*, 642 pp.

DE MARGERIE, E. 1936. Le Jura. Deuxième Partie: Commentaire de la carte structurale. Description tectonique du Jura français. *Ministère des Travaux publics, Paris.*

DE MONTMOLLIN, M.A. 1839. Carte géologique du Jura Neuchâtelois. Topographie de la carte de la Principauté de Neuchâtel dressée par Osterwald. *Mém. Soc. neuchâtel. Sci. nat.* T. II.

DE PURY, P. 1963. Etude géologique de la région des Combes-Dernier-Pouette-Combe sur le territoire des Ponts de Martel. *Travail de Diplôme, Université de Neuchâtel.*

DESOR, E. 1854. Quelques mots sur l'étage inférieur du groupe néocomien (étage valanginien). *Bull. Soc. neuchâtel. Sci. nat.* 3, 172-180.

DESOR, E. & GRESSLY, A. 1859. Etudes géologiques sur le Jura neuchâtelois. *Mém. Soc. neuchâtel. Sci. nat.*, T. IV (1), 159 pp.

DESSOULAVY, A. 1952. Les Gorges de la Vaux de Vaumarcus. Le passage de En Vaulery. *Travail de Diplôme, Université de Neuchâtel.*

DICKINSON, W.R. 1974. Plate tectonics and sedimentation. In: DICKINSON, W.R. (ed.) Tectonics and Sedimentation. 22: 1-27. *Spec. Publ. Soc. Paleont. Mineral., Tulsa.*

DIEBOLD, P., NAEF, H. & AMMAN, M. 1991. Zur Tektonik der Zentralen Nordschweiz. (Technischer Bericht N°. NTB 90-04). *NAGRA (CEDRA). Wettingen.*

DIESLER, C. 1914. Stratigraphie und Tektonik des Rotliegenden und der Trias beiderseits des Rheins zwischen Rheinfelden und Augst. *Thèse de Doctorat, Université de Bâle.*

DIXON, J.M. & LIU, S. 1992. Centrifuge modelling of the propagation of thrust faults. In: MCCLAY, K.R. (ed.) Thrust tectonics. 53-68. *Chapman & Hall, London.*

DOBSON, J. & MCCLAY, K. 1992. 3-D modelling of fault-related folding, McConnel thrust sheet, southwest Alberta. *Amer. Ass. Petrol. Geol. Conf. Abstracts, Calgary.*

DREYFUSS, M. 1960. Le Plateau de Chantrans et le Faisceau salinois entre Nods et La Loue. *Bull. Carte Géol. France* 261, 67-74.

DROXLER, A. 1978. Etude tectonique et microtectonique des plis de second ordre dans le Jura neuchâtelois. Déformation par dissolution des calcaires. Carte Géologique de l'anticlinal de Pouillerel entre le Col des Roches et les Brenets. *Travail de Diplôme, Université de Neuchâtel.*

DROXLER, A. & SCHAER, J.-P. 1979. Déformation cataclastique plastique lors du plissement, sous faible couverture, de strates calcaires. *Eclogae geol. Helv.* 72, 551-570.

DU PASQUIER, L. 1893. Le glaciaire du Val de Travers. *Bull. Soc. neuchâtel. Sci. nat.* 22, 3-32.

ELMOHANDES, S.E. 1981. The central european Graben system: Rifting imitated by clay modelling. *Tectonophysics* 73, 69-78.

FALCONNIER, A. 1950. Les Plats - Marchairuz - Cure - Arzier - Gimel. Atlas géol. Suisse, feuille N°25. *Commission Géologique Suisse. Berne.*

FAVRE, J. 1911. Description géologique des environs du Locle et de la Chaux-de-Fonds. *Eclogae geol. Helv.* 11, 369-475.

FAVRE, J., BOURQUIN, P. & STEHLIN, H.G. 1937. Etudes sur le Tertiaire du Haut-Jura neuchâtelois. *Mém. Soc. paléont. suisse* 60, 1-47.

FAVRE, J. & JEANNET, A. 1934. Le Jura. In: WEPF, B. & CIE (ed.). Guide géologique de la Suisse. Fasc. 1: 42-56. *Société Géologique Suisse, Bâle.*

FISCHER, H. & LUTERBACHER, H. 1963. Das Mesozoikum der Bohrungen Courtion 1 (Kt. Fribourg) und Altishofen 1 (Kt. Luzern). *Matèr. Carte Gèol. Suisse.* [n.s.] 115, 40 pp. *Berne.*

FREI, E. 1925. Zur Geologie des südöstlichen Neuenburger Jura. *Matèr. Carte Gèol. Suisse* [n.s.] 55. *Berne.*

FREI, E. 1942. Carte géologique 1: 25'000 de la feuille N°279, Noiraigue, de l'atlas topographique de Siegfried. Non-publié. *Déposé au Service hydrologique et géologique national, Berne, Suisse.*

FREI, E. 1946. 3 coupes géologiques à travers la feuille N°279, Noiraigue, de l'atlas topographique de Siegfried. Non-publié. *Déposé à l'Institut de Géologie de l'Université de Neuchâtel, Suisse.*

FREI, E., MEIA, J., BECKER, F., BÜCHI, O., BUXTORF, R., RYNIKER, K. & SUTER, H. 1974. Neuchâtel. Atlas géol. Suisse, feuille N°67. *Commission Géologique Suisse. Berne.*

GLANGEAUD, L. 1947. Caractères structuraux principaux de la région de Mouthier. *Ann. Soc. géol. Belgique* 73, 121-124.

GLANGEAUD, L. 1949. Les caractères structuraux du Jura. *Bull. Soc. géol. France* 19, 669-688.

GLANGEAUD, L. & MATTAUER, M. 1955. A propos des chevauchements du faisceau bisontin. *Bull. Soc. Histoire nat. du Doubs* 59, 83-85.

GORIN, G.E., SIGNER, C. & AMBERGER, G. 1993. Structural configuration of the western Swiss Molasse Basin as defined by reflection seismic data. *Eclogae geol. Helv.* 86, 693-716.

GRATIER, J.-P. 1984. La déformation des roches par dissolution-cristallisation. *Thèse de Doctorat, Université de Grenoble.*

GRESSLY, A. 1837-41. Observations sur le Jura soleurois. *Nouv. Mèm. Soc. Helv. Sci. Nat.* 2, 4, 5 / 349 pp. *Neuchâtel.*

GROSHONG, R.H., PFIFFNER, O.A. & PRINGLE, L.R. 1984. Strain partitioning in the Helvetic thrust belt of eastern Switzerland from the leading edge to the internal zone. *J. Struct. Geol.* 6, 19-32.

GUELLEC, S., MUGNIER, J.L., TARDY, M. & ROURE, F. 1990. Neogene evolution of the western Alpine foreland in the light of ECORS data and balanced cross sections. In: ROURE, F., HEITZMANN, P. & POLINO, R. (eds.). Deep structure of the Alps. 1, 165-184. *Mém. Soc. géol. suisse, Zurich.*

GUILLAUME, S. 1966. Le Crétacé du Jura français. *Thèse de Doctorat, Université de Paris V.*

GYGI, R.A. & PERSOZ, F. 1986. Mineralostratigraphy, litho- and biostratigraphy combined in correlation of the Oxfordian (Late Jurassic) formations of the Swiss Jura range. *Eclogae geol. Helv.* 79, 385-454.

GYGI, R.A. & PERSOZ, F. 1987. The epicontinental sea of Swabia (southern germany) in late Jurassic - factors controlling sedimentation. *N. Jb. Geol. Paläont., Abh.* 176, 49-65.

HALL, J. 1815. On the vertical position and convolutions of certain strata, and their relation with granite. *Transactions of the Royal Society Edinburgh* 7, 79-108.

HARLAND, B.W., AMSTRONG, R.L., COX, A.V., CRAIG, L.E., SMITH, A.G. & SMITH, D.G. 1990. A geologic time scale 1989. *Cambridge University Press, Cambridge.*

HARRISON, J.C. 1995. Melville Island's salt-based fold belt, Arctic Canada. *Geol. Surv. Canada, Bull.* 472, 1-331.

HARRISON, J.C. & BALLY, A.W. 1988. Cross-sections of the Parry Islands Fold Belt on Melville Island, Canadian Arctic Islands: implications for the timing and kinematic history of some thin-skinned décollement systems. *Bull. Can. Petrol. Geol.* 36, 311-332.

HAUBER, L. 1993. Der Mittlere Muschelkalk am Hochrhein. *N. Jb. Geol. Paläont., Abh.* 189, 147-170.

HEARD, H.C. & RUBEY, W.W. 1966. Tectonic implications of Gypsum Dehydration. *Geol. Soc. Amer., Bull.* 77, 741-760.

HEIM, A. 1915. Die horizontalen Transversalverschiebungen im Juragebirge. Geol. Nachlese Nr.22,. *V. Natf. Ges. Zürich* 60, 597-610.

HEIM, A. 1921. Geologie der Schweiz. Band 1 Molasseland und Juragebirge. *Tauchniz, Leipzig,* 704 pp.

HOMBERG, C., ANGELIER, J., BERGERAT, F. & O., L. 1994. Nouvelles données tectoniques dans le Jura externe: apport des paléocontraintes. *C.R. Acad. Sci. Paris* 318, 1371-1377.

HOMEWOOD, P. 1986. Geodynamics and paleogeography of the western Molasse basin: a review. *Giornale di Geologia,* ser. 3a 48, 275-284.

HOMEWOOD, P., ALLEN, P.A. & WILLIAMS, G.D. 1986. Dynamics of the Molasse Basin of western Switzerland. *Spec. Publ. int. Ass. Sediment.* 8, 199-217.

HOMEWOOD, P., RIGASSI, D. & WEIDMANN, M. 1989. Le bassin molassique Suisse. In: ASSOC. SÉDIM. FRANÇAISE (ed.). Dynamique et méthodes d'étude des bassins sédimentaires, 299-314. *Technip, Paris.*

HOUSSE, B.A. 1982. Forage Hermrigen 1d, Informations intéressant la Géothermie recueillies au cours du forage et des essais. (Deposited at Neuchâtel University N°. 82/1534). *Office de l'Economie Hydraulique et Energétique du Canton de Berne. Berne.*

HURFORD, A.J. 1986. Cooling and uplift patterns in the Lepontine Alps South Central Switzerland and age of vertical movement on the Insubric fault line. *Contrib. Mineral. Petrol.* 92, 413-427.

ILLIES, J.H. 1981. Mechanism of graben transformation. *Tectonophysics* 73, 249-266.

JACKSON, M.P.A. & TALBOT, C.J. 1989. Seismic recognition of salt welds in salt tectonics regimes. In: 10th A. Res. Conf. Prog. Extended abstract. 66-68. *Houston, Texas.*

JACKSON, M.P.A. & TALBOT, C.J. 1994. Advances in Salt Tectonics. In: HANCOCK, P.L. (ed.). Continental Deformation. 159-179. *Pergamon Press Ltd, Oxford.*

JAMISON, W.R. 1987. Geometric analysis of fold development in overthrust terranes. *J. Struct. Geol.* 9, 207-219.

JENNY, J., BURRI, J.-P., MURALT, R., PUGIN, A., SCHEGG, R., UNGEMACH, P., VUATAZ, F.-D. & WERNLI, R. 1995. Le forage géothermique de Thônex (Canton de Genève): Aspects stratigraphiques, tectoniques, diagénétiques, géophysiques et hydrogéologiques. *Eclogae geol. Helv.* 88, 365-396.

JENYON, M.K. 1986. Salt tectonics. *Elsevier Applied Science Publishers LTD, London.* 187 pp.

JENYON, M.K. & TAYLOR, J.C.M. 1987. Dissolution effects and reef-like features in the Zechstein across the Mid North Sea High. In: PERYT, T.M. (ed.). The Zechstein Facies in Europe. 51-75. *Springer-Verlag, Berlin.*

JOHNSON, A.M. & BERGER, P. 1989. Kinematics of fault-bend folding. *Engineering Geology* 27, 181-200.

JOHNSON, A.M. & FLETCHER, R.C. 1994. Folding of Viscous Layers. Mechanical Analysis and Interpretation of Structures in Deformed Rock. *Columbia University Press, New York,* 459 pp.

JORDAN, P. 1992. Evidence for large scale decoupling in the Triassic evaporites of Northern Switzerland: an overview. *Eclogae geol. Helv.* 85, 677-693.

JORDAN, P. 1994. Evaporite als Abscherhorizonte. Eine gefügekundlich-strukturgeologische Untersuchung am Beispiel der Nordschweizer Trias. *Matér. Carte Géol. Suisse* [n.s.] 164, 79 pp., *Berne.*

JORDAN, P. & NOACK, T. 1992. Hangingwall geometry of overthrusts emanating from ductile décollements. In: MCCLAY, K.R. (ed.). Thrust tectonics. 311-318. *Chapman & Hall, London.*

JORDAN, P., NOACK, T. & WIDMER, T. 1990. The evaporite shear zone of Jura boundary thrust - new evidence from Wiesen well (Switzerland). *Eclogae geol. Helv.* 83, 525-542.

JORDAN, P. & NÜESCH, R. 1989a. Deformation Structures in the Muschelkalk Anhydrites of the Schafisheim Well (Jura Overthrust, Northern Switzerland). *Eclogae geol. Helv.* 82, 429-454.

JORDAN, P. & NÜESCH, R. 1989b. Deformational behavior of shale interlayers in evaporite detachment horizons, Jura overthrust, Switzerland. *J. Struct. Geol.* 11, 859-871.

JORDI, H.A. 1955: Geologie der Umgebung von Yverdon, Jurafuss und Mittelländische Molasse. *Matér. Carte Géol. Suisse* [n.s.] 99, 1-84. *Berne.*

JORDI, H.A. 1990: Tektonisch-strukturelle Übersicht Westschweizerisches Molassebecken. *Bull. Ver. Schweizer. Petrol.-Geol. u. Ing.* 56, 1-11.

JORDI, H.A. 1993. Tectonique du bassin molassique et de son substratum jurassique-crétacé dans la région Orbe-Yverdon-Grandson. *Bull. Soc. Vaud. Sc. Nat.* 82, 279-299.

JORDI, H.A. 1994. Yverdon-les-Bains. Atlas géol. Suisse, feuille N°94. *Service hydrologique et géologique national, Berne.*

JORDI, H.A. 1995. Yverdon-les-Bains. Atlas géol. Suisse, feuille N°94. Notice explicative. *Service hydrologique et géologique national, Berne.*

JOUANNE, F. & MENARD, G. 1994. Quantification des mouvements verticaux actuels du Sud du Jura et des Alpes nord-occidentales par comparaison de nivellements: première analyse. *C.R. Acad. Sci. Paris* 319, 691-698.

JOUANNE, F., MENARD, G. & JAULT, D. 1994. Present-day deformation of the French northwestern Alps/southern Jura mountains: comparison between historical triangulations. *Geophys. J. Int.* 119, 151-165.

KÄLIN, D. 1993. Stratigraphie und Säugetierfaunen der oberen Süsswassermolasse der Nordwestschweiz. *Thèse de Doctorat, ETH Zurich.*

KÄLIN, D. 1997. Litho- und Biostratigraphie des mittel- bis obermiozänen Bois de Raube-Formation (Nordwestschweiz). *Eclogae geol. Helv.* 90, 97-114.

KARNER, G.D. & WATTS, A.B. 1983. Gravity anommalies and flexure of the lithosphere at mountains ranges. *J. Geophys. Res.* 88, 10'449-10'447.

KELLER, B. 1989. Fazies und Stratigraphie der oberen Meeresmolasse (unteres Miozän) zwischen Napf und Bodensee. *Thèse de Doctorat, Université de Berne.*

KELLER, B. 1990. Wirkung von Wellen und Gezeiten bei der Ablagerung der Oberen Meeresmolasse. *Mitt. Natf. Ges. Luzern* 31, 245-271.

KILIAN, W. 1893. Sur la constitution géologique du Jura du Doubs et des régions voisines. In: *Assoc. Fr. Av. Sc., C.R. 22ème sess., Besançon,* 442-445.

KIRALY, L. 1969. Bref commentaire à la carte structurale de la surface Argovien-Séquanien dans le canton de Neuchâtel. *Bull. Soc. neuchâtel. Sci. nat.* 92, 71-72.

KÜBLER, B. 1962a. Etude de l'Oehningien (Tortonien) du Locle. *Bull. Soc. neuchâtel. Sci. nat.* 85, 1-42.

KÜBLER, B. 1962b. Etude pétrographique de l'Oehningien (Tortonien) du Locle. *Schweiz. Mineral. Petrogr. Mitt.* 8, 267-314.

KÜHNI, A. 1993. Strukturgeologische Untersuchung in der Chasseral-Kette südlich von Corgémont/Sonceboz (BE). *Diplomarbeit, Unpublished, Universität Bern.*

LANGENBERG, W. 1992. Styles of deformation in the Rocky Mountain Foothills and Front Ranges, Alberta, Calgary. *Amer. Assoc. Petrol. Geol. Conf. Abstracts, Calgary.*

LAUBSCHER, H.P. 1961. Die Fernschubhypothese der Jurafaltung. *Eclogae geol. Helv.* 54, 221-280.

LAUBSCHER, H.P. 1965. Ein kinematisches Modell der Jurafaltung. *Eclogae geol. Helv.* 58, 232-318.

LAUBSCHER, H.P. 1972. Some overall aspects of Jura dynamics. *Amer. J. Sci.* 272, 293-304.

LAUBSCHER, H.P. 1973a. Faltenjura und Rheingraben: zwei Grossstrukturen stossen zusammen. *Jber. Mitt. oberrh. geol. Ver., N.F.* 55, 145-158.

LAUBSCHER, H.P. 1973b. Jura Mountains. In: DE JONG, K.A. & SCHOLTEN, R. (eds.). Gravity and Tectonics. 217-227. *Wiley, New York.*

LAUBSCHER, H.P. 1977. Fold development in the Jura. *Tectonophysics* 37, 337-362.

LAUBSCHER, H.P. 1979. Elements of Jura kinematics and dynamics. *Eclogae geol. Helv.* 72, 467-483.

LAUBSCHER, H.P. 1985. The eastern Jura: relations between thin-skinned and basement tectonics, local and regional. Technischer Bericht N°. NTB 85-53. *NAGRA (CEDRA), Wettingen.*

LAUBSCHER, H.P. 1986. The eastern Jura: Relations between thin-skinned and basement tectonics, local and regional. *Geol. Rdsch.* 75, 535-553.

LAUBSCHER, H.P. 1992. Jura kinematics and the Molasse basin. *Eclogae geol. Helv.* 85, 653-676.

LE PICHON, X., BERGERAT, F. & ROULET, M.-J. 1988. Plate kinematics and tectonics leading to the Alpine belt formation; a new analysis. In: CLARK-SYDNEY, P.J., BURCHFIEL, B.C. & SUPPE, J. (eds.). Processes in continental lithospheric deformation. 111-131. *Geol. Soc. Amer., Boulder.*

LEMCKE, K. 1959. Das Profil der Bohrung Chapelle 1. *Bull. Ver. Schweizer. Petrol.-Geol. u. Ing.* 26, 25-29.

LEMCKE, K. 1963. Die Ergebnisse der Bohrung Savigny 1 bei Lausanne. *Bull. Ver. Schweizer. Petrol.-Geol. u. Ing.* 30, 4-11.

LEMCKE, K. 1974. Vertikalbewegungen des vormesozoischen Sockels im nördlichen Alpenvorland von Perm bis zur Gegenwart. *Eclogae geol. Helv.* 71, 121-133.

LEMCKE, K. 1988. Das bayerische Alpenvorland vor der Eiszeit I, Geologie von Bayern. *Schweizerbart, Stuttgart,* 175 pp.

LIENHARDT, G. 1962. Géologie du bassin houiller stéphanien du Jura et de ses morts terrains. *Orléans,* 449 pp.

LLYOD, A.J. 1964. Cover folding in the Sonmartel chain (Jura Neuchâtelois). *Geol. Rdsch.* 53, 551-580.

LOUP, B. 1992a. Evolution de la partie septentrionale du domaine helvétique en Suisse occidentale au Trias et au Lias: contrôle par subsidence thermique et variations du niveau marin. *Thèse de Doctorat, Université de Genève. Publ. Départ. Géol. Paléont.*

LOUP, B. 1992b. Mesozoic subsidence and streching models of the lithosphere in Switzerland (Jura, Swiss Plateau and Helvetic realm). *Eclogae geol. Helv.* 85, 541-572.

LUGEON, M. 1941. Une hypothèse sur l'origine du Jura. *Bull. Lab. Géol. Univ. Lausanne* 73, 1-14.

MANCKTELOW, N. 1989. Stereoplot. Programme Macintosh. *Geologisches Institut. ETH, Zürich.*

MARGOT, J.-M. 1962. Géologie de la partie W de Chaumont. *Travail de Diplôme, Université de Neuchâtel.*

MARQUER, D. 1990. Structure et déformation alpine dans les granites hercyniens du massif du Gothard (Alpes centrales suisses). *Eclogae geol. Helv.* 83, 77-97.

MARTIN, J. 1987. Les replis crétacés, indicateurs de raccourcissements dans le Jura: application au Risoux. *Ann. sci. Univ. Besançon Géol.* 4, 47-54.

MARTIN, J., CHAUVE, P. & SEQUEIROS, F. 1986. Le contexte polyphasé du faisceau salinois. *Ann. sci. Univ. Besançon Géol.* 4, 43-47.

MARTIN, J., PHARISAT, A. & RANCHEARD, Y. 1991. Le synclinal des Verrières (Haute-Chaîne jurasienne): nouvelle interprétation structurale. *Ann. sci. Univ. Besançon Géol.* 4, 99-112.

MATHEY, B. 1976. Hydrogéologie des bassins de la Serrière et du Seyon. *Thèse de Doctorat, Université de Neuchâtel.*

MATTER, A., PETERS, T., BLÄSI, H.-R., SCHENKER, F. & WEISS, H.-P. 1988. Sondierbohrung Schafisheim Geologie Beilagenband. Technischer Bericht N°. NTB 86-03. *NAGRA (CEDRA), Wettingen.*

MATTHEY, F. 1971. Contribution à l'étude de l'évolution tardi- et postglaciaire de la végétation dans le Jura central. *Matériaux pour le levé géobotanique de la Suisse* 53. *Ed. Hans Huber. Berne.*

McClay, K.R. 1992. Thrust tectonics. *Chapman & Hall, London,* 447 pp.

MEIA, J. 1969. Géologie du Mont Aubert et de l'anticlinal Soliat-Montagne de Boudry au Nord du lac de Neuchâtel (Jura vaudois sud-oriental et Jura neuchâtelois méridional, Suisse). *Thèse de Doctorat, Université de Neuchâtel.*

MEIA, J. 1986. Carte géologique de la région des Gorges de l'Areuse. In: Les Gorges de l'Areuse. *A la Baconnière, Neuchâtel,* 66-67.

MEIA, J. 1987. Derniers regards sur la Mine d'asphalte de La Presta (Val-de-Travers, Jura neuchâtelois, Suisse). *Bull. Ver. Schweizer. Petrol.-Geol. u. Ing.* 53, 47-56.

MEIA, J. 1992. Géologie des tunnels de la Béroche et de la Vue des Alpes. *Publications de la Société Suisse de Mécanique des Sols et des Roches* 126, 1-8.

MITCHUM, R.M. & VAIL, P.R. 1977. Seismic stratigraphic interpretation procedure. In: PAYTON, C.E. (ed.). Seismic stratigraphy-applications to hydrocarbon exploration. Memoir 26, 135-144. *Amer. Ass. Petrol. Geol.*

MITRA, S. 1986. Duplex Structures and Imbricate Thrust Systems: Geometry, Structural Position, and Hydrocarbon Potential. *Amer. Ass. Petrol. Geol. Bull.* 70/9, 1087-1112.

MITRA, S. 1992. Balanced Structural Interpretations in Fold and Thrust Belts. In: MITRA, S. & FISCHER, G.W. (eds.). Structural Geology of Fold and Thrust Belts. 53-77. *Johns Hopkins University Press, Baltimore.*

MITRA, S. & NAMSON, J. 1989. Equal-area balancing. *Amer. J. Sci.* 289, 563-599.

MORNOD, L. 1970. Rapport hydrogéologique sur une campagne de recherches par forages au Val de Ruz, dans le secteur des Prés Royer. *Centre d'hydrogéologie souterraine, Bulle.*

MOSAR, J., STAMPFLI, G.M. & GIROD, F. 1996. Western Préalpes Médianes Romandes: timing and structure. A review. *Eclogae geol. Helv.* 89, 389-425.

MOSAR, J. & SUPPE, J. 1992. Role of shear in fault-propagation folding. In: MCCLAY, K.R. (ed.). Thrust tectonics. 123-132. *Chapman & Hall. London.*

MOUCHET, P. 1995. Le Kimméridgien du Jura Central. Microfaciès, minéralogie et interprétation séquentielle. *Thèse de Doctorat, Université de Neuchâtel.*

MUHLETHALER, C. 1930. Les Verrières - La Chaux. Atlas géol. Suisse, feuille N°2. *Commission Géologique Suisse. Berne.*

MÜLLER, J. 1958. Etude géologique de l'Anticlinal Creux du Van-Montagne de Boudry. *Travail de Diplôme, Université de Neuchâtel.*

MÜLLER, M., NIEBERDING, F. & WANNINGER, A. 1988. Tectonic style and pressure distribution at the northern margin of the Alps between Lake Constance and the River Inn. *Geol. Rdsch.* 77, 787-796.

MURALT, R., VUATAZ, F.D., SCHÖNBORN, G., SOMMARUGA, A. & JENNY, J. 1997. Intégration des méthodes hydrochimiques, géologiques et géophysiques pour la prospection d'une nouvelle ressource en eau thermale. Cas d'Yverdon-les-Bains, pied du Jura. *Eclogae geol. Helv.* 90.

NAEF, H. & DIEBOLD, P. 1990. Interprétation géologique de la sismique réflexion. *Cédra informe* 2, 16-28.

NAEF, H. & DIEBOLD, P. & SCHLANKE, S. 1985. Sedimentation und Tektonik im Tertiär der Nordschweiz. Technischer Bericht N°. NTB 85-14. *NAGRA (CEDRA), Wettingen.*

NEUGEBAUER, H.J., BRÖTZ, R. & RYBACH, L. 1980. Recent crustal uplift and the present stress field in the Alps along the Swiss Geotraverse Basel Chiasso. *Eclogae geol. Helv.* 73, 489-500.

NOACK, T. 1989. Computergestützte Modellierung geologischer Strukturen im östlichen Jura; Konstruktion balancierter Profile, Gravimetrie, Refraktionsseismik. *Thèse de Doctorat, Université de Bâle.*

NOACK, T. 1995. Thrust development in the eastern Jura Mountains related to pre-existing extensional structures. *Tectonophysics* 252, 419-431.

NÜESCH, R. 1991. Das Mechanische Verhalten von Opalinuston. *Mitt. geol. Inst. ETH u. Univ. Zürich* 293.

OLGAARD, D.L. & DELL'ANGELO, L.N. 1991. Rheology of fine-grained anhydrite at high temperatures. *Terra Abstracts* 3, 81.

PAVONI, N. 1961. Faltung durch Horizontalverschiebung. *Eclogae geol. Helv.* 54, 515-534.

PAVONI, N. 1984. Seismotektonik Nordschweiz. Technischer Bericht N°. NTB 84-45. 1-45. *NAGRA (CEDRA), Wettingen.*

PERSOZ, F. 1982. Inventaire minéralogique, diagenèse des argiles et minéralostratigraphie des séries jurassiques et crétacées inférieures du Plateau suisse et de la bordure Sud-Est du Jura entre les lacs d'Annecy et de Constance. *Matér. Carte Géol. Suisse* [n.s.] 155. *Berne.*

PERSOZ, F. & REMANE, J. 1973. Evolution des milieux de dépôt au Dogger supérieur et au Malm dans le Jura neuchâtâlois méridional. *Eclogae geol. Helv.* 66, 41-70.

PFIFFNER, O.A. 1990. Kinematics and intrabed-strain in mesoscopically folded limestone layers: examples from the Jura and the Helvetic Zone of the Alps. *Eclogae geol. Helv.* 83, 585-602.

PFIFFNER, O.A. 1994. Structure and evolution of the Swiss Molasse Basin in the transect Aar Massif-Bern-Central Jura. *Géologie Alpine* 4, 85.

PFIFFNER, O.A., ERARD, P.-F. & STÄUBLE, M. 1997a. Two cross sections through the Swiss Molasse Basin (line E4-E6, W1, W7-W10). In: PFIFFNER, A.O., LEHNER, P., HEITZMANN, P., MÜLLER, S. & STECK, A. (eds.). Deep structure of the Swiss Alps, results of NRP 20. Chapter 8, 64-72. *Birkhäuser Verlag, Basel.*

PFIFFNER, O.A., LEHNER, P., HEITZMANN, P., MÜLLER, S. & STECK, A. (eds.) 1997b. Deep structure of the Swiss Alps, results of NRP 20. *Birkhäuser Verlag, Basel.* 448 pp.

PHILIPPE, Y. 1994. Transfer Zone in the Southern Jura Thrust Belt (eastern France): Geometry, development and comparison with analogue modelling experiments. In: MASCLE, A. (ed.). Hydrocarbon and petroleum geology of France. 4, 327-346. *Europ. Ass. Petrol. Geol. Spec. Publ.*

PHILIPPE, Y. 1995. Rampes latérales et zones de transfert dans les chaînes plissées: géométrie, conditions de formation et pièges structuraux associés. *Thèse de Doctorat. Université de Chambéry (Savoie, France).*

PLESSMANN, W. 1972. Horizontal-Stylolithen im französisch-schweizerischen Tafel-und Faltenjura und ihre Einpassung in den regionalen Rahmen. *Geol. Rdsch.* 61, 332-347.

POMEROL, C. 1975. Stratigraphie et Paléogéographie. Ere mésozoïque. *Doin. Paris.* 383 pp.

PRICE, R.A. 1973. Large-scale gravitational flow of supracrustal rocks, southern Canadian Rockies. In: DE JONG, K.A. & SCHOLTEN, R. (eds.). Gravity and tectonics (Ed. by. *Wiley and Sons. New York.* 491-502.

RAMBERG, H. 1964. Selective Buckling of Composite Layers with Contrasted Rheological Properties: a Theory for Simultaneous Formation of Several Orders of Folds. *Tectonophysics* 1, 307-341.

RAMSAY, J.G. 1967. Folding and Fracturing of Rocks. *Mc Graw-Hill, New York,* 568 pp.

REID, H.F., DAVIS, W.M., LAWSON, A.C. & RANSOME, F.L. 1913: Report of the Committee on the nomenclature of faults. *Geol. Soc. Amer., Bull.* 24, 163-186.

REMANE, J. 1982. Die Kreide des Neuenburger Juras (Exkursion D am 15. April 1982). *Jber. Mitt. oberrh. geol. Ver., N.F.* 64, 47-59.

RENEVIER, E. 1854. Carte géologique du Mont de Chamblon. *Bull. Soc. Vaud. Sc. Nat.* 8.

RENEVIER, E. 1894. Chronologie géologique. Congrès géologique international de Zurich. *Imprimerie Georges Bridd. Lausanne.* 523-695.

REYER, E. 1892. Ursachen der Deformationen und der Gebirgsbildung. *Wilhelm Englemann, Leipzig*, 40 pp.

RICH, J.L. 1934. Mechanics of low-angle overthrust faulting illustrated by Cumberland thrust block, Virginia, Kentucky and Tennessee. *Amer. Ass. Petrol. Geol. Bull.* 18, 1584-1596.

RICKENBACH, E. 1925. Description géologique du territoire compris dans les feuilles N°278 et N°280 de l'atlas topographique de Siegfried, savoir du Val-de-Travers, entre Fleurier et Travers, du cirque de Saint-Suplice et de la vallée de la Brévine. *Bull. Soc. neuchâtel. Sci. nat.* 50, 1-76.

RIGASSI, D.A. 1962. A propos de la tectonique du Risoux (Jura vaudois et franc-comtois). *Bull. Ver. Schweizer. Petrol.-Geol. u. Ing.* 29, 39-50.

RIGASSI, D.A. 1977. Genèse tectonique du Jura: une nouvelle hypothèse. *Paleolab News* 2, 1-27.

RIGASSI, D.A. & JACCARD, M. 1995. Ste-Croix. Atlas géol. Suisse, feuille N°95. *Service hydrologique et géologique national, Berne.*

RITTER, M.G. 1888. Lac glaciaire du Champ-du-Moulin. *Bull. Soc. neuchâtel. Sci. nat. 16*, 93-100.

RODGERS, J. 1990. Fold-and-thrust belts in sedimentary rocks. Part 1: typical examples. *Amer. J. Sci.* 290, 321-359.

ROLLIER, L. & FAVRE, J. 1910. Carte géologique des environs du Locle et de La Chaux-de-Fonds. Carte géol. spéc., feuille N°59. *Commission Géologique Suisse. Berne.*

RUTTER, E.H. 1974. The influence of temperature, strain rate and interstitial water in the experimental deformation of calcite rocks. *Tectonophysics* 22, 311-334.

SCHAER, J.-P. 1956. Carte géologique de l'anticlinal de Chaumont. Non-publié. *Déposé à l'Institut de Géologie de l'Université de Neuchâtel, Suisse.*

SCHAER, J.-P. 1994. La seconde Académie: 1866-1909. In: UNIVERSITÉ DE NEUCHÂTEL (ed.). Histoire de l'Université de Neuchâtel. Vol. 2, 381-442. *Editions Gilles Attinger, Hauterive.*

SCHAER, J.-P., BURKHARD, M., TSCHANZ, X., GUBLER, E. & MATHIER, J.-F. 1990. Morphologie, contraintes et déformations dans le Jura central externe. *Bull. Soc. neuchâtel. Sci. nat.* 113, 1-12.

SCHAER, J.-P., REIMER, G.M. & WAGNER, G.A. 1975. Actual and ancient uplift rate in the Gotthard region, Swiss Alps: a comparison between precise levelling and fission track apatite age. *Tectonophysics* 29, 293-300.

SCHÄR, U., RYNIKER, K., SCHMID, K., HÄFELI, C. & RUTSCH, R.F. 1971. Bieler See. Atlas géol. Suisse, feuille N°60. *Commission Géologique Suisse. Berne.*

SCHARDT, H. 1906. Deux coupes générales à travers la chaîne du Jura. *Arch. Sci. Phys. Nat. Genève* XXIII.

SCHARDT, H. 1908. Les causes du plissement et des chevauchements dans le Jura. *Eclogae geol. Helv.* X, 484-488.

SCHARDT, H. & DUBOIS, A. 1903. Description géologique de la région des Gorges de l'Areuse. *Bull. Soc. neuchâtel. Sci. nat.* 30, 195-352.

SCHEGG, R., LEU, W., CORNFORD, C. & ALLEN, P.A. 1997. New coalification profiles in the Molasse Basin of Western Switzerland: Implications for the thermal and geodynamic evolution of the Alpine Foreland. *Eclogae geol. Helv.* 90, 79-96.

SCHMIDT, C., BRAUN, L., PALTZER, G., MÜHLBERG, M., CHRIST, P. & JACOB, F. 1924. Die Bohrungen von Buix bei Pruntrut und Allschwil bei Basel. *Beitr. Geol. Schweiz, Geotechn. Ser.* 10, 74 pp., *Berne.*

SCHNEGG, P.-A. 1992. Testing a new multichannel controlled-source audio magnetotelluric method (CSAMT) on a borehole. *Eclogae geol. Helv.* 85, 459-470.

SCHNEGG, P.-A., LE QUANG, B.V., FISCHER, G. & WEAWER, J.T. 1983. Audio-Magnetotelluric Study of a Structure with a Reverse Fault. *J. Geomag. Geolelectr.* 35, 653-671.

SCHNEGG, P.-A. & SOMMARUGA, A. 1995. Constraining seismic parameters with a controlled-source audio magnetotelluric method (CSAMT). *Geophys. J. Int.* 122, 152-160.

SCHÖNBORN, G. 1995. Tectonic styles, general transects and transverse zone kinematics of three Alpine fold and thrust belts - a comparison. *Geol. Soc. Amer. Penrose Conf. Abstracts, Calgary.*

SCHUPPLI, H.M. 1950. Erdölgeologische Untersuchungen in der Schweiz, III. Teil. *Beitr. Geol. Schweiz, Geotechn. Ser.* 26, 41 pp., *Berne.*

SCHWAAR, D.C. 1959. Etude géologique de la zone de décrochement de la Tourne. *Travail de Diplôme, Université de Neuchâtel.*

SIGNER, C. & GORIN, G.E. 1995. New geological observations between the Jura and the Alps in the Geneva area, as derived from reflection seismic data. *Eclogae geol. Helv.* 88, 235-265.

SOMMARUGA, A. 1995. Tectonics of the central Jura and the Molasse Basin. New insights from the interpretation of seismic reflection data. *Bull. Soc. neuchâtel. Sci. nat.* 118, 95-108.

SOMMARUGA, A. & BURKHARD, M. 1997. Interpretation of seismic lines across the rhomb shaped Val-de-Ruz Basin (internal folded Jura). In: PFIFFNER, A.O., LEHNER, P., HEITZMANN, P., MÜLLER, S. & STECK, A. (eds.). Deep structure of the Swiss Alps, results of NRP 20. Chapter 7.1, 44-53. *Birkhäuser Verlag, Basel.*

SOPENA, J. & SOULAS, J.P. 1973. Déformations de calcaires sous contrainte tectonique; essai d'interprétation et de corrélation des résultats pour l'ensemble de la chaîne. *Thèse de doctorat de 3ème cycle, Université de Franche-Comté.*

STAUB, R. 1924. Der Bau der Alpen. *Matér. Carte Géol. Suisse* [n.s.] 52. *Berne.*

SUPPE, J. 1983: Geometry and kinematics of fault-bend folding. *Amer. J. Sci.* 283, 684-721.

SUPPE, J. 1985: Principles of Structural geology. *Prentice-Hall Inc, Englewood Cliffs, New Jersey*, 537 pp.

SUPPE, J. & MEDWEDEFF, D.A. 1990. Geometry and kinematics of fault-propagation folding. *Eclogae geol. Helv.* 83, 409-454.

SUTER, H. & LÜTHI, E. 1969. Val de Ruz. Atlas géol. Suisse, feuille N°51. Notice explicative. *Commission Géologique Suisse. Berne.*

SWISSPETROL 1992. Seismic Lageplan Schweiz. *Bull. Ver. Schweizer. Petrol.-Geol. u. Ing.* 59, plate.

SYLVESTER, A.G. 1988. Strike-slip faults. *Geol. Soc. Amer., Bull.* 100, 1666-1703.

TAYLOR, J.C.M. 1993. Pseudo-reefs beneath Zechstein salt on the northern flank of the Mid North Sea High. In: Petroleum Geology of Northwest Europe: *Proccedings of the 4th Conference.* 749-757.

THIEBAUD, C.-E. 1936. Carte géologique 1: 25'000 de la feuille N°281, Travers, de l'atlas topographique de Siegfried. Unpublished. *Deposited at the Service hydrologique et géologique national, Berne, Suisse.*

THURMANN, J. 1836a. Sur l'histoire des connaissances géologiques relatives à la chaîne du Jura. *Actes Soc. Helv. Sci. Nat., Soleure,* 31-35.

THURMANN, J. 1836b. Lettre à M.E. de Beaumont. *Bull. Soc. géol. France* 7, 207-211.

THURMANN, J. 1856. Essai d'orographie jurassique. Oeuvre posthume. *Mém. Inst. genev.* 4, 8-18 et 19-22, *Genève.*

TRÜMPY, R. 1980. Geology of Switzerland - a guide-book. Part A: An outline of the geology of Switzerland. Part B: Geological excursions. *Wepf, Basel, New York,* 334 pp.

TRUSHEIM, F. 1957. Über Halokinese und ihre Bedeutung für die strukturelle Entwicklung Norddeutschlands. *Z. dtsch. geol. Ges.* 109, 111-151.

TRUSHEIM, F. 1960. Mechanism of salt migration in northern Germany. *Bull. amer. Assoc. Petroleum Geol.* 44, 1519-1540.

TSCHANZ, X. 1990. Analyse de la déformation du Jura central entre Neuchâtel (Suisse) et Besançon (France). *Eclogae geol. Helv.* 83, 543-558.

TSCHANZ, X. & SOMMARUGA, A. 1993. Deformation associated with folding above frontal and oblique ramps around the rhomb shaped Val-de-Ruz basin (Jura Mountains). *Ann. Tect.* 7, 53-70.

TWISS, R.J. & MOORES, E.M. 1992. Structural Geology. W.H. *Freeman and Company, New York,* 531 pp.

VANN, I.R., GRAHAM, R.H. & HAYWARD, A.B. 1986. The structure of mountain fronts. *J. Struct. Geol.* 8, 215-227.

VENDEVILLE, B.C. & JACKSON, M.P.A. 1992. The rise of diapirs during thin-skinned extension. *Marine Petroleum Geol.* 9, 354-371.

VERNET, J.-P. 1972. Morges. Atlas géol. Suisse, feuille N°62. *Commission Géologique Suisse. Berne.*

VOLLMAYR, T. 1992. Strukturelle Ergebnisse der Kohlenwasserstoffexploration im Gebiet von Thun, Schweiz. *Eclogae geol. Helv.* 85, 531-539.

VOLLMAYR, T. & WENDT, A. 1987. Die Erdgasbohrung Entlebuch 1, ein Tiefenaufschluss am Alpennordrand. *Bull. Ver. Schweizer. Petrol.-Geol. u. Ing.* 53, 67-79.

VON BUCH, L. 1867. Gesammelte Schriften. *Georg Reimer, Berlin,* 739 pp.

WEBER, H.P., SATTEL, G. & SPRECHER, C. 1986. Sondierbohrungen Weiach, Riniken, Schafisheim, Kaisten, Leuggern - Geophysikalische Daten, Texband. (Technischer Bericht N°. NTB 85-50). *NAGRA (CEDRA), Wettingen.*

WEGMANN, E. 1963. Le Jura plissé dans la perspective des études sur le comportement des socles. In: Livre Mém. Prof. P. Fallot (*Ed. by Soc. Géol. France*). Mém. hors série 1, 99-104., *Paris.*

WEIDMANN, M. 1988. Lausanne. Atlas géol. Suisse, feuille N°85. *Service hydrologique et géologique national. Berne.*

WEIDMANN, M. 1992. Châtel-St-Denis. Atlas géol. Suisse, feuille N°92. *Service hydrologique et géologique national. Berne.*

WILDI, W., BLONDEL, T., CHAROLLAIS, J., JAQUET, J. & WERNLI, R. 1991. Tectonique en rampe latérale à la terminaison occidentale de la Haute Chaîne du Jura. *Eclogae geol. Helv.* 84, 265-277.

WILDI, W. & HUGGENBERGER, P. 1993. Reconstitution de la plate-forme européenne anté-orogénique de la Bresse aux Chaînes subalpines: éléments de cinématique alpine (France et Suisse occidentale). *Eclogae geol. Helv.* 86, 47-64.

WILTSCHKO, D.V. 1979. A mechanical model for thrust sheet deformation at a ramp. *J. Geophys. Res.* 84, 1091-1104.

WINNOCK, E. 1961. Résultats géologiques du forage Risoux 1. *Bull. Ver. Schweizer. Petrol.-Geol. u. Ing.* 28, 17-26.

WINNOCK, E., BARTHE, A. & GOTTIS, C. 1967. Résultats des forages pétroliers français effectués dans la région voisine de la frontière suisse. *Bull. Ver. Schweizer. Petrol.-Geol. u. Ing.* 33, 7-22.

WODDCOCK, N.H. 1986. The role of strike-slip fault systems at plate boundaries. *R. Soc. London Phil. Trans.* 317, 13-29.

WOODWARD, N., BOYER, S.E. & SUPPE, J. 1989. Balanced geological cross-sections: an essential technique in geological research and exploration. *Amer. Geophys. Union., Washington D.C.*

ZIEGLER, P.A. 1982. Geological Atlas of Western and Central Europe. *Shell Internationale Petroleum Maatschappij B.V., The Hague,* 130 pp.

ZIEGLER, P.A. 1988. Evolution of the Arctic-North Atlantic and the Western Tethys. *Amer. Ass. Petrol. Geol.*, Mem. 43, 1-198.

ZIEGLER, P.A. 1990. Geological Atlas of Western and Central Europe. *Shell Internationale Petroleum Maatschappij B.V., Mijdrecht, Netherlands,* 239 pp.

ZIMMERMANN, M.A., KÜBLER, B., OERTLI, H.J., FRAUTSCHI, J.-M., MONNIER, F., DERES, F. & MONBARON, M. 1976. "Molasse d'eau douce inféricure" du Plateau suisse. Subdivision par l'indice de détritisme. Essai de datation par nannofossiles. *Bull. Cent. Rech. Explor.-Prod. Elf-Aquitaine* 10, 585-625.

ZWEIDLER, D. 1985. Genèse des gisements d'asphalte de la Pierre Jaune de Neuchâtel et des calcaires urgoniens du Jura (Jura neuchâtelois et nord-vaudois, Suisse). *Thèse de Doctorat, Université de Neuchâtel.*

PANELS/PANNEAUX:

Remark: The reader will find here the captions of the Panels, which are fold outs of this Memoir.
Remarque: Le lecteur trouvera ci-dessous la légende des Panneaux qui se trouvent hors-texte.

Panel 1: Line drawings from migrated seismic lines of the Jura Mountains (Neuchâtel, Switzerland). Eastern dip lines. Sections 1, 3, 5 and 7 in TWT time.
Illustration des réflecteurs caractéristiques des profils sismiques (migrés) transversaux du Jura neuchâtelois oriental (Suisse). Profils 1, 3, 5 et 7 en temps double.

Panel 2: Line drawings from migrated seismic lines of the Jura Mountains (Neuchâtel, Vaud, Switzerland). Western dip lines. Sections 9, 11, 13, 15, 17 and 19 in TWT time.
Illustration des réflecteurs caractéristiques des profils sismiques (migrés) transversaux du Jura neuchâtelois occidental et vaudois (Suisse). Profils 9, 11, 13, 15 et 19 en temps double.

Panel 3: Line drawings from migrated seismic lines of the Jura Mountains (Neuchâtel, Vaud, Switzerland). Strike lines. Sections 2, 4, 6, 8, 10, 12 and 14 in TWT time.
Illustration des réflecteurs caractéristiques des profils sismiques (migrés) longitudinaux du Jura neuchâtelois et vaudois (Suisse). Profils 2, 4, 6, 8, 10, 12 et 14 en temps double.

Panel 4: Line drawings of the Molasse Basin (Vaud, Switzerland). Strike lines. Sections 22, 26, 28 and 30 in TWT time.
Illustration des réflecteurs caractéristiques des profils sismiques longitudinaux du Bassin molassique (Vaud, Suisse). Profils 22, 26, 28 et 30 en temps double.

Panel 5: Line drawings of the Molasse Basin (Vaud, Switzerland). Dip lines. Sections 27, 29, 37, 39, 43, 47, 45 and 49 in TWT time.
Illustration des réflecteurs caractéristiques des profils sismiques transversaux du Bassin molassique (Vaud, Suisse). Profils 27, 29, 37, 39, 43, 47, 45 et 49 en temps double.

Panel 6: Line drawings of the Molasse Basin (Vaud, Switzerland). N-S lines. Sections 34, 36, 38 and 48 in TWT time.
Illustration des réflecteurs caractéristiques des profils sismiques N-S du Bassin molassique (Vaud, Suisse). Profils 34, 36, 38 et 48 en temps double.

Panel 7: Line drawings of the Molasse Basin, Pontarlier tear fault zone (Vaud, Switzerland). Strike lines. Sections 46, 50 and 54 in TWT time.
Illustration des réflecteurs caractéristiques des profils sismiques longitudinaux de la région de la faille de Pontarlier (Vaud, Suisse). Profils 46, 50 et 54 en temps double.

Panel 8: Line drawings of the Risoux, Jura Mountains (Vaud, Switzerland). Strike lines. Sections 80, 82, 84 and 86 in TWT time.
Illustration des réflecteurs caractéristiques des profils sismiques longitudinaux de la région du Risoux (Jura vaudois, Suisse). Profils 80, 82, 84 et 86 en temps double.

Panel 9: Line drawings of the Risoux, Jura Mountains (Vaud, Switzerland, France). Dip lines. Sections 53, 55, 61, 81, 83, 85, 87, 89, 91, 95 and 111 in TWT time.
Illustration des réflecteurs caractéristiques des profils sismiques transversaux de la région du Risoux (Jura vaudois, Suisse). Profils 53, 55, 61, 81, 83, 85, 87, 89, 91, 95 et 111 en temps double.

Panel 10: Line drawings of the Champagnole-Mouthe area, Jura Mountains (France). Dip lines. Sections 107, 115, 117 in TWT time.
Illustration des réflecteurs caractéristiques des profils sismiques transversaux de la région de Champagnole-Mouthe (Jura français). Profils 107, 115, 117 en temps double.

PLATES/PLANCHES:

Remark: The reader will find here the captions of the Plates, which are fold outs of this Memoir.
Remarque: Le lecteur trouvera ci-dessous la légende des Planches qui se trouvent hors-texte.

Plate 1A: Uninterpreted, migrated seismic Section 1. Dip line, Neuchâtel Jura, Switzerland.
Profil sismique 1 migré, non interprété. Profil transversal, Jura neuchâtelois, Suisse.

Plate 1B: Line drawing of Section 1. Dip line, Neuchâtel Jura, Switzerland.
Illustration des réflecteurs caractéristiques du profil sismique 1. Profil transversal, Jura Neuchâtelois, Suisse.

Plate 2A: Uninterpreted, migrated seismic Section 3. Dip line, Neuchâtel Jura, Switzerland. See also SOMMARUGA & BURKHARD (1997).
Profil sismique 3 migré, non interprété. Profil transversale, Jura neuchâtelois, Suisse. Voir aussi SOMMARUGA & BURKHARD (1997).

Plate 2B: Line drawing of Section 3. Dip line, Neuchâtel Jura, Switzerland.
Illustration des réflecteurs caractéristiques du profil sismique 3. Profil transversal, Jura neuchâtelois, Suisse.

Plate 3A: Uninterpreted, migrated seismic Section 8. Strike line, Neuchâtel Jura, Switzerland. See also SOMMARUGA & BURKHARD (1997).
Profil sismique 8 migré, non interprété. Profil longitudinal, Jura neuchâtelois, Suisse. Voir aussi SOMMARUGA & BURKHARD (1997).

Plate 3B: Line drawing of Section 8. Strike line, Neuchâtel Jura, Switzerland.
Illustration des réflecteurs caractéristiques du profil sismique 8. Profil longitudinal, Jura neuchâtelois, Suisse.

Plate 4A: Uninterpreted, migrated seismic section 11. Dip line, Neuchâtel and Vaud Jura, Switzerland.
Profil sismique 11 migré, non interprété. Profil transversal, Jura neuchâtelois et vaudois, Suisse.

Plate 4B: Line drawing of Section 11. Dip line, Neuchâtel and Vaud Jura, Switzerland.
Illustration des réflecteurs caractéristiques du profil sismique 11. Profil transveral, Jura neuchâtelois et vaudois, Suisse.

Plate 5A: Uninterpreted, migrated seismic Section 14. Strike line, Neuchâtel and Vaud Jura, Switzerland.
Profil sismique 14 migré, non interprété. Profil longitudinal, Jura neuchâtelois et vaudois, Suisse.

Plate 5B: Line drawing of Section 14. Strike line, Neuchâtel and Vaud Jura, Switzerland.
Illustration des réflecteurs caractéristiques du profil sismique 14. Profil longitudinal, Jura neuchâtelois et vaudois, Suisse.

Plate 6A: Uninterpreted, seismic Section 43. Dip line, Molasse Basin, Vaud, Switzerland. See also GORIN *et al.* (1993).
Profil sismique 43 non interprété. Profil transversal, Bassin molassique, Vaud, Suisse. Voir aussi GORIN et al. (1993).

Plate 6B: Line drawing of Section 43. Dip line, Molasse Basin, Vaud, Switzerland.
Illustration des réflecteurs caractéristiques du profil sismique 43. Profil transversal, Bassin molassique, Vaud, Suisse.

Plate 7A: Uninterpreted, seismic Section 45. Dip line, Molasse Basin, Vaud, Switzerland.
Profil sismique 45 non interprété. Profil transversal, Bassin molassique, Vaud, Suisse.

Plate 7B: Line drawing of Section 45. Dip line, Molasse Basin, Vaud, Switzerland.
Illustration des réflecteurs caractéristiques du profil sismique 45. Profil transversal, Bassin molassique, Vaud, Suisse.

Plate 8A: Uninterpreted, seismic Sections 111, 85 and 87. Dip lines, Jura, Vaud, Switzerland and France. Section 111 see also BITTERLI (1972).
Profils sismiques 111, 85 et 87 non interprétés. Profils transversaux, Jura vaudois (Suisse) et France. Pour le profil 111 voir aussi BITTERLI (1972).

Plate 8B: Line drawing of Section 111, 85 and 87. Dip line, Jura, Vaud, Switzerland and France.
Illustration des réflecteurs caractéristiques des profils sismiques 111, 85 et 87. Profil transversal, Jura vaudois (Suisse) et français.

Plate 9: Large scale balanced cross-section and restored section from the external Jura to the Alps (external crystalline massif) across the Molasse Basin. Data of the Moho are from BAUMANN (1994). Modified from BURKHARD & SOMMARUGA (in press).
Coupe équilibrée à grande échelle allant du Jura externe aux Alpes (massifs cristallins externes) en passant par le Bassin molassique. Les données du Moho sont de BAUMANN (1994). Coupe modifiée de BURKHARD & SOMMARUGA (in press).

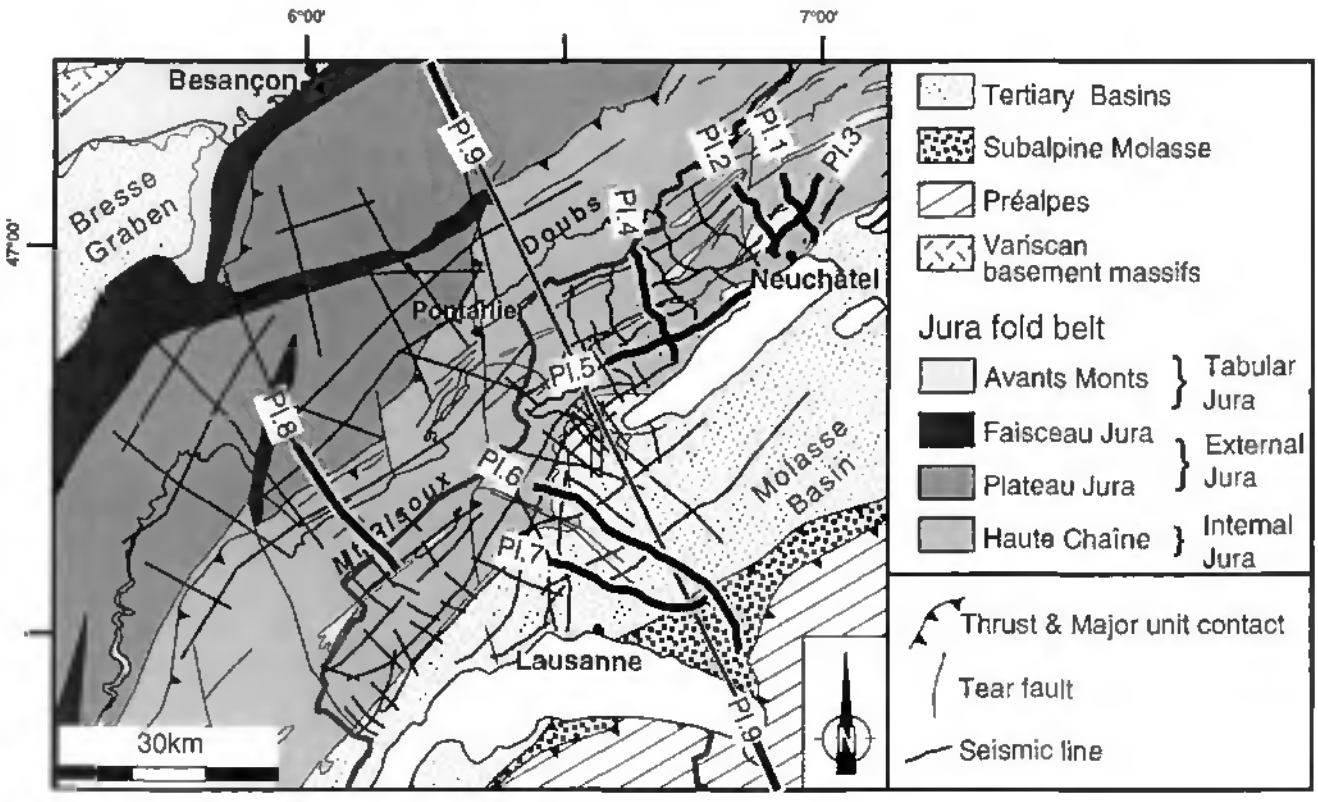

MÉMOIRES DE LA SOCIÉTÉ NEUCHÂTELOISE DES SCIENCES NATURELLES

Tome I, 1835, 199 pp. (épuisé).
Travaux de *L. Agassiz, F.-A. de Montmollin, A. de Montmollin, C. Nicolet, Ch. Allamand, J.F. de Castella, J.-L. Borel, L. Coulon, J.-F. d'Osterwald, H. Ladame.*

Tome II, 1839, 283 pp. (épuisé).
Travaux de *C. Nicolet, Ch.-H. Godet, J.-J. Tschumi, L. Agassiz, C.-L. Bonaparte, M. de Bosset, A. de Montmollin, A.-P. de Candolle.*

Tome III, 1845, 454 pp. (épuisé).
Travaux de *L. Lesquereux, L. Agassiz et C. Vogt, J. Marcou, J.-F. d'Osterwald, A. Guyot.*

Tome IV, 1ère partie, 1859, 206 pp.
E. Desor & A. Gressly - Etudes géologiques sur le Jura neuchâtelois.
Charles Kopp - Des variations du niveau du lac de Neuchâtel pendant les années 1835 à 1856.

Tome IV, 2e partie, 1874, 225 pp.
E. Desor & A. Gressly- Le bel âge du bronze lacustre en Suisse.
P. de Loriol - Description de quelques Astérides du terrain néocomien des environs de Neuchâtel.
P. de Loriol - Description de trois espèces d'Echinides appartenant à la famille des Cédéridées.
M. de Tribolet - Recherches géologiques et paléontologiques dans le Jura neuchâtelois.

Tome V, 1914, 1090 pp.
O. Fuhrmann & E. Mayor - Voyage d'exploration scientifique en Colombie.

Tome VI, 1938, 535 pp.
G. Dubois - Monographie des Strigeida (Trematoda).

Tome VII, 1943, 253 pp. (épuisé).
D. Vouga - Préhistoire du Pays de Neuchâtel des origines aux Francs.

Tome VIII, 1er fascicule, 1952, 121 pp.
V. Aellen - Contribution à l'étude des Chiroptères du Cameroun.

Tome VIII, 2e fascicule, 1953, 141 pp.
G. Dubois - Systématique des Strigeida, complément de la monographie.

Tome IX, 1958, 202 pp.
E. Mayor - Catalogue des Péronosporales, Taphrinales, Erysiphacées, Ustilaginales et Urédinales du canton de Neuchâtel.

Tome X, 1er fascicule, 1968, p. 1-258.
G. Dubois - Synopsis des Strigeidae et des Diplostomatidae (Trematoda).

Tome X, 2e fascicule, 1970, p. 259-727.
G. Dubois - Synopsis des Strigeidae et des Diplostomatidae (Trematoda).

Tome XI, 1989, 322 pp.
J. Remane et al. - Révision de l'étage Hauterivien (région-type et environs, Jura franco-suisse).

Les Mémoires de la S.N.S.N. peuvent être obtenus à l'adresse suivante: **Société neuchâteloise des Sciences naturelles, p. a. Bibliothèque publique et universitaire de la Ville, 2000 Neuchâtel (Suisse).**

PLATE 8B Line drawing
Section 111-87

LOCATION MAP

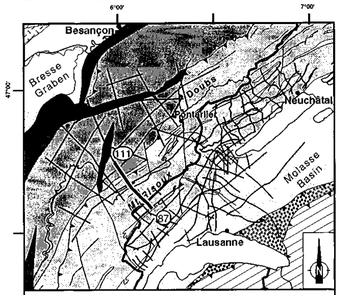

LEGEND

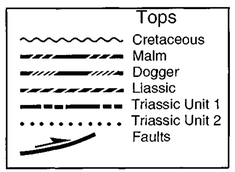

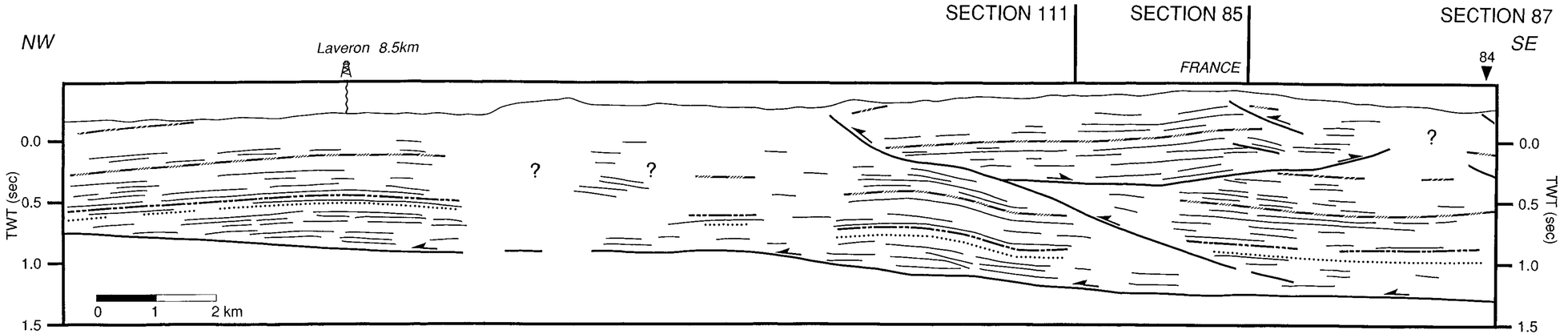

PLATE 8A Seismic line 111-87

LOCATION MAP

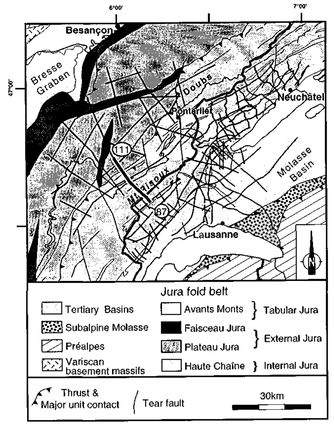

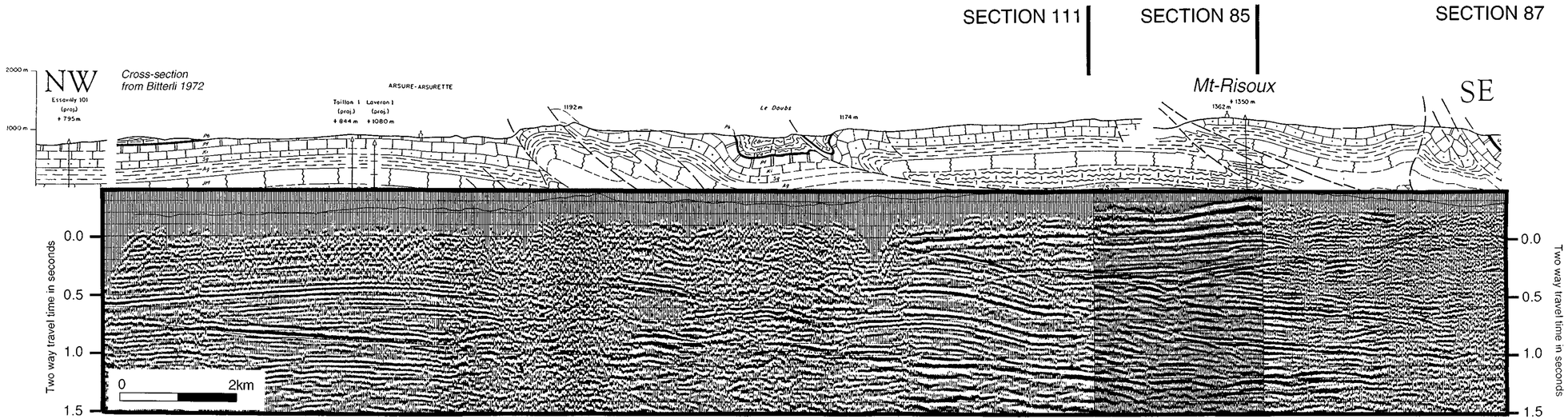

PLATE 7B Line drawing Section 45

LOCATION MAP

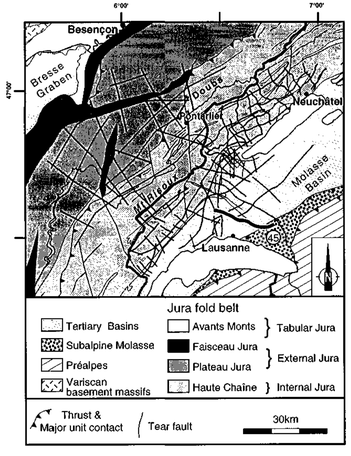

LEGEND

Tops
- Cretaceous
- Malm
- Dogger
- Liassic
- Triassic Unit 1
- Triassic Unit 2
- Faults

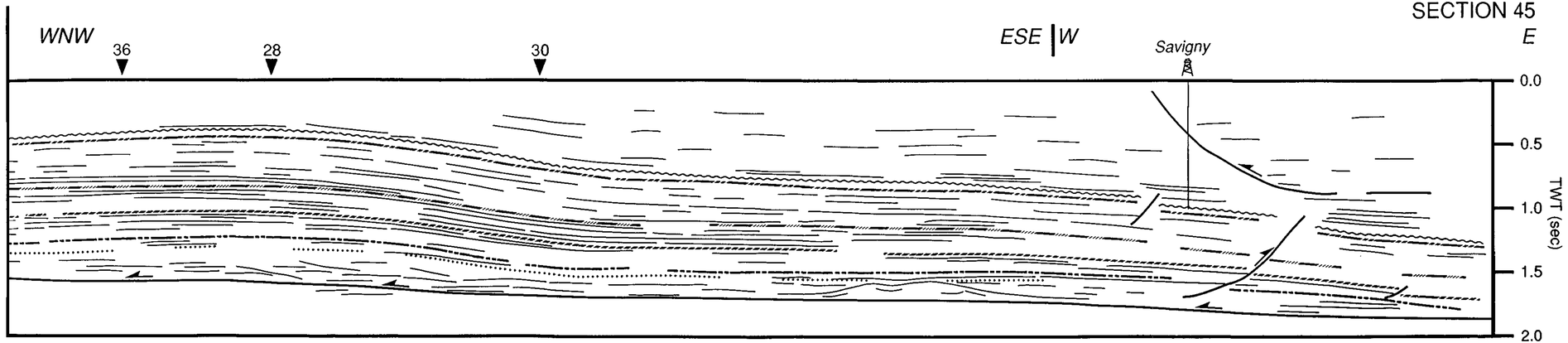

PLATE 7A Seismic Section 45

LOCATION MAP

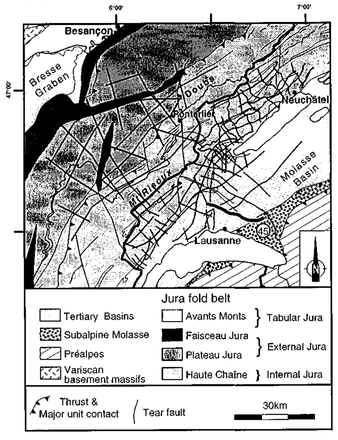

SECTION 45

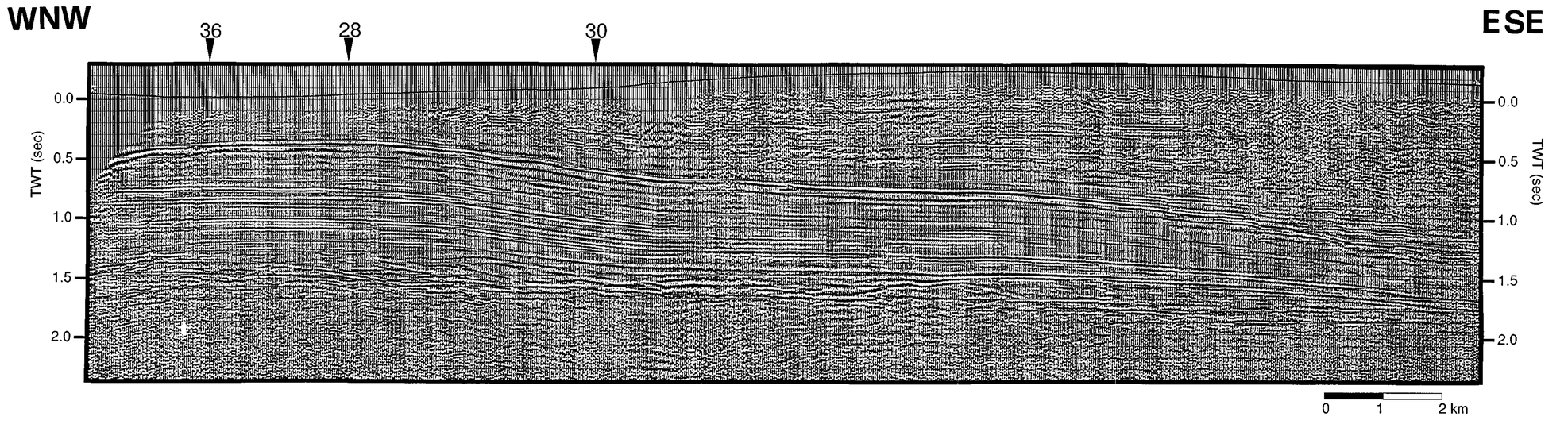

PLATE 6B Line drawing
Section 43

LOCATION MAP

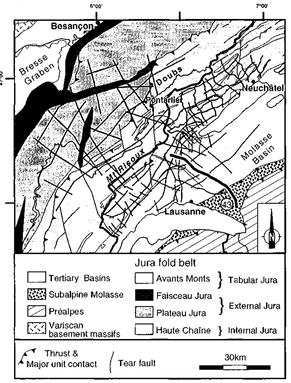

LEGEND

Tops
- Cretaceous
- Malm
- Dogger
- Liassic
- Triassic Unit 1
- Triassic Unit 2
- Faults

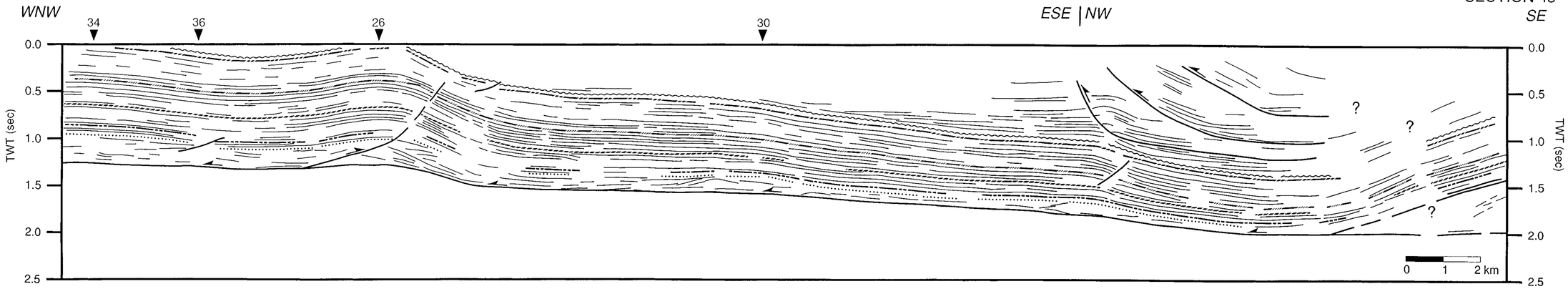

PLATE 6A Seismic Section 43

LOCATION MAP

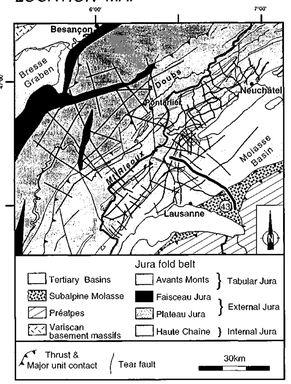

SECTION 43

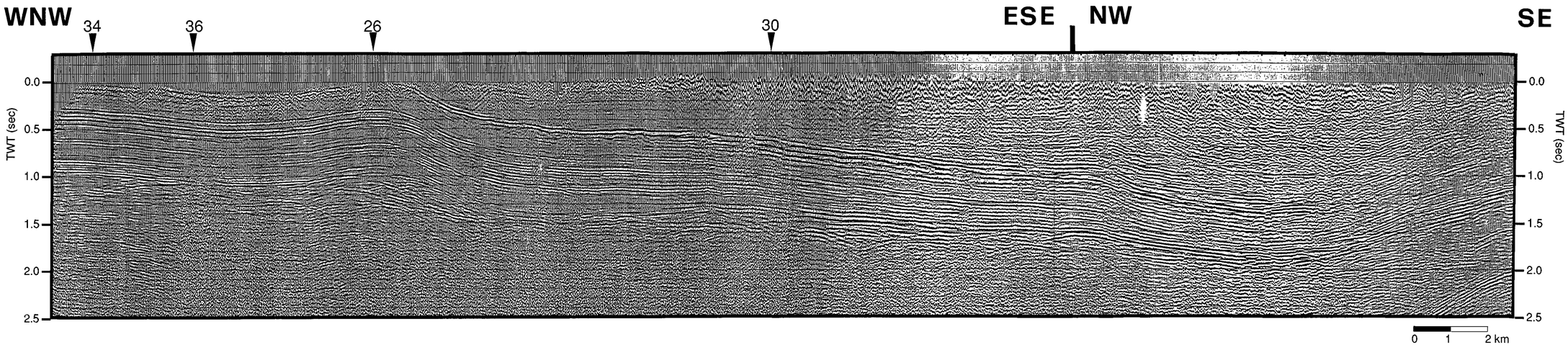

PLATE 5A Seismic Section 14

LOCATION MAP

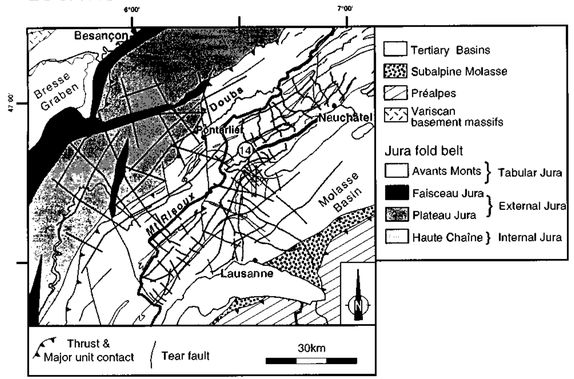

PLATE 5B Line drawing

LEGEND

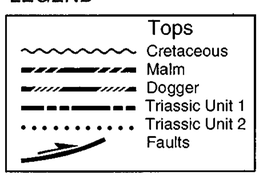

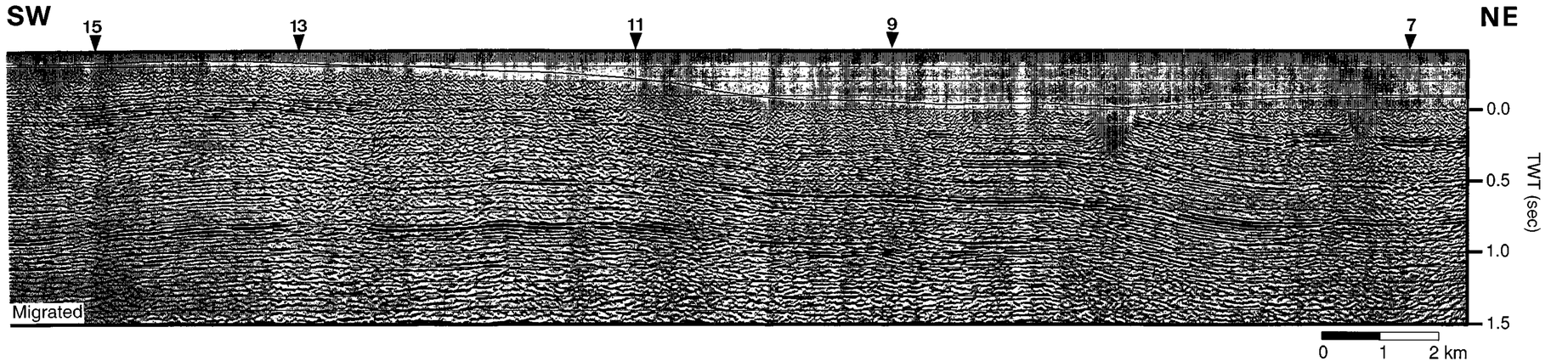

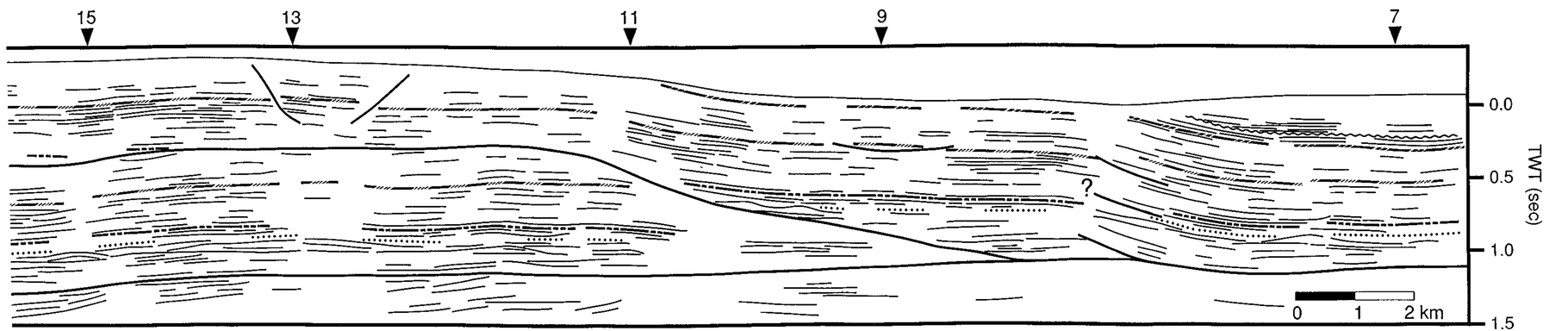

PLATE 4A Seismic Section 11

LOCATION MAP

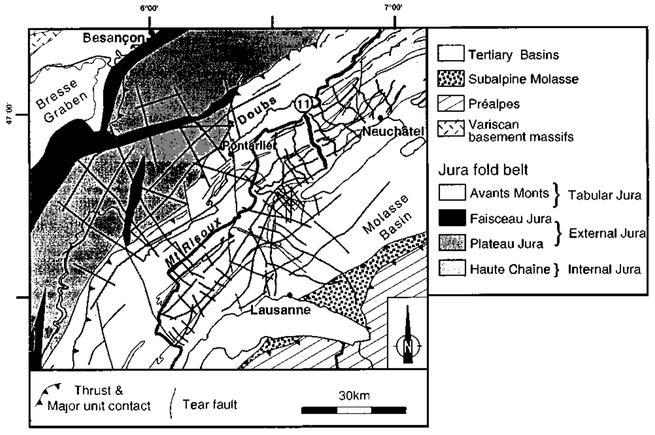

PLATE 4B Line drawing

LEGEND

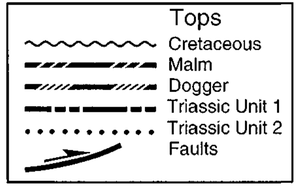

SECTION 11

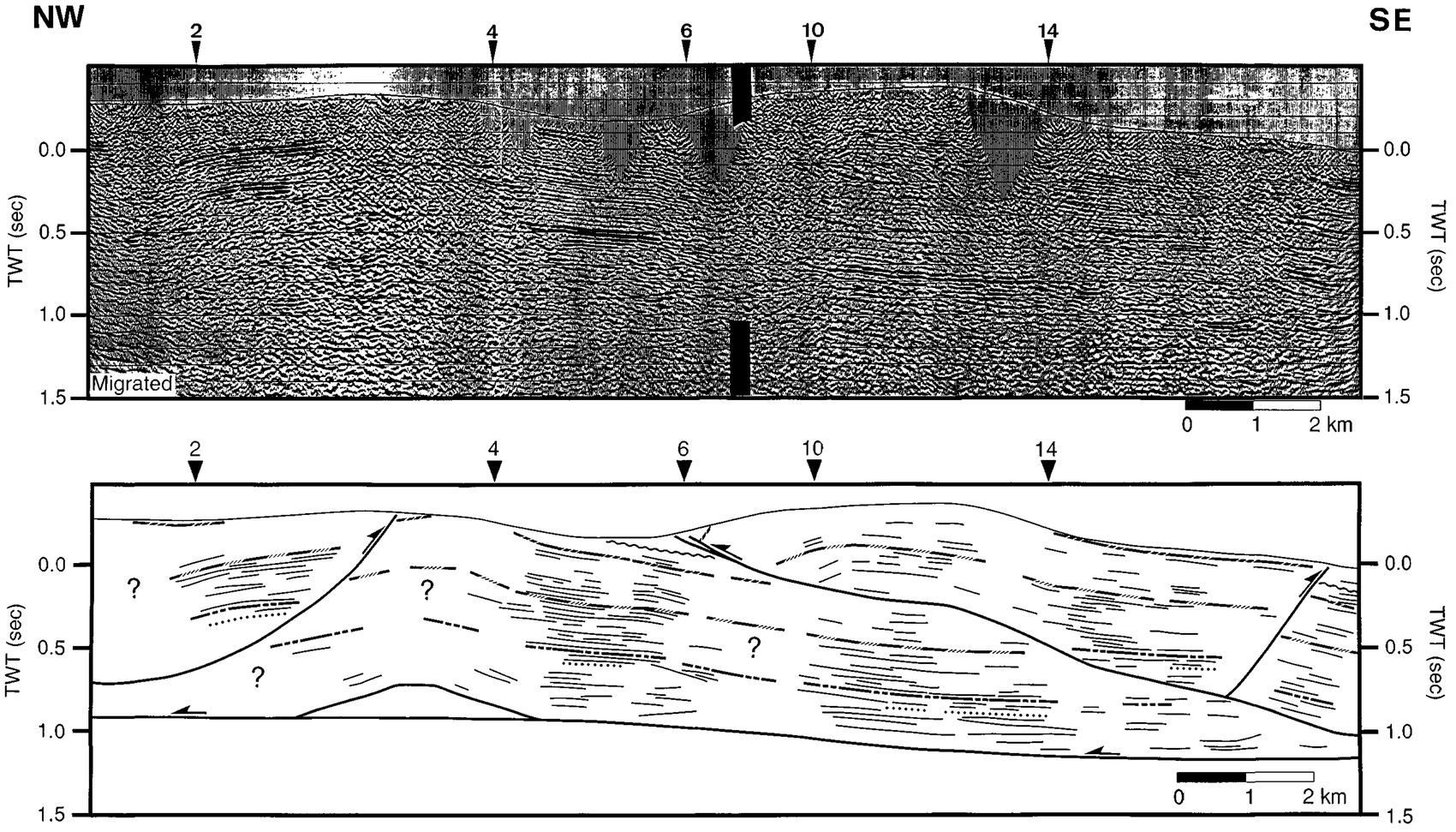

PLATE 3A Seismic Section 8

LOCATION MAP

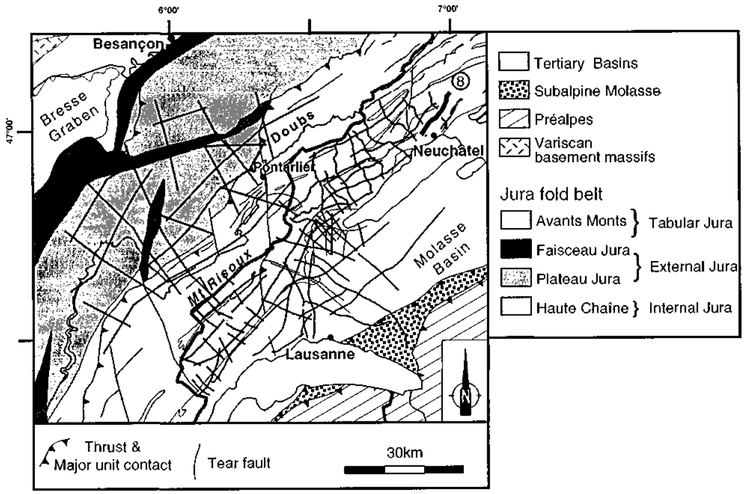

PLATE 3B Line drawing

LEGEND

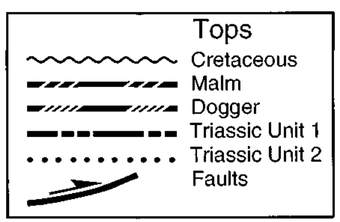

SECTION 8

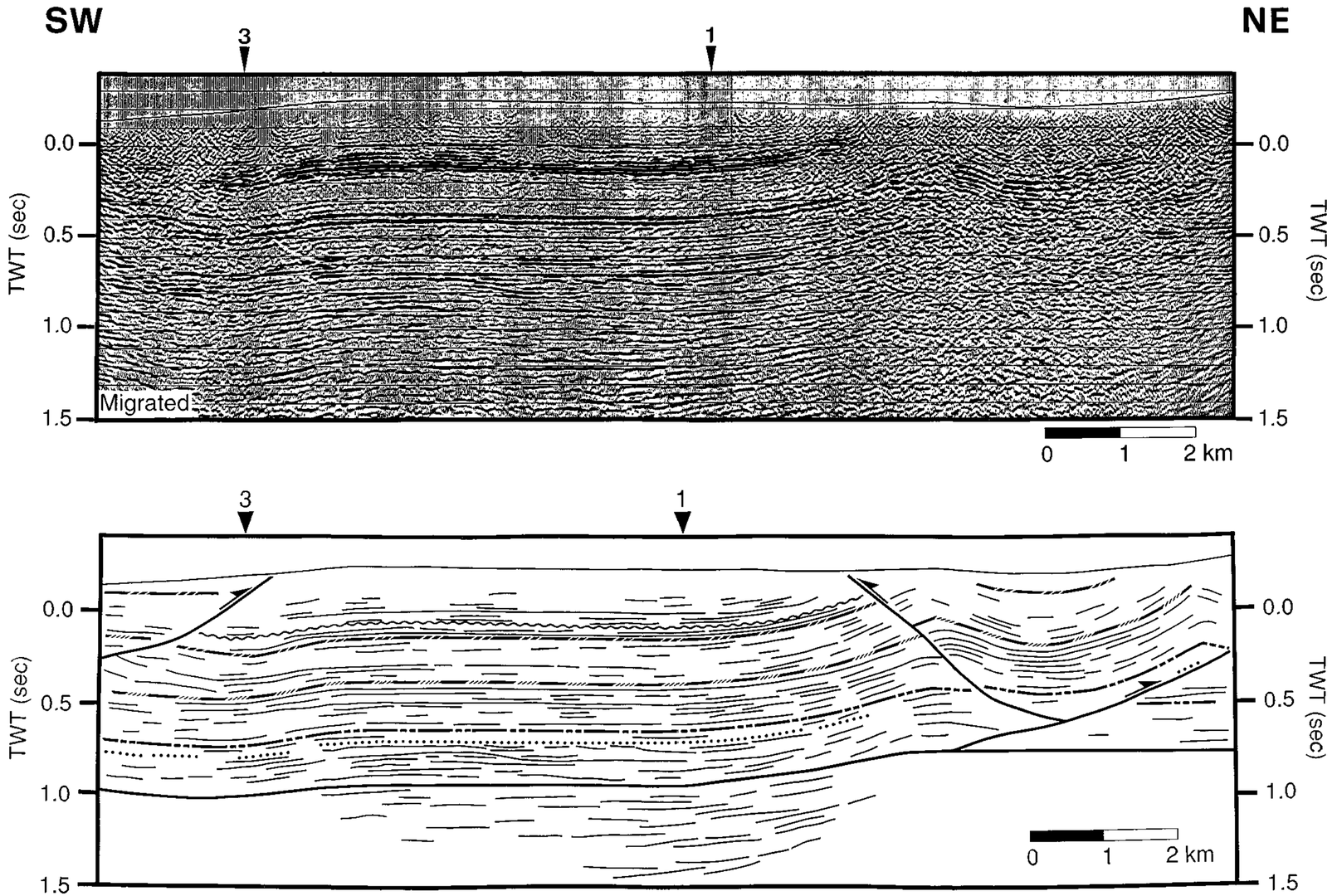

PLATE 2A Seismic Section 3

LOCATION MAP

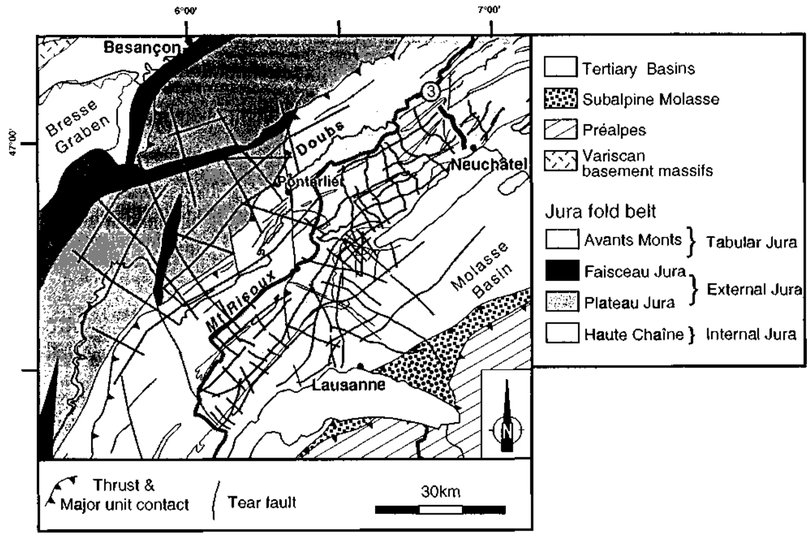

PLATE 2B Line drawing

LEGEND

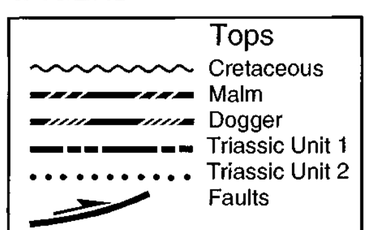

SECTION 3

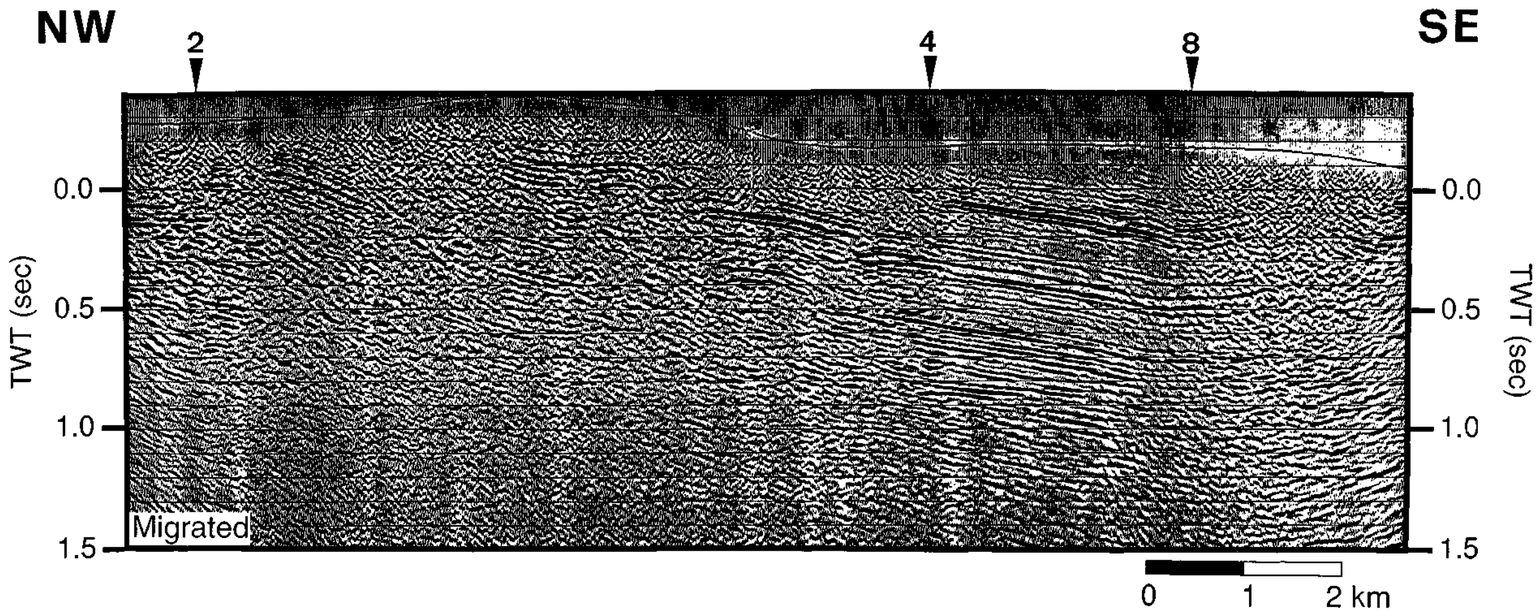

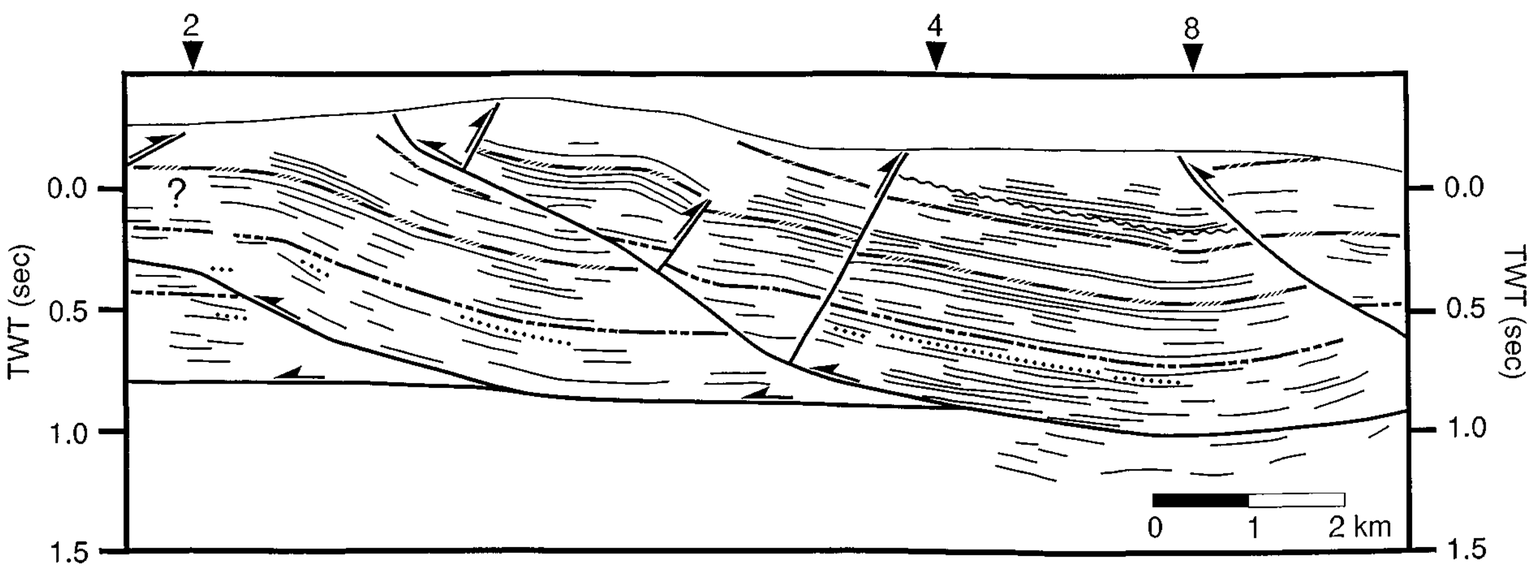

PLATE 1A Seismic Section 1

LOCATION MAP

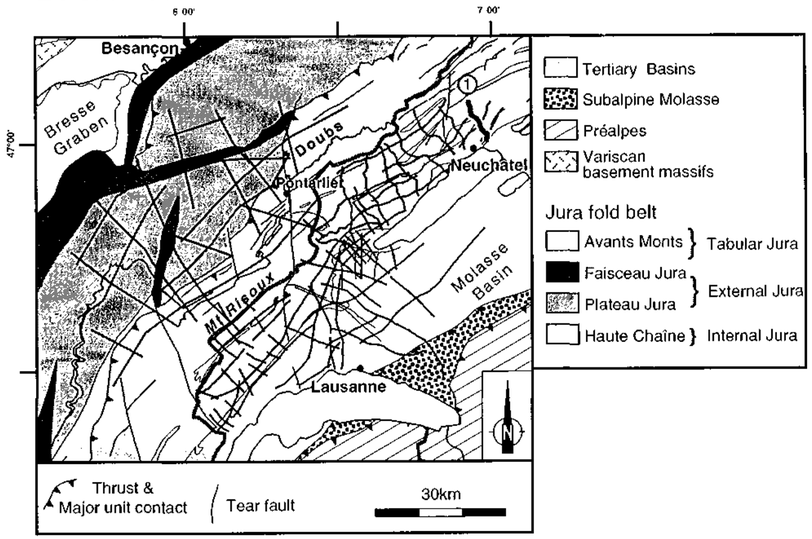

PLATE 1B Line drawing

LEGEND

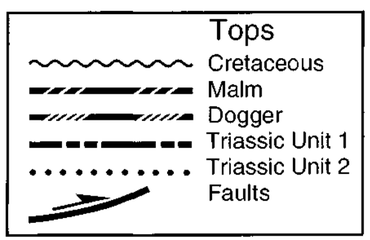

SECTION 1

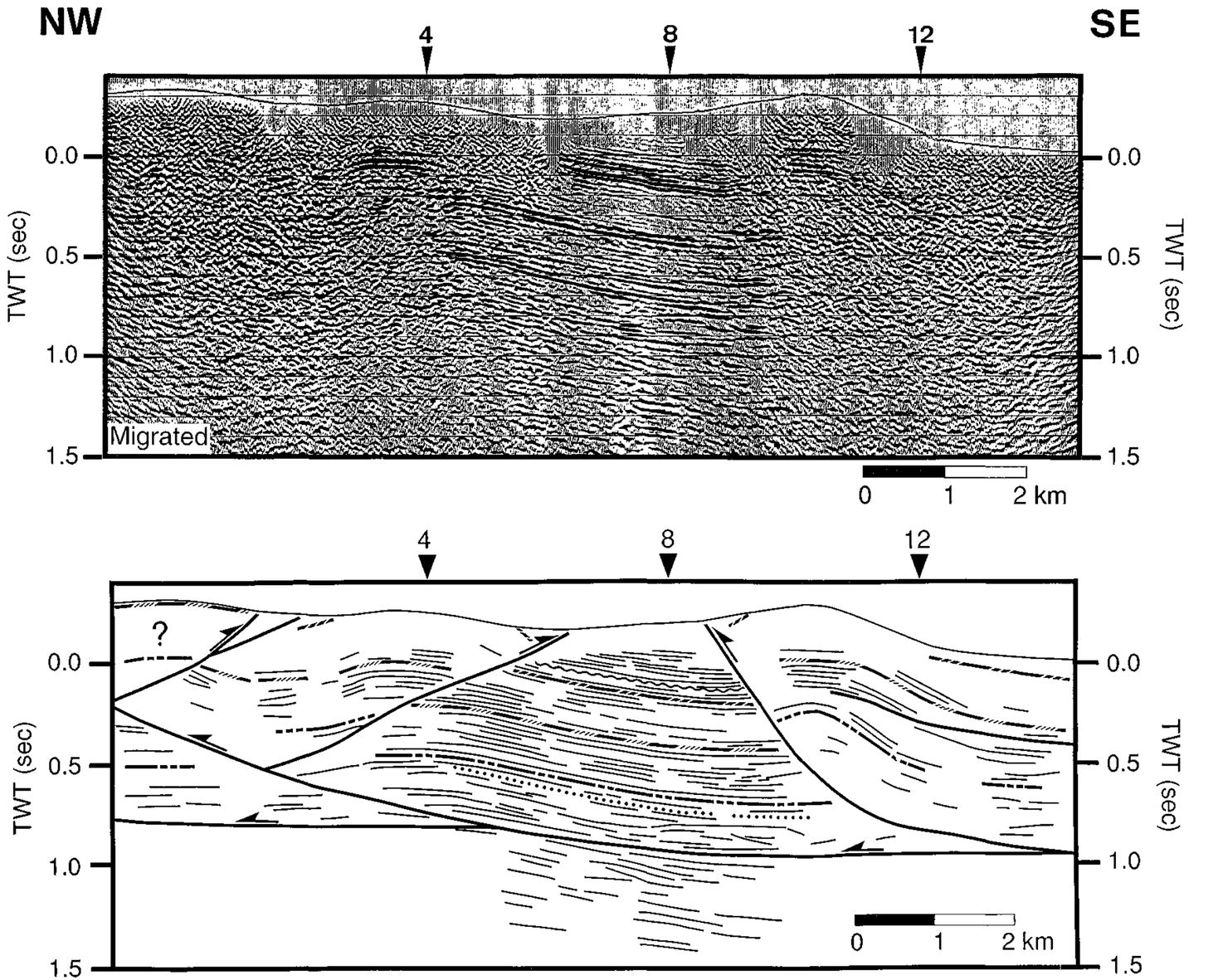

PANEL 10

DIP LINES

CHAMPAGNOLE-MOUTHE, JURA MTS. FRANCE

SECTION 107

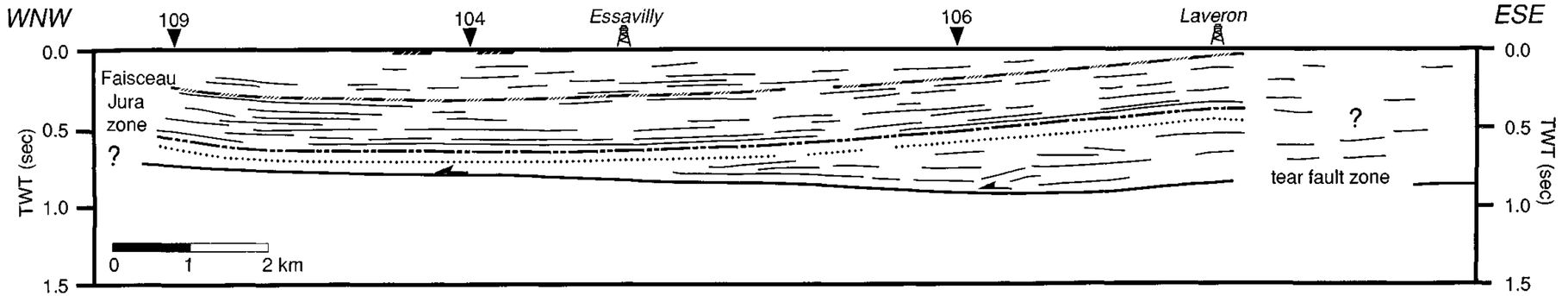

SECTION 115

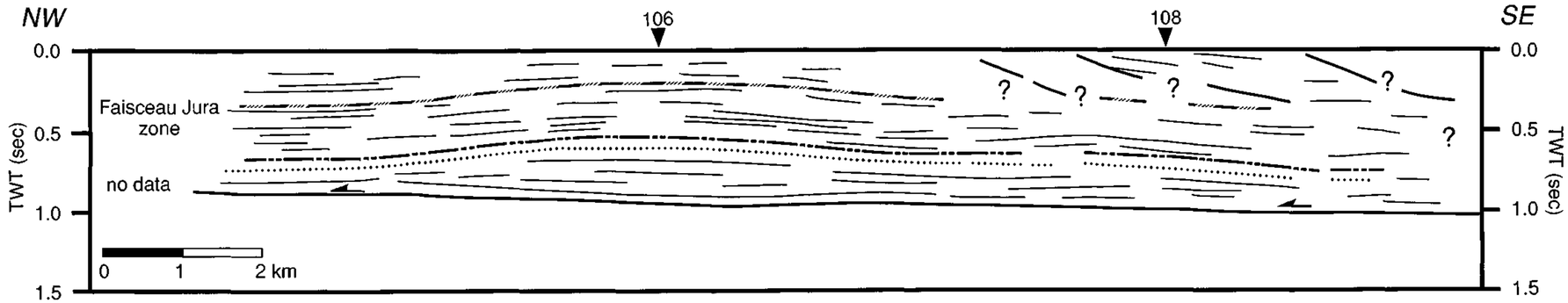

SECTION 117

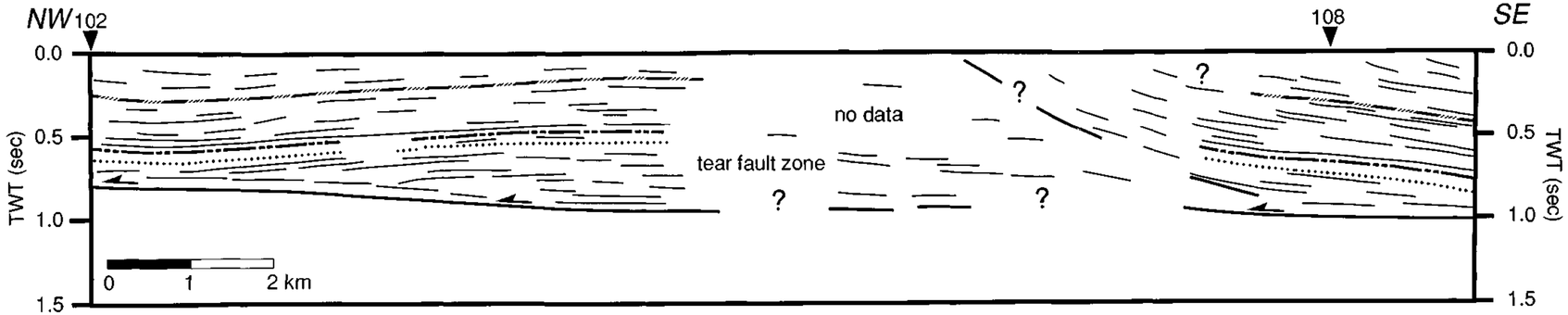

LOCATION MAP

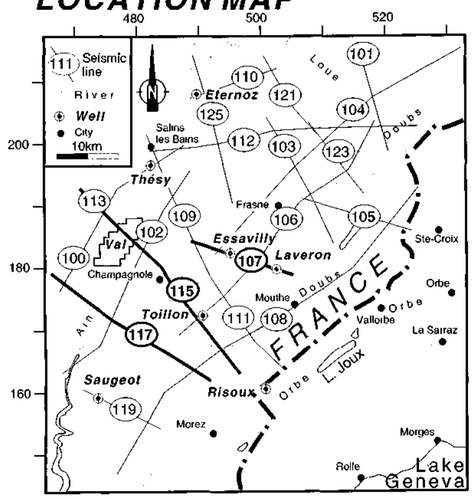

LEGEND

- Tops
- Malm
- Dogger
- Triassic Unit 1
- Triassic Unit 2
- Faults
- well

PANEL 9

DIP LINES

RISOUX, JURA MTS.
(VAUD)
SWITZERLAND
FRANCE

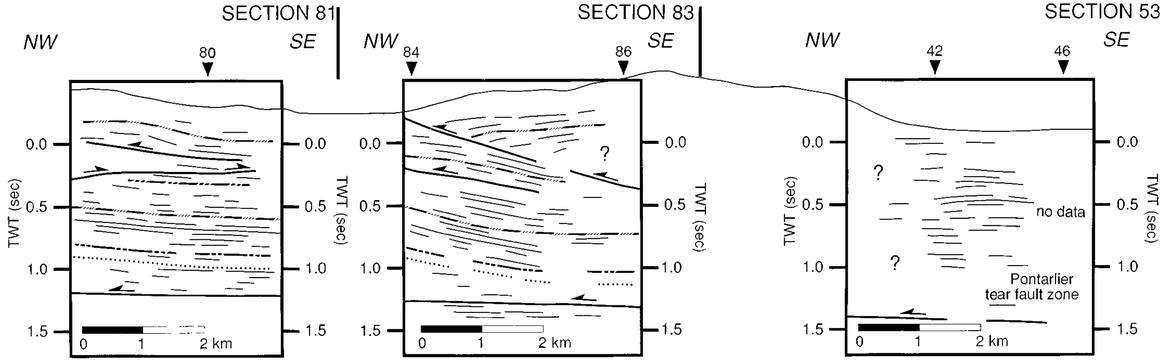

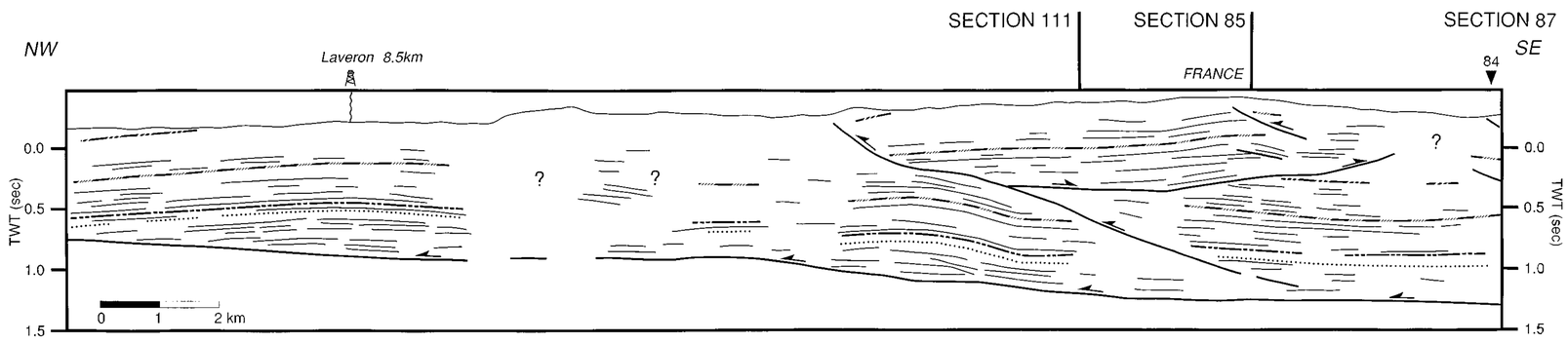

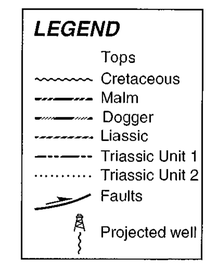

LOCATION MAP

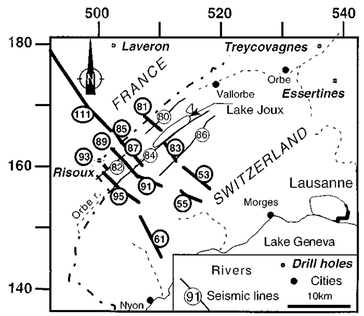

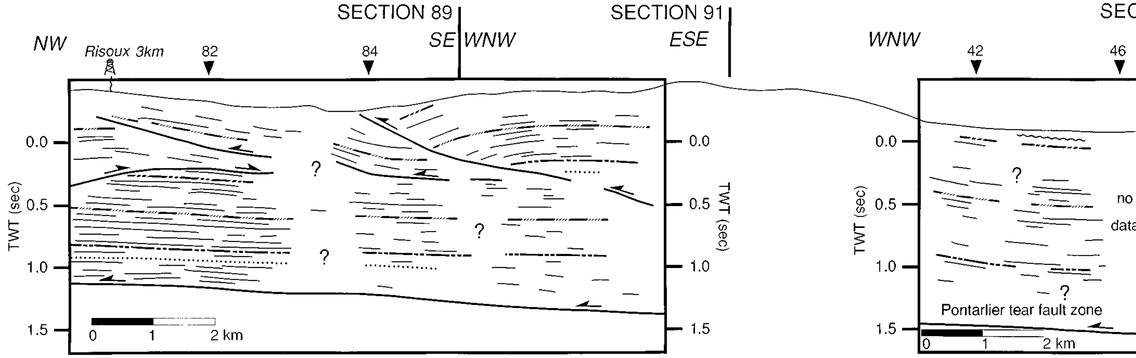

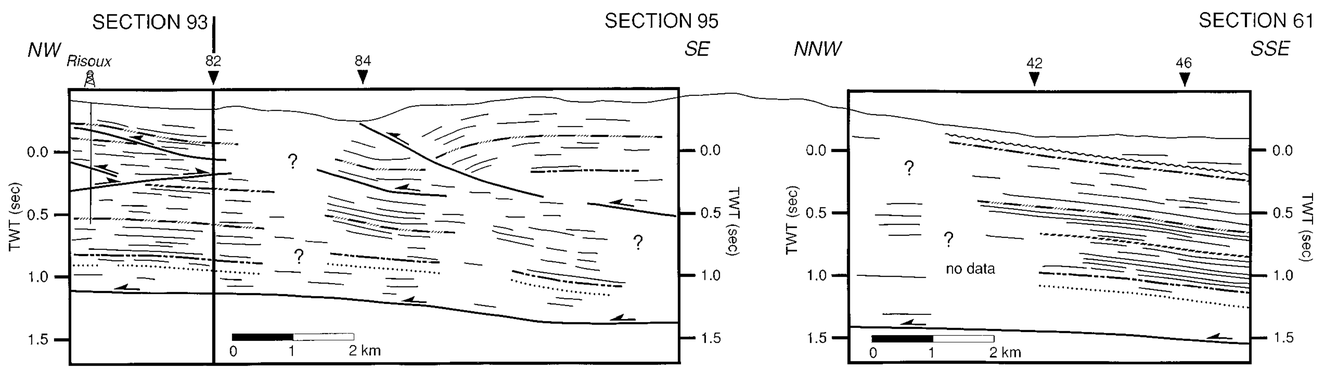

PANEL 8

STRIKE LINES

RISOUX, JURA MTS (VAUD) SWITZERLAND

SECTION 82

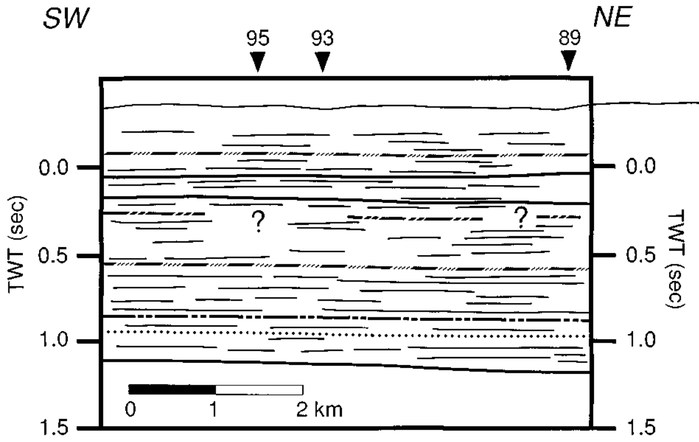

SECTION 80

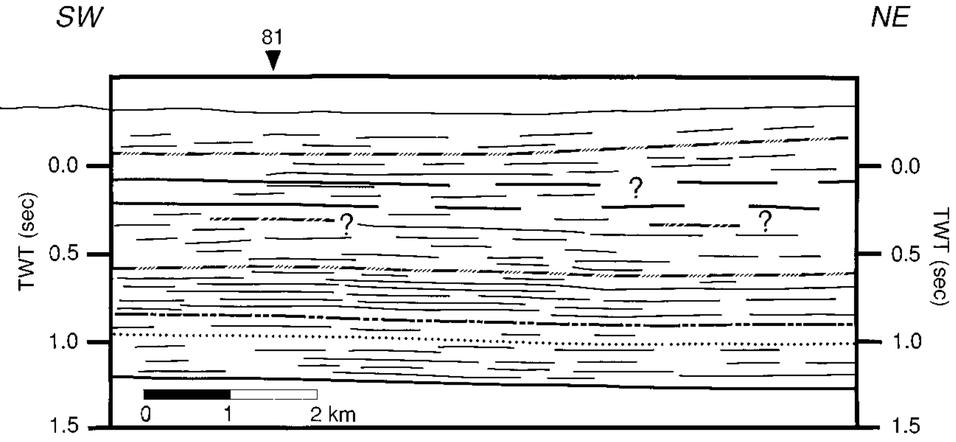

SECTION 84

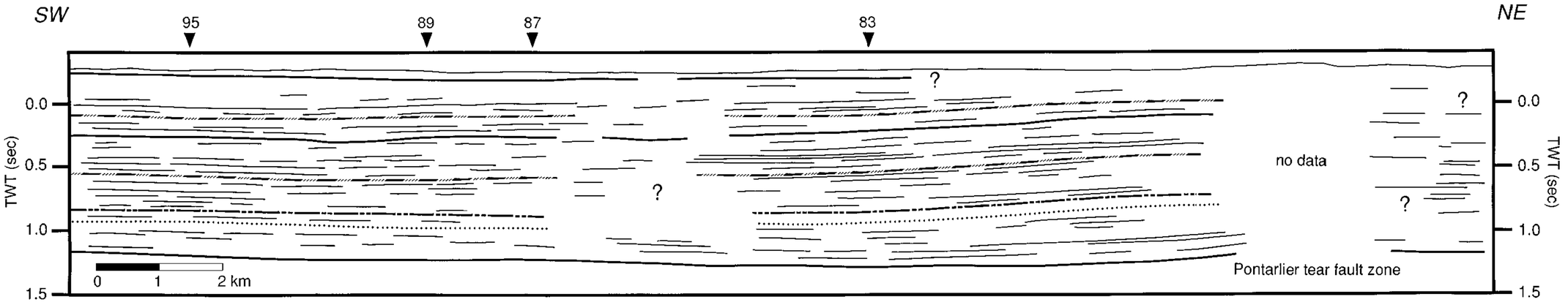

LEGEND

- Tops
- Cretaceous
- Malm
- Dogger
- Liassic
- Triassic Unit 1
- Triassic Unit 2
- Faults

LOCATION MAP

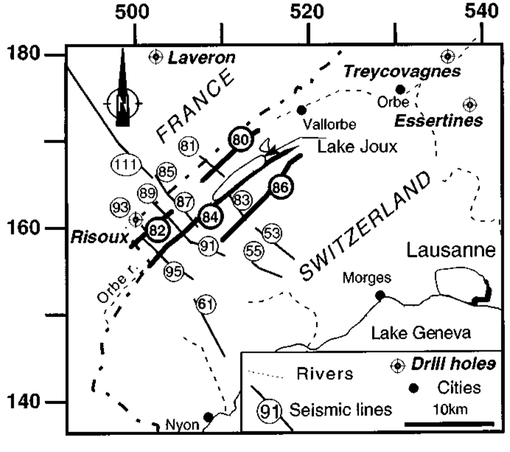

SECTION 86

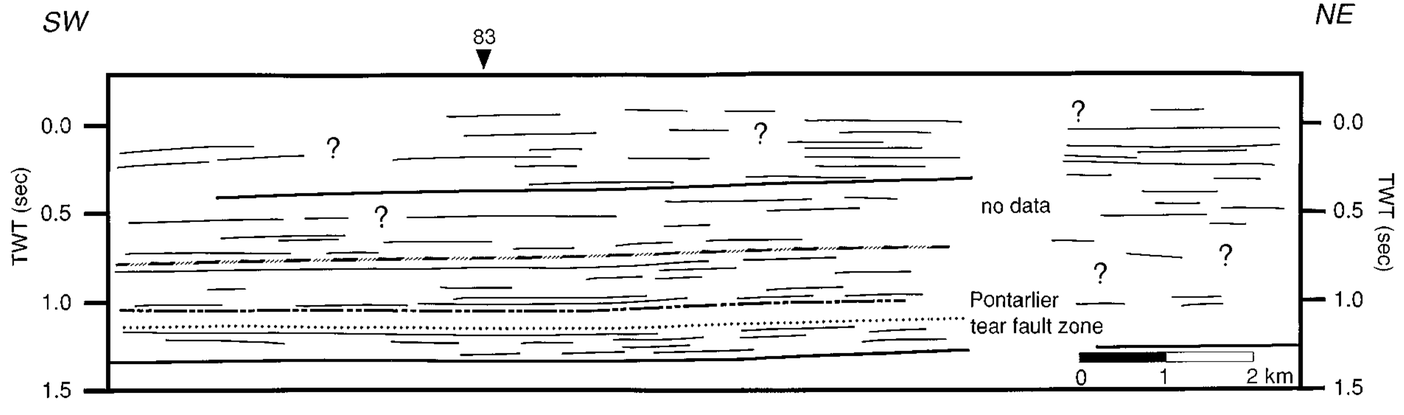

SECTION 46

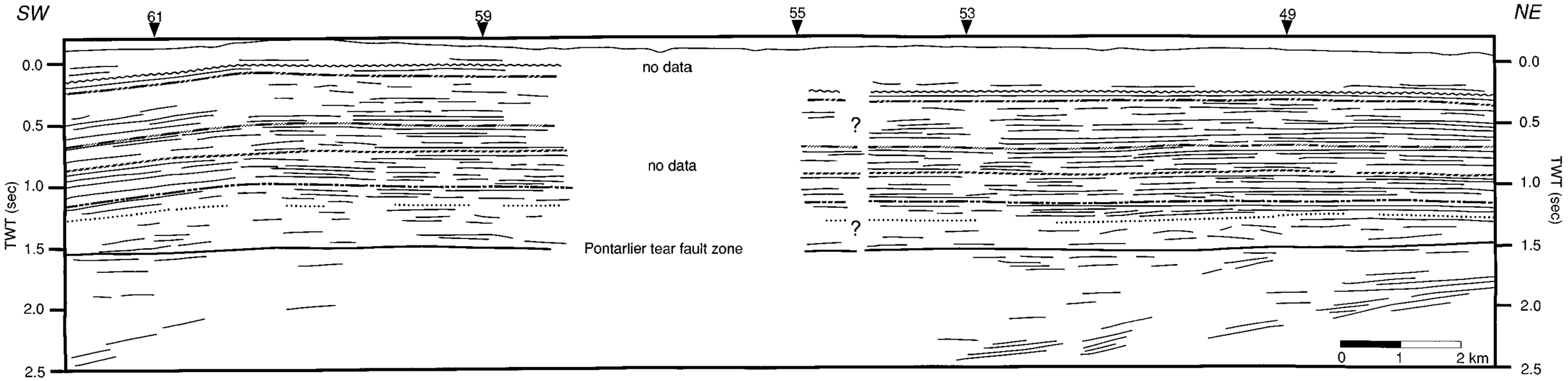

PANEL 7

STRIKE LINES

MOLASSE BASIN (VAUD) SWITZERLAND

Pontarlier tear fault zone

SECTION 50

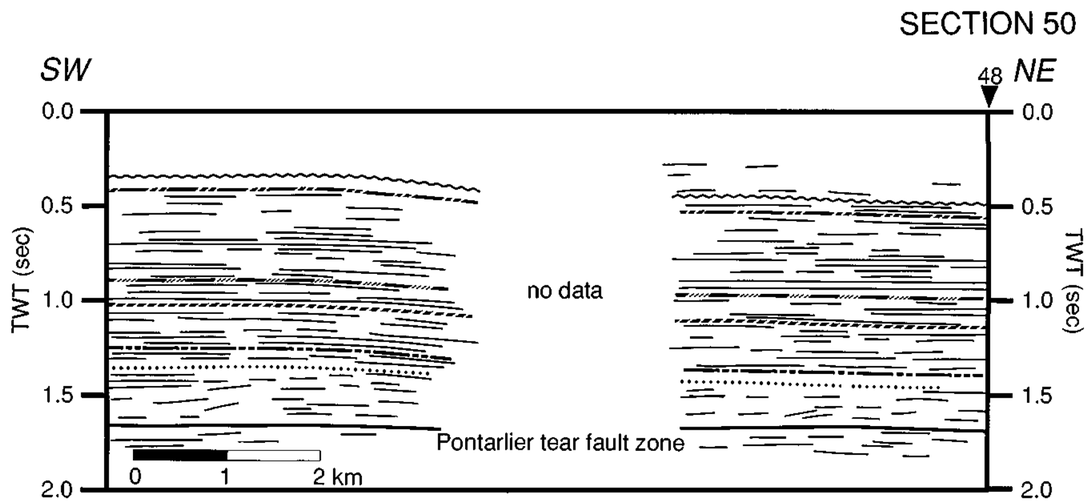

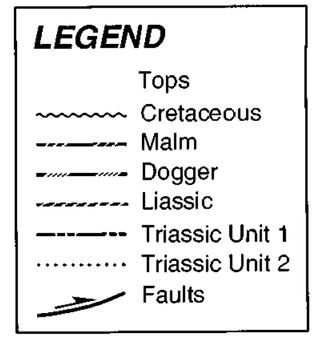

LOCATION MAP

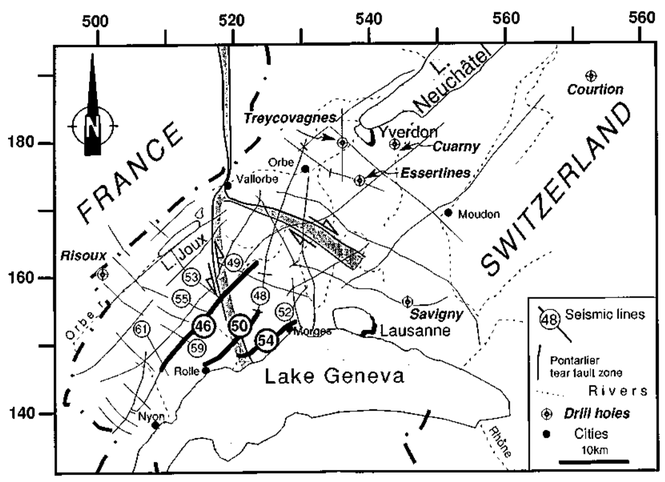

SECTION 54

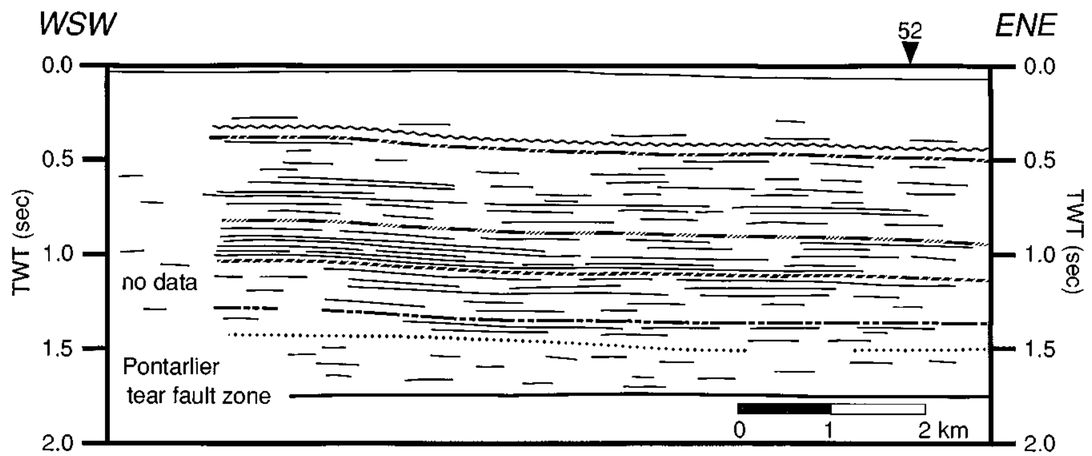

PANEL 6

N-S LINES

MOLASSE BASIN (VAUD) SWITZERLAND

LOCATION MAP

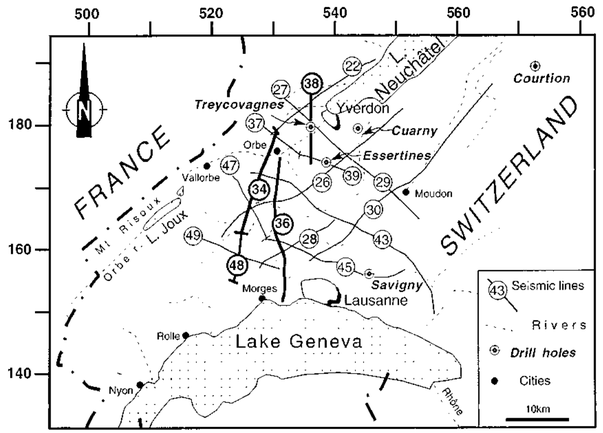

SECTION 38

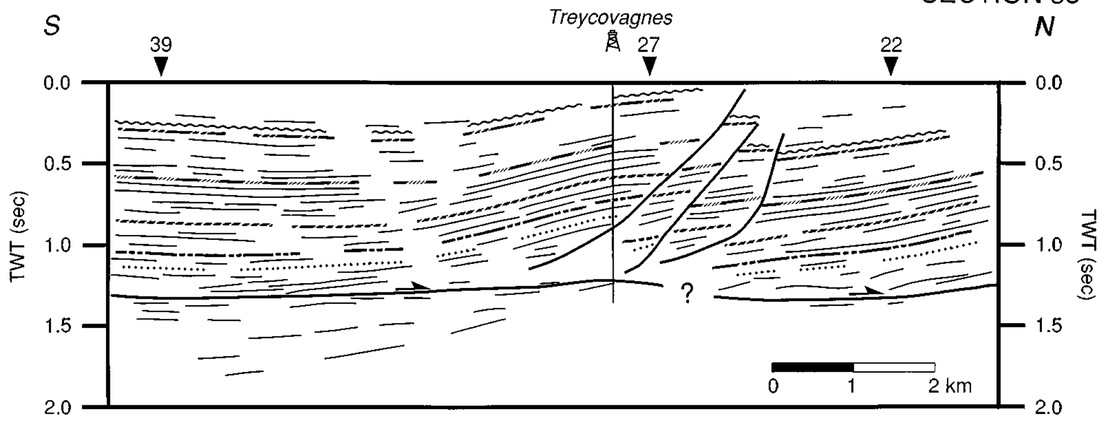

SECTION 36

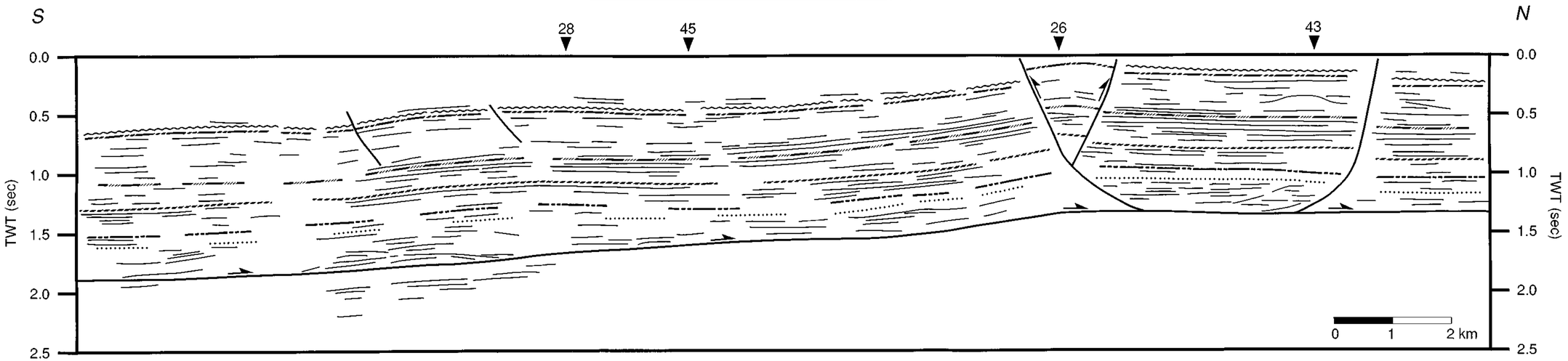

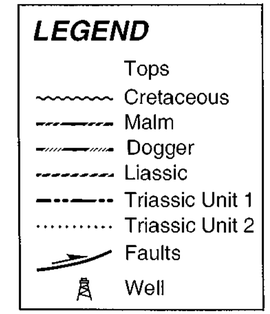

SECTION 48 — SECTION 34

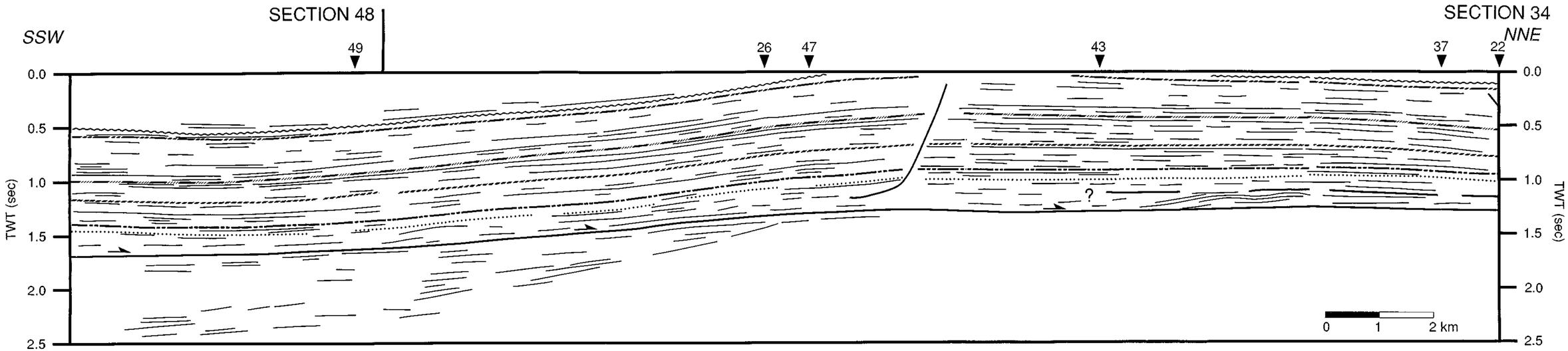

PANEL 5

DIP LINES

MOLASSE BASIN (VAUD) SWITZERLAND

SECTION 27

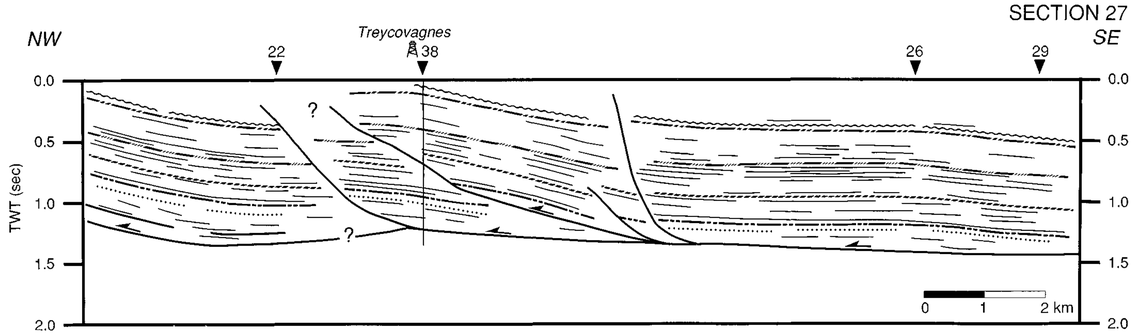

SECTION 29

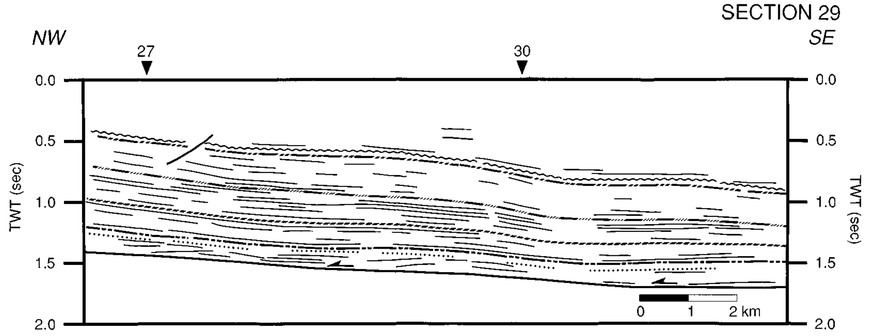

SECTION 37 | SECTION 39

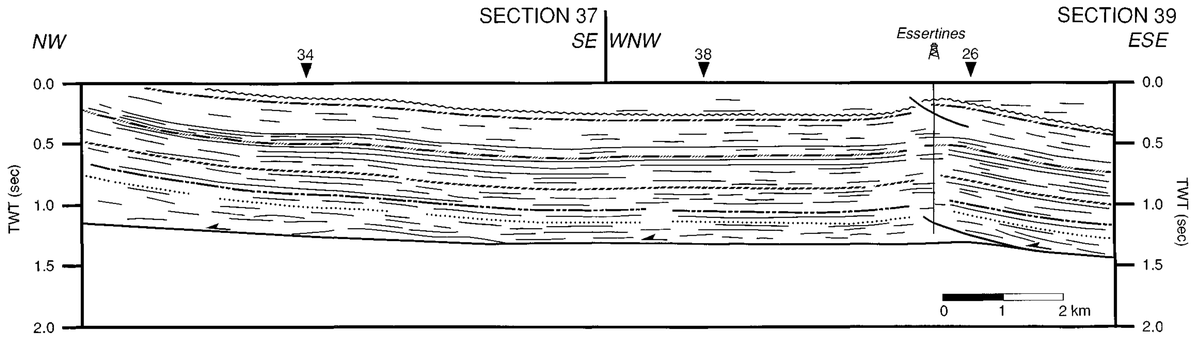

LOCATION MAP

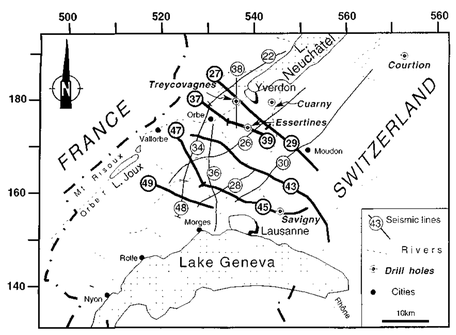

SECTION 43

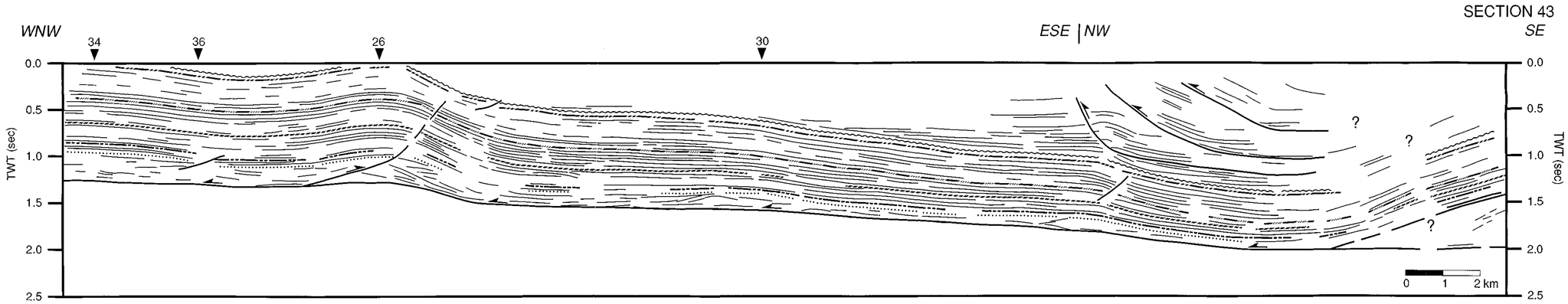

SECTION 47 | SECTION 45

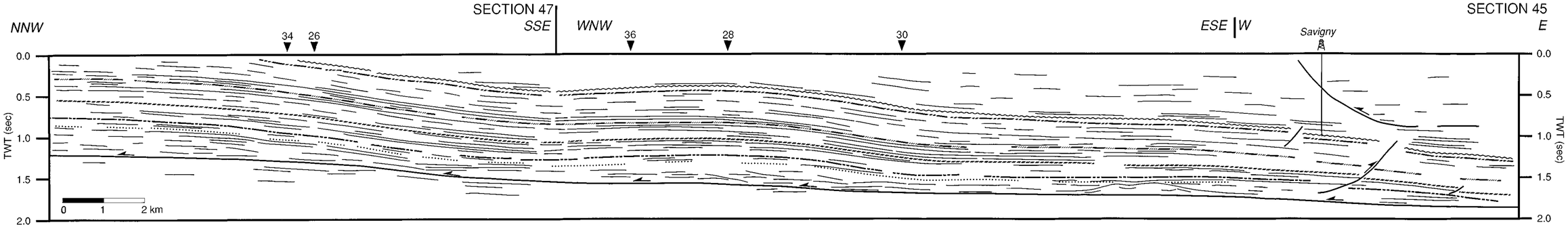

SECTION 49

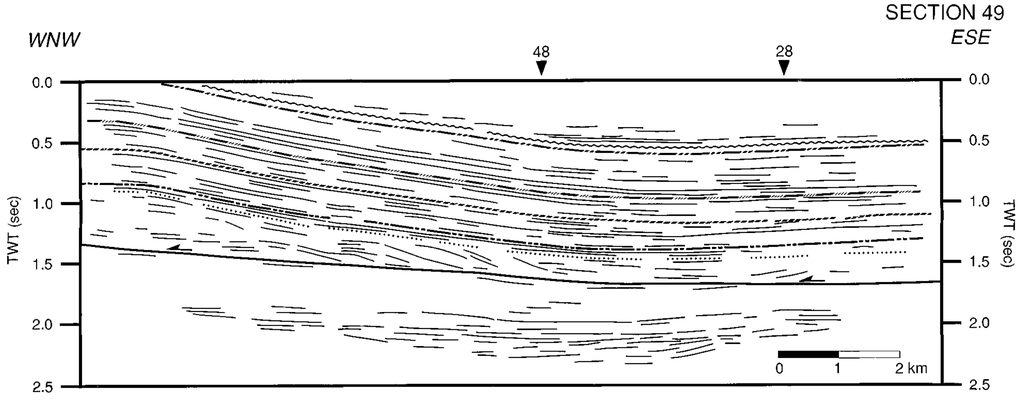

LEGEND

- Tops
- Cretaceous
- Malm
- Dogger
- Liassic
- Triassic Unit 1
- Triassic Unit 2
- Faults
- Well

PANEL 4

STRIKE LINES

MOLASSE BASIN (VAUD) SWITZERLAND

SECTION 22

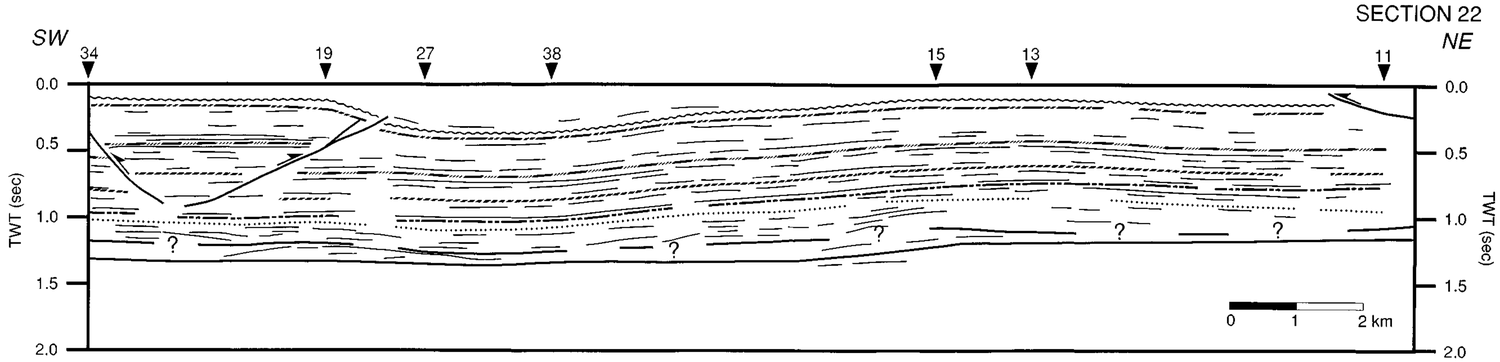

SECTION 26

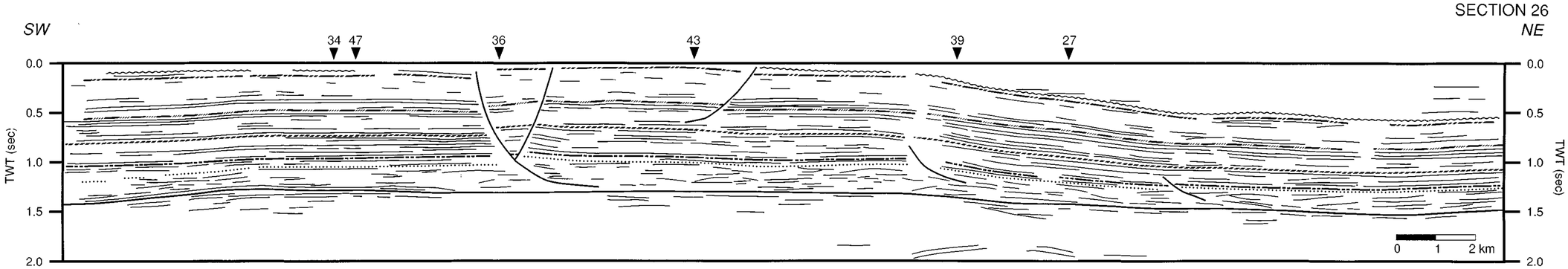

SECTION 28

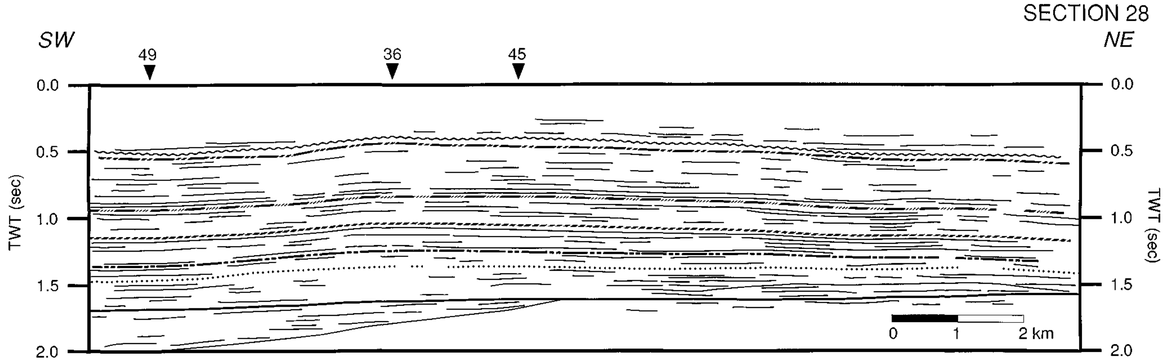

LOCATION MAP

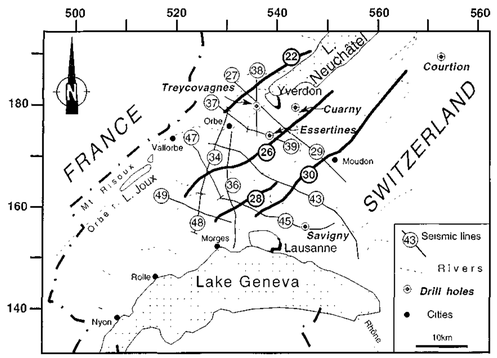

LEGEND

- Tops
- Cretaceous
- Malm
- Dogger
- Liassic
- Triassic Unit 1
- Triassic Unit 2
- Faults

SECTION 30

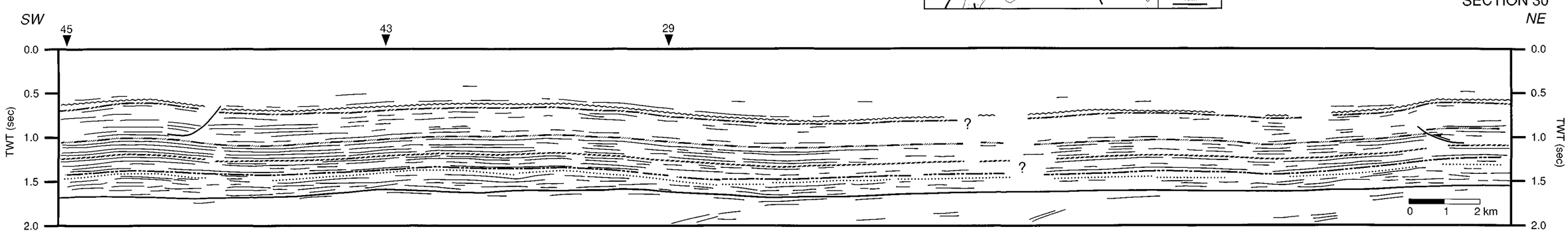

PANEL 3

STRIKE LINES
JURA MTS.
(NEUCHATEL, VAUD)
SWITZERLAND

LOCATION MAP

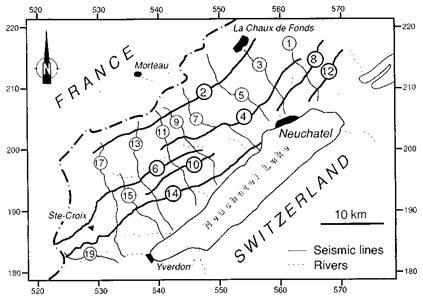

SECTION 2

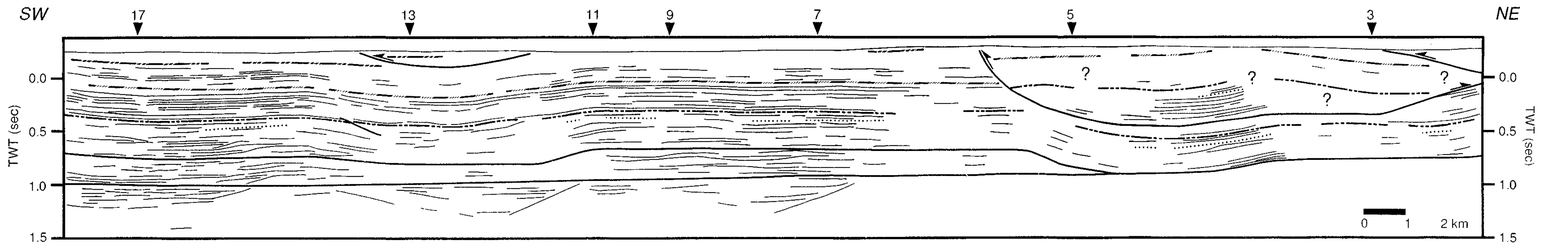

SECTION 4

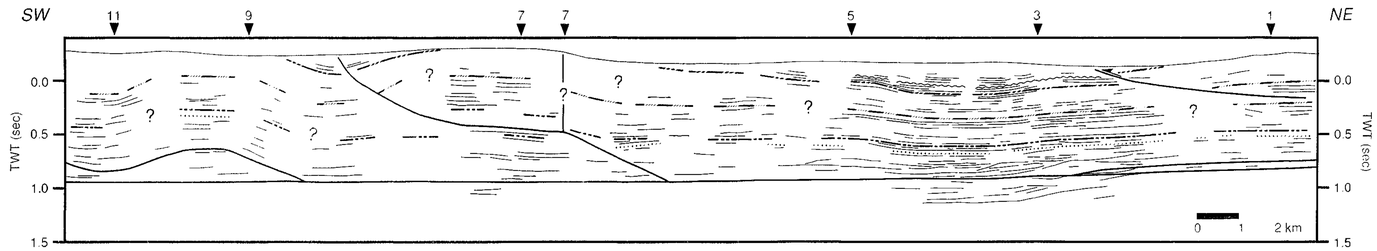

SECTION 6

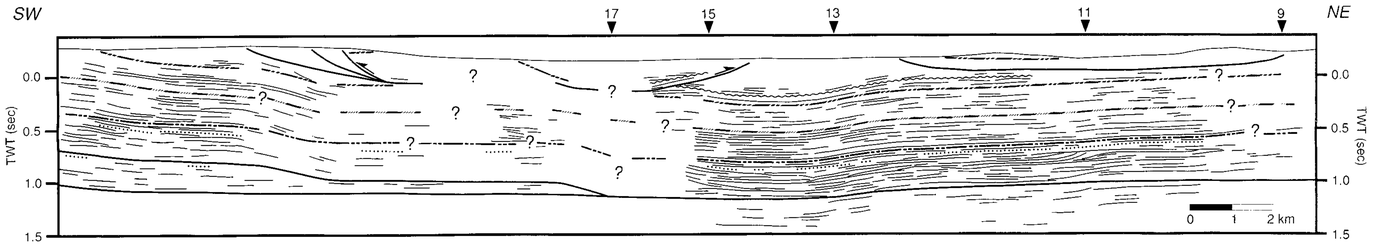

SECTION 8

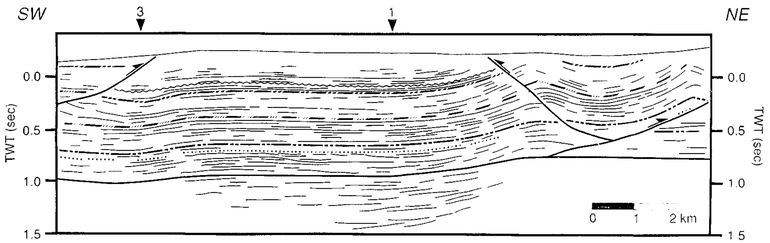

SECTION 10

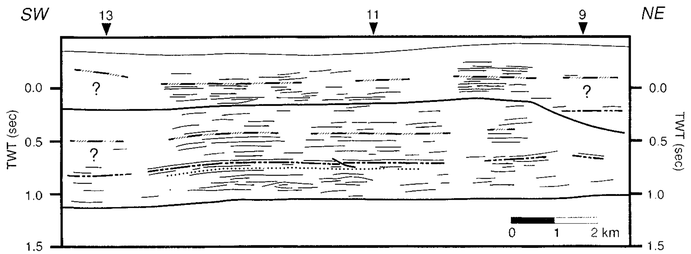

SECTION 12

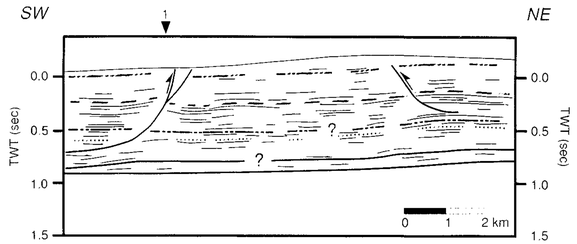

LEGEND

- Tops
- Cretaceous
- Malm
- Dogger
- Triassic Unit 1
- Triassic Unit 2
- Faults

SECTION 14

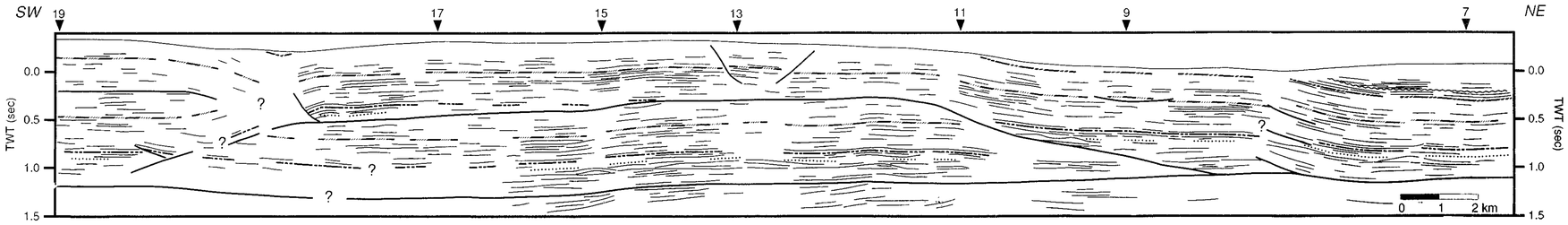

PANEL 2

DIP LINES

JURA MTS. (NEUCHATEL, VAUD) SWITZERLAND

SECTION 9

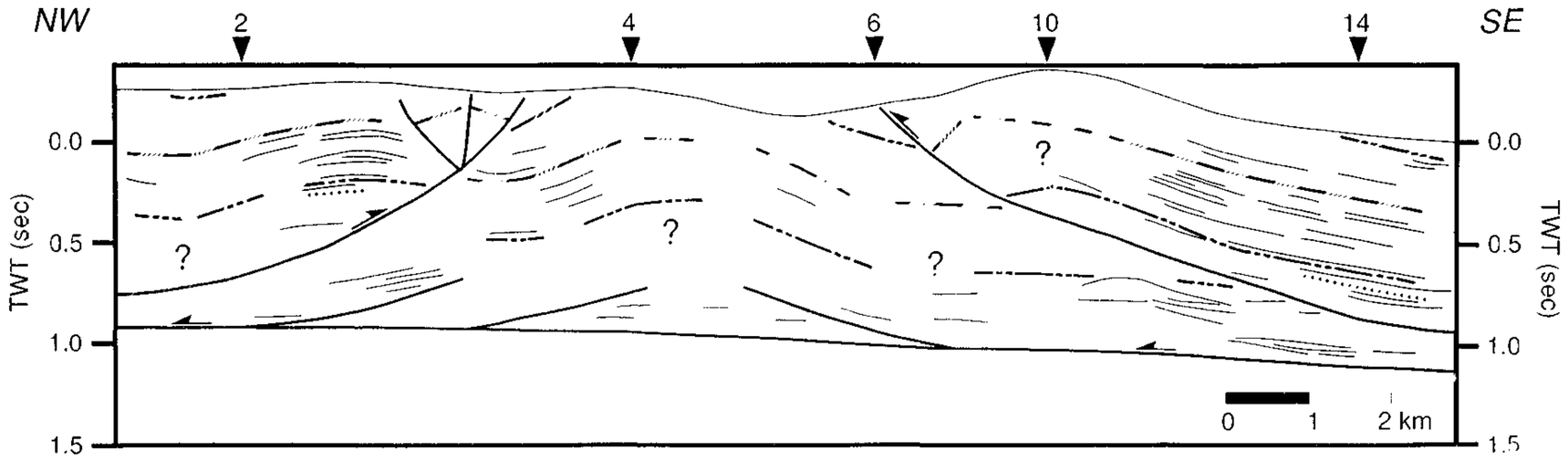

SECTION 11

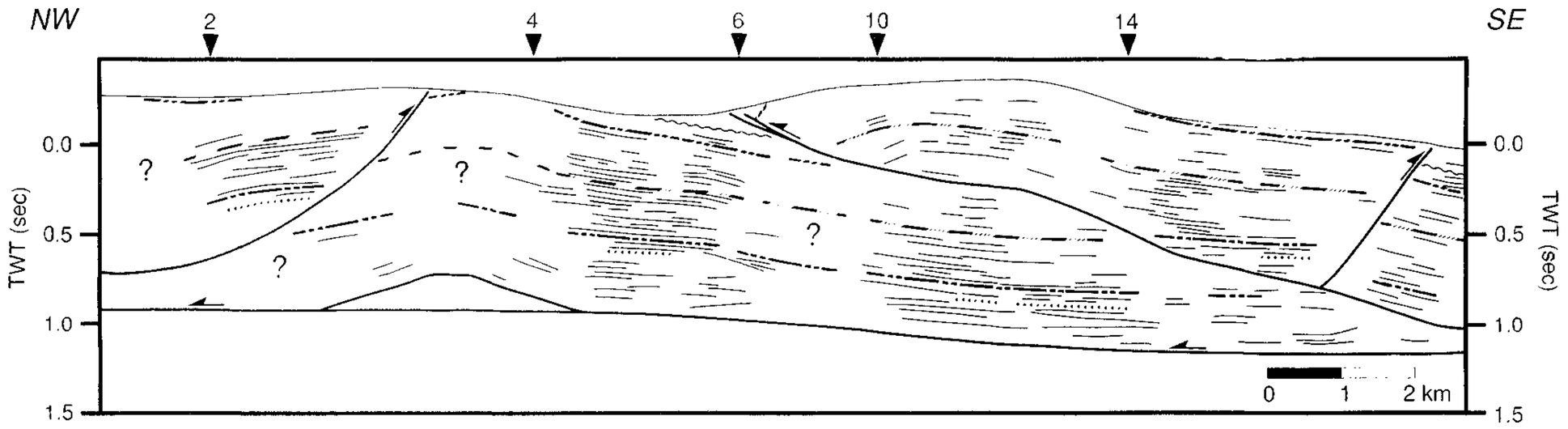

SECTION 13

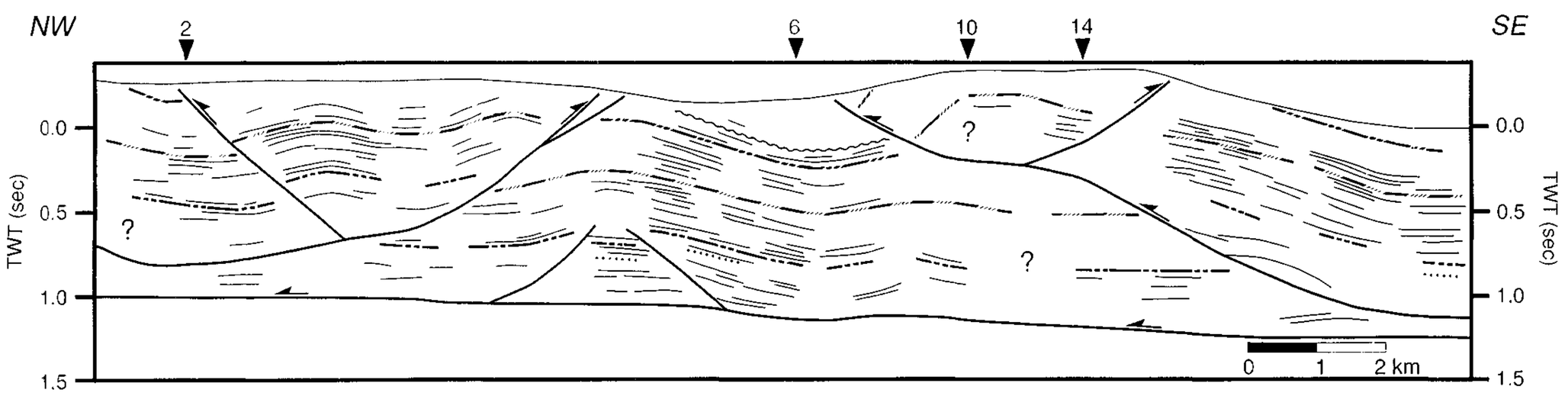

SECTION 15

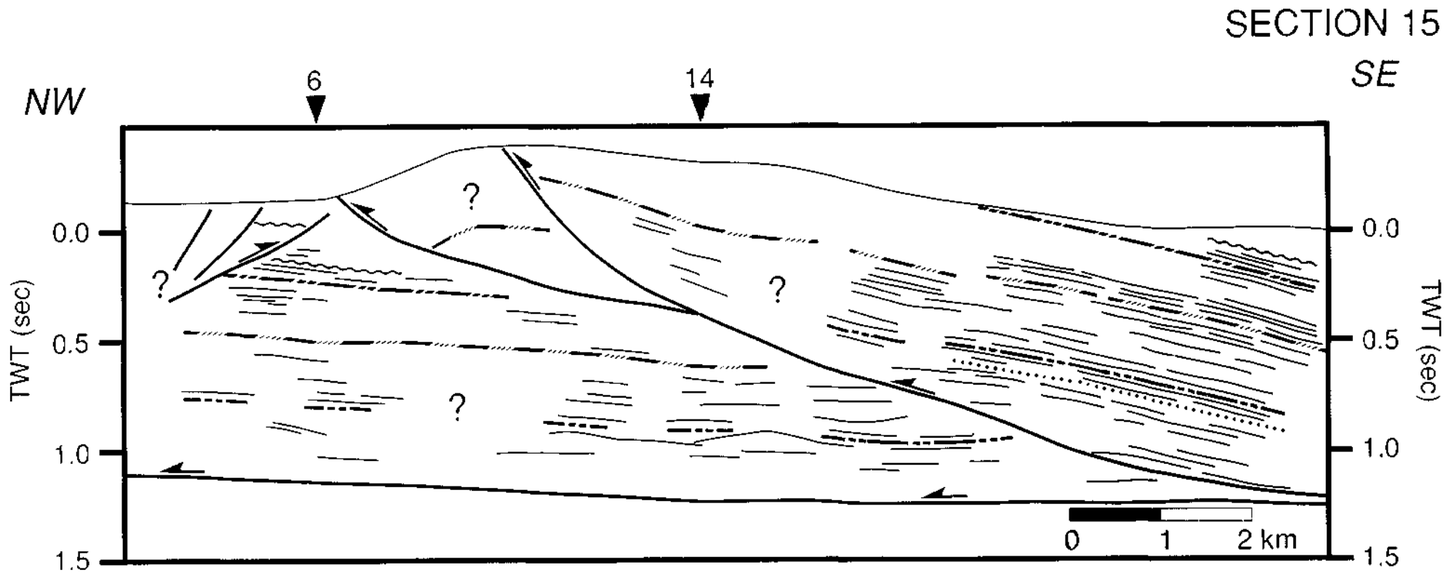

LEGEND

- Tops
- Cretaceous
- Malm
- Dogger
- Triassic Unit 1
- Triassic Unit 2
- Faults

SECTION 17

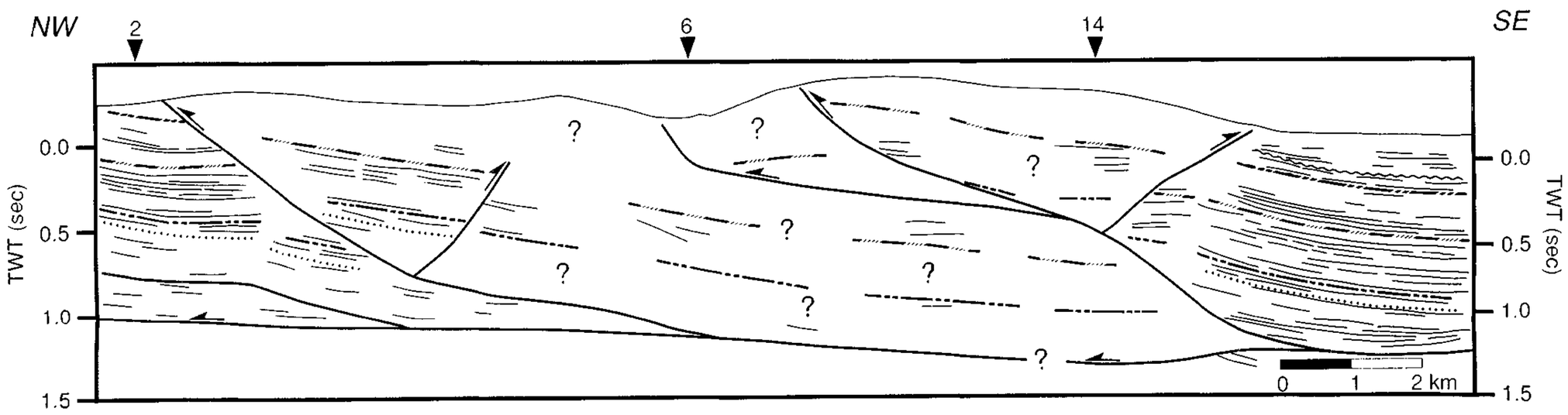

LOCATION MAP

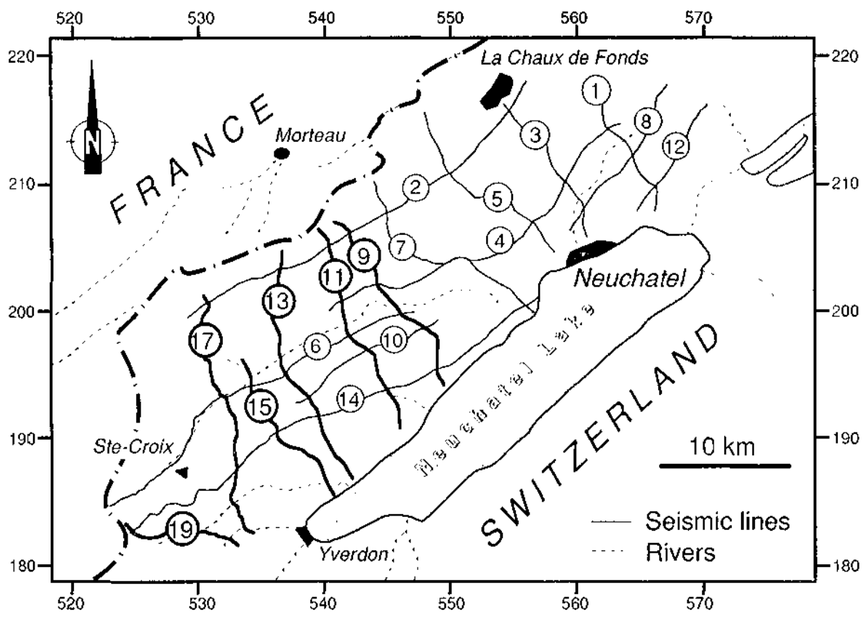

SECTION 19

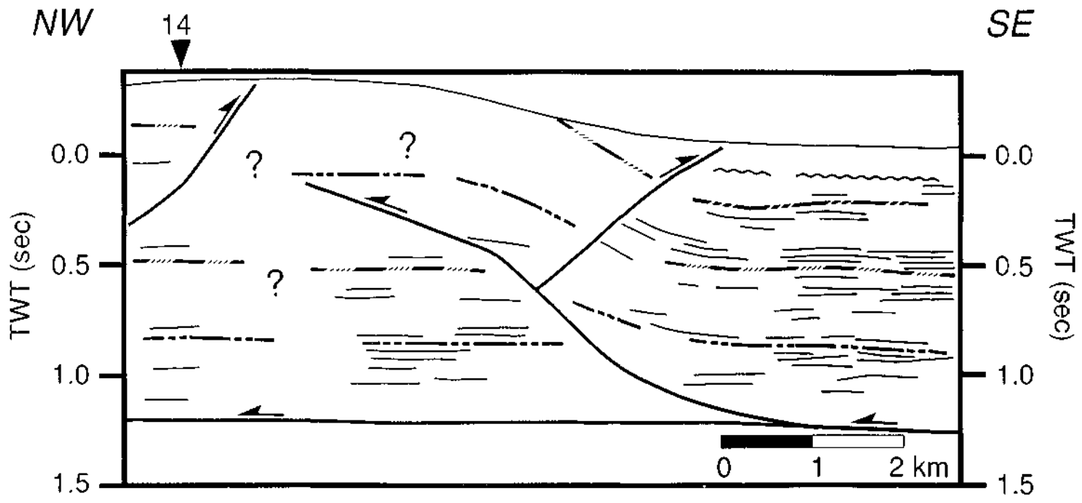

PANEL 1

DIP LINES
JURA MTS.
(NEUCHATEL)
SWITZERLAND

LOCATION MAP

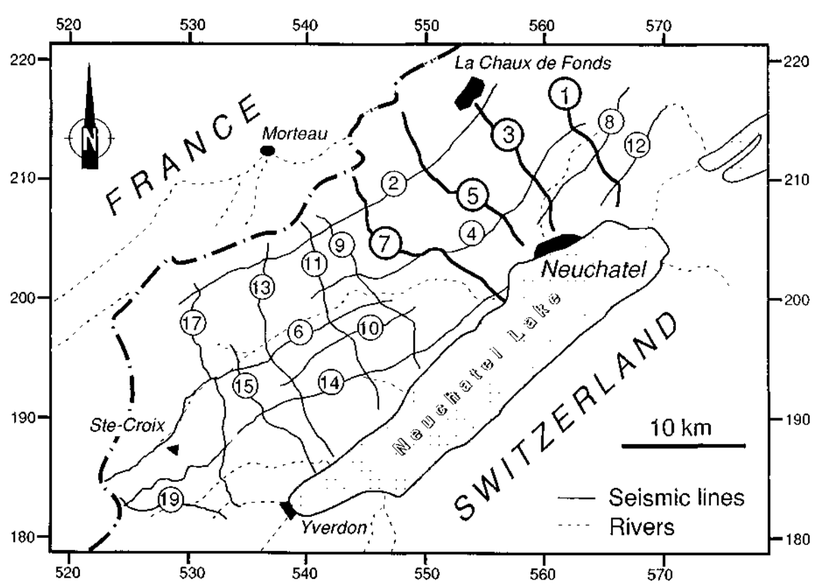

LEGEND

- Tops
- Cretaceous
- Malm
- Dogger
- Triassic Unit 1
- Triassic Unit 2
- Faults

SECTION 1

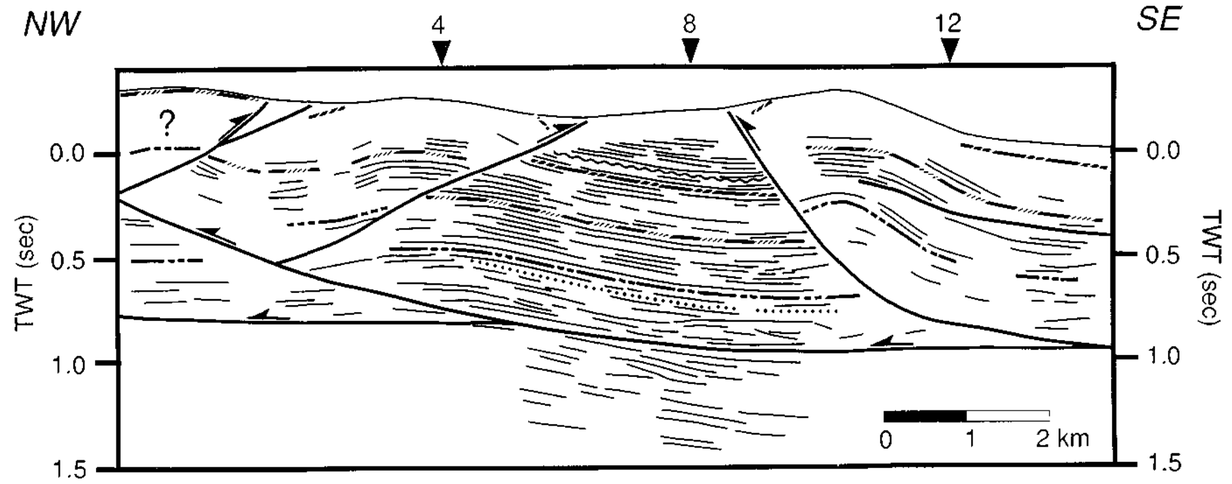

SECTION 3

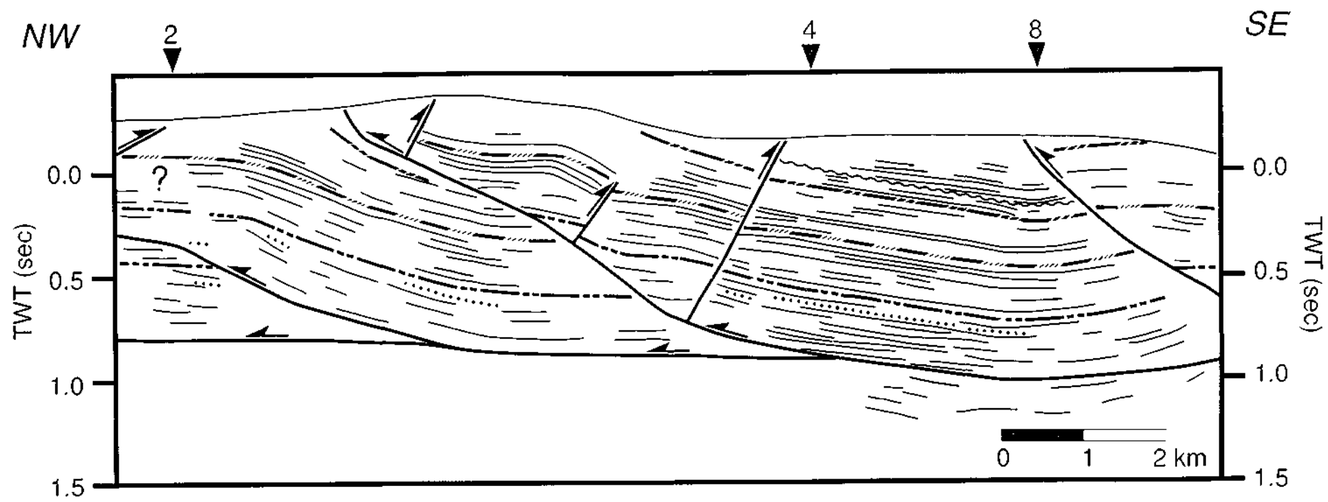

SECTION 5

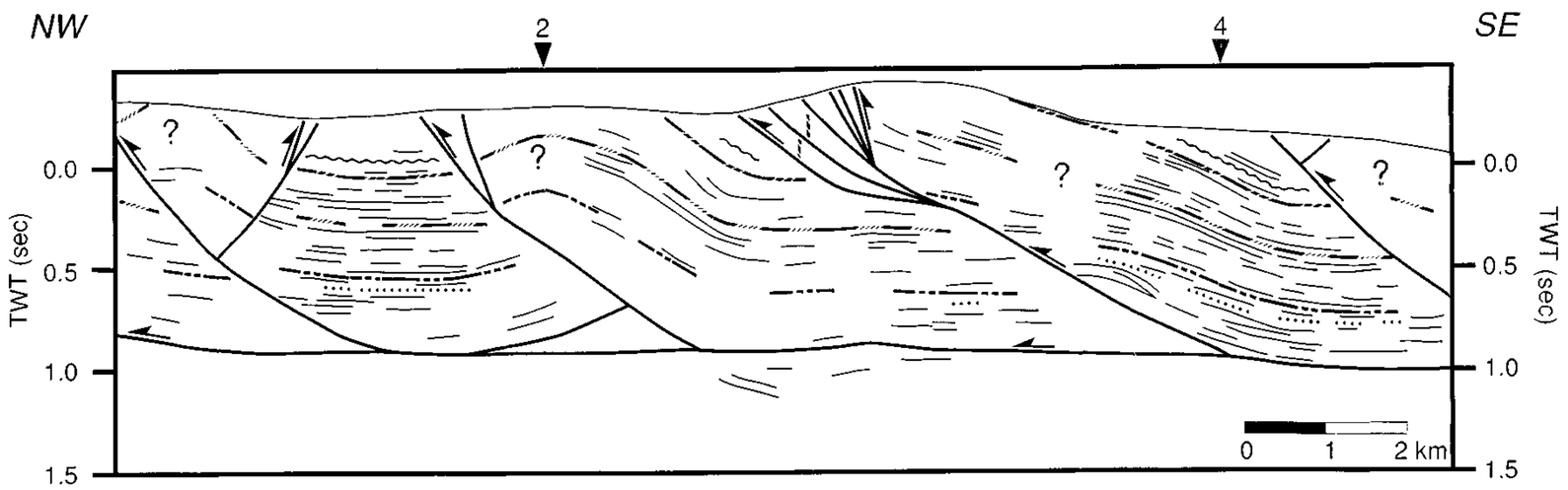

SECTION 7

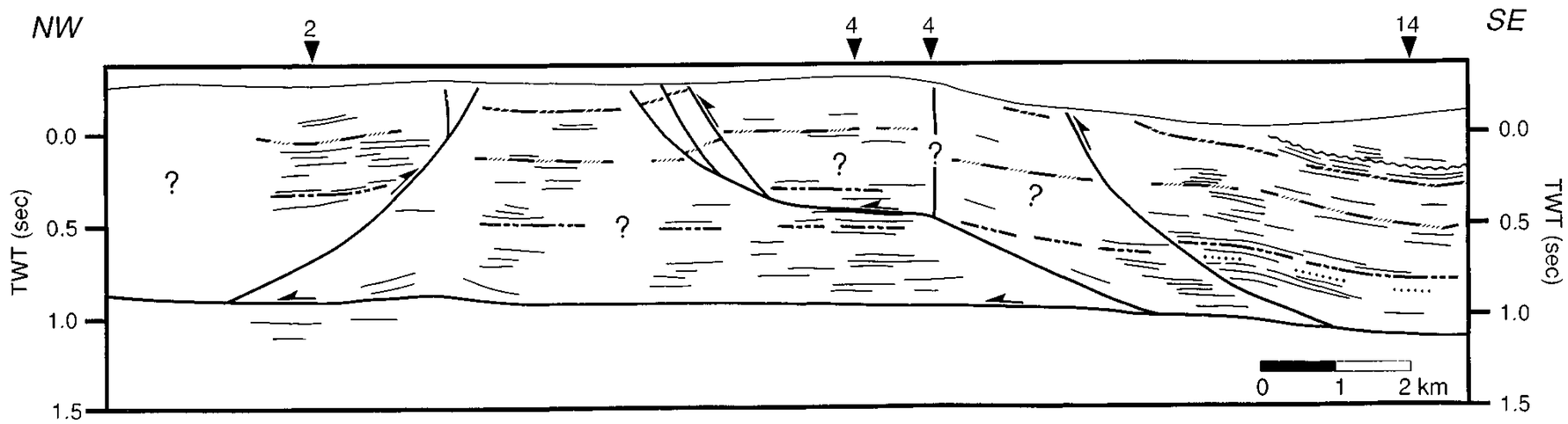

PLATE 9 Cross-section

LOCATION MAP

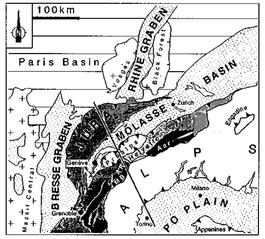

Restored section

NW (335°) *SE (155°)*